Mechanisms of Emplacement of Cone Sheets, Ardnamurchan, Argyll

by

Theresa Maria Jezierski

This thesis is presented to the C.N.A.A. in partial fulfilment of the requirements for the degree of Doctor of Philosophy.

This research was carried out at the Department of Geology,
City of London Polytechnic

March 1985

DEDICATION

I dedicate this work to the memory of my parents
Jan and Jean Jezierski

ACKNOWLEDGEMENTS

I would like to thank Professor R.R. Skelhorn for all his help throughout the duration of my research, Drs. J. Hossack and R.C. Standley for assistance during my research and for reading the manuscript. I also thank the technical staff of the City of London Polytechnic, for their photographic and thin sectioning services. I should like to express my thanks to Kym Hockings for helping me to master the PDP11 and for assistance with my experiments.

This research was supported by a N.E.R.C. Research Studentship (GT4/79/GS/54) which is gratefully acknowledged.

Finally, I would like to thank my family and my husband, Jon, for being a constant source of encouragement.

ABSTRACT

Mechanisms of Emplacement of Cone Sheets, Ardnamurchan, Argyll

by Theresa Maria Jezierski

Thin (1m), centrally inclined (cone) sheets of basic rock are a unique but common feature of the intrusive complexes within the Thulean Igneous Province. A field, structural, statistical and petrographic analysis of these sheets belonging to the Ardnamurchan Central Intrusive Complex has been made in order to determine their mode of emplacement.

Detailed field work involved the measurement of the dip, strike, thickness, distance between each cone sheet fracture, host rock type and rock type of each cone sheet contained within a number of traverses across all the cone sheet sets. Each of the traverses were divided into unit lengths of 100m, enabling ease of calculation and comparison both within and between traverses. Displacements of host rock structures were measured in order to determine opening directions of the cone sheets. The aggregate amount of uplift caused by the emplacement of the Ardnamurchan cone sheets is about 820m.

Statistical analysis of cone sheet parameters revealed the existance of five sets of cone sheets associated with the three igneous centres recognised by Richey *et al.* (1930). Centre One has one set, Centre Two has three sets and Centre Three has one set.

Hydraulic fracturing was the mechanism whereby cone sheet fractures were initiated. Their subsequent opening was predominantly through reversed shear movements although opening via normal shear and tension also occurred. Cone sheet emplacement not only resulted in vertical movements but also caused an anticlockwise rotation ($<1^{\circ}$) of the centrally uplifted rock mass.

Cone sheet at their terminations commonly pass latterally from a continuous sheet into a series of en echelon lenses of diminishing size. The existance of en echelon lenses assisted in the identification of an advancing cone sheet front and a vertical zonation of a cone sheet set.

As a culmination of the work an idealised cone sheet set has been modelled. The set has three vertical structural levels or zones. Zones 3 (proximal to the focus) to 1 (distal) show a progressive shallowing in dip angle and an increase in the number of termination structures. The two uppermost zones have been recognised in Ardnamurchan. Zone 3 is thought to lie beneath the present level of erosion.

CONTENTS

CONTENTS

ON THE FORM OF CONE SHEETS

LIST OF FIGURES

TABLES

LIST OF PLATES

CHAPTER 1

PREVIOUS INVESTIGATIONS

1.1 BRITISH TERTIARY IGNEOUS PROVINCE

For almost a century the genesis of cone sheet intrusions has been debated. "Centrally inclined sheets" were first identified and described in the Cuillins of Skye by Harker (1904). As a direct consequence of Harkers identification, other cone sheet complexes were recognised in other parts of the British Tertiary Igneous Province. Bailey et al. (1924) produced detailed maps of such intrusions in Mull, and Richey et al. (1930) identified cone sheets in Ardnamurchan (Fig.1.1.1). Anderson (in Bailey et al. (1924)) first postulated a mechanism of formation of cone sheets under high magma pressure.

Several authors have put forward theories of formation and general comments on the morphology of cone sheets and their emplacement. Judd (1874) commented on the ridges occurring in the Mesozoic sediments of Ardnamurchan which are now known to be cone sheets. Traill (1878) mapped a set of sheets belonging to the Carlingford Central Intrusive Complex, although he did not attach any significance to them and it was Richey (1932) who re-interpreted them as a series of inclined sheets (cone sheets). Bailey and Wright were shown the inclined sheets of the Cuillins by Harker in 1909, which led to the identification of the Mull cone sheet sets. Mapping of the Mull Central Intrusive Complex led to the publication of the Mull Memoir (1924) where Bailey et al. noted the large number of cone sheets and commented that few eruptive centres, in a world wide sense, contained cone sheets.

Anderson (in Bailey et al. 1924) was the first person to

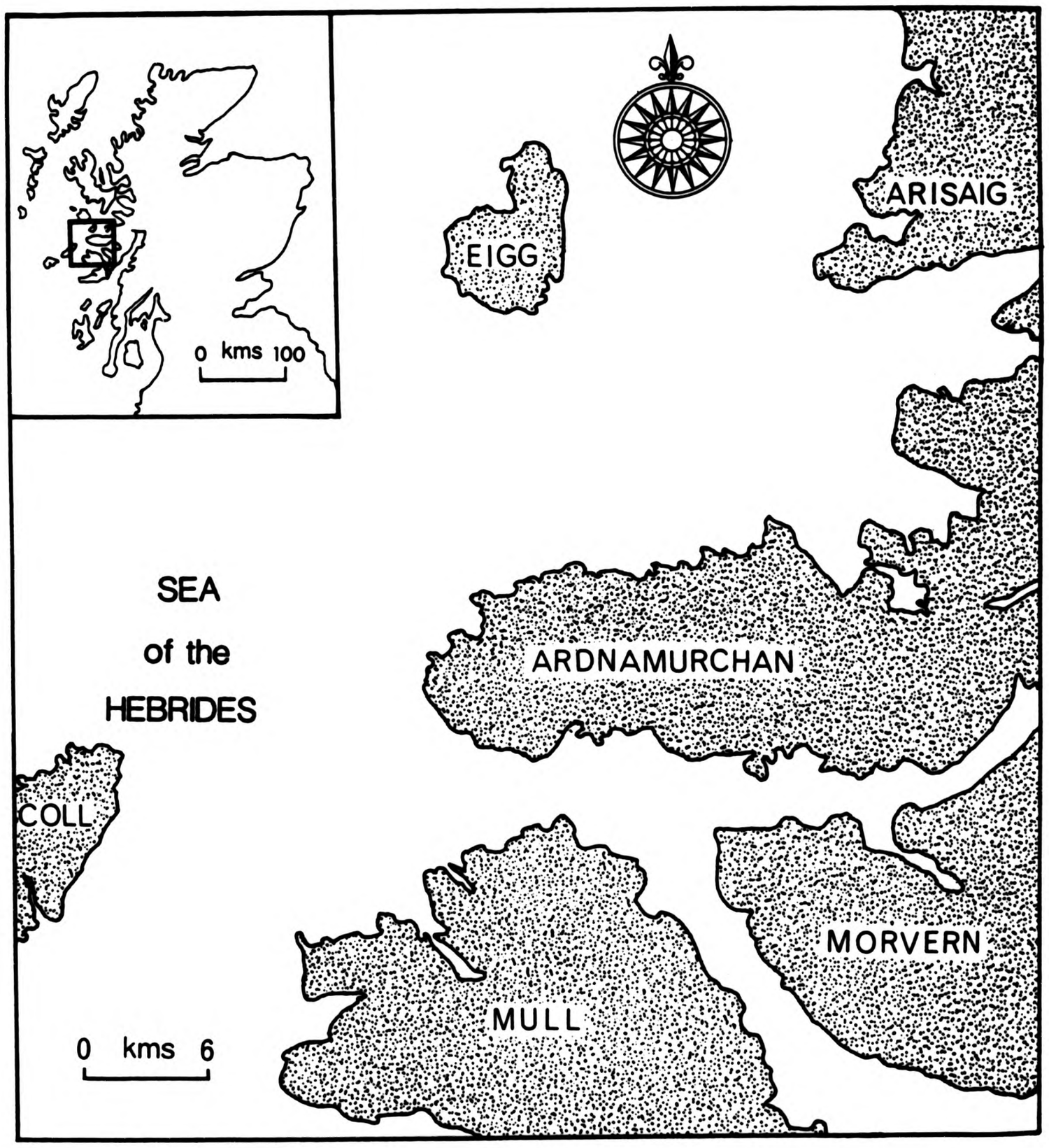

Fig.1.1.1. Location map of the Ardnamurchan Peninsula

put forward a mathematical theory of cone sheet formation. His model involved a parabola shaped magma chamber several miles below a horizontal ground surface. The magma has a specific gravity similar to the host rock and is at sufficient pressure to reach the surface if there was an outlet. If magma pressure were increased, a tensional regime would act across the area of the magma chamber, forming a set of fractures roughly conical in shape, which steepen towards the focus. Cutting these tension fractures orthogonally are a second set of tension fractures (Fig.1.1.2).

Further work on cone sheets during the 1930's shed more light on their mechanism of emplacement. In 1930 the Ardnamurchan, N W Mull and Coll Memoir was published, in which Richey *et al.* (1930) calculated the central uplift caused by the emplacement of the cone sheets as 4600ft, assuming that all displacement caused by the intrusion of the cone sheets was confined to the upper wall of the cone sheets. The total uplift was measured in a vertical sense and he made no reference to the actual type of opening displayed by the cone sheets in the field.

Anderson (1936) expanded his views on the distribution of stresses around a theoretical magma chamber (Fig.1.1.2). He calculated that the maximum principal stress (σ_1) is perpendicular to the host rock/magma interface, the intermediate principal stress (σ_2) is parallel to the strike of the cone sheets and the minimum principal stress (σ_3) is tangential to the host rock/magma interface and lies in radial planes. He concluded that cone sheets occupy tension fractures but that his theoreti-

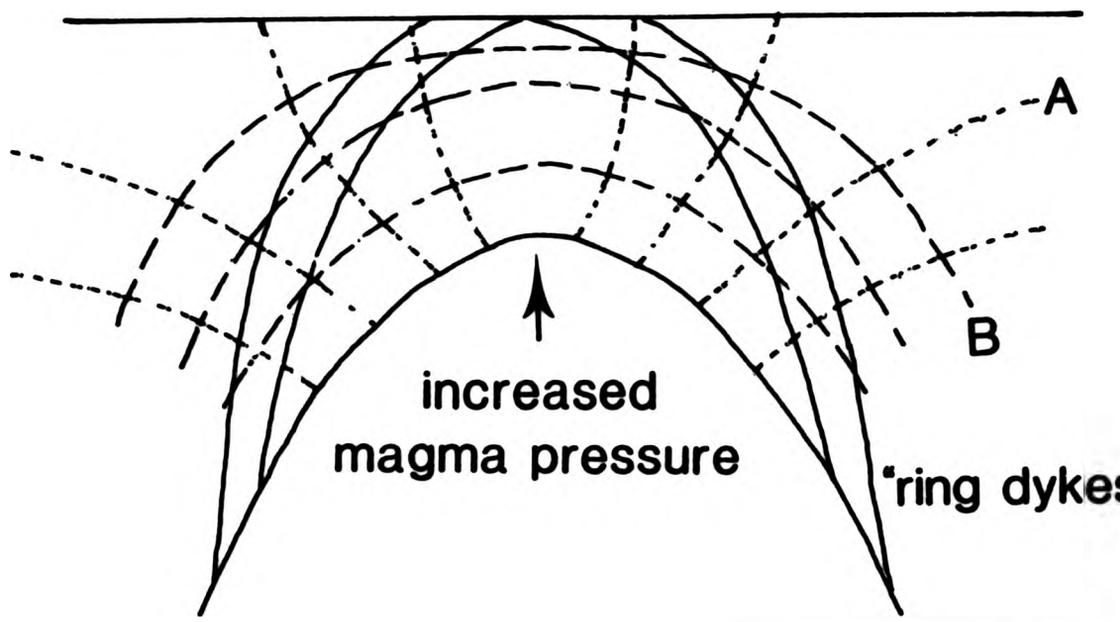

A system of tensions ,conical in shape - cone sheet fractures

B superimposed set of tensions

Fig.1.1.2 Diagram showing Anderson's (1936) model of tension distribution around a parabolic magma chamber, resulting in the formation of cone sheets
The increased magma pressure and B result in opening of fractures A to form cone sheets

cally derived shear planes were too steep to account for the low dipping sheets seen in the field.

Keunen (1937) took a close look at the type of uplift, as indicated by the displacement of marker horizons on either side of individual cone sheets in the field, and points out that Anderson gave no evidence of central uplift. With no evidence of subsequent movement along the cone sheet fractures, Keunen (1937) gave a number of examples of Ardnamurchan cone sheets in which the hanging wall is lifted. Plate 1.1 shows the section to which Keunen refers, where a cone sheet fracture is parallel to a joint set. With reference to this example, Keunen (p180) states:-

"The intruding cone-sheets made use of the joints that happened to coincide with their direction, in the same manner as offshoots

followed the fissility provided by the bedding planes to form small sills."

As to the cause of fracturing, he used the analogy of a sharp blow punching a conical hole in glass in contrast to the shattering caused by a thrown stone. Following fracturing, a low viscosity magma intruded the fractures. He estimated that the Ardnamurchan cone sheets were emplaced over a period of 100,000 yrs, with a rate of magma advance of 1" per year that is:

"...one cone sheet every few hundred years."

The cause of fracture as proposed by Anderson (1936) did

Plate 1.1 Cone sheet emplaced parallel to well developed joint set in Jurassic limestones, west of Mingary Pier, Outer Centre Two, as referred to by Keunen (1937).

Plate 1.1 Cone sheet emplaced parallel to well developed joint set in Jurassic limestones, west of Mingary Pier, Outer Centre Two, as referred to by Keunen (1937).

not explain the lack of cone sheets in the central area of the complexes. Jeffries (1936), working on fractures in glass and flint, recognised that conical fractures caused by percussion had features similar to cone sheet complexes, there being a central zone with no fractures and a definite outer limit to the intensity of fracture formation.

Garson (1959) describes cone sheets in Nyasaland (Malawi) which have low dips and shear movements along their fractures. Robson and Barr (1964) investigated the stress field around a simple magma body and from this derived theoretical stress figures for cone sheet formation. They concluded that cone sheets occupy normal shear fractures, such that the central block is displaced downwards and therefore take the completely opposite view to Anderson's original hypothesis.

Hills (1968) interpreted the work of Tolansky and Howes (1954) on fractures in glass as being similar to the development of cone sheet fractures and concluded that cone sheets developed in a spiral and that perhaps some cone sheets were spiral fractures. Working on the Ardnamurchan Complex, Durrance (1967) adopted the spiral cone sheet hypothesis in his photoelastic analysis of the cone sheet complex. His hypothesis, in essence, is that of a single centre causing a dominant fracture pattern that has been subsequently been exploited by the four cone sheet sets of Ardnamurchan. This single centred hypothesis opposes the triple centred hypothesis of Richey et al. (1930). In addition to this, Durrance (1968) suggests the existance of a torsional force (Chapter 7) acting during the emplacement of the cone sheets.

Phillips' (1974) hypothesis of cone sheet formation begins with retrograde boiling in the magma chamber, resulting in the expansion of the magma and increased magma pressure, and the formation of hydraulic shear fractures in areas of rotational strain (Fig.1.1.3). On cessation of expansion a decrease in deviatoric stress occurs and the resultant increased magma pressure on the cone sheet fractures causes them to pass into simple hydraulic tension fractures, thus resulting in trumpet-shaped cone sheets (in vertical cross-section), the lower part forming in shear, the more distal part forming in tension.

Walker (1975), with reference to the British Tertiary Igneous Province, describes an all embracing theory of a rising acid diapir, ahead of a basic cylinder, which would dome the surface and act to divert the rising basic magma to form cone sheets, rather than dykes, due to the change in pattern of excess hydrostatic pressure surfaces.

Bahat (1979) simulated cone sheet fractures in glass by using a liquid (mercury) as an indenter and noted the spiral development of the fracture, similar to those produced by a solid indenter. He, like Phillips, believes that different stress regimes exist at different depths, shear at greater depths, tension at shallower depths and suggests that this explains the cone sheet sets of Homa Mountain, Kenya whose large number of cone sheet foci of activity lie at different depths beneath the present land surface. Throughout Bahat's (1979) experiments only one fracture is created with each "indentation". Thus, for a large number of cone sheets, as in the Ardnamurchan peninsula, the indenter would have to indent

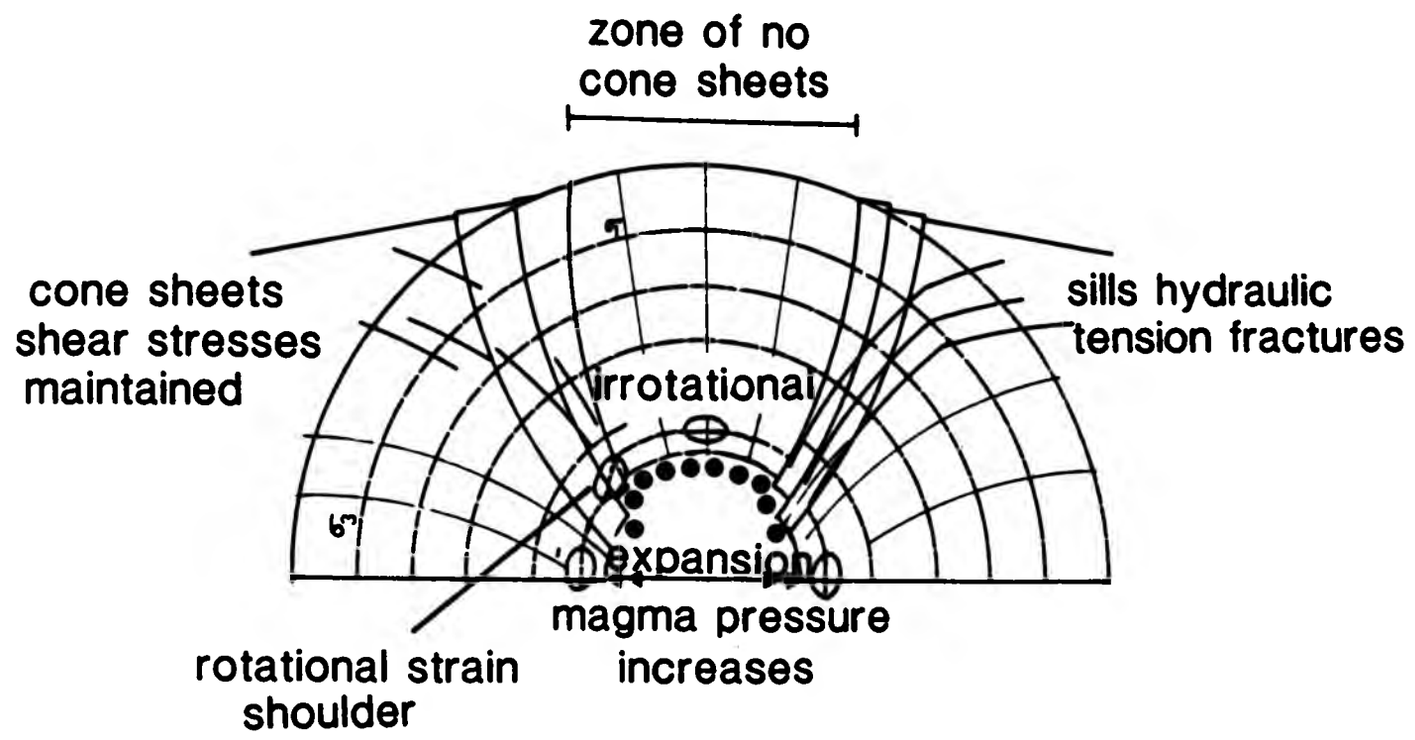

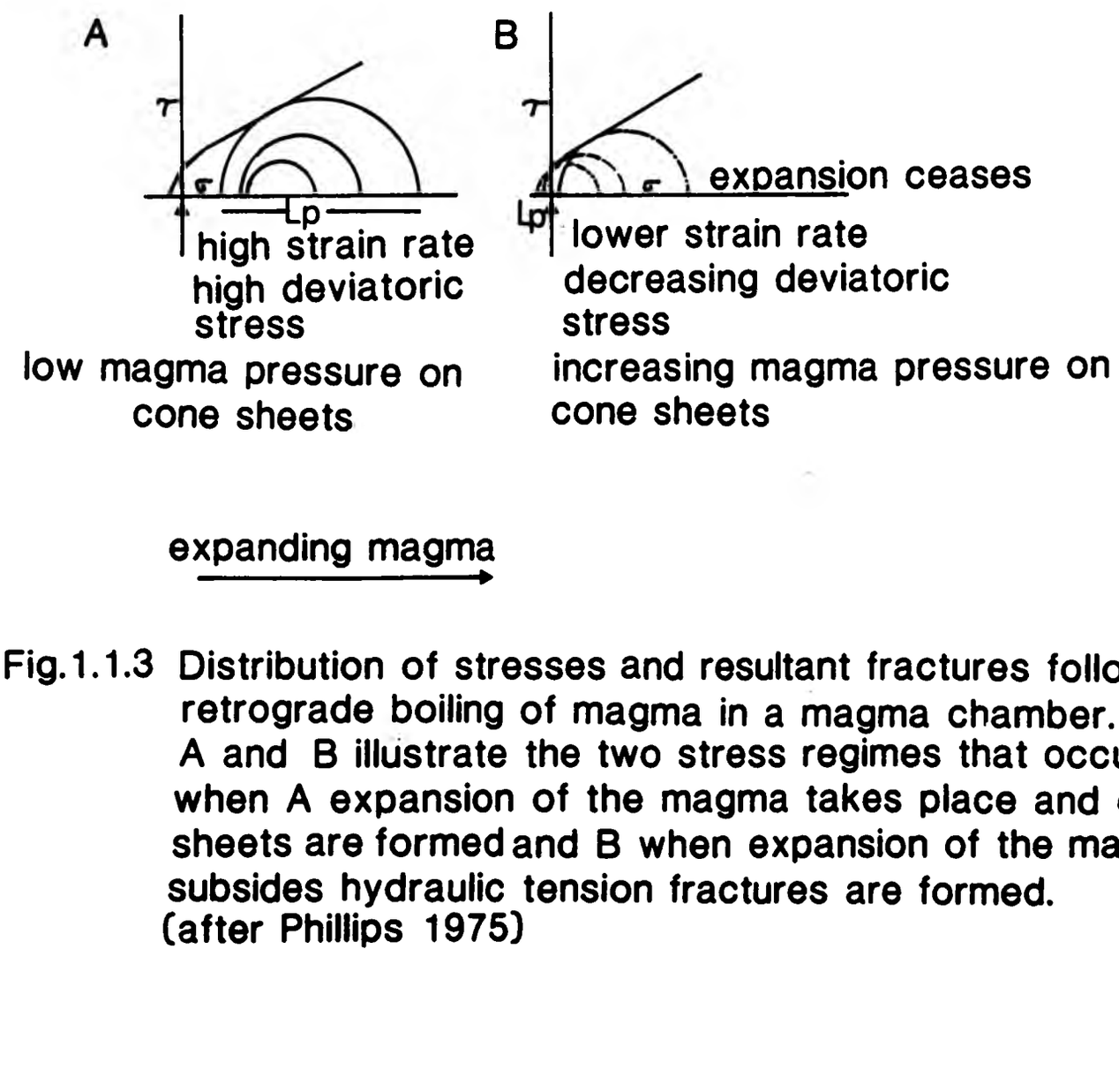

Fig.1.1.3 Distribution of stresses and resultant fractures following retrograde boiling of magma in a magma chamber. A and B illustrate the two stress regimes that occur when A expansion of the magma takes place and cone sheets are formed and B when expansion of the magma subsides hydraulic tension fractures are formed. (after Phillips 1975)

the surface a large number of times.

Following Walker (1975), Bahat (1980) derives two models for the development of the British Tertiary Intrusive Complexes. Using an acid diapir ahead of a basic cylinder the two models (Fig.1.1.4) involve conical fracture, doming and acid volcanism. The first model differs from the second in that cone sheets develop fully after doming, although both cone sheet emplacement and doming are intimately associated in both models (Chapter 8).

Each of the above works are either purely theoretical or have been concerned with the cone sheets of the British Tertiary Igneous Province. This is understandable because of the intense development of cone sheet sets within this classic province.

1.2 WORLD WIDE OCCURRENCES

A variety of cone sheet type intrusions have been identified in Finland, St. Helena, Galapagos Islands, Gran Canaria, North and West Iceland, Kenya, Norway, Nyasaland (Malawi) and Sicily.

Kaitro (1953) describes what to the present author are cone sheets from the Åva complex, Finland, a well developed circular, Precambrian complex. The granite filled cone sheets, varying in thickness from 15 to 40m, dip towards the centre of the complex at 70° - 80°. However, following Cloos (1936), Kaitro prefers to use the term "ring dyke" to cover all manner of circular intrusions despite the important difference in the attitude of the dip between cone sheets and ring dykes. It is therefore

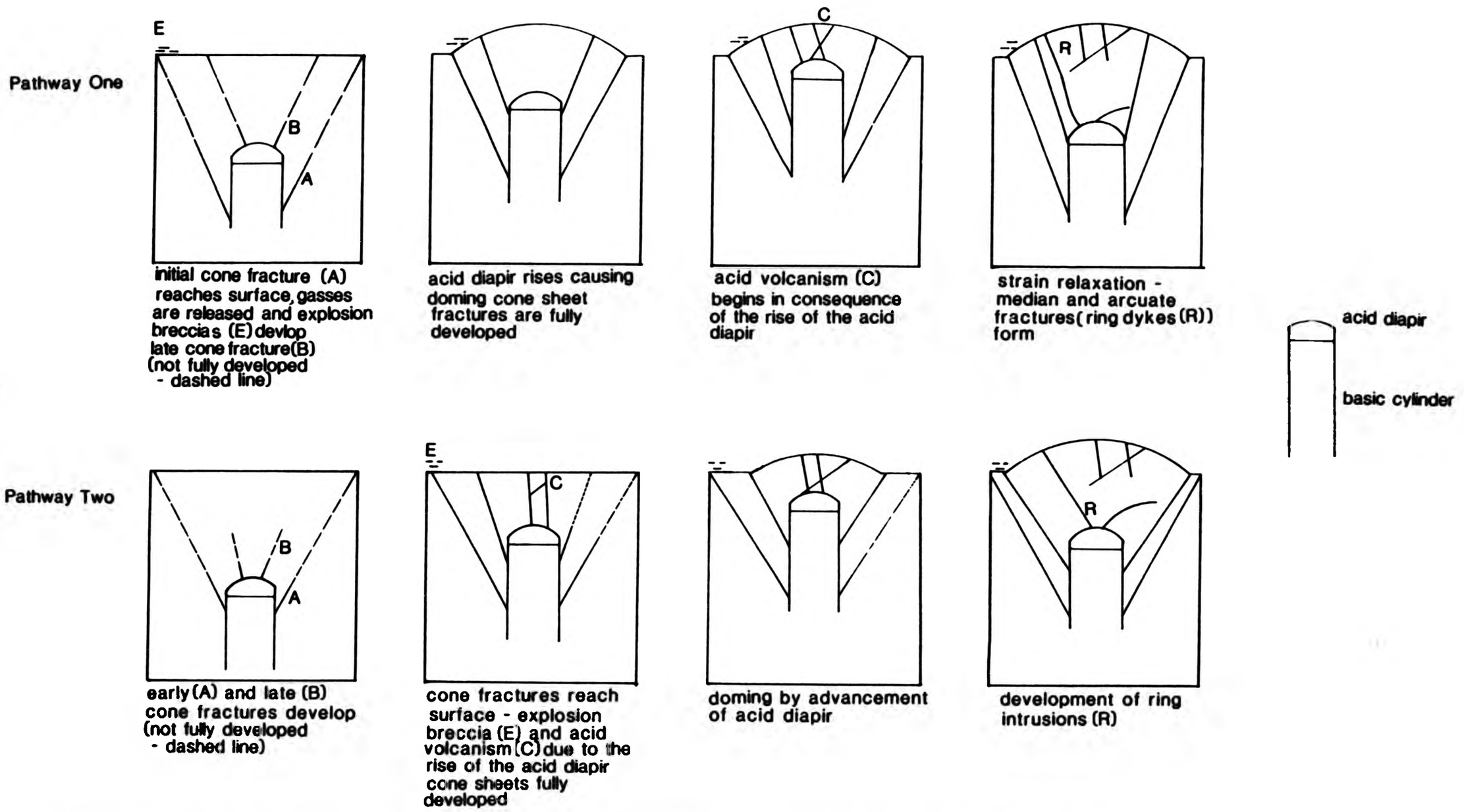

Fig. 1.1.4 Sequential diagrams showing Bahat's (1980) two pathways for the development of a British intrusive centre based on conic fractures

difficult to determine to which type of intrusion Kaitro is refering. What are presumed to be cone sheets dip towards a common focus and occur all around the complex. Although individual sheets can be followed for hundreds of metres none form a complete circle. Kaitro describes cross joints at the locations of offset sheets and states that a concentric arc of closely spaced, conical shear fractures were filled by magma that forced the overlying host rock upwards.

A present day example of possible cone sheet structures occur in the Sierro Negro Volcano, Galapagos Islands (Banfield, 1956). Spectacular circumferential fissures occur on the surface and contain no magma. It is thought that these fissures develop after the main extrusive event, and therefore are collapse structures.

Schminke (1967) describes a cone sheet complex from the Tejeda Caldera, Gran Canaria. Closely spaced tachylite cone sheets cross cut a syenite stock that is thought to have been partly solidified at the time of cone sheet emplacement. Very little country rock remains between the cone sheets which have caused a doming of the caldera.

In the Snaefellsnes area, Western Iceland (Siggurdsson, 1966) a large number of basaltic and rhyolitic cone sheets occur. They range in thickness from 25cm to 20m, with a predominant thickness of 1 metre. The sheets which transgress basaltic flows show a flow lineation and pipe vesicles that indicate flow up the dip of the sheets. A 7km diameter, central area contains few sheets, with the majority of sheets occurring

in a 2km wide band around this area, although sheets occur throughout an area of up to 11km diameter.

Hald et al. (1971) describe a cone sheet complex in the Kroksfjordur area of Iceland which has suffered post-intrusion tilting. The tholeiitic basalt sheets are mostly 0.5m-1m thick, with the thickest sheets being 2-3m thick. Granophyric sheets are up to 30m thick, a thickness which is similar to acidic sheets in other complexes.

Le Bas (1977) described some East African carbonatite cone sheets. These differ from those of Ardnamurchan. The differences are firstly, a number of twin centres are described which were simultaneously active, and show a combined outline of a figure of eight pattern in plan (Fig.1.2.1) resulting in the two cone sheet sets showing no cross cutting relationships. Secondly, 11 individual centres, the foci of which are thought to lie in a spiral, have been identified as occurring in an area of 2km radius around Homa Mountain (Fig.1.2.2). Similarities to the Ardnamurchan complex include the following, the thicknesses of individual cone sheets vary from 2cm (thin alvikite cone sheets) to 6m. The dip of the cone sheets varies from 30° in some sets to vertical in others. In the Homa Mountain complex the dip changes from 60° in the centre of the complex to 30° in the peripheral areas. Also, flow banding, often parallel to the cone sheet margins is marked by minerals and xenoliths (cf. Chapter 4).

Based on dip data, Kresten (1980) subdivided the cone sheets of the Alno complex, Norway, into 4 groups which form two

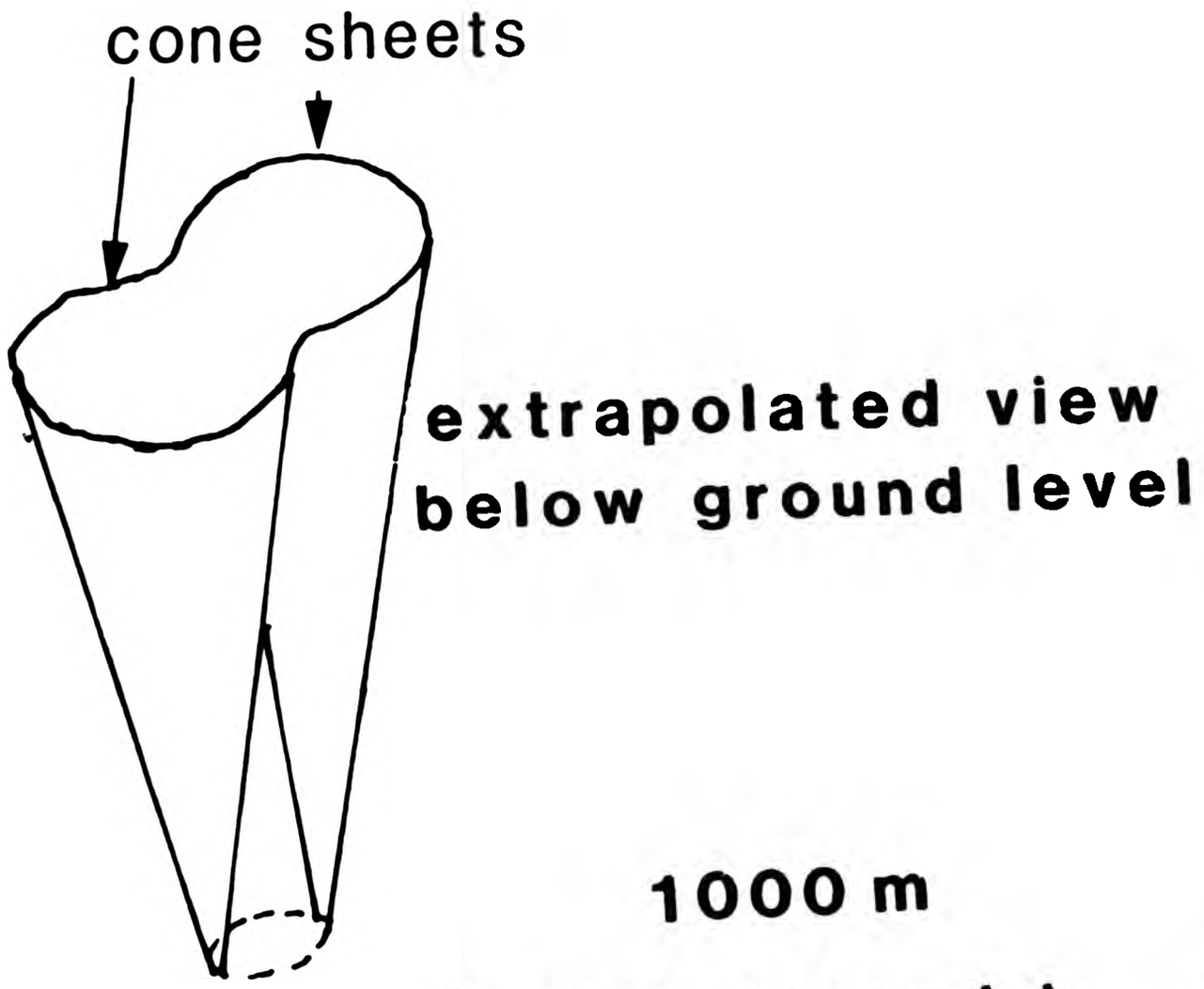

Fig.1.2.1 Twin cone sheet centres resulting in a double structure Nyasanja carbonatite cone sheet complex, Kenya (after Le Bas, 1977)

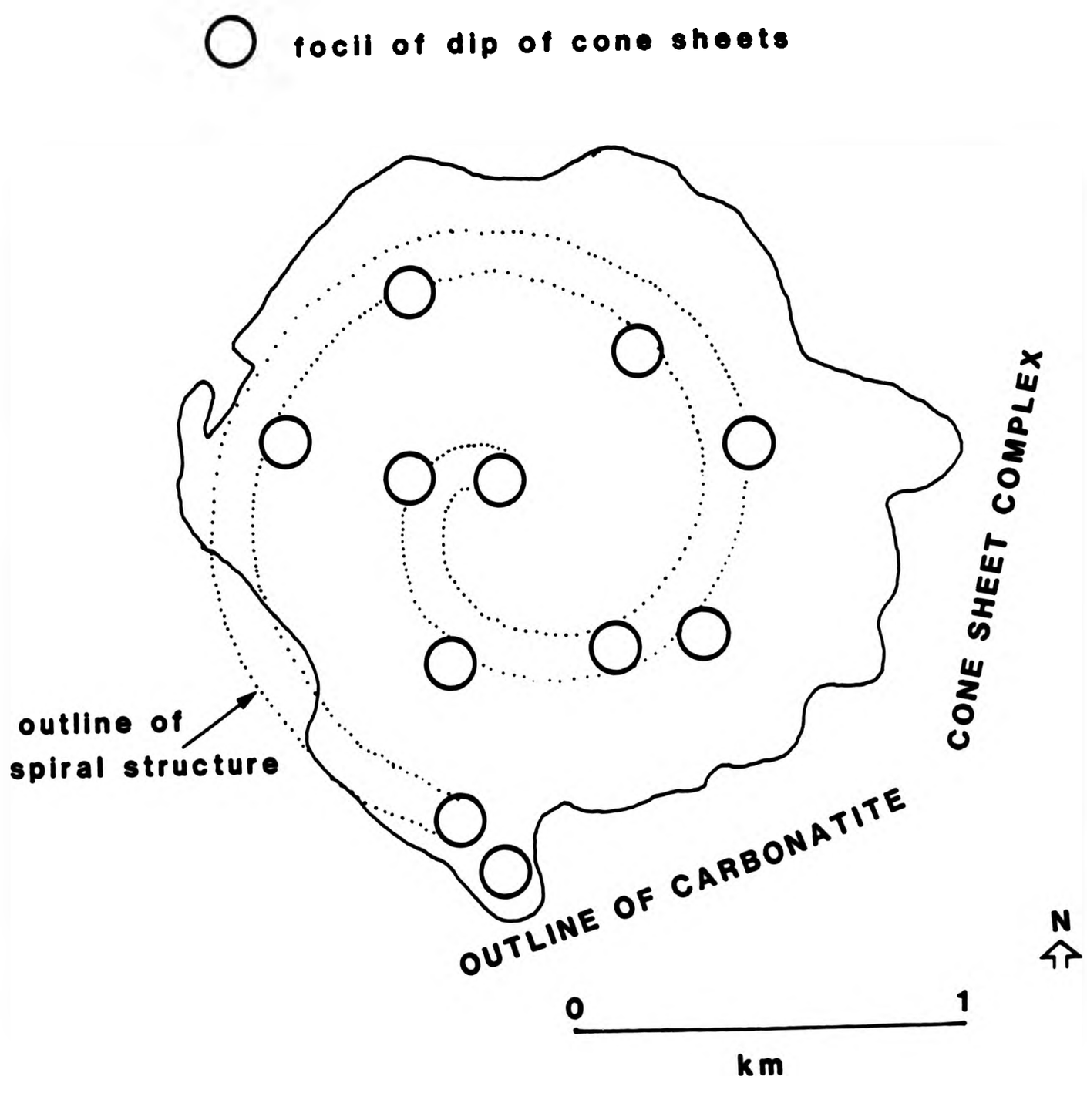

Fig.1.2.2 Spiral structure of the cone sheet complex of Homa Mountain, Kenya (after Le Bas, 1977)

pairs. Two of the groups dip towards the centre, whilst the other two dip away from the centre, by definition the latter are not cone sheets. Kresten's explanation for the formation of one pair is that following an initial upward push by the magma, conjugate joints were formed, dipping at 45° to a horizontal surface. One group dips towards the magma chamber, whilst the other group dips away. Magma emplaced into these fractures form two of the groups of "cone sheets". The loss of pressure caused by the emplacement of magma resulted in cauldron subsidence. As a result of the cauldron subsidence the second pair of fractures developed, one group dipping at 60° towards the centre and one group dipping shallowly at 30° away from the magma chamber; this accounts for the second pair of congugate cone sheets.

Baker (1968) describes from St. Helena a series of arcuate, trachytic intrusions which dip steeply inward and have diameters ranging from 150m to 45m. The form of the intrusions indicates that the estimated origin is at approximately 500m below the present surface. Baker explains the variation in the completeness of the arcs in terms of a "stick of celery", which is almost circular in cross section at the leaf end, whilst the root end has an open arcuate form.

From the above survey of the occurrences of cone sheets, it can be seen that there is a variation in rock types, thicknesses of individual cone sheets but, most important of all, there is a large variation in theories of their formation and development within each complex. All but one of the cone sheet sets described are Tertiary to Recent in age with one Precambrian set being described. It is possible that cone sheet sets of other

ages have not yet been described.

1.3 GENESIS OF CONE SHEETS-PREVIOUS HYPOTHESES

Previous investigations have highlighted a number of points relating to the mechanisms of cone sheet emplacement :-

1. Mechanism of host rock indentation,
2. Type of initial fracture,
3. Subsequent development and propagation of the fracture,
4. Processes involved in opening the cone sheet fracture,
5. Shape of the cone sheet fracture,
6. One or more major foci of activity,
7. Subsidiary foci of cone sheet formation.

Many authors have forwarded hypotheses to explain the formation of cone sheet fractures via an upward push originating in the magma chamber. Anderson (1924, in Bailey et al.) invokes a point push, whereas Field (1964) invokes a percussion fracture resulting in a central area devoid of cone sheets, and therefore resembling the field evidence more closely. Bahat (1980) uses a non-solid indenter to produce conic fractures with a central area containing no fractures, similar to Field (1964). Walker (1975) invokes a rising acid diapir to indent the country rock and thus produce cone sheet fractures. Only Phillips (1975) postulates expanding gases to increase pressure in the magma chamber to produce fractures, in such a system fractures particularly occur in the "shoulder" areas, and these fractures are subsequently exploited by magma to form cone sheets. All the theories discussed above involve an upward push, of some sort, and are therefore similar. However, the effects of this upward push differ. The major discrepancy between Anderson's hypothesis and field observation is that the former predicts cone sheets in the central area whereas observations in the

field show that the central area lacks cone sheets. Bahat's slow, non-solid indenter produces a single fracture at a time and therefore repeated indentation is necessary to produce the large number of fractures seen in areas of cone sheet occurrence and thus differs from Field's (1964) solid indentor, which produces a number of fractures with a single indentation. Walker's (1975) acid diapir is very similar to Andersons (in Bailey et al. 1924) basic magma indenter in that fracture distribution is homogeneous and therefore discrepancies with field evidence occur. Phillips' (1975) method, by using increased gas pressure, dissipates the pressure distribution and therefore forms a major distinction between his method and that of the previous authors. It also allows for a central area of no cone sheets. The theories of Field, Bahat and Phillips all predict a central zone of no fractures, with only the intensity of fracturing varying in the different theories.

Increased pressure in the magma chamber, either derived from the expansion of gases (retrograde boiling) or by physical indentation, creates a series of tensions across the magma chamber roof which features in Anderson's (in Bailey et al., 1924) hypothesis. This hypothesis has been sustained throughout the sucession of subsequent investigations. It can, therefore, be agreed that the original fracturing of the host rock is under a regime of tension.

Secondary exploitation of cone sheet fractures has not received much attention from previous authors. However, propagation mechanisms of other minor igneous intrusions have been discussed in the literature (Pollard 1973; Pollard et al.

1975). Principally, wedging, some stoping and assimilation can be identified (Chapter 4) in the Ardnamurchan cone sheets as methods of propagation. Secondly, Pollard (1973) and Pollard et al. (1975) highlight propagation mechanisms along sheets, developing a three-dimensional movement theory, which may be applied to the Ardnamurchan cone sheets (Chapter 7).

Another facet of the emplacement mechanisms of cone sheets is the relative displacement along the cone sheet fracture. Anderson's (in Bailey et al., 1924) hypothesis, which was followed by Richey (1930), indicates that the central area of the complex is uplifted and is therefore indicative of shear movements, although they give no evidence of this. Kennen (1937) records examples of reversed shear movements along cone sheets of Ardnamurchan and Mull, whilst Garson (1968) gives examples of shear movement along cone sheets in Nyasaland (Malawi). Phillips (1974) suggests that the cone sheet fractures are shear planes, then as pressure decreases in the magma chamber the shear planes pass into ones of tension (cf Chapter 6).

The shape of cone sheet with depth varies in the theories, this is principally related to the opening mechanism, that is whether cone sheets occupy tension or shear fractures. Anderson's model (Fig.1.3.1) depicts cone sheets which are steeply inclined when in close proximity to the focus of activity (e.g. Inner Centre Two Cone Sheet Set, Ardnamurchan) and more shallowly inclined when more distal from the focus of activity (e.g. Outer Centre Two Cone Sheet Set, Ardnamurchan). Phillips (1974) derived a model of cone sheet formation which combines both shape profiles as given by Anderson (1936). Similar pro-

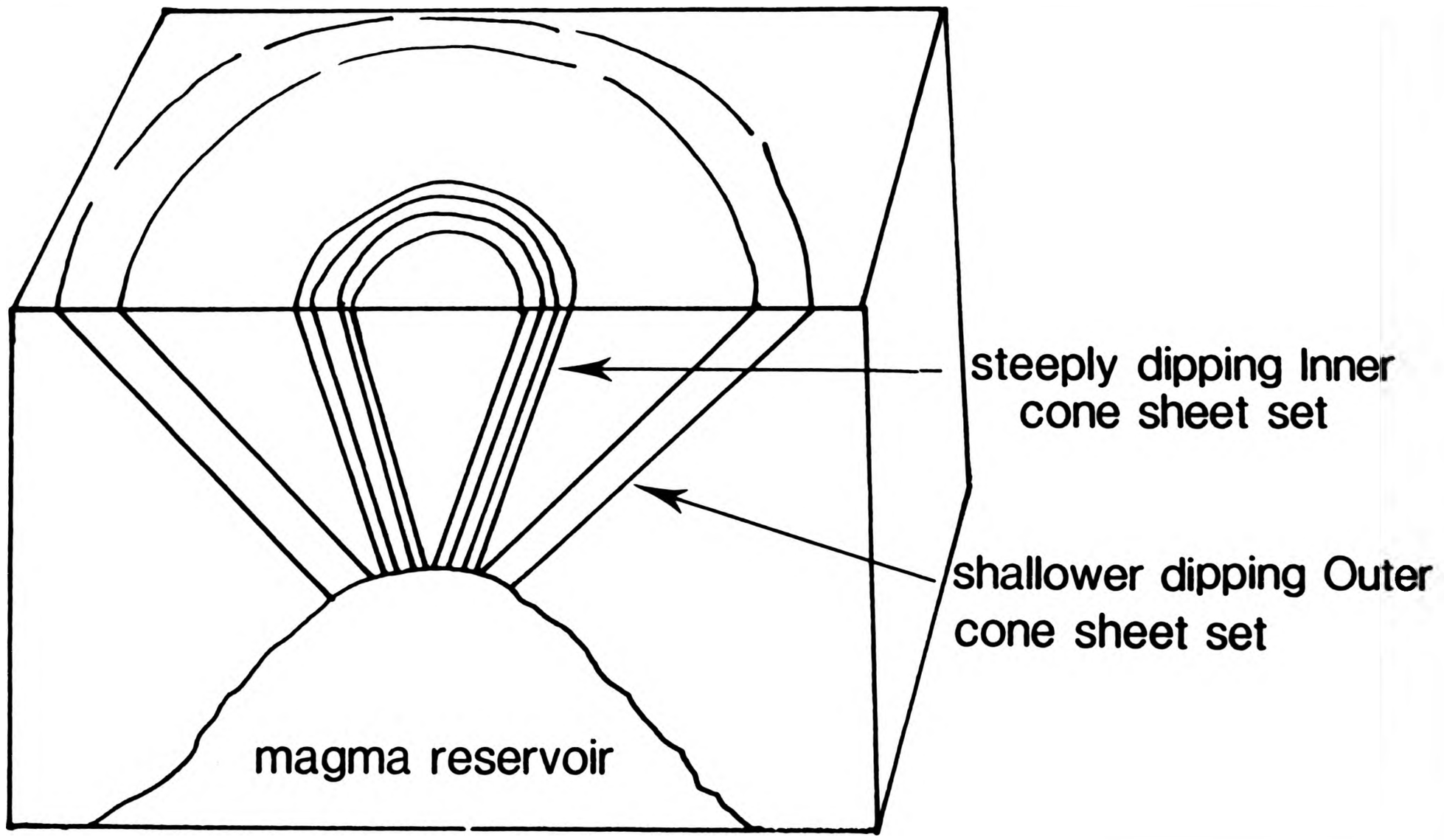

Fig.1.3.1 Andersons interpretation of the cone sheets of Centre Two Ardnamurchan (Richey et al.,1930)

files have been derived in photoelastic experiments carried out by the present author (Chapter 9). As magma is emplaced along the fractures the central area is uplifted (Fig.1.3.2), the net result is therefore an increase in height of the land surface. The majority of sheets measured both for this study and in other studies (Garson (1959) in Nyasaland (Malawi), Kresten (1980) in Norway) have average dips of 40° to 50°, with dip varying between 10° and 90°. Therefore, any model of emplacement requires some mechanism to allow for the formation of different shaped cone sheet fractures with different angles of dip. Kresten's model suggests an explanation for four different groups of dips, however, two of the congugate sets of cone sheets form under different pressure systems. Durrance (1968), working on the Ardnamurchan complex, derives his "single centred" hypothesis from photoelastic models (see below) in which he envisages one fracture system predominating throughout the emplacement of cone sheets, the cone axis being inclined to the NW, despite the periodic intrusion of the major ring intrusions. The cone sheet sets are spatially separated and also separated by the major ring intrusions, that is after each cone sheet set was emplaced a period of major ring intrusion took place, thus relieving the cone sheet stress system completely.

Perhaps the question of one or more foci of activity is confined to the Ardnamurchan complex only. Based on the observations of Richey et al. (1930) and field work of this study, it can be stated that the different cone sheet sets can confidently be identified as separate groups, from cross cutting evidence. Also, each cone sheet set has a series of specific characteristics (Chapter 5), the most prominent being that each

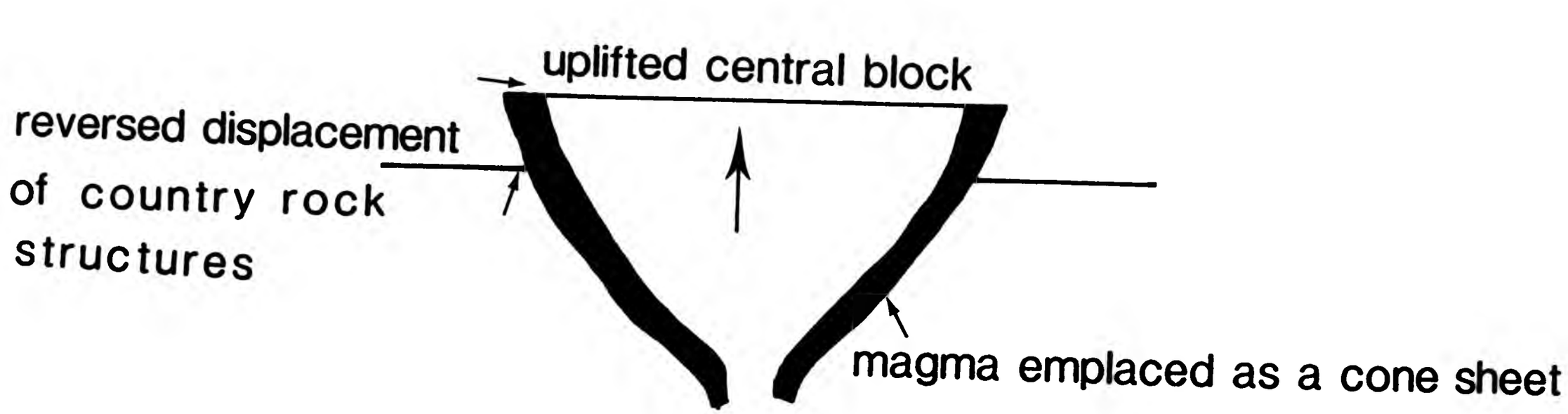

Fig.1.3.2 Emplacement of a cone sheet resulting in the uplift of the central block

set dips towards a common focus, which therefore demonstrates multiple centred activity.

However, Le Bas (1978) and Bahat (1980) develop the spiral fractured hypothsis and tie this together with multiple centres, that is seperate foci develop along a spiral pathway. A more simple explanation is perhaps a series of "small" magma blips rising in the crust to create the fractures for cone sheet formation.

1.4 PRESENT INVESTIGATIONS

Previous investigations of cone sheet intrusions have raised a number of points, ranging from the regional stress regimes to the shape of the intrusions with depth. It may also be noted that since the original Geological Survey work in the British Tertiary Igneous Complexes, little intense field work has been carried out on the cone sheet complexes to substantiate the numerous theoretical models. Consequently, a large part of this thesis is field based with subsequent interpretation of the data collected, together with some theoretical investigations using photoelasticity.

1.4.1 Field Studies

The present studies were planned to investigate cone sheets on two levels, that is a) cone sheet sets in general and b) the Ardnamurchan cone sheet sets in particular.

One of the principal characteristics of cone sheets is their mineralogical composition and therefore the petrography of a number of cone sheets has been investigated. However, during petrographic studies it became obvious that the great majority of the Ardnamurchan cone sheet rocks have undergone thermal metamorphism by later members of the central complex. Also they have undergone greenschist facies metamorphism due to meteoric hydrothermal systems associated with the central intrusive complex (Taylor and Forester, 1971).

The number of sheets, their dip, strike and individual thicknesses have been analysed for individual traverses and also in relation to the centre of activity. Cumulative thickness of cone sheets have been used to analyse strain caused by their emplacement. Also, the type of dilation and sense of relative displacement of individual cone sheets has been analysed in order to establish whether tension or shear, or both, processes predominate as a mechanism of formation and emplacement. Mechanisms of propagation are perhaps best illucidated by the form and attitude of the terminations of intrusions and their relationships to the adjacent host rocks. Exploitation or utilization of pre-existing country rock structures have been examined a) on a regional scale (doming) and b) on a local scale (joints and bedding).

In terms of the Ardnamurchan peninsula as a specific example, Richey et al. (1930) established a three centred hypothesis based on cross cutting relationships to explain the configuration of cone sheet sets. Durrance (1968), based on theoretical work, explains the system of cone sheet fractures, which emanate from a spiral pattern, as belonging to a single centre of activity and thus contrasting with the work of Richey et al. (1930). In consequence, the question of one or more multiple centres for the Ardnamurchan cone sheet sets has been prominant throughout the investigation. A refinement of the centred hypothesis has been made with the additional identification of subsidiary foci.

Field data has been applied to a number of theories proposed by previous investigators as follows:-

THEORY	FIELD DATA
1. Magma Indentor–point push, percussion fracture, retrograde boiling, acid diapirs,	Distribution of cone sheets within each cone sheet set,
2. Fracture mechanism– Hertzian fracture, hydraulic fracture,	Distrribution of cone sheet fractures,
3. Propagation of fractures,	Location and form of termination structures,
4. Emplacement mechanism,	Movements on cone sheet fractures,
5. Utilization of host rock structures,	Relationship of cone sheets to joints, bedding, foliation, distribution of host rock types,
6. Idealised cone sheet sets,	Analysis of dip, strike, thickness of each cone sheet.

1.4.2 Model Studies

Three types of models have been designed in order to study various aspects of cone sheets and their emplacement. The three

In terms of the Ardnamurchan peninsula as a specific example, Richey et al. (1930) established a three centred hypothesis based on cross cutting relationships to explain the configuration of cone sheet sets. Durrance (1968), based on theoretical work, explains the system of cone sheet fractures, which emanate from a spiral pattern, as belonging to a single centre of activity and thus contrasting with the work of Richey et al. (1930). In consequence, the question of one or more multiple centres for the Ardnamurchan cone sheet sets has been prominant throughout the investigation. A refinement of the centred hypothesis has been made with the additional identification of subsidiary foci.

Field data has been applied to a number of theories proposed by previous investigators as follows:-

THEORY	FIELD DATA
1. Magma Indentor—point push, percussion fracture, retrograde boiling, acid diapirs,	Distribution of cone sheets within each cone sheet set,
2. Fracture mechanism- Hertzian fracture, hydraulic fracture,	Distrribution of cone sheet fractures,
3. Propagation of fractures,	Location and form of termination structures,
4. Emplacement mechanism,	Movements on cone sheet fractures,
5. Utilization of host rock structures,	Relationship of cone sheets to joints, bedding, foliation, distribution of host rock types,
6. Idealised cone sheet sets,	Analysis of dip, strike, thickness of each cone sheet.

1.4.2 Model Studies

Three types of models have been designed in order to study various aspects of cone sheets and their emplacement. The three

model types are 1) photoelastic models, 2) mechanical models and 3) numerical models.

A series of photoelastic experiments have been designed to investigate different oriented indentors to determine the stress distributions around a magma chamber. Further experiments were designed to determine the distribution of regional stresses in the area, and their effect on several closely spaced igneous centres. Fracture propagation has also been studied.

A mechanical model has been studied in order to determine the type and conditions of fracture which would result when a water-saturated host was subjected to sudden impact.

Numerical models have been designed and applied to the collected data in order to test the distributions of strike and dip of cone sheets within and between individual cone sheet sets. Also, these studies have assisted in the identification of an idealised cone sheet set.

CHAPTER 2

AREA OF STUDY

2.1 INTRODUCTION

The Ardnamurchan peninsula contains the only mainland igneous complex of Tertiary age in Scotland. Other Tertiary centres of activity, including lava piles, are Skye, Mull, Rhum, Arran, St.Kilda, Rockall, Blackstones, Lundy, N.Ireland, Mourne Mts, Slieve Gullion and Carlingford. Collectively these are termed the British Tertiary Igneous Province (B.T.I.P) and this province belongs to the larger North Atlantic (Thulean) Province which includes Jan Mayen, Faeroes, Iceland and the east and west coasts of Greenland.

Richey (1937,p13) said of the Thulean Province, "the present surface gives a comprehensive view of the volcanic phenomena since it provides cross sections at various levels between the tops of the volcanic mountains of bygone days and the reservoirs of molten rock from which the volcanoes were fed".

The B.T.I.P. extends from Skye in the north through the igneous centres of the west coast of Scotland, N.Ireland, Carlingford to Lundy in the Bristol Channel. For convenience of description the igneous activity within the province has been divided into three groups:

a)Lava eruption, predominantly basaltic (1500m thick in Mull, 600m thick in Skye, 100m thick in Ardnamurchan).
b)Emplacement of central intrusive complexes.
c)Dyke swarms.

This sequence is not chronological. For instance, the dyke swarms which are thought to have fed the lava piles, were intruded throughout the evolution of the central intrusive com-

plexes. Each of the loci of the B.T.I.P. show different degrees of development and intensity; Skye has four intrusive centres whilst Mull and Ardnamurchan (Richey et al., 1930) have three. Richey et al. (1930) thought that Ardnamurchan depicted cross sections of volcanoes at three different levels, relative to the present day land surface.

2.2 VOLCANO - TECTONIC SETTING

Previous studies of the B.T.I.P. have resulted in the identification of a number of characteristics which are associated with the locations of the central intrusive complexes (Vann, 1971):-

a)They lie in an area of Mesozoic subsidence
b)They occur along a line (Fig.2.2.1 after Speight et al., 1982)
c)They are associated with intense dyke swarms
d)There are in close associations with major faults

a)Although the Thulean Province is in an area of Mesozoic subsidence the area is traversed by a number of ridges. Ardnamurchan lies at the eastern extremity of the Coll-Tiree ridge, separating the Minch and Mull Mesozoic basins, all of which trend NE-SW (Hallam, 1972).

b)Richey (1932) noted that the closely spaced intrusive centres from Skye to Carlingford and the more distant centre of Lundy form a north to south alignment, with additional outlying centres of St.Kilda and Rockall.

c)Fig.2.2.1, taken from Speight et al. (1982) shows the location of the axes of the dyke swarms and the percentage dila-

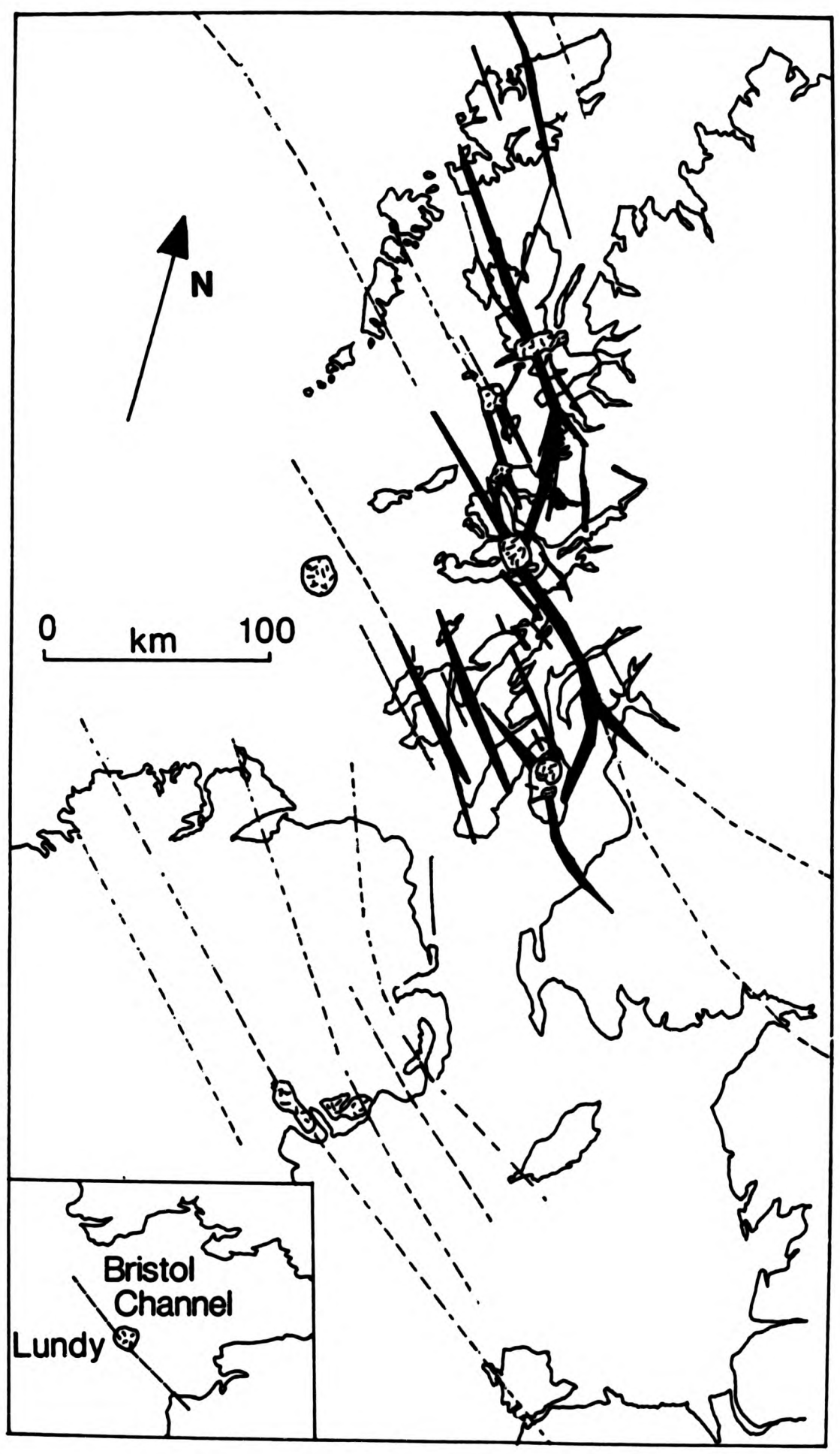

---------- uncertain dyke swarm axes

main dyke swarm axes

central complexes

Fig.2.2.1 Dilation axes of the Tertiary dyke swarms of Britain located along the North West coast (after Speight et. al. in Sutherland 1982)

tion. Each of the dyke swarms is believed to be underlain by a basaltic ridge.

d)The central intrusive complexes are believed to be located at the intersection of the basaltic ridges with prominent NE-SW trending faults. For example, the Skye centre is located adjacent to the Camasunary fault, whilst the Ardnamurchan centre lies close to the Strath Conon fault (Fig.2.2.2 from Speight et al., 1982). The assumption is that the intersection of the basaltic ridge and fault causes a crustal weakness up which there rises a cylinder of basaltic magma from which the central intrusive complexes evolve.

Igneous activity in the Thulean Province is thought to be associated with the opening of the Atlantic Ocean. Present day volcanic activity occurs on Iceland and Jan Mayen which both lie astride the Mid Atlantic Ridge. This modern activity marks the junction of two oceanic plate margins, whereas the igneous activity of the B.T.I.P. took place within a continental margin.

2.3 GEOLOGY OF ARDNAMURCHAN

Richey et al. (1930) in the NW Mull, Ardnamurchan and Coll Memoir (hereafter referred to as the Memoir) described the rocks of the Ardnamurchan peninsula. This was summarised in the Regional Guide (Richey,1961)(Plate 2.1).

Gribble et al. (1976) in a guide to field excursions, include summaries of more recent research carried out on the

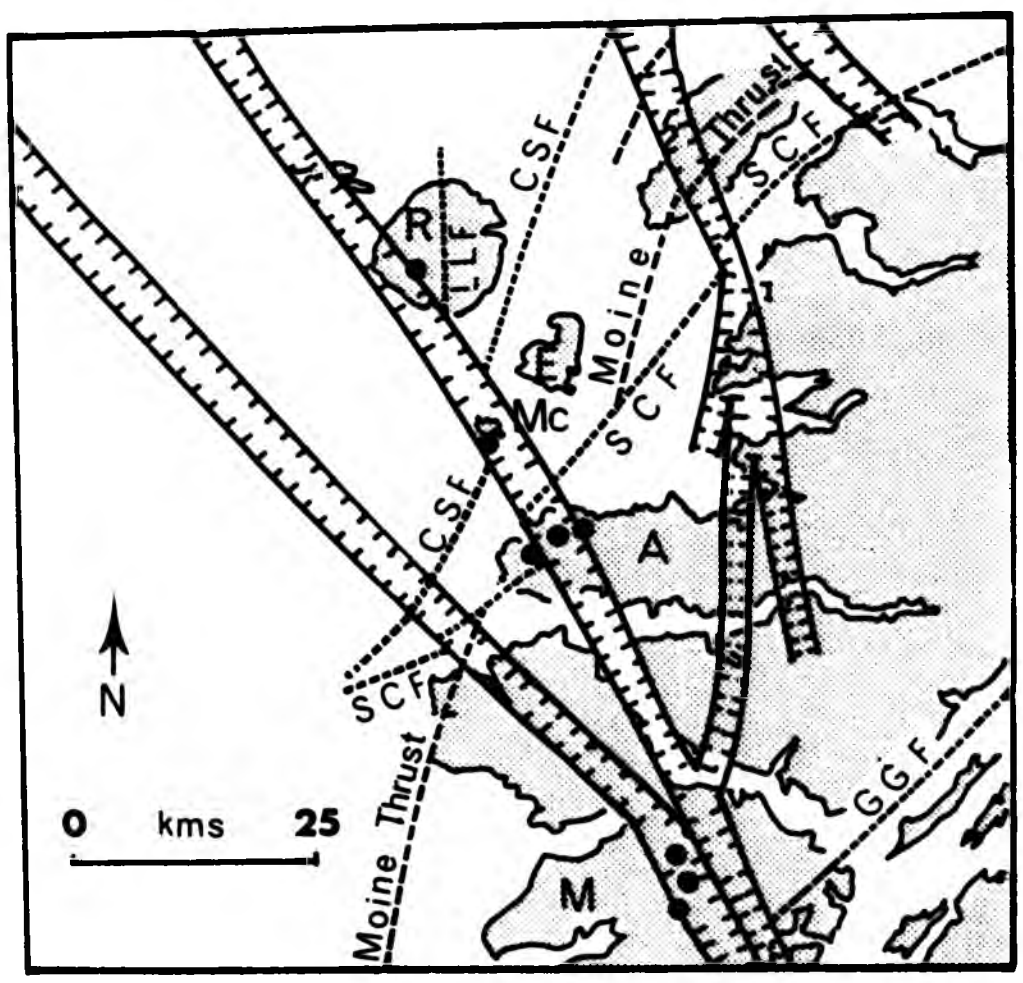

Moine Thrust

SCF Strath Conon Fault

CSF Camasunary Fault

GGF Great Glen Fault

basaltic ridges

● Igneous Centres

R Rhum E Eigg

Mc Muck M Mull

A Ardnamurchan

Fig.2.2.2 Map to show the intersections of the crests of basaltic ridges and zones of sinistral displacement with pre-Tertiary faults in the area of the Small Isles, Ardnamurchan and Mull (after Speight 1972)

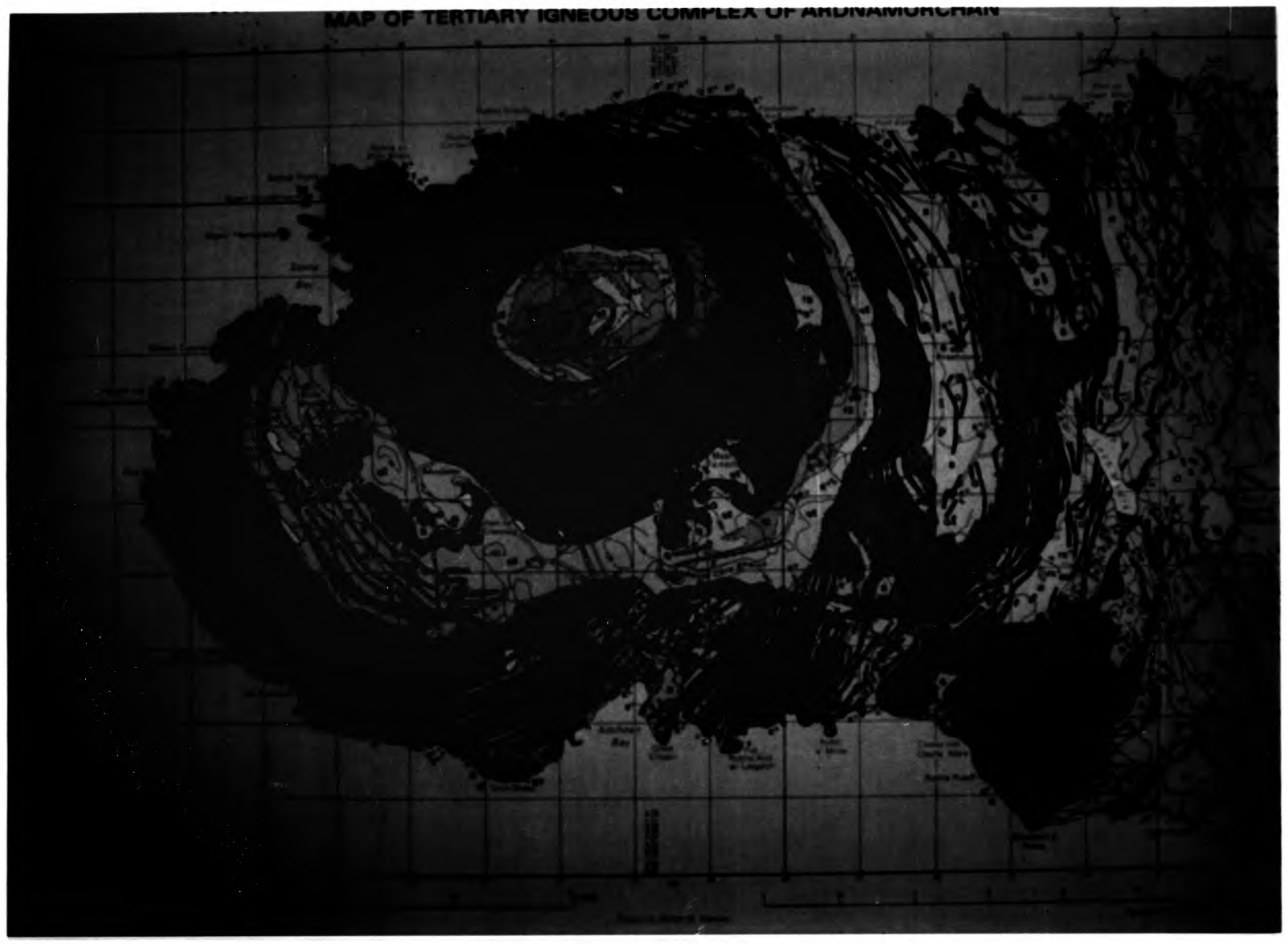

Plate 2.1A Geological map of Ardnamurchan (Gribble et al., 1976).

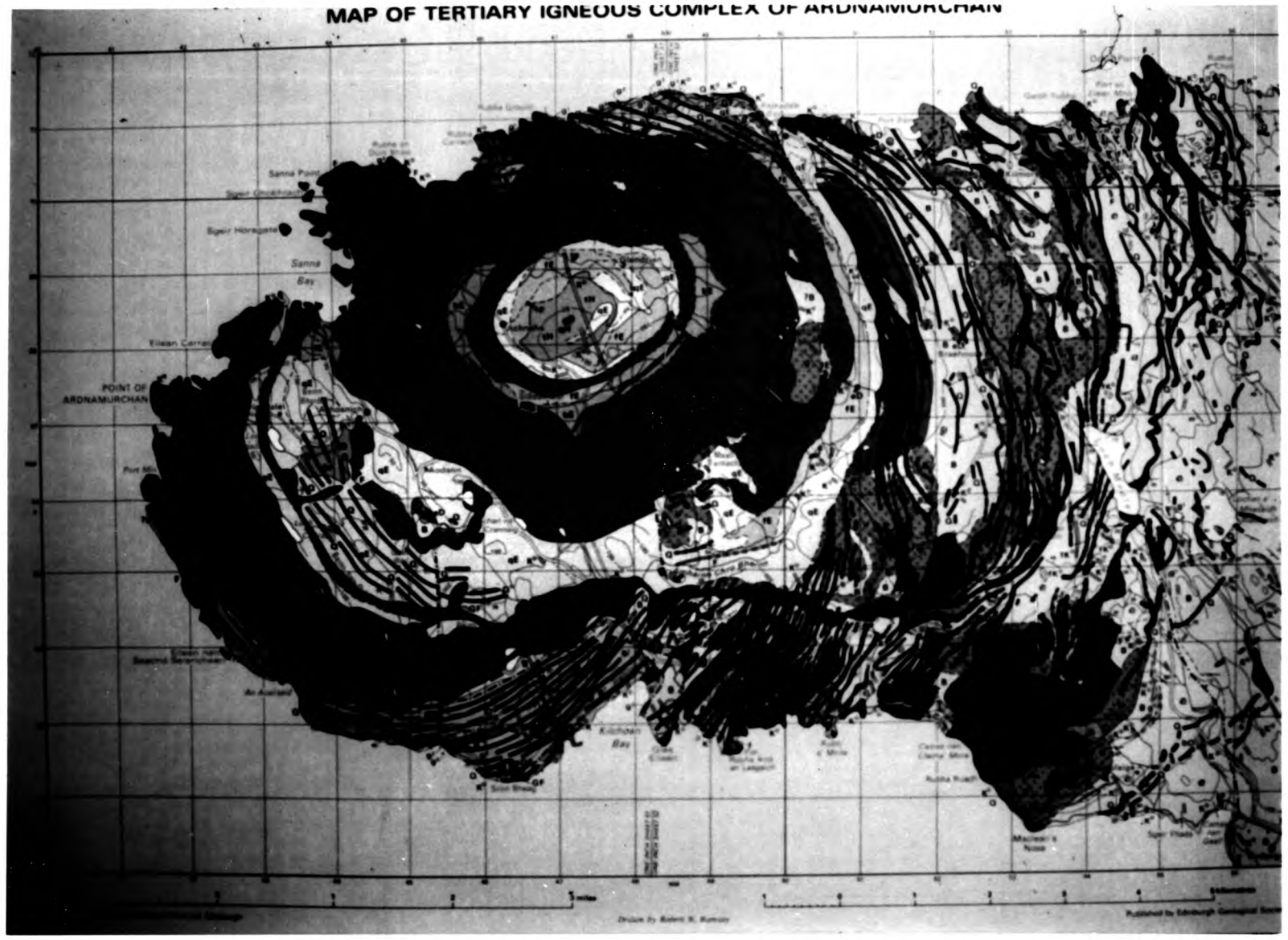

Plate 2.1A Geological map of Ardnamurchan (Gribble et al., 1976).

MAP OF TERTIARY IGNEOUS COMPLEX OF ARDNAMURCHAN

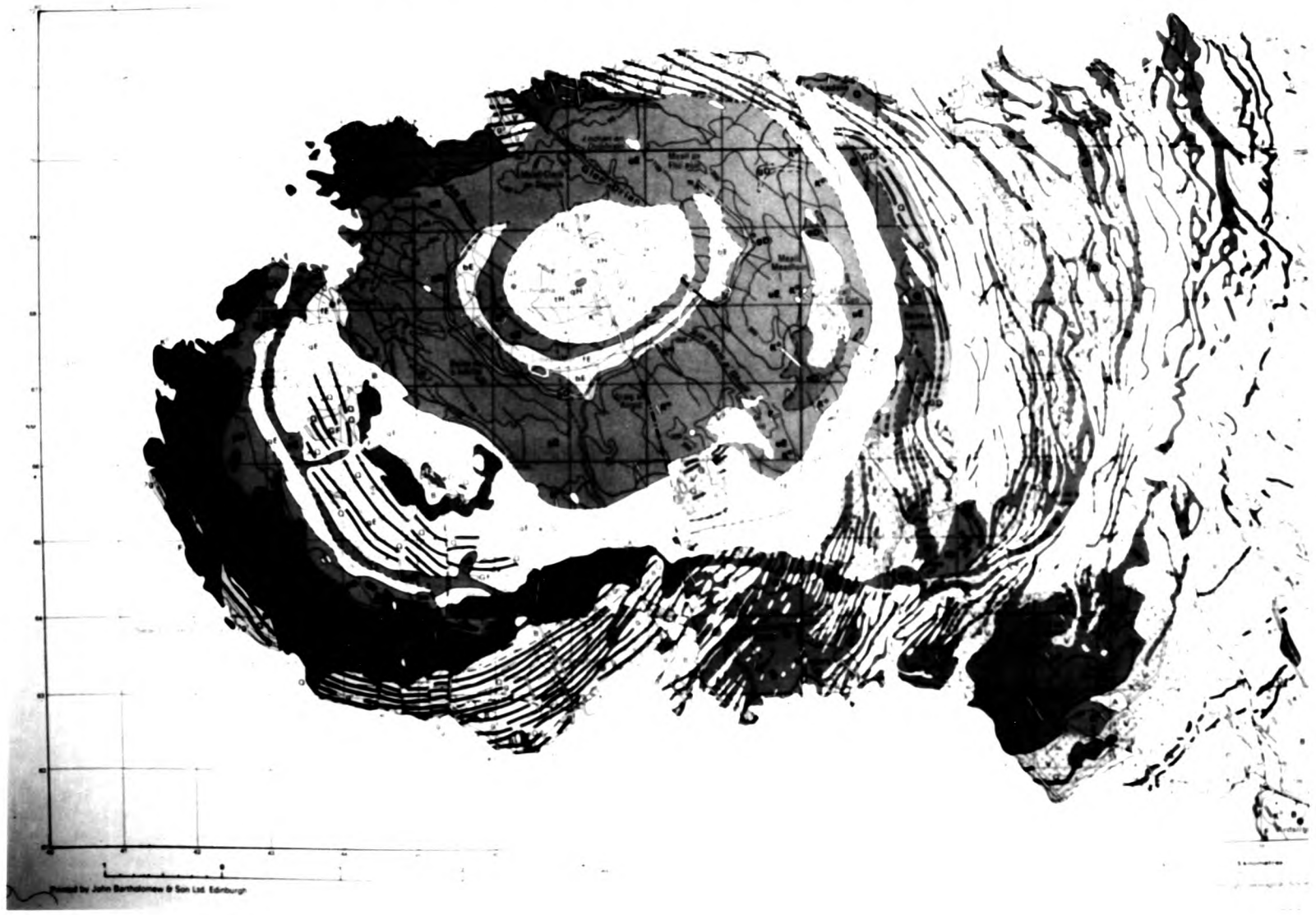

Plate 2.1A Geological map of Ardnamurchan (Gribble et al., 1976).

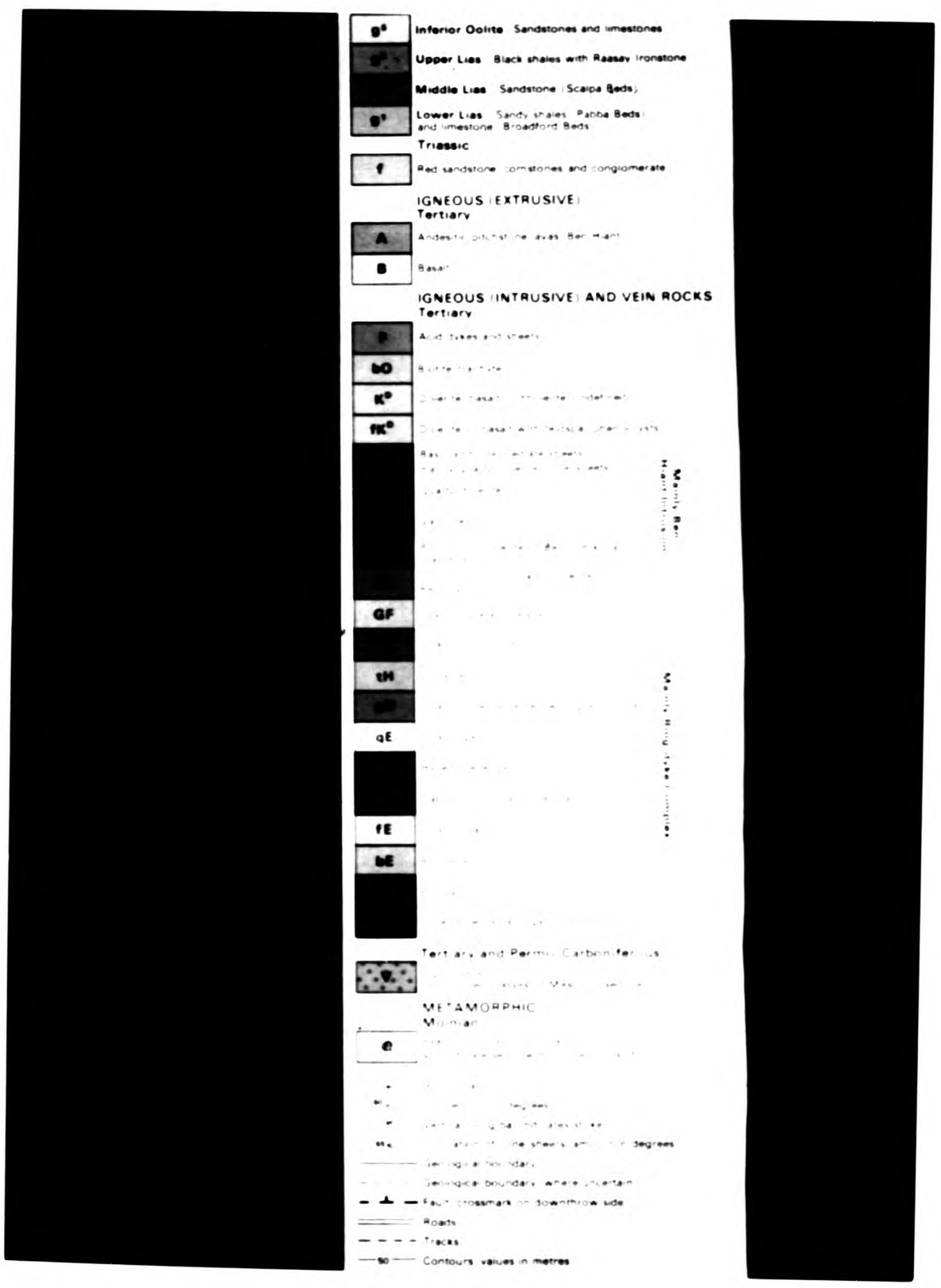

Plate 2.1B Key to the geological map of Ardnamurchan (Plate 2.1A) (Gribble et al., 1976).

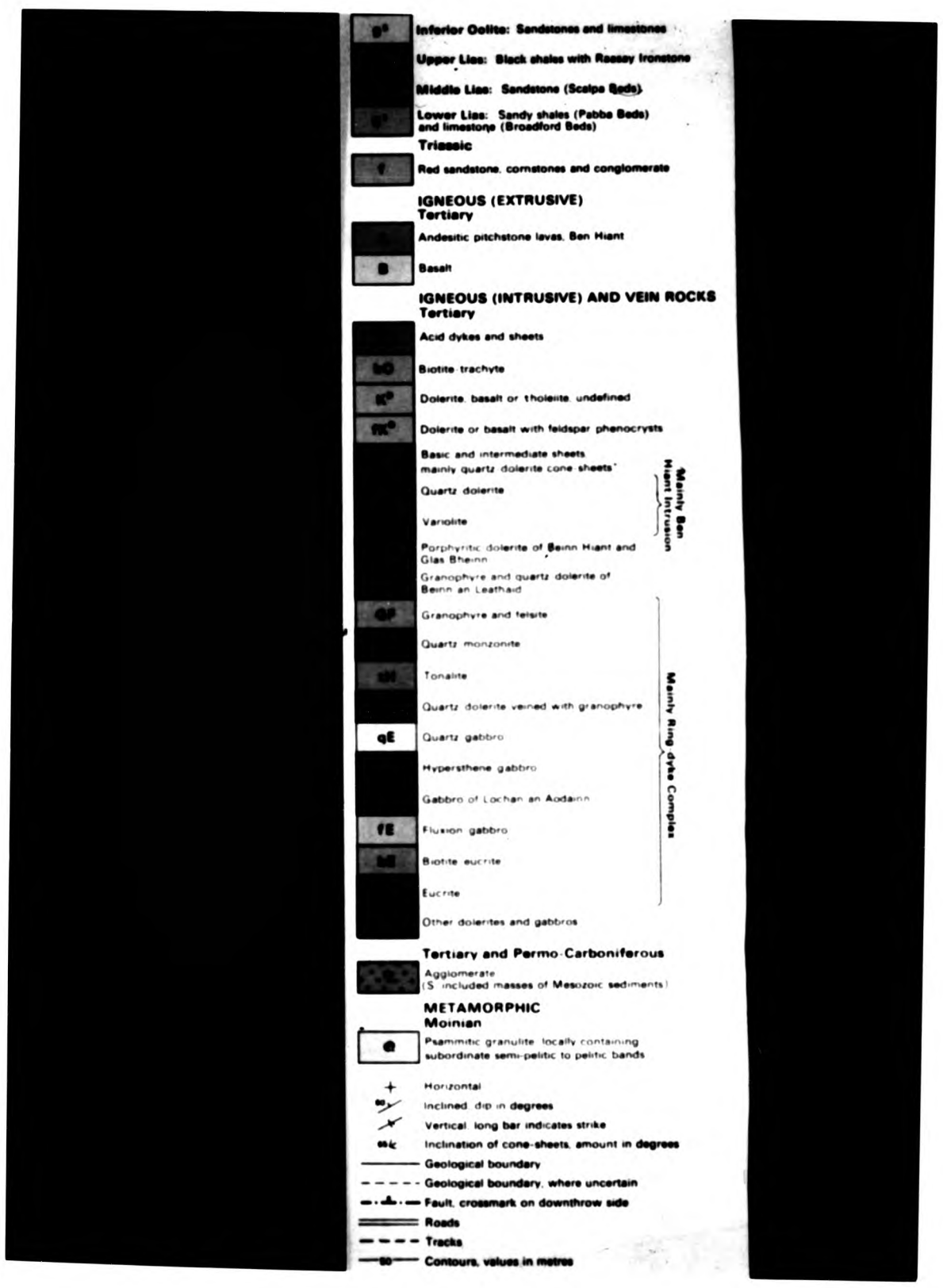

Plate 2.1B Key to the Geological map of Ardnamurchan (Plate 2.1A) (Gribble et al., 1976).

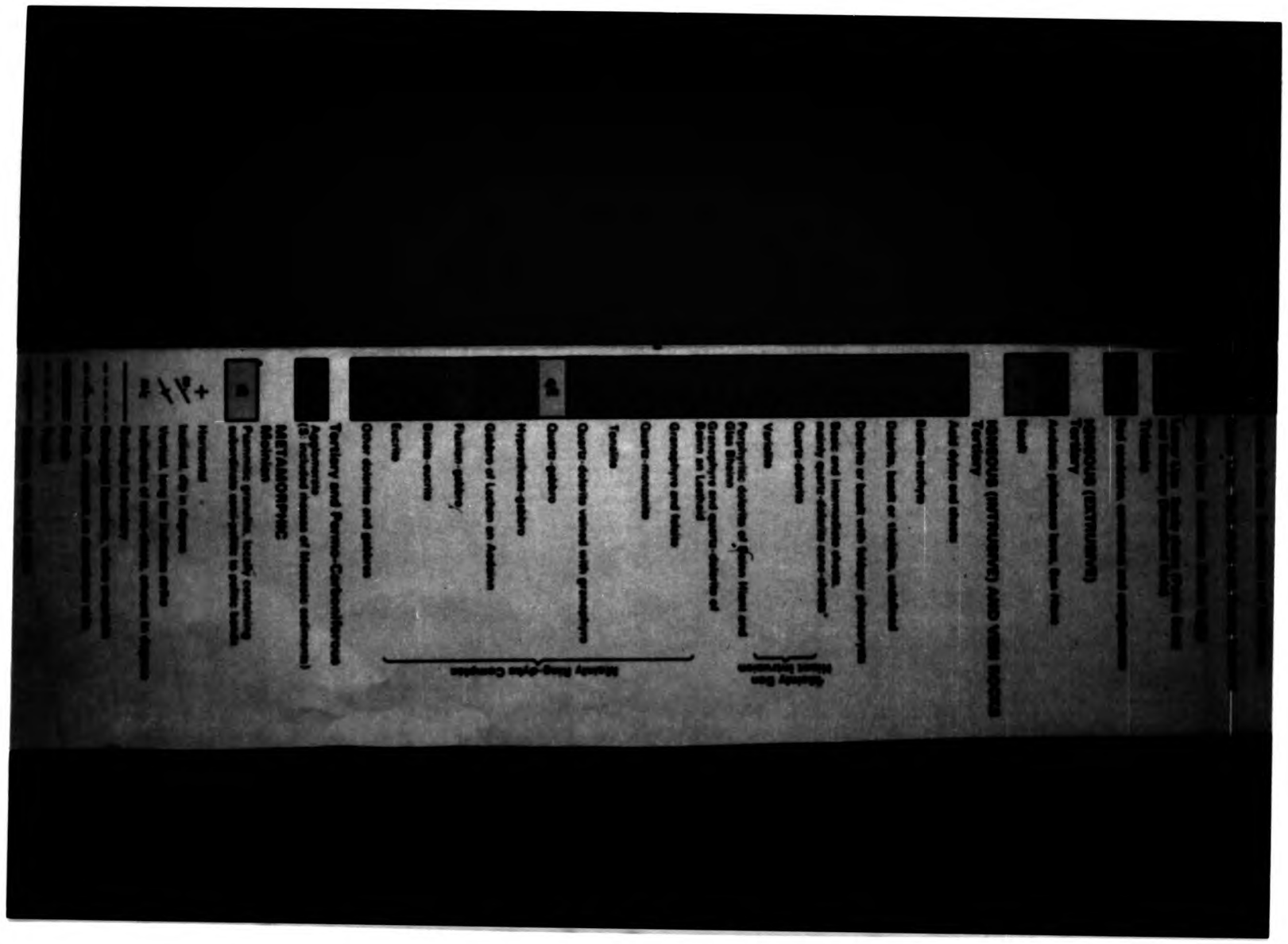

Plate 2.1B Key to the Geological map of Ardnamurchan (Plate 2.1A) (Gribble et al., 1976).

Ardnamurchan Tertiary complex. Thus, since detailed lithological descriptions already exist there follows a resume of the geology of the Ardnamurchan peninsula. Emphasis is placed on the Moine, Triassic, Jurassic and the central intrusive complex which form the host rocks to the four cone sheet sets.

2.3.1 Precambrian

The western half of the peninsula is dominated by the Tertiary central igneous complex, with few exposures of Pre-Tertiary rocks (Plate 2.1). Forming the country rocks to the Tertiary complex east of Kilchoan and, in particular, east of easting 54, are a group of metamorphosed Precambrian rocks belonging to the Moine succession. These rocks are mainly arkosic psammites that consist of feldspar grains (1-2 mm in length), quartz and chlorite. Mica gives a flaggy character to some psammites and is a major component of the pelitic layers. East of Mingary Castle and near Ockle (553705) the Moine rocks are stained red where they occur adjacent to the Triassic unconformity.

To the east of the Tertiary Loch Mudle Fault (Richey et al., 1930; MacGregor, 1967) are the Eastern Moines, a term introduced by Richey et al. (1930) to distinguish these garnet grade psammites from the biotite grade Moines which are found around Kilchoan. Another difference between these two groups of Moine rocks, which I have noted, is that the pelites of the Eastern Moines have a macroscopic crenulation cleavage (e.g. at Rubha a'Choit (55357135)), whilst the Kilchoan Moines exhibit only a microscopic cleavage.

The Moine rocks have a prominent foliation which in the east, near Ockle, has been folded and subsequently exploited by the Centre One cone sheets (Plate 8.1:Fig.8.5.1). Near Mingary Pier, intensive jointing in the Moines has influenced the form of the margins of the cone sheets which are irregular where bounded by joint surfaces (Chapter 4)

2.3.2 Triassic

Exposures of Triassic rocks are small and scattered; the principal ones are at Mingary Pier and to the west, Port an Eilean Mhor, Rubh'a'Mhile and east of Ockle. At Rubh'a'Mhile the unconformity between Moine and Triassic rocks is exposed. The Triassic sediments are cornstones, red sandstones and conglomerates which contain Moine fragments (Table 2.1). The total thickness of Triassic rocks is less than 5 metres (Table 2.1). Because these rocks contain few planar structures e.g. recognisable bedding, they are of little use as marker horizons to enable resolution of direction of cone sheet opening.

2.3.3 Jurassic

Rocks belonging to the Lias and Inferior Oolite attain a maximum thickness of 176m (Table 2.1). The Lower Lias is approximately 120m thick and the principal exposures are at Rubh'a'Mhile (506629), Mingary Pier (494627), Ormsaigbeg (468625), Swordle (546709), south of Rubha Carrach (465744) and 2km west of Faskadale (485714). Only 12m of Middle Lias occurs on the peninsula and is exposed to the west of Kilchoan Bay

Table 2.1 Mesozoic rocks of the Ardnamurchan Peninsula

SYSTEM	SERIES THICKNESSES + LOCALITIES	STAGES	ROCK TYPES
Jurassic	Great Esturine Series 3m at Sron Bheag	Bathonian and topmost Bajocian	black fissile shales
		Lower Bajocian	blue shales,flags and limestones
	Inferior Oolite, 35m at Maoll Bhuidhe 2km SW of Kilchoan	Aalenian	hard white limestone, blue, sandy and hard limestones
	Upper Lias 6m western shore of Kilchoan Bay	Toarcian	dark flags and shales fine-grained purplish shales with limey ironstone (Raasay ironstone)
	Middle Lias 12m 3km east of Rubha Groulin Western side of Kilchoan Bay	Domerian	sandstone often baked
		Lower Pliensbachian	sandy,well bedded shales
	Lower Lias 120m south of Mingary Pier	Sinemurian	
		Hettangian	hardened shales and thin limestones
Triassic	<5m at Mingary Pier, Rubha'a' Mhile and east flank of Ben Hiant		red sandstones, conglomerates, schist, breccias and cornstones

(469625), 1km west of Sron Bheag (454625), Rubha Carrach (462705) and also east of Rubha Carrach (479712). Exposures of the Upper Lias have a maximum thickness of 6m and occur adjacent to those of the Middle Lias; except at Rubha Carrach. Inferior Oolite outcrops at Sron Bheag and much of Ormsaigbeg, and has a maximum thickness of 35m.

These Jurassic rocks consist principally of sandstones, limestones, micaceous sandstones and shales; the bed thicknesses vary from 0.5cm to >30cm. Both west of Mingary Pier and west of Faskadale cone sheets are intruded into Lower Lias rocks consisting of well-banded, nodular limestones with sandy partings which enables the direction of movement along cone sheet fractures to be determined (Chapter 6). At Swordle (546707), the Lower Lias sediments are massively bedded, with few cone sheets and such sediments are of little use for determining the direction and amount of movement along cone sheet fractures. For a similar reason the Middle and Upper Lias rocks are of little use. However, in the cliff sections at Sron Bheag the Inferior Oolite is exposed and because it is well bedded the vertical displacements along cone sheet fractures can be determined.

Well-developed joint sets occur throughout the Jurassic rocks. Keunen (1937), after noting the parallel nature of the joints with some cone sheets, suggested that the joint fractures may represent unfilled cone sheet fractures. This is discussed in Chapter 10.

A prominent feature of the Jurassic rocks is that they dip radially away from the central intrusive complex. Wells (1953)

proposed that the radial dip was imposed largely, or perhaps completly, before the cone sheets were injected, the doming being produced by localised magma pressure of the Hypersthene Gabbro. Bahat (1980) interpreted doming as one of the integral process of cone sheet emplacement (Chapter 1).

2.3.4 Tertiary

2.3.4.1 Lavas and sediments -

Tertiary mudstones on the Ardnamurchan peninsula outcrop beneath the basalt lavas at Sron Bheag (462623) and Glebe Hill (484644). Thin coal and clay layers are found beneath the lavas near Ardslignish (565612) and from this locality Simpson (1961) obtained plant spores which he used to date the sediments as Miocene (Section 2.4).

Ardnamurchan retains only a few remnants of lavas which are thought to belong to the Mull-Morven lava pile. The thickness of the lavas in Ardnamurchan is 100m, whereas Mull has a thickness of more than 1,500m. Outcrops of basaltic lavas are found mainly to the east of the central intrusive complex, in the area of the Northern Vents (Braehouse), Ardslignish and east of Ben Hiant. Scattered outcrops of lavas occur within the central complex.

Subsequent to the lava outpourings, the series of vents called the Northern Vents (520710 - 525650) were formed and form part of the screen of Meall nan Con (545680). The Ben Hiant

agglomerates are bedded and may represent the surface manifestation of the Northern Vents.

2.3.4.2 Central Intrusive Complex -

As a result of mapping the peninsula the Officers of the Geological Survey recognised that many of the intrusions, particularly the cone sheets, were centred on three different foci, termed Centres One, Two and Three, which were dated relative to each other by cross cutting relationships. Centre One is located near Brachouse, Centre Two is near Aodann and Centre Three at Achnaha (Fig.3.1.1). Durrance (1967), however, attributed the distribution pattern of the cone sheets to a single spiral, with a centre located near to Sanna (435694).

Centre One cone sheets are the first series of intrusions of the Ardnamurchan central intrusive complex (Table 2.2) and outcrop from Rubha a' Choit (557715) to Faskadale (499709). In general, these cone sheets are fewer in number, in comparison to the Outer Set of Centre Two. In the east, near Rubha a' Choit, the cone sheets are concordant to the Moine foliation and dip at 70° to the west (Chapter 5). The main mass of dolerite that constitutes Ben Hiant is thought (Gribble, 1974) to be a series of stacked cone sheets belonging to Centre One.

Table 2.2, which lists the major intrusions, is based on Richey et al. (1930) and it should be noted that Gribble et al. (1976) dispute the validity of some of these intrusions.

The Outer Set of Centre Two cone sheets cut the Centre One

Table 2.2

Intrusions of the Tertiary Central Intrusive Complex of Ardnamurchan with emphasis on the timing of the emplacement of the Cone Sheet Sets. (after Richey et al., 1930)

	Quartz Monzonite
	Tonalite
	Fluxion Gabbro of Glendrian
	Quartz Gabbro
	Quartz Dolerite veined with Granophyre
	Quartz Granophyre of Meall an Tarmachain
CENTRE THREE	Biotite and Inner Eucrite
	Great Eucrite
	Porphyritic Gabbro of Meall nan Con
	Gabbro of Plocaig
	Fluxion Gabbro of Faskadale
	SET OF CENTRE THREE CONE SHEETS
	Quartz Gabbro of Faskadale
	Aodann Felsite
	Fluxion Gabbro of Portuairk
	Younger Quartz Gabbro of Beinn Bhuidhe
	Quartz Gabbro of Loch Caorach and Beinn na Seilg
	Eucrite of Beinn nan Ord
	INNER SET OF CENTRE TWO CONE SHEETS
CENTRE TWO	Granophyric Quartz Dolerite of Sgurr nam Meann
	Quartz Gabbro of Aodann
	Older Quartz Gabbro of Beinn Bhuidhe
	Granophyre of Grigadale
	Quartz Gabbro of Garbdhail
	Older Gabbro of Lochan an Aodain
	Hypersthene Gabbro
	OUTER SET OF CENTRE TWO CONE SHEETS
	Porphyritic Dolerite of Glas Bheinn
	Granophyre of Beinn an Leithaid
	Augite Diorite of Camphouse
	Quartz Gabbro of Faskadale
CENTRE ONE	Gabbro of Meall nan Con
	Gabbro of Faskadale
	Ben Hiant Dolerite
	Porphyritic Dolerite of Ben Hiant
	Quartz Dolerite of Camphouse
	SET OF CENTRE ONE CONE SHEETS
	Northern Vents

intrusions and lavas (Table 2.2) and the Kilchoan Moines, the Lias and Inferior Oolite.

Marking the end of the intrusive episode of the Outer Set of Centre Two cone sheets was the emplacement of the Hypersthene Gabbro. The gabbro was followed by a series of intrusions (Table 2.2) that are in turn cut by the Inner Set of Centre Two cone sheets, which outcrop from Beinn Bhuidhe (437672) to Beinn na Seilg (458642). A period of emplacement of major intrusions followed (Table 2.2) before Centre Three became the focus of activity. South of Meall an Tarmachain (486655) are the exposures of the partially developed set of Centre Three cone sheets which intrude the Quartz Gabbro of Faskadale, agglomerates and lavas. Subsequent Centre Three major intrusions conclude the development of the Central Intrusive Complex (Table 2.2). Dykes were emplaced throughout the evolution of the Central Intrusive Complex.

2.4 DATING THE IGNEOUS ACTIVITY

Tertiary igneous activity in Ardnamurchan has been dated at approximately 60My ago mainly using potassium - argon isotope techniques.

Simpson (1962) described and dated the flora of a lignite seam which occurs at the base of the basalts at Ardslignish (566613). He concluded that the flora could not be older than the Oligocene or Lower Miocene, thus implying a much younger date than had previously been proposed for the igneous activity. However, Boulter (in Curry et al., 1978) states that the palino-

morphs illustrated by Simpson (1962) and those described by Strivastava (1975) from inter-basaltic horizons from the Island of Mull, suggest a Palaeocene age, that is 65 - 55My ago; this agrees with the isotopic age dates.

Table 2.3 Isotopic age dates for the three centres of igneous activity of Ardnamurchan by Mitchell and Reen (1973)

CENTRE	AGE	NO OF SAMPLES	NO OF INTRUSIONS
One	58.9±2.0My	6	5
Two	59.1±2.2My	8	6
Three	59.0±1.8My	9	5

K-Ar isotopic age dating has been undertaken on the Ardnamurchan Central Intrusive Complex by Mitchell and Reen (1973). In collating their results, they averaged values for each centre (Table 2.3).

A comparison of the average values shows that the value for each of the three centres is, within experimental error, the same, and therefore the question posed is what event is being recorded? It is possible that the cooling event after Centre Three activity has overprinted all earlier dates, therefore all intrusions give a similar age. Mitchell and Reen (1973) conclude that either :-

a)Due to the large range of dates within a single centre there has been minor argon loss and therefore assign the oldest age determination, that of 61My, to mark the complete evolution of the complex.
b)By assuming no argon loss and therefore accepting the average values for each centre, they assign an age of >59My, emplacement lasting 1 million years.
c)The age recorded is that of cooling, which is post Centre Three.

Palynological and isotopic evidence seem to agree on a date for the whole Ardnamurchan complex, whilst the relative dating of the cone sheet sets enables a distincion in time.

2.5 MAGNETO - STRATIGRAPHY

A magnetostratigraphic survey undertaken in Mull by Mussett et al. (1980) resulted in the establishment of a sequence of reversed and normal polarities. Samples measured were taken from both plateau lavas and the central intrusive complex. The resultant sequence could be either R-N-R or an extended sequence of R-N-R-N-R. Further, unpublished work by these authors indicates that the sequence for the Mull Tertiary complex is most probably R-N-R. A detailed palaeomagnetic survey of the Ardnamurchan central intrusive complex by Mussett et al. (1984) reveals that all the intrusions sampled are reversely magnetized. This may indicate a fairly short period of activity, unlike the Mull igneous complex, or that overprinting or very slow cooling has taken place so that the magnetic sequence merely records the cooling event which occured after the intrusion of Centre Three.

2.6 DEEP STRUCTURE BENEATH THE COMPLEX

A gravity survey by Bott and Tuson (1973) of the igneous complexes of Skye, Mull and Ardnamurchan reveal maximum positive Bouguer anomalies of 70mgal, up to 70mgal and 40mgal respectively, against a regional anomaly of 20mgal. The Bouguer anomaly associated with the Ardnamurchan central intrusive complex is much smaller and less well defined than those associated with the other two complexes. These positive Bouguer anomalies have been interpreted as indicating a cylinder of ultrabasic/basic rock at depth. The model proposed for Ardnamurchan is that of a cylinder of 6km radius extending to a depth of 2.1km (assuming a density contrast of 0.35gmcm) or to 4.5km (assuming a density contrast of 0.21gmcm). The Ardnamurchan central intrusive complex covers a smaller area at the earths surface than the central intrusive complexes of Skye and Mull and this smaller size seems to continue at depth.

CHAPTER 3

METHODS OF ANALYSIS

This chapter outlines the methods used to collect and analyse cone sheet data, together with a discussion of some of the problems encountered.

3.1 FIELD CRITERIA

In order to collect data from the four cone sheet sets a number of field criteria must be defined, these are:-

a) Definition of a cone sheet
b) Location of traverses
c) Division of the traverses into unit lengths

3.1.1 Definition of a cone sheet

Harker (1904) first recognised a series of centrally inclined sheets in the Cuillins of Skye. Bailey (1958) describes how he and Wright were introduced in 1909 by Harker to these (Skye) inclined sheets in the field and they realised that they had begun to map similar intrusions in Mull, where they coined the synonymous term cone sheet.

Harker (1904, p366) defines the term centrally inclined sheet as follows ".....this very remarkable set of intrusions consist....of a vast number of roughly parallel sheets of basic rocks....having a general inward dip at moderate angles.....". He emphasized the fact that they intersect various rock types, although in general they have a restricted outcrop and that they " dip towards a certain point in the interior ". Bailey et al. (1924, p221) used the term cone sheet because when the "sheets are viewed as members of a suite, they suggest the partial infilling of a number of coaxial cone shaped fractures with

inverted apices united underground".

Richey et al. (1930, p56) defined the term cone sheet as "a suite of intrusions occupying conical fissures that have a common apex and common vertical axis....The apex at which they converge may be designated the cone sheet focus....collectively the outcrop pattern is a series of idealized, concentric circles....the central area is devoid of sheets ".

I prefer Harker's term, centrally inclined sheets, but because of present day usage I will use the term cone sheet, here defined as:-

An annular outcropping igneous sheet, inclined towards a central focus.

In the field, the annular nature of individual intrusions cannot always be proved. However, the circular outcrop is evident from the way in which the sets are distributed on a regional basis. Dip of the cone sheets varies from vertical to sub-horizontal and can therefore be confused with dykes and sills respectively, although it could be argued that cone sheets are a variety of sill.

3.1.2 Location of traverses

Richey et al. (1930) identified four cone sheet sets, based on their geographical distribution and their time relationships with other intrusions of the central intrusive complex. Fig.3.1.1 shows the generalized location of each cone

sheet set; each set is truncated by later ring intrusions (Table 2.2), thus restricting their distribution. Richey et al. (1930) noted some possible areas of geographical overlap of the four sets; for example, on the shore east of Mingary Castle two sets of sheets, trending ENE and NNE, are exposed and possibly belong to the Outer set of Centre Two and the set of Centre One, respectively. In order to examine the variations in the four cone sheet sets the following traverses were chosen (Fig.3.1.1):-

CENTRE ONE :- North coast, from Faskadale (501707) to Rubha a' Choit (557715)

OUTER SET OF CENTRE TWO :- North coast, Rubha an Duin Bhain (448705) to Faskadale (501707)

South coast, West side of Sron Bheag (454627) to (461623)

Kilchoan section, Glas Eilean (485630) to Sgurr nan Eun (511631)

INNER SET OF CENTRE :- Beinn Bhuidhe (438674)
Garbhdhail (445657)
Upper Garbhdhail (445649)
Beinn na Seilg (457642)
Lighthouse (416674)
Sgurr nam Meann (433678)
An Acairseid (435631)

CENTRE THREE :- Northern slopes of Abhain Chro Bheinn (487652)

Location of the traverses was governed by exposure and the orientation of the sheets. Traverses for the sets of Centre One

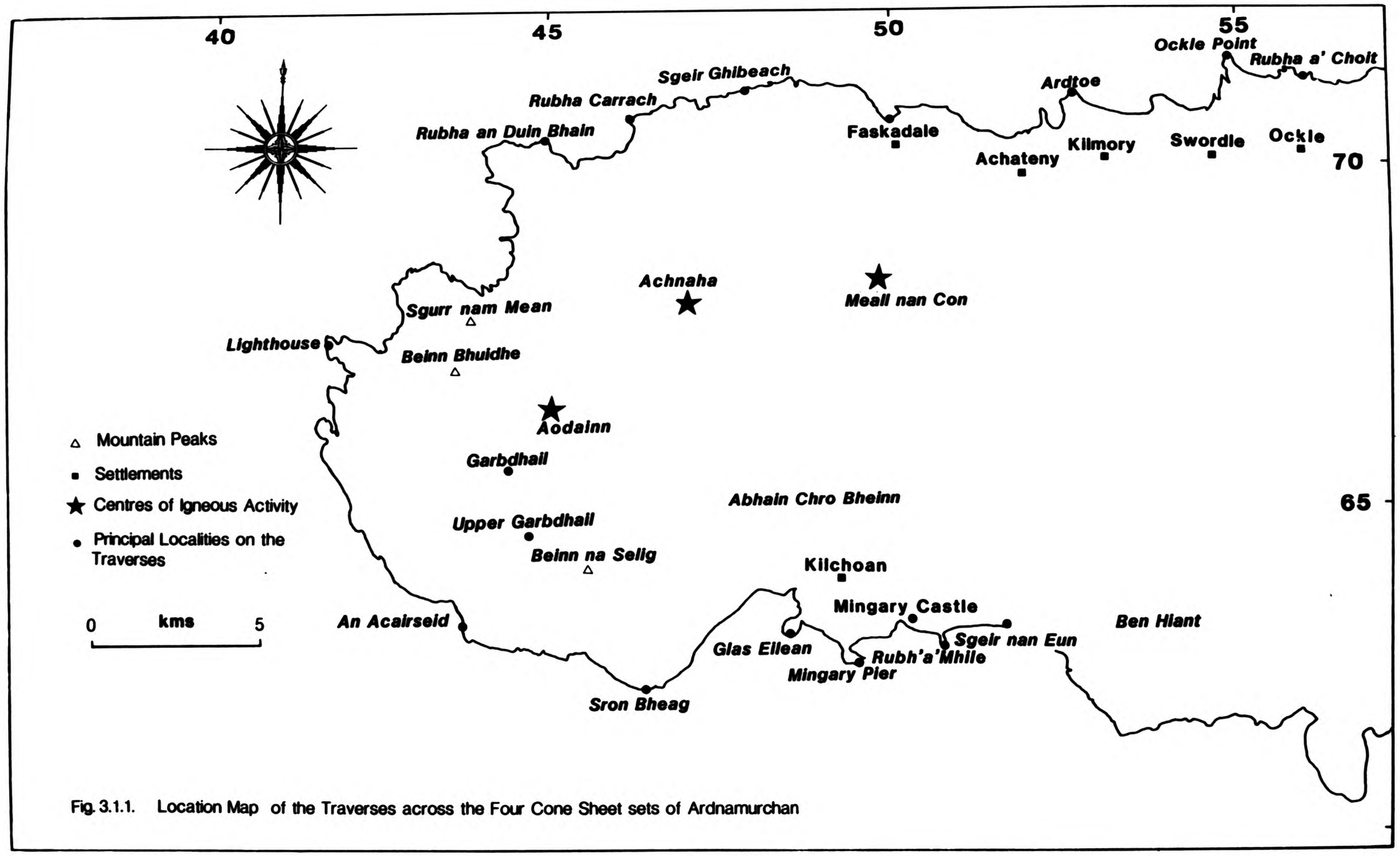

Fig. 3.1.1. Location Map of the Traverses across the Four Cone Sheet sets of Ardnamurchan

and Outer Centre Two are located on the coast, where exposure is excellent and the sheets trend roughly perpendicular to the coastline. On the north coast, traverses in the west are parallel to the coast, whereas farther east the traverses are at a small angle to the coastline.

In general, coastline sections predominate and consequently the whole of the Ardnamurchan coastline has been sampled, excepting from An Acairseid to Port Garbh, which is inaccessable. Fortunately, this area contains few cone sheets and it's exclusion from analysis will not affect the result.

Although Centre One cone sheets crop out over a large area (Fig.3.1.1) they do not show a well developed annular form because they have been truncated by younger intrusions. This contrasts sharply with the three-quarter circle of the Outer Set of Centre Two, which also is excellently exposed and therefore dominates the data. Only one-quarter of the presumed circle now remains of the Inner Centre Two cone sheets, whilst the Centre Three cone sheets are very restricted in their occurrence and, therefore, do not give a realistic view of the annular nature of the sheets.

3.1.3 Division of the traverses into unit lengths

Subdivision of the traverse length into units is determined by the following factors:-

Area over which the cone sheets occur

Exposure

Homogeneous strain

3.1.3.1 Area over which cone sheets occur -

The abundance of the cone sheets in the geology of Ardnamurchan is obvious from Plate 2.1. Despite the truncation by later Centre Three ring intrusions, the Centre One Set and the Outer Set of Centre Two cone sheets outcrop almost continuously along the north and south coasts to easting 57. The Inner Set of Centre Two and Centre Three cone sheets are less well developed than the earlier cone sheet sets and only occur from Beinn Bhuidhe to Beinn na Seilg (Inner Centre Two) and on the northern slopes of Abhain Chro Bheinn (Centre Three).

3.1.3.2 Exposure -

As stated above, Centre One cone sheets are exposed along the coast, therefore accessibility to the majority of the area is unhindered. However, gullys, which result from erosion of dykes and a number of vertical cliffs make parts of the traverse inaccesible. In general, therefore, the Centre One traverse is continuous from Rubha a' Choit to Faskadale. Several inland exposures have been studied but because they are discontinuous they add little to the information gained from the coastal sections.

The north coast sections of the Outer Centre Two cone sheets consist of a narrow foreshore backed by steep cliffs and, therefore, the measured sections are taken from valleys which are at right angles to the coast and to the trend of the sheets. From Sgeir Ghibeach to Faskadale a number of subsets of cone sheets are exposed, such that the strike of the cone sheet sets

varies over 90°. In consequence, the section line from Sgeir Ghibeach to Faskadale has been stepped, so that the section lines are perpendicular to the trend of the cone sheets.

On the south coast, wide foreshores occur at Sron Bheag and between Glas Eilean and Mingary Pier, whereas east of Mingary Pier there exists only a narrow foreshore. At Rubha'a'Mhile (Fig.3.1.1) a small promontory occurs which facilitates data collection. Farther east along this section, towards Sgeir nan Eun, although the exposure is generally poor, a few thick sheets are well exposed.

Exposures showing the Inner Centre Two cone sheets are only accessible in early spring, before vegetation obscures the exposures, especially those of the Garbhdhail sections.

The main exposures of the set of Centre Three cone sheets outcrop on the northern slopes of the Abhain Chro Bheinn (Fig.3.1.1) and in the agglomerate cap south of Meall an Tarmachain.

3.1.3.3 Homogeneous strain -

To calculate the homogeneous strain produced by the emplacement of cone sheets along a 100m section (unit length) all cone sheet thicknesses are added together, as each cone sheet represents one strain. Holmes (1924) calculated that homogeneous strain would be achieved over an area 100 times the strain marker. For the cone sheets along the Kilchoan section the average sheet thickness is 1m. Despite the fact that the

cone sheets belonging to the Centre One set are thicker (Chapter 5), the 100m unit length has been maintained to facilitate calculations.

3.2 DATA COLLECTED

The dip, strike, thickness, rock type, presence or absence of phenocrysts and terminations, were recorded for each sheet encountered along a traverse. The type of dilation and sense of relative movement is, unfortunately, not available for each sheet measured because of a lack of suitable marker horizons in the country rocks. Where present, the following information has been collected from the country rocks; fracture systems, relationships between host rock type and the structure of the margins of the sheets and the number of unfilled cone sheet fractures.

3.3 STRAIN MEASUREMENT

There are a number of methods of determining the amount of strain, which, in this case, has been produced by the emplacement of cone sheets. However, the applicability of these methods varies according to the data being measured. Described below are three methods which I have used with a discussion of the errors generated by each method.

3.3.1 Method 1

This is method 4 of Ramsay (1967, p80). Both the orienta-

tion of the principal strains and values for the principal extensions can be found by computing the quadratic elongations of three known lines and the angles between them in the strained state. The construction, which is in two parts is as follows: Construction 4a of Ramsay (1967, p80)(Fig.3.3.1)

i. Draw three lines A_1B_1, B_1C_1 and C_1A_1 of any length but having the correct angular relationships of the lines i, j, k, in the deformed state.

ii.Calculate the undeformed lengths of the lines A_1B_1, B_1C_1 and C_1A_1 ($AB=A_1B_1 0\ (\lambda i)^{0.5}$ etc.) and construct the triangle A B C representing A^1 B^1 C^1 in an undeformed state

iii.Drop a perpendicular CD onto AB, and a perpendicular AE onto BC.

iv.Locate the positions of D and E in the deformed state (D_1 and E_1, respectively) knowing that $A_1D_1/D_1B_1 = AD/DB$, and $B_1E_1/E_1C_1 = BE/EC$. Draw C_1D_1 and A_1E_1. The deflections of angles $A_1D_1C_1$ and $B_1E_1A_1$ from the perpendicular give the angular shear strain ui and uj for the directions of A_1B_1 and B_1C_1 respectively. For the lines i and j both the quadratic elongation (λ_i, λ_j) and shear strain ($\gamma_i = \tan u_i, \gamma_j = \tan u_j$) can be calculated. It is now possible to construct a Mohr diagram and determine the orientations and amounts of principal strains.

The second part of the construction (4b of Ramsey, 1967 p80)(Fig.3.3.2) is as follows

i. Draw two perpendicular co-ordinate axes λ' and γ'.

ii.Calculate values of λ'_i, λ'_j, $\gamma'_j = \gamma_i/\lambda_i$, and γ_j. Plot the points $P_i(\lambda'_i, \gamma'_i)$ and $P_j(\lambda'_j, \gamma'_j)$; these must both lie on the Mohr strain circle and therefore the right bisector of the line joining them will intersect the λ' axis at X, the centre of

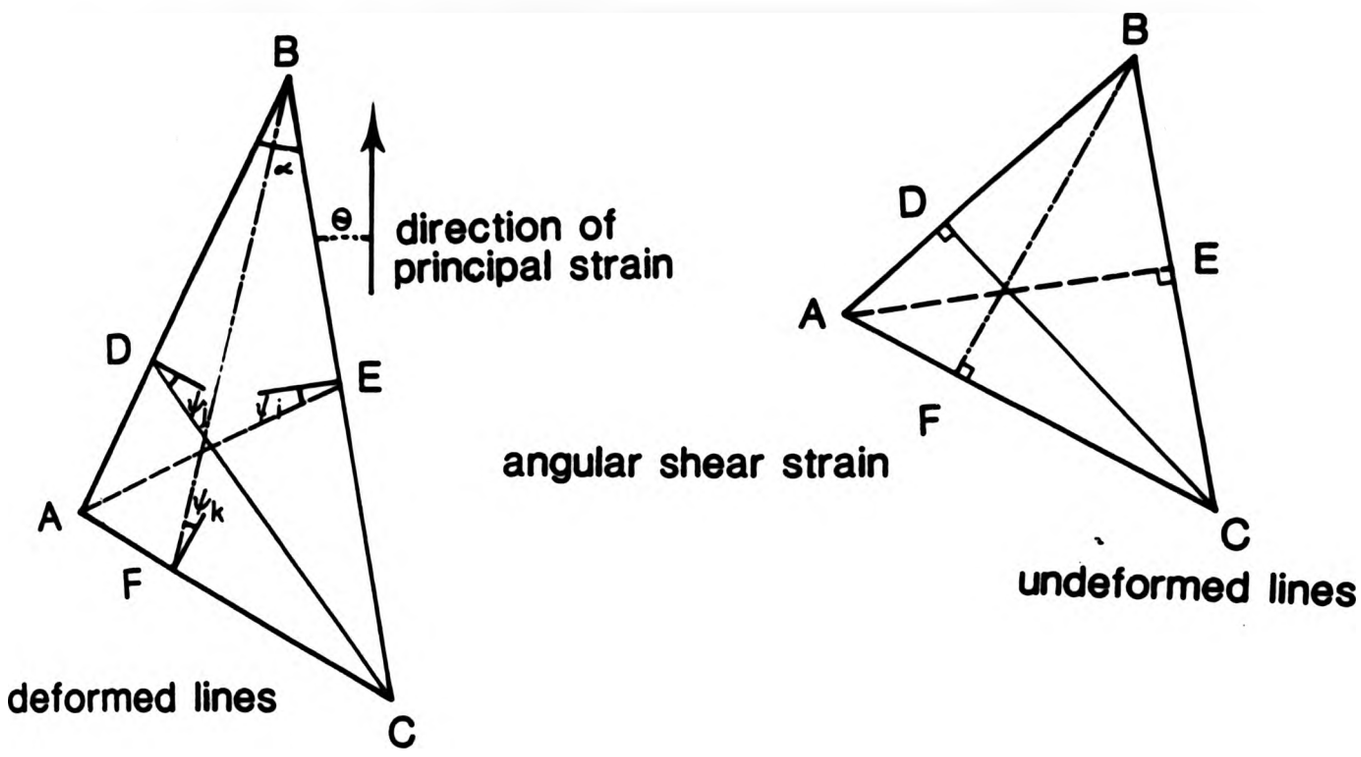

Fig.3.3.1 Mohr construction to determine the values of shear strain when the extensions along three lines are known (after Ramsay, 1967)

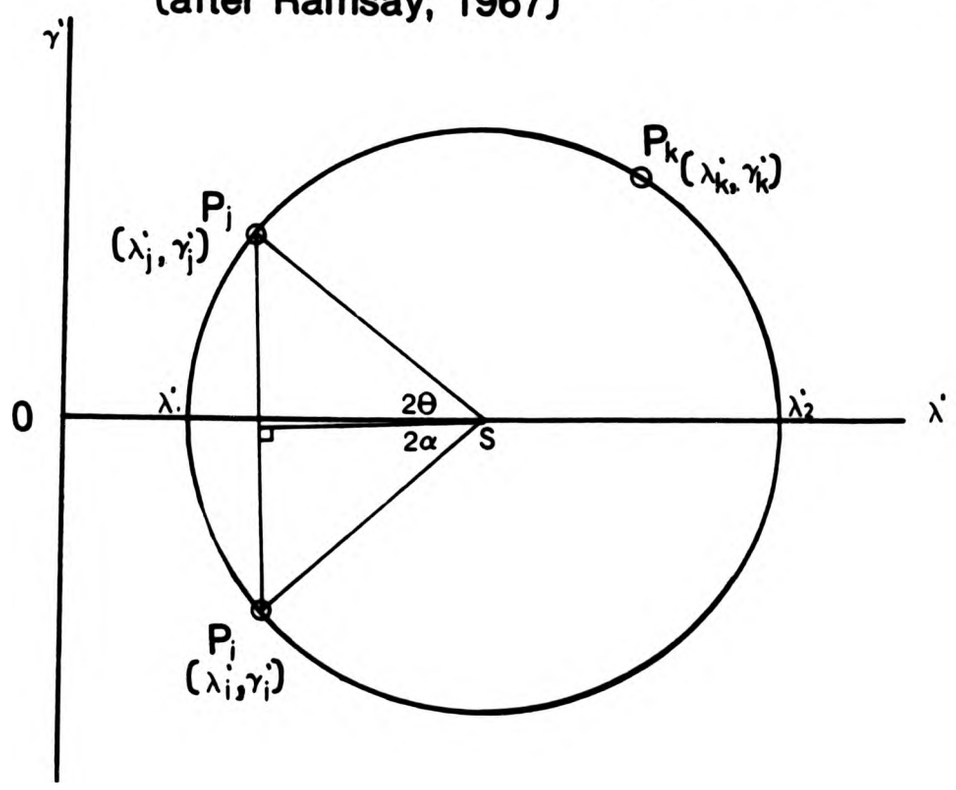

Fig.3.3.2 Mohr construction to determine the principal strains, using the information derived from Fig.3.3.1 (after Ramsay, 1967)

the circle. Draw the circle of radius X P_i. Check that angle P_i X P_j = $2\alpha'$.

iii.The angle P∞CO is $2\theta_i$ where θ'_i is the angle between the principal axis of longitudinal strain and the line i, the values of principal strains λ'_1 and λ'_2 are found where the Mohr circle cuts the λ' axis.

This method is particularly applicable for measuring horizontal strain caused by the emplacement of cone sheets, as the extension along three lines may be either measured from a scaled plan view or directly in the field. For each line the orientation must be recorded plus the true thickness of each cone sheet perpendicular to the line (Fig.3.3.3) and the length of the line. The results can then be tabled (Table 3.1). Thus the extension along the three differently orientated lines and the angles between them may be ascertained and used to determine the principal strains. In addition, values for the principal extensions can be found for the area.

3.3.2 Method 2

This method measures bulk strain, that is the sum of all strains resulting from the emplacement of cone sheets in a unit length. Fig.3.3.4 is a series of diagrams which summarise this method.

i. Fig.3.3.4a depicts, in the strained state, a cliff section at Rubha Carrach in agglomerate country rock cut by a number of cone sheets.

ii.Firstly, all cone sheets are removed by cutting them out from a tracing or photograph of the chosen section. To recon-

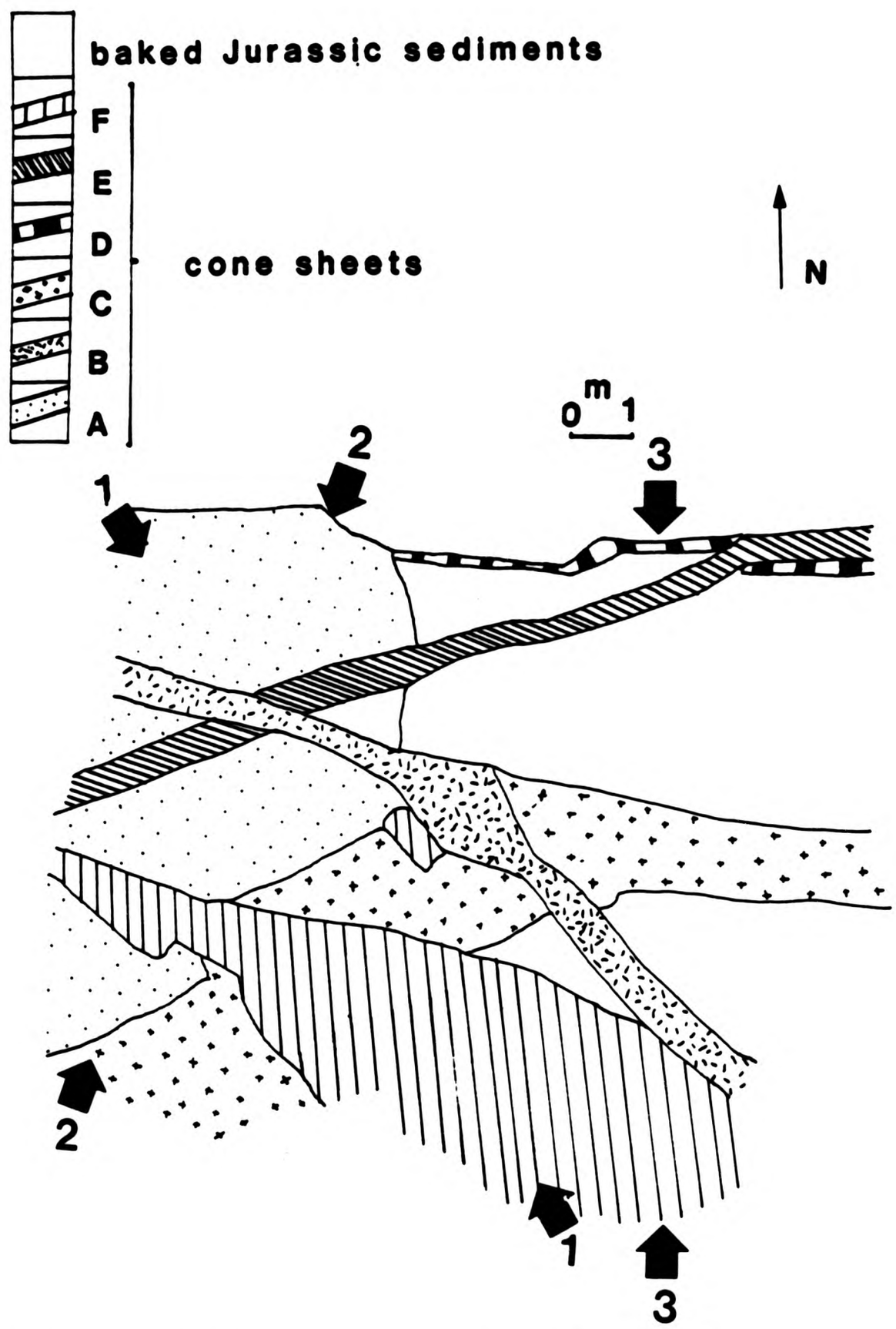

Fig.3.3.3 Diagram of the cone sheets of Rubha Dubh an Aige, north coast Outer Centre Two. By measuring the cone sheets perpendicular to the lines (1-1, 2-2, 3-3) and the orientation of the lines, Ramsay's (1967) method 4 may be used

Table 3.1 Determination of strain using the extension along three lines (Method 3)

	Line 1	Line 2	Line 3
Orientation of each line	324°	025°	360°
Sheets contained within each line	E C	A F	D

Plate 3.1 Part of the cliff section at Rubha Carrach showing cone sheets of the Outer Set of Centre Two intruded into agglomerates.

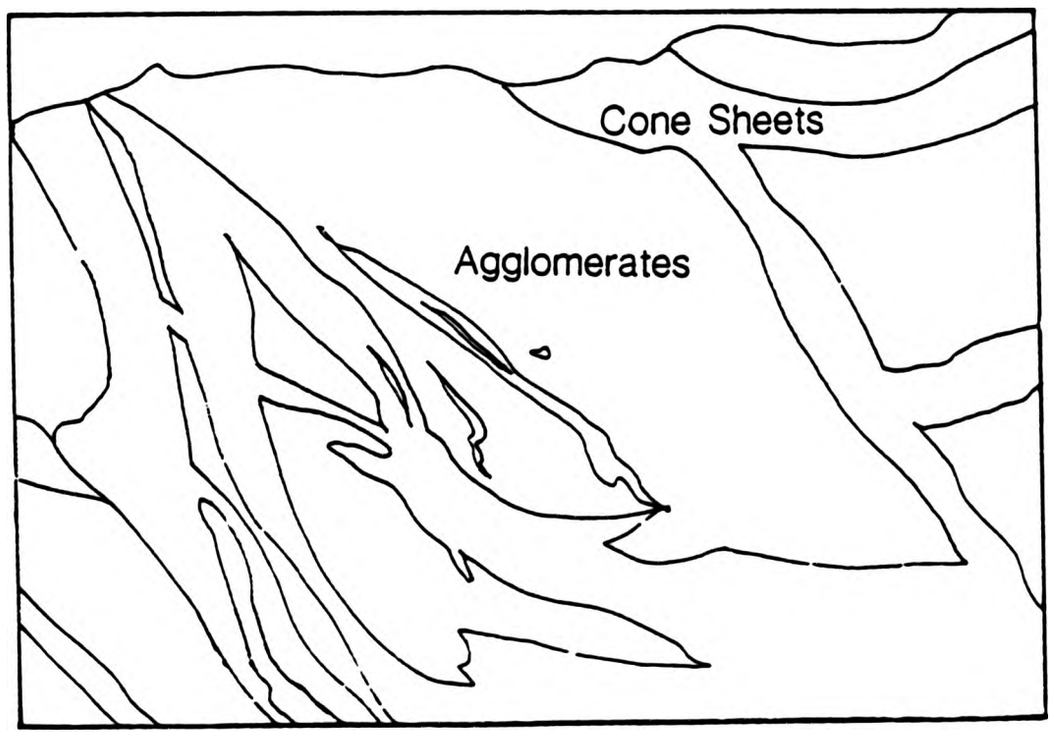

Fig3.3.4a Tracing of the cliff section depicting the main rock units shown in Plate 3.1

Plate 3.1 Part of the cliff section at Rubha Carrach showing cone sheets of the Outer Set of Centre Two intruded into agglomerates.

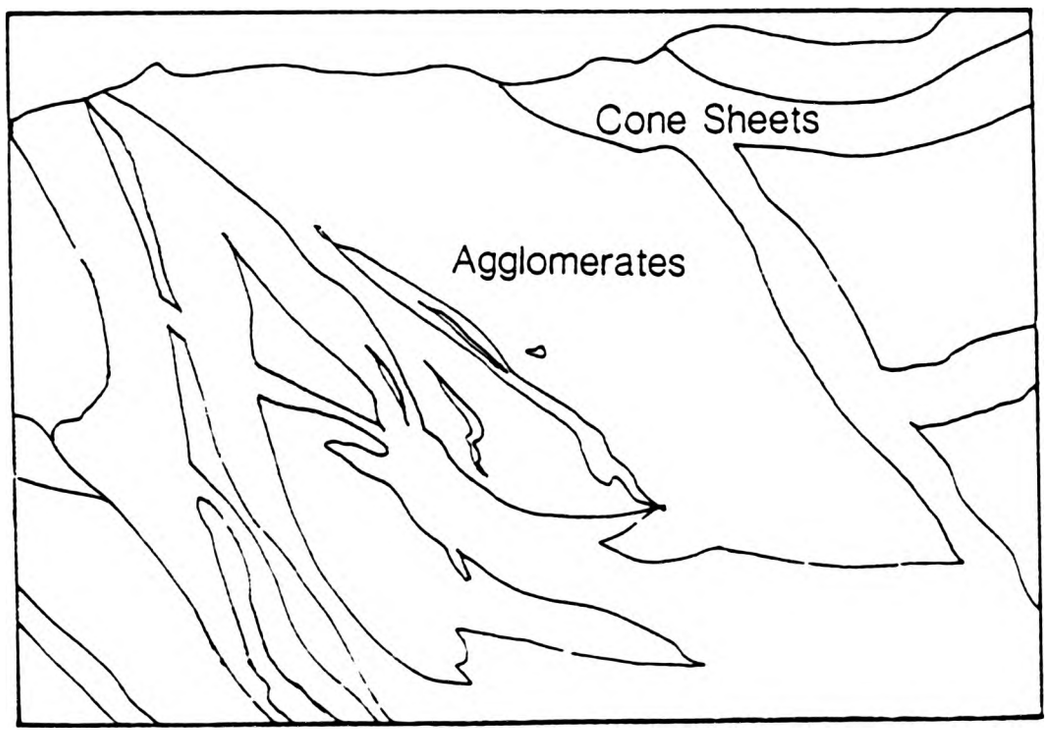

Fig3.3.4a Tracing of the cliff section depicting the main rock units shown in Plate 3.1

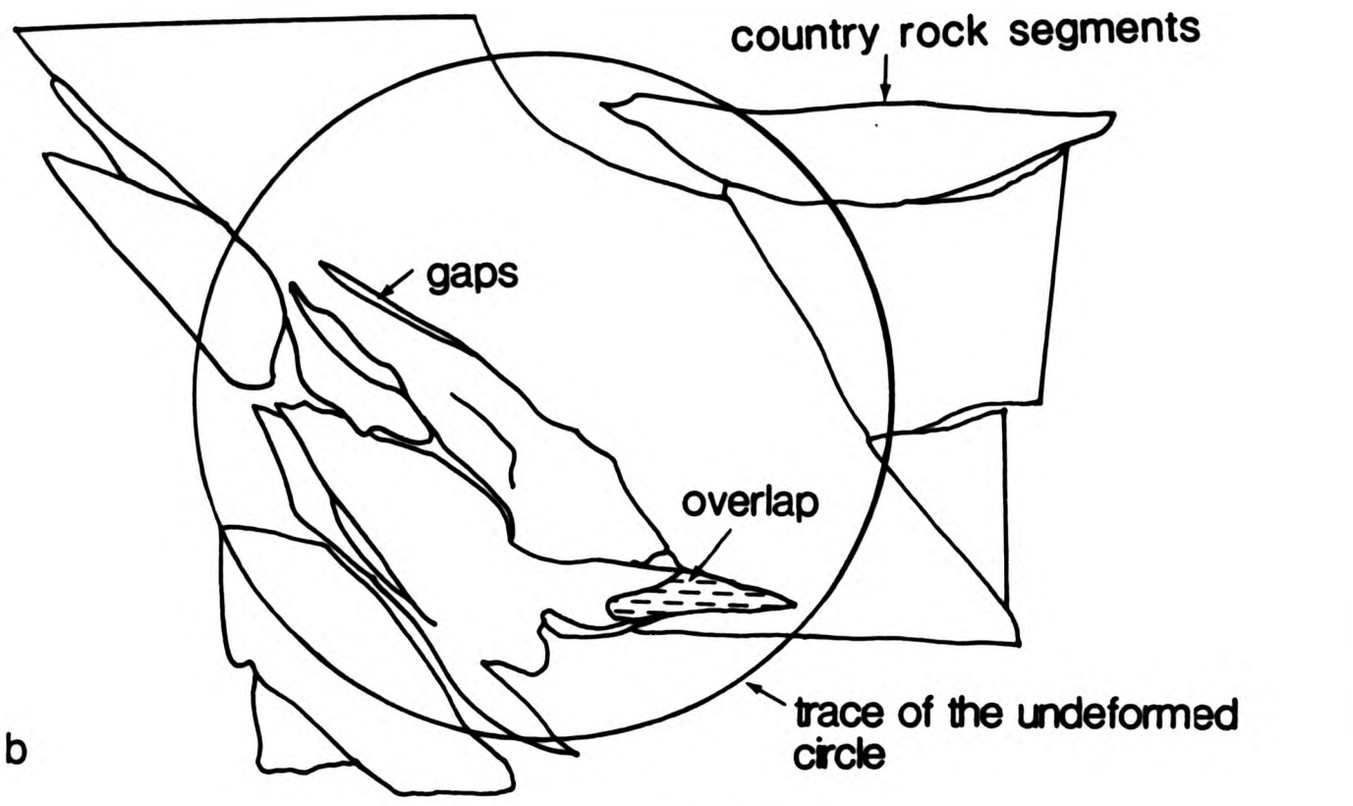

Fig.3.3.4

b Reconstruction of the undeformed state, minus the cone sheets, plus the trace of the undeformed circle

c Re-strained section bearing the trace of the circle and the outline of the best fit ellipse

struct the unstrained state fit together, with as little overlap as possible, all the country rock segments (Fig.3.3.4b). Draw a circle on the unstrained country rock, the radius is not critical, although it should include all sections of the country rock.

iii.Re-insert the cone sheets into the country rock bearing the circle, the new circle represents the strained state (Fig.3.3.4c).

iv.The bulk strain is determined by the best fit ellipse through the parts of the original circle. The ratio of the ellipse axes to those of the original circle determines the amount of strain. Also, the directions of the axes and the orientation of the bulk strain can be determined.

3.3.3 Method 3

This method, like method 2, measures strain throughout 360°, although method 3 is more systematic (Fig.3.3.5a). The procedure is as follows:-

i. A series of radial lines, 10cm long, spaced at 20° intervals of compass, is centred on a small scaled drawing (1cm = 5m) of a unit length or photograph.

ii.The true thickness of all sheets whose strike is normal to each radius is measured and recorded (Fig.3.3.5b), each sheet being measured only once.

iii.Calculate the extension i.e. the sum of all the sheet thicknesses per radius, as a percentage of each radii (Fig.3.3.5c).

iv.Construct an ellipse (Fig.3.3.5d) by joining the incremental strains along each radii, thus determining the maximum

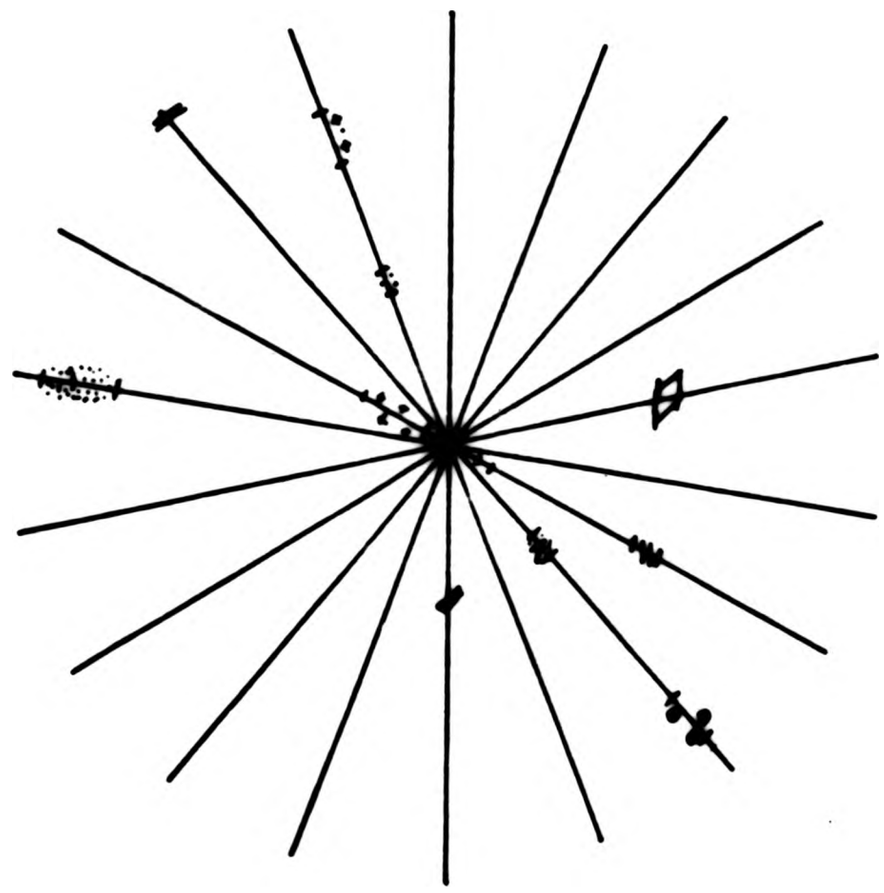

Fig.3.3.5b Radial grid superimposed on a scaled drawing, to measure the strain caused by the emplacement of cone sheets

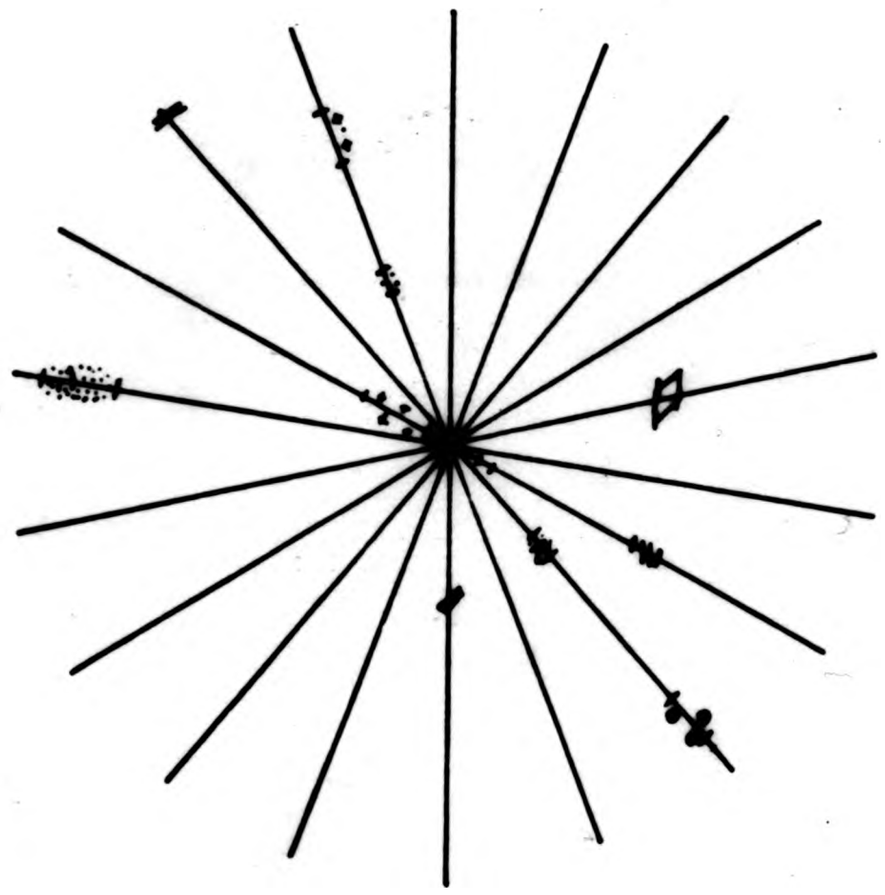

Fig.3.3.5b Radial grid superimposed on a scaled drawing, to measure the strain caused by the emplacement of cone sheets

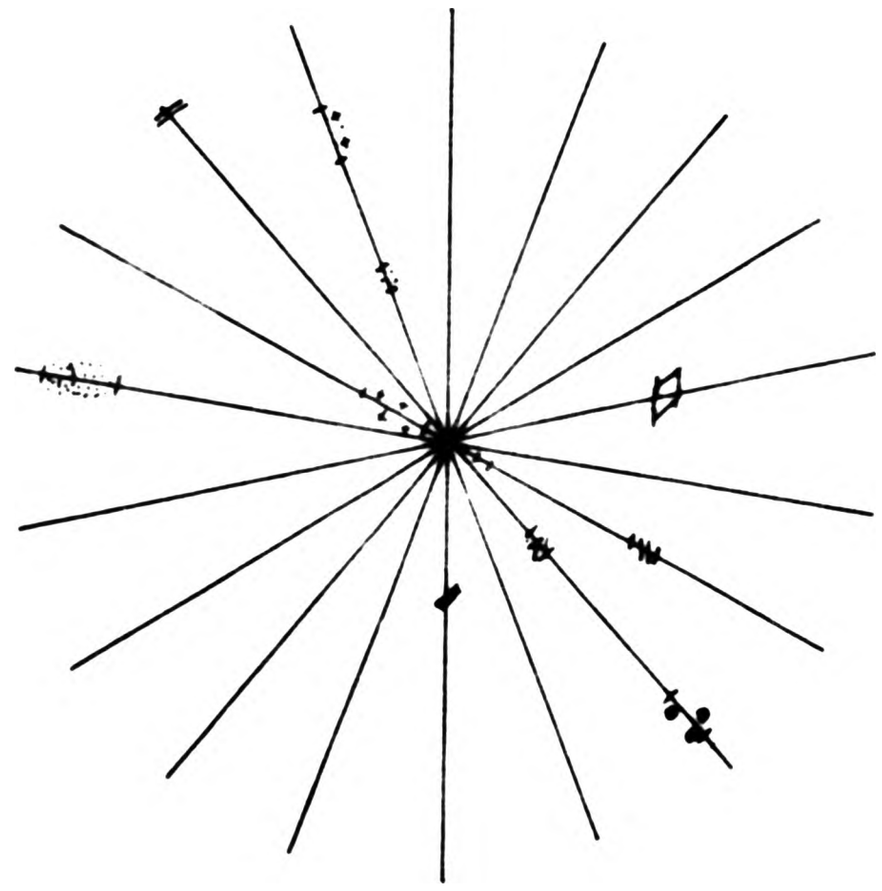

Fig.3.3.5b Radial grid superimposed on a scaled drawing, to measure the strain caused by the emplacement of cone sheets

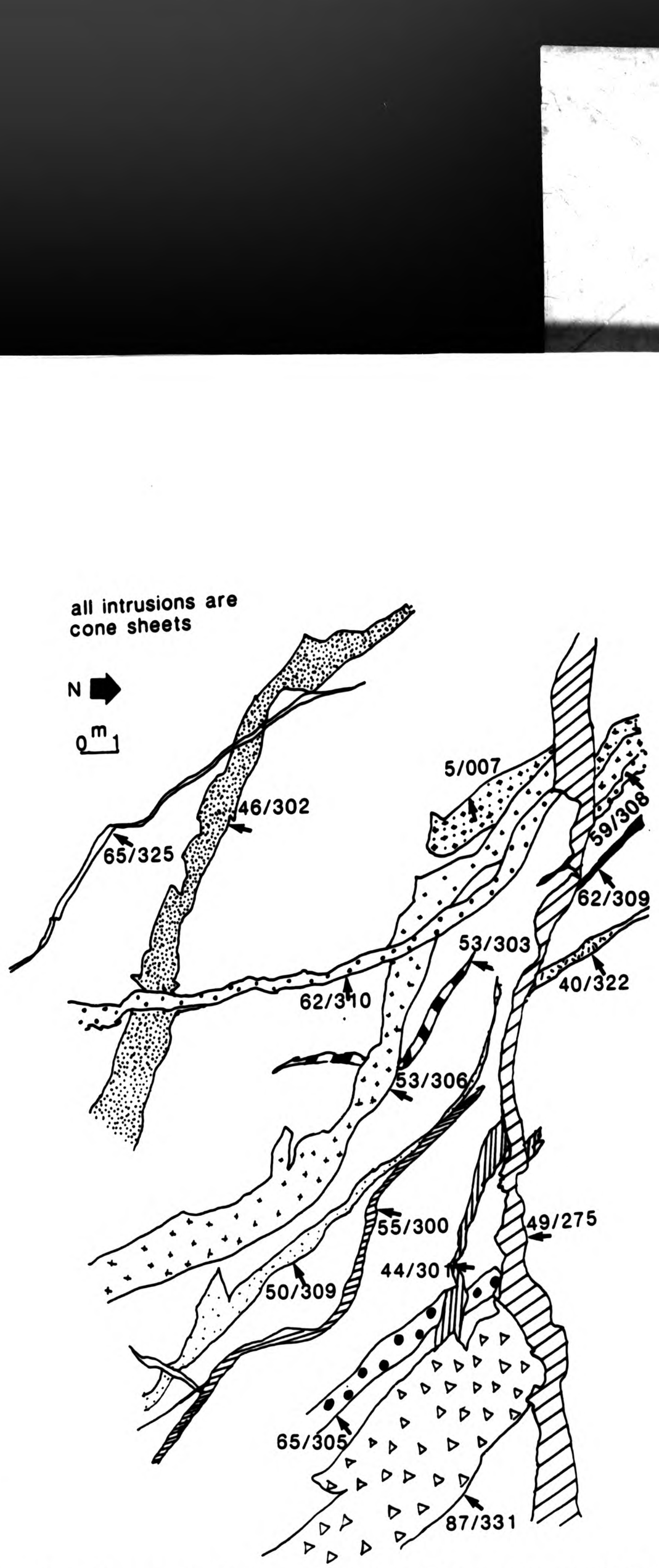

Fig.3.3.5a Map of Outer Centre Two cone sheets intruded into Jurassic limestones at Sgeir Ghibeach

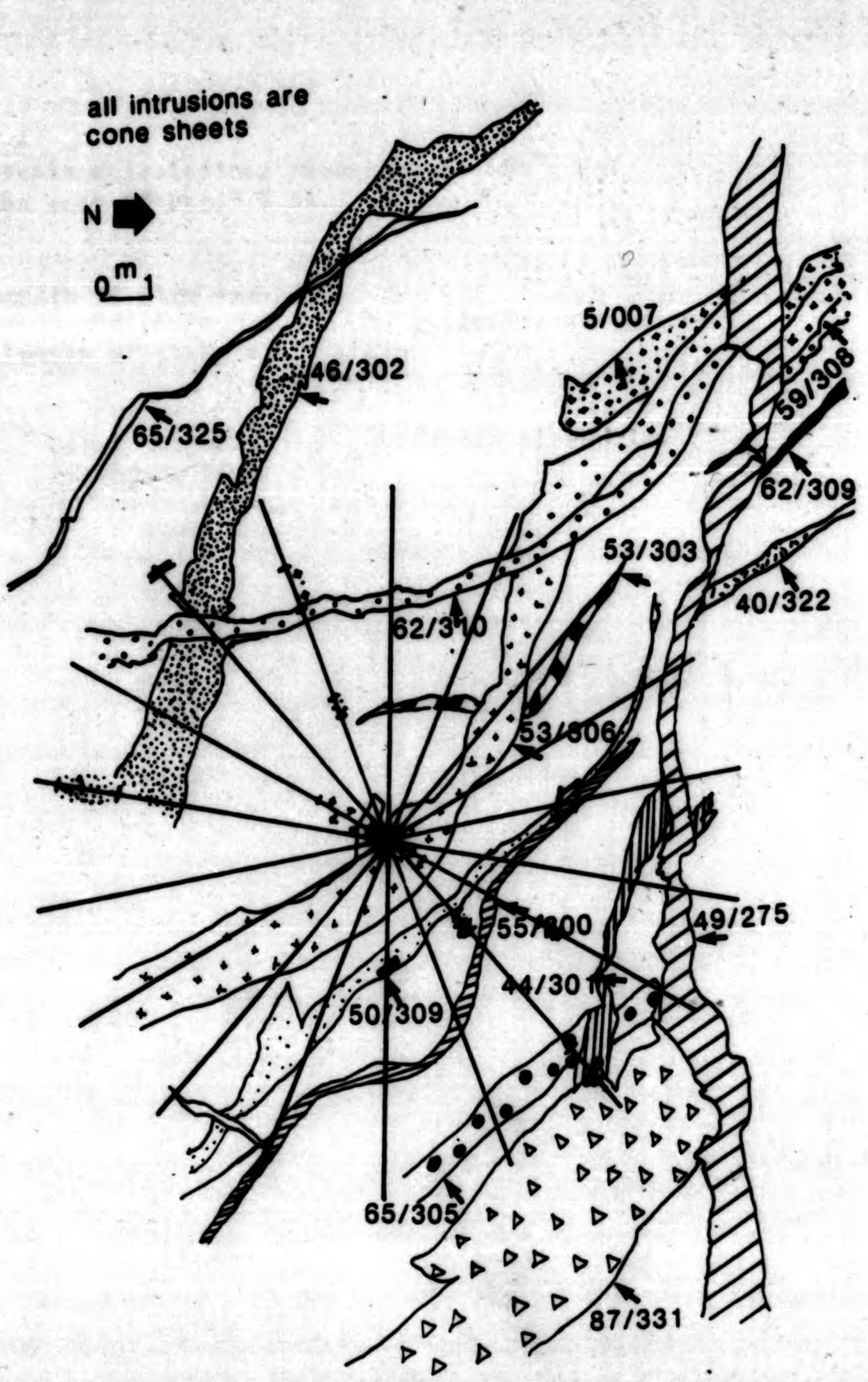

Fig.3.3.5a Map of Outer Centre Two cone sheets intruded into Jurassic limestones at Soeir Glaibeach

Fig.3.3.5b Radial grid superimposed on a scaled drawing, to measure the strain caused by the emplacement of cone sheets

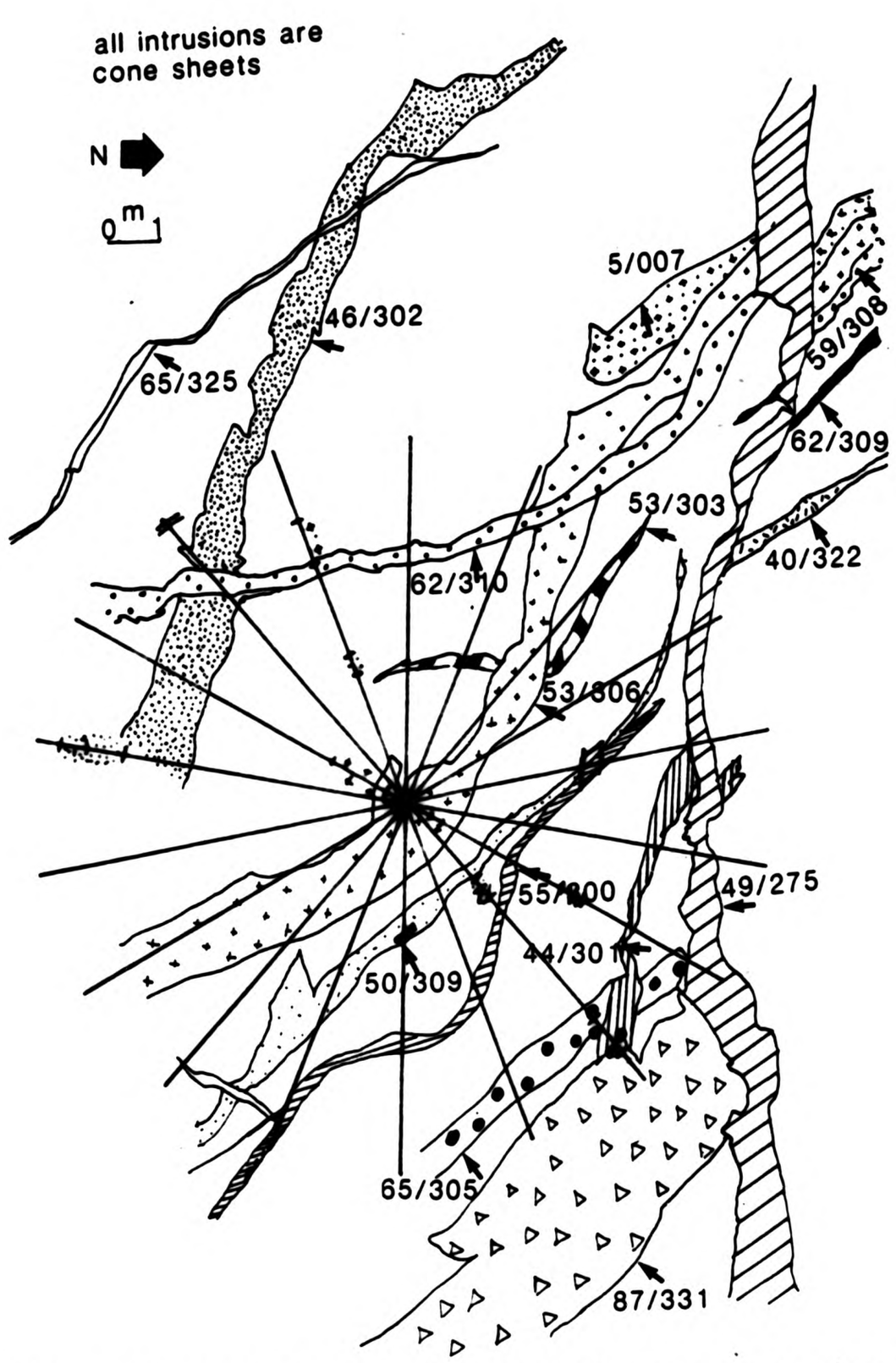

Fig 3.3.5a Map of Outer Centre Two cone sheets intruded into Jurassic limestones at Soir Chaibeach

Fig3.3.5b Radial grid superimposed on a scaled drawing, to measure the strain caused by the emplacement of cone sheets

Fig.3.3.5c Strain calculations throughought 360°, for the area of Fig.3.3.5a.

$$\frac{\text{deformed length of diameter}}{\text{undeformed length of diameter}}^{2} = \text{quadratic elongation}$$

orientation of diameter	total thickness of sheets in m	quadratic elongation
020	0.00	0.00
040	0.00	0.00
060	0.00	0.00
080	0.90	1.19
100	1.30	1.32
120	1.40	1.35
140	1.25	1.31
160	1.25	1.31
180	0.25	1.00

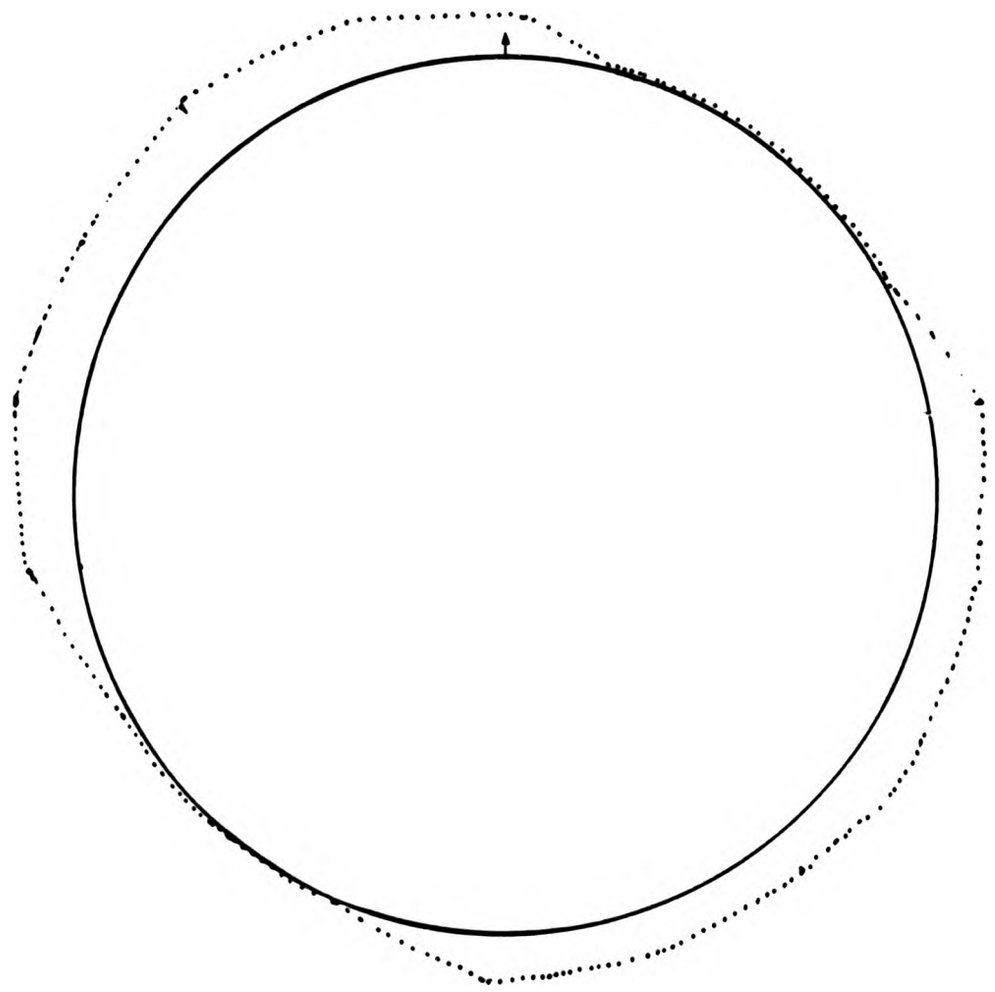

Fig.3.3.5 Calculated strain ellipse for the area (Fig.3.3.5a) caused by the emplacement of cone sheets

extension directions and the amount and direction of the strain.

3.3.4 Comparison of the three methods of strain measurement

In method 1 (Fig.3.3.1) extensions along the three lines should lie on the perimeter of the Mohr circle. However, Fig.3.3.1 shows that only two of the three points fall on the circle. Consequently, two circles can be drawn (using the minimum value plus one of the other extensions), each recording an incremental strain. By multiplying the axes of the two incremental ellipses together a resultant finite ellipse is formed, which has the same axes as the ellipse derived by method 3. Ramsay's (1967) method of construction of the strain ellipse should give a finite ellipse and, in addition, it apparently picks out incremental strains. This is probably because the area measured is one of inhomogeneous deformation.

Problems arising from the use of method 2 are indicated in Fig.3.3.4b. These consist primarily of gaps and overlaps when a reconstruction of the unstrained state is performed. It is possible that the gaps are due to either the mechanical erosion of the wall rock during the intrusion of the sheets, the assimilation of the wall rocks or that dilation of the sheet has a component of shear, that is movement in a plane at an angle to the one undergoing analysis. Secondly, in re-calculating the strained state the ellipse is "fitted by eye" and this introduces an error into the calculations.

In measuring the radial distribution of strain in method 3 a finite ellipse is obtained, and no strain is omitted as can

happen in method 2. Timing of sheet emplacement is not accounted for in method 3, in contrast to method 2, where cross-cutting relationships and therefore timing of sheet emplacement are required in order to re-construct the unstrained state of the country rock, consequently minimizing errors of the unstrained state in method 3. In addition to the finite ellipse, method 3 also records incremental strains and directions (Fig.3.3.5), similar to method 1, whereas the finite ellipse smooths out all irregularities.

It is concluded that method 3 combines the best characteristics of all three methods, and it is this method which has been used most commonly in the present study.

3.4 PIERCING POINTS

Most displacements measured in a two-dimensional plane are apparent displacements. However, with sufficient two-dimensional data for a single cone sheet it is possible to compute the three-dimensional displacements.

The three-dimensional displacement along a cone sheet fracture can be calculated by means of a piercing point technique as follows:- two intersecting planes form a line (Fig.3.4.1) and if these two planes are cut by a third plane, in this case a cone sheet, the line will intersect the plane of the sheet as a point which is termed the piercing point. If the position of the piercing point can be determined on either side of the sheet, the true amount and direction of displacement can be calculated, that is net slip. With such evidence the opening direction of

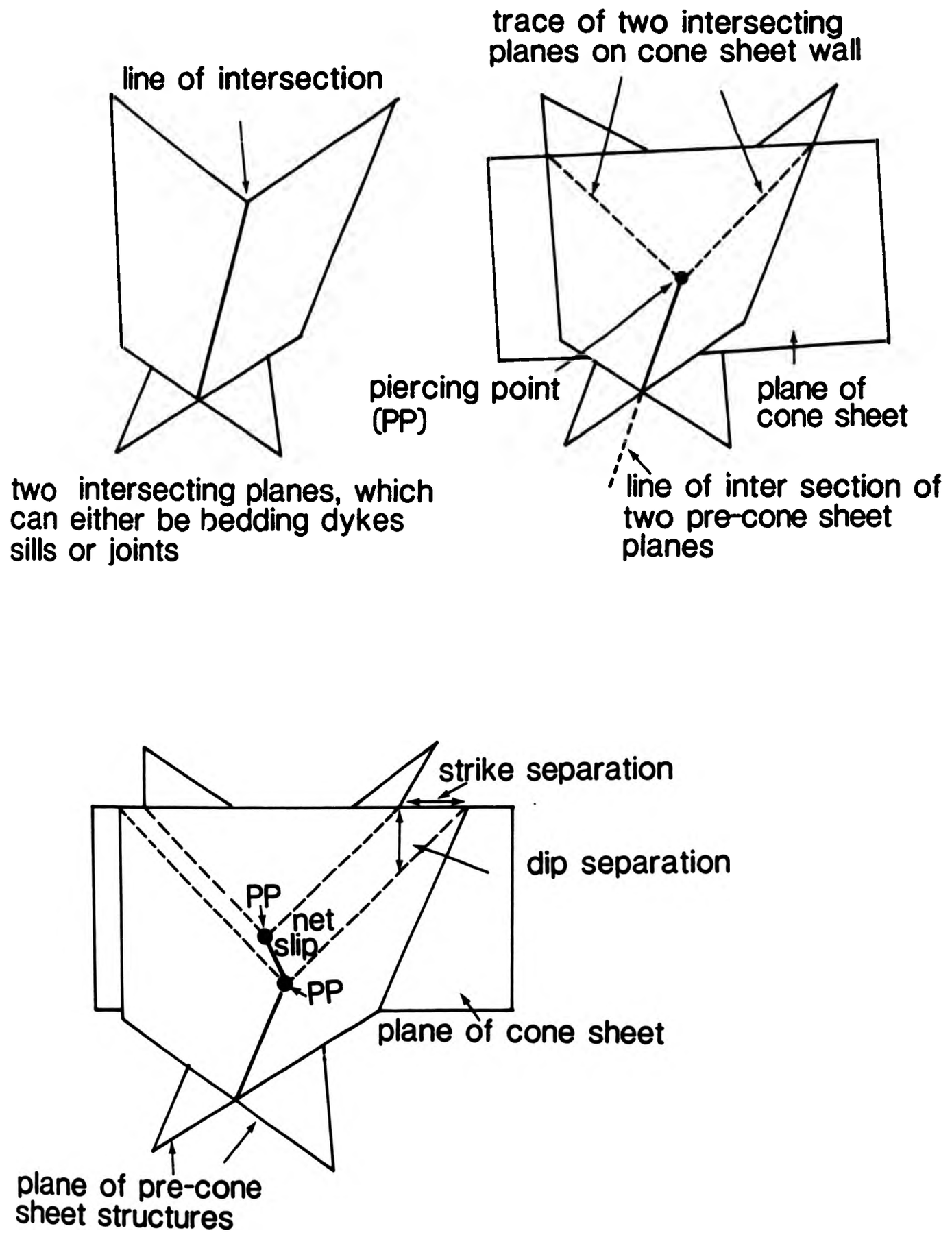

Fig. 3.4.1 A series of diagrams illustrating the nomenclature and the displacement of the piercing points across a cone sheet and the estimates of net slip.

the sheet fracture can be determined.

Two methods of how to calculate the positions of piercing points are given below. The data required are two cross cutting planes which predate dating the sheet and which are cross cut by the sheet. A detailed field drawing, a photograph and spot heights above a reference plane for each intersection of the sheet and the two pre-dating planes (Fig.3.4.2a) are required in order to determine the net slip.

3.4.1 Calculation 1

Using the collected data, structural contours for each surface (planes A_1,B_1, C_1,A_2,B_2 and C_2 of Fig.3.4.2b) are constructed. A line of intersection for planes A_1B_1 and A_2B_2 can then be constructed and where these lines intersect planes C_1 and C_2 respectively marks the location of the piercing points (D_1 and D_2). On a scaled drawing the vector between points D_1 and D_2 may be ascertained (Chapter 6), the distance between the points on the plan view gives the horizontal displacement whilst the structural contour values give the vertical separation. With these values, the angle and dip direction of the net slip may be ascertained by trigonometry and the azimuth can be measured directly from the scaled drawing. The net slip, plane of the cone sheet and the pole to the plane of the cone sheet (π pole) are plotted on a stereonet. If the net slip is contained within the plane of the sheet, the sheet opened by shear (Fig.3.4.3a) whereas if the net slip is in the direction of the π pole the sheet opened by tension (Fig.3.4.3b).

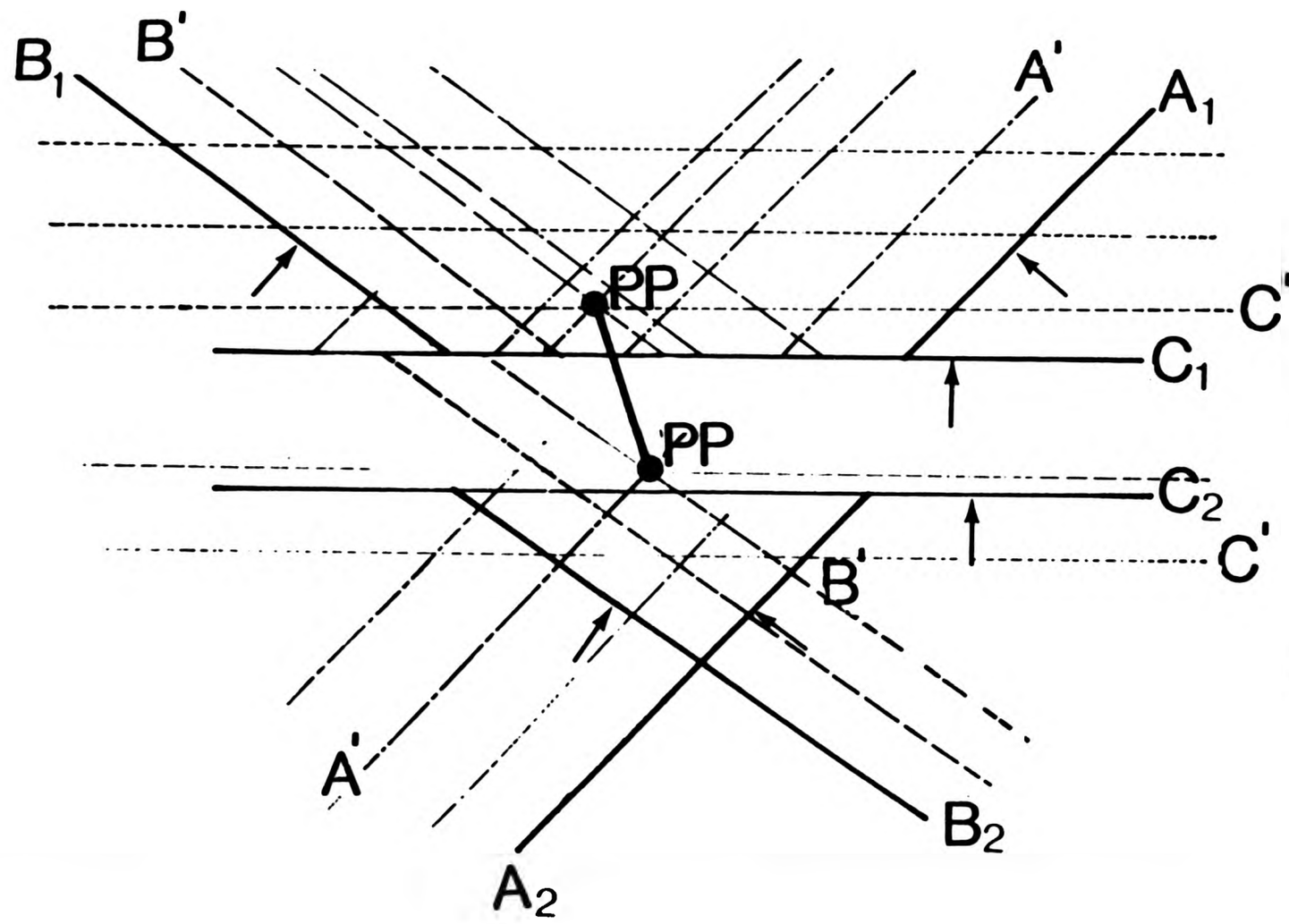

structural contours
A'B' for the pre-cone sheet planes
C' for the cone sheet plane
PP piercing point

Fig.3.4.2Construction for piercing point analysis method 1 (description of method Chapter 3.3)

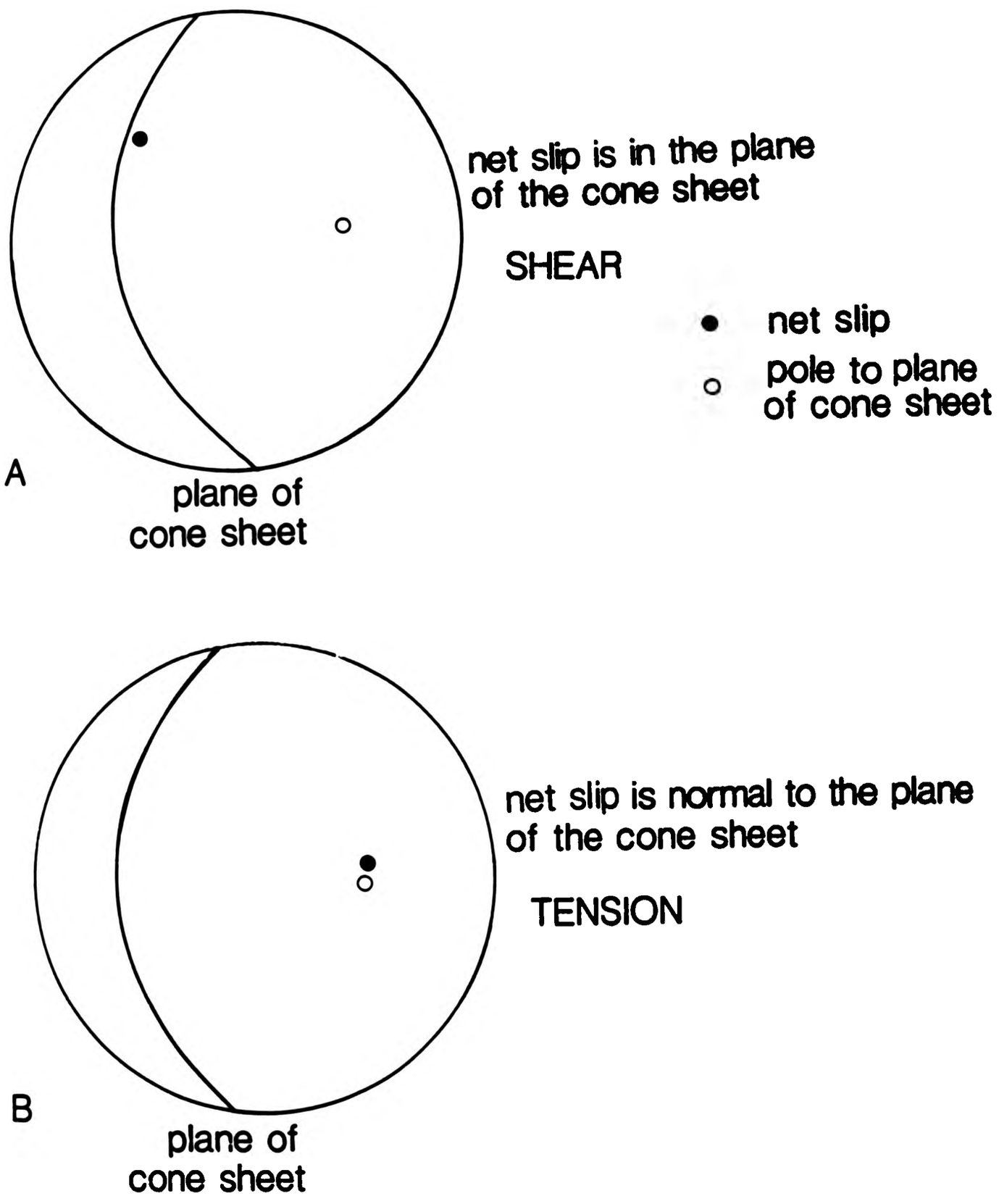

Fig.3.4.3 Stereographic projections of piercing point solutions for cone sheets opening in (A) shear and (B) tension

3.4.2 Calculation 2

Draw on a stereographic projection the great circles of each of the two pre-cone sheet planar structures and of the cone sheet itself. Then the pitch of the two pre-cone sheet planar structures (A and B of Fig.3.4.4a) on the cone sheet plane may be ascertained.

Using the pitch angles on the plan view draw off the angles of pitch in the direction of dip. Where the two planes E_1 and F_1 (Fig.3.4.4a) intersect is the trace of the piercing point H (Fig.3.4.4b) on the northern plane of the sheet. The intersection of lines E_2F_2 (Fig.3.4.4b) is the trace of the piercing point I on the southern plane of the sheet. By constructing a line joining points H and I and measuring the angle it makes with the cone sheet plane (Fig.3.4.4c)(on the plan view) the angle of pitch of the net slip (x)is measured. By plotting the pitch of the net slip on the stereographic projection the azimuth may be determined (Fig.3.4.4). Thus the angle, orientation and amount of net slip can be determined.

3.5 DETERMINATION OF CRUSTAL STRAIN

In this study, because of the degree of exposure, most of the data has been obtained from coastal sections and the inland regions have been neglected. However, I have attempted an analysis of the distribution of the inland cone sheets using copies of the 6 inch field slips of the I.G.S., as follows:-

i. Overlay a grid of regularly arranged points, in the style of hexagonal close packing, on a copy of the 6 inches to the

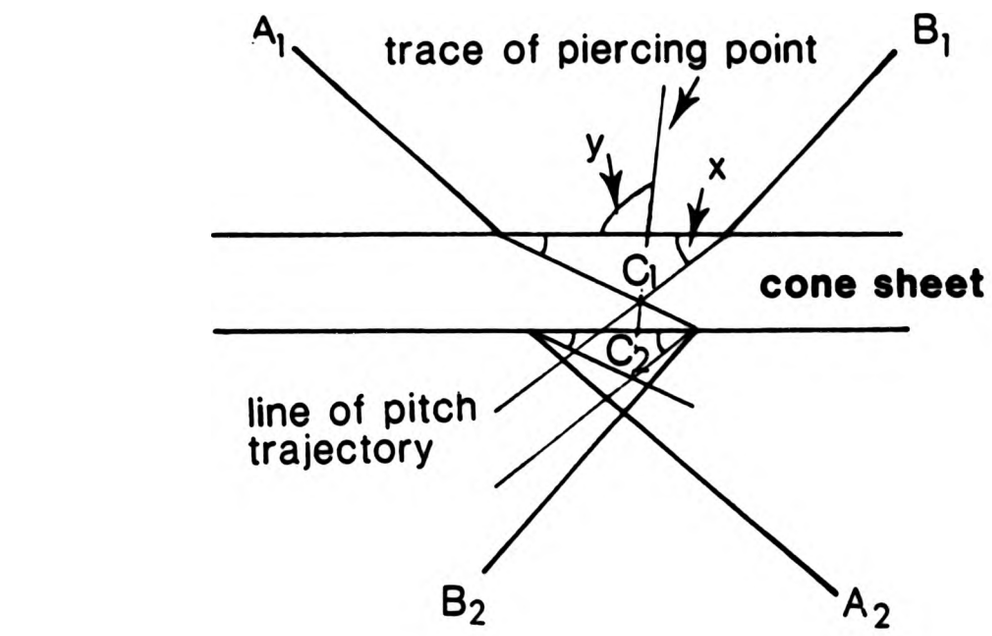

C intersection of pitch trajectories of pre - dating planes

x angle of pitch of the pre - dating planes

■ net slip piercing point

y angle of pitch of net slip

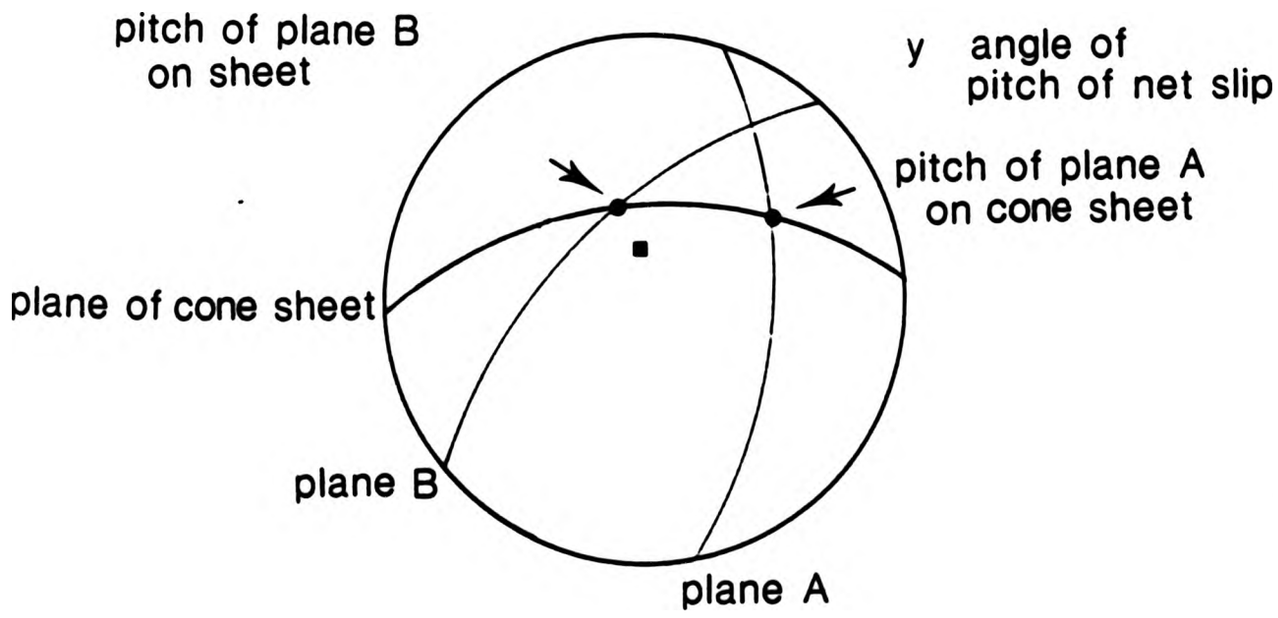

Fig. 3.4.4 Diagram to show the determination of a piercing point using angles of pitch of early planar structures

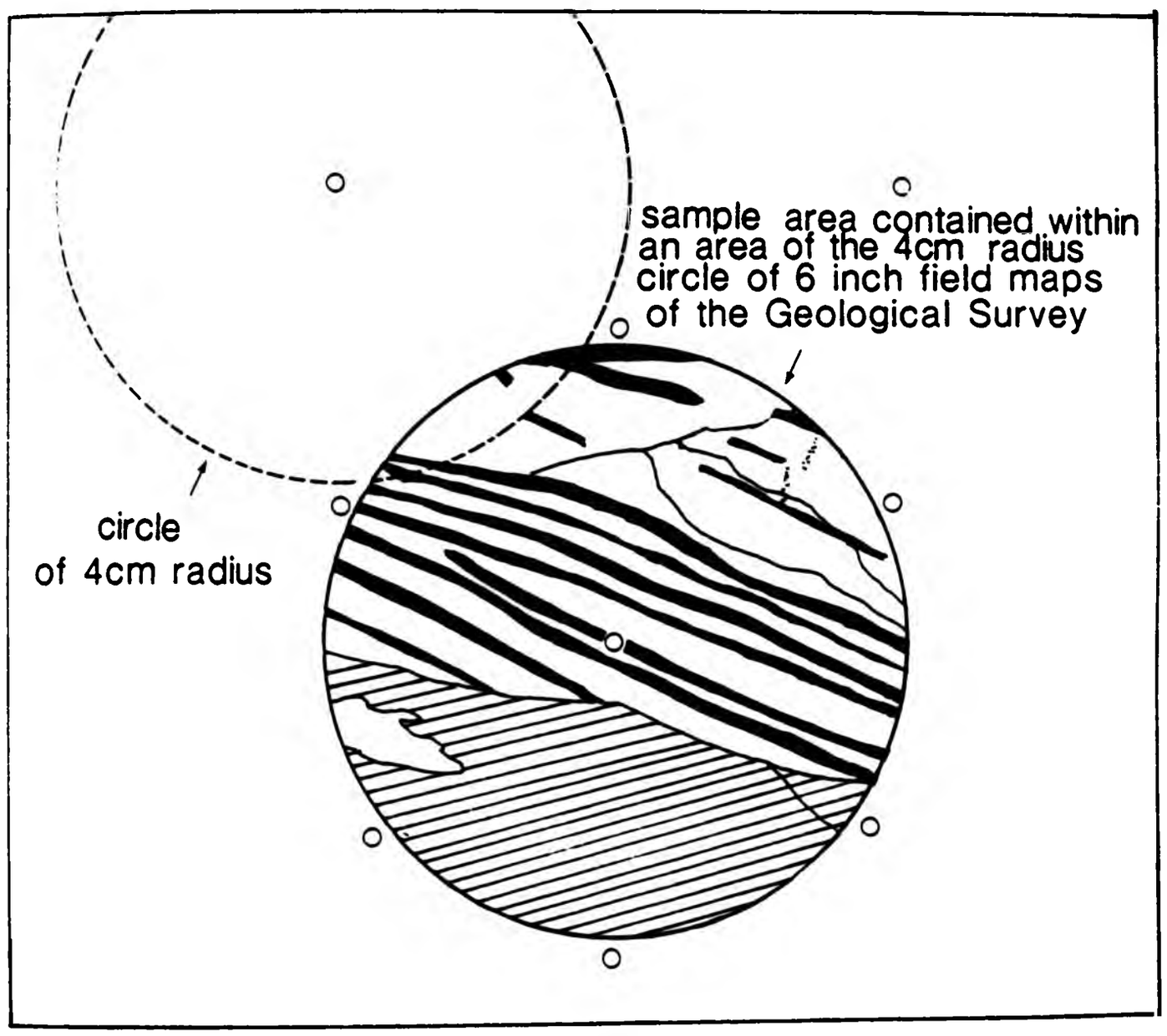

○ hexagonally arranged grid points

cone sheets
dykes
igneous host rocks pre-cone sheet emplacement
igneous host rocks post-cone sheet emplacement

Fig.3.5.1 Diagram to illustrate the measurement of strain caused by the emplacement of cone sheets throughout the Ardnamurchan peninsula, by using a series of hexagonally arranged sample areas superimposed on the 6 inch field of the Geological Survey

mile field maps of the Ardnamurchan peninsula (Fig.3.5.1). In view of the fact that the cone sheets have, in places, been drawn diagrammatically on the 6" maps, I have, for consistency, accepted that the depicted cone sheets represent actual exposures and, also, where cone sheets can be seen to continue on either side of drift patches that they are continuous.

ii. Place the centre of a 4cm radius circle upon each of these grid points.

iii. Determine a) the area within each circle that consists of country rock, and b) the area occupied by cone sheets within each circle.

iv. Measure the orientation of the widest sheet.

v.Calculate the area occupied by cone sheets as a percentage of each circle.

vi. Plot on a 1:50000 map of the Ardnamurchan peninsula the percentage area occupied by cone sheet intrusions for each of the 550 circles. This data, i.e. percentage dilation and orientation of the sheets, can then be contoured for the whole peninsula.

3.6 MEAN STRIKE OF CONE SHEETS:TUKEY CHI TEST

To determine the mean strike of cone sheets presents difficulties because of their circular, non-linear arrangement. Tukey (1957) suggested a modification of the Chi^2 test used by Harrison (1957) and Rusnak (1957). The Tukey Chi^2 test determines the mean orientation and gives the level of significance against isotropy. Table 3.2 illustrates the test as applied to the Centre One cone sheets.

a) Classify the strike of the cone sheets into classes of 20°,

this being termed the observed data = 0

b) Calculate an estimated distribution, that is if the cone sheets were distributed equally throughout the classes:-

$$\frac{\text{total number of sheets in sample}}{\text{number of classes}} = \frac{N}{K} = E$$

$$= \frac{134}{18} = 7.44$$

c)Calculate x, the statistical difference between the observed and expected frequency for each class:-

$$x = \frac{O - E}{E}$$

This would give the Chi^2 for each class if the distribution of the data was linear. However, as stated above, the Tukey Chi^2 analysis takes into account the angular nature of the distribution.

d)By multiplying x by cos θ and sin θ respectively, where θ is the minimum value of the class and summing the results, C and S are obtained.

Determine :- C the Cosine of the distribution

$$C = \frac{\sum x \ \cos\{\theta\}}{\sum x \cos^2 \theta}$$

S the Sine of the distribution

$$S = \frac{\sum x \sin \theta}{\sum x \sin^2 \theta}$$

e) To determine the level of significance of the pattern for two degrees of freedom = $C^2 + S^2$.

f) Determine tan θ = S/C the sign of which determines whether the tan θ value is added or subtracted from 0° or 180° (sign sin θ = sign S).

g) Tan θ is added to the mid point of the class interval (i.e. 10°)

h) The result is the mean orientation of the distribution (Fig.3.6.1).

Table 3.2 Determination of average orientation of Centre One cone sheets by Chi^2 analysis

Strike	θ	O	O-E	x	cos θ	sin θ
0 - 20	0	4	-3.4	-1.25	1.00	0.00
21 - 40	20	3	-4.4	-1.60	0.94	0.34
41 - 60	40	4	-3.4	-1.25	0.76	0.64
61 - 80	60	2	-5.4	-2.00	0.50	0.87
81 - 100	80	0	--	--	0.17	0.98
101 - 120	100	0	--	--	-0.17	0.98
121 - 140	120	4	-3.4	-1.25	-0.50	0.87
141 - 160	140	2	-5.4	-2.00	-0.76	0.64
161 - 180	160	1	-6.4	-2.40	-0.94	0.34
181 - 200	180	1	-6.4	-2.40	-1.00	0.00
201 - 220	200	3	-4.4	-1.60	-0.94	-0.34
221 - 240	220	2	-5.4	-2.00	-0.76	-0.64
241 - 260	240	5	-2.4	-0.90	-0.50	-0.87
261 - 280	260	6	-1.4	-0.50	-0.17	-0.98
281 - 300	280	18	10.6	3.90	0.17	-0.98
301 - 320	300	34	26.6	9.90	0.50	-0.87
321 - 340	320	30	22.6	8.40	0.76	-0.64
341 - 360	340	16	8.6	3.20	0.94	-0.34

where n = 134
E = 7.4
E = 2.7

$$\sum x \cos\theta = 20.661$$

$$\sum x \sin\theta = -22.069$$

$$C = \frac{\sum x \cos\theta}{\sum (\cos^2\theta)^{0.5}} = \frac{20.661}{2.994} = 6.9 \quad \text{therefore } C^2 = 47.6$$

$$S = \frac{\sum x \sin\theta}{\sum (\sin^2\theta^{0.5}} = \frac{-22.069}{2.994} = -7.37 \quad \text{therefore } S^2 = 54.3$$

$$S^2 + C^2 = 101.9$$

$$\tan\theta = \frac{S}{C} = -1.068$$

$\theta = -46.8^\circ$ if θ is +ve then it is added to 180/360
if θ is -ve then it is subtracted from 180/360

therefore the average orientation is :
$313.2 + 10^\circ = 323.2^\circ$

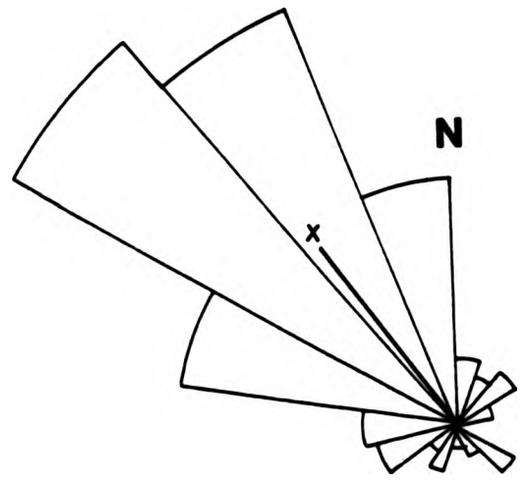

number of samples - 134

x mean orientation - 323° at the 99.5% confidence level

Fig. 3.6.1 A rose diagram showing the mean orientation, as determined by Chi^2 analysis, for the Centre One cone sheets (Table 3.1).

CHAPTER 4

FIELD CHARACTERISTICS AND PETROLOGY OF THE CONE SHEETS

4.1 INTRODUCTION

"The Ardnamurchan peninsula is probably the most spectacular region of the world for viewing concentric patterns of cone sheets" (Holland and Brown, 1972). This statement is particularly applicable as the central intrusive complex possesses four cone sheet sets, each being developed to a different degree. This study of the cone sheet sets has a bias towards their structural aspects. Given below are field characteristics of the cone sheets, along with some comments on the differences between each set.

Since the publication of the Ardnamurchan Memoir (Richey et al., 1930), little field based work has been carried out on the Ardnamurchan cone sheets. Kennen (1937) commented on the possibility that certain joint sets are unfilled cone sheet fractures. Durrance (1968) applied a mechanical analysis to the cone sheets and ring intrusions of Ardnamurchan. The work of both these authors is discussed in Chapter 1. Geochemically, the B.T.I.P. has been extensively studied (Thompson, 1982), although the cone sheets have for the most part been neglected. However, Holland and Brown (1972) analysed 98 specimens from the Ardnamurchan cone sheets and attempted to substantiate the four structural sets on geochemical grounds (Chapter 4.4).

4.2 FIELD CHARATERISTICS

4.2.1 Chilling

Almost all of the basic (basalt - dolerite) sheets possess chilled margins (Plate 4.1) which may either be tachylitic or fine-grained material grading into a coarser-grained rock towards the centre of the sheet (Fig.4.2.1). Tachylite margins are approximatly 0.5cm-1cm thick and are characterised by an immense number of closely spaced joints (Plate 4.1). Often the fine-grained chilled margin is the only discernable feature that enables the recognition of individual cone sheets within a mass of sheets.

4.2.2 Form of the contacts

Three main types of contact have been observed:-

a)Large scale (greater than 1m) planar surface controlled,

b)Small scale (less than 1m) joint controlled,

c)Cuspate,

d)Irregular.

a) Many of the cone sheet contacts are planar and parallel sided (Plate 4.2).

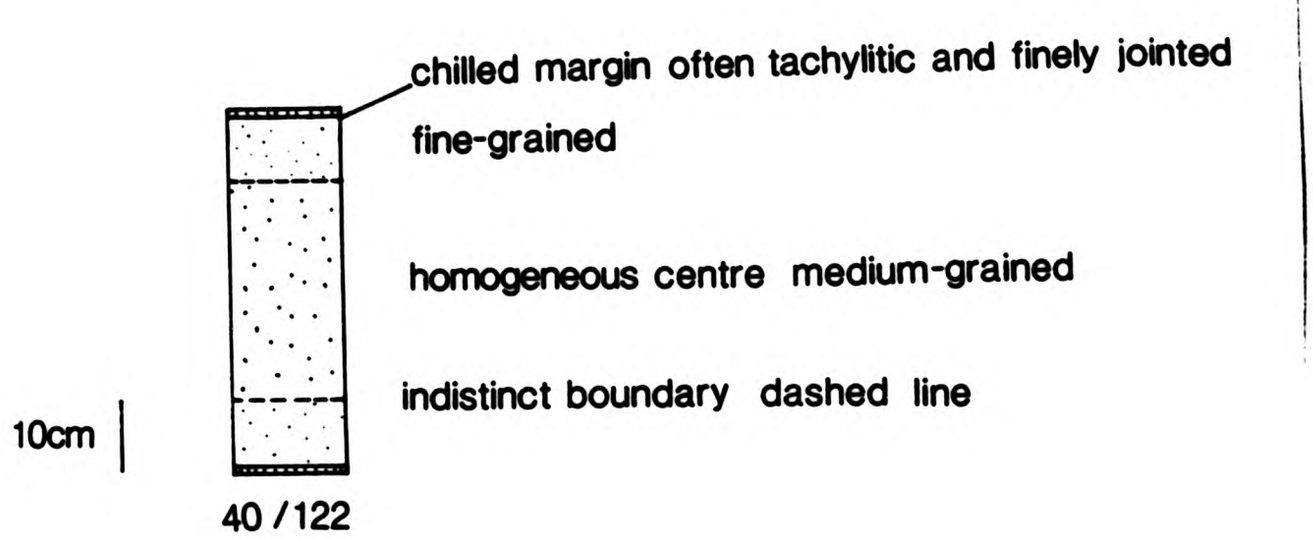

Fig.4.2.1 A cross section through a non-porphyritic cone sheet showing the increase of grain size from the margins to the centre of the basic sheet
Centre One, east of Ardtoe

Plate 4.1 A thin, fine-grained cone sheet with tachylitic margins and closely spaced joints intruded into Hypersthene Gabbro host rock. Inner Centre Two, Lighthouse.

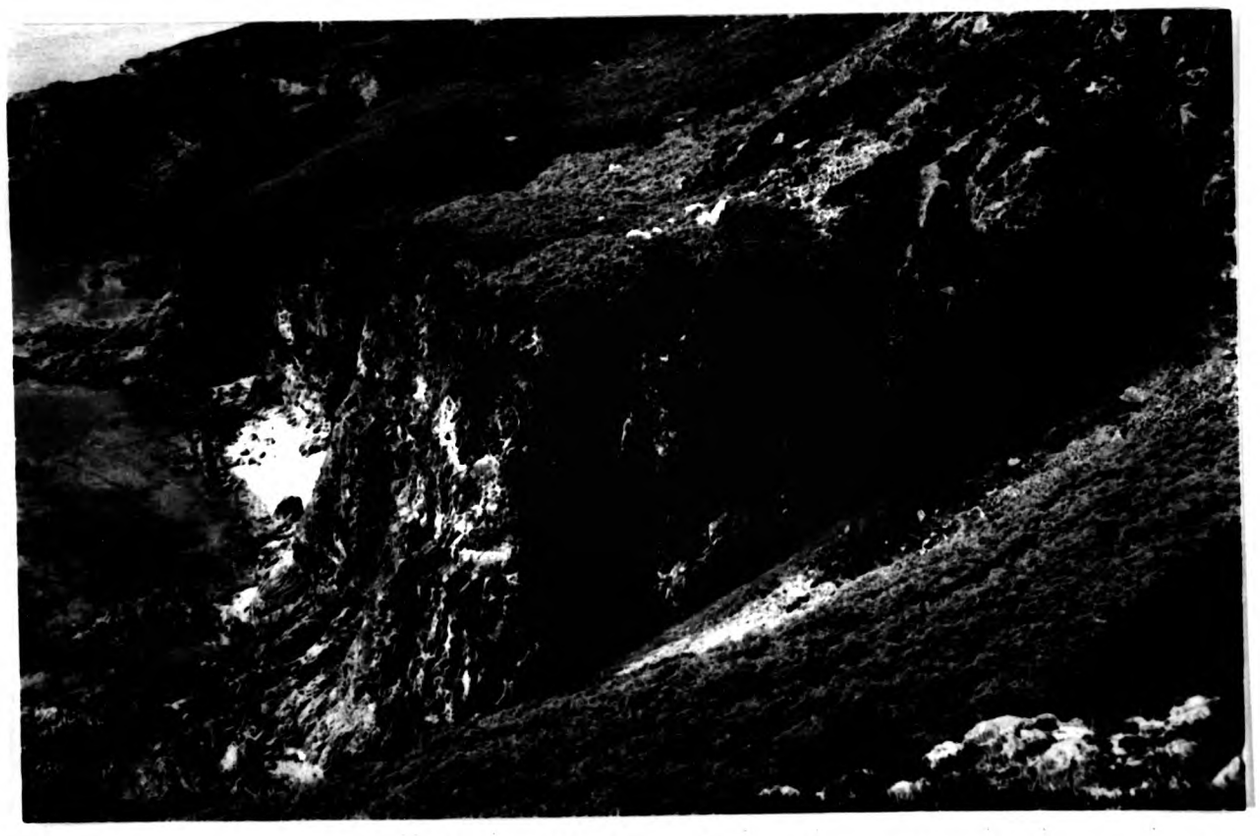

Plate 4.2 Several parallel sided cone sheets emplaced in Jurassic limestones in a vertical cliff at Sron Bheag, Outer Centre Two.

Plate 4.1 A thin, fine-grained cone sheet with tachylitic margins and closely spaced joints intruded into Hypersthene Gabbro host rock. Inner Centre Two, Lighthouse.

Plate 4.2 Several parallel sided cone sheets emplaced in Jurassic limestones in a vertical cliff at Sron Bheag, Outer Centre Two.

Plate 4.1 A thin, fine-grained cone sheet with tachylitic margins and closely spaced joints intruded into Hypersthene Gabbro host rock. Inner Centre Two, Lighthouse.

Plate 4.2 Several parallel sided cone sheets emplaced in Jurassic limestones in a vertical cliff at Sron Bheag, Outer Centre Two.

b) Control of cone sheet contacts on a small scale by pre-existing joints in the host rocks are well demonstrated (Plates 4.3-4.5). The extent to which the joints influence the form of the contact varies. Plate 4.3 shows a zigzag form resulting from joint control whereas Plate 4.4 demonstrates slip along a joint plane. Plate 4.5 shows an irregularity in the margin of a cone sheet intruded into Moine host rock. A large number of small joints exploited by a sheet results in an irregular contact (Plate 4.6).

c) In cross section some cone sheets show cuspate shaped margins (Plate 4.7). In Chapter 7 it is shown that this is possibly the remnants of fingers of magma which have coalesced to form a continuous sheet.

d) Plate 4.6 shows an irregular margin of a sheet, varying from sinusoidal to angular resulting in the cone sheet having variable thickness.

4.2.3 Apophyses

Thin branches or offshoots from the main body of a cone sheet are termed apophyses. Two types of apophyses have been identified:-

a)Single apophysis, on one margin (Plate 4.8),

b)Paired apophyses, one on either margin (Plate 4.9).

Plate 4.3 Cone sheet controlled by joints resulting in a zigzag form intruded into Hypersthene Gabbro. Inner Centre Two, Lighthouse.

Plate 4.4 A conjugate joint set developed in Jurassic rocks which has been utillized by a cone sheet, giving a stepped profile in cross section. Outer Centre Two, east of Mingary Pier.

Plate 4.3 Cone sheet controlled by joints resulting in a zigzag form intruded into Hypersthene Gabbro. Inner Centre Two, Lighthouse.

Plate 4.4 A conjugate joint set developed in Jurassic rocks which has been utillized by a cone sheet, giving a stepped profile in cross section. Outer Centre Two, east of Mingary Pier.

Plate 4.3 Cone sheet controlled by joints resulting in a zigzag form intruded into Hypersthene Gabbro. Inner Centre Two, Lighthouse.

Plate 4.4 A conjugate joint set developed in Jurassic rocks which has been utillized by a cone sheet, giving a stepped profile in cross section. Outer Centre Two, east of Mingary Pier.

Plate 4.5 Stepped, lower contact of an Outer Centre Two cone sheet, controlled by pre-existing joints, Mingary Pier.

Plate 4.6 A sinusoidal to irregular, upper contact of a cone sheet controlled by pre-existing joints, emplaced in Quartz Gabbro host rock, Centre Three, Abhain Chro' Beinn.

Plate 4.5 Stepped, lower contact of an Outer Centre Two cone sheet, controlled by pre-existing joints, Mingary Pier.

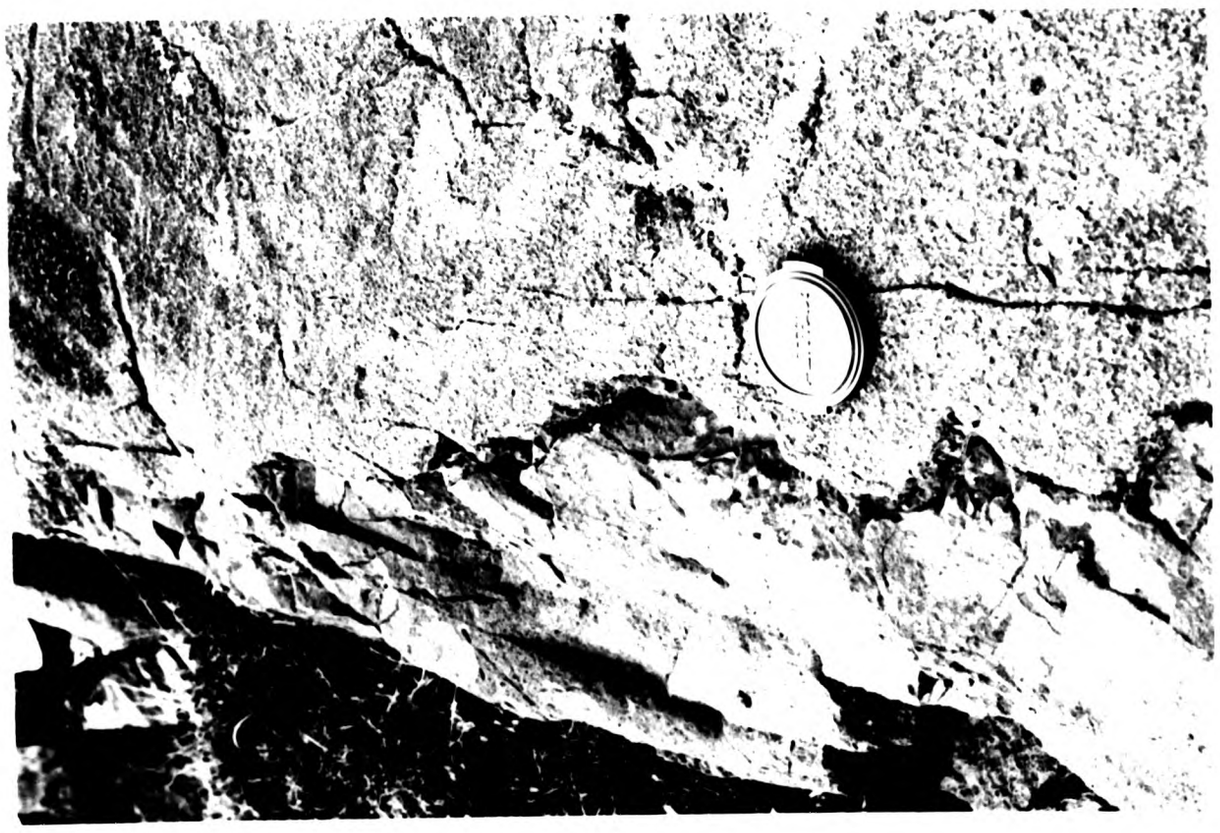

Plate 4.6 A sinusoidal to irregular, upper contact of a cone sheet controlled by pre-existing joints, emplaced in Quartz Gabbro host rock, Centre Three, Abhain Chro' Beinn.

Plate 4.5 Stepped, lower contact of an Outer Centre Two cone sheet, controlled by pre-existing joints, Mingary Pier.

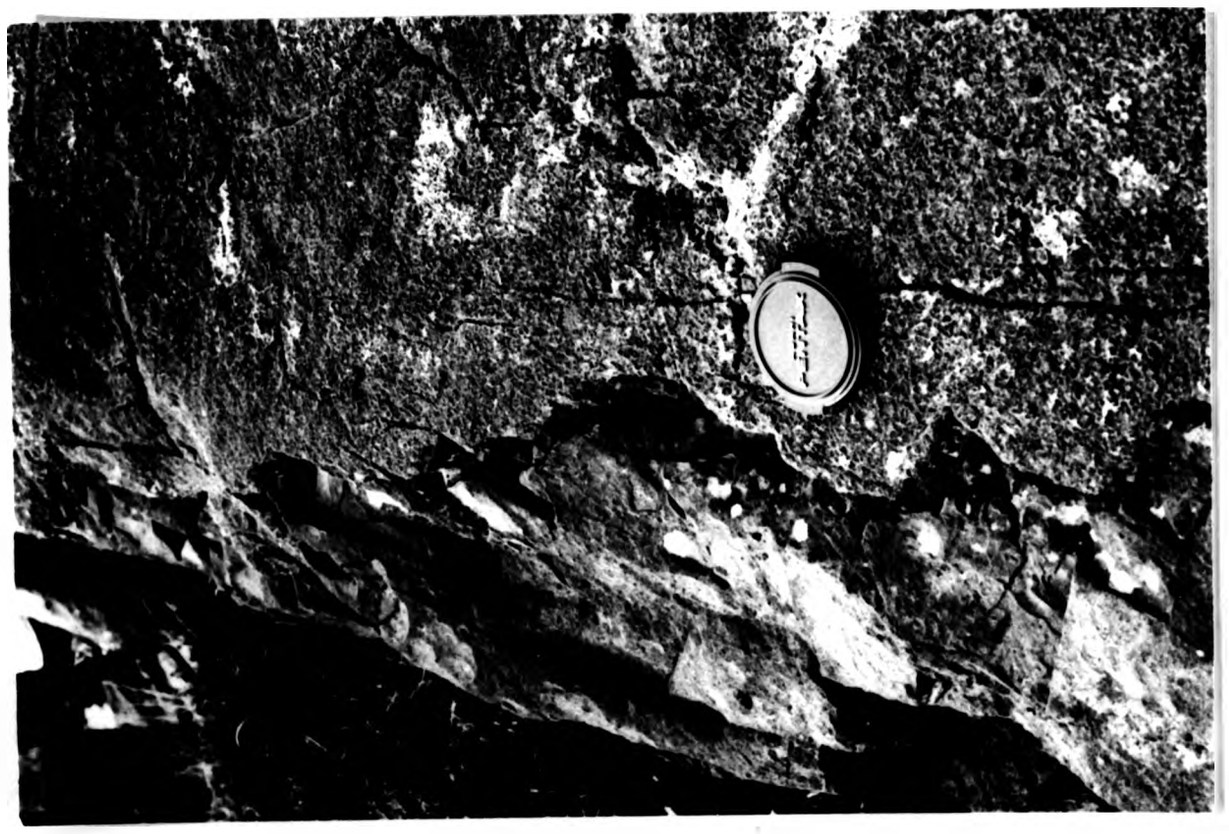

Plate 4.6 A sinusoidal to irregular, upper contact of a cone sheet controlled by pre-existing joints, emplaced in Quartz Gabbro host rock, Centre Three, Abhain Chro' Beinn.

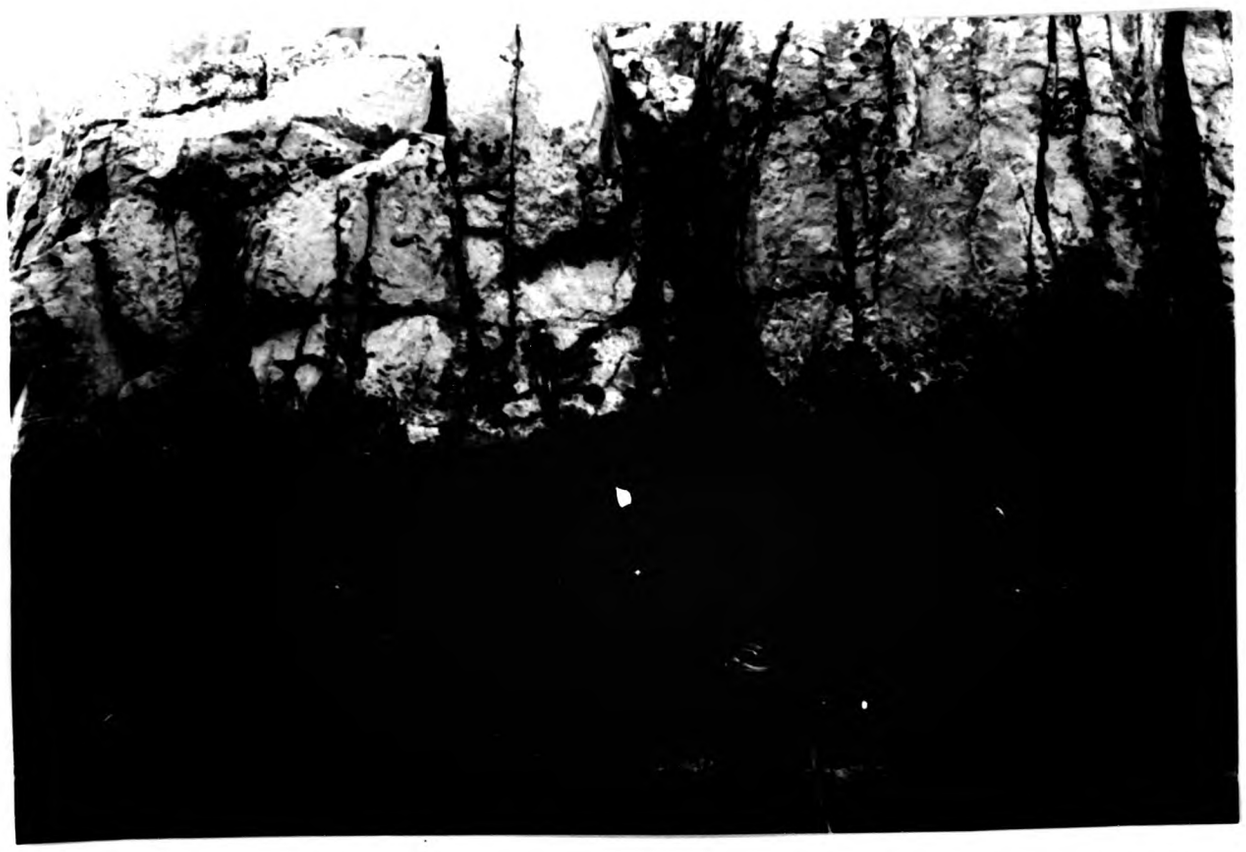

Plate 4.7 Cuspate lower margin of a cone sheet, marking a remnant of a magma finger, intruded into Lias host rock. Centre One, Swordle Bay.

Plate 4.8 Apophysis on the lower margin of a cone sheet intruded in Lias host rock. Centre One, Ockle Point.

Plate 4.7 Cuspate lower margin of a cone sheet, marking a remnant of a magma finger, intruded into Lias host rock. Centre One, Swordle Bay.

Plate 4.8 Apophysis on the lower margin of a cone sheet intruded in Lias host rock. Centre One, Ockle Point.

Plate 4.7 Cuspate lower margin of a cone sheet, marking a remnant of a magma finger, intruded into Lias host rock. Centre One, Swordle Bay.

Plate 4.8 Apophysis on the lower margin of a cone sheet intruded in Lias host rock. Centre One, Ockle Point.

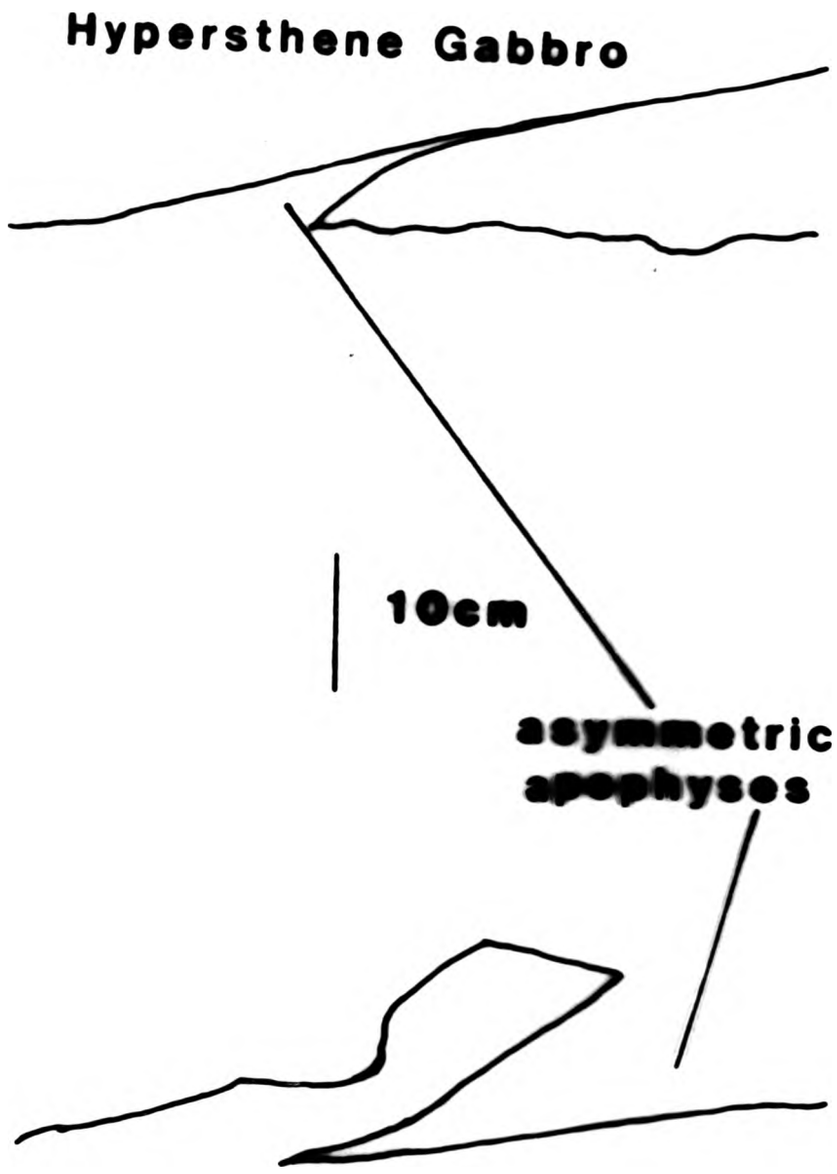
Hypersthene Gabbro
10cm
asymmetric
apophyses

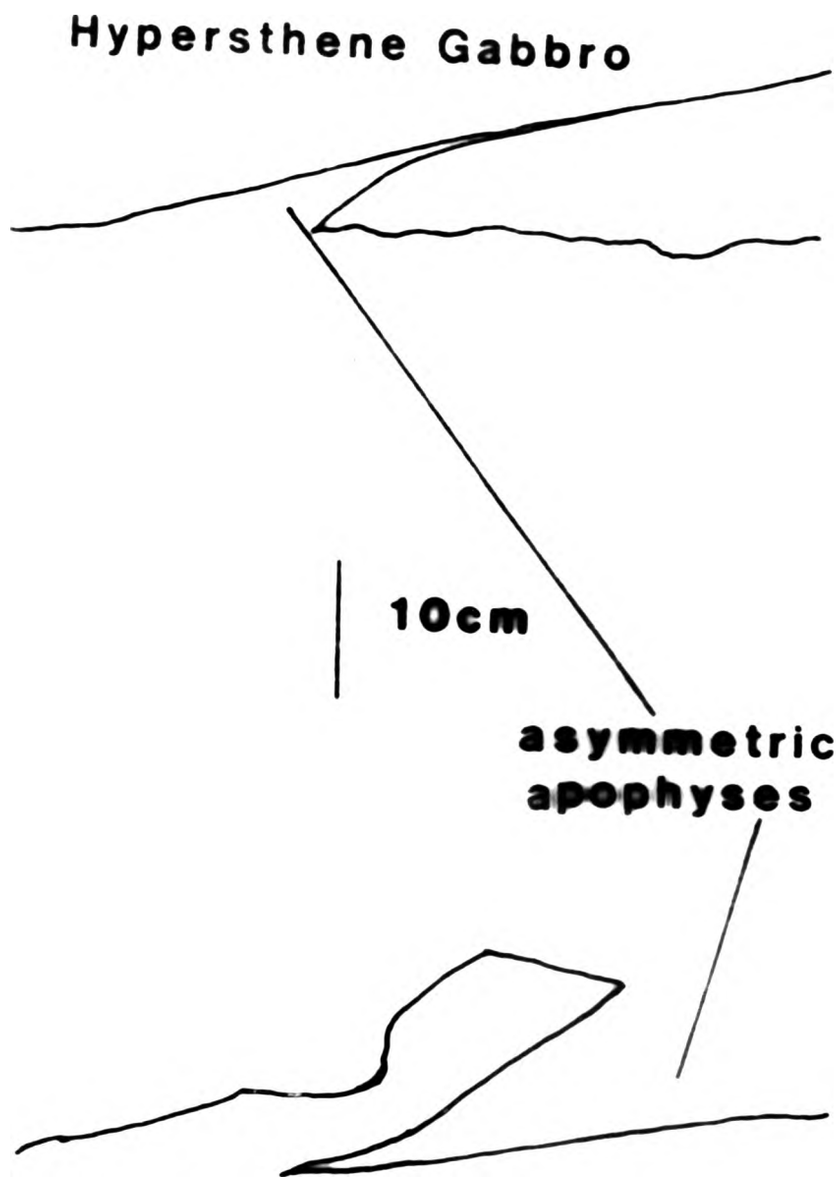
Hypersthene Gabbro
10cm
asymmetric
apophyses

Plate 4.9 Apophyses on both the upper and lower margins, which are dextral and sinistral respectively, intruded into Hypersthene Gabbro, Inner Centre Two, Lighthouse.

Plate 4.9 Apophyses on both the upper and lower margins, which are dextral and sinistral respectively, intruded into Hypersthene Gabbro, Inner Centre Two, Lighthouse.

Plate 4.9 Apophyses on both the upper and lower margins, which are dextral and sinistral respectively, intruded into Hypersthene Gabbro, Inner Centre Two, Lighthouse.

Plate 4.9 Apophyses on both the upper and lower margins, which are dextral and sinistral respectively, intruded into Hypersthene Gabbro, Inner Centre Two, Lighthouse.

Plate 4.9 Apophyses on both the upper and lower margins, which are dextral and sinistral respectively, intruded into Hypersthene Gabbro, Inner Centre Two, Lighthouse.

Plate 4.9 Apophyses on both the upper and lower margins, which are dextral and sinistral respectively, intruded into Hypersthene Gabbro, Inner Centre Two, Lighthouse.

a)This first grouping may be subdivided according to either:-

i.The apophysis exploits a previous structure.

ii.The apophysis occurs where the main body of the sheet changed orientation.

i. Exploitation of pre-existing structures, for example, joint planes, by apophyses. The sheet depicted in Fig.4.2.2 shows a combination of both i. and ii. type apophyses.

ii. Plate 4.10 illustrates a sheet displaying a geniculation from which a number of narrow (1cm thick) apophyses emanate. Fig.4.2.3 shows a sheet with a number of side steps, at each of the side steps an apophysis maintains the orientaiton of the sheet before the side step.

b) Plates 4.9 and 4.11 illustrate paired apophyses, one occurring on each cone sheet margin and pointing in opposite directions to each other. This phenomenon is probably due, in part, to the same torsion forces which have produced the en echelon cone sheet fractures observed at a number of locations (Chapter 7).

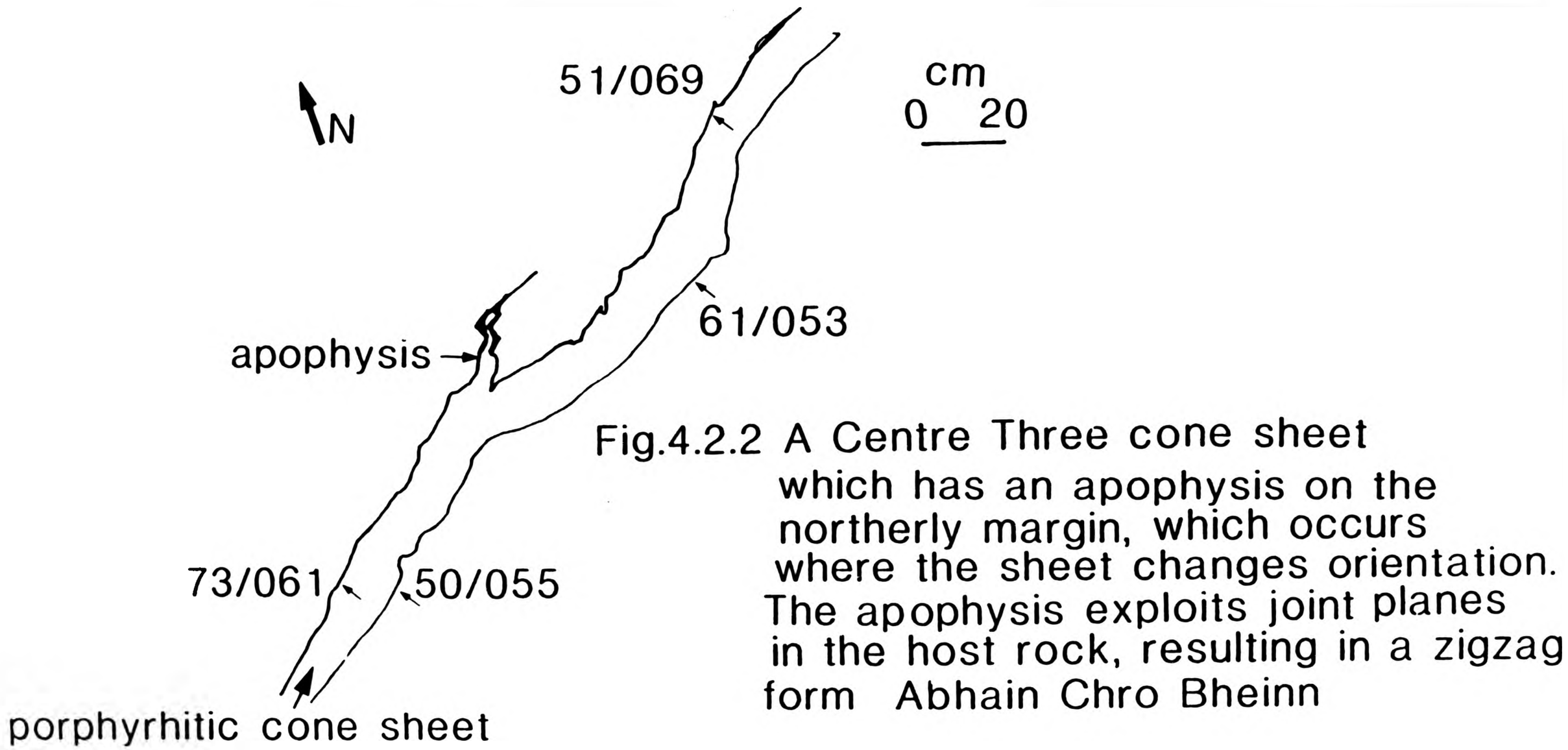

Fig.4.2.2 A Centre Three cone sheet which has an apophysis on the northerly margin, which occurs where the sheet changes orientation. The apophysis exploits joint planes in the host rock, resulting in a zigzag form Abhain Chro Bheinn

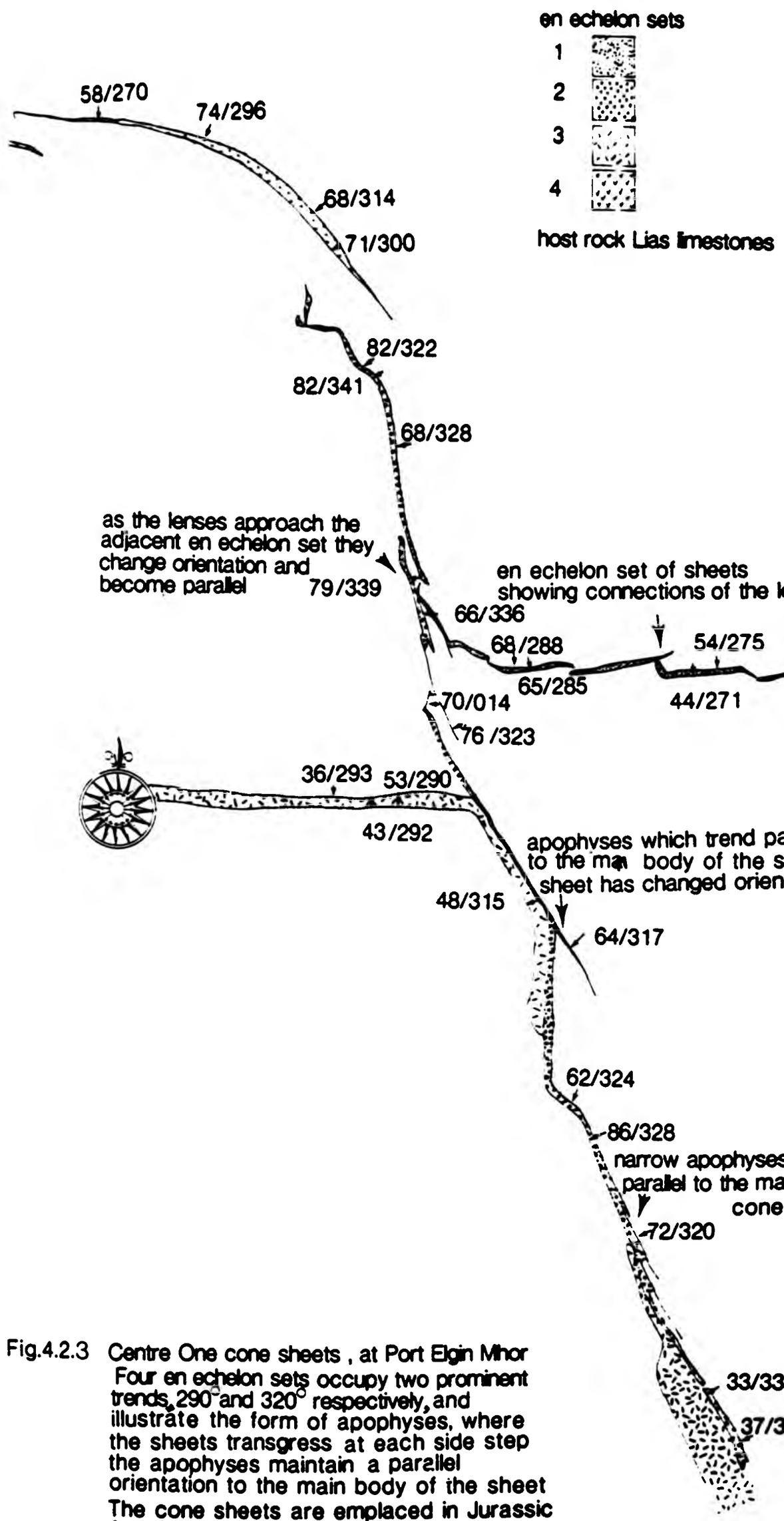

Fig.4.2.3 Centre One cone sheets , at Port Elgin Mhor
Four en echelon sets occupy two prominent trends, 290° and 320° respectively, and illustrate the form of apophyses, where the sheets transgress at each side step the apophyses maintain a parallel orientation to the main body of the sheet
The cone sheets are emplaced in Jurassic (Lias) limestones

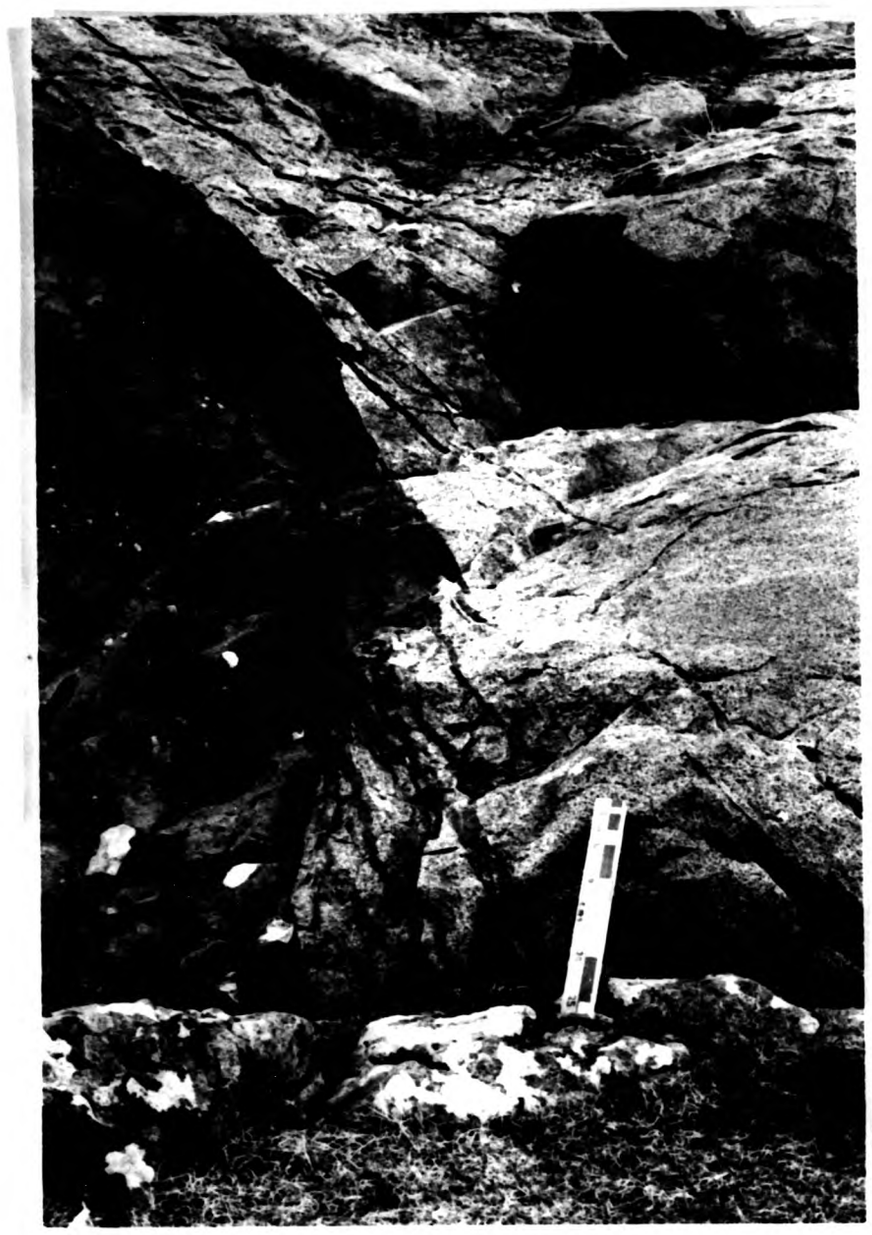

Plate 4.10 A number of thin apophyses emanate from the geniculation of a cone sheet intruded into the Hypersthene Gabbro. Inner Centre Two, Lighthouse.

Plate 4.10 A number of thin apophyses emanate from the geniculation of a cone sheet intruded into the Hypersthene Gabbro. Inner Centre Two, Lighthouse.

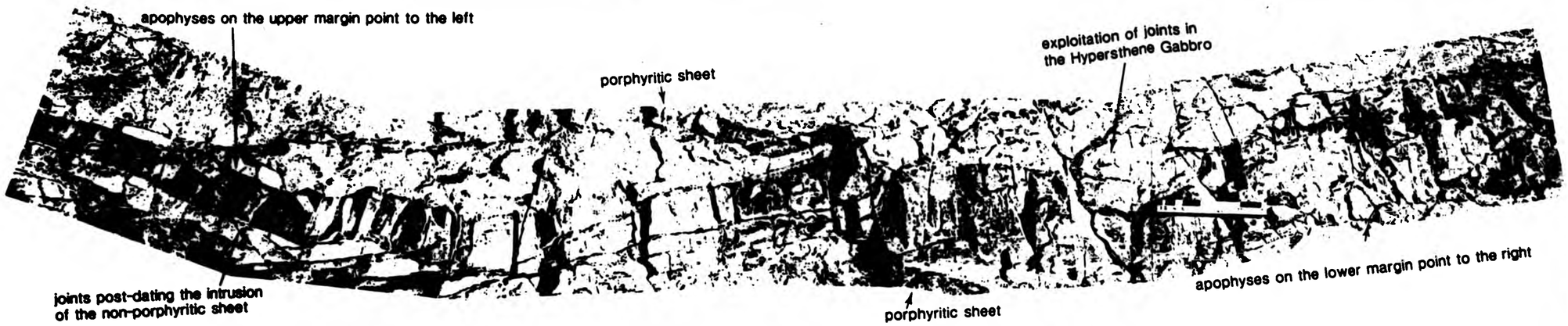

Plate 4 11 Illustrating the relationships between the joint planes and the margins of a cone sheet Inner Centre Two, Lighthouse section

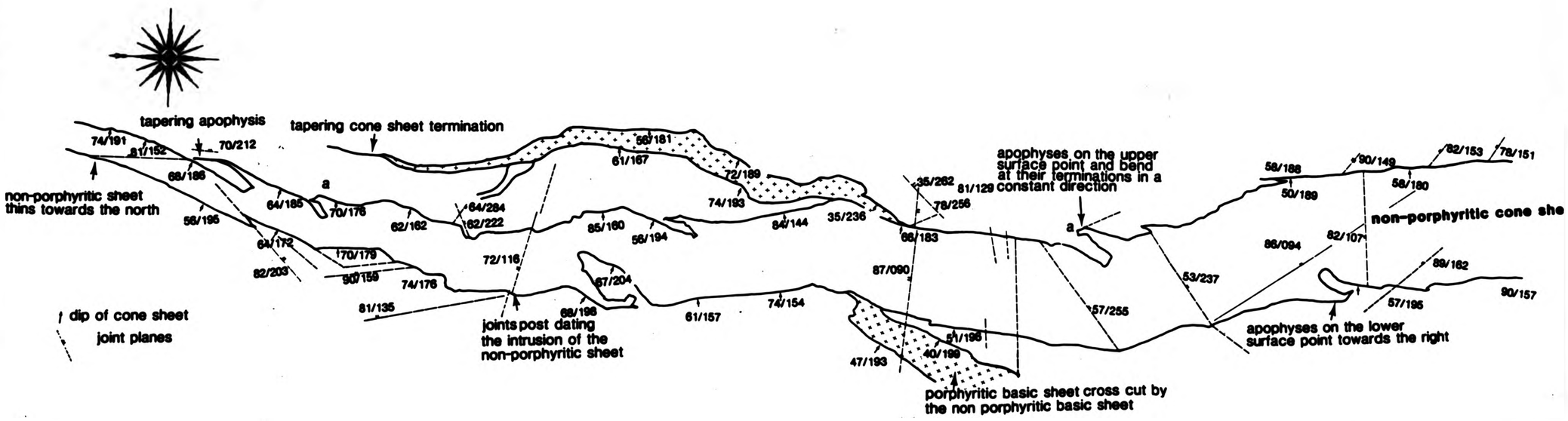

A tracing of the non-porphyritic sheet of Plate which shows tapering apophyses, paired apophyses the exploitation of pre-exitsting joints, thinning of individual cone sheets and their tapering terminations. Inner Centre Two, Lighthouse section

4.2.4 Xenoliths

Xenoliths are rarely found in the cone sheets, the majority of examples are cognate, with relatively few accidental xenoliths. Plate 4.12 shows cognate xenoliths of anorthosite in a Centre One composite intrusion which occurs at Ockle Point (549717). In this large, 20m thick, sheet all xenoliths are contained in the lower basic margin and range in size from 3.20m x 1.20m to 1cm x 1cm. Plates 4.13 and 4.14 show the top and bottom of a cone sheet which is exposed at Sron Bheag, with cognate anorthosite fragments occurring in two seperate layers which are located approximately 30cm from either margin. In this case, the largest fragments, up to 30cm in diameter, occur in the layer near to the upper margin. All xenoliths are irregular in shape.

Anorthosite xenoliths occur in the cone sheets of Centre One and Outer Centre Two Sets. In a thin section it is observed that an anorthosite xenolith, occuring within an Centre One cone sheet, consists of 70% plagioclase (An_{64}) and 10% serpentonized olivines (Plate 4.15) set in a fine-grained matrix consisting of 7.5% plagioclase, 7.5% pyroxenes and 5% opaques.

West of Mingary Pier is a cone sheet intruded into Lower Lias

Plate 4.12 Cognate xenoliths of anorthosite contained above the base of a composite cone sheet. Centre One, Ockle Point.

Plate 4.12 Cognate xenoliths of anorthosite contained above the base of a composite cone sheet. Centre One, Ockle Point.

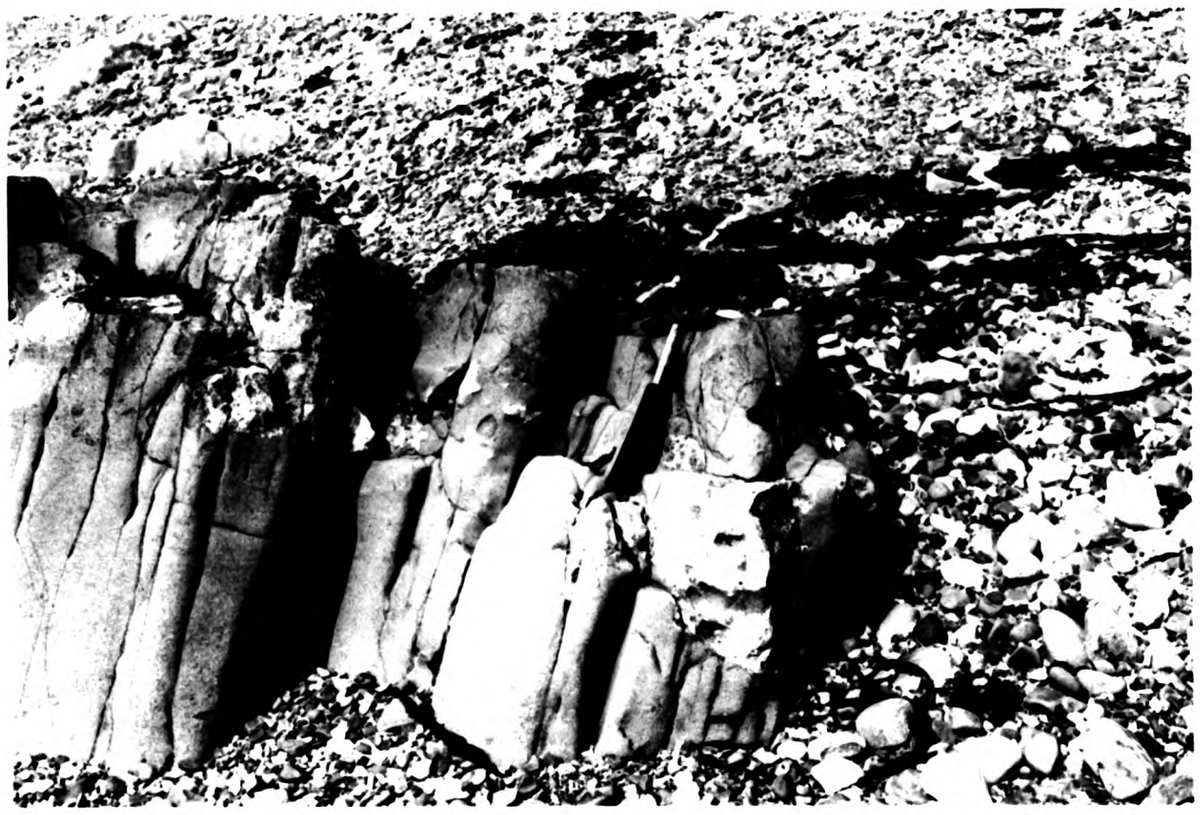

Plate 4.13 Upper margin of a cone sheet, containing numerous anorthosite xenoliths. Outer Centre Two, Sron Bheag.

Plate 4.14 Lower margin of the cone sheet in 4.13 showing an horizon of anorthosite xenoliths. Outer Centre Two, Sron Bheag.

Plate 4.13 Upper margin of a cone sheet, containing numerous anorthosite xenoliths. Outer Centre Two, Sron Bheag.

Plate 4.14 Lower margin of the cone sheet in 4.13 showing an horizon of anorthosite xenoliths. Outer Centre Two, Sron Bheag.

Plate 4.15 Photomicrograph, of an anorthosite xenolith serpentenized olivine and plagioclase (An_{64}) Xenolith occurs in a Centre One basic cone sheet, Ockle Point

Plate 4.16 Xenolith of Moine psammite contained within a fine-grained cone sheet. The cone sheet thickens around the xenolith. Outer Centre Two, west of Mingary Pier.

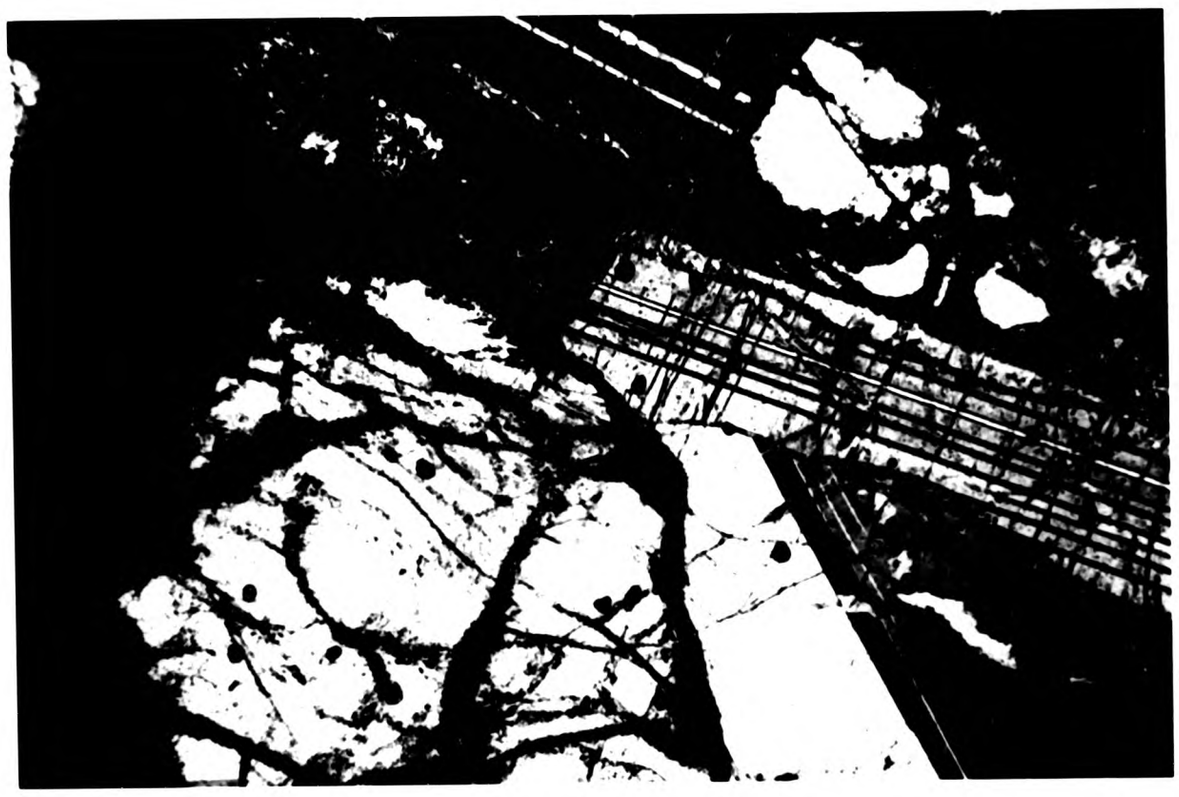

Plate 4.15 Photomicrograph, of an anorthosite xenolith serpentenized olivine and plagioclase (An_{64}) Xenolith occurs in a Centre One basic cone sheet, Ockle Point

Plate 4.16 Xenolith of Moine psammite contained within a fine-grained cone sheet. The cone sheet thickens around the xenolith. Outer Centre Two, west of Mingary Pier.

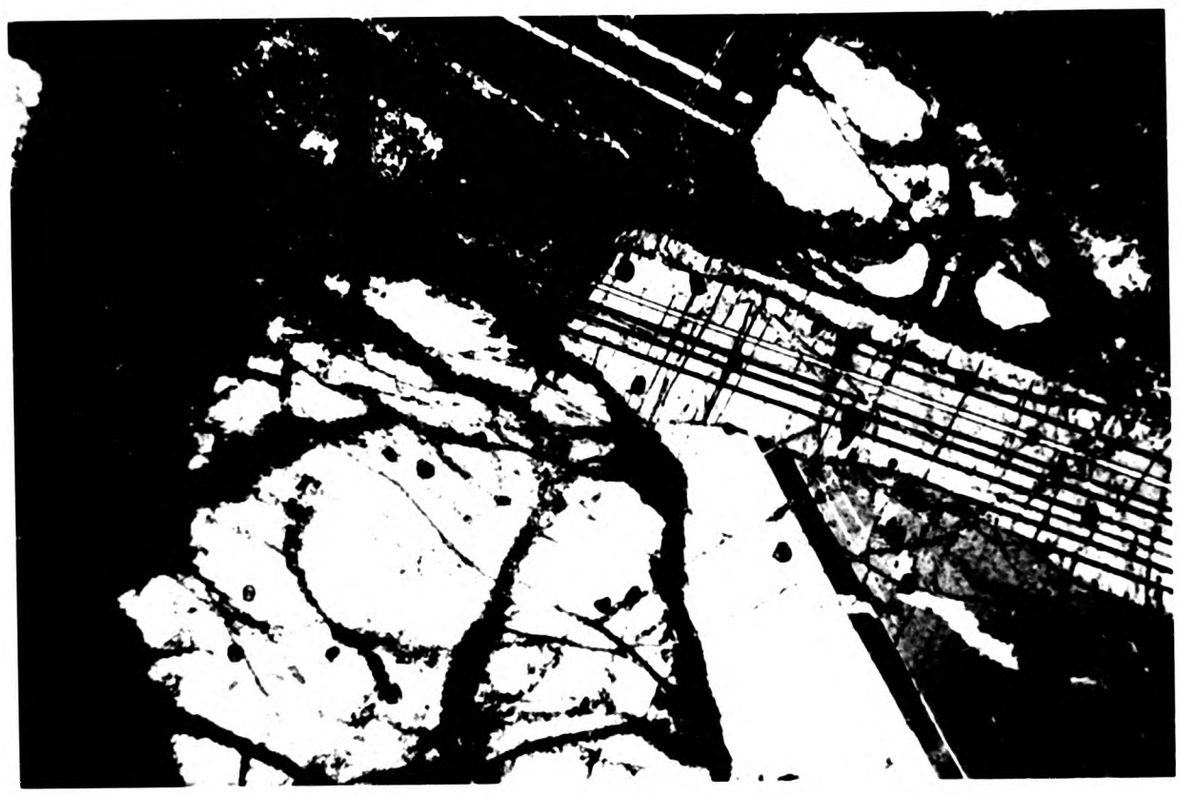

Plate 4.15 Photomicrograph, of an anorthosite xenolith serpentenized olivine and plagioclase (An_{64}) Xenolith occurs in a Centre One basic cone sheet, Ockle Point

Plate 4.16 Xenolith of Moine psammite contained within a fine-grained cone sheet. The cone sheet thickens around the xenolith. Outer Centre Two, west of Mingary Pier.

which contains a xenolith of Moine psammite (120cm x 34cm) (Plate 4.16). It can been seen that the sheet thickens around the xenolith (Plate 4.16). Thickening around large xenoliths is not common, two examples are shown in Fig.4.2.4.

Plate 4.17 shows a xenolith of Hypersthene Gabbro frozen in the process of being wedged from the host rock. Few examples of wedging have been identified in the four cone sheet sets.

The fact that few xenoliths of host rock occur together with the paucity of wedging occurrences indicates that stoping and wedging contribute little to the production of space for the emplacement of cone sheets.

4.2.5 Banding

The term banding will be used as defined by Irvine (1982) to describe planar structures in igneous rocks. Few examples of banded structures are seen in the cone sheet rocks. The best examples of banding occur in the feldspar porphyritic sheets of the Inner Set of Centre Two and the Centre Three cone sheets.

An example of banding from a Centre One cone sheet (Plate 4.18)

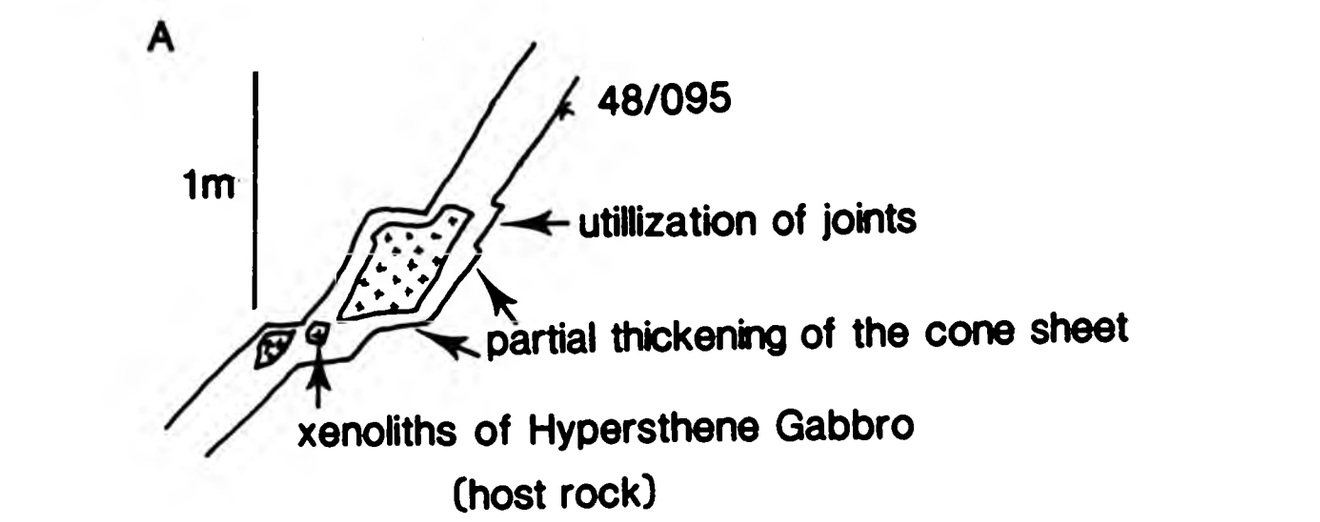

Fig.4.2.4 Two examples of basic cone sheets, containing large xenoliths of country rock. The cone sheets have increased thicknesses where xenoliths occur.

Plate 4.17 Xenolith of Hypersthene Gabbro being wedged off at the margin of a cone sheet. Inner Centre Two, Lighthouse.

Plate 4.18 Banding marked by plagioclase crystals at the margin of a thin, fine-grained cone sheet. Centre One, Swordle Bay.

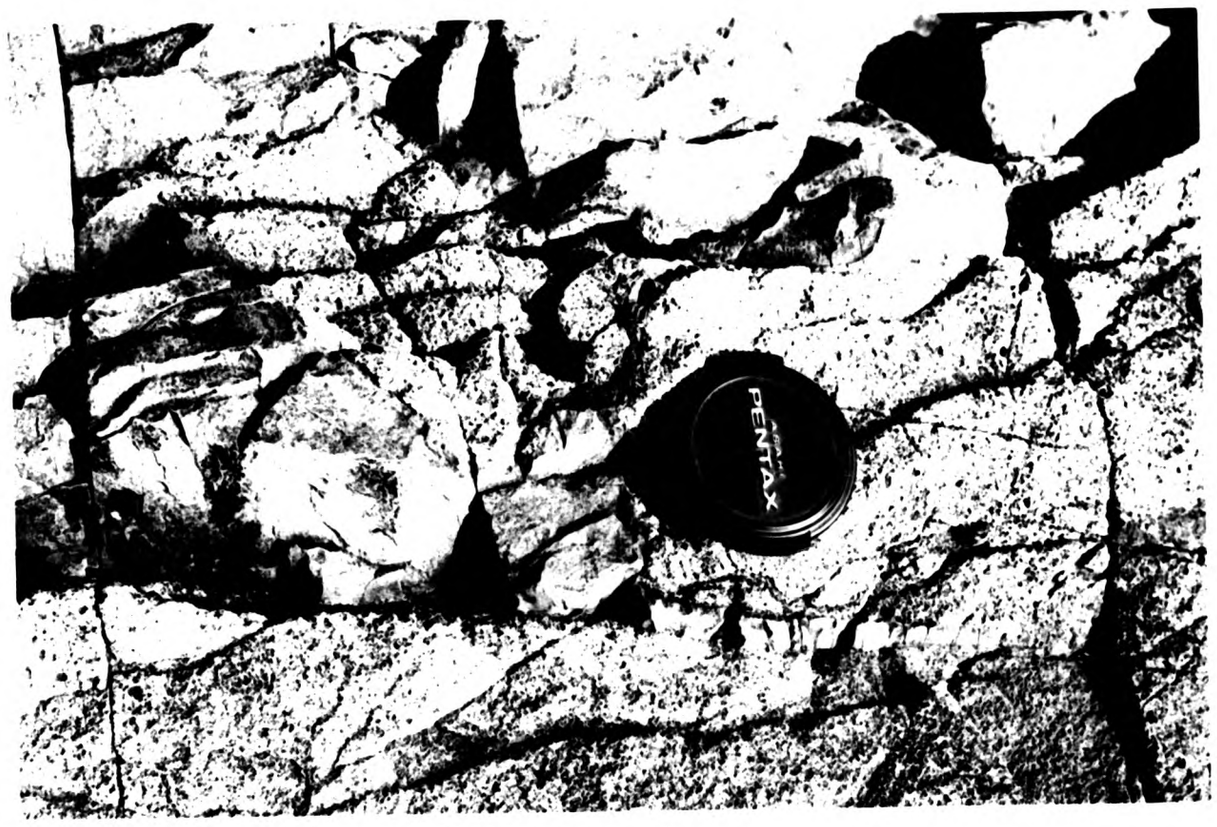

Plate 4.17 Xenolith of Hypersthene Gabbro being wedged off at the margin of a cone sheet. Inner Centre Two, Lighthouse.

Plate 4.18 Banding marked by plagioclase crystals at the margin of a thin, fine-grained cone sheet. Centre One, Swordle Bay.

shows, 1cm above the lower margin, a thin band of plagioclase crystals and above this a second band with sparse phenocrysts in a fine-grained matrix.

One example of asymmetric banding where amygdales of varying size and intensity form 15 bands within the sheet is depicted in Fig.4.2.5. A diagramatic cross section through a banded cone sheet (Fig.4.2.6) shows three, possibly four, bands which exhibit grading, that is the larger amygdales occur towards the base of the band whilst the smaller ones occur towards the top of the band. Bands four and five have a more uniform grain size, with the former coarser grained than the latter.

The most common form of banding is symmetrical about a central axis parallel to the margin of the cone sheet (Fig.4.2.7). From the margin the sequence of bands is; a fine-grained chilled layer (5mm-1cm thick), 13cm of fine-grained basic rock with sparse feldspar phenocrysts, 60cm of coarser-grained material containing 30% feldspar phenocrysts, with the central 50cm being coarse-grained and containing up to 50% feldspar phenocrysts. Symmetrical banding is thought to be the result of flow differentiation, although flow differentiation can produce an asymmetrical distribution of bands. As magma is emplaced within an intrusion crystallization begins at the margins, whilst the majority of the magma and any phenocrysts it contains flow along

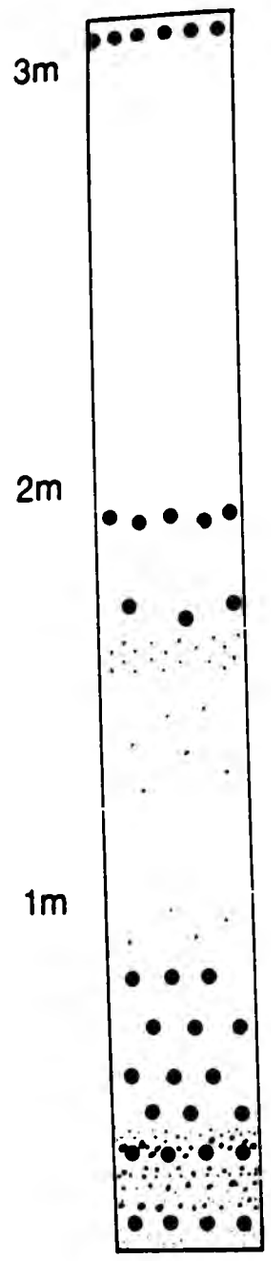

size of amygdales

small less than 2mm

medium 2mm to 5mm

large 5mm up to 2cm

graded bands

no amygdales

Fig4.2.5 Section across a cone sheet which demonstrates banding, the bands are marked by different sized amygdales Outer Centre Two west of Mingary Pier

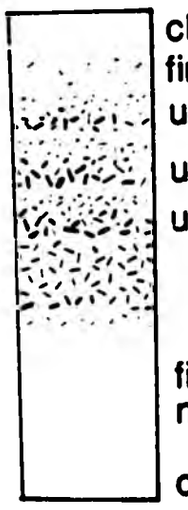

Larger phenocrysts at the base wiith smaller phenocrysts towards the top of the band

Fig.4.2.6 A section across a cone sheet showing asymmetric banding which is defined by various sizes and concentrations of plagioclase feldspar phenocrysts Outer Centre Two Mingary Pier

10 cm

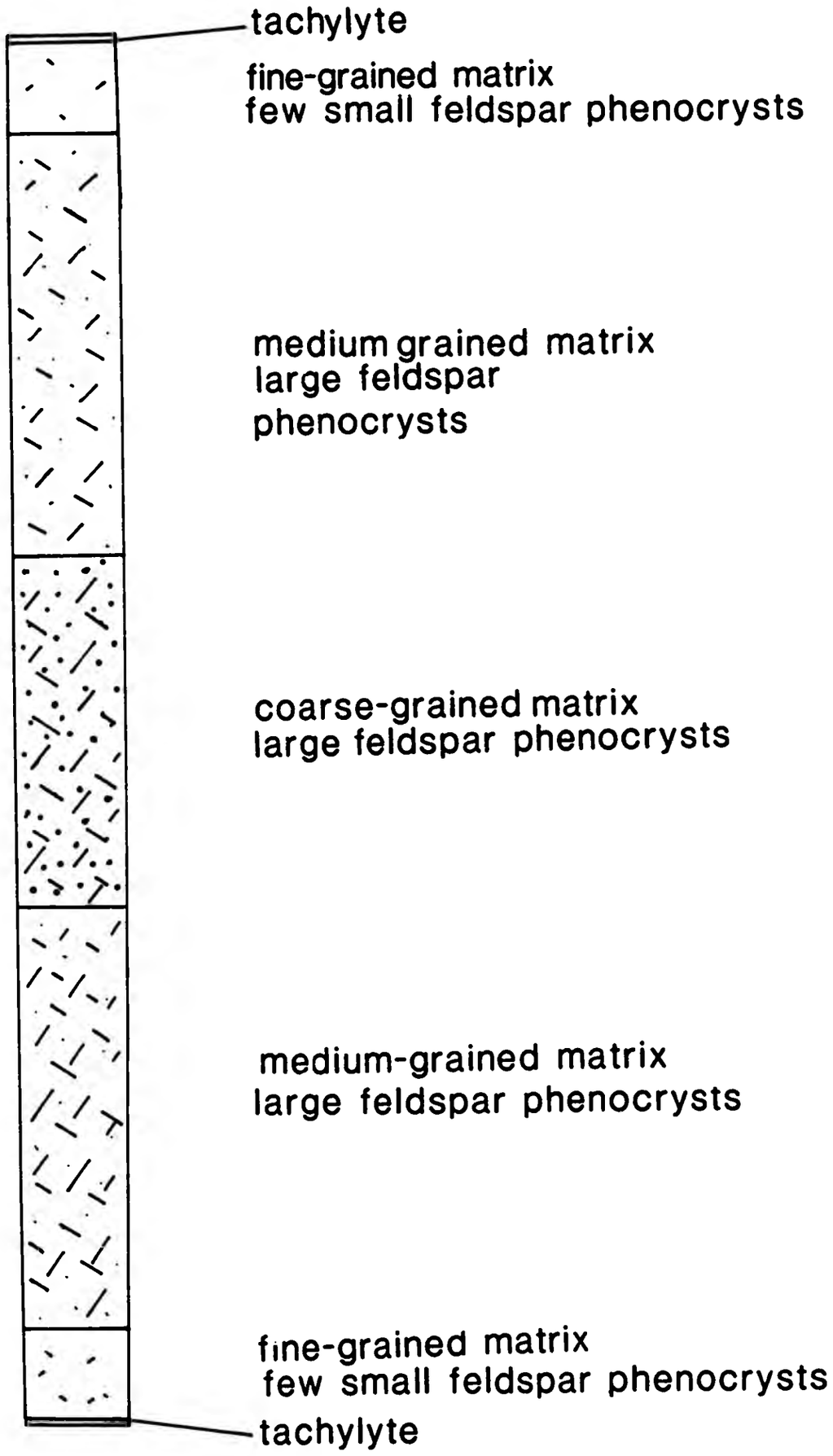

Fig.4.2. 7 An example of symmetrical banding, the bands are emphasized by the presence of feldspar phenocrysts. Centre Three north of Abhain Chro Bheinn

the central area.

Two factors influence the distribution and size of the phenocrysts, the first is that the entrained particles flow towards the centre of the conduit and secondly the longer the time the phenocrysts spend in the magma the larger they become. Thus, as the intrusion begins to crystallize the phenocrysts are moving too fast along the conduit to become entrained in the fine grained outer zone. As the crystalizing front advances the conduit becomes narrower and the flow rate is reduced, thus increasing the incidence of phenocrysts in the bands. Finally, the central area crystallizes with the largest crystals being found in this region. Phenocrysts only occur in the outer region if the crystallizing front advances faster than the "flow-regime" in the central area of the sheet (Platten and Watterson, 1969).

Table 4.1 illustrates the differences and similarities of the four cone sheet sets. In general, the differences are slight, the greatest variation is seen in the type of apophyses in each set. Differences in banding is perhaps best attributed to the presence of phenocrysts and vesicles in each set.

Table 4.1 Table of the field characteristics of the four cone sheet sets of Ardnamurchan

	Centre One	Outer Centre Two	Inner Centre Two	Centre Three
Chilled margins	x	x	x	x
Planar contacts				
a)large scale	x	x	x	x
b)small scale	x	x	x	x
Irregular contacts	x	x	x	x
Apophyses				
i.exploiting a pre-existing fracture	x	x	x	x
ii.at the change in orientation of the sheet		x	x	
b)paired			x	x
Xenoliths				
a)Accidental		x	x	x
b)Cognate	x	x		
Banding				
a)Plagioclase phenocrysts			x	x
b)Amygdaloidal	x	x		

4.3 PETROLOGY

A total of 90 rock specimens have been collected from the four cone sheet sets and subsequently sectioned. Despite a large variation in hand specimen, Richey et al. (1930) divided the cone sheets into two broad compositional groups, that is acid/felsites and intermediate/basic. Because the present investigation is structurally based it was found practical to maintain this simple division even though the grain size varies from glass to medium-grained (1mm crystals) and the colour index varies between 80% and 50% in the basic rocks. Richey's classification has been modified by dividing the sheets into three groups; 1) aphyric basic/intermediate, 2) phyric basic/intermediate and 3) acid. A brief mineralogical and textural description of the three groups is given below and, based on previous authors work, the geochemistry of the cone sheets will be briefly discussed.

4.3.1 Aphyric basic/intermediate

The majority of the cone sheet rocks fall into this category, a typical thin section of one of these rocks consists of plagioclase feldspar (60%), clinopyroxene (30%), magnetite(5%),chlorite(5%) (Plate 4.19). Plagioclase and clinopyroxene show a poorly developed ophitic texture, the 1mm

Plate 4.19 Photomicrograph of a medium-grained, aphyric, basic cone sheet. Outer Centre Two, west of Mingary Pier. (x4, xpl)

Plate 4.20 Skeletal feldspars containing glass inclusions, the matrix consists of chlorite, magnetite and pyroxene all of which have been thermally metamorphosed, Inner Centre Two, Lighthouse. (x4, xpl)

Plate 4.19 Photomicrograph of a medium-grained, aphyric, basic cone sheet. Outer Centre Two, west of Mingary Pier. (x4, xpl)

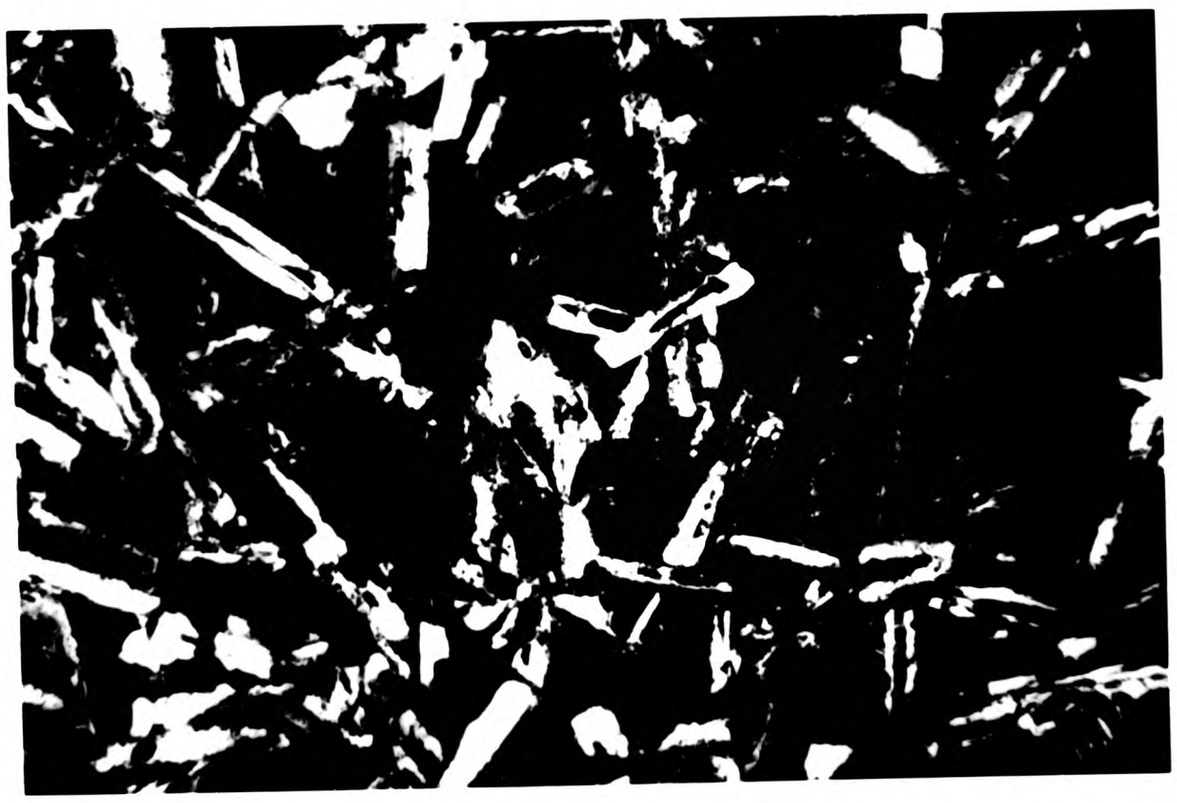

Plate 4.20 Skeletal feldspars containing glass inclusions, the matrix consists of chlorite, magnetite and pyroxene all of which have been thermally metamorphosed, Inner Centre Two, Lighthouse. (x4, xpl)

Plate 4.19 Photomicrograph of a medium-grained, aphyric, basic cone sheet. Outer Centre Two, west of Mingary Pier. (x4, xpl)

Plate 4.20 Skeletal feldspars containing glass inclusions, the matrix consists of chlorite, magnetite and pyroxene all of which have been thermally metamorphosed, Inner Centre Two, Lighthouse. (x4, xpl)

feldspar laths ($An_{,,}$) partly enclosed in small clinopyroxene crystals. The feldspars are often skeletal and contain inclusions of glass (Plate 4.20). Pyroxenes are typically 0.05mm in diameter.There are two forms of Fe-Ti oxide in the glassy interstices one as acicular needles and the other as octahedra. Quenched textures are common in the form of poorly developed or hollow feldspar terminations (Plate 21), acicular magnetites and the commonly devitrified glass.

Variation of the mineralogy within this group is slight, although the relative amounts of each mineral show a large range. Olivine pseudomorphs up to 1mm in diameter consist of serpentine and magnetite. Feldspar compositions range from $An_{,,}$ to $An_{2,}$. Twinned, skeletal and zoned feldspars are commonly observed and interstitial quartz is often present up to 5%.

Textures vary from quenched glass to subophitic (Plate 4.22). Quenched textures include spherulites composed of plagioclase, chlorite and magnetite (Plate 4.21), acicular magnetite and skeletal, swallow tailed feldspars. Such textures occur either throughout the rock, confined to interstices or within small patches up to 3mm in diameter (Plate 4.21). The presence of acicular magnetite increases the colour density particularly in the devitrified patches. Ophitic texture is more common in medium-grained rocks, whereas in the fine-grained rocks the

Plate 4.21 Photomicrograph of quenched textures; spherulites, acicular magnetites, very fine- grained, now devitrified, glass patches. Outer Centre Two, west of Mingary Pier. (x4, xpl)

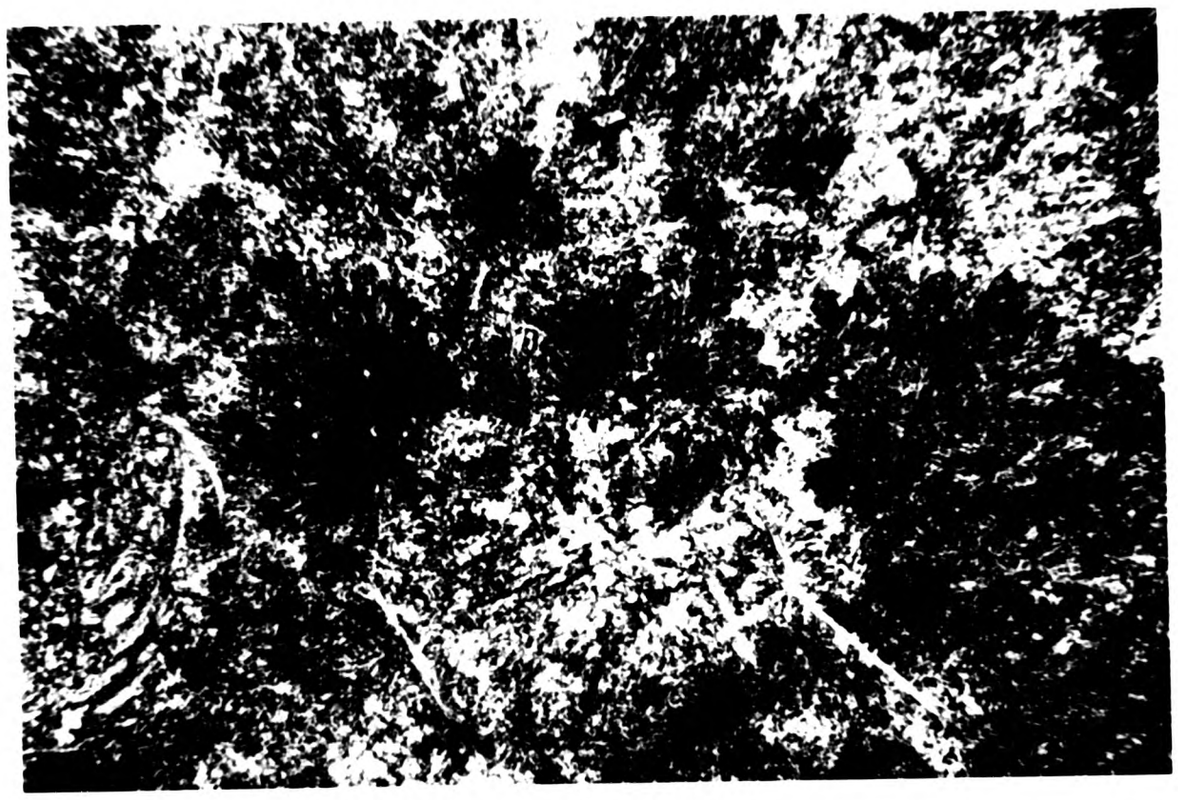

Plate 4.21 Photomicrograph of quenched textures; spherulites, acicular magnetites, very fine- grained, now devitrified, glass patches. Outer Centre Two, west of Mingary Pier. (x4, xpl)

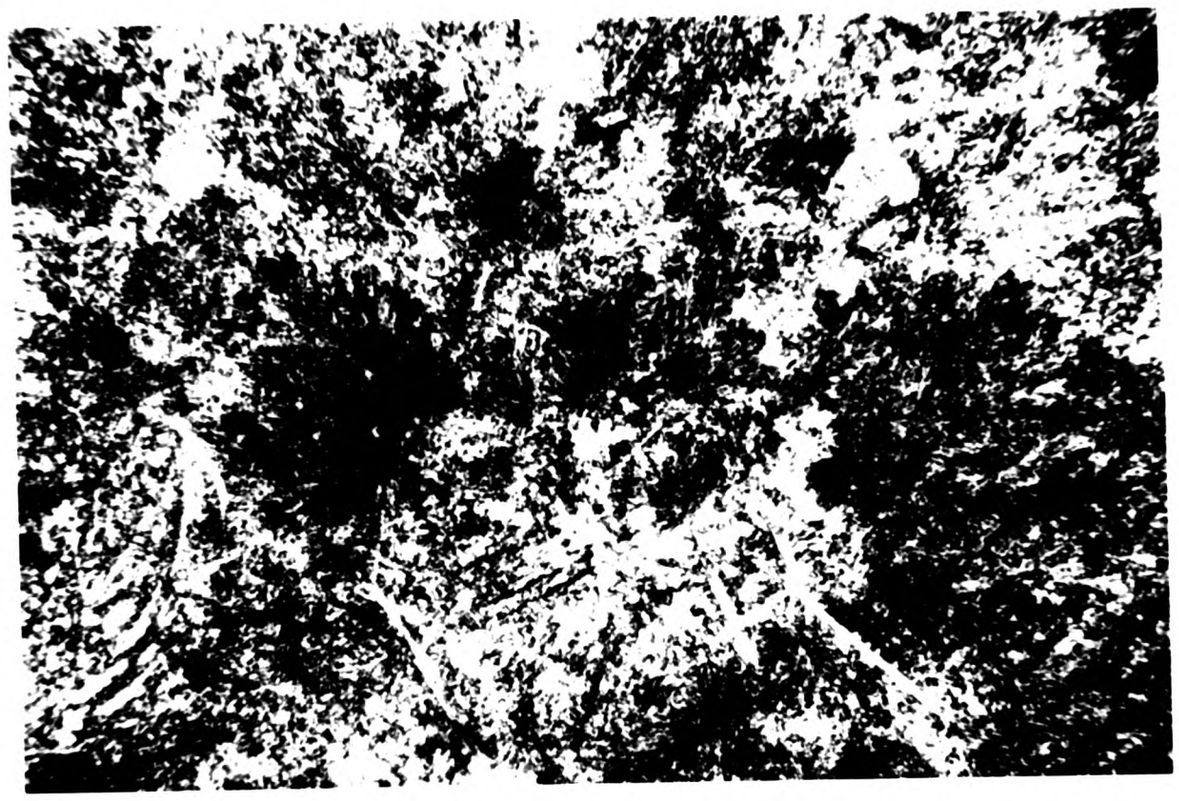

Plate 4.21 Photomicrograph of quenched textures; spherulites, acicular magnetites, very fine- grained, now devitrified, glass patches. Outer Centre Two, west of Mingary Pier. (x4, xpl)

Plate 4.22 Medium-grained, aphyric, basic cone sheet with small, sub-ophitic pyroxene crystals. Outer Centre Two, west of Mingary Pier. (x4, xpl)

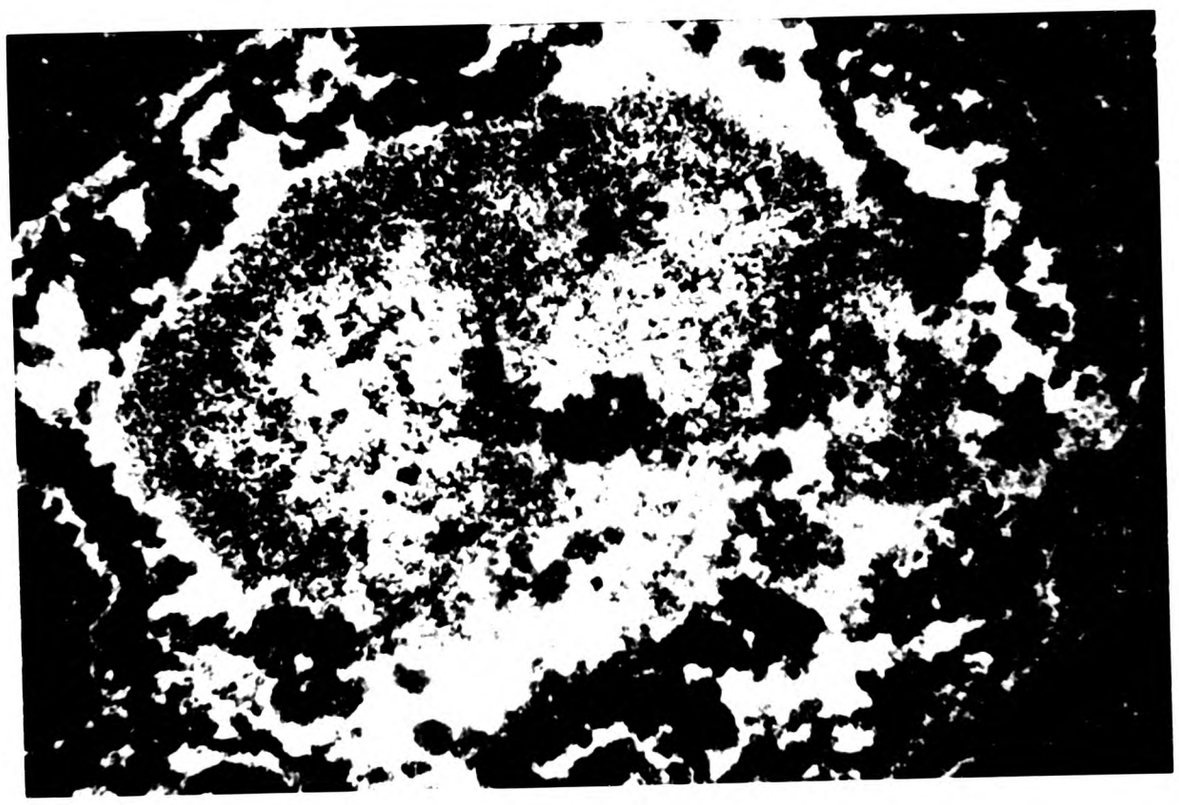

Plate 4.23 Photomicrograph of an amygdaloidal dolerite showing an amygdale infilled with concentric bands of magnetite and calcite. Outer Centre Two, west of Mingary Pier.

Plate 4.22 Medium-grained, aphyric, basic cone sheet with small, sub-ophitic pyroxene crystals. Outer Centre Two, west of Mingary Pier. (x4, xpl)

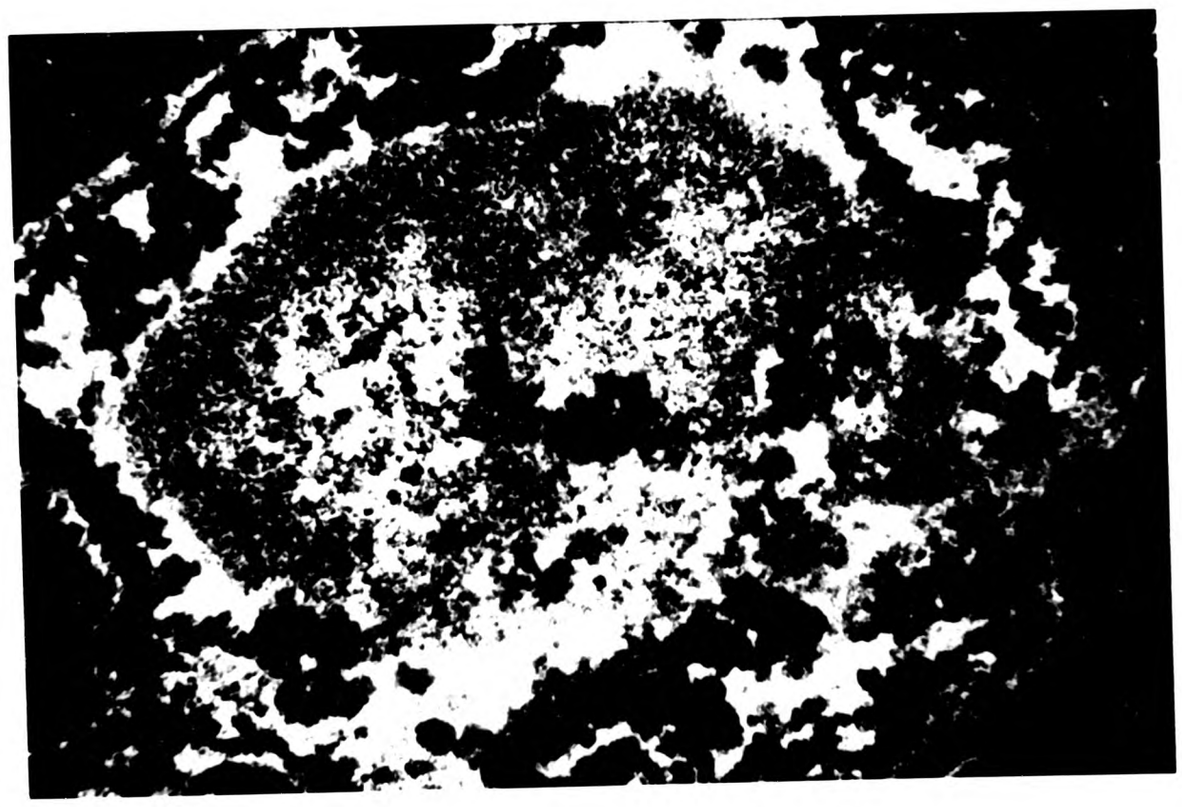

Plate 4.23 Photomicrograph of an amygdaloidal dolerite showing an amygdale infilled with concentric bands of magnetite and calcite. Outer Centre Two, west of Mingary Pier.

Plate 4.22 Medium-grained, aphyric, basic cone sheet with small, sub-ophitic pyroxene crystals. Outer Centre Two, west of Mingary Pier. (x4, xpl)

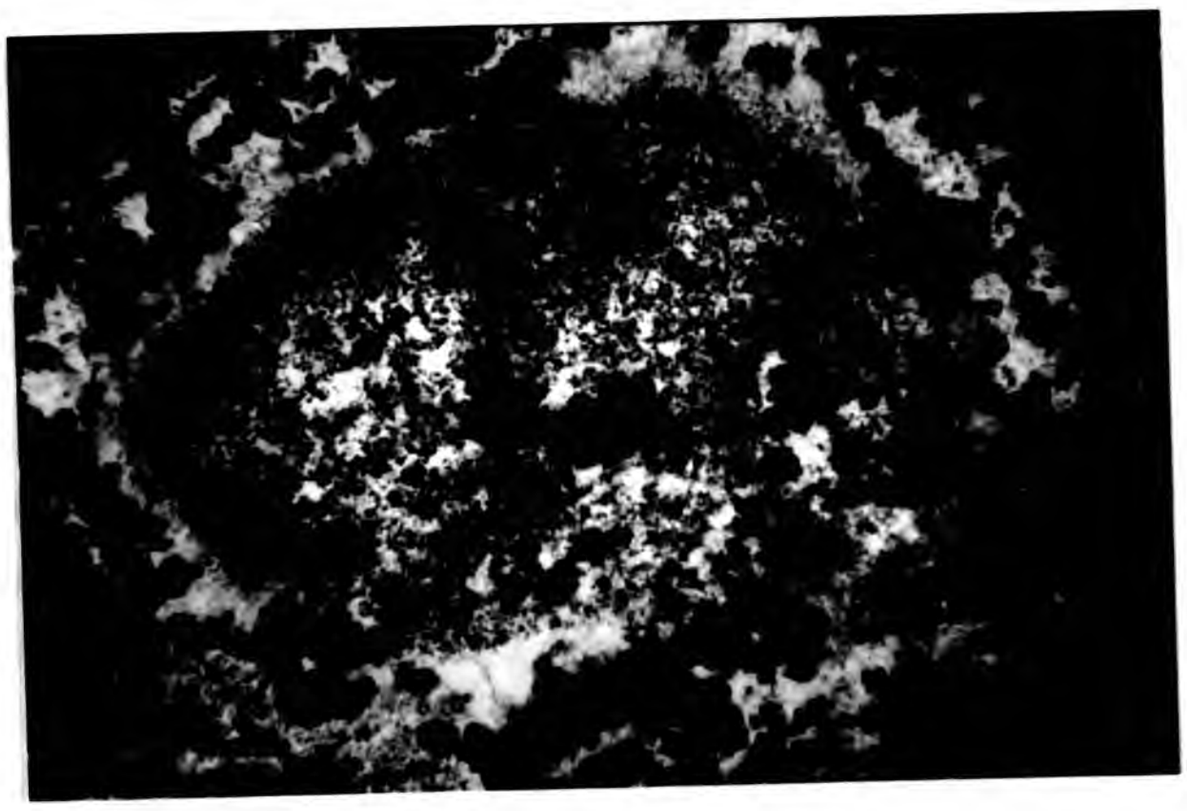

Plate 4.23 Photomicrograph of an amygdaloidal dolerite showing an amygdale infilled with concentric bands of magnetite and calcite. Outer Centre Two, west of Mingary Pier.

pyroxene occurs in the form of grains. In general, pyroxene crystals tend to occur in clusters, rather than being evenly distributed throughout the rock.

Amygdaloidal cone sheets are rare, only three examples have been found, one is a Centre One cone sheet near Ockle Point, the other two are Outer Centre Two sheets and occur west of Mingary Pier at (492627) and (491627), the latter is figured in Fig.4.2.5. Fig.4.2.5 shows a section of a rhythmic banded sheet, the bands being defined by the change in size of amygdales. In thin section, the host rock matrix is composed of plagioclase, pyroxenes and Fe-Ti oxides. The amygdales (up to 11mm in length) are infilled in a layered manner and consist of calcite,epidote and opaque minerals with the amount of epidote being less common towards the centre of the amygdales (Plate 4.23). Other sections show irregular shaped amygdales infilled with chlorite and calcite or quartz. The presence of so few amygdaloidal cone sheets suggests that the cone sheets were intruded under a moderate overburden.

Modal proportions of three typical thin sections of the aphyric basic/intermediate group illustrates the variation in composition of the rocks are as follows:-

Plagioclase	60 (An_{28})	55	25(An_{50})
Pyroxene	20	15-20	60

Chlorite	10	10	5
Fe-Ti oxides	8	15	10
Quartz	2	--	--

Aphyric basic/intermediate sheets occur in all four cone sheet sets, though less frequently in the Inner Centre Two and Centre Three cone sheet sets.

4.3.2 Phyric basic/intermediate

Phyric sheets commonly occur in the Inner Centre Two and Centre Three cone sheet sets and show mineral banding (Banding 4.2). Sparsely porphyritic sheets attributed to Centre One have a low frequency of occurrence, the porphyritic phase is generally plagioclase (An_{50}). Similarly, few Outer Centre Two sheets are porphyritic, with plagioclase forming the porphyritic phase; the majority of these pophyritic sheets occur along the Sron Bheag section. A large proportion of Inner Centre Two sheets are porphyritic and exhibit the whole range of porphyritic species, that is plagioclase, pyroxene, olivine and spinel. Cone sheets of Centre Three are also porphyritic and show the most dense occurrence of plagioclase phenocrysts (Fig.4.2.7). The fine-grained matrix of these sheets is very similar in composition to the aphyric sheets described above, and consists of feldspar laths, clinopyroxene, Fe-Ti oxides and chlorite with

Plate 4.24 Photomicrograph of a porphyritic doleritic cone sheet showing a partial developed feldspar phenocryst. Inner Centre Two, Lighthouse.

Plate 4.25 Photomicrograph of a plagioclase phenocryst, from a porphyritic dolerite cone sheet, showing an irregular core and a rim of oscillatory zones. Inner Centre Two, Lighthouse.

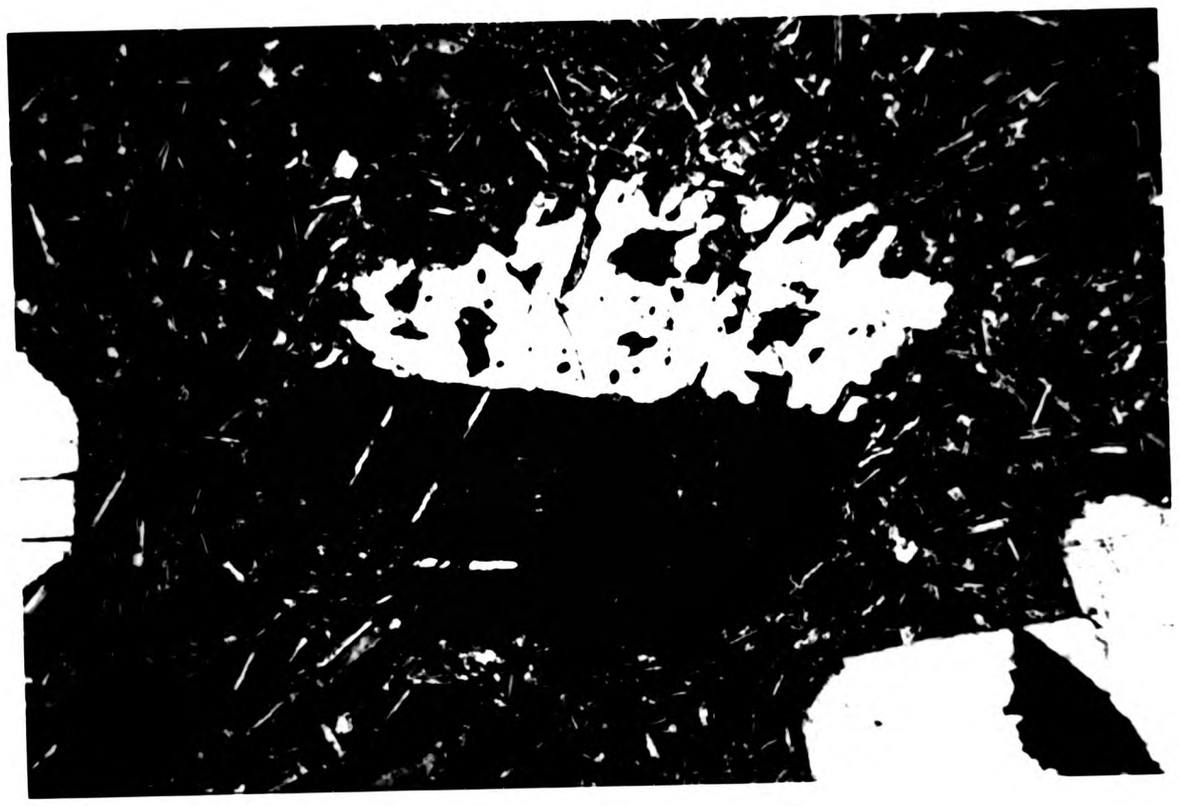

Plate 4.24 Photomicrograph of a porphyritic doleritic cone sheet showing a partial developed feldspar phenocryst. Inner Centre Two, Lighthouse.

Plate 4.25 Photomicrograph of a plagioclase phenocryst, from a porphyritic dolerite cone sheet, showing an irregular core and a rim of oscillatory zones. Inner Centre Two, Lighthouse.

Plate 4.24 Photomicrograph of a porphyritic doleritic cone sheet showing a partial developed feldspar phenocryst. Inner Centre Two, Lighthouse.

Plate 4.25 Photomicrograph of a plagioclase phenocryst, from a porphyritic dolerite cone sheet, showing an irregular core and a rim of oscillatory zones. Inner Centre Two, Lighthouse.

5-30% of the total rock being composed of plagioclase phenocrysts and 3% clinopyroxene.

The most abundant phenocryst species is plagioclase forms between 5% and 30% of the total rock and frequently they occur in clusters (glomerophyric). The phenocrysts often contain glass inclusions. Some of the feldspar crystals reach a length of 1.5mm, some are partially developed and others are irregular in shape and are often cracked, probably in response to abrasion during emplacement. Plate 4.25 shows a plagioclase phenocryst, the centre of which is irregularly shaped whilst the rim consists of thin oscillatory zones.

Other phenocrysts are not common but pyroxene phenocrysts have well formed euhedral faces (Plate 4.26). Phenocrysts of spinel and pseudomorphed olivines occur, only rarely although they account for less than 5% of the total rock.

Compositional variation from olivine-bearing to quartz-bearing rocks can be seen, as in the non-porphyritic rocks. Quenched textures similar to those seen in the non-porphyritic rocks are common.

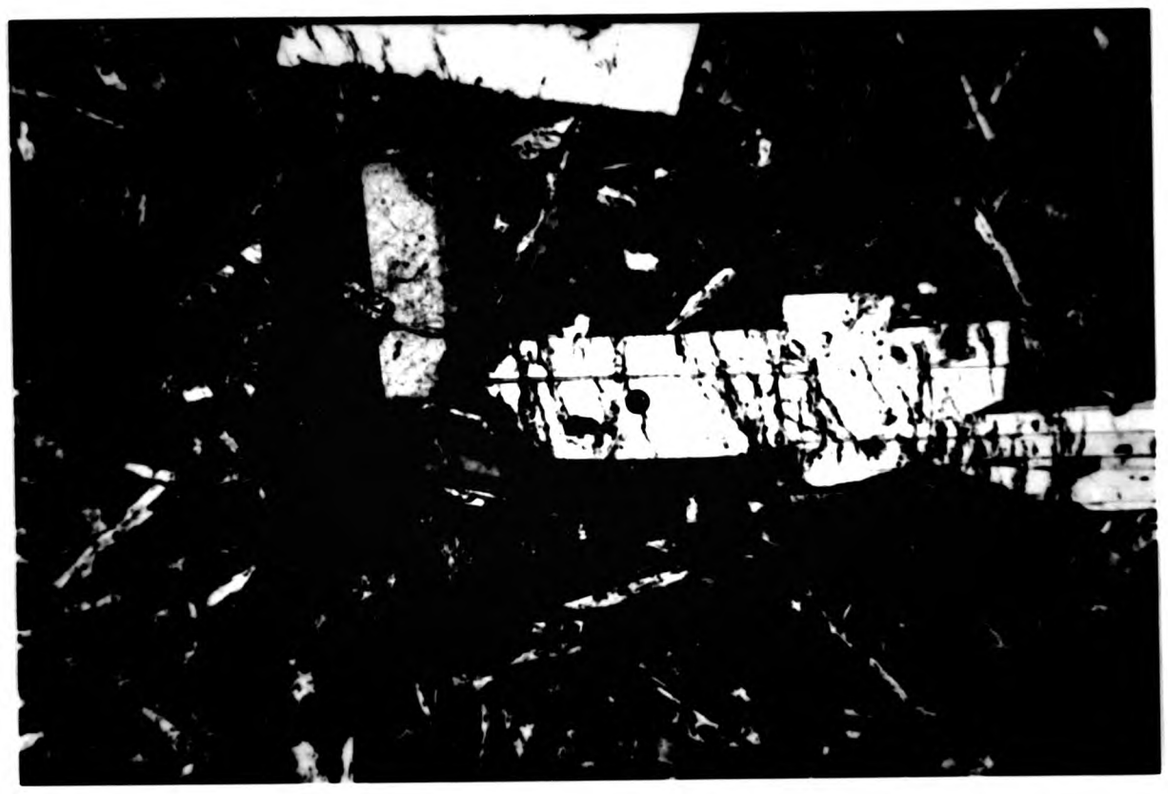

Plate 4.26 Photomicrograph of euhedral pyroxene phenocrysts, one contains a small early formed plagioclase crystal (An ^{35}). The plagiclase phenocrysts are cracked. Inner Centre Two, Lighthouse.

Plate 4.26 Photomicrograph of euhedral pyroxene phenocrysts, one contains a small early formed plagioclase crystal (An ^{35}). The plagiclase phenocrysts are cracked. Inner Centre Two, Lighthouse.

Plate 4.26 Photomicrograph of euhedral pyroxene phenocrysts, one contains a small early formed plagioclase crystal (An ^{35}). The plagiclase phenocrysts are cracked. Inner Centre Two, Lighthouse.

Hydrothermal alteration of both the porthyritic and non-porphyritic rocks has produced epidote, pyrite in the form of a string of small cubes emanating from a line or a single point,and chlorite replacing both pyroxene and glass.

4.3.3 Acid

Acid cone sheets are very much less common than basic ones. Usually, they occur as the central component of composite sheets, bordered by thin basic margins. A typical example is seen 400m west of Mingary Pier. It appears that within each cone sheet set, acid ones are early in the sequence, for example, east of Faskadale a composite sheet forms the host rock to a large number of thin basic sheets.

Features discernable in hand specimen include xenoliths, feldspar phenocrysts, chloritic patches (relics of pyroxenes) and pyrite cubes set in a pale-grey, fine-grained matrix (colour index 20-30%). The xenoliths are small, basic and have a composition similar to the lower basic margins that form the basic intrusions, and are generally confined to an area adjacent to the lower basic margin.This seems to indicate that the basic material had consolidated before the acid component was intruded.

In thin section, it is seen that 1mm turbid feldspar phenocrysts are set in a devitrified matrix, composed of very fine grained granules of feldspar and quartz with occasionally feathery alkali feldspars and quartz occuring as a graphic intergrowth. Accessory minerals are acicular Fe-Ti oxides and late stage apatite. Chlorite and Fe-Ti oxides frequently pseudomorph pyroxenes. In one rock a brownish hornblende has been found.

Alteration is ubiquitous and prominently takes the form of glass being converted to chlorite, feldspars to sericite and pyroxenes to chlorite and Fe-Ti oxides. Due to the very fine-grained nature of the rocks coupled with the ubiquitous alteration the modal proportions of the acid rocks cannot be asertained with any confidence.

4.4 GEOCHEMISTRY

No geochemical analyses have been performed in this study, therefore, the important aspects of the geochemical studies by Holland and Brown (1972) and Gribble (1974) will be summarised.

Holland and Brown (1972), who analysed 98 samples taken from the Ardnamurchan cone sheets, designed their investigation to asses the three centred hypothesis of Richey *et al.* (1930) as against

Table 4.2 Promax oblique primary pattern matrix for two primary factors which account for 70% of the variation of 15 elements in geochemical analysis of cone sheet rocks (after Holland and Brown, 1972)

Element	Factor 1	Factor 2
Si	0.83	0.38
Al	-0.50	
Fe		
Fe	-0.22	-0.94
Mg	-0.89	
Ca	-0.87	
Na		
K	0.93	
Ti		-0.58
Mn		-0.98
S		
P	0.69	-0.58
Rb	0.98	
Sr		
Ba	0.90	
Zr	0.86	
Cu	-0.96	-0.40
Ni	-0.97	
Zn	0.54	-0.64

the single centred spiral fracture hypothesis of Durrance (1967). By computing a principal factor matrix (Table 4.2, after Holland and Brown,1972) and plotting the two most influential factors,

F1 (Si,Al,Fe,Mg,Ca,K,P,Rb,Ba,Zr,Cu,Ni,Zn)

and F2 (Si,Fe,Ti,Mn,P,Cu,Zn) (Fig.4.4.1 after Holland and Brown, 1972),

it became apparent that the cone sheet sets could be divided chemically. From the F1 and F2 plots they were able to conclude that there is no geochemical evidence to discriminate between the Centre One and the Outer Centre Two cone sheets, especially those on the Kilchoan section, although they differ in 10 components. Cone sheets on the north coast section have an intermediate composition, whilst the Inner Centre Two cone sheets have the most basic composition of the sheets analysed.

Gribble (1974) analysed several dolerites in which the cone sheet dolerites sampled were collected on the basis of the three centred hypothesis. Fig.4.4.2 (after Gribble (1974)) shows an AFM plot, where the trend for each centre shows slight iron-enrichment. When the norms of the rocks are plotted on an Olivine-Nepheline-Quartz diagram (Fig.4.4.3) data from all three centres overlap.

It therefore seems that the principal factor matrix of Holland

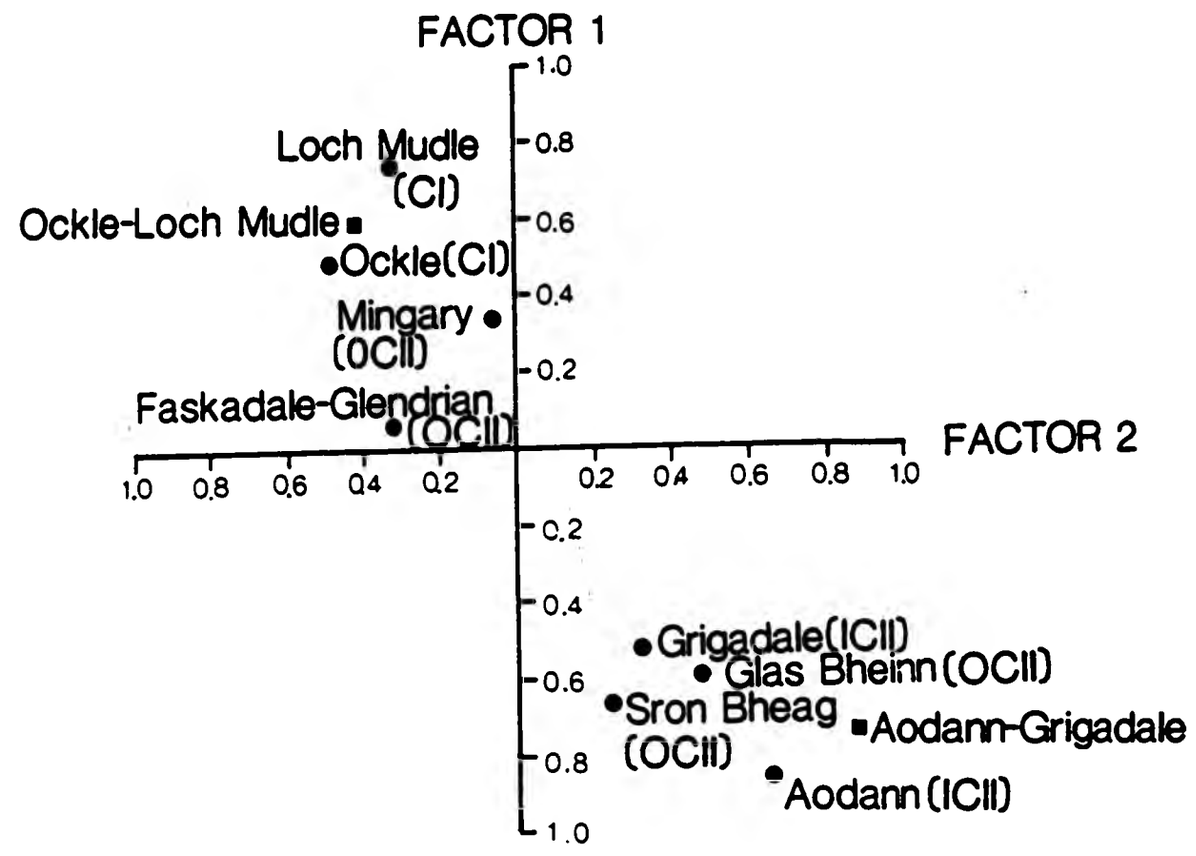

Fig.4.4.1 Geochemical classification of cone sheets from several sample areas of the Ardnamurchan peninsula based on a principal component factor analysis by Holland and Brown (1972)
F1 consists of elements Si, Al, Fe , Mg, Ca, K, P, Rb, Ba, Zr, Cu, Ni, Zn
F2 consists of elements Si, Fe , Ti, Mn, P, Cu, Zn

- average values were calculated for Centre One (Ockle-Loch Mudle) and Inner Centre Two (Aodann-Grigadale).

CI Centre One
OCII Outer Centre Two
ICII Inner Centre Two

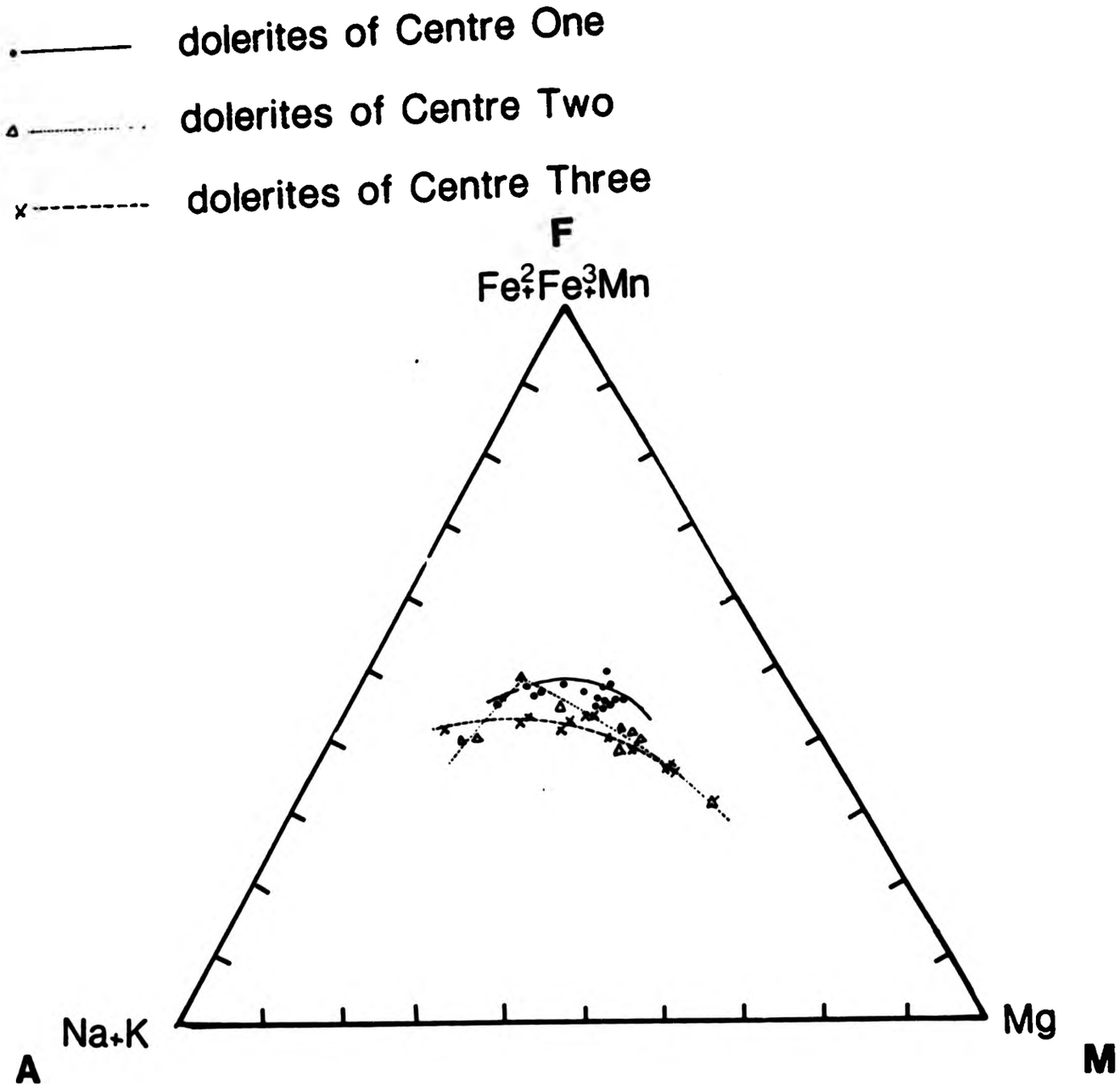

Fig.4.4.2 AFM plot of the dolerites from each of the three centres . Each centre shows a slight iron enrichment trend from basic to intermediate rocks . Not all of the dolerites were obtained from cone sheets (after Gribble, 1974).

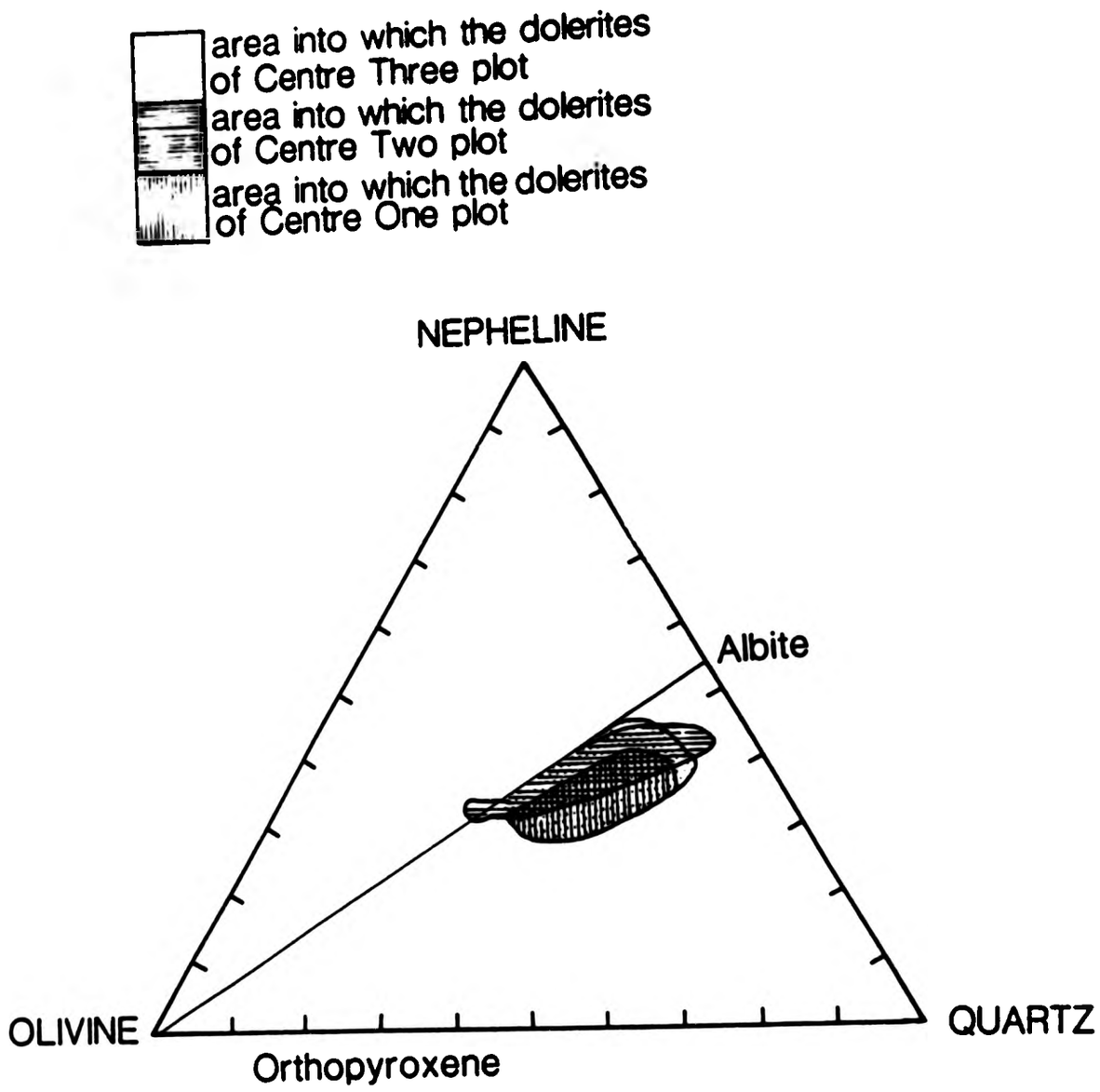

Fig.4.4.3 Normative distribution of the dolerites plotted on an Olivine-Nepheline-Quartz diagram. Not all of the dolerite samples were obtained from cone sheets (after Gribble, 1974).

and Brown (1972) enables a finer distinction between various cone sheet groups, that is not apparent in normative plots. The principal factor matrix analysis has highlighted a number of groupings of the collected cone sheet rocks. One of the most notable results is that the Inner Centre Two analyses plot close to the Sron Bheag (Outer Centre Two) analyses and therefore suggests a possible closer link between the Outer and Inner of Centre Two cone sheets sets (Chapter 5 and 6). Also, the principal factor matrix shows that the Centre One cone sheets and those of the Kilchoan section are similar, which tends to support the theory that the emplacement of both sets overlapped, possibly utilizing the same magma source.

The Outer Centre Two cone sheets of Faskadale differ from all the other cone sheets analysed, a possible explanation is discussed in Chapter 10.

CHAPTER 5

CONE SHEET CHARACTERISTICS

5.1 INTRODUCTION

The physical parameters of the four cone sheet sets have been collated (Appendix A) and statistically analysed. To the authors knowledge only one other cone sheet complex, the Snaefell complex, Western Iceland (Sigurdsson, 1966), has been analysed quantitatively. Richey et al. (1930) give average figures for dip and thickness of the Ardnamurchan cone sheets, although no statement is given about the number of samples. Sigurdsson (1966) attempted a quantative study in several well-exposed sections of cone sheet sets in the Setberg area, Western Iceland. He observed a decrease in the number and volume of sheets with increasing altitude, for example, at 100m above sea level the cone sheets make up 30% of the rock outcrop, whilst at 300m above sea level they form only 5%. However, only figures for dip and thickness are given; the sheets have a modal thickness of 1m and a modal dip of 30°. Kresten (1980), following the work of von Eckerman (1948, 1958) on the cone sheets of the Alnö Complex, Norway, investigated the dip angles of the sheets and concluded that two sets of cone sheets were superimposed on each other.

5.2 METHODS

As indicated in Chapter 3, each line of traverse has been divided into 100m unit lengths; Centre One has 24 unit lengths, Outer Centre Two 68, Inner Centre Two 16 and Centre Three 2 unit lengths. The number of unit lengths is a direct consequence of the exposure, development and distribution of the sheets at the present level of erosion. Table 5.1 illustrates the bivariate

Table 5.1 Bivariate and multivariate analyses carried out on the cone sheet characteristics

BIVARIATE ANALYSIS

Dip	-	Distance from centre
Dip	-	Distribution per unit length
Dip	-	Strike
Dip	-	Thickness
Average Dip	-	Per unit length
Average Dip	-	Cumulative thickness per unit length
Number	-	Per unit length
Number	-	Dip
Strike	-	Distribution per unit length
Strike	-	Thickness
Strike	-	Distance from centre
Strike	-	Chi^2
Strike	-	Number (per centre)
Thickness	-	Number per unit length
Thickness	-	Distance from centre
Av Thickness	-	Per unit length
Av Thickness	-	Cumulative thickness

MULTIVARIATE ANALYSIS

	Strike	Thickness	Dip	Distance
Strike	x	x	x	x
Thickness	-	x	x	x
Dip	-	-	x	x
Distance	-	-	-	x

parameters that have been statistically analysed, the letter C indicates analysis using a cluster analysis program (Clustan; Table 5.1).

RESULTS

5.3 NUMBER OF SHEETS PER UNIT LENGTH

Distribution of the number of cone sheets per unit length for each cone sheet set are given in Figs.5.3.1-5.

5.3.1 Centre One

Figure 5.3.1 illustrates the distribution from Faskadale to Rubha a' Choit and, in general, the frequency of sheets is low with eight unit lengths containing no sheets: the population varies from 0 to 13 sheets per unit length. The number of sheets in unit lengths 1 to 4 varies between 8 and 13, differing from the low frequencyof sheets over the the remaining parts of the traverse. The cumulative frequency curve which has an initial steep gradient then shallows towards the east (Fig.5.3.1) also amplifys the higher frequency of sheets occurring in the unit lengths 1 to 4.

In summary, therefore, there are two distinct groupings along the traverse consisting of a) unit lengths 1 to 4 and b) unit lengths 5 to 43, with sheets being more common in the sections 1 to 4 to the east of Faskadale.

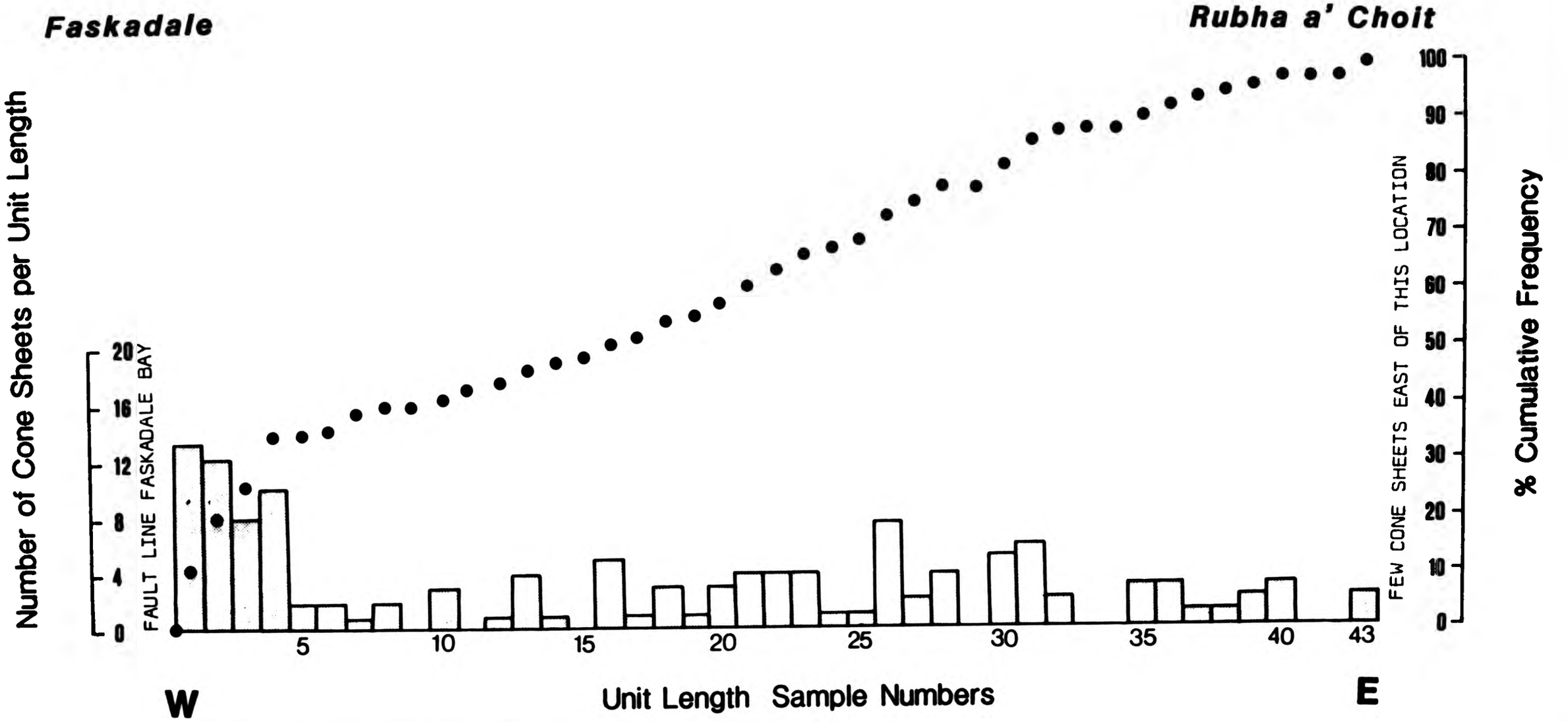

Fig.5.3.1. Centre One Distribution of sheets per Unit Length

5.3.2 Outer Centre Two

North Coast. Figure 5.3.2 shows that a large number of sheets (maximum 40) are present in some unit lengths, particularly in sections 1 to 16 (Rubha an Duin Bhain to Sgeir Ghibeach). To the east of Sgeir Ghibeach the frequency of sheets is lower per unit length and resembles the distribution of the south coast section (Fig.5.3.3). This difference is emphasized where the cumulative frequency curve (Fig.5.3.2) changes slope at unit length 4.

South Coast. Frequencies of cone sheets range from 0 to 23 per unit length (Fig.5.3.3). Lows in the frequency distibution occur west of Sron Bheag, Mingary Pier and Rubh'a'Mhile. Generally there is a larger number of sheets per unit length in the west than in the east and this is shown by a change of slope in the cumulative frequency curve.

5.3.3 Inner Centre Two

From Beinn Bhuidhe (unit length 4) to Beinn na Seilg (unit length 15) there is a general increase in the number of cone sheets per unit length (Fig.5.3.4). Intensity of the sheets ranges from 3 to 23 per unit length.

5.3.4 Centre Three

The two unit lengths contain 11 and 7 cone sheets respectively (Fig.5.3.5).

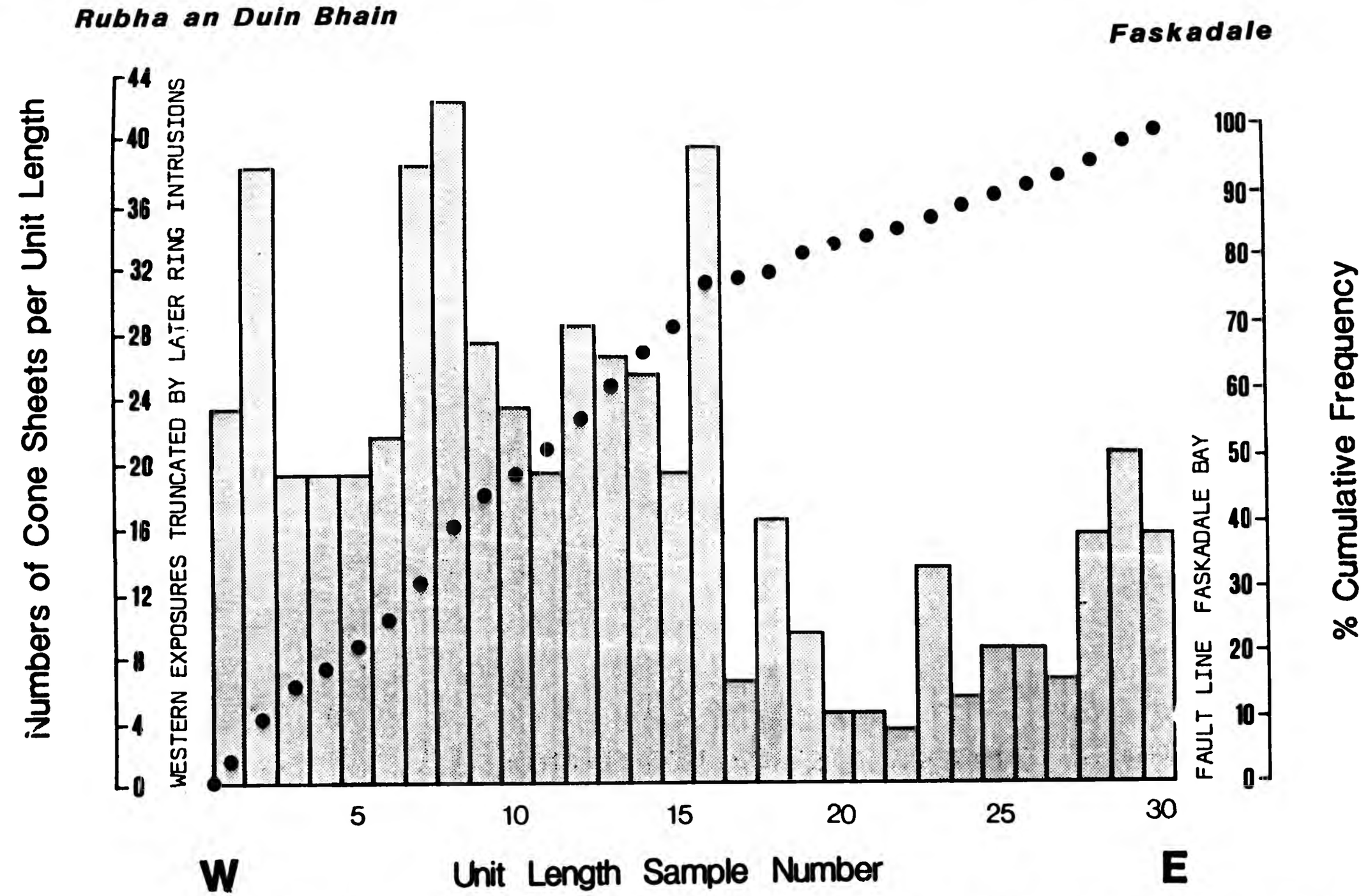

Fig.5.3.2. Outer Centre Two North Coast Distribution of Sheets per Unit Length

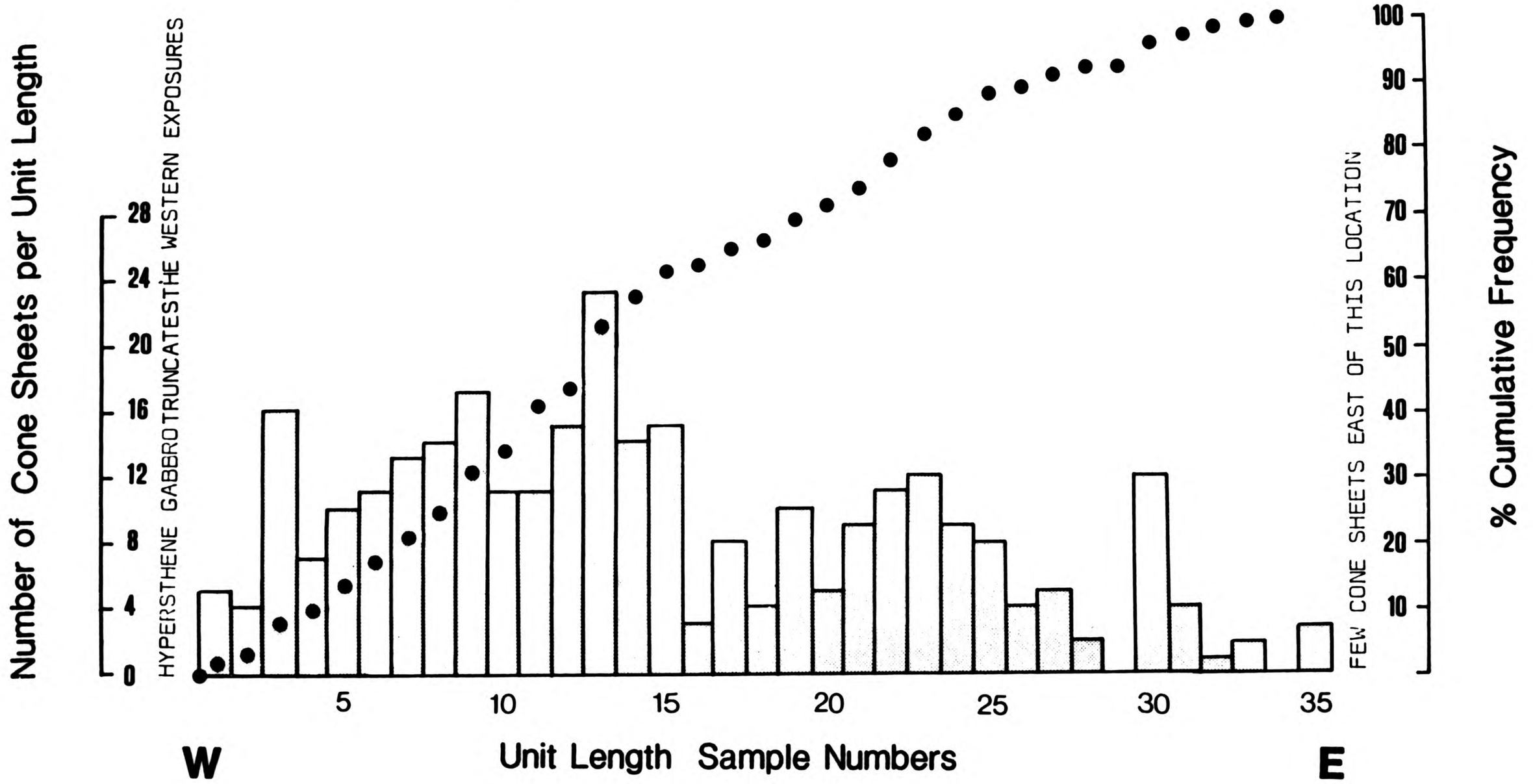

Fig.5.3.3. Outer Centre Two South Coast Distribution of Sheets per Unit Length

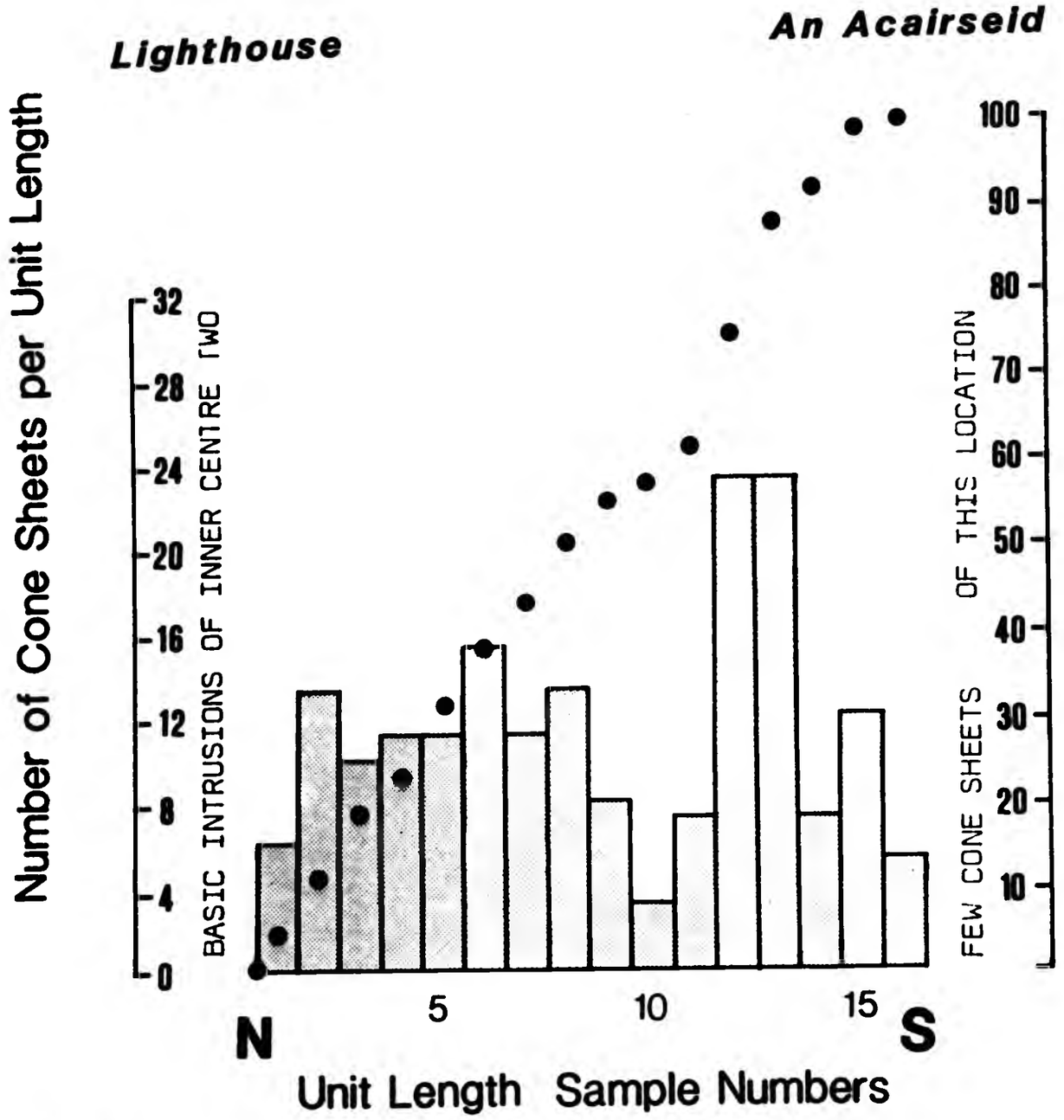

Fig.5.3.4. Inner Centre Two
Distribution of Sheets per Unit Length

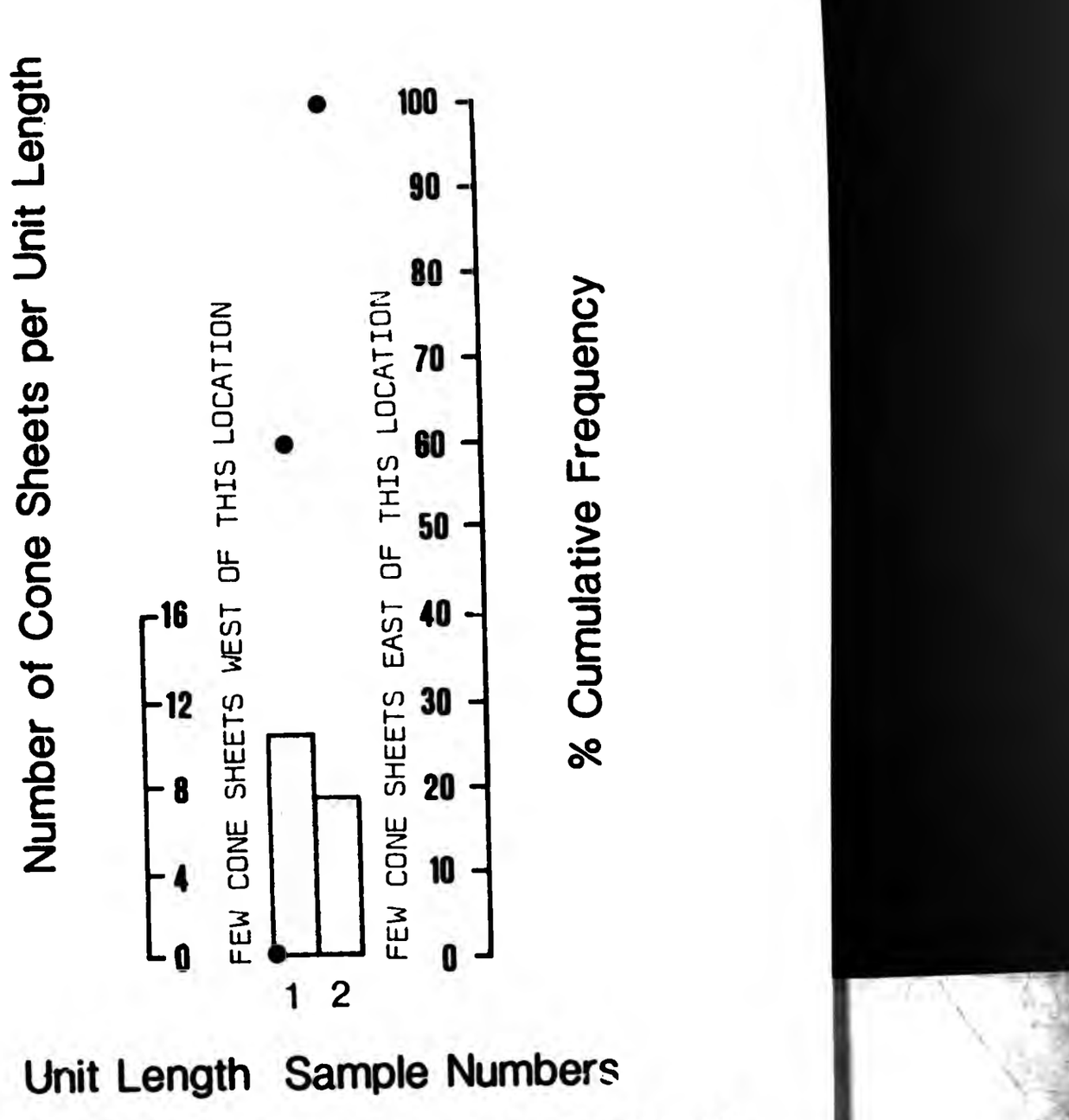

Fig.5.3.5. Centre Three Distribution of
Sheets per Unit Length

5.3.5 Mean Number of Sheets per Unit Length

Table 5.2 gives the mean number of cone sheets per unit length for all the cone sheet sets. The Outer Centre Two (north coast) cone sheet set has the greatest number of sheets per unit length (24), Centre One has the fewest cone sheets per unit length (3), whilst Outer Centre Two (south coast), Inner Centre Two and Centre Three have similar values (11). The two extreme types of cone sheet intensity are a) the Centre One sheets which occur as very low frequencies over a large geographical area (Chapter 3) and b) the Outer Centre Two distribution with its large number of cone sheets over a small geographical area. The Outer Centre Two set has been subdivded into two, as the traverses are geographically separated, and this has highlighted the differences within this set; the average number of sheets per unit length on the north coast is 18 and on the south coast is 9.5.

SPATIAL DISTRIBUTION OF CONE SHEETS

Figure 5.3.6 is a contoured plot of cone sheet intensity with contours at intervals of 5 sheets.

5.3.6 Centre One

The Centre One distribution has a low frequency in comparison to the Outer Set of Centre Two located to the west of Faskadale Bay. However, 0.5 km east of Faskadale the frequency of sheets increases, resembling the distribution of sheets west of Faskadale. It is probable that Faskadale marks the overlap

Table 5.2 Mean number of cone sheets per unit length for each of the cone sheet sets

	Mean number of sheets
Centre One	0.5
Outer Centre Two	
north coast	18.0
south coast	9.5
Inner Centre Two	11.8
Centre Three	9.0

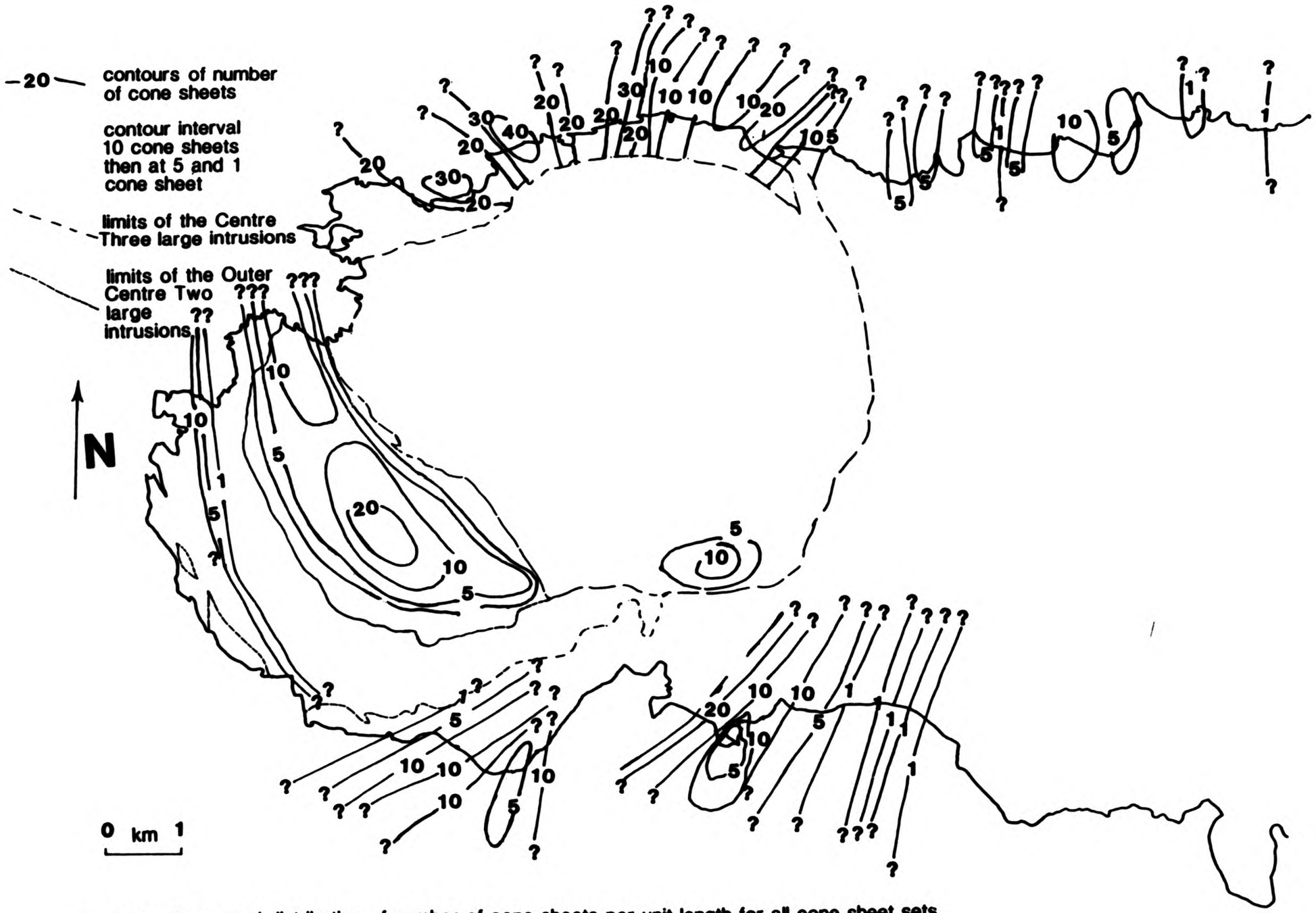

Fig.5.3.6 Contoured distribution of number of cone sheets per unit length for all cone sheet sets

of these two sets. The low intensity characteristic of Centre One may indicate periodic emplacement over a large area, though each episode was geographically localised. It is possible that this area marks either the extremities of the intrusions at a high level within the volcanic ediface, or that it is just an area of low intensity intrusive activity. Evidence given in a later chapter (7) tends to support the theory that the Centre One traverse is at a high structural level within the volcanic ediface and depicts both the vertical and lateral extremities of a cone sheet set.

5.3.7 Outer Centre Two

A peak in the distribution of cone sheets (n=20 where n is the number of sheets at the peak) is located along the south coast section midway between Glas Eilean and Mingary Pier, with subsidiary peaks (n=15) occurring on either side, with the number of sheets decreasing towards both extremities of the section line. On the north coast, there is a maximum peak (n=40) at Rubha Groulin, with two subsidiary peaks (n=30) occurring on either side; the north coast peaks being twice the value of those of the south coast.

5.3.8 Inner Centre Two

These cone sheets fall into two distinct groups, an Outer Group (n = 10) located at the Lighthouse, Sgurr nam Meann and An Acairseid and an Inner Group (n=20) located close to the focus of Centre Two activity.

5.3.9 Centre Three

These cone sheets form a small high, maximum 10 sheets, located on the northern slopes of Abhain Chro Beinn.

5.3.10 Summary

Assuming that a single intrusive episode of cone sheet emplacement will be concentrated in a relatively restricted area with the intensity decreasing with distance away from this area, a normal distribution will result. The Inner Set of Centre Two shows two distinct normal groupings (Fig.5.3.6). However, the Outer Centre Two sections show 3 to 4 peaks which may be interpreted as a number of separate episodes of activity.

5.4 DIP

5.4.1 Centre One

The dip data has been divided into classes of 10° and Fig.5.4.1 shows the dip distribution along each unit length. There is no systematic variation in dip towards the centre, or a single predominating dip throughout the traverse. However, localised areas show common modal classes, for example, unit lengths 1 to 5 have a modal class of 31°-40°. In the more easterly parts of the traverse, the sheets show a greater range in the amount of dip per unit length. Fig.5.4.5 shows the average dip values across the section with a decrease in the angle of dip from 50° to 30° from east to west, a variation which is not

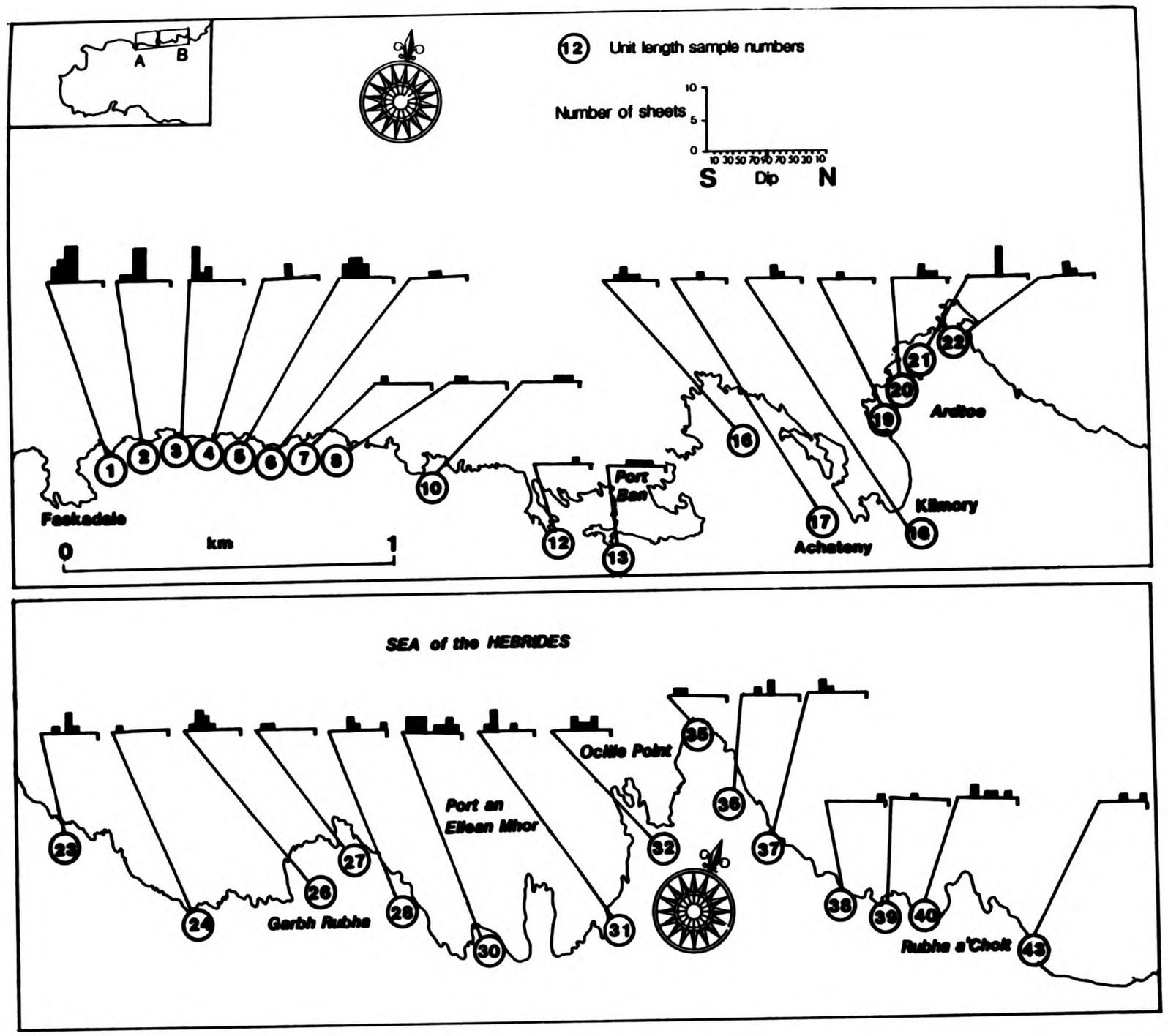

Fig.5.4.1 Centre One cone sheets Distribution of dip of cone sheets per unit length

seen in the total distribution of dip per unit length. Standard deviation (σn)of the average values indicates a dispersion of 1°-24°, and such a large variation renders an average value for the whole traverse as being unrepresentative of the data.

5.4.2 Outer Centre Two

North Coast. The dip distribution of sheets per unit length shows no clear modal class (Fig.5.4.2). However, 800m west of Faskadale the sections indicate a normal distribution about the 51°-60° class. From Sgeir Ghibeach westward the modal class is 31°-40°, with a subsidiary high in the 61°-70° class which is particularly emphasized at Rubha Carrach. At (404732), the sheets dip towards the north at 81°-90° in contrast to the majority of the section in which the regional dip of the sheets is towards the south. The average dip (Fig.5.4.6) of the cone sheets along the traverse shows a wave like form with three peaks, the first at the most westerly extremity where the average dip is 71°, the second at Sgeir Ghibeach where the average dip is 63° and the third, 0.5km west of Faskadale, where the average dip is 72°.

South Coast. Cone sheets of the Sron Bheag section have a modal value of 50° (Fig.5.4.3). From Glas Eilean to Mingary Pier the 41°-50° class predominates, whereas east of Mingary bimodality of the dip is encountered, with peaks at 50° and 80°. The existance of a peak with a high angle of dip, 80°, may indicate the presence of dykes. In summary, most sheets on the south coast dip northwards at 41°-50°; this modal value is from a skewed distribution. The Sron Bheag sections and those to the

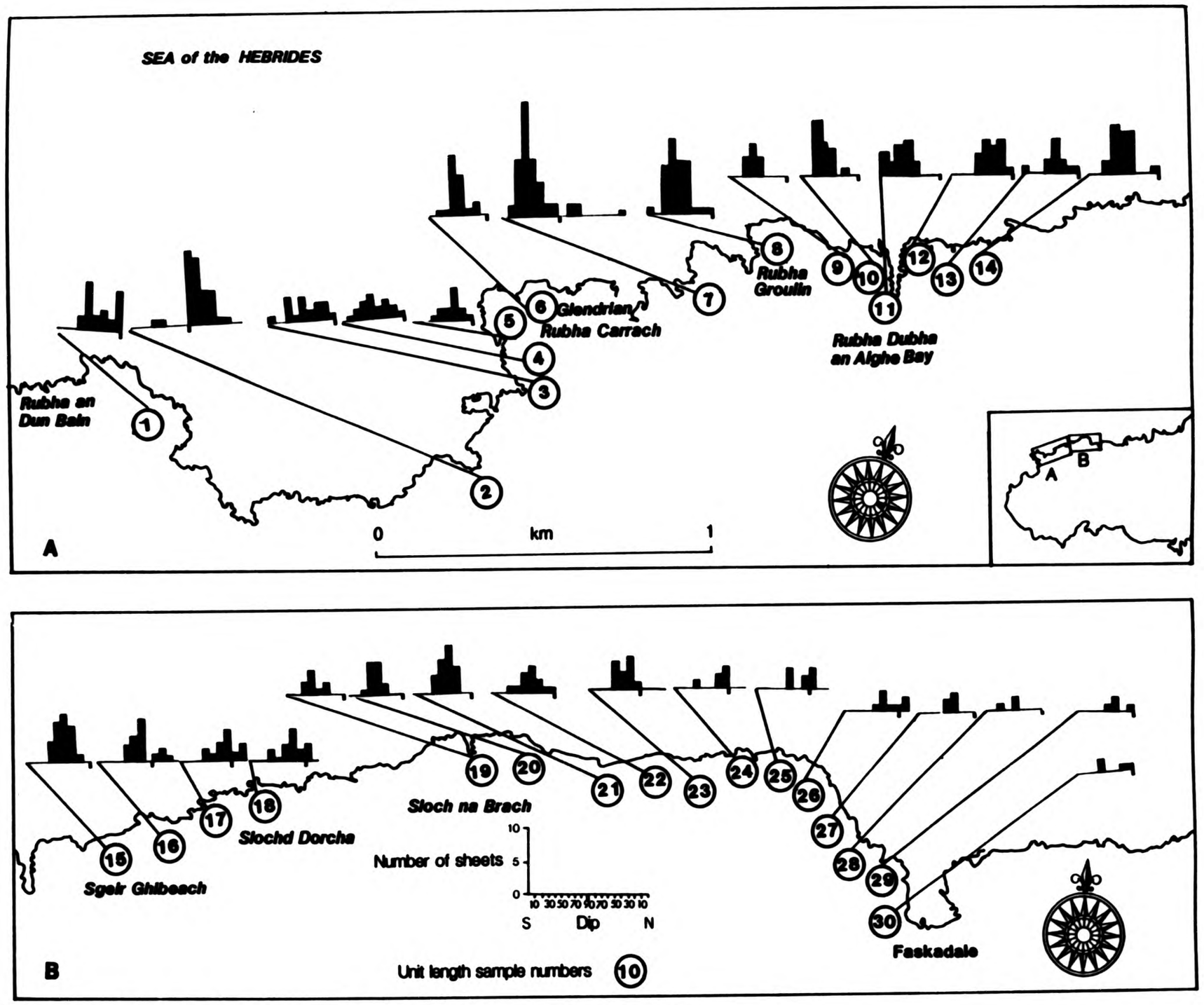

Fig.5.4.2 Outer Centre Two North Coast Distribution of dip of cone sheets per unit length

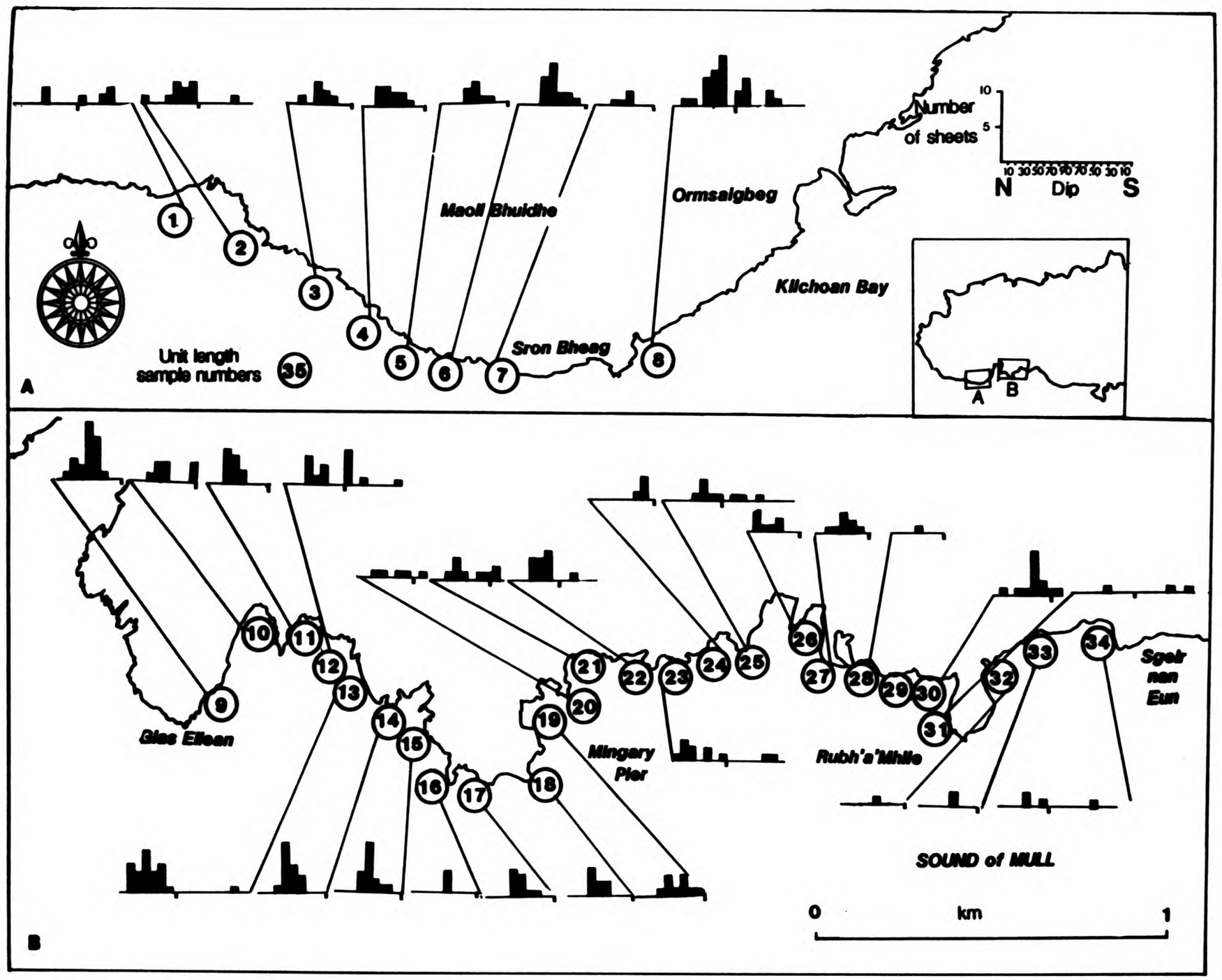

Fig.5.4.3 Outer Centre Two South Coast Distribution of dip of cone sheets per unit length

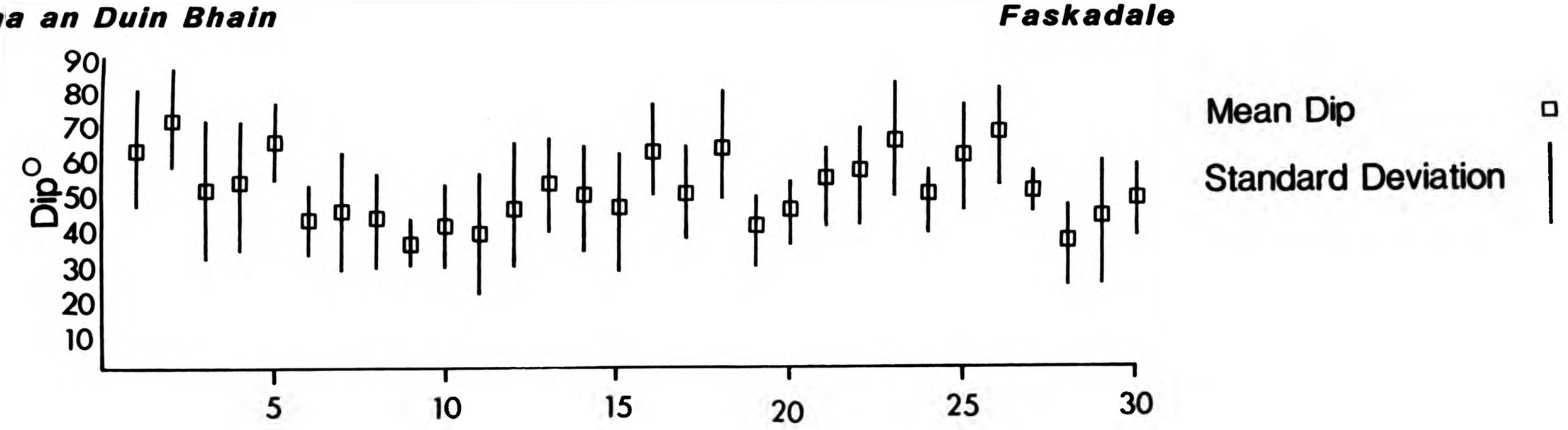

Fig.5.4.6. Outer Centre Two North Coast Average Dip per Unit Length in a W to E traverse

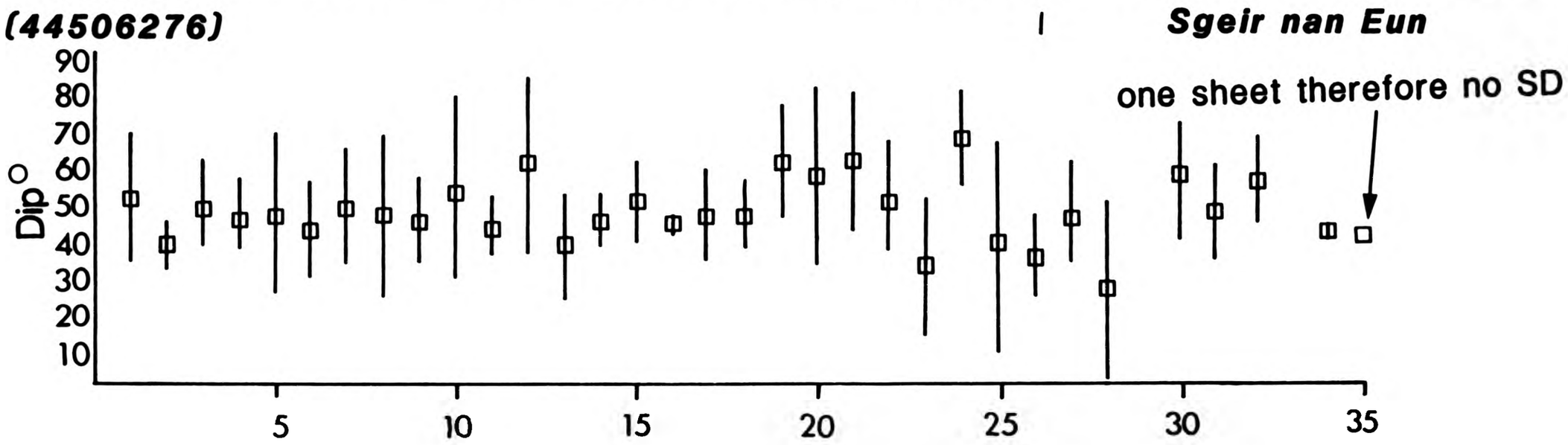

Fig.5.4.7. Outer Centre Two South Coast Average Dip per Unit Length in a W to E traverse

west of Mingary Pier have average dips of 45° and show little variation. However, east of Mingary Pier the average dip is 60°, which decreases eastward, with a dip of 26° being calculated as the average value for the Rubh'a'Mhile section (Fig.5.4.7).

Standard deviation (σn) from the mean for both north and south coast sections is approximately 10°-20° (8°-20° north coast, 2°-24° south coast), reflecting the dispersion of dips found within each sample section line. Figures 5.4.6 and 7 show groups of unit lengths where average dip increases towards the east, for example, from unit lengths 19-23 in Fig.5.4.6 the average dip increases by 20°. It is possible that these may represent separate sets of sheets.

5.4.3 Inner Centre Two

There is a great variation in the dip of the sheets (Fig.5.4.4) and consequently there is a low frequency distribution in each unit length. However, to eliminate this effect all sheets within each traverse have been grouped together, and from these groupings modal values can confidently be identified. A modal dip of 80° characterises the Beinn Bhuidhe and Garbdhail sections, whilst a modal dip of 70° describes the population at Upper Garbdhail. Within both the Garbdhail and Upper Garbdhail sections the sheets dip both to the west and east thus differing from the other sections. For the Sgurr nam Meann and Lighthouse sections the dips show widespread variation and no modal class can be identified, with confidence. The sheets of the An Acairseid section show a normal distribution about the 51° - 60°

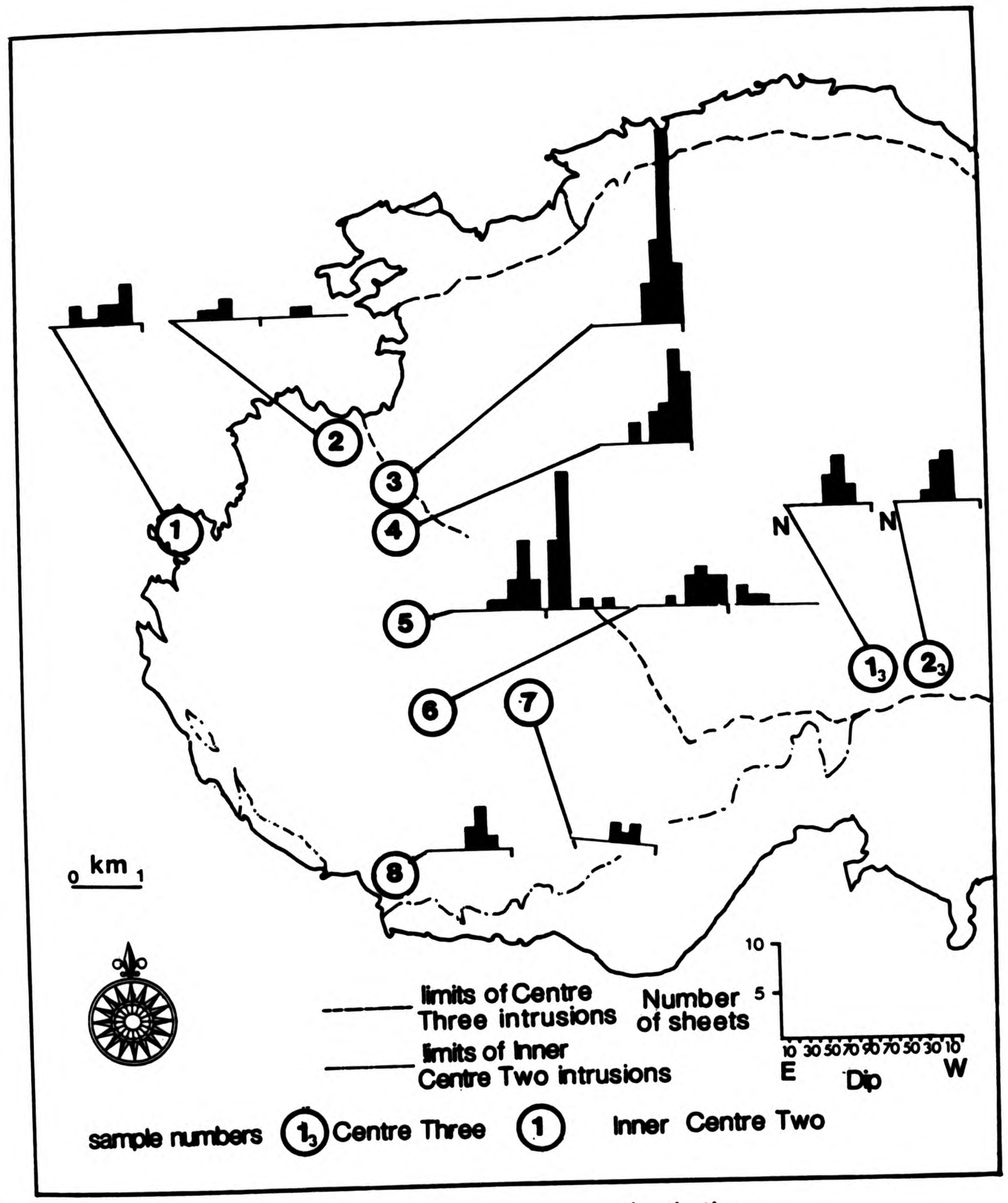

Fig.5.4.4 Distribution of dip of cone sheets per traverse of both the Inner Centre Twoand Centre Three sets

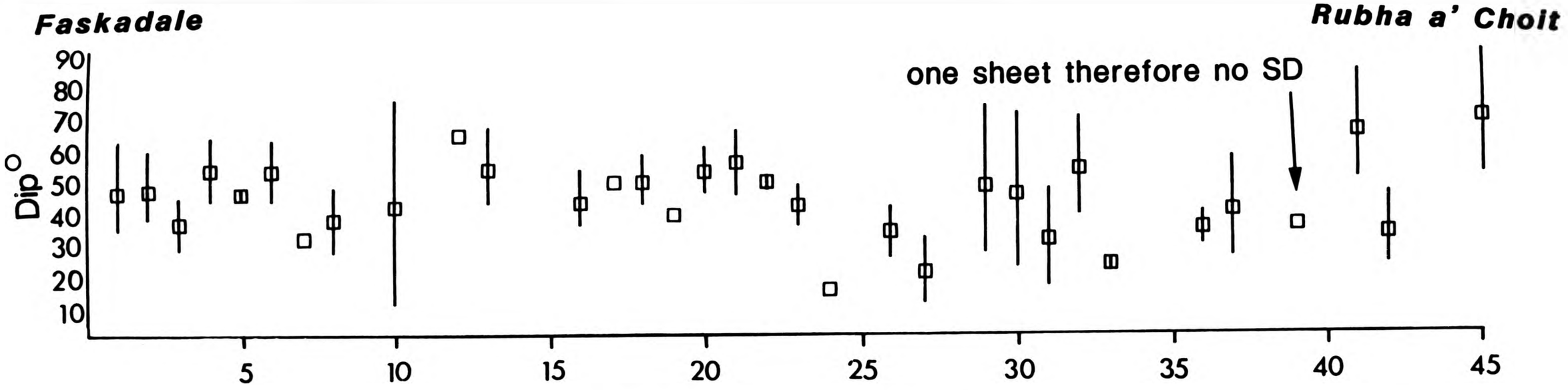

Fig.5.4.5 Centre One

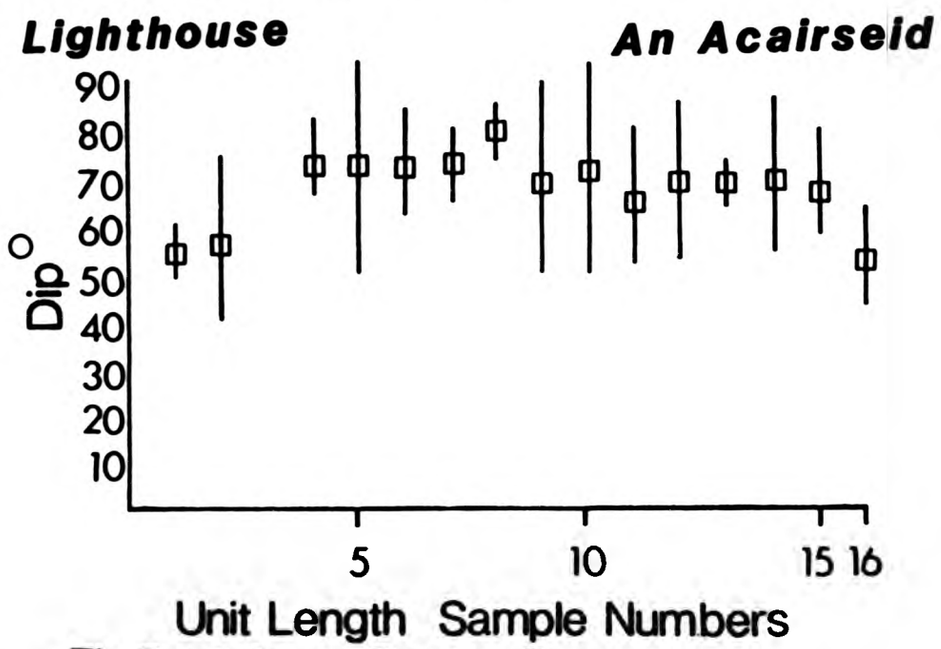

Fig.5.4.8. Inner Centre Two

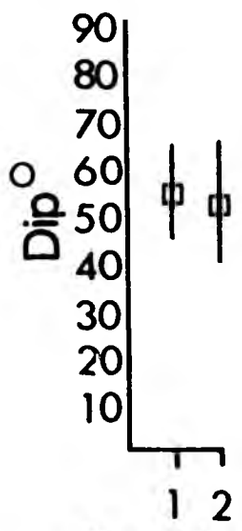

Fig.5.4.9. Centre Three

Mean Dip □

Standard Deviation |

Figs.5.4.5.,8.,9. Average Dip per Unit Length in a W to E traverse, N to S for Inner Centre Two

class. The average dip values for the majority of the Inner Set of Centre Two sections are 70°, whereas for the Sgurr nam Meann, Lighthouse and An Acairseid sections the average dip occurs between 54° and 56° (Fig.5.4.7). Figure 5.4.8 shows the standard deviation for all Inner Centre Two sections, indicating the large range within the sample. The Outer and Inner Groups mentioned above are prominent in Fig.5.4.8, with the Outer Group of sheets having lower mean dips than the sheets forming the Inner Group.

5.4.4 Centre Three

For both unit lengths the modal class is 51°-60°, although in the second unit length the peak tends to spread into the 41°-50° class (Fig.5.4.4). Mean dips show a decrease in the second section, with respect to the first, that is 52° to 57°, with the standard deviation being larger in the second section (Fig.5.4.9).

5.4.5 Summary

Centre One unit lengths show multimodality of dip and a large range of standard deviation and in comparison with the Outer Centre Two unit lengths (Fig.5.4.2 and 3) the whole of the Centre One traverse shows a large variation in dip. Both the north and south coast sections of Outer Centre Two show a similar range in dip and standard deviation, the distribution having a wave-like form. The Inner Centre Two section shows two groupings (Fig.5.4.7). All the unit lengths measured for each cone

sheet set have a range of σn from 5° to 20°, which may reflect true variation, although the size of the unit length used could be a reason for the wide range. I believe that true variation is shown.

5.4.6 Dip Distribution for each Cone Sheet Set

The dip distribution for each cone sheet set is illustrated in Fig.5.4.10. The Centre One distribution is slightly skewed, with most sheets occurring in the lower angled dip classes. Sheets are present in all but the lowest angled dip class, that is 0°-10° and the modal class is 41°-50°. The Outer Centre Two cone sheets are by far the most numerous (n = 847) and it is perhaps in consequence of this that the dip approaches a normal distribution. The Outer Centre Two cone sheets have a modal class of 41° - 50°, the steepest part of the cumulative frequency curve occurs between classes 21° - 30° and 61° - 70°.

The dip of the Inner Centre Two cone sheets is skewed towards the higher angles of dip, the modal class being 71° - 80°. Although sheets occur in all classes the majority occur between 51° - 60°, with the distribution being slightly skewed towards this class.

In general, the dip distributions of the four cone sheet sets are skewed with only the Outer Set of Centre Two having a normal distribution, which may be due to the comparitively large population present in this set. All the sets, except Centre Three, show a widespread distribution of dip angle, the dip of almost all sets ranges from 0° - 90°. Despite the different

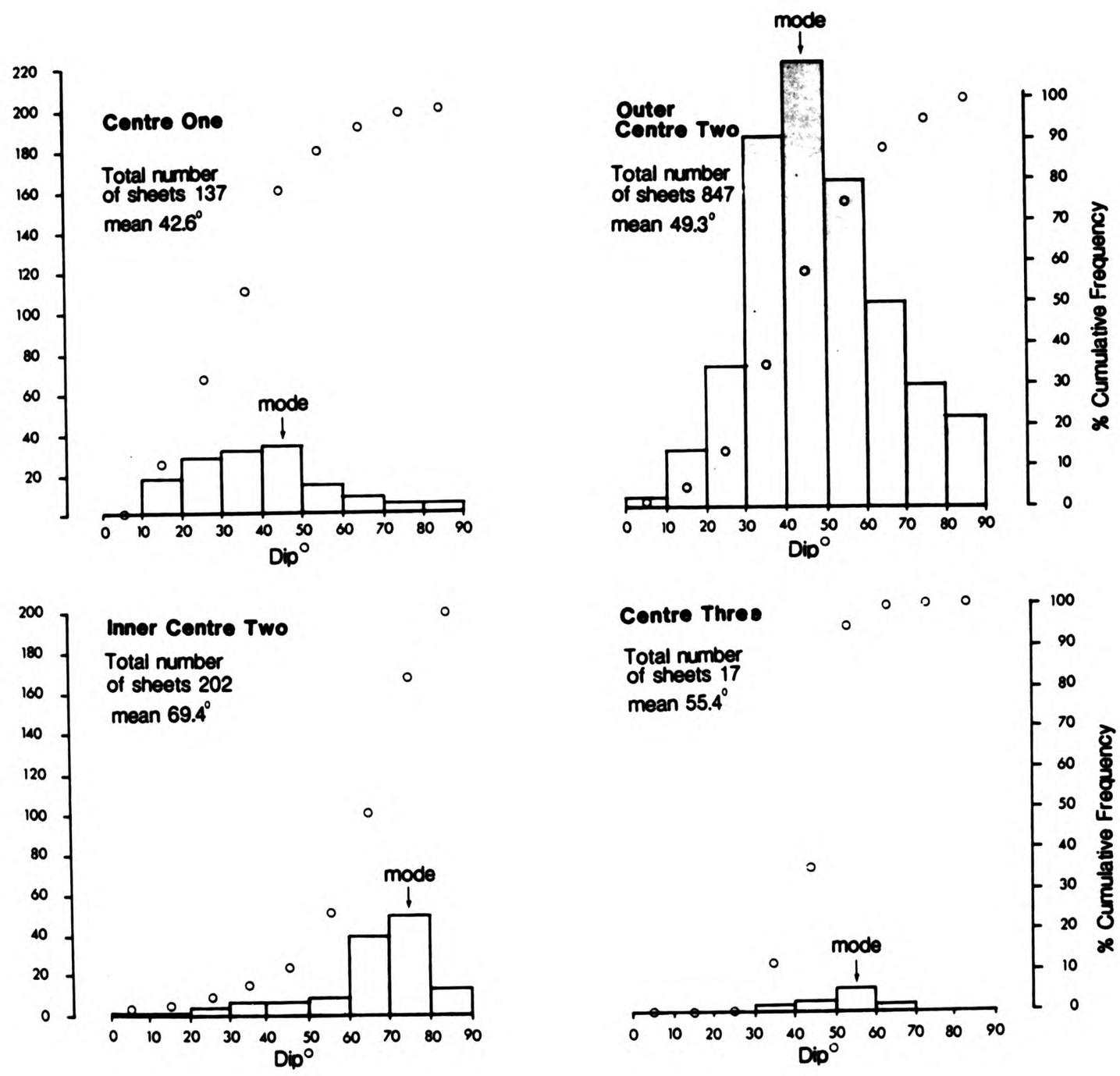

Fig.5.4.10 Dip Distribution for the Four Cone Sheet Sets of Ardnamurchan

total distributions, Centre One and Outer Centre Two have the same modal class (41° - 50°), whereas Inner Centre Two (71° - 80°) and Centre Three (51° - 60°) have steeper angled modal dips. Richey et al. (1930) commented on the difference in dip of the Outer and Inner Centre Two cone sheets and attributed the difference to the rising of the magma chamber after the intrusion of the Outer Centre Two cone sheets, and that the more steeply inclined Inner Centre Two cone sheets illustrate the shape of the cone sheets at a deeper level, thus indicating that cone sheets are trumpet shaped in vertical section (Chapter 5.11).

5.5 DIP AND STRIKE

These two primary measurements are plotted as poles to the igneous contact on a Wulff stereonet, then contoured using a Kalsbeek counting net at 0-5, then at intervals of 10 (Fig.5.5.1-3).

5.5.1 Centre One

The data has been plotted on two stereonets (Fig.5.5.1), the first consists of data collected between Faskadale and Ardtoe, the second consists of data collected between Ardtoe and Rubha a' Choit. The first group shows a widespread arc situated in the NE and SE area of the stereonet whereas the second group indicates a tighter clustering of the poles in the NE quadrant. The change in orientation of the clusters may demonstrate either a change of dip and/or strike towards the centre of activity, or

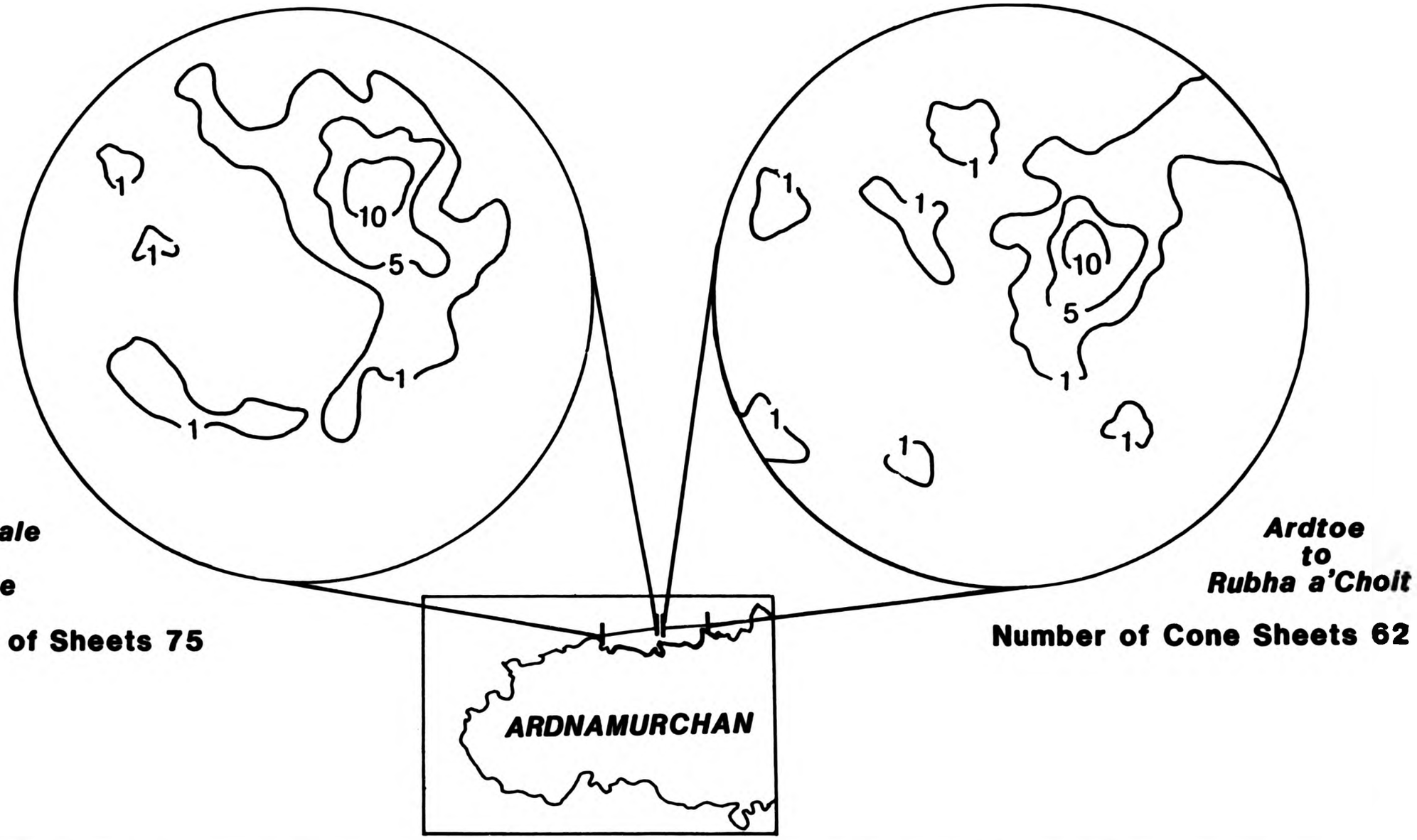

Fig.5.5.1. Centre One Cone Sheets Contour density plots of poles to cone sheet contacts for two subsections

the presence of sheets belonging to the Outer Set of Centre Two, or the presence of a subsidiary set of cone sheets, or the influence of the structure of the host rock i.e. steeply dipping Moine psammites compared to shallowly dipping Liassic limestones (Chapter 8).

5.5.2 Outer Centre Two

Fig.5.5.2 shows stereograms of five sub-regions. The first of these diagrams (Rubha an Duin Bhain to Sgeir Ghibeach) shows a large cluster of readings, the axis of which extends to the west, the second diagram (Sgeir Ghibeach to Faskadale) indicates a gradual change in orientation, with variable dip, along the traverse, that is, the orientation changes with distance from the centre. Data from the south coast section shows a similar gradual extension of the cluster axis in each of the sequential diagrams (Fig.5.5.2 Sron Bheag, Glas Eilean to Mingary Pier and Mingary Pier to Sgurr nan Eun). Figure 5.5.3 illustrates the distribution of cone sheet orientations for each of the four cone sheet sets. The diagram representing the whole of the south coast section demonstrates the form of a well developed arc. Despite the constant change in strike with distance from the centre, the dip variation is large, as evident from the large spread around the cluster axis. Ideally, if one considers that a cone sheet in three-dimensions forms a cone, then the variation in dip and strike may be accounted for in the following ways;

a) the spread of readings may be attributed to the presence of a number of cone sheet axes of different inclinations, with their apices located at similar depths beneath the surface, thus the dip would vary and the strike would show a more eccentric elliptical shape

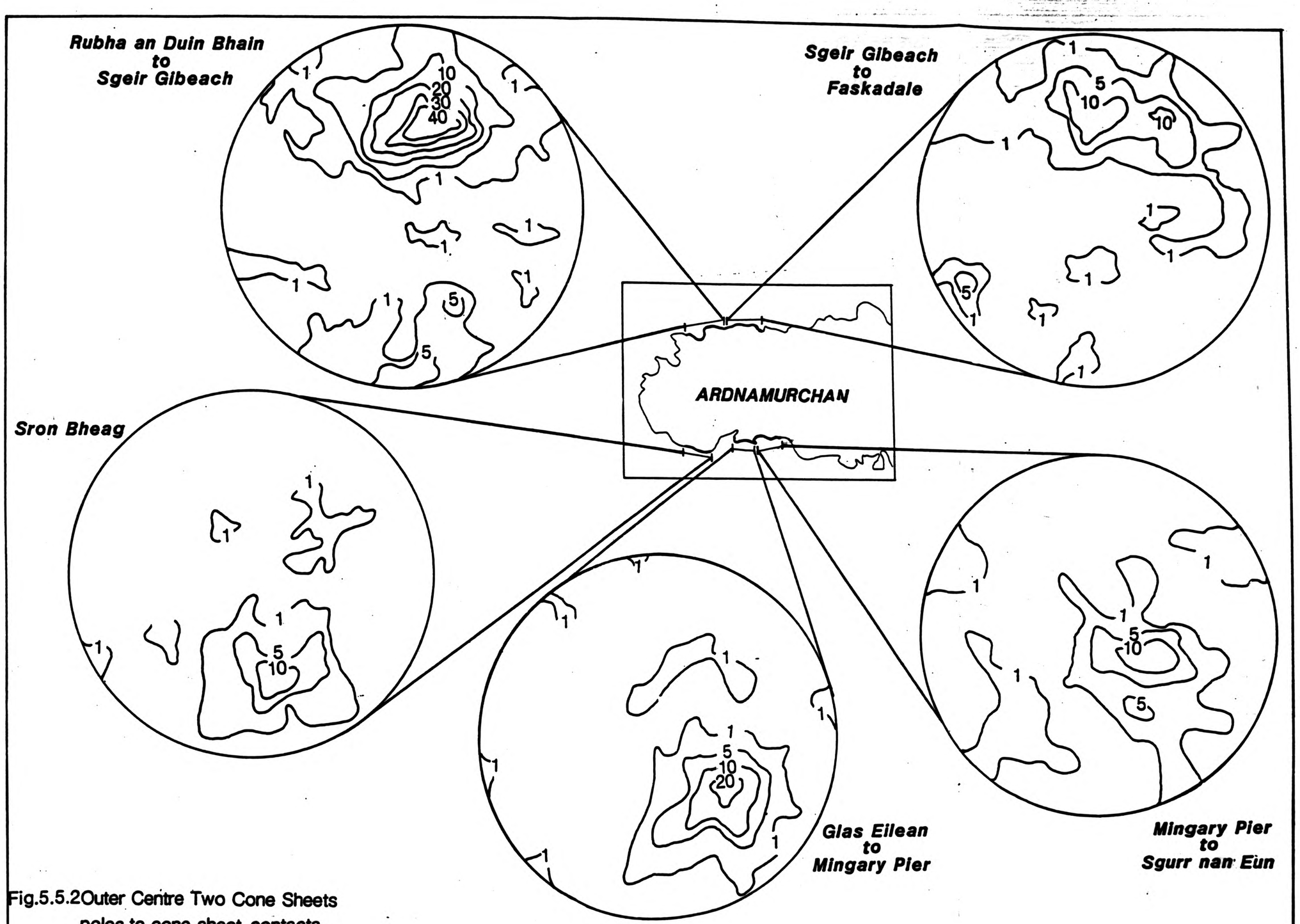

Fig.5.5.2Outer Centre Two Cone Sheets
poles to cone sheet contacts
for five sub sections

(Chapter 9).

b)a number of cone apices located at various depths beneath the surface and assuming that the dip of a sheet varies with depth then cone sheet apices located at different levels will result in a variation in dip but the strike would remain the same.

c)the dip and strike of a cone sheet is locally controlled by country rock structures (Chapter 8).

Within any one cone sheet set it is most probable that the dip and strike variation may be attributed to a) and to a lesser extent c).

5.5.3 Inner Centre Two

Fig.5.5.3 shows that the dip and strike data for these cone sheets differ from those of the Outer Set of Centre Two sheets. The poles to the sheets are located close to the perimeter of the hemisphere, due to their steep dips, combined with their conjugate pattern. As most of the sheets in a cone sheet set exploit one member of a conjugate set of fractures whilst only a few exploit the second direction (Chapter 8), the presence of a conjugate set of cone sheets in the Inner Centre Two section (Fig.5.5.3) is emphasized by the low total frequency of sheets in the Inner Centre Two cone sheet set.

5.5.4 Centre Three

These sheets form a small cluster in the SE quadrant (Fig.5.5.3).

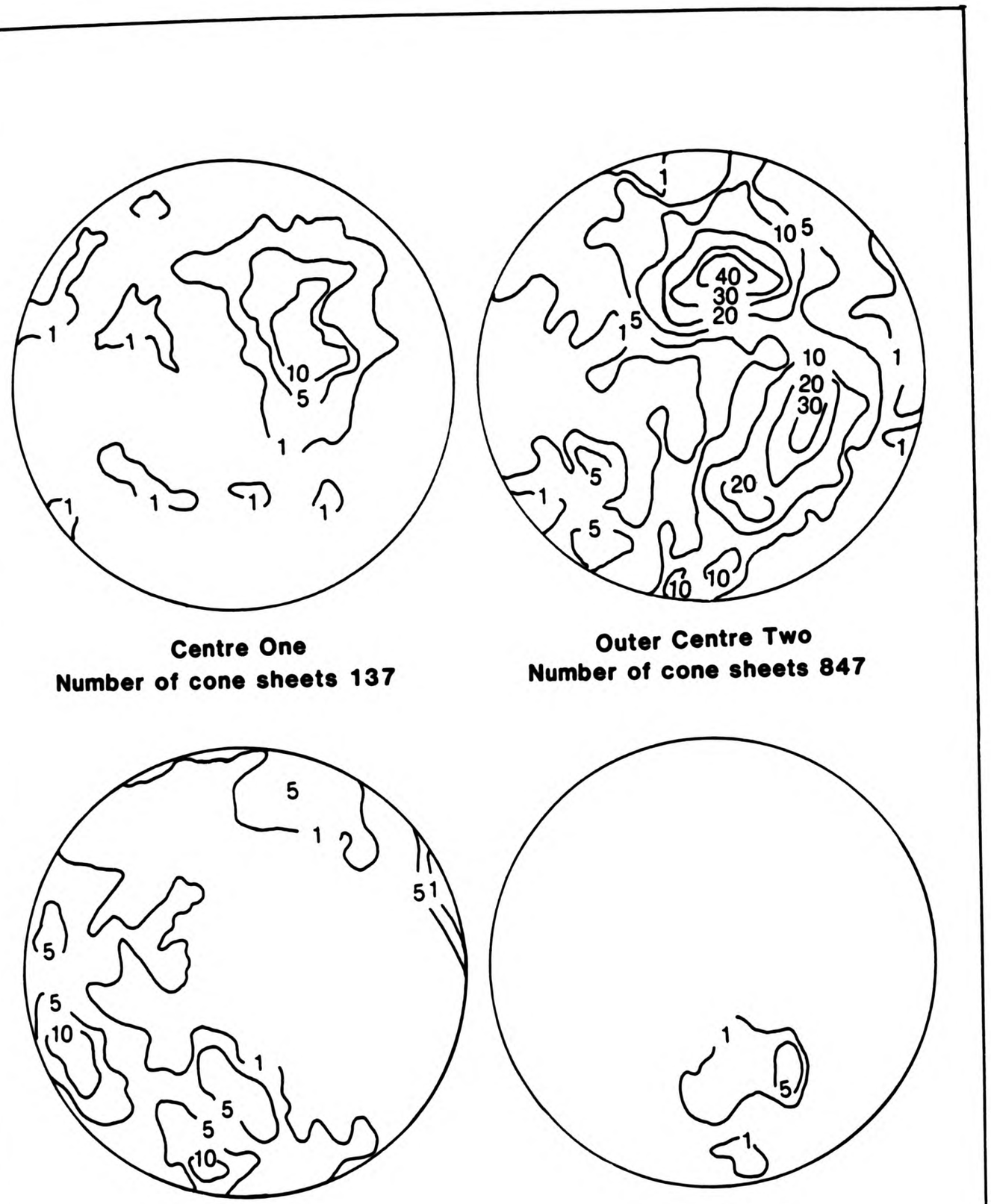

Centre One
Number of cone sheets 137

Outer Centre Two
Number of cone sheets 847

Inner Centre Two
Number of cone sheets 202

Centre Three
Number of cone sheets 17

Fig.5.5.3. Contoured density plots of poles to cone sheet contacts for the four cone sheet sets of Ardnamurchan.

5.5.5 Summary

Data for each of the sets shows an arc (Fig.5.5.3) with the degree of development depending largely on the intensity of sheet numbers in each set. A subsidiary grouping often occurs on the plots, for example, within the Outer Set of Centre Two (Fig.5.5.2) and the Inner Set of Centre Two (Fig.5.5.3), indicating the presence of a conjugate set of sheet fractures. Contoured plots of the poles to sheet contacts result in the rough outlines of small circles which define a cone (Fig.5.5.3). Assuming that the sheets dip at a constant angle with depth, the spread of the readings may indicate a number of slightly offset cones. Or, if it is assumed that sheets do not dip at a constant angle with depth, then the spread of readings may depict the variation in dip of cone sheets that intersect the surface at different levels of their profile (Chapter 10).

Centre One data forms a small circle, the axis of which dips to the NW, with a cone apical angle of 60° (plunge of axis 260/68°W) (Fig.5.5.4). Despite the large spread of readings for the Outer Centre Two data, Fig.5.5.4 demonstrates a small circle, the axis of which dips to the SW which has an apical angle of 60° (plunge of axis 280/60°W). The apical angle of the Inner Centre Two small circle is 5° (plunge of axis 056/60°) Because the Centre Three data is limited to a single cluster no axis can be determined.

As the axes of the cones determined by the dip and strike distributions are inclined at different plunge angles and in different directions they lend credit to Richey's *et al.* (1930)

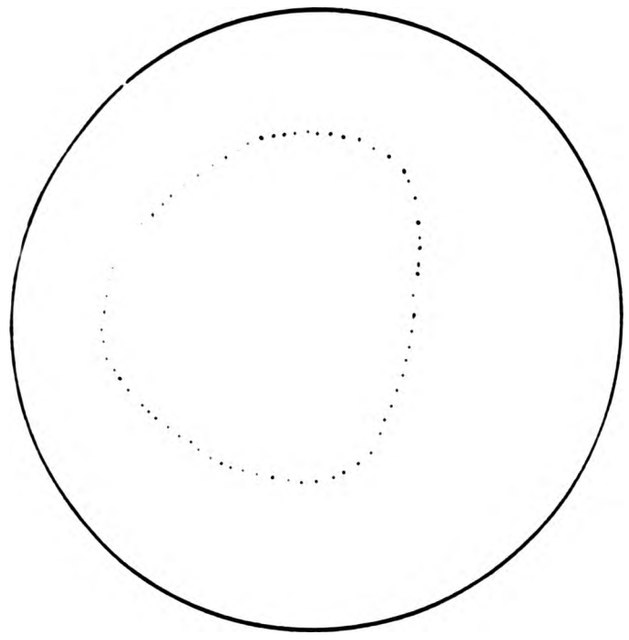

Centre One
plunge of cone axis 260/68°W

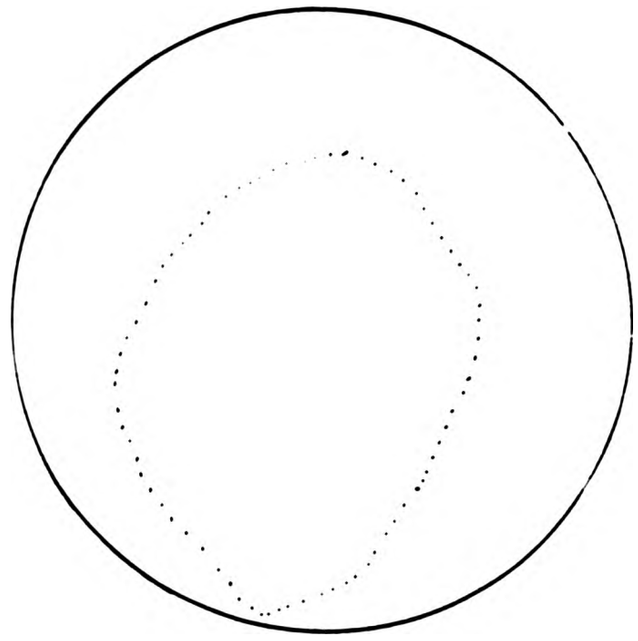

Outer Centre Two
plunge of cone axis 280/60°W

Fig.5.5.4 Small circles constructed for each cone sheet set (without Centre Three) based on the stereographic projections of dip and strike data (Fig.5.5.3)

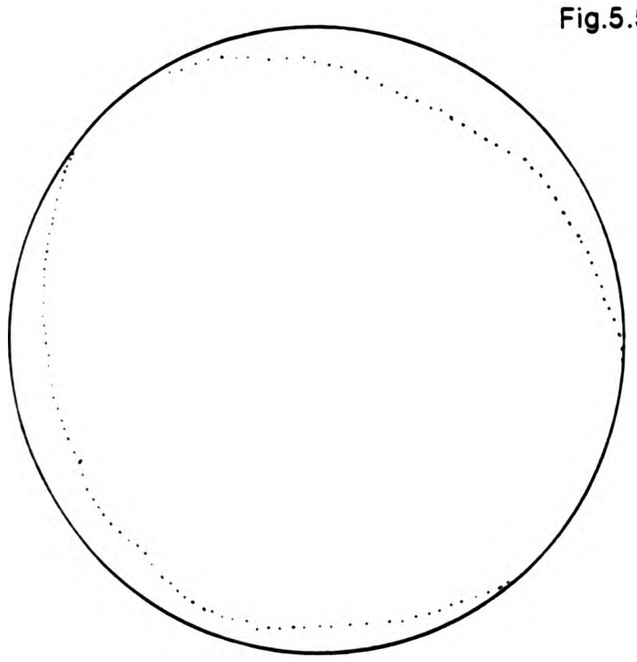

Inner Centre Two
plunge of cone axis 056/60°N

three centred hypothesis (Fig.9.2.1) arrived at by field relationships and, conversely, refute Durrance's (1967) single centred hypothesis (Fig.9.2.2).

All three small circles are derived from raw data and show a great amount of spread, which may be due to:-

a)large number of readings

b)measuring error

c)presence of sub-sets of cone sheets

d)the axis of the cone is inclined

The number of readings, even when small e.g. Inner Centre Two (Fig.5.5.3) where the total number of samples is 202, are widely distributed on the plot. Because the measuring error is ~2°, the 20° variation must be accounted for. A number of sub-sets occurring within the areas defined (Chapter 3) may be masked by the collation of all data on one diagram. It is demonstrated in Chapter9 how the shape of the cone becomes a more eccentric ellipse as a result of the intersection of the erosion surface with the cone or by varying the inclination of the cone axis. Thus, if the land surface and the cone intersect at different angles then a number of closely spaced sheets with a variety of elliptical profiles would result (Chapter 9).

5.6 STRIKE

Mapping of the geology of the Ardnamurchan peninsula by Richey et al. (1930) resulted in the recognition of the arcuate outcrop of the cone sheets. Therefore the strike of individual cone sheets and their position relative to the presumed centre

of activity to which they belong are important characteristics.

Distribution of Strike (Orientation) per Unit Length

5.6.1 Centre One

Figure 5.6.1 shows 35 strike diagrams for the 6km section. In an east to west traverse, the modal strike changes from 330° at Rubha a' Choit in Moine host rock, to 300° at Port an Bain in agglomerate host rock. A variation of strike is seen in the unit lengths from Rubha a' Choit to Ockle Point; the modal strike at Rubha a' Choit is 330° and 320° at Ockle Point. The change in strike within this traverse (Fig.5.6.1) may be due to the exploitation of the prominent host rock structures (Chapter 8) eg. the bedding in the Mesozoic rocks which are unconformable on the Moine rocks exposed at Ockle Point. West of Ockle Point the strike of the sheets varies from 270° to 310°. Most of the Swordle Bay sheets occur in Lias limestones, the Moines being exposed farther to the west. In the volcanic agglomerates at Ardtoe, a modal strike is difficult to ascertain, because the sheets are few in number and have widely variable strike, contrasting sharply with those cone sheets which occur in the Swordle Bay sections, which are intruded into Moine and Lias rocks. Continuing along the east to west traverse the sheets around Achateny strike at 310° which changes to 300° at Port an Bain. The traverse west from Port an Bain for 1.5km is characterised by a low frequency of sheets and inconsistent strike, for example, 310°, 290°, 030°. However, the four sections immediately east of Faskadale show a large number of sheets

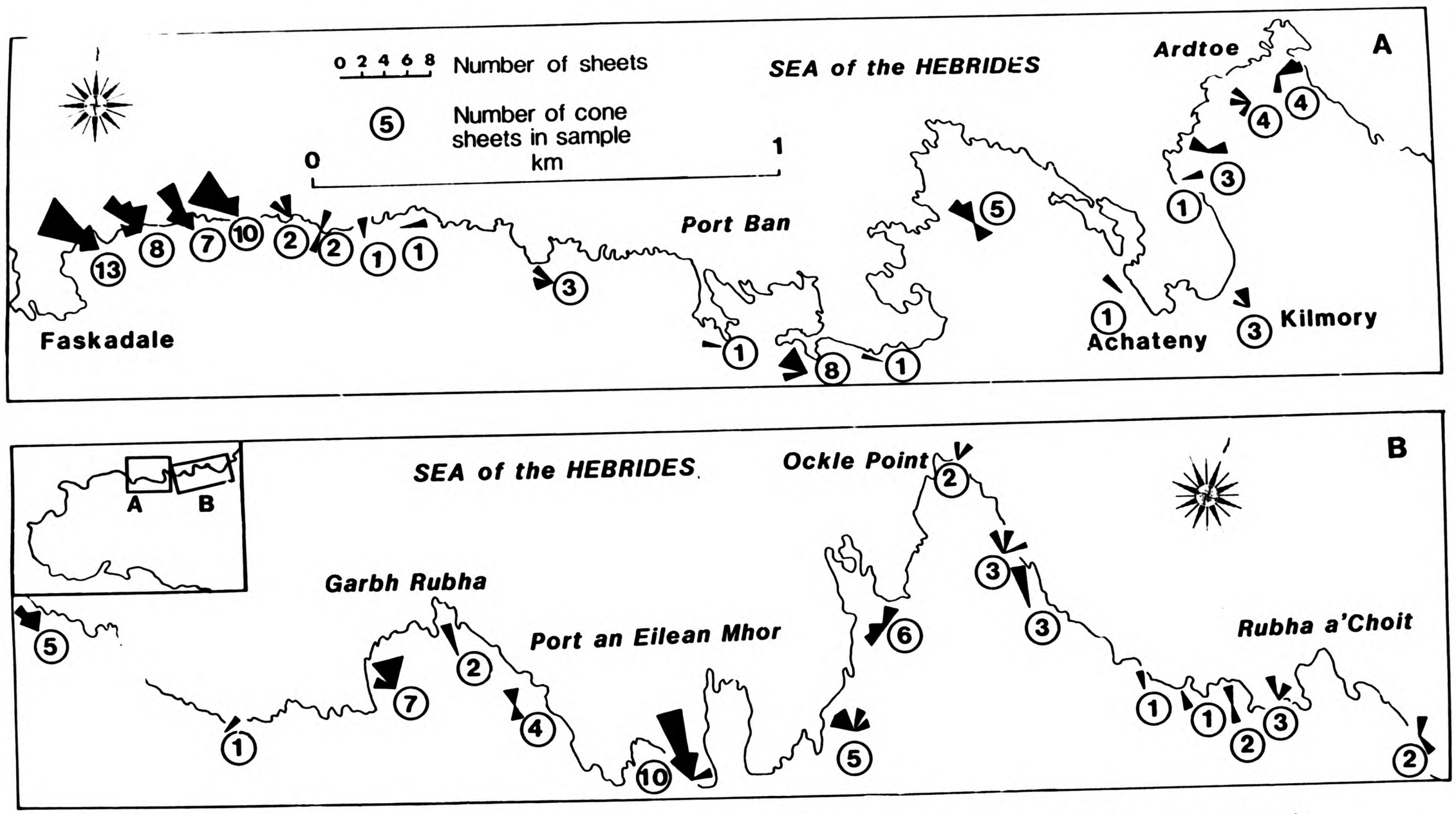

Fig.5.6.1. Centre One Distribution of Orientation (measured clockwise from dip) of Cone Sheets per Unit Length

which have a modal strike of 300°-310°, although the strike ranges from 300° to 360°.

Summary: Strike of the Centre One cone sheet set may be characterised by their modal value, which is 300°-310°.

5.6.2 Outer Centre Two

North Coast. Figure 5.6.2 displays the strike of the sheets measured. For the Rubha an Duin Bhain and Rubha Carrach sections the modal value is 270°. Continuing the traverse towards Sgeir Ghibeach the modal value oscillates between 270° and 310°. The sections that occur between eastings 46 and 48 are characterised by a large number of samples. On the western side of Rubha Dubh an Aighe the readings are spread between the 290°, 270° and 250° classes. From Sgeir Ghibeach to Faskadale the number of samples per unit length are lower than those farther west, consequently a modal value does not represent the distribution very well. However, the unit lengths at Sloch na Bracha (484713), (488714), (489713) and (492713) give resultant diagrams similar to those located farther west and have modal values of 250°, 250°, 270° and 250°, respectively. At Faskadale the strike of the sheets shows a more generalised spread.

Summary: The main trend of the strike of the cone sheets along the north coast changes from 290° in the west to 270° in the east with localised variations in modal strike up to 40°.

South Coast. A modal strike of 080° represents the strike of the 600m section of Sron Bheag (453627) (Fig.5.6.3). East of Sron Bheag (466624) the strike of sheets is inconsistent and differs from the unit lengths to the west.

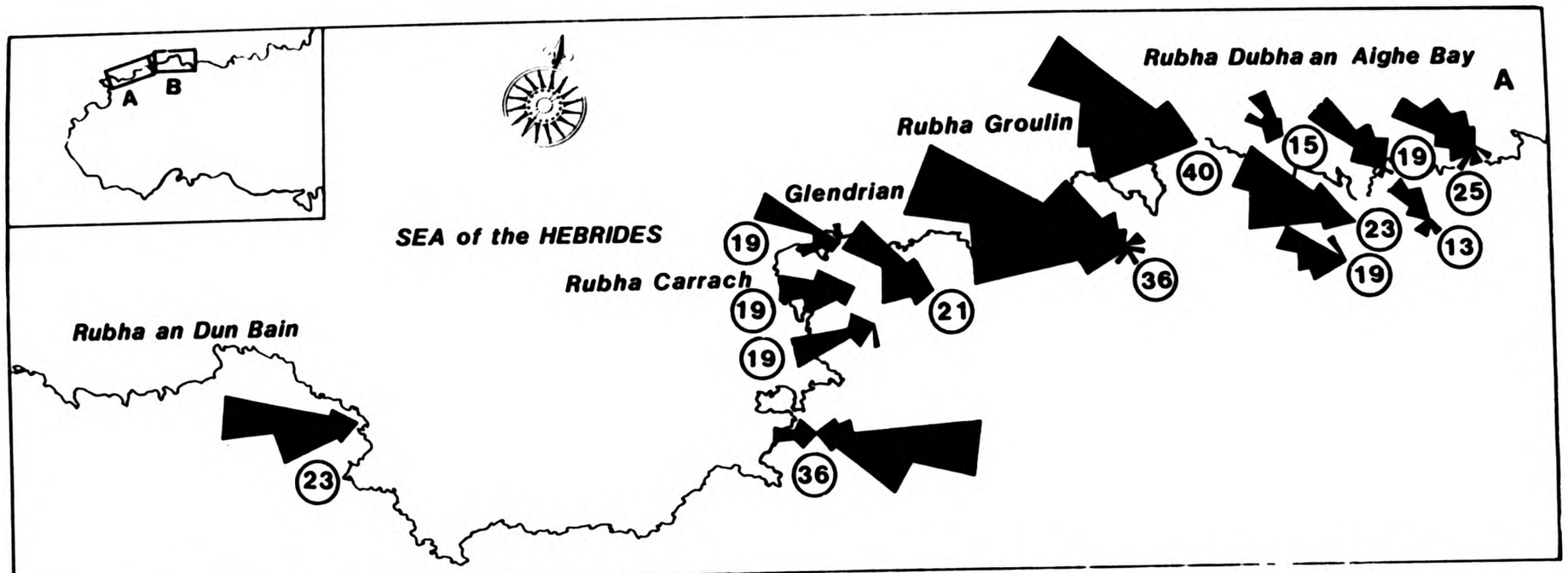

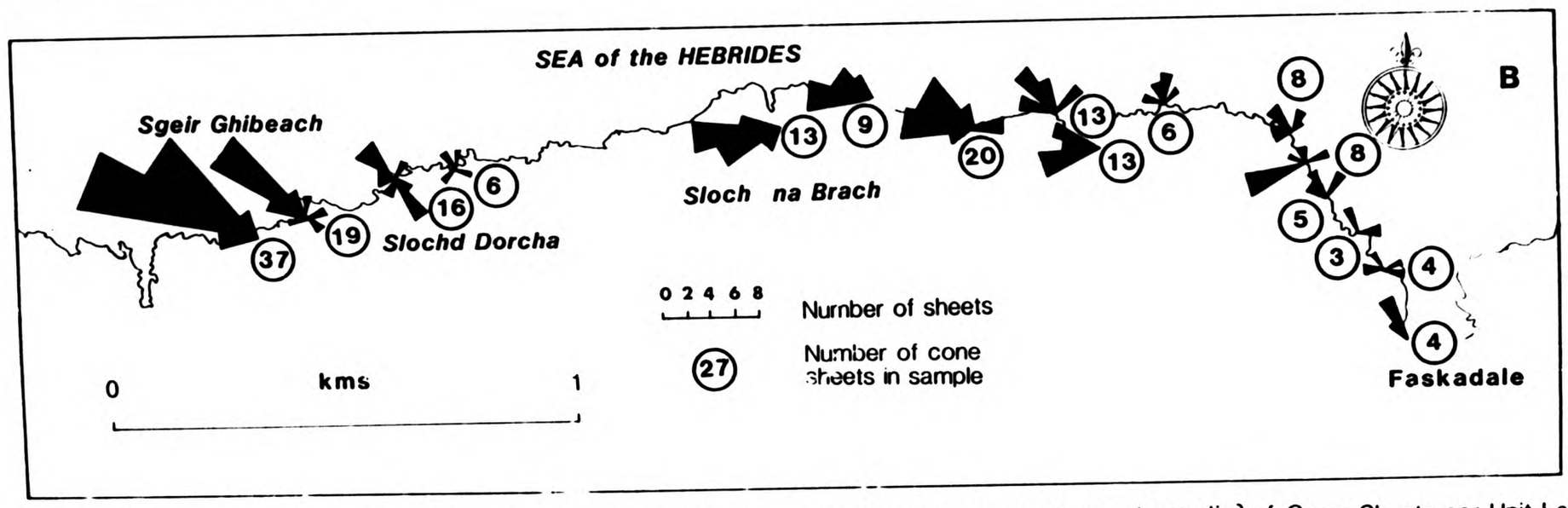

Fig.5.6.2. Outer Centre Two North Coast Distribution of Orientation (measured clockwise from dip) of Cone Sheets per Unit Length

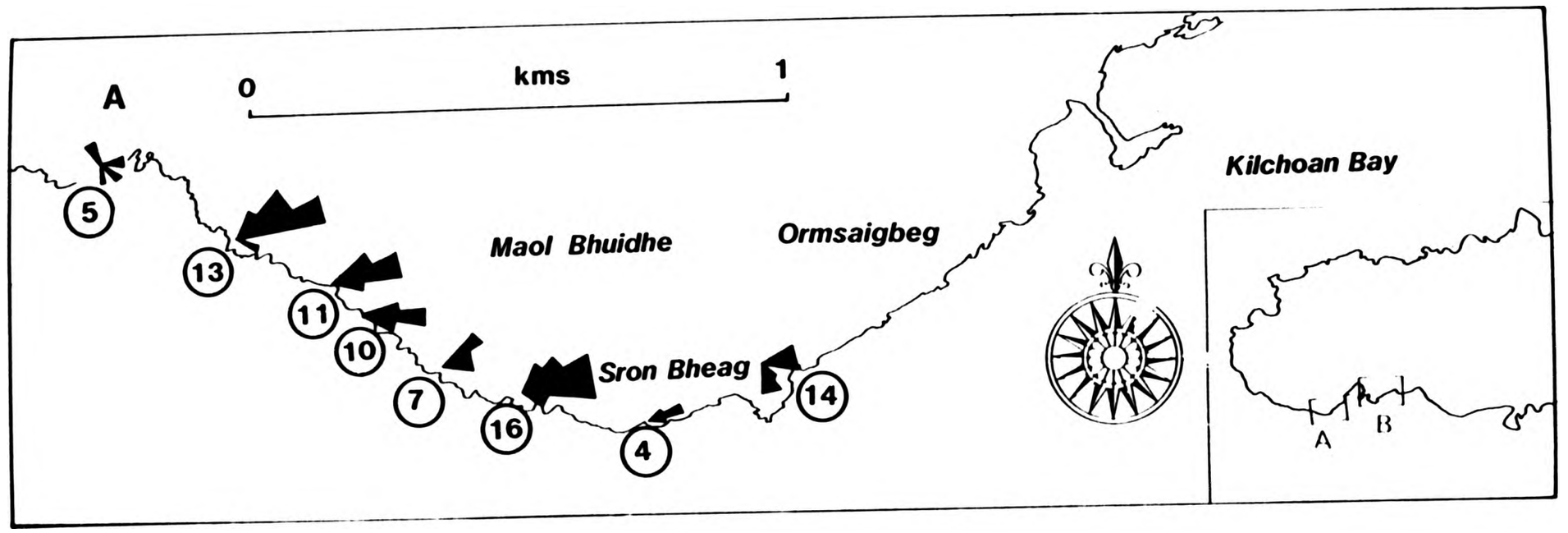

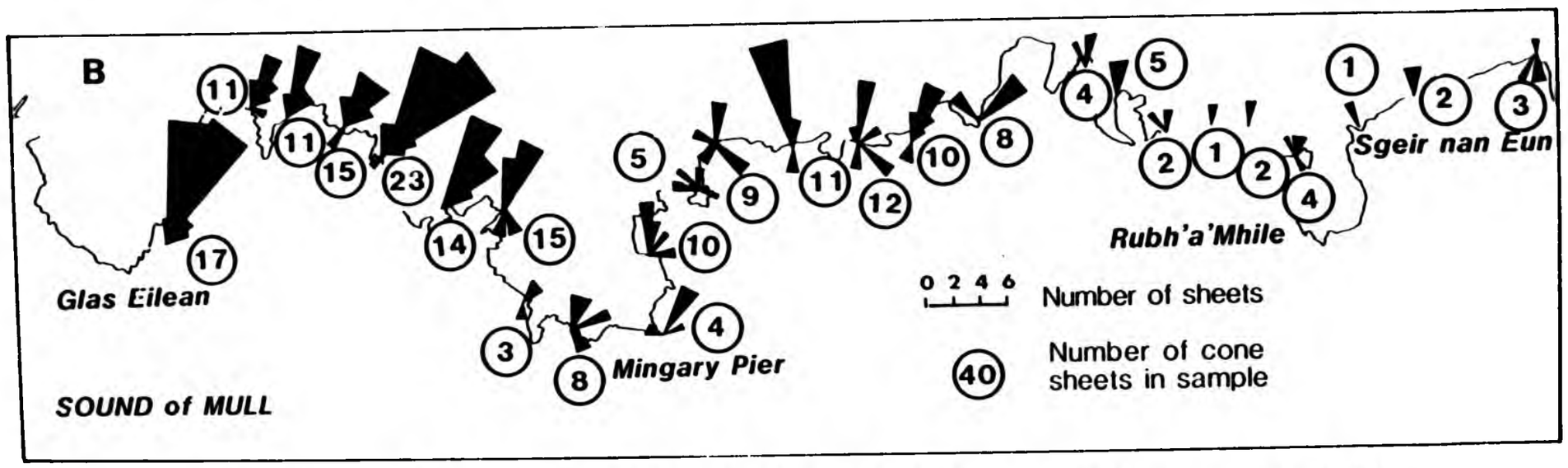

Fig.5.6.3. Outer Centre Two South Coast Distribution of Orientation (measured clockwise from dip) of Cone Sheets per Unit Length

Few cone sheets characterise the coastal strip around Kilchoan Bay, i.e. from Ormsaigbeg to Glas Eilean, as the trend of the cone sheets is parallel to the coast. From Glas Eilean to Mingary Pier the modal strike value is 030°, although at (492627) the modal class has a strike of 050°. East of Mingary Pier the modal value oscillates between 350° and 010° with the strike readings spread among the classes on either side of the modal class, similar to the north coast section. Inconsistency characterises the strike of the cone sheets to the east of Mingary Pier, a fact which is emphasised by the small number of cone sheets per unit length in this area (Fig.5.6.2).

A change in modal orientation occurs from 030° to 050° towards Rubh'a'Mhile, where the mode swings back to 010°. Although the sample size is small at this location, there does appear to be a link between percentage dilation (Chapter 6) and this change in strike (Fig.6.3.2) which is thought to mark the boundary between the cone sheet sets of Centre One and the Outer Set of Centre Two. In order to substantiate this hypothesis the Allt Choire Mhuilinn valley and a section from Sgeir nan Eun to Rubh' a' Mhile have been investigated. As indicated in Fig.5.6.2 few cone sheets occur. However, the Sgeir nan Eun section gives results weighted towards the assumption of a more northerly trending set of sheets, that of Centre One. The Allt Choire Mhiulinn section gives a more generalised distribution and therefore was of little help in elucidating the limits or overlaps of the two adjacent cone sheet sets.

Summary: From Sron Bheag to Rubh' a' Mhile the modal strike of the cone sheets of the south coast section changes from 080° to 010°, a gradual change in orientation of 70°.

5.6.3 Inner Centre Two

Three unit lengths termed the Outer Group occur just within the Hypersthene Gabbro, whereas the remaining 13 sections termed the Inner Group are located towards the focus of Centre Two activity. For the Outer Group the modal value at An Acairseid is 070°, whilst at the Lighthouse and Sgurr nam Meann sections the modal strike is 190° (Fig.5.6.4). The Inner Group form a north to south traverse, begining in the north, on the upper slopes of Beinn Bhuidhe, a modal value of 160° is obtained, whereas the strike of sheets on the lower slopes of Beinn Bhuidhe show a wide spread of readings with no clear modal class (Fig.5.6.4). The most southerly extent of the Inner Group is in the Garbdhail valley sections, where the modal strike is 110°, and an almost identical result is obtained from the slopes of Beinn na Seilg.

Summary:Figure 5.6.4 illustrates the gradual change in strike of the Inner Group from 160° in the north to 110° on Beinn na Seilg, although a number of sheets on the lower slopes of Beinn Bhuidhe and Garbdhail have strike values of other orientations. The unit lengths comprising the Outer Group seem to form a separate set of sheets.

5.6.4 Centre Three

Both unit lengths measured on the northern slopes of Abhain Chro Bheinn indicate a change of strike from 070° to 090°, from east to west, respectively (Fig.5.6.5).

Summary:Figure 5.6.6 shows the distribution of strike of cone sheets for each of the cone sheet sets each showing, in varying

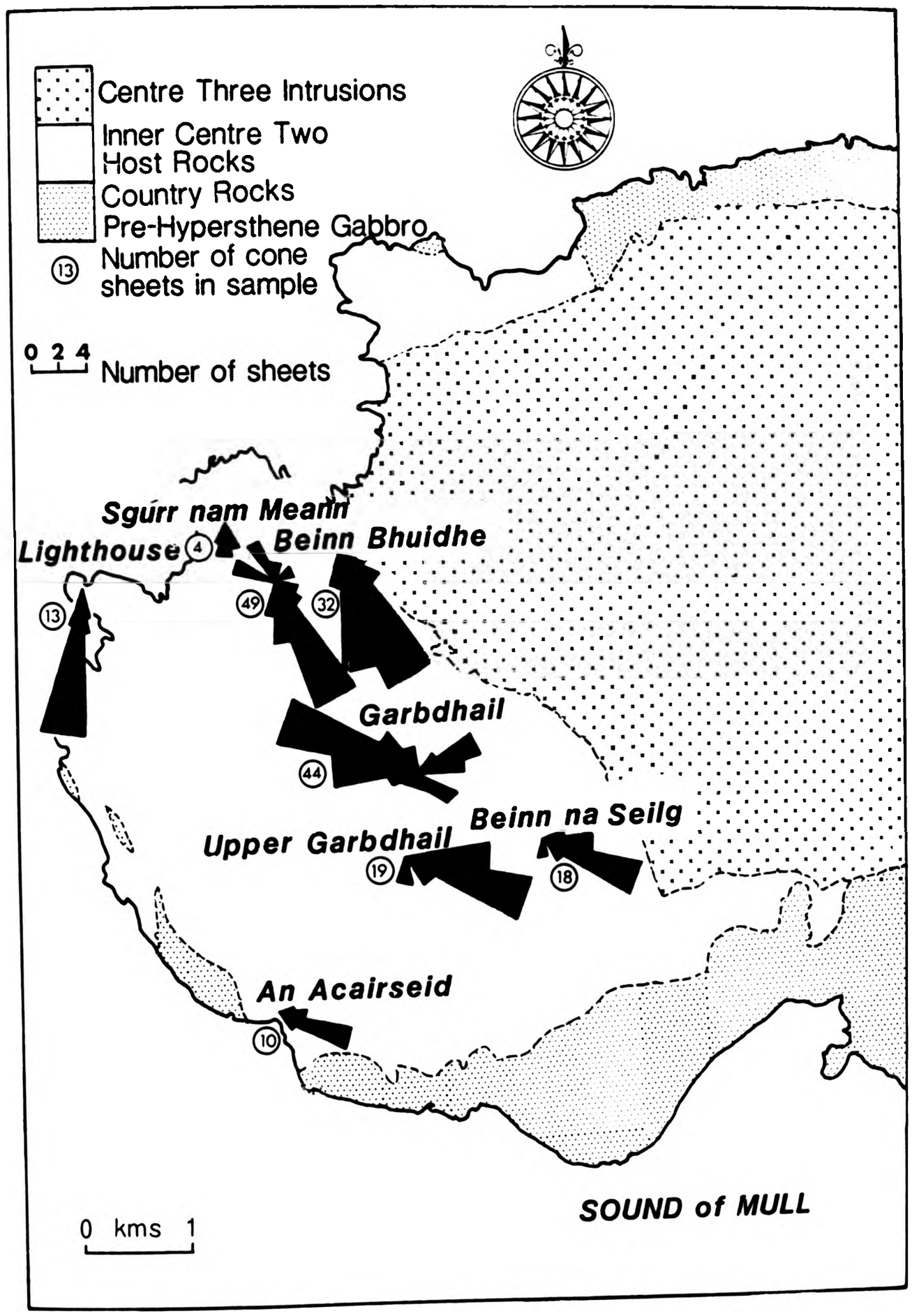

Fig.5.6.4. Inner Centre Two Distribution of Orientation (measured clockwise from dip) of Cone Sheets per Unit Length

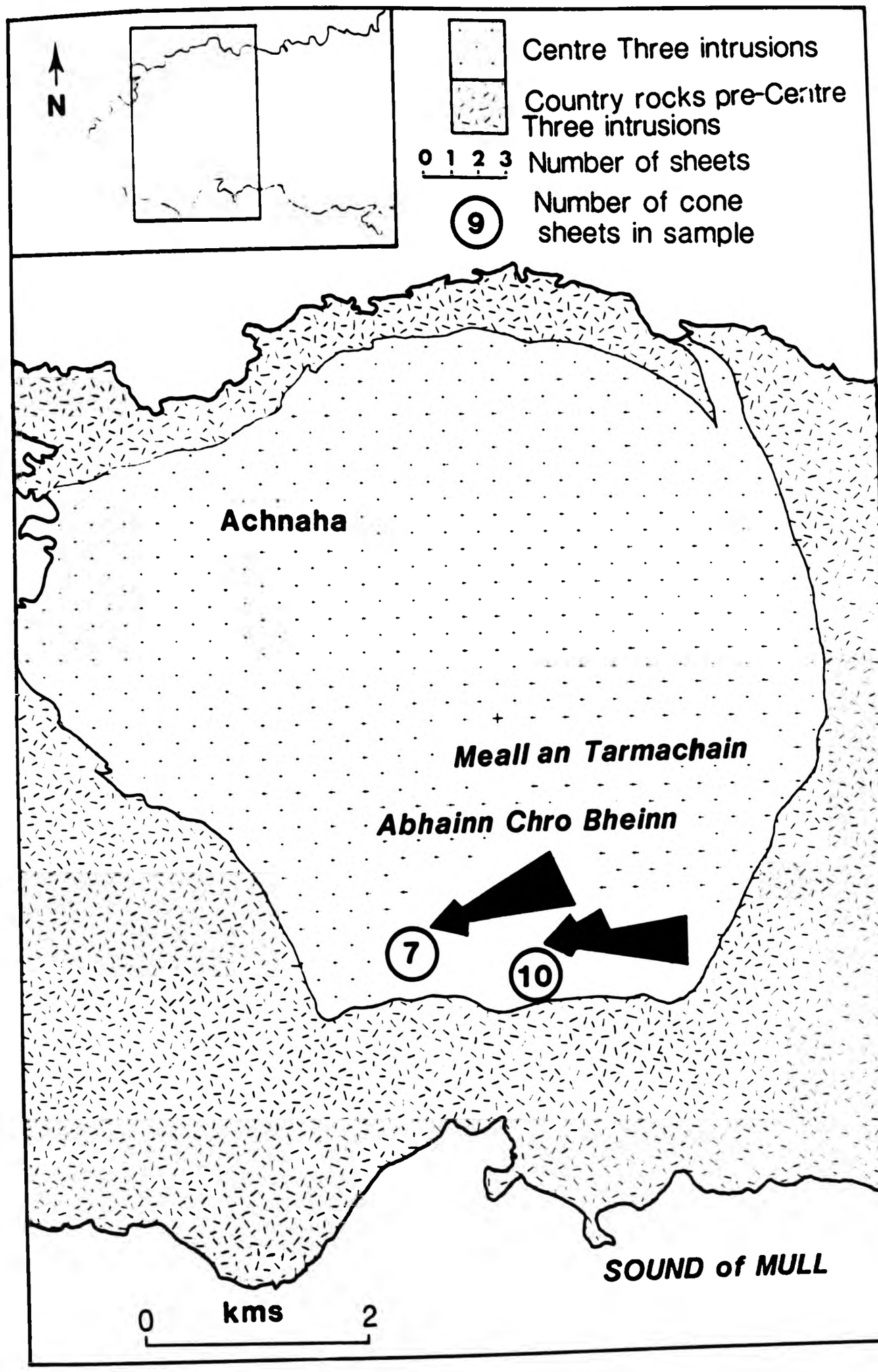

Fig.5.6.5 Centre Three Distribution of Orientation (measured clockwise from dip) of Cone Sheets per Unit Length

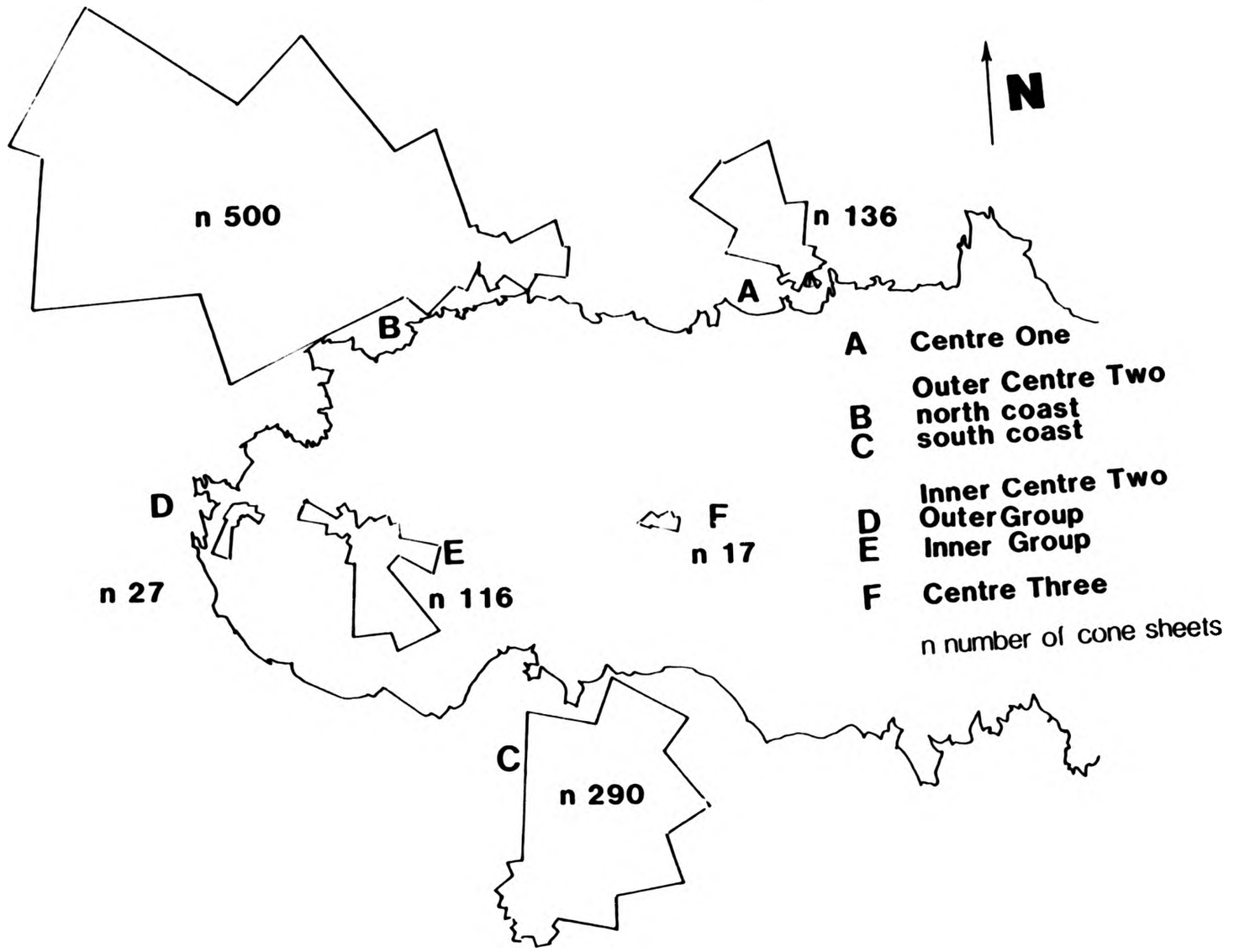

Fig.5.6.6 Orientation (measured clockwise from dip) distribution of each cone sheet set

degrees, the spread of orientation of sheets over several classes. This is particularly prominent in the Outer Centre Two cone sheet set.

5.7 MEAN STRIKE

Arithmetic mean, median and geometric mean (mode) values are used to describe the population from which they are derived. To determine an average value of a 360° distribution neccessarily requires a different method, therefore the Tukey Chi^2 test has been used (Chapter 3).

5.7.1 Centre One

The Chi^2 results emphasize a change in orientation from 340° to 310° along the east to west traverse. The marked change in orientation in the western extremities may be due to the presence of sheets belonging to the Outer Centre Two.

5.7.2 Outer Centre Two

North Coast. The Chi^2 results tend to refine the oscillations illustrated by the modal distributions. For example, from Rubha Carrach to Glen Drian, the modes indicate a sharp change in orientations from 250° to 310°, whereas the Chi^2 values are 289° to 301°, thus indicating a more gradual change. Conversely, it may be stated that the Chi^2 method merely masks the true variation of the orientations of the cone sheet sets. However, oscillations along the west to east traverse are iden-

tified in both mode and Chi^2 distributions. The first two sections of the traverse have mean strike values that trend to the west and the second two switch back to the more northerly direction (301°). Over the next six sections an overall increase to 308° is noted. When the traverse nears Faskadale, there is a slight reversion to a more westerly strike (266°). These oscillations may indicate that the Outer Centre Two cone sheet suite consists of a number of discrete subsets which were perhaps intruded at slightly different times.

South Coast. From Sron Bheag to Mingary Pier the sheets change orientation from ENE to NNE. In general, the strike of the cone sheets at the eastern extremities of the south coast section possess a more northerly trend.

5.7.3 Inner Centre Two

Chi^2 values for sections located near the focus of Centre Two activity, at Aodainn, illustrate a gradual change in orientation of the cone sheets, as do the modal values, although it should be noted that the strike of sheets in the Garbdhail section differs greatly from the other sections. Chi^2 values seem to support the existence of a subset of cone sheets located at the perimeter of the Hypersthene Gabbro.

5.7.4 Centre Three

Chi^2 values of the data within the west and east unit lengths are 066° and 076°, respectively. These values reflect

the modal distributions of the data and illustrate a slight shift in the strike of the sheets towards a more northerly strike in the eastern unit length.

5.8 THICKNESS DISTRIBUTION

5.8.1 Centre One

Due to the low frequency of sheets in the east the thickness distribution per unit length is scattered (Fig.5.8.1), although most sheets occur in the <0.5m, 0.5-1m and 1-1.5m classes. 1.5km east of Rhuba Choit cone sheet numbers increase and further illustrates the prominence of thin sheets (<0.5m thick). The maximum thickness recorded for a sheet is 15m (unit length 32). The scattered thickness distribution reflects the low frequency distribution of the sheets. In unit lengths 2,3 and 4, east of Faskadale, the 0.5-1m class, marginally, contains the most sheets, the sheets contained in unit length 1 have a modal class thickness of <0.5m. Figure 5.9.1 shows the thickness distribution for the whole cone sheet set and emphasizes the predominance of the thinner sheets, that is sheets from 0.1m to 1.5m thick. This squewed distribution is further emphasized by the cumulative frequency curve, 70% of the data occur in the first three classes of thickness.

5.8.2 Outer Centre Two

North Coast. Thickness distribution of all sheets contained in the north coast traverse is between 0.1m and 11m, with

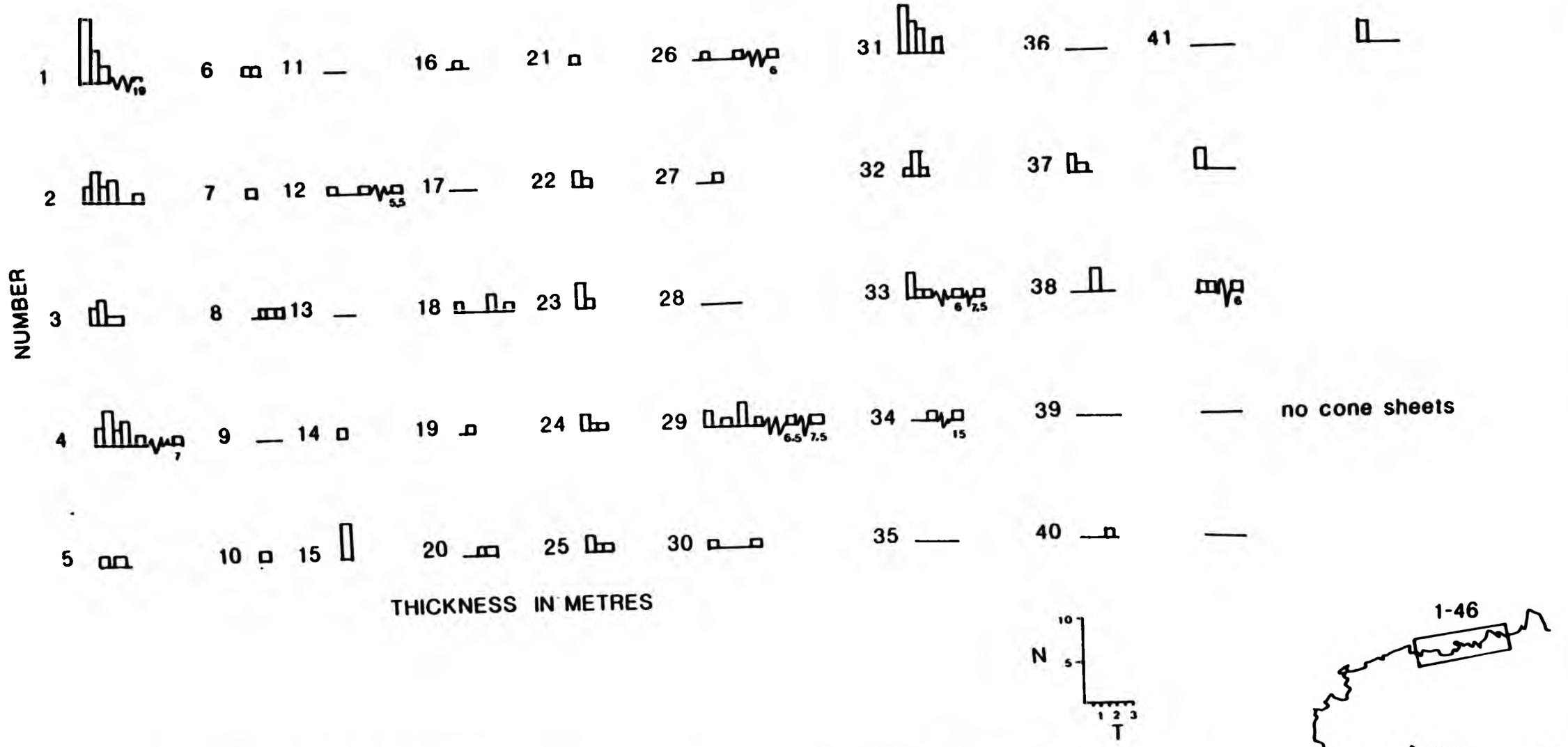

Fig.5.8.1 Distribution of thickness of cone sheets per unit length across the Centre One traverse

almost all sheets being less than 6m thick. All, except one, unit lengths contain sheets which are <0.5m thick and this is the modal class in all unit lengths except 2,6,11,17 and 25, in which case the 0.5-1m class is the modal class (Fig.5.8.2). Unit lengths to the west of Sgeir Ghibeach contain more sheets in the 2.5-6m range than the unit lengths to the east of Sgeir Ghibeach. Cone sheets east of Sgeir Ghibeach principally occur in the 0.1-3m range. Figure 5.9.1 shows the total distribution for this traverse and emphasizes the prominence of the first two classes, combined they contain 72% of the data, the three adjacent classes (sheet thicknesses up to 3m) account for 23% of the sheets with the remaining 5% of cone sheets having thicknesses of >3m.

South Coast. The modal thickness class of the majority of the unit lengths is <0.5m except unit lengths, 1,7,15,16,17,19 and 26 in which the modal class is 0.5-1m thick (Fig.5.8.3). Most sheets of the Sron Bheag section (unit lengths 1-8) occur in the first three thickness classes that is <2m thick, whilst from Glas Eilean to the east of the traverse, most unit lengths have sheets which range in thickness up to 6m. Maximum thickness of sheets contained in this traverse is 35m. Figure 5.9.1 summarises the thickness distribution of all cone sheets of the traverse and emphasizes the concentration of sheets in the first three thickness classes (from 0-1.5m thick) which account for 71% of the cone sheets with 89% of the cone sheets being <3m thick.

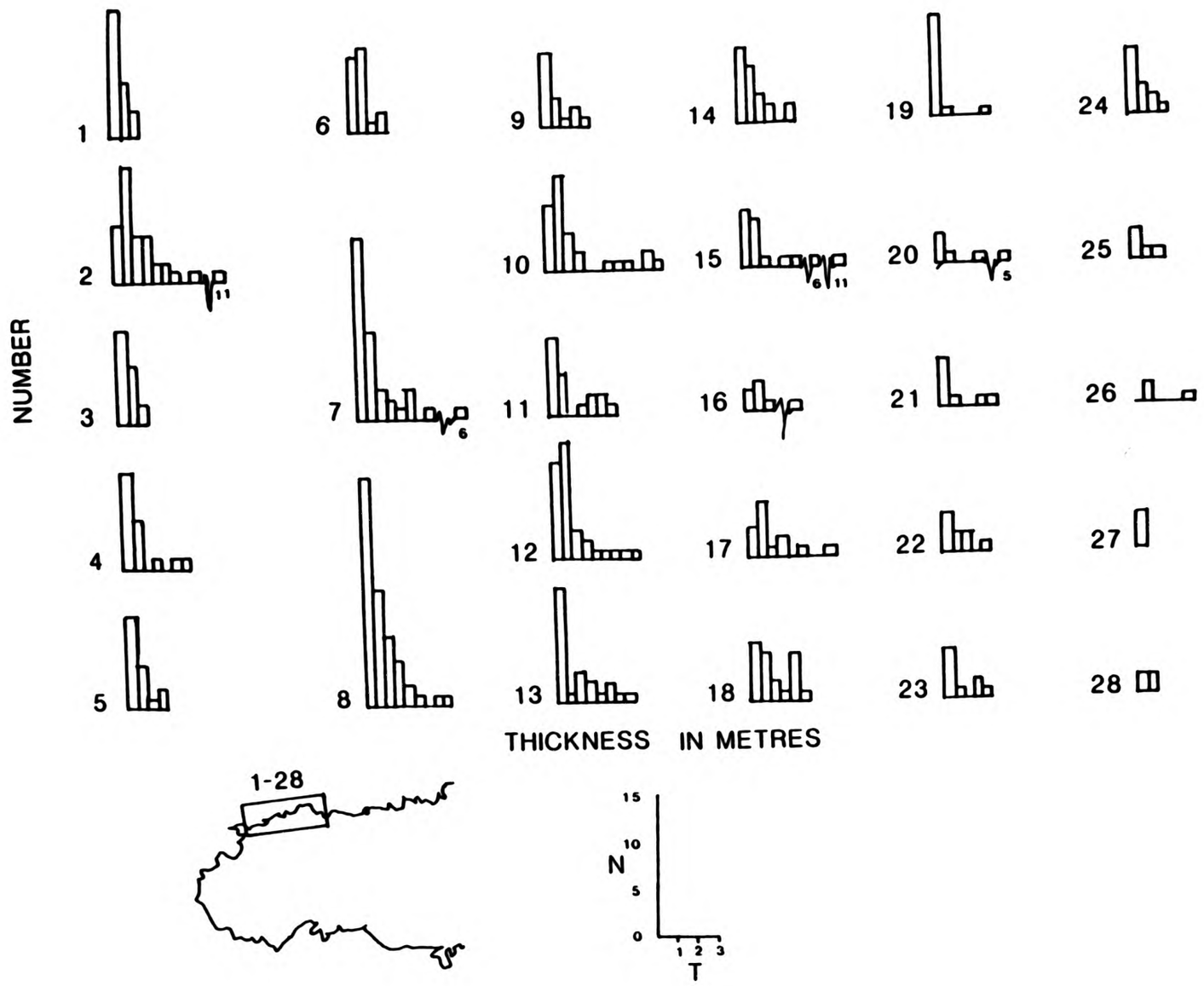

Fig.5.8.2 Distribution of thickness of cone sheets per unit length across the Outer Centre Two north coast traverse

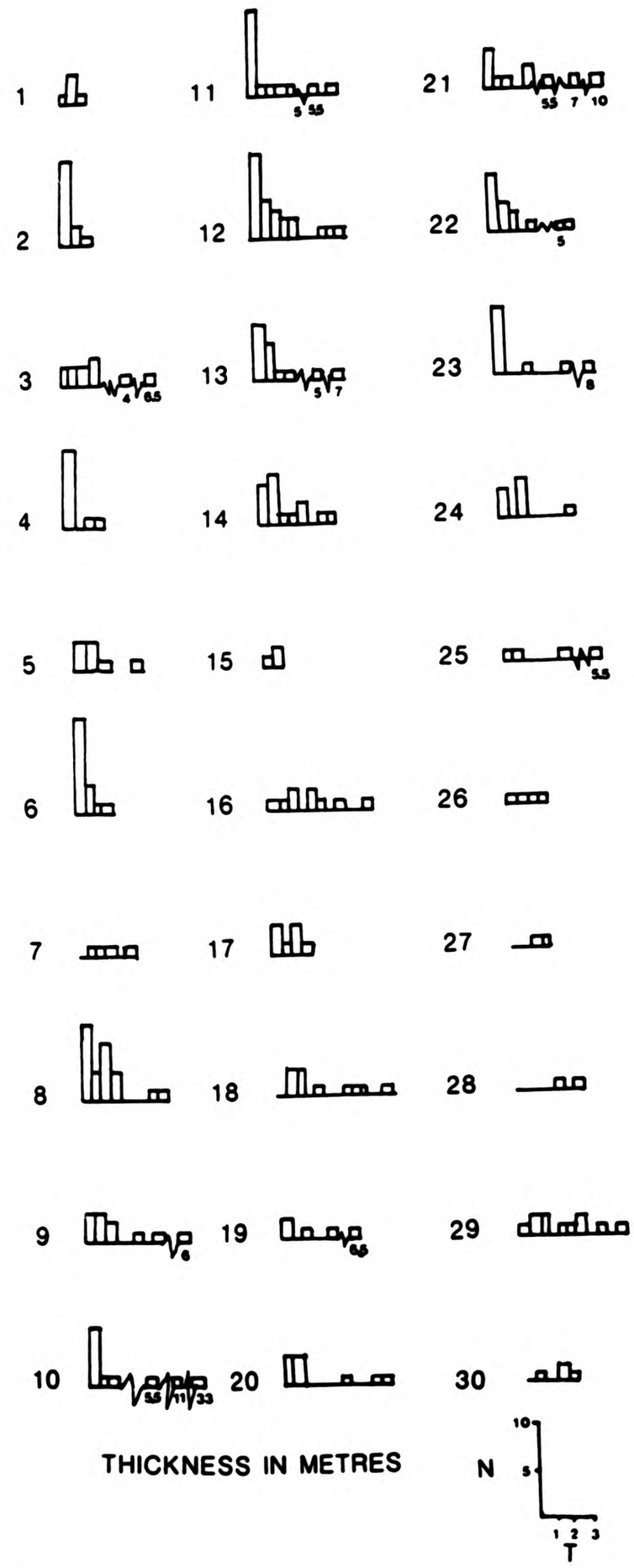

Fig.5.8.3 Distribution of cone sheet thickness per unit length across the Outer Centre Two south coast traverse

5.8.3 Inner Centre Two

The <0.5m class is the modal class for all, except one (unit length 12, Upper Garbdhail), unit lengths of this traverse. Unit length 12 has a modal class of 0.5-1m. The maximum thickness of Inner Centre Two cone sheets is 4m, although most sheets are <3m thick (Fig.5.8.4). Figure 5.9.1 shows the total thickness distribution and cumulative frequency curve for the whole of the set and shows that 76% of the sheets are <1m thick and 90% are <2m thick.

5.8.4 Centre Three

The modal thickness of the two unit lengths of this set are 1.5-2m and 2-2.5m respectively (Fig.5.8.5). Seventy percent of the sheets of this set are <2m thick and 90% of the sheets are <3m thick.

5.9 COMPARISON OF THE CONE SHEET THICKNESS OF EACH CONE SHEET SET

The distribution of thickness of cone sheets in sets of Centre One, Outer Centre Two north and south coast traverses and Inner Centre Two, are very similar in that the modal class is <5m thick. Also each set shows a well-marked decrease in the number of sheets of increasing thickness (Fig.5.9.1). In each of the sets, except Centre Three, one increase in the distribution is noted at 6m,3m,4m,3m in Centre One, Outer Centre Two north coast, Outer Centre Two south coast and Inner Centre Two, respectively. Centre Three cone sheet thickness data differs

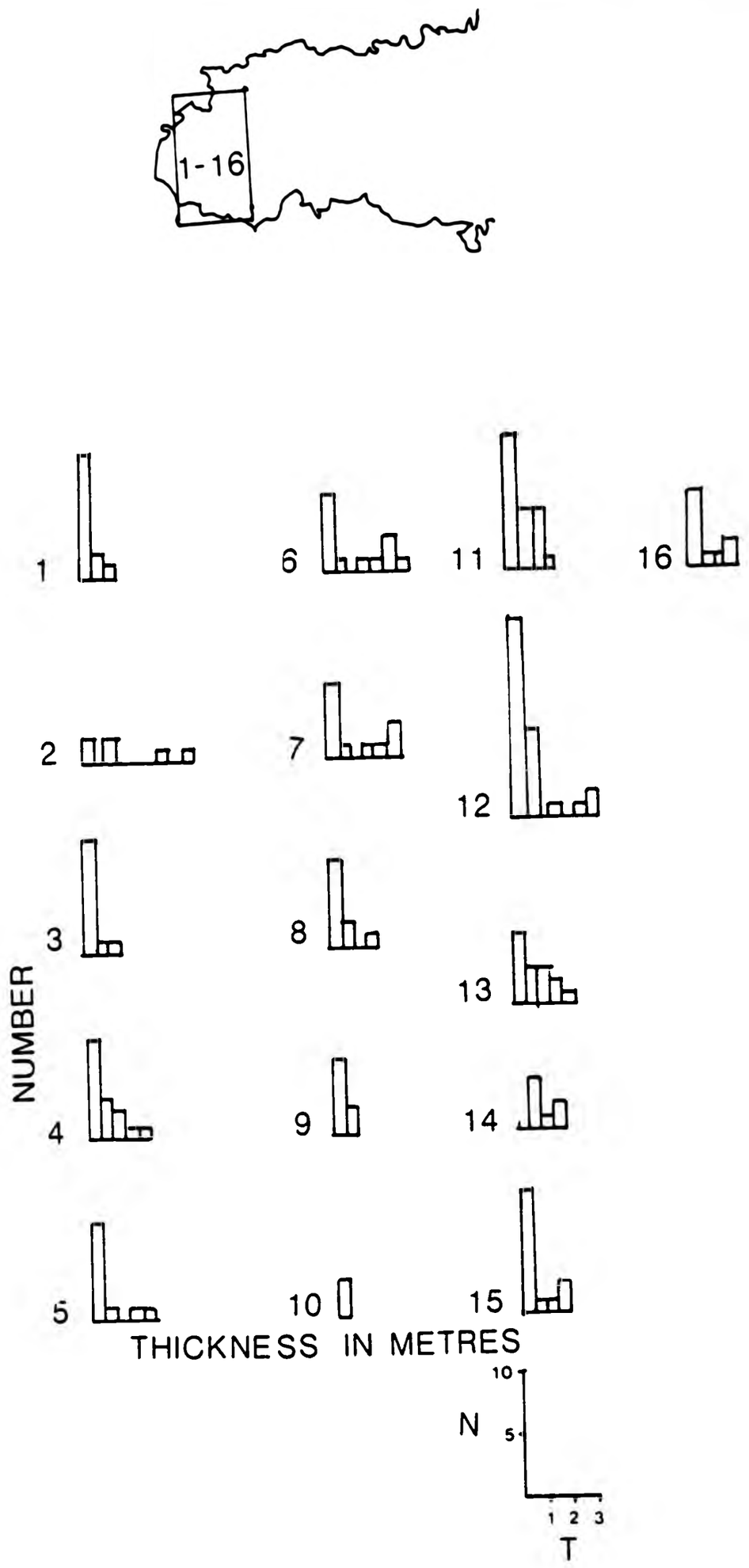

Fig.5.8.4 Distribution of cone sheet thicknesses per unit length across the Inner Centre Two traverse

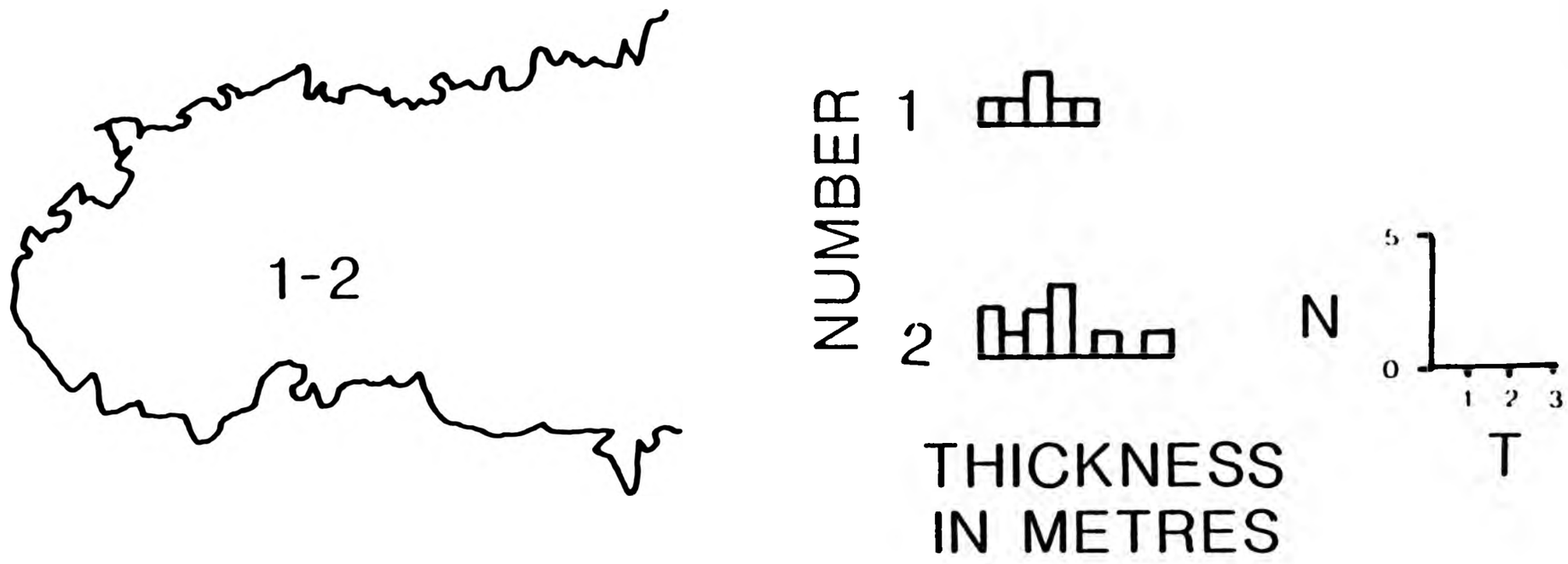

Fig.5.8.5 Distribution of cone sheet thicknesses across the Centre Three traverse

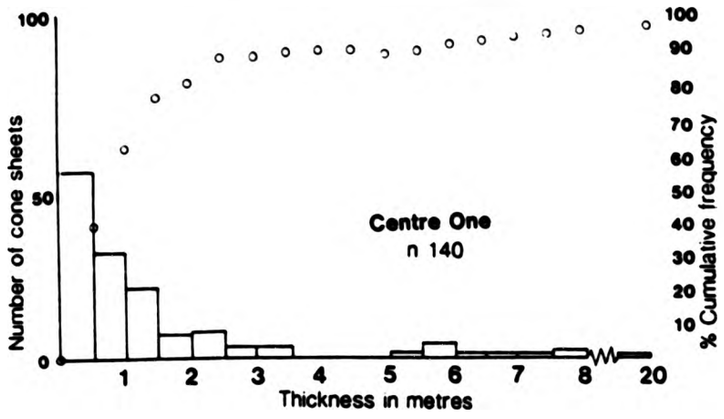

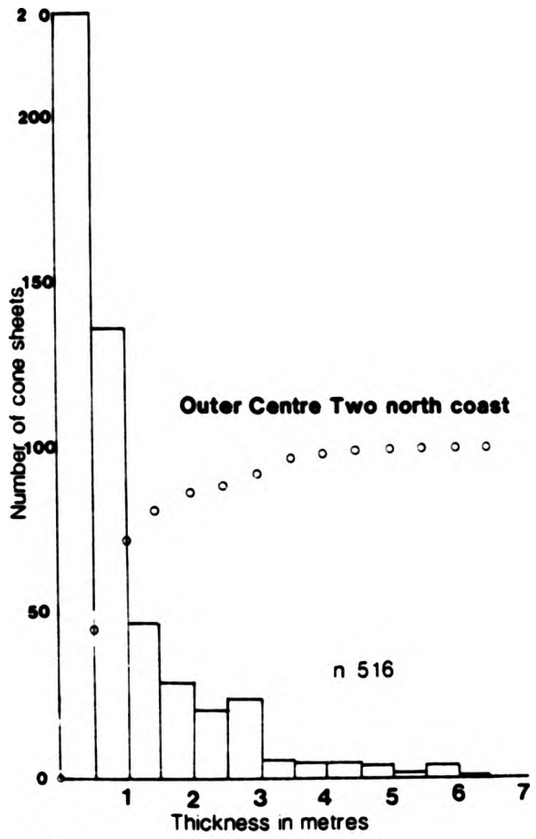

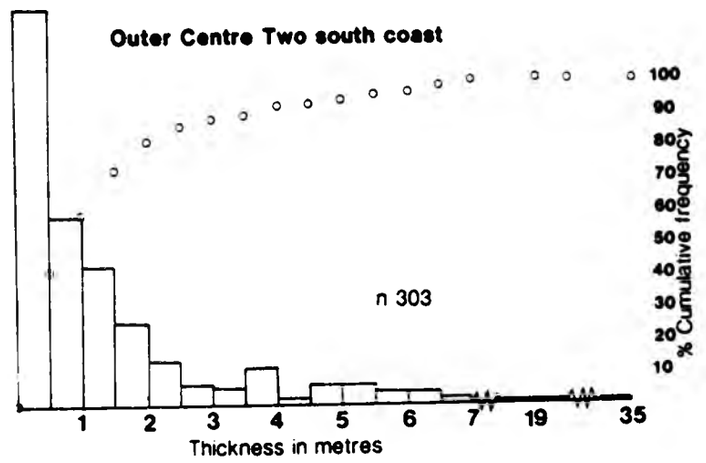

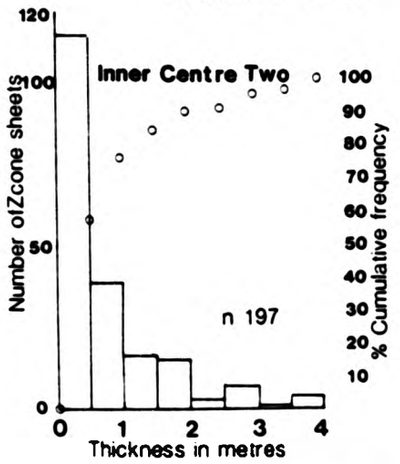

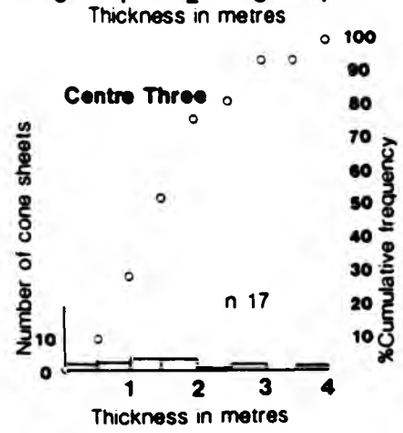

Fig.5 9.1 Distribution of cone sheet thicknesses for each cone sheet set

n - total number of sheets

from that of all the other sets in that the modal thickness is the 1-2m thick class. Also, the distribution of Centre Three sheets is almost equally spread over the thickness classes, this is perhaps due to the low frequency of sheets in this poorly developed set. In general there is no systematic change in thickness with distance from the centre of activity for any of the cone sheet sets.

5.10 THICKNESS AND STRIKE

Aggregate thickness of all cone sheets have been plotted (Figs. 5.10.1-5) as a percentage (%T) per unit length against strike (in intervals of 20°) for sub-regions for each cone sheet set. On the same graph the percentage number (%N) of sheets in each class have also been plotted. By plotting the two parameters, %T and %N, it may be possible to pick out conjugate sets, or other sub-sets, which may be highlighted by either aggregate thickness and/or number of cone sheets throughout a 360° distribution.

5.10.1 Centre One

Figure 5.10.1 shows the collated aggregate thickness and distribution of strike data for two sub-regions of Centre One; the first diagram (Ardtoe to Rubha a' Choit) has a maximum total thickness peak of 52% at a strike of 340°, the remaining 48% of the data is distributed as 4 small peaks at 020°, 160°, 220° and 260°. Where the strike is 020°, 160° and 220° the number of sheets is greater than the percentage total thickness, that is

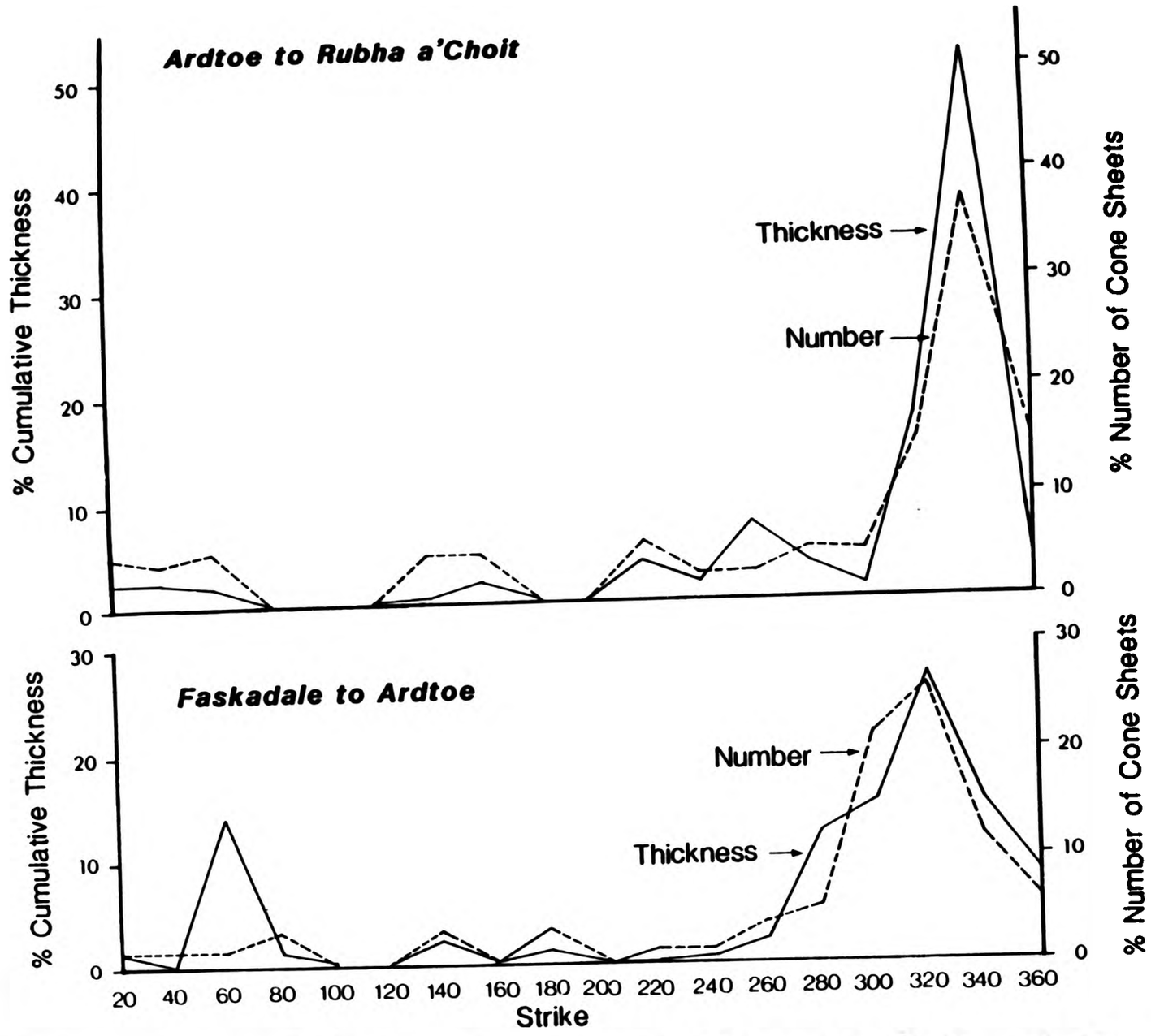

Fig.5.10.1. Centre One % Cumulative Thickness of Cone Sheets per 20° intervals of Strike and % Number of Cone Sheets

the sheets are thin. However, the reverse is the case for the 260° and 340° strike directions. From Faskadale to Ardtoe the main peak tends to spread over several classes of strike from 280° to 360°, with a second peak at 060°. Again the smaller peaks show a greater percentage number of sheets than total thickness, whilst the large peaks illustrate the reverse.

5.10.2 Outer Centre Two

North Coast. The two sub-sections of the north coast demonstrate a widespread peak (Fig.5.10.2). From Rubha an Duin Bhain to Sgeir Ghibeach the maximum total thickness of sheets (30% total thickness) occurs at 300° and 18% total thickness at 260°. Both profiles of percentage thickness of number of cone sheets and percentage total thickness of sheets become out of phase at a strike of 160°, where T > N and at 260° where N > T and at 300° where T > N. From Sgeir Ghibeach to Faskadale the majority of the sheets form a group from 220° to 360°, which shows a double peaked distribution of aggregate thickness at 280° and 320°; the intervening low at 300° representing 13% of the total thickness. Both percentage thickness and percentage number profiles are in phase over the distribution, indicating a constant thickness of sheets, except at strike 100° where T > N and from 300° where N > T to 340° where T > N.

South Coast. The Sron Bheag distribution pattern (Fig.5.10.3a) shows two main peaks at 60° and 100° with 28% and 27% total thickness, respectively. This bimodal distribution is similar to that seen on the north coast (Fig.5.10.2). Figure 5.10.3a shows two of the subsections for the Outer Centre Two

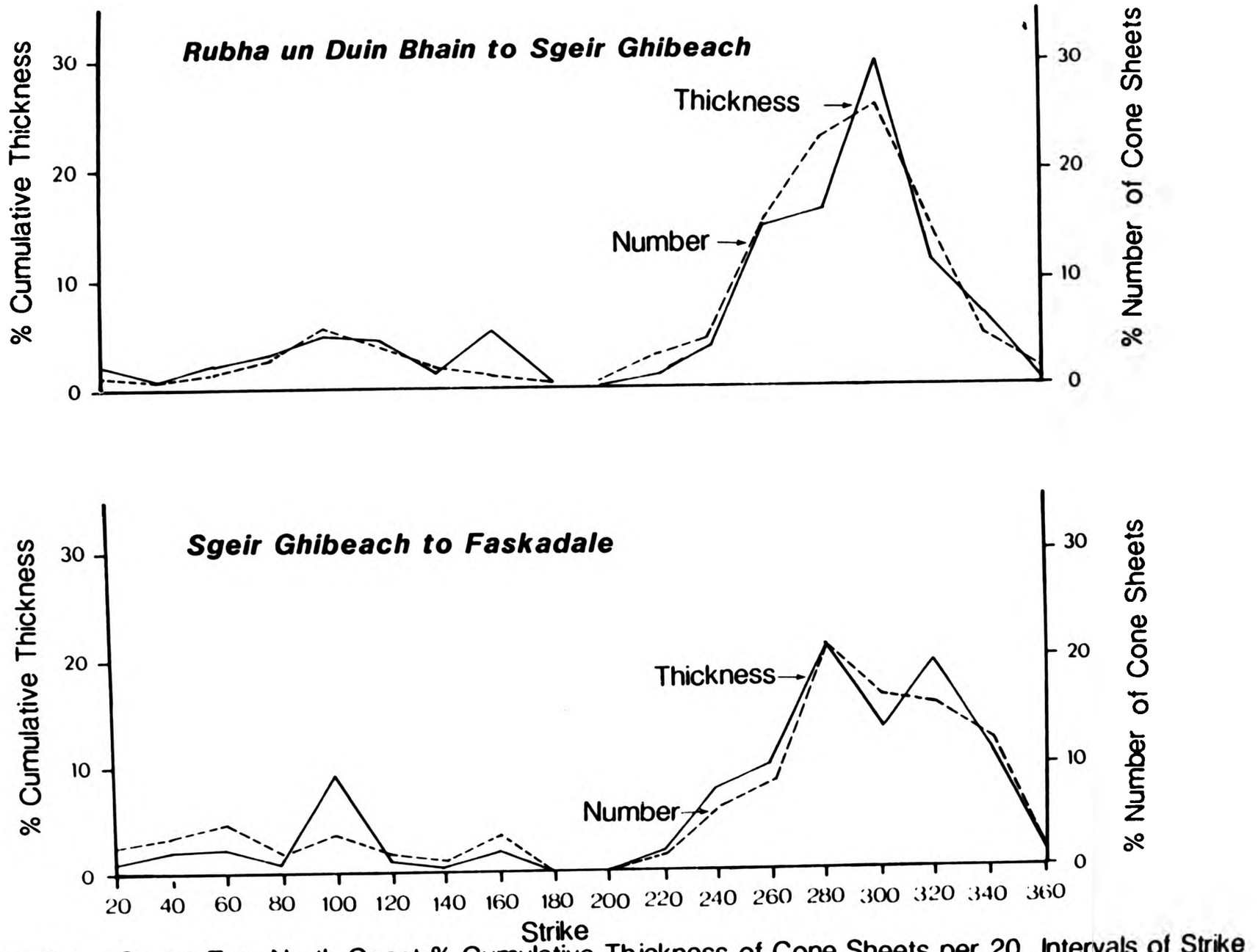

Fig.5.10.2. Outer Centre Two North Coast % Cumulative Thickness of Cone Sheets per 20 Intervals of Strike and % Number of Cone Sheets

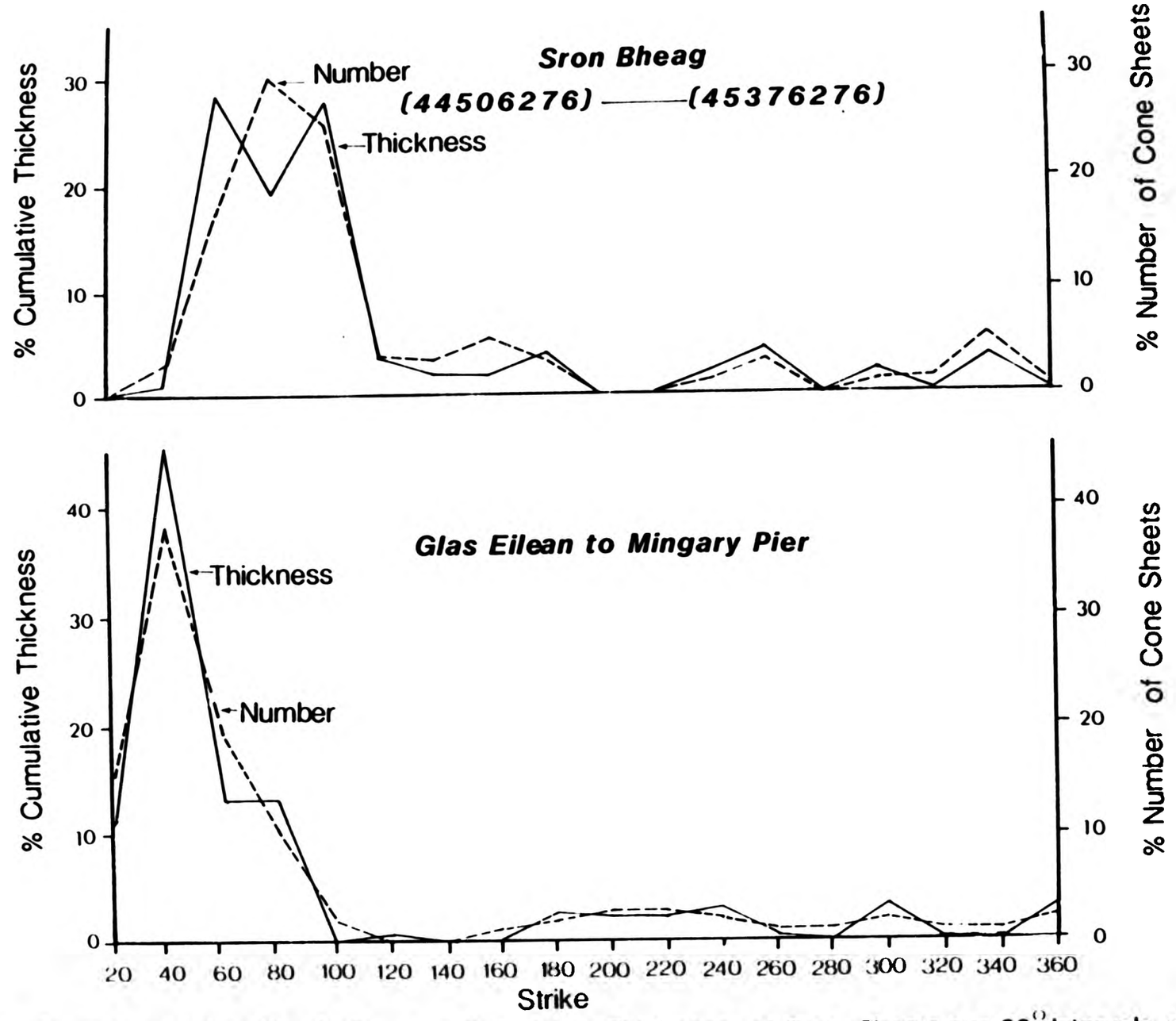

Fig.5.10.3a. Outer Centre Two South Coast % Cumulative Thickness of Cone Sheets per 20° Intervals of Strike and % Number of Cone Sheets

section. From Glas Eilean to Mingary Pier a dominant single peak at 040° occurs, although the spread is from 020° to 100°. From Mingary Pier to Sgeir nan Eun (Fig.5.10.3b) the main peak of % total thickness occurs at 020°, with subsidiary peaks at 60° (13% total thickness), 140° (5% total thickness), 200° (7% total thickness) and 320° (4% total thickness). Both % number and % thickness profiles are quite closely spaced in the region of the peak of the distribution and become out of phase from 160° to 360°. Despite the very prominent peak, the distribution of % thickness is more evenly spread than in the sections depicted in Fig.5.10.3a. A gradual migration of the main peak towards the north is noted in each successive diagram for the west to east traverse along the south coast section.

5.10.3 Inner Centre Two

Two diagrams have been produced, one containing data from the Inner Group and one containing data for the Outer Group of the Inner Centre Two cone sheets (Fig.5.10.4).

The Outer Group data shows two peaks of %T at 120° (37% T) and 200° (35% T) which correspond to the prominence of data collected from the An Acarseid and Lighthouse unit lengths respectively. The similarities in the %T from these two locations indicates an equal development of cone sheets within a set, as might be expected from an idealised cone sheet set.

A maximum peak of 15% occurs at 140° for the Inner Group data, although the majority of the data forms a widespread, low amplitude peak between 100° and 180° strike. This overall dis-

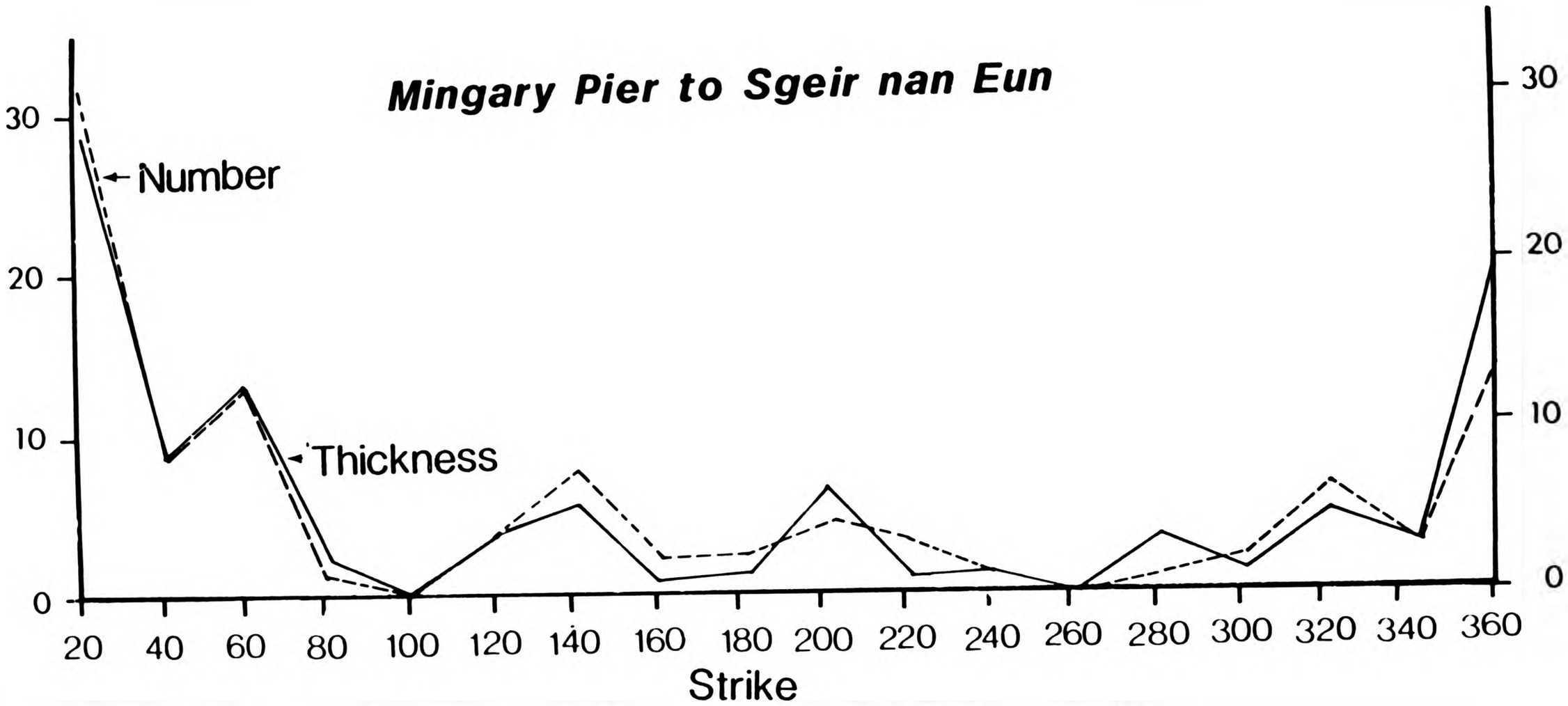

Fig.5.10.3b. Outer Centre Two South Coast % Cumulative Thickness of Cone Sheets per 20° Intervals of Strike and % Number of Cone Sheets

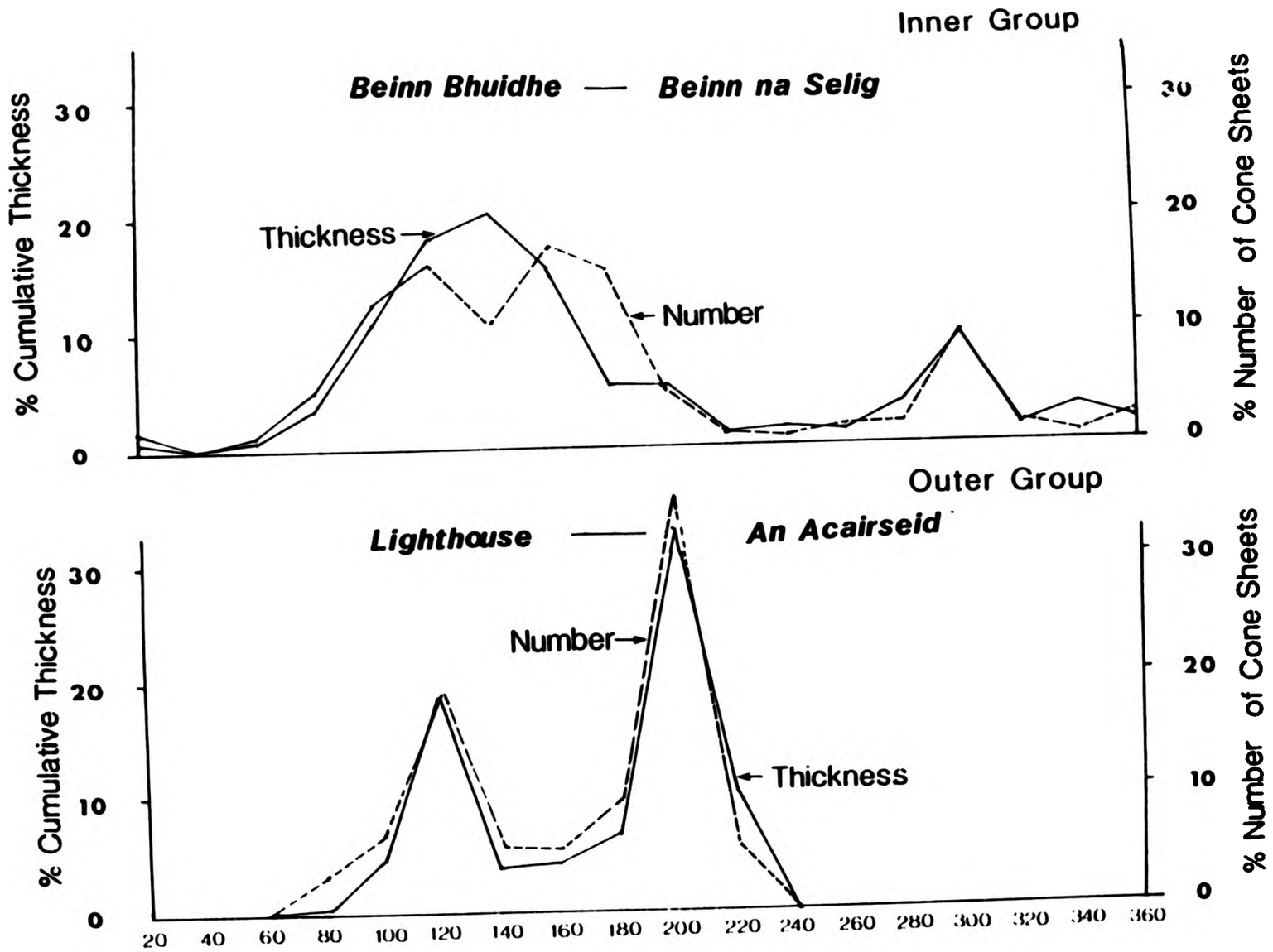

Fig.5.10.4. Inner Centre Two % Cumulative Thickness of Cone Sheets per 20° Intervals of Strike and % Number of Cone Sheets

tribution of equal intensity of cone sheets within the group may indicate the intrusion of a single cone sheet set.

5.10.4 Centre Three

Centre Three data (Fig.5.10.5) occurs between the 040° to 140° classes, and the peak of the distribution is at 100° strike (59% T). The % total thickness profile is only greater than % number of sheets at the peak.

5.10.5 SUMMARY

The four cone sheet sets, with the exception of Centre Three, have similar distributions of the % total thickness and % number of sheets, in that they have either a single dominant peak or one main peak with several smaller highs, although some classes are missed out. In general, where the % T peaks, it is greater than the % N of sheets, with three exceptions, these being the two sections of Inner Centre Two (Fig.5.10.4 and 5) and the Outer Centre Two Sron Bheag section (Fig.5.10.3a). Bimodal peaks of % T occur at Sron Bheag and Sgeir Ghibeach to Faskadale which may mark the presence of two closely spaced sub-sets. Often a subsidiary peak occurs, for example, the section from Faskadale to Ardtoe (Fig.5.10.1) has a well developed secondary peak at 060°, denoting a well developed subsidiary cone sheet set.

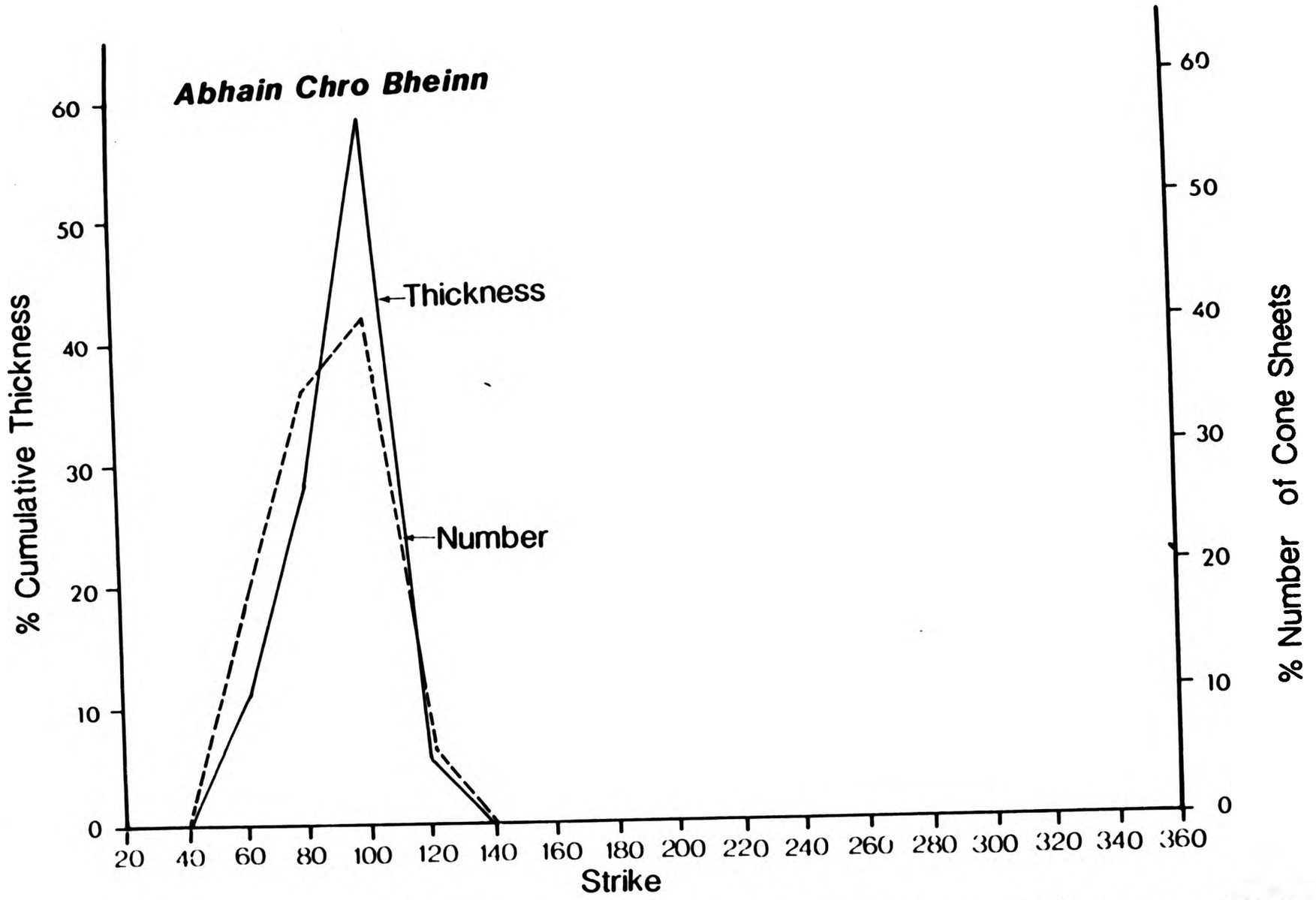

Fig.5.10.5. Centre Three % Cumulative Thickness of Cone Sheets per 20° Intervals of Strike and % Number of Cone Sheets

5.11 CLUSTER ANALYSIS

Cluster analysis is an objective approach to the analysis of the characteristics of cone sheets, that is dip, strike, thickness and distance from centre of activity, by which all the characteristics can be analysed in relation to each other.

5.11.1 Introduction

Due to the large number of cone sheets present in the area of study, various regions have been subdivided to facilitate analysis, thus subjecting the data to an inherent classification before analysis begins. In order to alleviate this subjective classification an objective analysis, cluster analysis, has been applied to the collected data. However, the number of cone sheets (cases) measured over the whole area of study exceeds the maximum number of cases that the cluster analysis program (Clustan; Wishart, 1978) is capable of analysing in it's present form. This, therefore, imposes some of the restraints that the cluster analysis is designed to alleviate. Thus, all the cone sheet data cannot be analysed together. Since Centre One, Inner Centre Two and Centre Three cone sheet sets form incomplete groups of data, in that only a small part of the circumference of the cone sheet set can be measured, they have been left out of the analysis. However, analysis has been performed on the Outer Centre Two data set, in order to identify any "within sample" variation. The Outer Centre Two data set consists of 843 samples; incomplete cases , where one or more of the analysed characteristics, dip, strike, thickness or distance from centre, could not be measured or calculated were omitted from the ana-

lysis.

5.11.2 Method

Appendix B contains all relevant details of cluster analysis, with reference to the Clustan programme.

As a result of a Clustan run, 10 terminal clusters were produced, which is perhaps a larger number than is usually produced in a cluster analysis, however, the number specified was the one recommended as a starting point for analysis in the Clustan manual (Wishart, 1978). A later discussion points out that if left to continue the clustering procedure would continue and produce fewer clusters, eventually producing just one cluster. This, therefore, necessitates a stopping point, i.e. 10 clusters.

Dip, strike, thickness and distance from the location of Centre Two activity, for each cone sheet form the variables for the analysis. Distance from the centre of Centre Two activity may be interpreted as distance from a fixed reference point and therefore may be treated as an objective characteristic. Cluster analysis, in general terms, takes all the cases and plots them in multidimensional space, in this example 4 dimensions. Each case is assigned to a cluster, and at the start of the analysis each case forms a separate cluster. Clustering of the most similar clusters is carried out and this relocation of each cluster continues until the designated number of terminating clusters is formed.

Mean, standard deviation, t (the distance between clusters) and f (the tightness / closeness of clusters) values are given for each cluster (Table 5.3) so that the similarities between clusters may be established. Figure 5.11.1 is a dendrogram of the relationships between the 10 clusters. The smaller the distance between clusters indicates the degree of similarity, the clusters that have the greatest distances between them, show the least similarity.

5.11.3 Interpretation

Two megagroups are formed from the 10 clusters;

Megagroup A = 4,5,6 and 7 (Fig.5.11.1)

Megagroup B = 1,2 and 8; clusters 3 and 9 are most similar to group B (Fig.5.11.1)

Cluster 10, however, is most unlike any of the 9 clusters and has an f value of 4. Any cluster with an f value of greater than 1.5 exceeds confidence limits and is therefore not considered viable.

Figure 5.11.2 shows the distribution of the cases within the clusters in a regional context. Group A, which comprises clusters 4 to 7, shows a uniformly high frequency for the south coast cases and highlights the main Outer Centre Two distribution. The north coast cases are most well developed in clusters 4,5 and 6, although few occur in cluster 5. Clusters 4 and 6 have similar strike values (Table 5.3) but differ in their dip

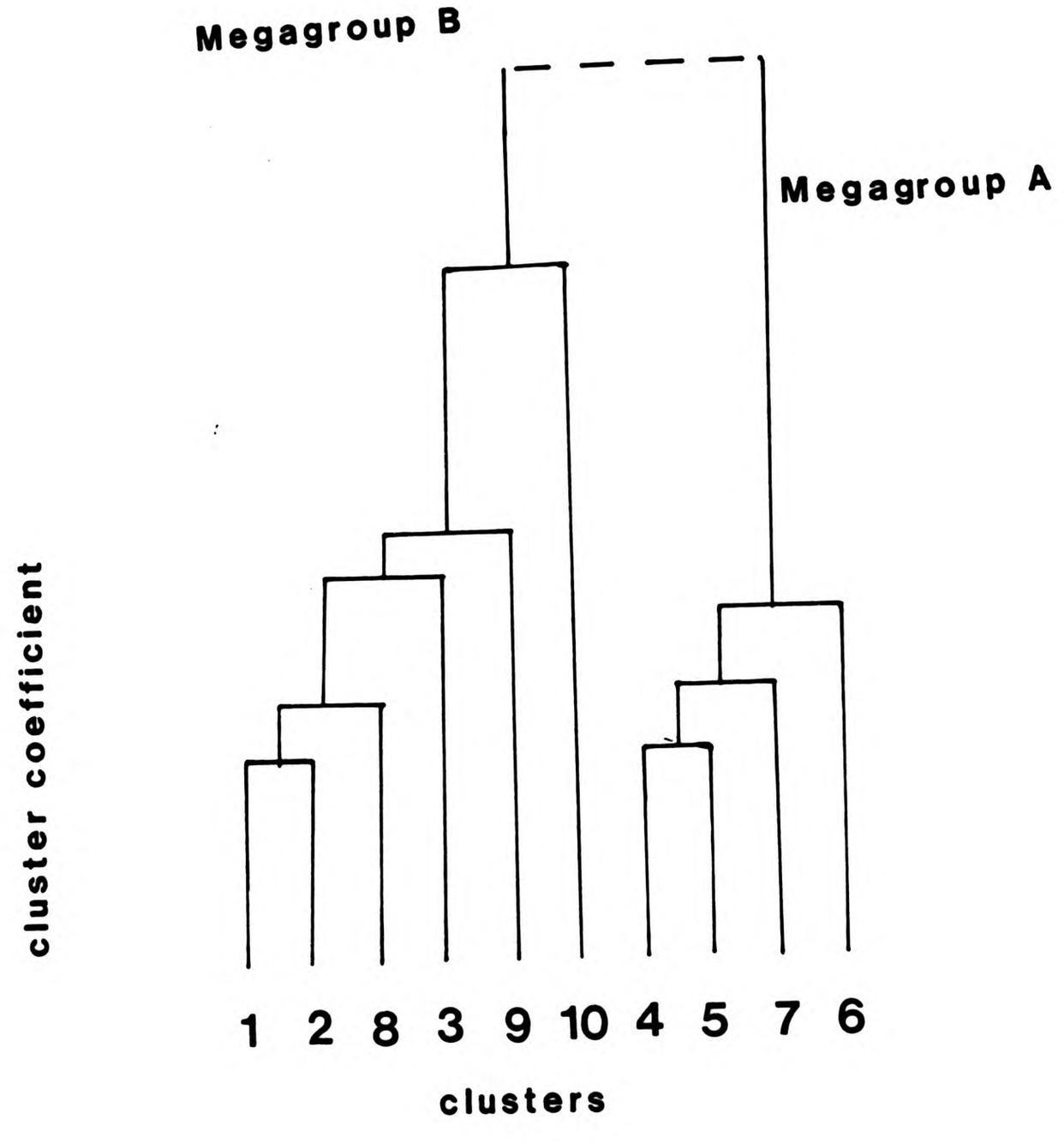

Fig. 5.11.1 Dendrogram of the 10 clusters produced by cluster analysis of the Outer Centre Two cone sheet data

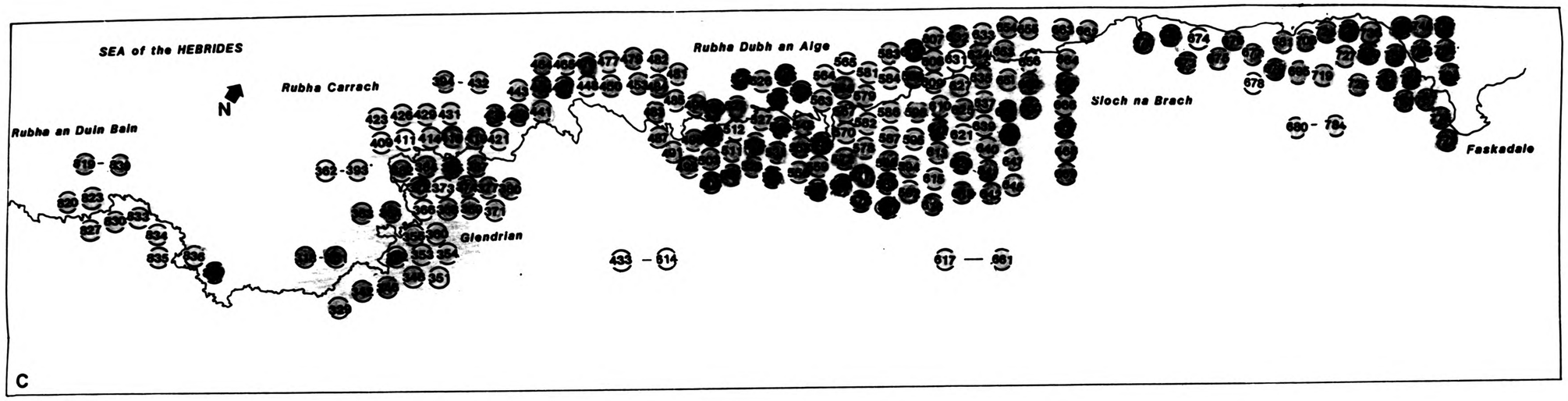

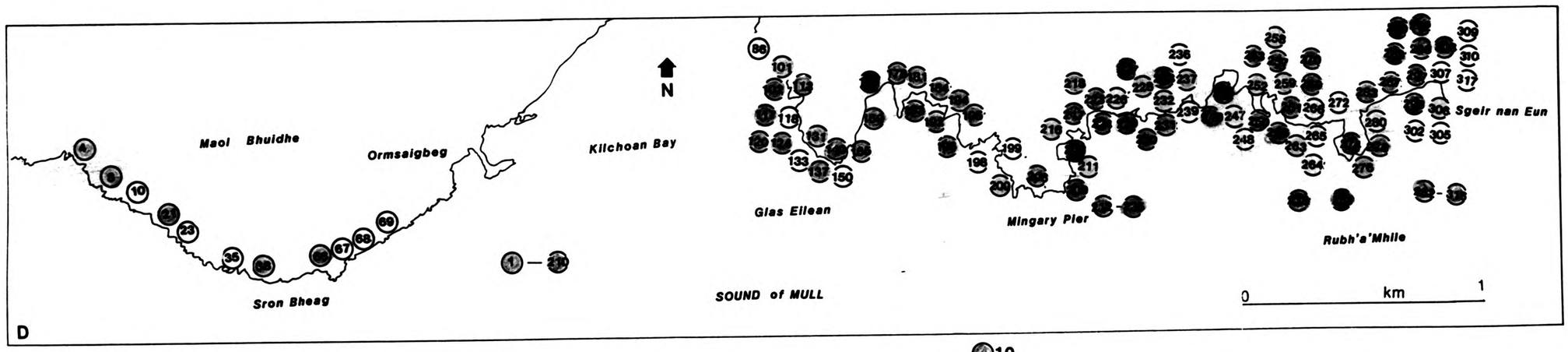

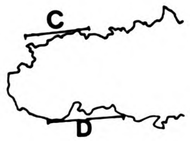

10
9
8
7
6
5
4
3
2
1

CLUSTERS

(31) cone sheet number as in Appendix A

Fig.5.11.2 Spatial distribution of the ten clusters produced by cluster analysis of the Outer Centre Two data
The background shading is where one cluster predominates

Table 5.3 Results of Cluster Analysis

where VAR variable

1 Dip

2 Orientation

3 Thickness of sheet in metres

4 Distance from focus of activity

MN-ORIG mean of the cone sheet data

SD-ORIG standard deviation of the cone sheet data

CLUSTER ONE NUMBER OF CASES = 82
CLUSTER DIAGNOSIS

VAR	F-RATIO	T	MN-ORIG	STD-ORIG
4	0.0574	1.5662	6.1085	0.1679
2	0.1326	0.8225	282.5122	41.6031
3	0.1922	-0.1849	0.9369	0.8482
1	0.3633	-0.1590	47.4878	10.7097

CLUSTER TWO NUMBER OF CASES = 13
CLUSTER DIAGNOSIS

VAR	F-RATIO	T	MN-ORIG	STD-ORIG
2	0.0533	0.9331	295.1538	26.3813
3	0.0893	-0.3087	0.6969	0.4018
1	0.1459	0.3374	56.3077	6.7871
4	0.3284	0.7038	5.5038	0.4018

CLUSTER THREE NUMBER OF CASES = 98
CLUSTER DIAGNOSIS

VAR	F-RATIO	T	MN-ORIG	STD-ORIG
3	0.1311	-0.2660	0.7796	0.7006
1	0.2938	1.3475	74.2551	9.6306
2	0.3742	0.5670	253.3265	69.8716
4	0.5606	-0.3503	4.7648	0.5250

CLUSTER FOUR NUMBER OF CASES = 140
CLUSTER DIAGNOSIS

VAR	F-RATIO	T	MN-ORIG	STD-ORIG
2	0.0731	0.8270	283.0357	30.89.05
3	0.1693	-0.1963	0.9144	0.7960
1	0.2337	-1.0524	31.6143	8.5894
4	0.4061	-0.0857	4.9504	0.4468

Table 5.3 contd.

CLUSTER FIVE NUMBER OF CASES = 9
CLUSTER DIAGNOSIS

VAR	F-RATIO	T	MN-ORIG	STD-ORIG
3	0.0342	-0.3600	0.5978	0.3578
2	0.1620	-0.3045	153.7778	45.9722
4	0.5647	0.1595	5.1222	0.5268
1	0.6866	-0.7305	37.3333	14.7224

CLUSTER SIX NUMBER OF CASES = 109
CLUSTER DIAGNOSIS

VAR	F-RATIO	T	MN-ORIG	STD-ORIG
2	0.0483	0.8275	283.0826	25.0950
3	0.1230	-0.2674	0.7769	0.6785
1	0.2213	-0.0760	48.9633	8.3588
4	0.2685	-0.5514	4.6239	0.3633

CLUSTER SEVEN NUMBER OF CASES = 270
CLUSTER DIAGNOSIS

VAR	F-RATIO	T	MN-ORIG	STD-ORIG
2	0.1082	-1.1428	58.0259	37.5663
3	0.1648	-0.2066	0.8945	0.7855
4	0.7425	-0.4512	4.6941	0.6041
1	1.0010	0.0132	50.5481	17.7767

CLUSTER EIGHT NUMBER OF CLUSTERS = 17
CLUSTER DIAGNOSIS

VAR	F-RATIO	T	MN-ORIG	STD-ORIG
2	0.1523	0.8252	282.8235	44.5775
3	0.1846	0.9263	3.0865	0.8313
1	0.2465	0.0983	52.0588	8.8209

CLUSTER NINE NUMBER OF CASES = 28
CLUSTER DIAGNOSIS

VAR	F-RATIO	T	MN-ORIG	STD-ORIG
3	0.0428	-0.3489	0.6193	0.4001
1	0.4011	1.1100	70.0357	11.2529
4	0.4255	1.1618	5.8250	0.4573
2	0.4306	-0.6553	113.7143	74.9572

CLUSTER TEN NUMBER OF CASES = 74
CLUSTER DIAGNOSIS

VAR	F-RATIO	T	MN-ORIG	STD-ORIG
1	0.7755	0.0333	50.9054	15.6469
2	1.0546	-0.3447	149.1892	117.3033
4	1.1071	0.7571	5.5412	0.7377
3	4.7251	2.0935	5.3447	4.2057

angle and their distribution, cluster 4 groups the cases which occur towards the east of the north coast traverse (Fig.5.11.2). If the cone sheets (cases) were distributed symmetrically at constant dip around the complex then two groups should be identifiable within the clusters. Assuming an apical angle of 80° for a vertical cone (Fig.5.11.3) the average dip of the north and south coast cone sheets should be 50°, therefore, cluster 7 on the south coast is equal to cluster 6 on the north coast. Cluster 4 predominates among the northern cases (Table 5.3) and has a shallower dip angle (31°) than cluster 6 (48°). It is possible that the shallowing in the angle of dip represents an inclination of the axis of the cone towards the south (Figure 5.11.4). If the apical angle is 80°, the southern limb, corresponding to the 31° dip of the northern limb, i.e. cluster 4, would dip at 69° towards the centre of activity. Figure 5.11.4 shows the calculation for the projected exposure of the inclined cone. The southern limb should be exposed 2.27km farther to the north i.e. towards the centre of activity of Centre Two, than the location of the cone sheets of cluster 7. This northern move coincides, approximately, with the exposure of Inner Centre Two cone sheets, which dip at approximately 70° towards the focus of Centre Two activity. Alternatively, the apical angle may be larger than 80° and if this was so the resulting cone sheets would occur 4.89km to the south of the cone sheets of cluster 7, that is in the Sound of Mull. Limited, yet conclusive field evidence can be given to support the theory of a tilted cone. However, two cross cutting relationships (Figs.6.8.7 and 8) indicate that the shallower dipping sheet post dates the more steeply inclined sheet.

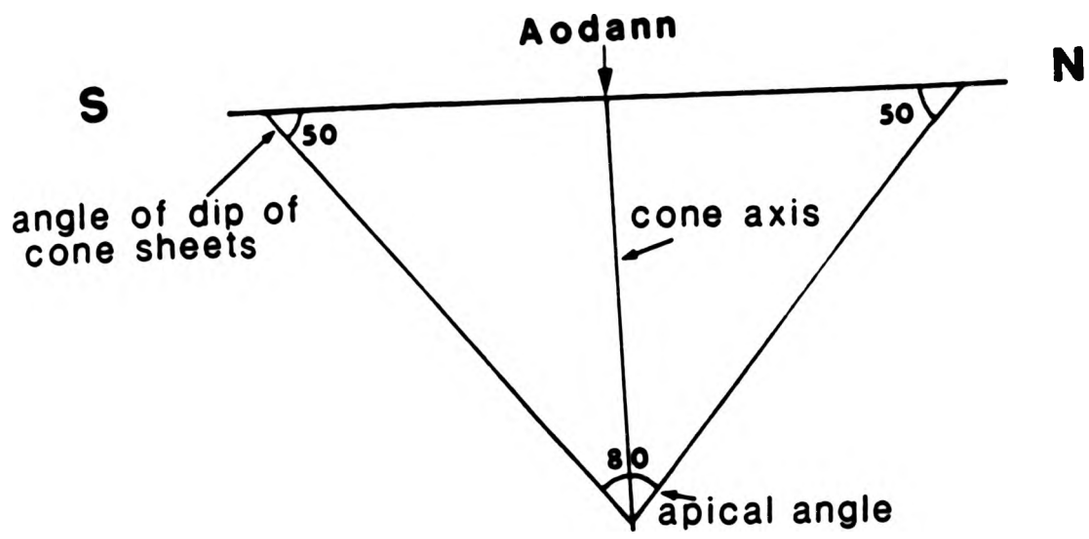

Fig.5.11.3 Cross section of a vertical cone, with both limbs dipping at 50

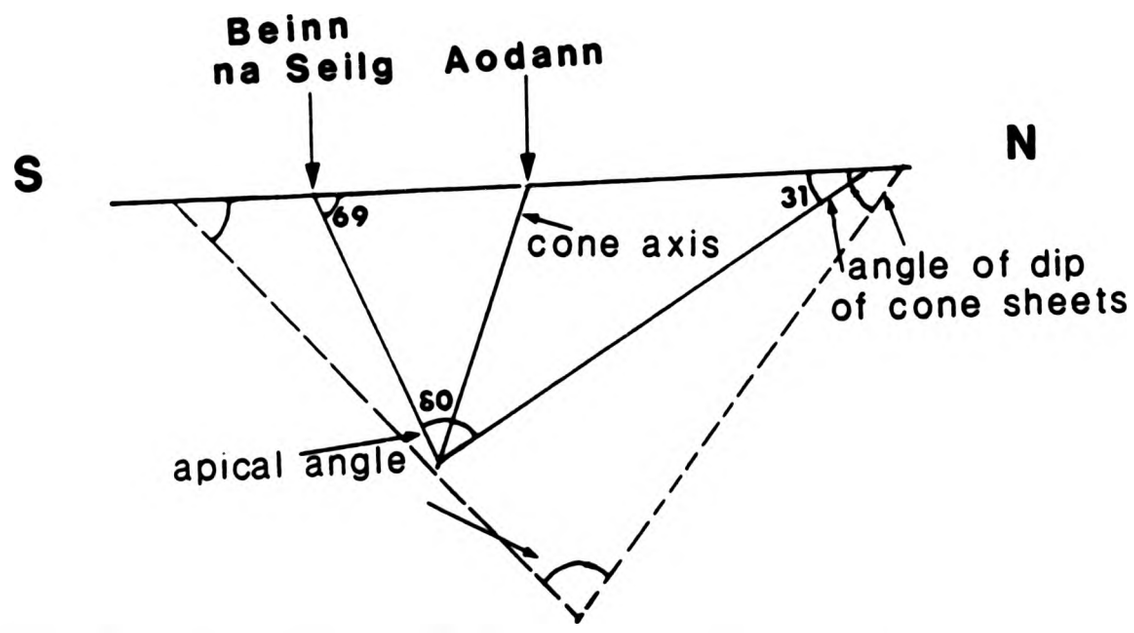

Fig.5.11.4 Cross sections of both a vertical and an inclined cone to illustrate the different angles of dip and the distribution of sheets

In addition to the main distribution of Megagroup A, a subsidiary distribution occurs which is particularly well developed in cluster 4, which emphasizes cases that dip away from the centre of activity i.e. towards the south on the south coast. It is possible that this set represents the exploitation of a set of fractures conjugate to the main distribution of Outer Centre Two cone sheets.

The second group of clusters, 1,2 and 8, forming Megagroup B, tend to cluster cases which occur in the east of the north coast traverse, especially in the last 5km of the traverse. Mean dip and strike values of Megagroup B are similar to cluster 6, although they differ in the two other variables, thickness and distance from centre. It is possible that Megagroup B shows the change in thickness with distance from the centre, even though the mean strike shows little change. The mean dip of clusters 2 and 8 is steeper than those of cluster 6 and perhaps represents a lateral increase in dip towards the east of the traverse.

Clusters 3 and 9 show the steepest average dips, 74° and 70°, respectively (Table 5.3), with both clusters containing sheets at the extremities of the north coast traverse. If the inclined cone theory, described above, is applied, it is possible that cases in clusters 3 and 9 represent the exploitation of conjugate fractures.

Cluster 10 tends to group the thicker sheets together and contains a large number of cases on the south coast traverse. The number of cases increases towards the east of the traverse

and may indicate the presence of Centre One sheets.

5.12 SUMMARY AND CONCLUSIONS

To a limited extent each of the characteristics discussed above assists in the delineation of each of the cone sheet sets. Together the characteristics have also served to highlight the differences within each set and those between the sets. The analysis of these characteristics leads one to suggest that within a cone sheet set a number of closely spaced intrusions were emplaced in rapid succession: a cone sheet set may be built up by a number of sub-sets.

The increased number and thickness of cone sheets within the 400m section to the east of Faskadale, relative to the distribution of sheets to the east of this location, marks the overlap of the Outer Centre Two and Centre One cone sheet sets.

The eastern limits of the Centre One traverse probably marks the natural end of the series of intrusions. Similarly, on the south coast section, for the Outer Centre Two Set, the intensity, marked by the number of sheets and their cumulative thickness, decreases towards the east. The change in dip and strike of the cone sheets noted to the east of Mingary Castle is equated with the overlap of the Centre One set of cone sheets. The Inner Centre Two cone sheets are subdivided into an Outer Group and an Inner Group. The Outer Group (at An Acairseid) show many similarities with the westerly extensions of the Outer Centre Two cone sheet set at Sron Bheag. The Inner Group show some characteristics which are similar to those of the cone

sheets on the north coast of the Outer Centre Two traverse. Both of these statements will be discussed in Chapter 10.

CHAPTER 6

DILATION CAUSED BY THE EMPLACEMENT OF CONE SHEETS

6.1 INTRODUCTION

Dilation is a general term used to describe the expansion of the country rock to accommodate the emplacement of intrusive bodies, which in this case are cone sheets.

Figure 6.3.4 shows the amount of dilation caused by the intrusion of the cone sheets within the peninsula. To obtain an ideal result (Chapter 3) it is necessary to determine the dilation in three-dimensions for each cone sheet. This cannot be done because there is a lack of suitable marker horizons in the country rocks which can be used as reference planes to determine the opening directions of individual sheets. Consequently, the number of dilation determinations is less than 10% of the total number of measured cone sheets.

6.2 TWO-DIMENSIONAL DILATION

Richey *et al.* (1930) calculated the total dilation caused by the emplacement of cone sheets by assuming:-

1. Space for each cone sheet was provided by the displacement of it's roof and not the floor,
2. That the intrusions are equally distributed around the complex,
3. The uplift produced by the emplacement of each cone sheet was considered to be vertical (Fig.6.2.1).

Richey *et al.* (1930) calculated the aggregate thickness of cone sheets in a well exposed sample section, that of the Outer Centre Two cone sheets SE of Kilchoan. Total uplift of the complex resulting from cone sheet emplacement was calculated using the following equation:-

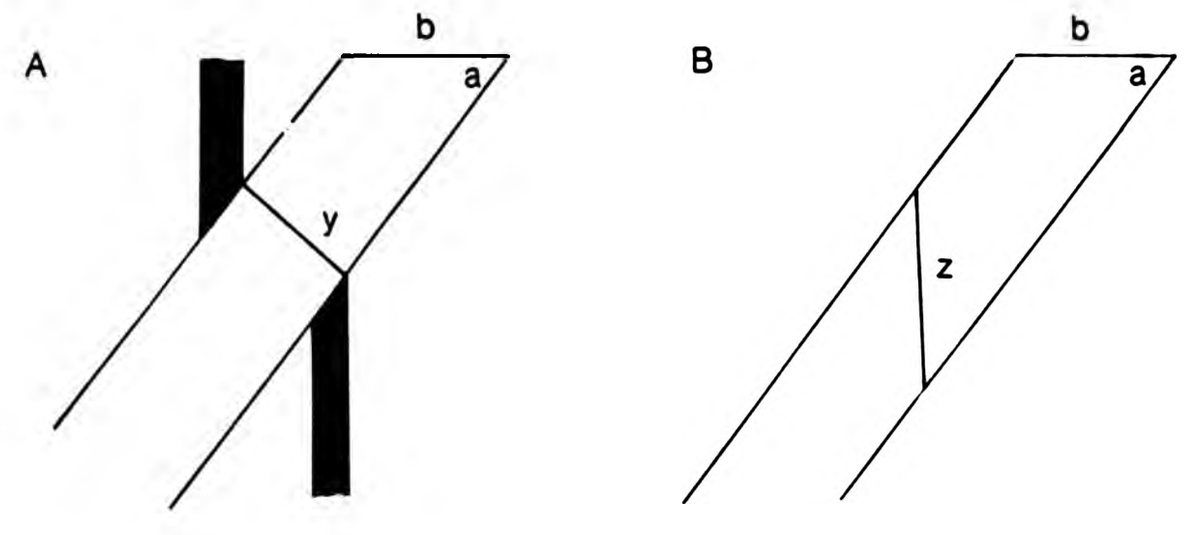

opening by extension, displacement is normal to the cone sheet margin

(Tension only)

Amount of uplift $y = b \times \sin a$ as depicted by Richey et.al. (1930) (Fig.6.2.2)

Calculation of total uplift used by Richey et.al.(1930) $z = \frac{b}{\cos a}$

when $a = 47$ (average values for Glas Eilean
$b = 1.5m$ to Mingary Pier (Fig.6.2.2))

$y = 1.09m$

$z = 2.19m$

Fig.6.2.1 Diagram to compare the types of displacement A. shown by Richey et al. (1930) and B. that used by Richey et al. (1930) to calculate the total uplift caused by the emplacement of the cone sheet sets of Ardnamurchan.

$$Z = \frac{B}{\cos a}$$

where Z = total uplift caused by the emplacement of the whole belt of cone sheets
B = aggregate thickness of cone sheets forming the belt
a = average angle of inclination of the cone sheets

Figure 6.2.2 (after Richey et al.) depicts the Kilchoan coastal section used as the sample section in the calculation. It should be noted, that in this figure cone sheets are depicted as displacing an earlier dyke and other cone sheets normal to their margins, i.e. extension. However, the calculations by Richey et al. (1930) for uplift assumes a vertical sense of movement (Fig.6.2.1B). Given below are Richey's et al. (1930) calculations and measurements. The Kilchoan section which is approximately half a mile long and the aggregate thickness of cone sheets within this section is 950ft. By using the Kilchoan section as an average measurement, they estimated that the total area occupied by all the Ardnamurchan cone sheets is equal to a belt 2 miles wide and the total aggregate thickness (true thickness) of the cone sheets across this 2 mile belt was calculated to be 3800ft. Assuming an average dip angle of 35° for the cone sheets, the calculated uplift is 4600ft. These calculations first involved the calculation of the true thickness of each cone sheet and then another calculation assuming vertical uplift (Fig.6.2.1). The result obtained by Richey et al., 4,600 ft, is for the vertical expansion caused by the emplacement of the cone sheets, However, this is not the maximum extension direction, which would give an upper limit to the dilation caused by the cone sheets. As Richey's figure represents the value of an

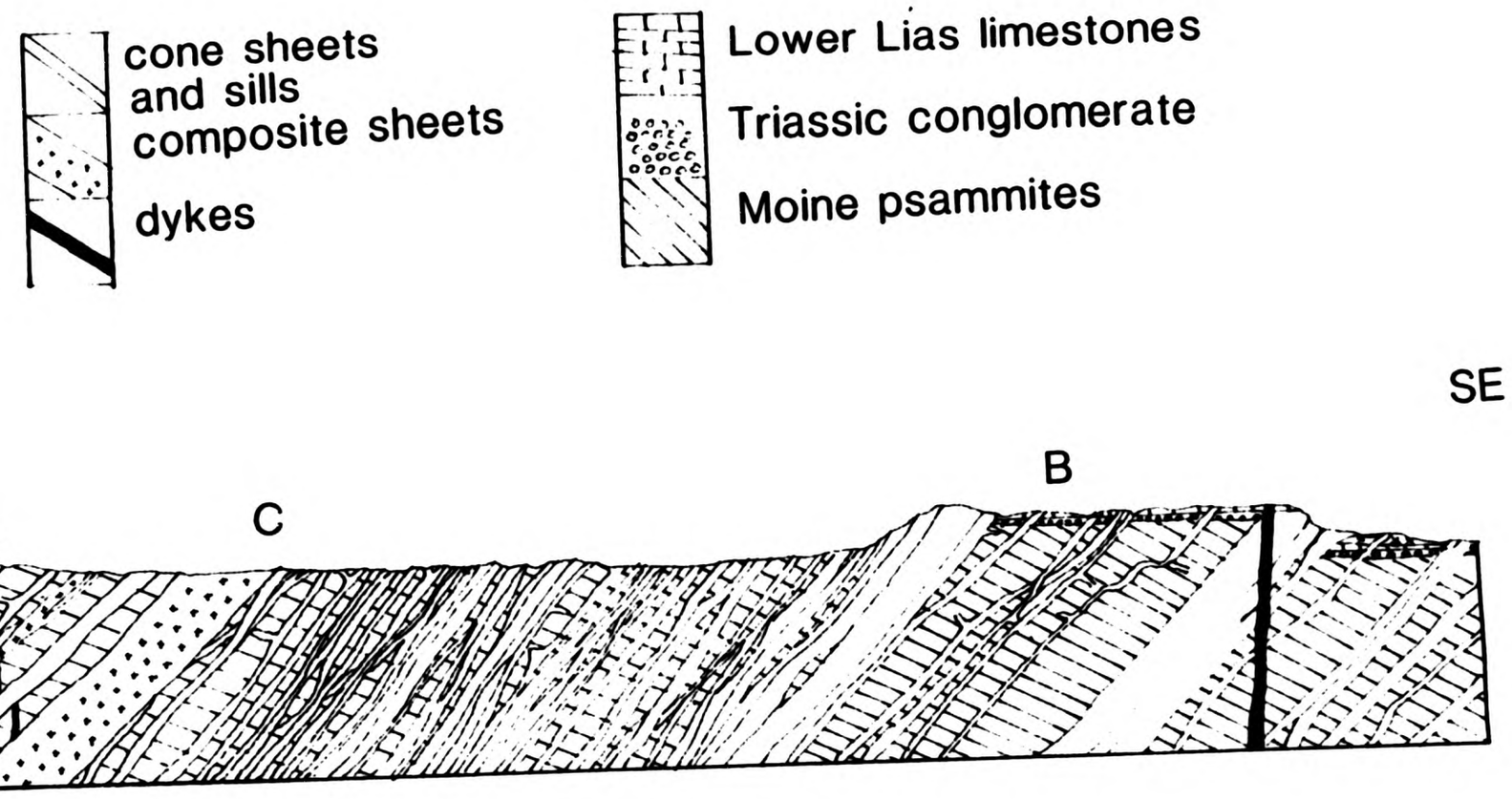

Fig.6.2.2 Cross section of the shore line exposures south of Kilchoan used by Richey et. al. (1930) to calculate the average amount of uplift for the whole complex. At A a dyke is cross cut by several cone sheets, the displacement is normal to the cone sheet margins. Other examples are seen at B and C

intermediate dilation there is no maximum or minimum for comparison. Maximum extension for all cone sheet traverses, using the true thickness of each sheet have been calculated for this study.

6.3 TOTAL DILATION CAUSED BY THE EMPLACEMENT OF THE FOUR CONE SHEET SETS

The collection of data has been confined, in general, to coastal sections (Chapter 3). Having checked the 6" field slips of the Geological Survey in the field, I decided that remapping on 1:10,000 scale would not improve the existing maps, particularly where the inland exposure is poor. Therefore, two dilation maps have been constructed, one based on data collected by myself (coastal sections) and the other on data obtained from the 6" field slips of the Geological Survey.

6.3.1 The amount of dilation calculated from designated traverses

The percentage dilation per unit length has been calculated as follows:-

$$\frac{\text{total thickness of sheets (true thickness)}}{\text{length of section}} \times 100 = \% \text{ dilation}$$

For each unit length the calculated dilations have been plotted and subsequently contoured (Fig.6.3.1-5).

6.3.1.1 Centre One -

PAGINATION ERROR

intermediate dilation there is no maximum or minimum for comparison. Maximum extension for all cone sheet traverses, using the true thickness of each sheet have been calculated for this study.

6.3 TOTAL DILATION CAUSED BY THE EMPLACEMENT OF THE FOUR CONE SHEET SETS

The collection of data has been confined, in general, to coastal sections (Chapter 3). Having checked the 6" field slips of the Geological Survey in the field, I decided that remapping on 1:10,000 scale would not improve the existing maps, particularly where the inland exposure is poor. Therefore, two dilation maps have been constructed, one based on data collected by myself (coastal sections) and the other on data obtained from the 6" field slips of the Geological Survey.

6.3.1 The amount of dilation calculated from designated traverses

The percentage dilation per unit length has been calculated as follows:-

$$\frac{\text{total thickness of sheets (true thickness)}}{\text{length of section}} \times 100 = \% \text{ dilation}$$

For each unit length the calculated dilations have been plotted and subsequently contoured (Fig.6.3.1-5).

6.3.1.1 Centre One -

Along the west-east traverse three highs occur, against a general background of 1-5% dilation (Fig.6.3.1). Located at the western extremity of the traverse i.e. nearest to the presumed centre of intrusion, is the largest of the highs, 40% dilation. This high, on the east side of Faskadale Bay, differs markedly from the low dilation values (1-5%)recorded along most of the traverse. It is possible that the fault which trends NW - SE through Faskadale Bay has been exploited by the intruding magma resulting in an anomalously high dilation (40%) on one side of the fault. Alternatively, the fault may have juxtaposed two different structural levels of the same cone sheet set.

6.3.1.2 Outer Centre Two -

North Coast. The crustal dilation per unit length ranges from 48% to 1% (Fig.6.3.2). In general, there is a decrease in dilation from west to east, punctuated by a series of highs and lows.

South Coast. The maximum crustal dilation, 93%, occurs midway along the Glas Eilean to Mingary Pier traverse. At the western extremities of the south coast traverse dilation is 8%, gradually increasing to 90% near Kilchoan and decreasing to 10% near Mingary Pier (Fig.6.3.2). Two localised highs (both 30%) occur between Mingary Pier and Rubha Mhile, with zero dilation being recorded east of Mingary Castle.

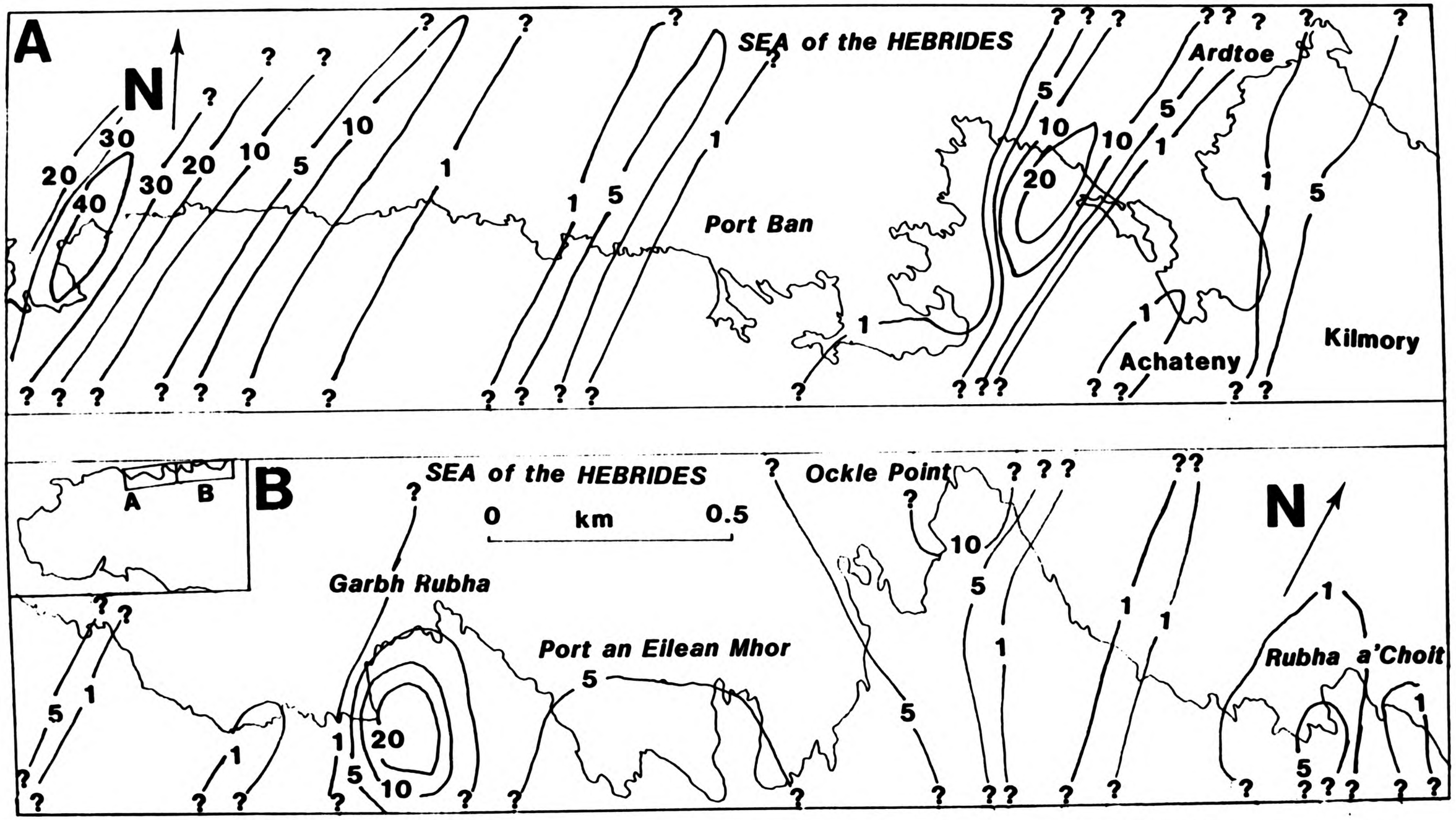

Fig.6.3.1 Percentage crustal dilation caused by the emplacement of cone sheets of the Centre One traverse

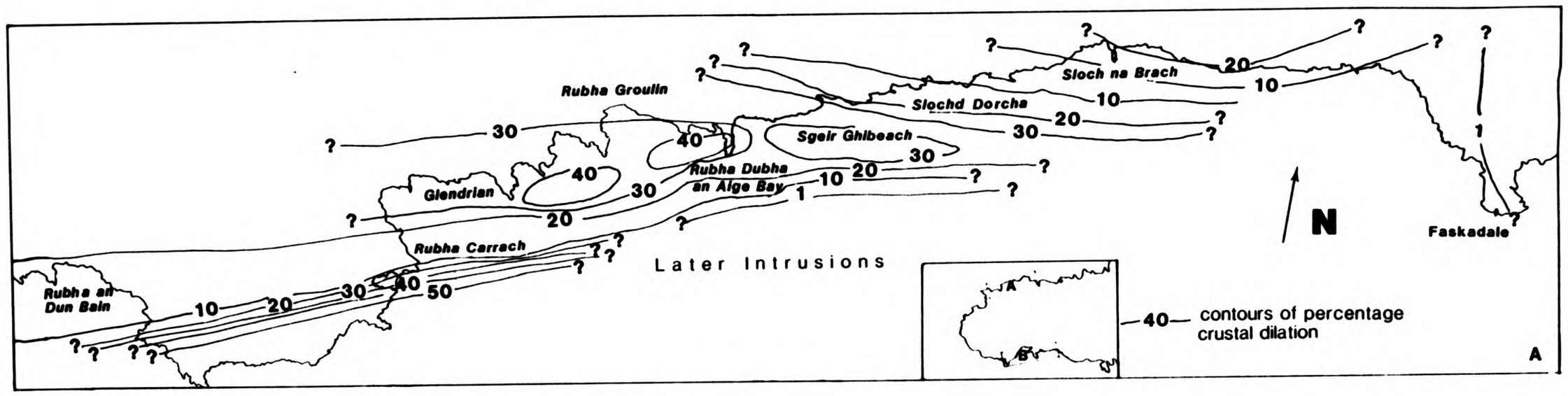

Fig.6.3.2 Percentage crustal dilation caused by the emplacement of cone sheets on the North and South coast Outer Centre Two traverses based on data collected for this study

6.3.1.3 Inner Centre Two -

Figure 6.3.3 shows that the maximum crustal dilation, 21%, occurs in the area of the Garbdhail valley, close to the focus of Centre Two activity. An Outer Group of cone sheets forms an arc of dilation, maximum 10%, close to the western coast of the peninsula. In general, the Inner Centre Two dilation is much smaller than either the Centre One or Outer Centre Two cone sheet traverses.

6.3.1.4 Centre Three -

This poorly developed set of cone sheets exhibits a maximum crustal extension of 10% (Fig.6.3.3).

6.3.2 Crustal dilation based on field slips of the Geological Survey

Although the method by which crustal dilation figures have been calculated has been described earlier (Chapter 3), it is important to stress that the cone sheets have in many places been drawn diagramatically on the field slips and therefore the figures gained from them must be interpreted with some caution. The calculated dilation figures based on the field slips of the Geological Survey have been plotted and contoured (Fig.6.3.4) and the most prominent features shown are a series of ridges which may incorporate a series of minor highs and lows. A particularly good example of such a ridge belonging to the Outer Set of Centre Two cone sheets is seen to be truncated by the ring intrusions of Centre Three. The ridges, including their

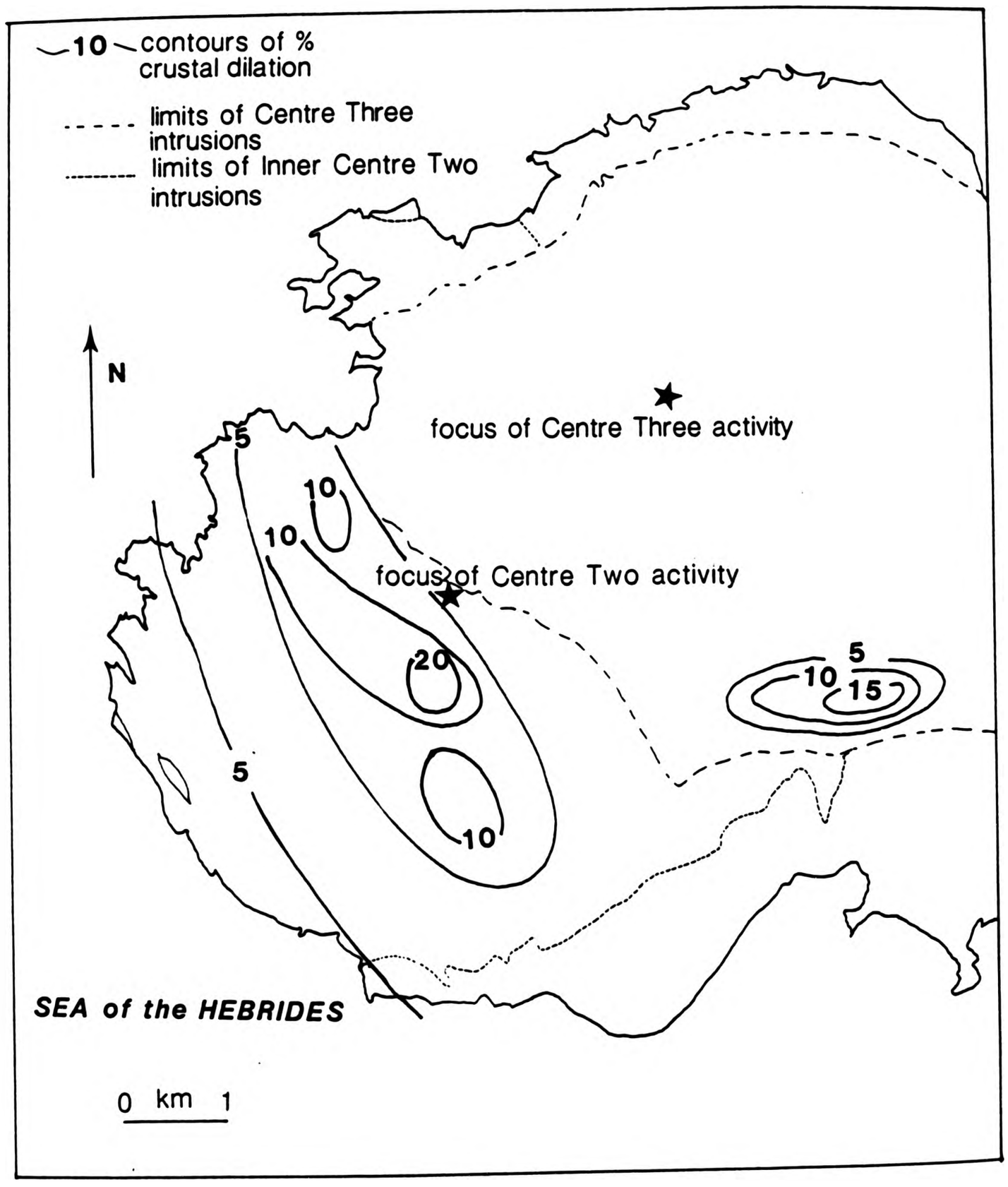

Fig.6.3.3 Percentage crustal dilation per unit length caused by the emplacement of the Inner Centre Two and Centre Three Cone Sheets contoured at intervals of 5%, based on data collected for this study

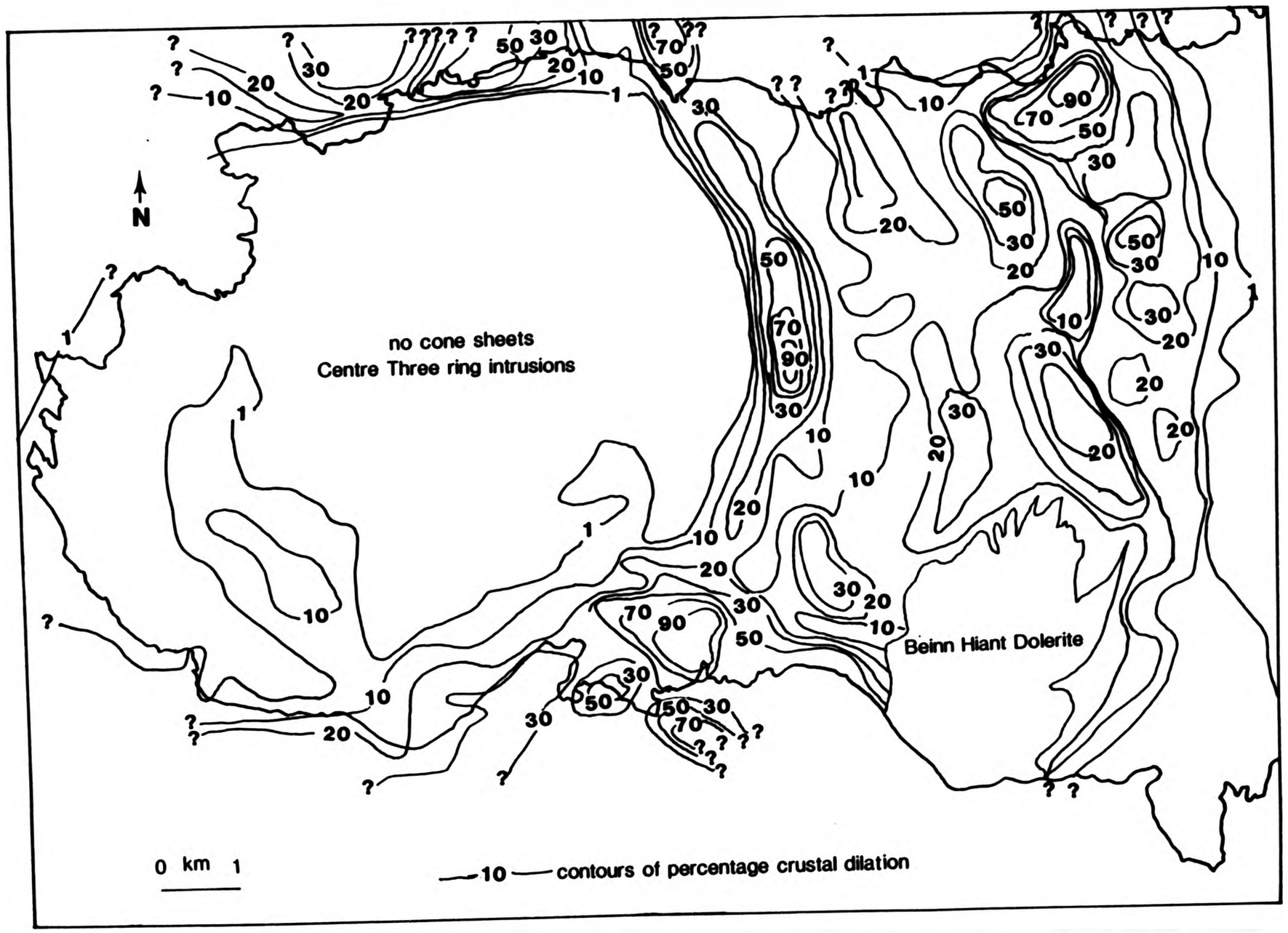

Fig.6.3.4 Percentage crustal dilation caused by the emplacement of cone sheets over the whole peninsula, data derived from the 6" field maps of the Geological Survey.

oscillating highs and lows, indicate that even within the most intensively developed area of a cone sheet complex (Chapter 5) the cone sheets are not uniformly distributed. In addition to the great difference in amount of dilation, each centre can be picked out by a change in orientation of the contour trend, for example, as shown by the Outer Centre Two and Centre Three cone sheet sets. The western extremity of the Outer Centre Two cone sheets on the south coast section and the southerly extent of the Inner Centre Two cone sheets are indistinguishable as seperate sets on the dilation map. This may indicate that the Outer Set of Centre Two and the Outer Group of Inner Set of Centre Two form a series of intrusions that were continuously emplaced, that is, cone sheet emplacement may not have halted during the emplacement of the Hypersthene Gabbro. The chemistry of the marginal facies of the Hypersthene Gabbro is similar to that of many of the Outer Centre Two cone sheets (Wells, 1954) and therefore supports the idea that cone sheets were emplaced before, during and after emplacement of the Hypersthene Gabbro.

Crustal dilation varies both within and between centres; Centre One has two highs, one of 50% and the other of 100% at Ockle Point (cf. Fig.6.3.1), the latter decreasing to less than 1% at Rubha a' Choit. In general, the level of dilation for the Centre One area varies between 10% and 20%, however, areas of zero dilation do occur. Centre One shows the lowest % dilation values of all the cone sheet sets. A discontinuous series of highs (90%-60%) and lows (20%) occur within the Outer Centre Two section along the north coast and these continue around Beinn an Leithaid where the contours form a prominent arc. A similar maximum dilation occurs along the south coast section, which

falls to 30% at Sron Bheag. The main outcrop of Inner Centre Two cone sheets have a maximum dilation of 10% which is centred on the more southerly located sheets. A small, maximum 5% dilation ridge, marks the partially developed set of Centre Three cone sheets.

6.4 COMPARISON OF CRUSTAL DILATION FIGURES

In spite of the differences in dilation values, when compared with the field based studies, the study based on the 6" field slips gives a good overall picture of crustal dilation throughout the peninsula. The map based study tends to over emphasize the Centre One distribution of dilation (Fig.6.3.4), when compared with the figures obtained from the coastal sections, for example, the maximum extension derived from the coastal section data is 40% (Fig.6.3.1) compared to the 100% (Ockle) derived from the map based study (Fig.6.3.4). This large difference can be accounted for by the presence of thick, low-dipping sheets in this area, with their top surfaces being exposed for long distances. Consequently, when mapped these sheets cover a large area of the map.

The Outer Centre Two north coast data tends to be overemphasized in the map based study (Fig.6.3.4), giving a maximum 60% dilation compared to the 40% obtained from the detailed traverse, a 50% exaggeration. Conversely, the variations identified by the detailed traverse maps (Figs.6.3.1-3) occur as discrete parallel bands across the north coast and tend to emphasize localised high dilations, thus somewhat obscurring the more general pattern depicted by the map based study

(Fig.6.3.4).

Both maps (Fig.6.3.1-3 and Fig.6.3.4) give the same general distribution of high dilations, although they differ in the values of the dilations. One point which is emphasized by the map based study (Fig.6.3.4) is the discontinuity of the dilation around the main arc of Outer Centre Two cone sheets. Also, the 50% high crustal dilation which occurs to the east of Faskadale is depicted on both maps and contrasts greatly with the 5% crustal dilation on the west of Faskadale Bay.

6.4.1

Together with the distribution of crustal strain a number of characteristics (listed below) can be used to identify individual cone sheet sets:-

1. Normal distribution of crustal dilation about a central point,
2. Gradual change in mean orientation about a central point,
3. Time relationships, i.e. cross-cutting relationships,

Therefore, based mainly on strain distributions, two cone sheet sets can be identified along the south coast of Ardnamurchan, the first occurring from Sron Bheag to Mingary Castle, the second occurring to the east of Mingary Castle. To the east of Mingary Castle a change in orientation of the dilation contours (Fig.6.3.4), also marked by zero crustal dilation, has been interpreted as a product of the Centre One cone sheet set. On the north coast section, the Outer Centre Two cone sheets in the western extremities of the traverse have been truncated by the later ring intrusions of the central complex, principally the Hypersthene Gabbro. Consequently, the crustal dilation figures

begin at high values (20-30%). The area from Rubha Carrach to Rubha Dubh an Aighe consists of a region of highs (40%), whose values decrease towards the east, possibly marking the termination of a series of sheets towards Faskadale.

6.5 STRAIN CAUSED BY THE EMPLACEMENT OF CONE SHEETS

6.5.1 Introduction

Ramsey (1967, p51) describes strain as:-

> " A distortion, deformation or change in the position of particles relative to each other " is termed a "strain."

In terms of cone sheet emplacement a single resultant strain is defined as that resulting in a deformation caused by the emplacement of a set of cone sheets, that is anything ranging from a single cone sheet to a large number of cone sheets of parallel orientation within a unit length; the net result is an extension in a single direction. Figure 6.5.1 demonstrates the change in shape of the finite strain ellipse when more than one set of cone sheets occur in one section. By calculating the strain ellipse for each unit length of each cone sheet set, the distribution of strains is obtained.

6.5.2 Methods

Method 3, in which the strain caused by the emplacement of

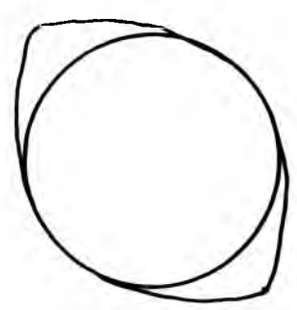

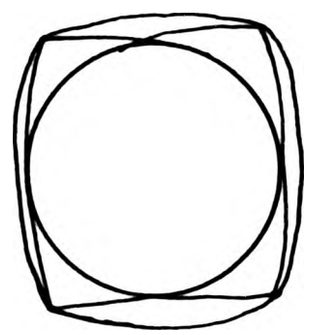

Plan view

one cone sheet or a number of parallel cone sheets results in a single extension direction

Plan view

a number of non parallel cone sheets results in an equal number of extensions

Fig.6.5.1 Diagram to illustrate the change of the shape of the strain ellipse caused by the emplacement of non parallel cone sheets

each sheet can be measured, was chosen for the computation of the finite ellipse (Chapter 3). Data collected from each unit length has facilitated the computation of strain along the horizontal surface. Few vertical strain profiles have been calculated because of the lack of suitable cliff sections. However, two well documented cliff sections have been studied at Rubha Carrach and Sron Bheag, both of these contain sheets belonging to the Outer Set of Centre Two and illustrate strains in a number of directions in vertical section.

6.5.3 Horizontal strain

Horizontal strain is the strain caused by the emplacement of cone sheets as seen at the present erosion level.

6.5.3.1 Centre One -

Figure 6.5.2 illustrates the component strain ellipses. The most prominent strain direction which occurs all across the section is in the direction of 040°. In sections 1 to 4, strains in the 020° and 060° directions also occur with a strain in the 080° direction being present in the east.

6.5.3.2 Outer Centre Two -

North Coast. Figure 6.5.3 shows the distribution of strains for both north and south coastal sections. However, on the north coast section there is a wide range in strain orientations. From Rubha an Duin Bain, where the strain is in a

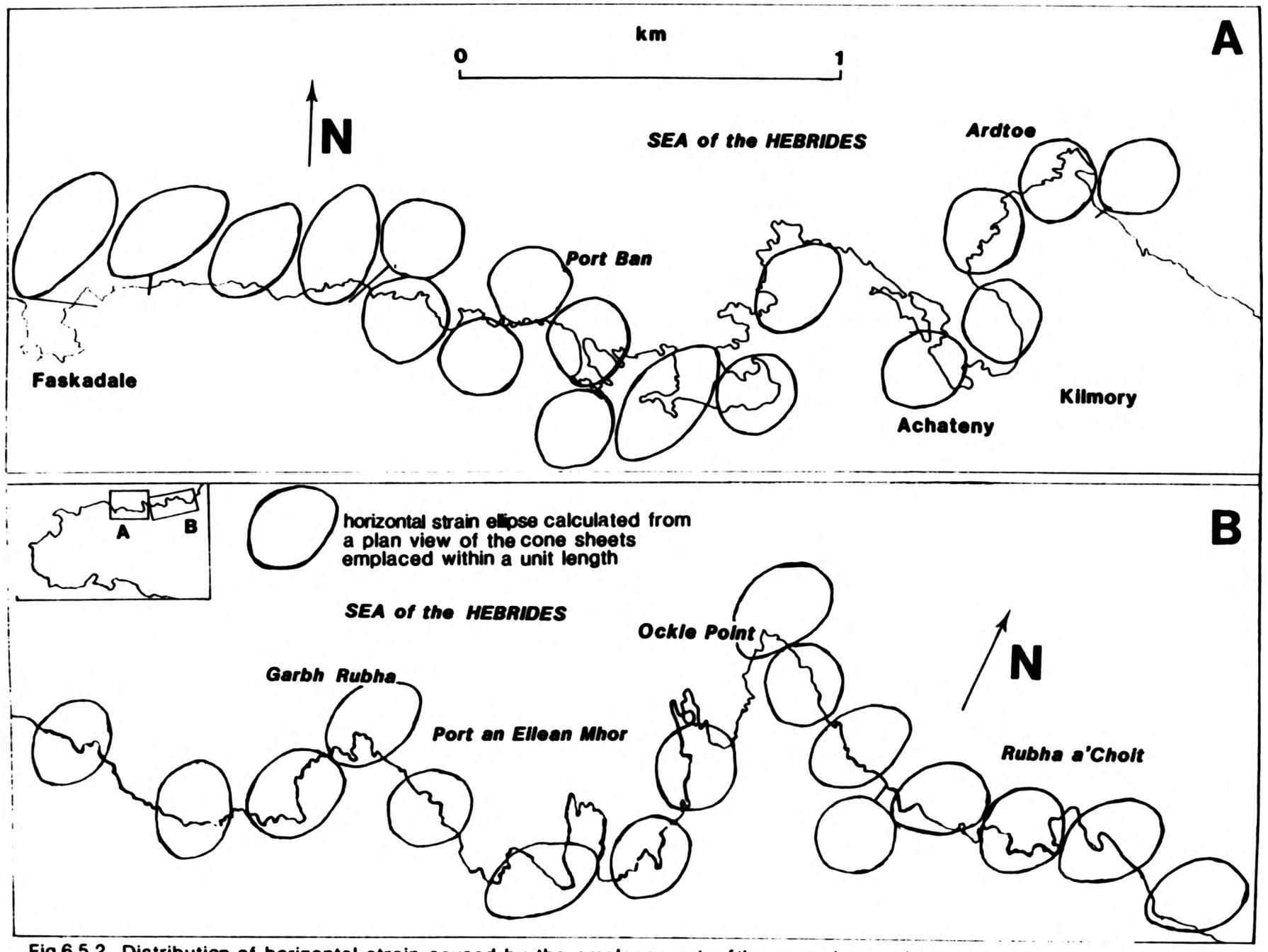

Fig.6.5.2 Distribution of horizontal strain caused by the emplacement of the cone sheets of the Centre One traverses

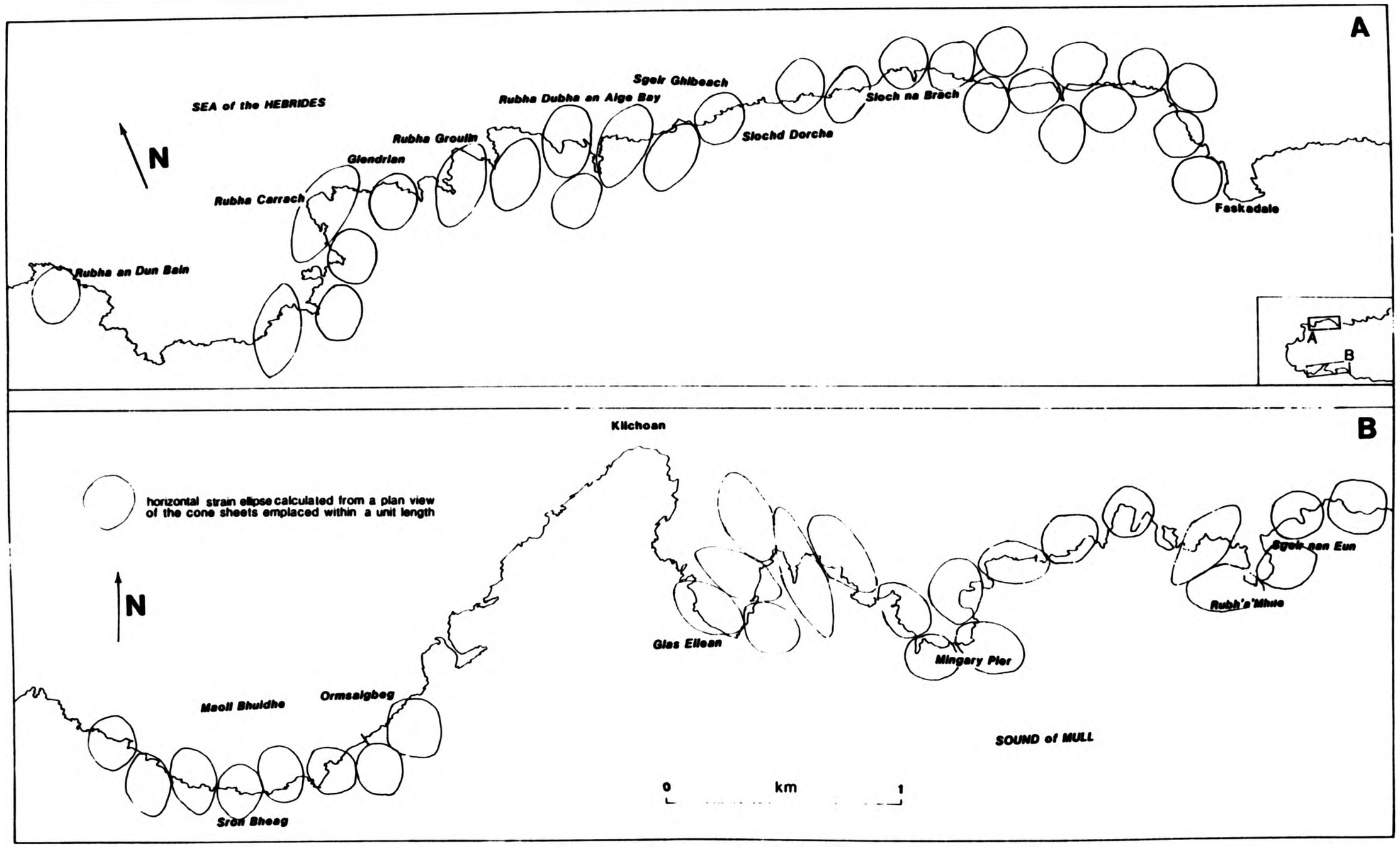

Fig.6.5.3 Distribution of horizontal strain caused by the emplacement of cone sheets for both the north and south coast Outer Centre Two traverses

north-south direction, to Sgeir Ghibeach a number of strain directions can be identified, these being 020°, 040°, 060° and 160°, although each strain direction does not necessarily occur in every unit length. To the east of Sgeir Ghibeach each unit length shows less variation in the strain orientations which are 020°, 040° and 140°, which perhaps demonstrates a gradual change in orientation of two strains from 000° in the west of the section to 020° in the east and from 020° in the west of the section to 040° in the east and two additional strain directions orientated at 140° and 160°. The presence of the strain orientated at 040° to the west and east (Centre One, above) of Faskadale, emphasizes the possibility of overlap of the two cone sheet sets (Centre One and Outer Centre Two).

South Coast. The western extremities of the Sron Bheag traverse show a strain direction of 000° (Fig.6.5.3), unlike the strains farther to the east which are 060°. It is possible that some Inner Centre Two cone sheets are present in the western part of the traverse. Along the west to east traverse a gradual change in strain orientation occurs from 160° (Sron Bheag) to 120° (Mingary Pier). Midway along the Glas Eilean to Mingary Pier traverse a 160° orientation strain occurs and it is possible that the change in strain orientation to the east of this location marks another set of cone sheets.

6.5.3.3 Inner Centre Two -

The overall strain profile is rather low for the Inner Centre Two traverses and shows a number of strain directions

(Fig.6.5.4). The Beinn Bhuidhe sections show strains in the 060° and 080° directions which gradually changes orientation to 000° and 020° at Upper Garbdhail. Each of the two cone sheet groups recognised (Inner Group and Outer Group, see Chapter 5) has a distinguishable strain, emphasized by the geographical distribution. The Inner Group show two strain directions as indicated above, whilst the Outer Group has a strain orientated at 110° at the Lighthouse and at 010° at An Acairseid.

6.5.3.4 Centre Three -

The strain for the cone sheet set is low and changes from 020° to 010° over the two unit lengths (Fig.6.5.4).

6.5.4 Vertical Strain

Figure 6.5.5 shows the cliff section at Sron Bheag. The Inferior Oolite host rocks are cross cut by a number of cone sheets and, based on cross cutting relationships, at least six phases of emplacement can be recognised. Based on their angle and direction of dip, they can be subdivided: two dip to the north and one to the south. The sheets dipping south are more shallowly inclined (35°) than the majority that dip to the north (30°-50°). Although the maximum extension is in the 350° direction (maximum 6% extension), three strain directions can be identified, 340°, 010° and 030°. The horizontal strain at this location (Fig.6.5.3) shows only one strain direction, implying that no differentiation between the three groups seen in cross section can be made from the plan view. This provides further

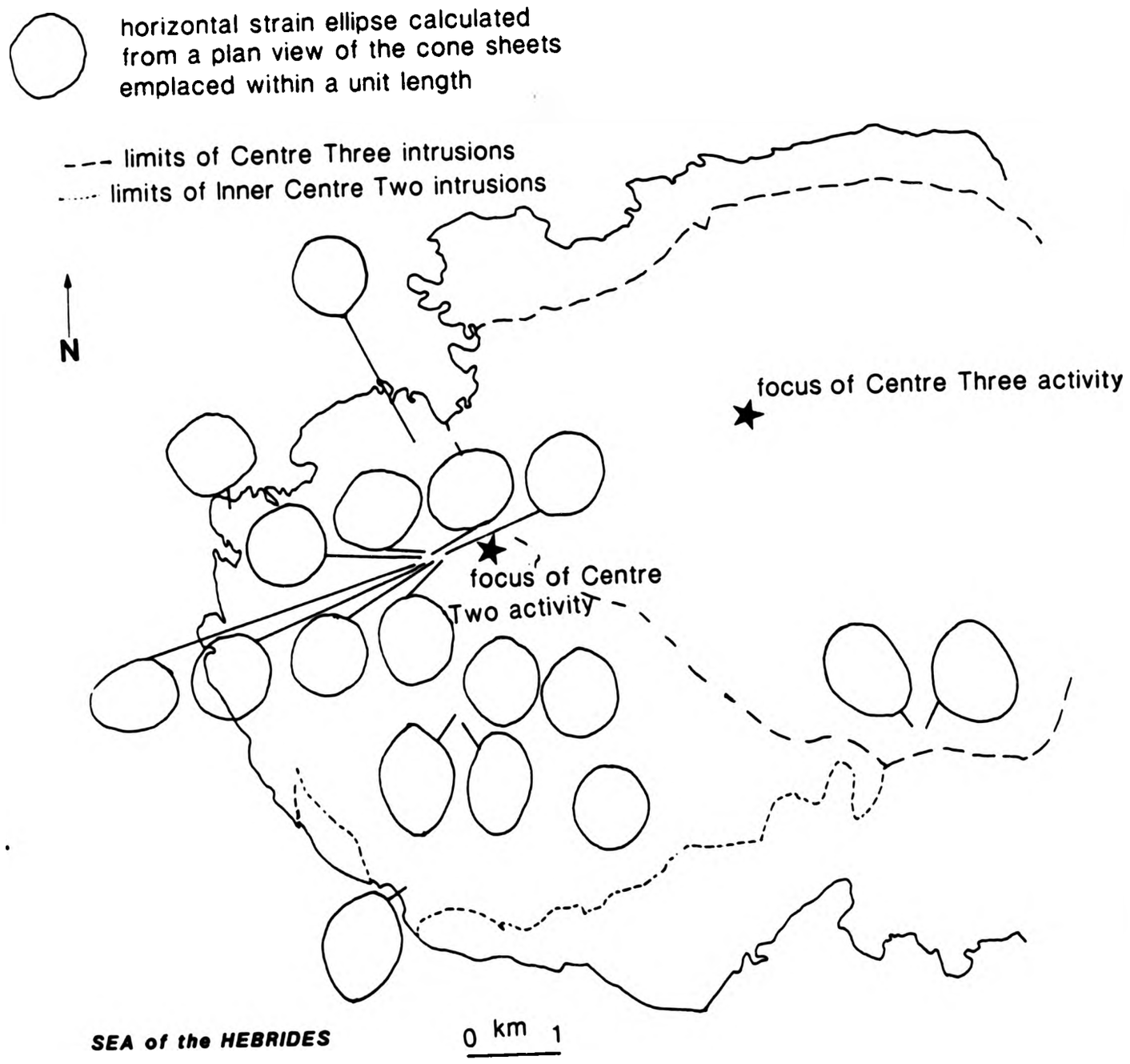

Fig.6.5.4 Distribution of horizontal strain caused by the emplacement of cone sheets of the Inner Centre Two and Centre Three traverses

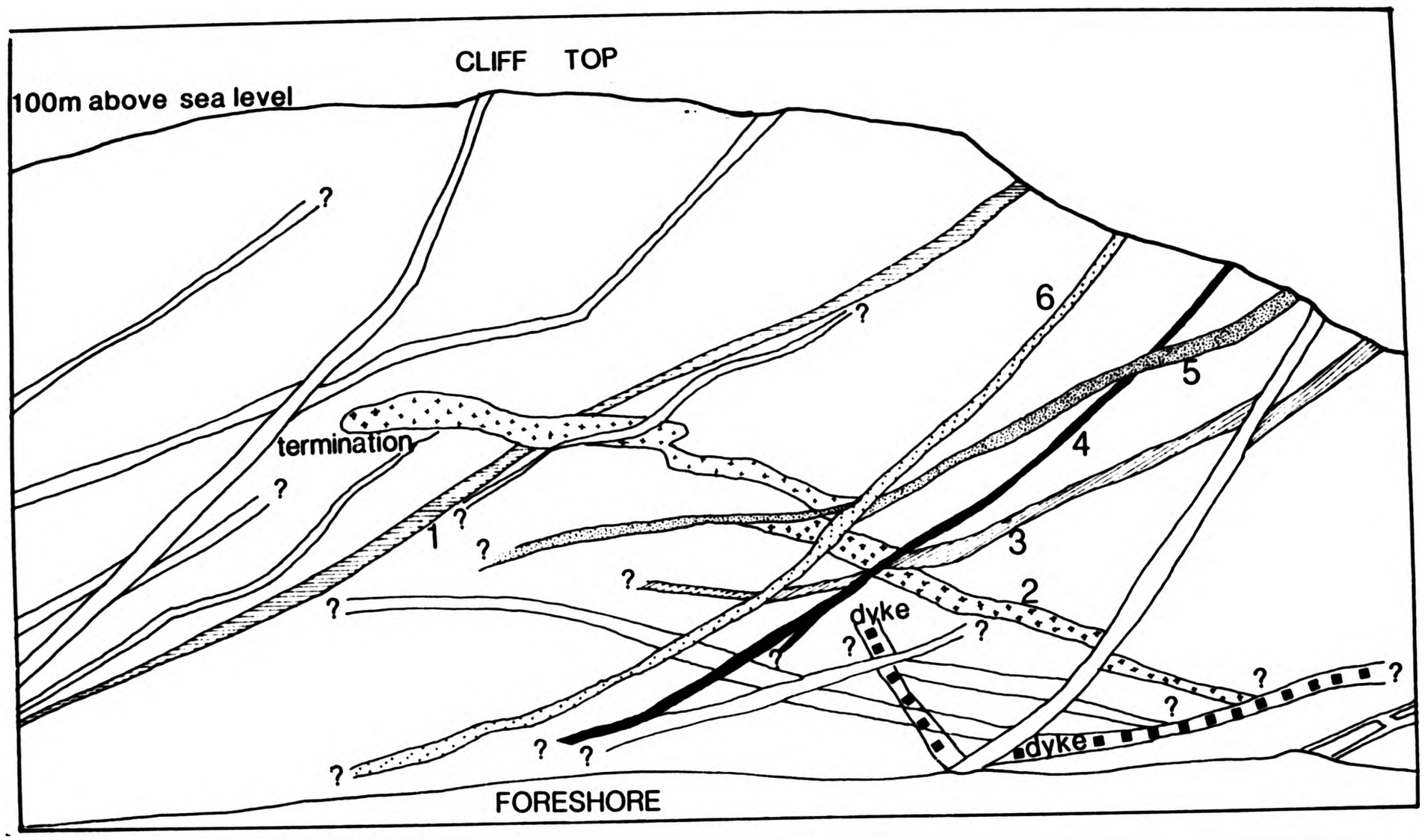

Fig.6.5.5 Diagram of the cliff section at Sron Bheag, showing Outer Centre Two cone sheets emplaced into Inferior Oolite sandstones and limestones (Plate6. 1). At least 6 phases (ornamented cone sheets 1-6) of emplacement can be recognised from cross cutting relationships

evidence for the models described in Chapter 9, that is, although cone sheet sets may show very similar annular outcrop patterns, their focii are located at different levels within the crust and their axes may dip at different angles.

6.6 TWO-DIMENSIONAL MOVEMENTS ALONG CONE SHEET FRACTURES

Richey et al. (1930) described the movement along cone sheet fractures as reversed, resulting in uplift of the central block. This has been accepted by most subsequent authors e.g. Le Bas (1979) and Bahat (1979,1980). However, Richey et al. (1930) does not quote specific examples of this phenomenon but Keunen (1937) does quote a number of examples in Mull and Ardnamurchan of cone sheet fractures which exhibit reversed movements. In contrast, Robson and Barr (1964) concluded, from a theoretical study, that cone sheets are normal shear fractures and that therefore the central block would descend.

6.6.1 Examples of two dimensional displacement in Ardnamurchan

Throughout the complex the sense of opening along 84 cone sheets, that is approximately 10% of the total number of cone sheets studied, can be ascertained. In most of the measured examples shear movements, both normal and reversed, predominate. However, in six examples the displacement of the wall rocks is orthogonal to the igneous contacts indicating tensional fractures (Plate 6.2 and Fig.6.6.1).

Of the cone sheets which have opened by shear, 24 (29%) show normal displacement (Plate 6.3) and 54 (64%) show reversed

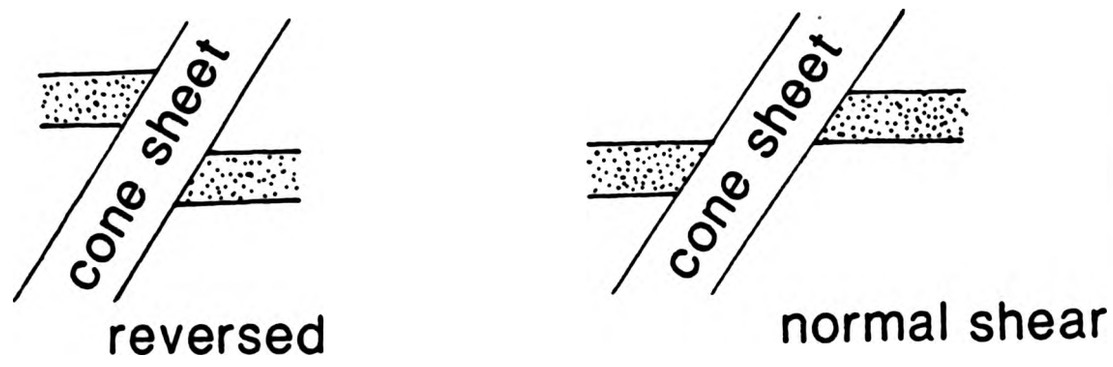

Fig.6.6.1Nomenclature used in this study for the description of cone sheet opening directions

Plate 6.1 A quartz veim (A) displaced normal to the margins of a sheet indicating that the cone sheet opened by extension (tension). Inner Centre Two, Beinn na Seilg.

Plate 6.2 The displaced layering in the Hypersthene Gabbro on either side of a cone sheet indicates normal shear displacement of the country rock, the downthrown block is on the left of the photograph. Inner Centre Two, Garbdhail.

Plate 6.1 A quartz vein (A) displaced normal to the margins of a sheet indicating that the cone sheet opened by extension (tension). Inner Centre Two, Beinn na Seilg.

Plate 6.2 The displaced layering in the Hypersthene Gabbro on either side of a cone sheet indicates normal shear displacement of the country rock, the downthrown block is on the left of the photograph. Inner Centre Two, Garbdhail.

displacement (Plate 6.4). As the majority of these examples occur in the Outer Centre Two cone sheet set a comparison can be made between the north and south coast traverses, to determine if any spatial differences occur. Figure 6.6.2 shows the spatial distribution of reversed and normal opening directions for the Outer Centre Two cone sheets. Cone sheets on the north coast sections show that 8% more sheets on the north coast traverse open by normal shear compared with those on the south traverse. Both the north and south coast sections have a reversed to normal shear opening directions ratio of 3:1, therefore indicating no difference in the spatial distribution of opening mechanisms despite the difference in number of examples, that is examples are more numerous on the north coast. Normal opening directions may be accommodated by the subsidence following doming. Alternatively it is possible that the normal opening directions are the result of a superimposed tensional regime associated with the regional emplacement of the dyke swarm and therefore accommodating the decending block. However, the regional dyke swarm has a greater effect on the north coast of the peninsula (Speight, 1972) and therefore some of the normal movements along the cone sheet fractures must arise from the descending of the central block, which differs from the Anderson theory of cone sheet formation. Both theories probably operated to cause the normal opening directions seen.

To produce the three types of cone sheet fracture opening different stress systems are required, which could be as follows:-

1. External tensional system,
2. A tensional system produced by a pressure reduction in the magma chamber.
3. A shear system produced by increased pressure on the magma chamber roof.

Plate 6.3 A cone sheet intruded into Lias limestones displaces a basic sill indicating reversed movement; the upthrown block occurs on the left of the photograph. Outer Centre Two, west of Mingary Pier.

Plate 6.4 A small cone sheet emplaced into Lias limestones displaces an earlier intruded basic sill. Displacement of the sill indicates a reversed movement. Outer Centre Two, west of Mingary Pier.

Plate 6.3 A cone sheet intruded into Lias limestones displaces a basic sill indicating reversed movement; the upthrown block occurs on the left of the photograph. Outer Centre Two, west of Mingary Pier.

Plate 6.4 A small cone sheet emplaced into Lias limestones displaces an earlier intruded basic sill. Displacement of the sill indicates a reversed movement. Outer Centre Two, west of Mingary Pier.

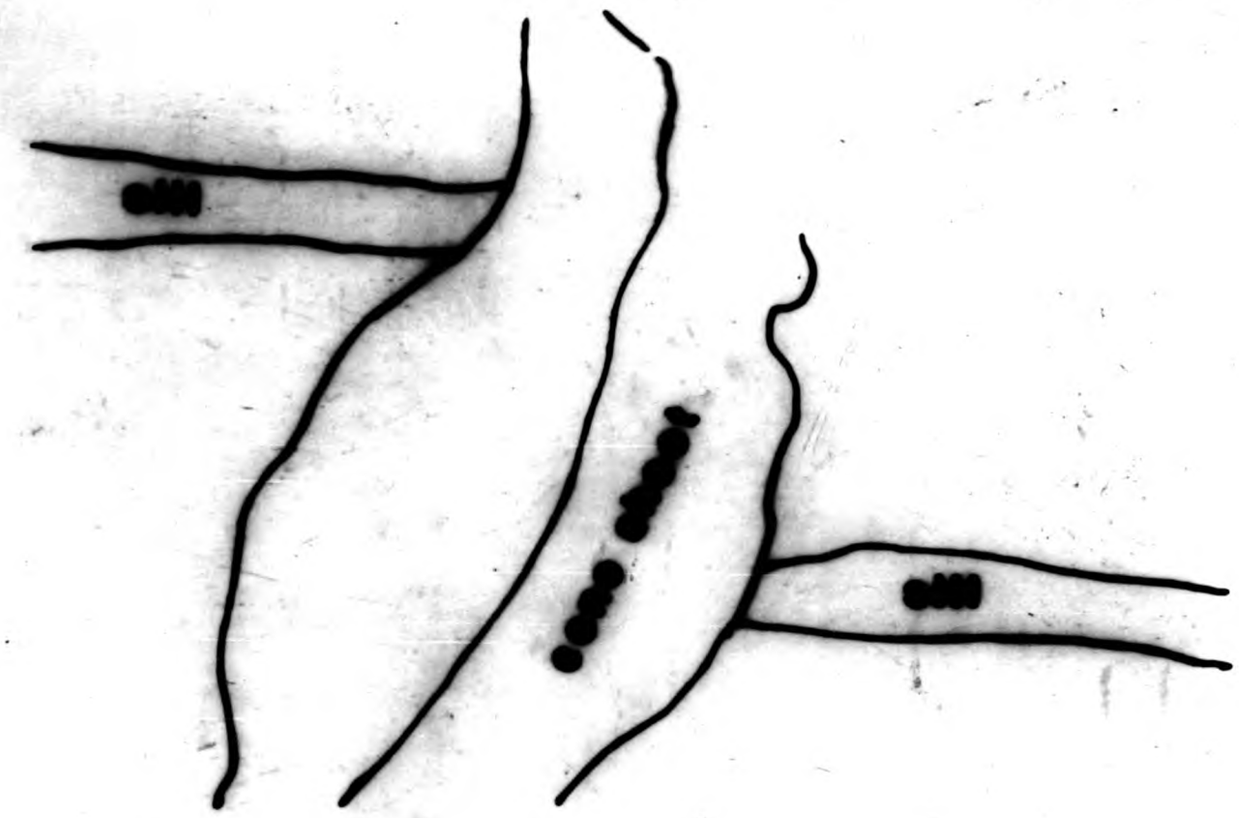

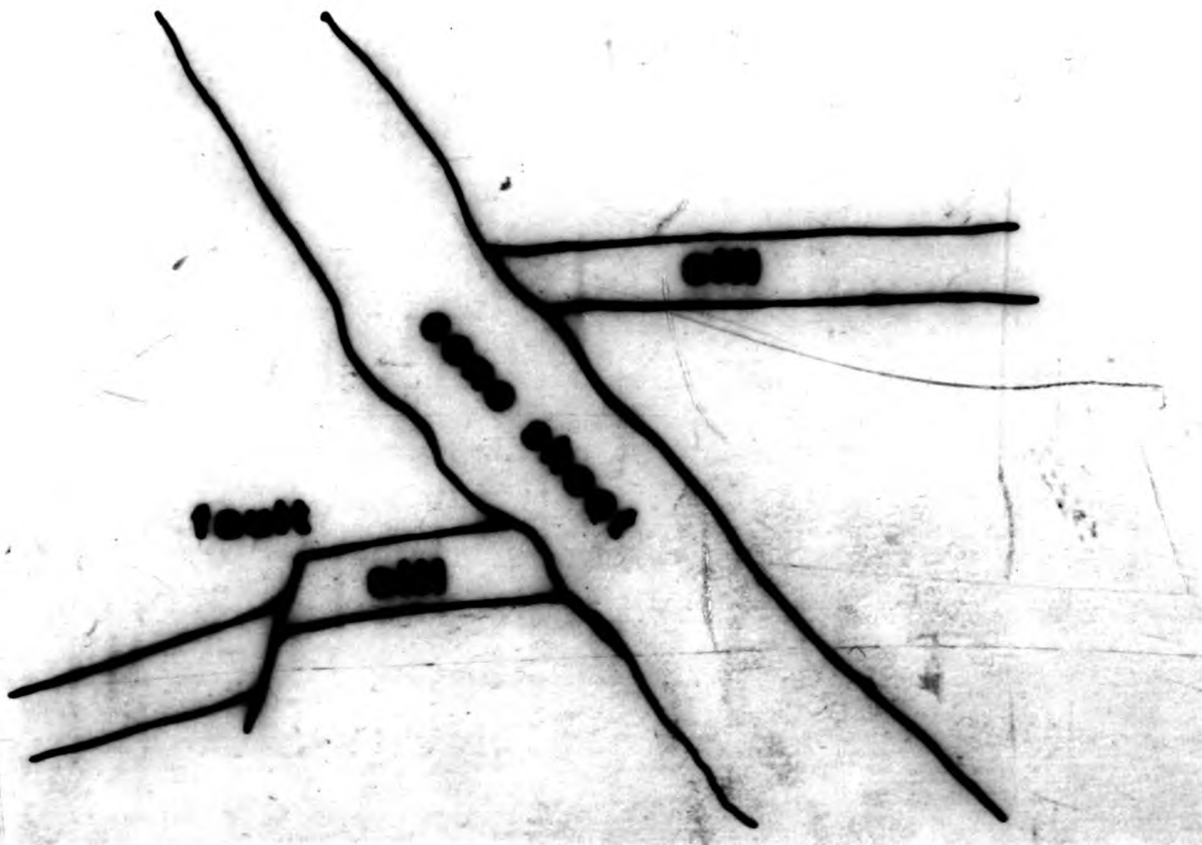

Plate 6.3 A cone sheet intruded into Lias limestones displaces a basic sill indicating reversed movement; the upthrown block occurs on the left of the photograph. Outer Centre Two, west of Mingary Pier.

Plate 6.4 A small cone sheet emplaced into Lias limestones displaces an earlier intruded basic sill. Displacement of the sill indicates a reversed movement. Outer Centre Two, west of Mingary Pier.

Plate 6.3 A cone sheet intruded into Lias limestones displaces a basic sill indicating reversed movement; the upthrown block occurs on the left of the photograph. Outer Centre Two, west of Mingary Pier.

Plate 6.4 A small cone sheet emplaced into Lias limestones displaces an earlier intruded basic sill. Displacement of the sill indicates a reversed movement. Outer Centre Two, west of Mingary Pier.

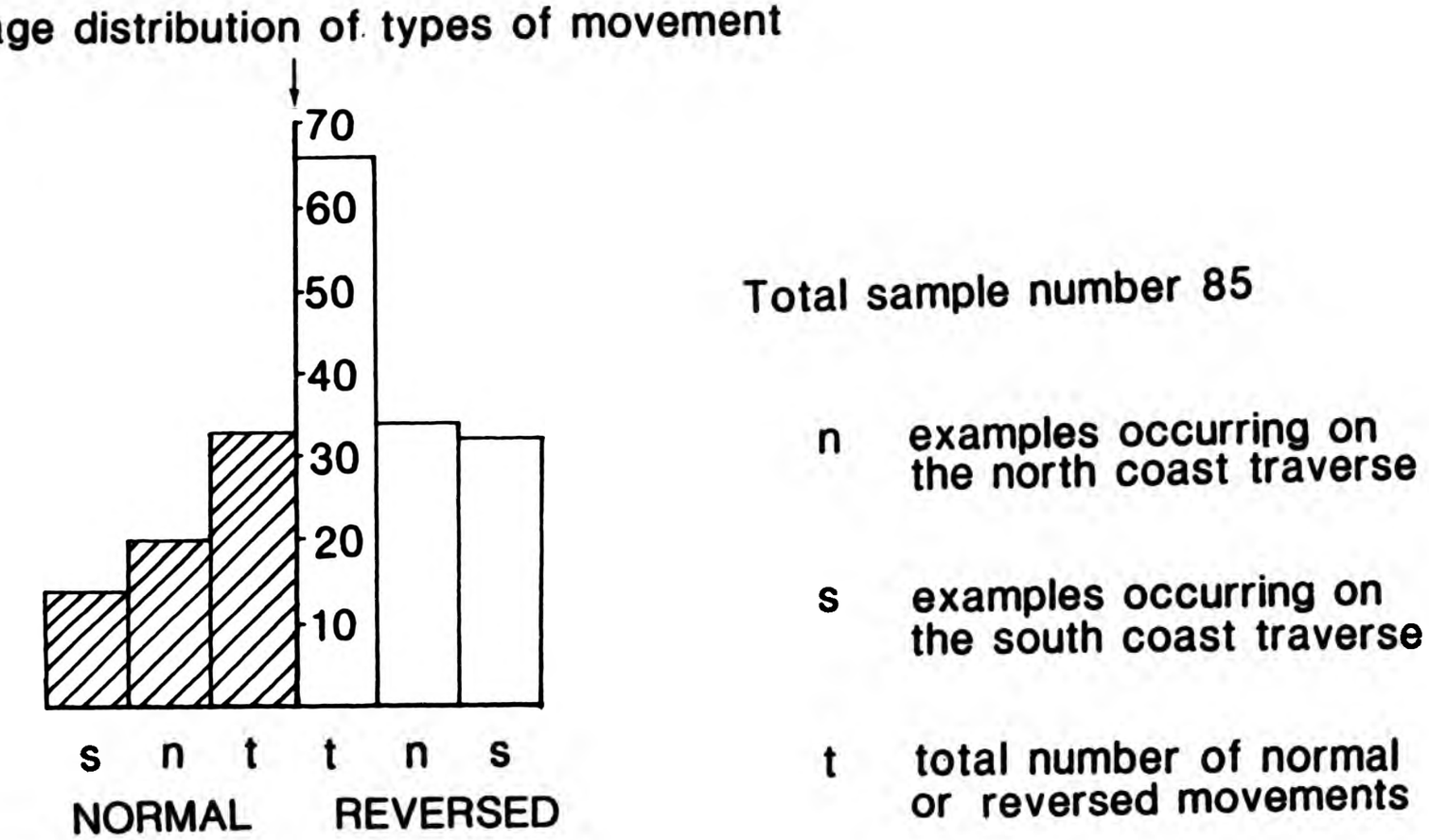

Fig.6.6.2 Percentage distribution of types of movement along cone sheet fractures along the north and south coast traverses of the Outer Centre Two cone sheet set

Phillips' (1975) hypothesis accounts for hydraulic tension fractures occurring at the upper extremities of hydraulic shear fractures. At the cessation of expansion of magma, due to retrograde boiling, the deviatoric stresses decrease and therefore magma pressure on the cone sheet fractures increases and the fractures pass into simple hydraulic tension fractures or sills. This is a possible explanation for the attitude of some of the Centre One sheets in Swordle Bay (Plate 7.20) which are parallel to low-angle bedding.

Robson and Barr (1964) and Kresten (1980) have proposed that shear fractures, with steep inward dips, develop in the country rock following down faulting of a central block during cauldron subsidence; Kresten (1980) further envisages the development of a second set of fractures congugate to the first set, which are tension joints and possess horizontal to gentle outward dips.

Most previous authors invoke an "upward push" to form the fracture system in the roof of the magma chamber, subsequently exploited by magma to form cone sheets. This "upward push" may result from increased pressure on the magma chamber roof caused by upward movement of the magma or retrograde boiling (Chapter 10). However, retrograde boiling is unlikely to occur in a basic magma chamber. As described above, three-quarters of the Ardnamurchan cone sheets apparently form in a stress regime which causes reversed shear fractures with central uplift.

6.7 THREE-DIMENSIONAL DISPLACEMENTS

The mechanisms of cone sheet emplacement has been argued since Anderson (in Bailey et al. 1924) first postulated that cone sheets occupied tensional fractures. Robson and Barr (1964) thought that cone sheets occupied shear fractures. Similarly, Phillips' (1975) mechanism for cone sheet emplacement involved the formation of hydraulic shear fractures. However, neither Robson and Barr (1964) nor Phillips (1975) give field evidence to support their theories.

In order to resolve the argument it is necessary to provide well documented field evidence, preferably in the form of three-dimensional displacements for the type of movements associated with the emplacement of cone sheets. However, the present day fracture, as represented by a cone sheet, incorporates two elements of the opening mechanism, that is one element relating to the fracture development and the other caused by the emplacement of the magma along the fracture. It is possible that the two elements may overprint the effects of each other. Piercing point analysis (Chapter 3), however, gives the amount and direction of movement along the fracture, that is the net result of the opening mechanisms.

6.7.1 Piercing Points

Examples of cone sheets that can be used for piercing point analysis are few in number, due to the prerequisites required for such an analysis (Chapter 3). Seventeen examples have been found. A number of the piercing point analyses are illustrated

in Figs.6.7.3-10 which also show the different types of marker horizons used. A number of characteristics associated with the opening of cone sheet fractures have become prominent during analysis and these include the amount and direction of opening, relationships between thickness of sheet and amount of displacement. The majority of piercing point examples occur in Jurassic host rock, with 4 in Moine rocks, 1 in basic host rock and 1 in granophyre host rocks. All the sheets used in the piercing point analysis belong to the Outer Set of Centre Two, this is due to the prominence of bedding in the Jurassic combined with the large number of intersecting cone sheets in the Outer Centre Two sections.

As described in the Memoir the mode of emplacement of cone sheets involves fractures opening in a reversed direction, and only the roof moves during the formation of cone sheets. However, it can be shown for the cone sheets analysed in three-dimensions that both normal and reversed movements occurred during the formation of cone sheets. Two of the cone sheets analysed by the piercing point technique show normal displacement and therefore when compared to those which show reversed displacement, they indicate different stress systems. Five examples of piercing point analysis indicate reversed shear displacement. The seven examples which show tension as the dominant process of opening also indicate some shear movement. This is discussed in chapter 10.

When the piercing point data is analysed it becomes obvious that there is not a simple division between a shear controlled opening and a tension controlled opening, yet as a result of the

analyses a dominant processes can be assigned. Piercing point analysis shows that seven of the analysed sheets opened in tension, seven under shear and three examples in which both tension and shear seem to operate. The amount of displacement resulting from shear movements ranges from 2.5m (1.9m thick sheet) to 8.25m (2m thick sheet). Shear movements are commonly associated with thicker sheets. The thinner sheets tend to open by tension, displacements range from 5cm (20cm thick sheet) to 90cm (50cm thick sheet). In order to compare the amount of movement of each sheet in relation to the thickness of the sheet a displacement index (H) has been calculated:-

$$\frac{\text{amount of movement}}{\text{thickness of sheet}} = H$$

Table 6.1 shows the results calculated for the displacement index. Sheets opening under tension have H values of 0.1 to 1.8, whereas sheets opening under shear have H values of 1.3 to 4.1. It is interesting to note the amount of overlap of the H values for the two processes, that is between 1 and 2. There are two possible reasons for this, the first is that all sheets involve both tension and shear processes in the opening of their fractures and therefore the H values form one continuous scale or, secondly, that the two processes are independent of each other and that the overlap of the H values is of no significance (Fig.6.7.1). A plot of H against sheet thickness (Fig.6.7.2) tends to support the former suggestion, whereas a plot of the amount of movement against thickness of sheet (Fig.6.7.1) shows that the shear and tension examples form two separate trends.

Table 6.1 Table of piercing point results showing the thickness, amount of movement, type of movement and H value for each sheet

where T tension
R reversed shear
N normal shear

Thickness	Movement	H	T/R/N
0.20m	0.05m	0.25	T
2.00m	8.25m	4.13	R
1.90m	2.50m	1.32	R
0.08m	0.07m	0.98	T
1.50m	2.30m	1.53	T
0.06m	0.06m	0.00	T
0.50m	0.90m	1.80	T
1.00m	3.20m	3.20	N
1.00m	2.83m	2.83	R
1.00m	3.00m	3.00	T
0.85m	2.31m	2.72	N
0.90m	1.25m	1.47	T
1.00m	0.37m	0.37	N
0.12m	0.34m	2.80	R
0.12m	0.21m	1.75	R
0.05m	0.10m	2.00	R

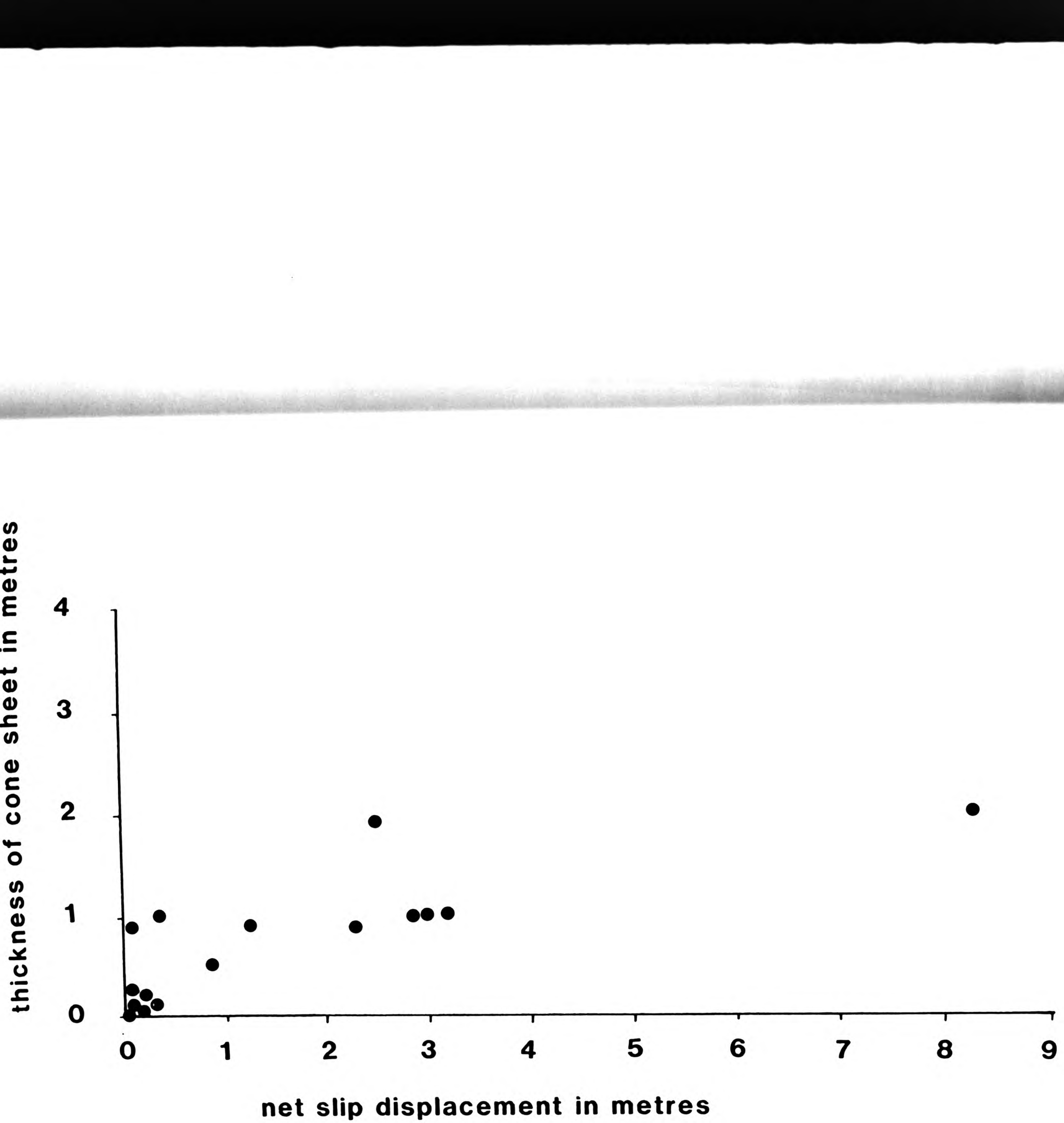

Fig.6.7.1 Diagram to show the relationship between sheet thickness and the amount of displacement of the country rock (net slip) for all piercing point analyses

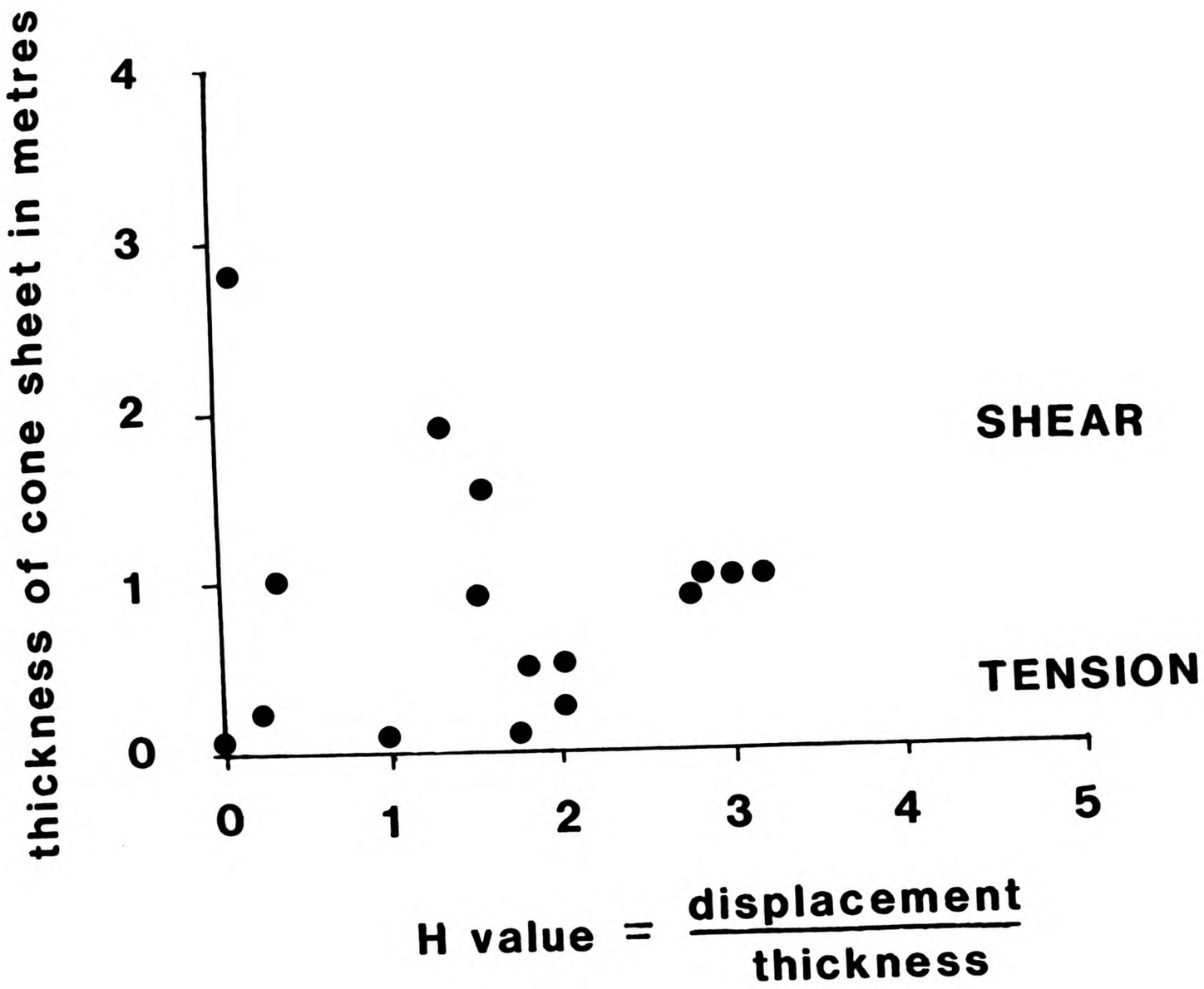

Fig.6.7.2 Diagram to show the relationship between thickness of cone sheets and H for all piercing point analyses

However, on the basis that tension is required to open the fracture it is most probable that the two processes are closely linked.

Figure 6.8.2 shows the position and direction of the vectors as determined by the piercing point analyses. Despite their variation in amount of dip (16°-77°) most of the vectors are almost parallel to the strike of the sheets. The pitch direction of the vectors describe an anticlockwise movement over the whole area of the complex, possibly indicative of a torque force. Further evidence of the existence of this force is seen in Plate 4.8 which shows a profile of a sheet at the Lighthouse section, in which the apophyses indicate a shear force, plus the presence of en echelon sets at the same location (Fig.7.3.1). Two notable exceptions to this are those piercing point solutions located at Sron Bheag, which trend perpendicular to the strike of the sheets.

Figure 6.7.3 demonstrates two examples of cone sheets which opened by reverse shear, one from the north coast section and the other from the south coast section. Both piercing point analyses show that net slip lies close to the plane of the cone sheet, although not precisely in the plane. This may possibly indicate that a tensional force was involved during opening (see later) or it may possibly be the result of an error in either field measurements or analysis of the data. The precision of the piercing point technique is difficult to assess in general as more than one analysis would be necessary for each cone sheet measured, and this would therefore require the presence of three or four intersecting planes which pre-dated cone sheet emplace-

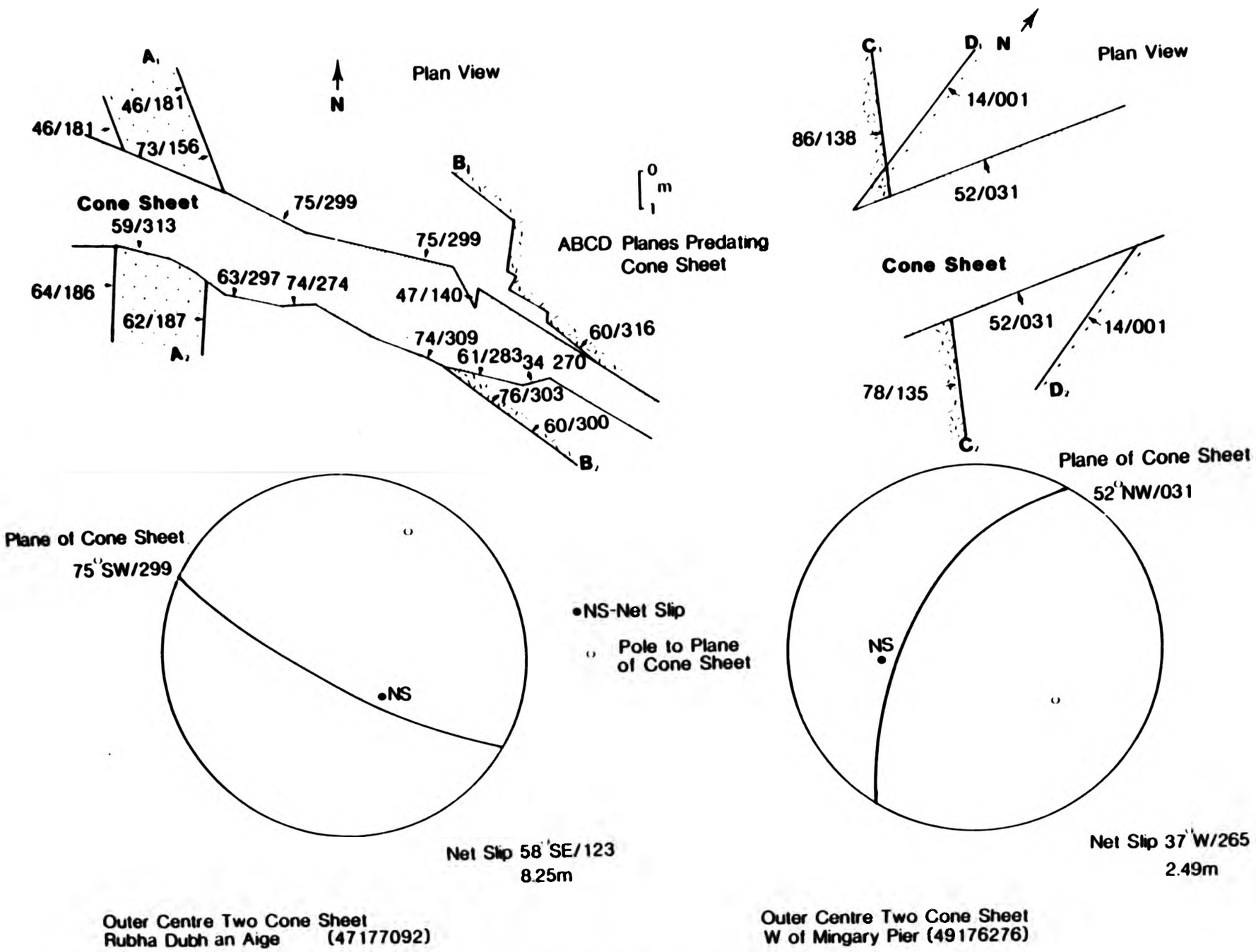

Outer Centre Two Cone Sheet
Rubha Dubh an Aige (47177092)

Outer Centre Two Cone Sheet
W of Mingary Pier (49176276)

Fig.6.7.3 Piercing Point solutions for two examples of reversed shear opening directions of cone sheets

ment.

The three types of opening mechanism are illustrated in Fig.6.7.3, reversed shear, Fig.6.7.4 normal shear and Fig.6.7.5 tension. Figs 6.7.5 and 6 and Plates 6.5 and 6.6 show piercing point solutions for two thin cone sheets emplaced in Moine host rock. Both sheets are steeply inclined (72° and 75°) and opened by extension. The net slip for both sheets lies close to the pole of the cone sheet plane indicating tension. Figure 6.7.7 shows two piercing point solutions for moderately inclined sheets (45° to 50° dip) which opened by extension. The sheet located to the west of Faskadale shows the net slip located between the plane of the cone sheet and the pole to the cone sheet. The main process involved is tension, although again the net slip does not lie very close to the pole to the plane of the cone sheet. Fig.6.7.8 shows two piercing points solutions of cone sheets located at Sgeir Ghibeach, B involves shear, whereas A involves both shear and tension. Figure 6.7.9 shows a piercing point solution for a sheet which involves reversed shear.

Figure 6.7.10 shows the piercing point solutions to the small geniculate cone sheet illustrated in Plate 6.6. On Fig.6.7.10 the pivot point of the hinge of the termination of the sheet can be seen, along with the two piercing point analyses for the two parts of the cone sheet. The first part of the sheet (A) opened by extension, whereas the parts of the sheet more distant from the hinge (B) open by shear, showing how both processes occur in close proximity within the same cone sheet.

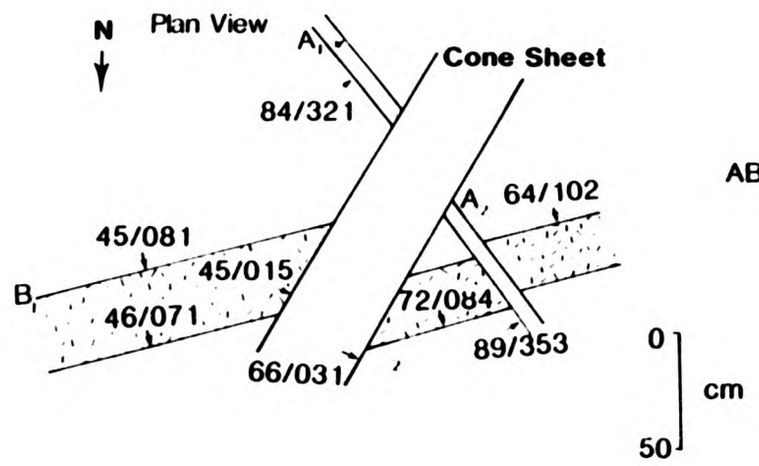

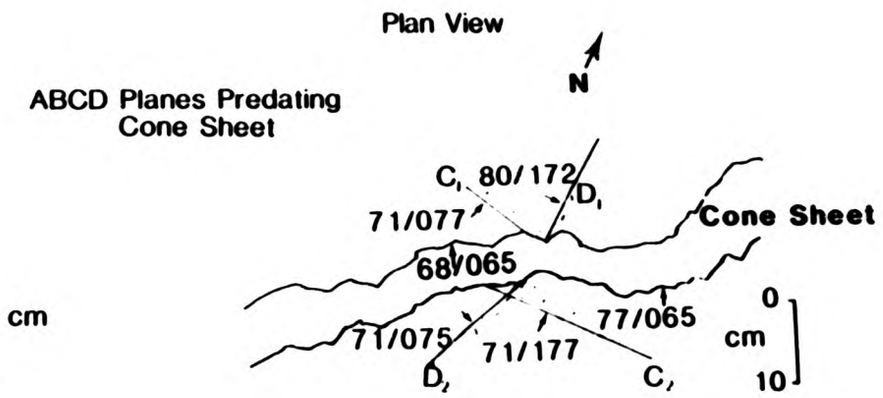

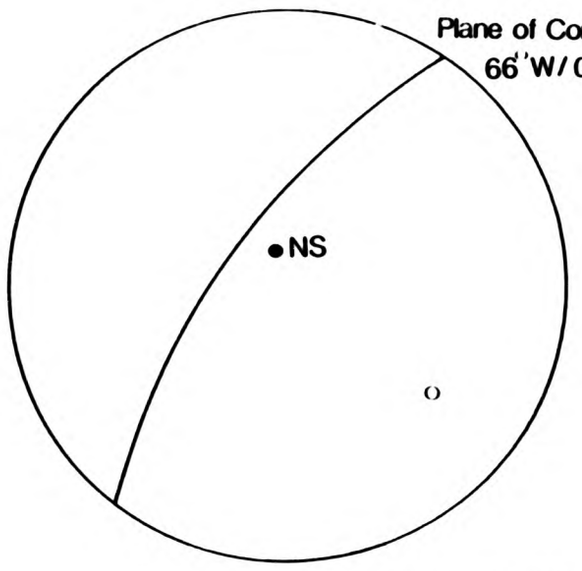

Outer Centre Two Cone Sheet
W of Mingary Pier (49126387)

Net Slip 77°N/351
2.3m

● NS Net Slip
o Pole to Plane
of Cone Sheet

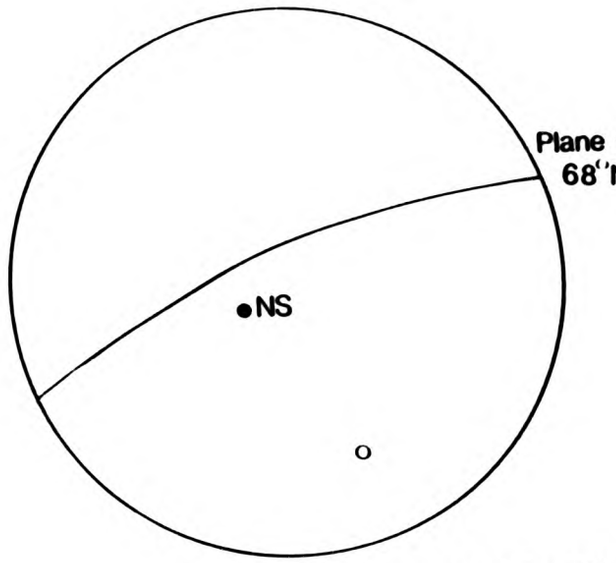

Outer Centre Two Cone Sheet
W of Faskadale (49557120)

Net Slip 68°S/226
10cm

Fig.6.7.4 Piercing Point solutions for two cone sheets which opened by normal shear

Plate 6.[5] Cone sheet intruded into Moine country rocks , two pre-cone sheet planes A and B have been used to determine the piercing point in Fig.6.

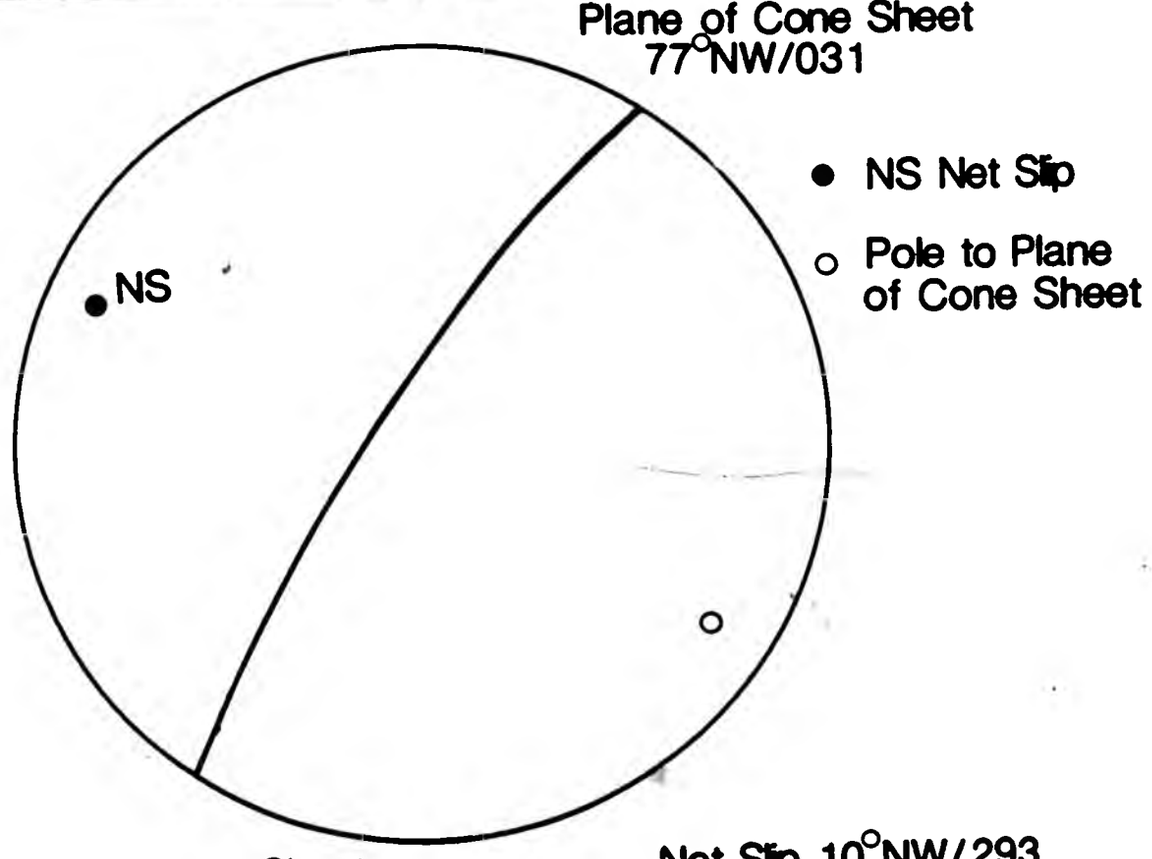

Fig.6.7.5 Piercing Point solution for the cone sheet of Plate 6. indicating that the sheet opened by tension

Plate 6.[5] Cone sheet intruded into Moine country rocks, two pre-cone sheet planes A and B have been used to determine the piercing point in Fig.6.

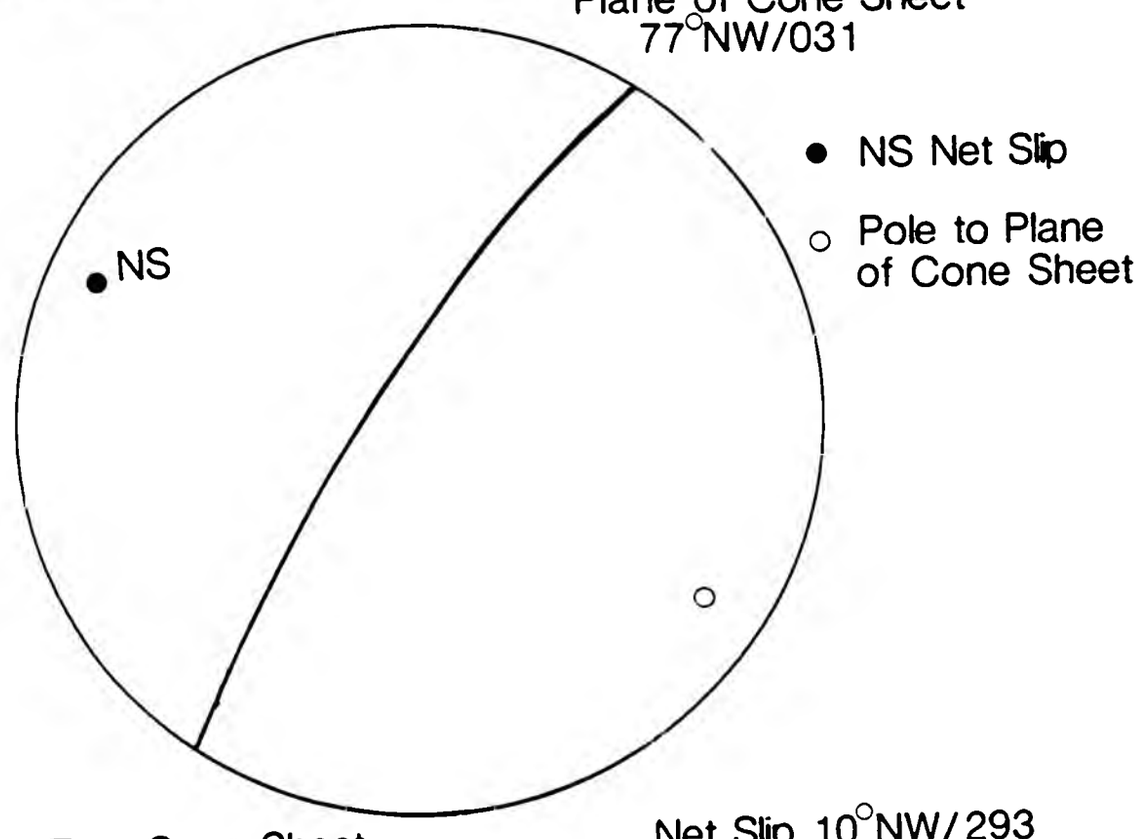

Fig.6.7.5 Piercing Point solution for the cone sheet of Plate 6. indicating that the sheet opened by tension

Plate 6.[6]Cone sheet intruded into Moine country rock two pre-cone sheet planes A and B have been used to determine the piercing point in Fig.6.

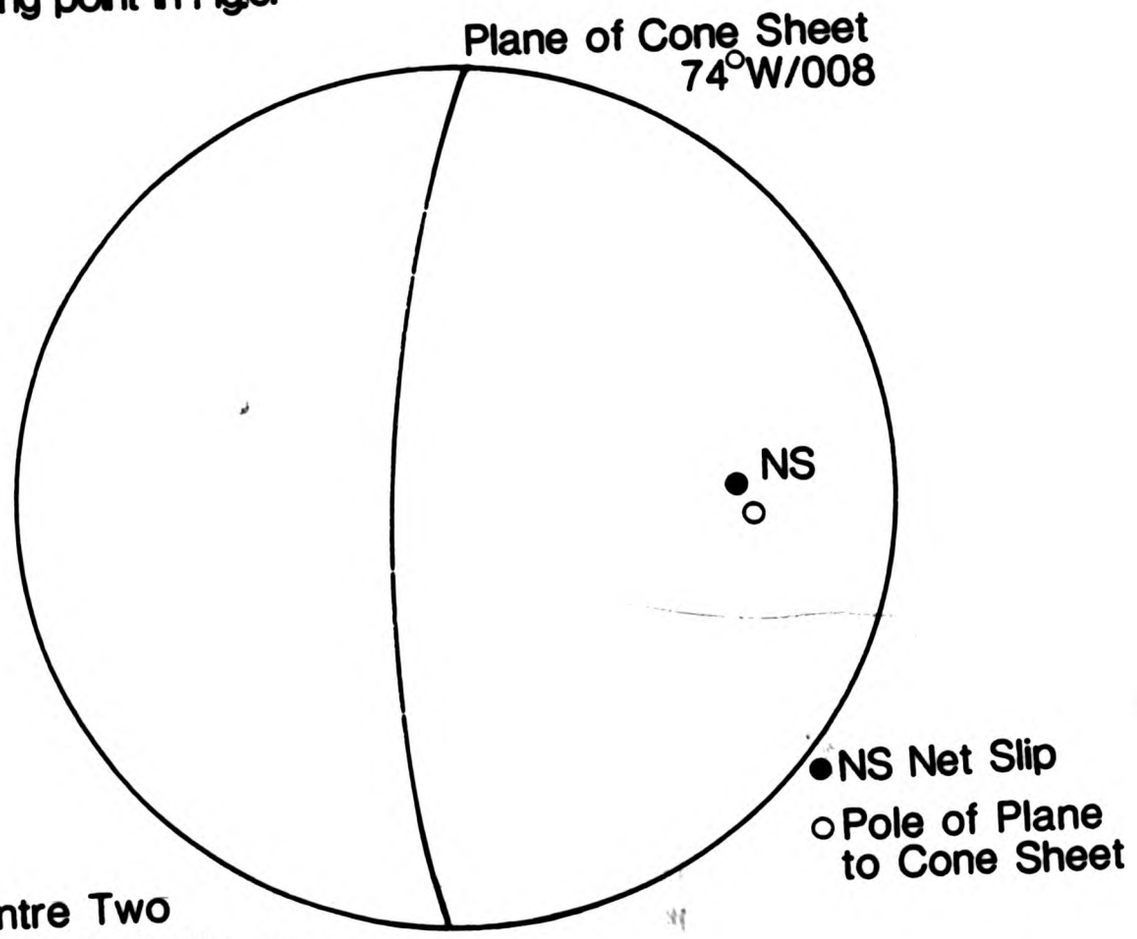

Fig.6.7.6 Piercing Point solution for the cone sheet of Plate 6. indicating that the sheet opened by tension

Plate 6.6 Cone sheet intruded into Moine country rock two pre-cone sheet planes A and B have been used to determine the piercing point in Fig.6.

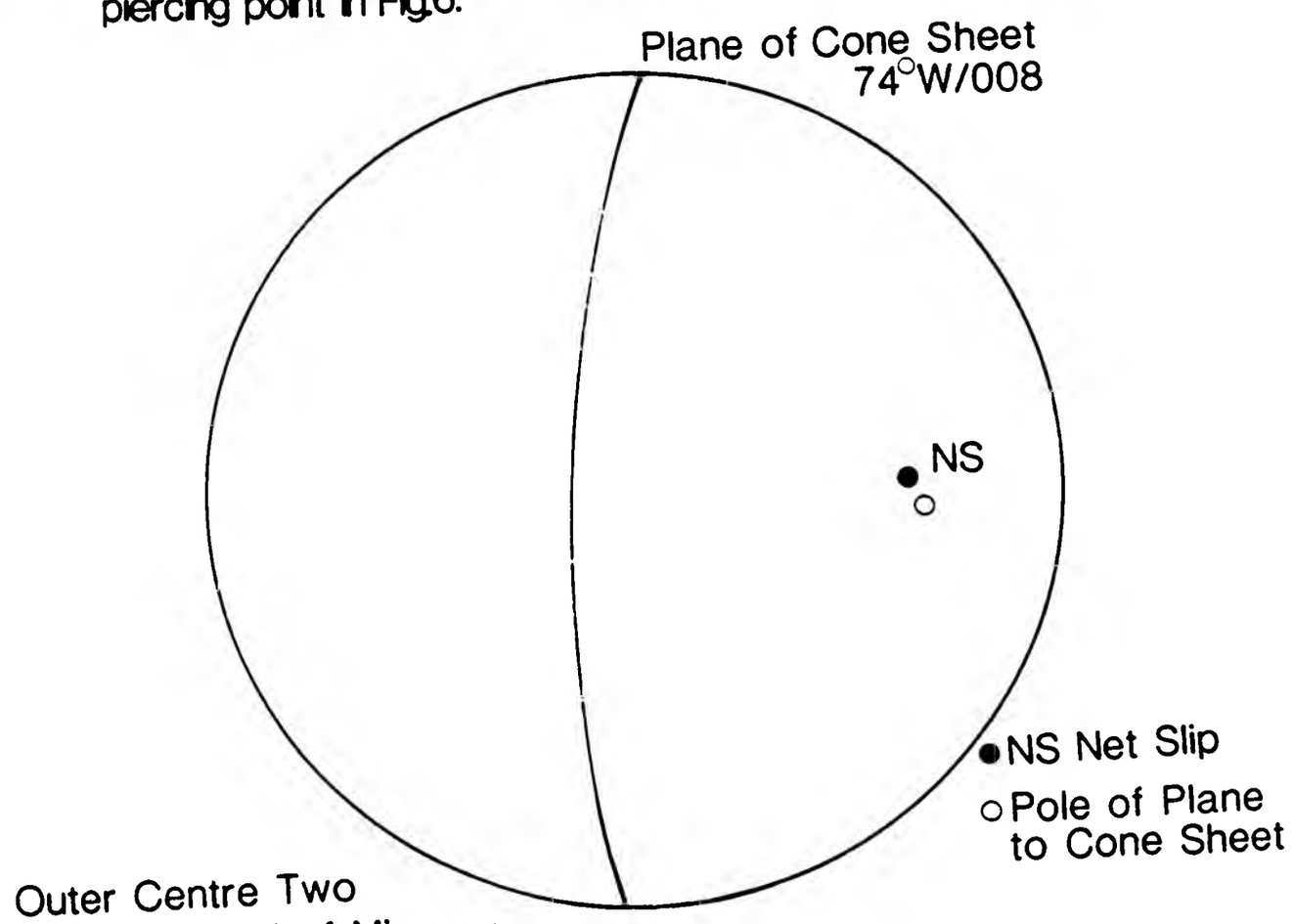

Fig.6.7.6 Piercing Point solution for the cone sheet of Plate 6. indicating that the sheet opened by tension

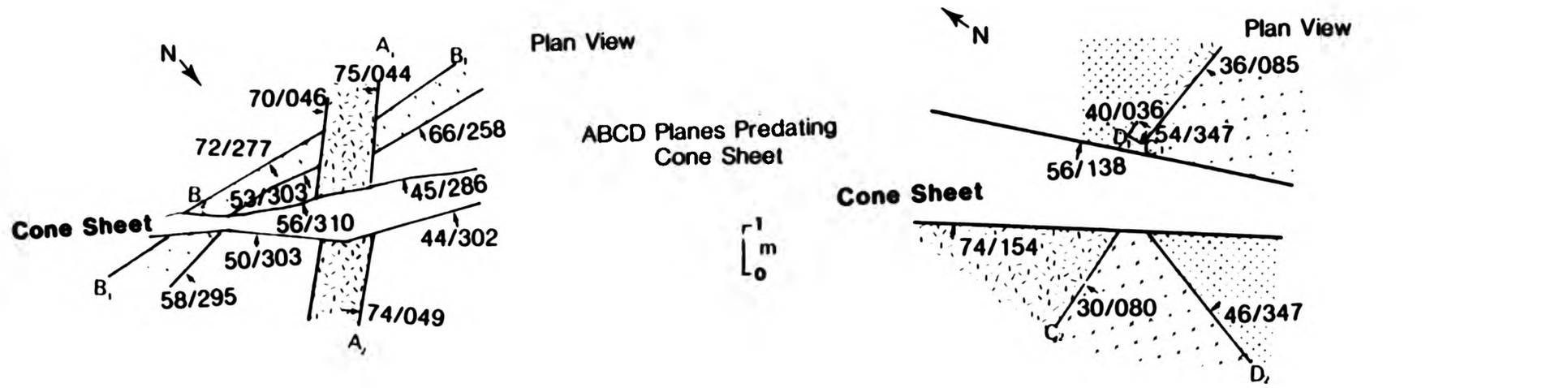

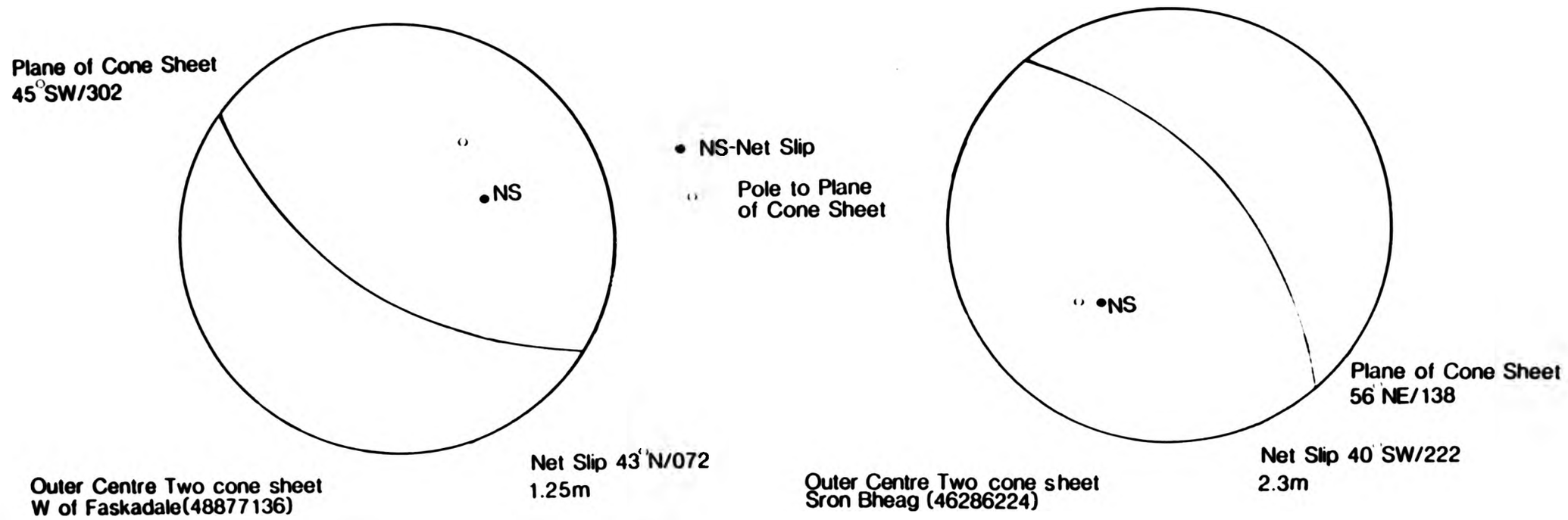

Fig6.7.7 Piercing Point solutions for two examples of cone sheets which opened by tension

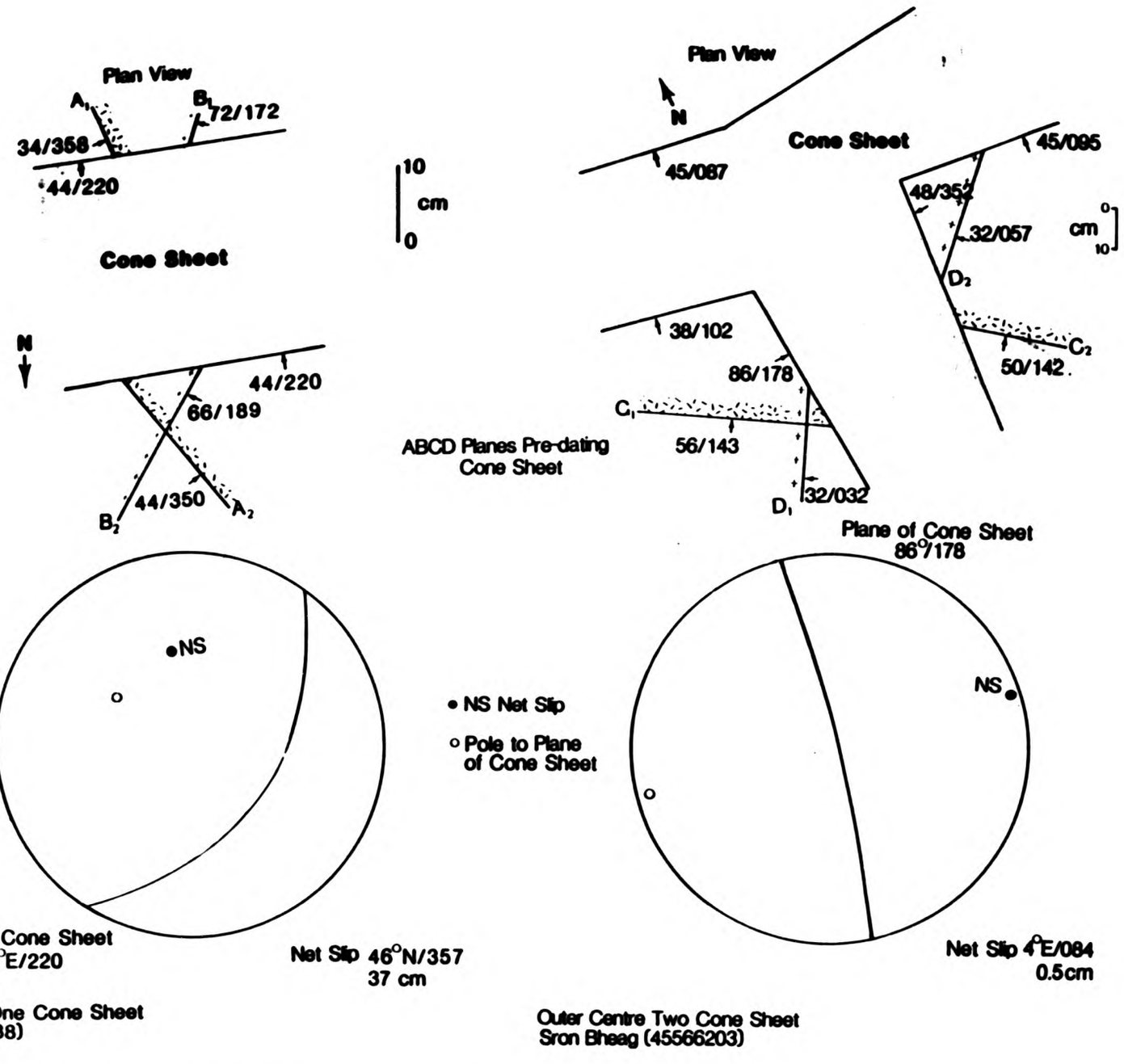

Fig.6.7.8 Piercing Point solutions for two cone sheets, one which opened by tension and one which opened by tension and shear

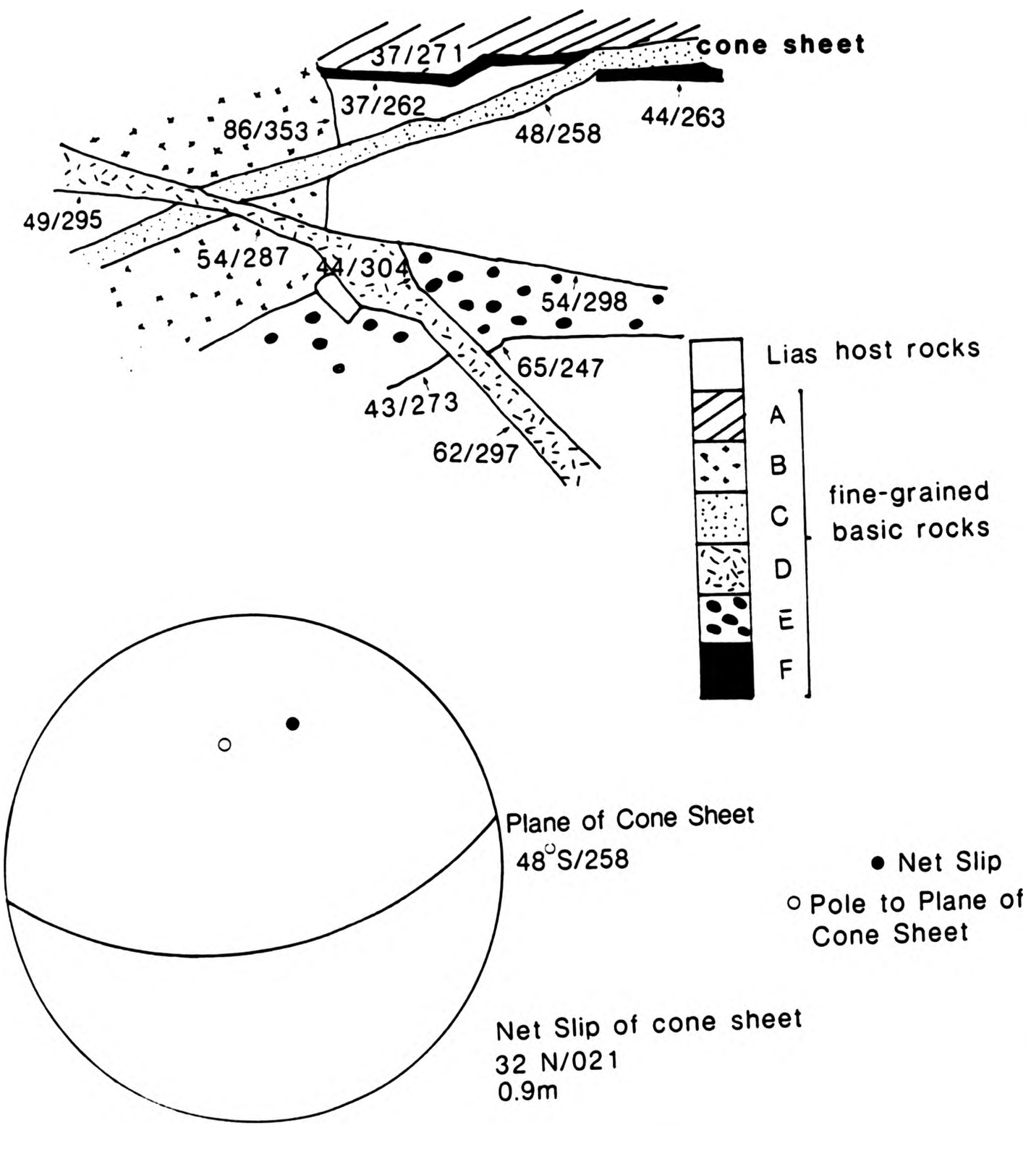

Fig.6.7.9 Piercing Point solution for a cone sheet which occurs at (47187104)

Cone sheet intruded into Moine country rocks, three planes, (ABC) pre-dating the cone sheet have been used to determine the opening direction of the genuflecting sheet, which terminates towards the right of the photograph

ABC Planes Pre-dating Cone Sheet

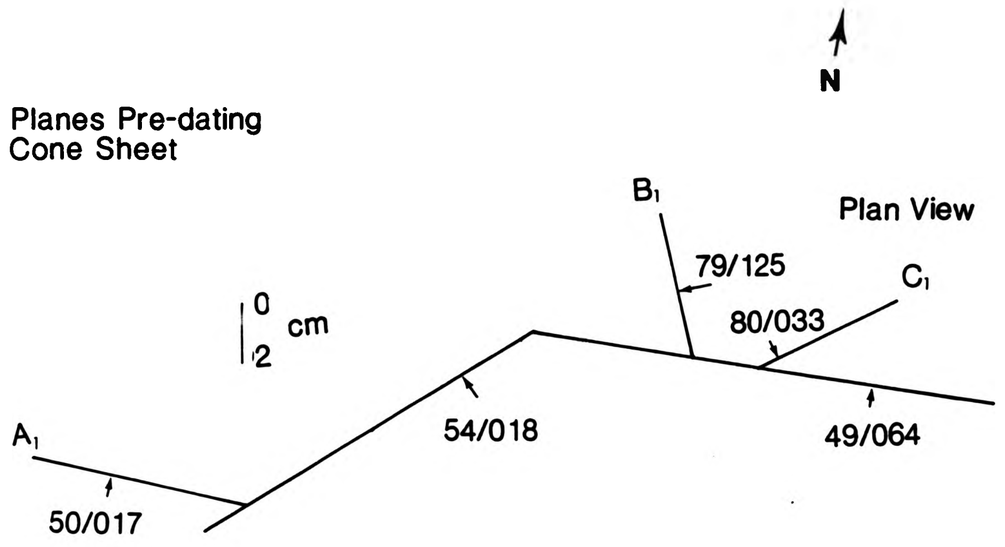

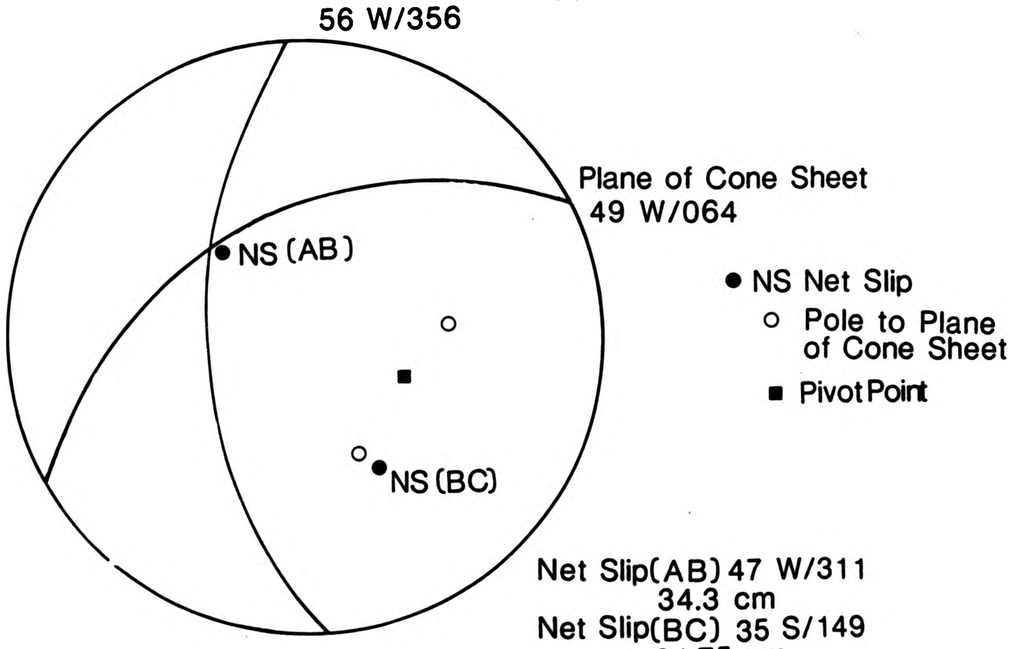

Cone Sheet

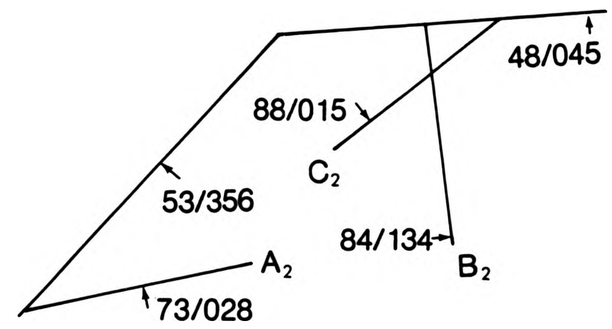

drawing of the cone sheet

Fig. 6.7.10 Piercing Point solution for a cone sheet which is intruded into Moine host rocks which shows two types of opening mechanisms Planes B and C indicate tensile opening of the sheet E of the genuflection to the W of the genuflection planes A and B indicate a shear mechanism

Cone sheet intruded into Moinecountry rocks, three planes,(ABC) pre-dating the cone sheet have been usedto determine the opening direction of the genuflecting sheet, which terminates towards the right of the photograph

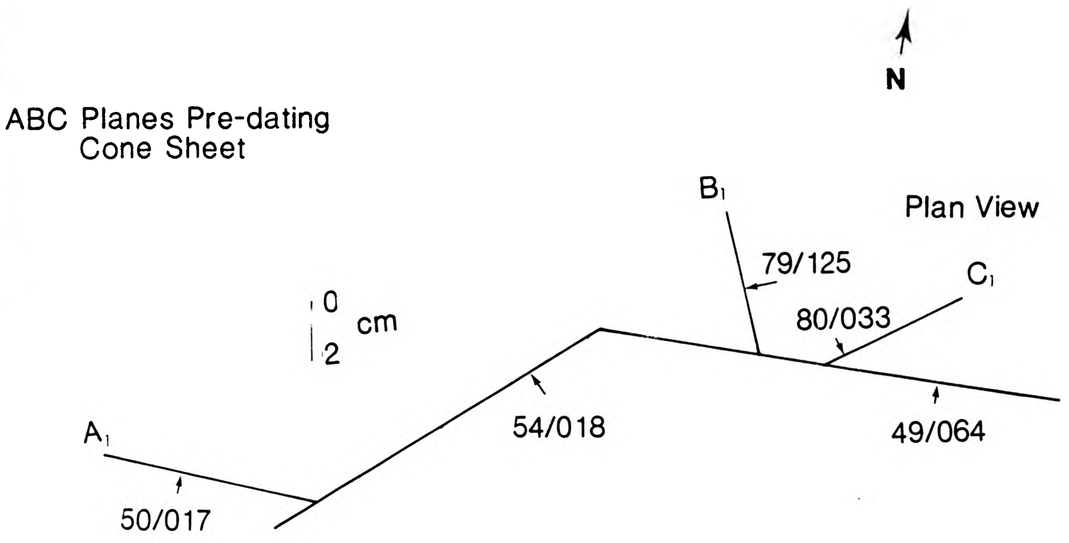

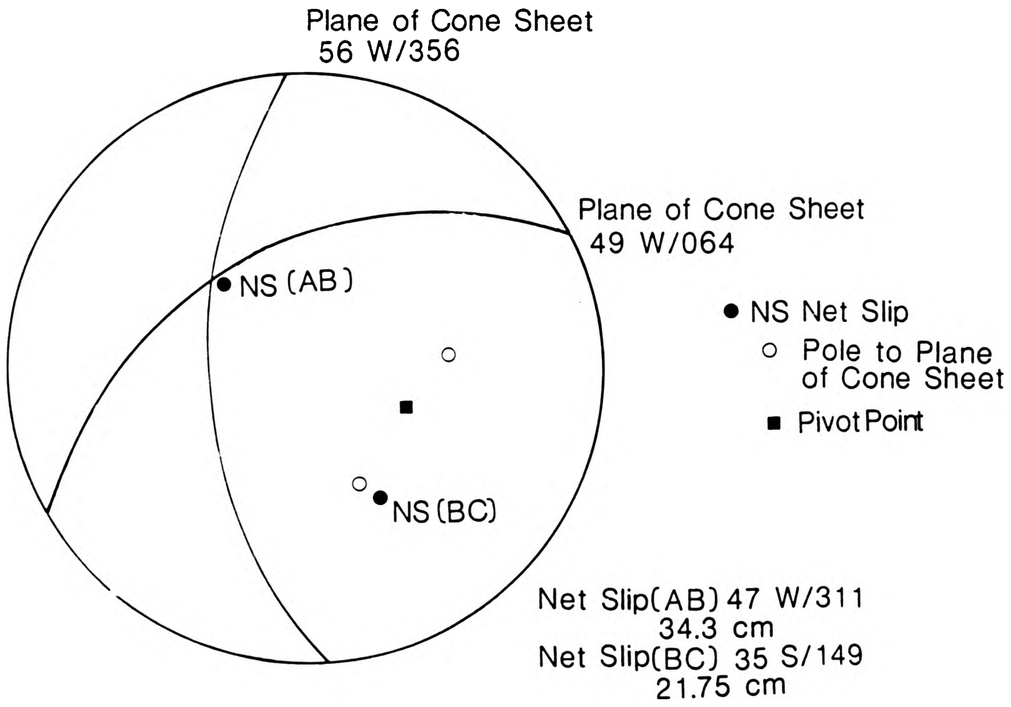

Cone Sheet

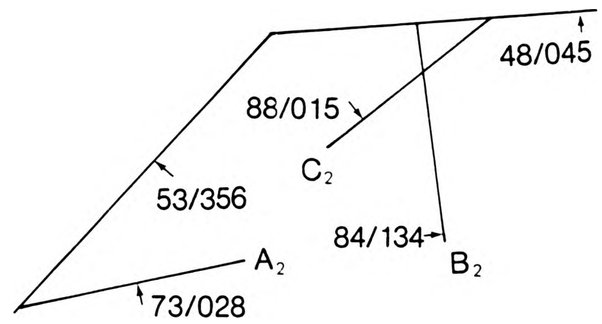

drawing of the cone sheet

Fig. 6.7.10 Piercing Point solution for a cone sheet which is intruded into Moine host rocks which shows two types of opening mechanisms Planes B and C indicate tensile opening of the sheet E of the genuflection to the W of the genuflection planes A and B indicate a shear mechanism

6.8 CONCLUSIONS

In contrast to the conclusions of the authors of the Memoir (1930) and all subsequent authors, the piercing point analyses have highlighted a number of factors involved in the types of opening of cone sheet fractures. That is, there are two extremes, shear and tension, with a series of examples which fall between these. The existence of a normal shear stress system indicates the possible influence of the emplacement of dyke swarms (Chapter 2) creating a regional system of tension at the time of cone sheet emplacement. The alternative explanation is that offered by Robson and Barr (1964) which proposes that all cone sheet fractures are normal shear fractures. This is refuted, because the majority of piercing point analyses indicate that reversed shear movements predominated.

Tension is an essential process involved in the mechanism of emplacement of cone sheets as without it no magma could be emplaced within the fracture. Therefore, the opening of all cone sheet fractures involves some tension (Fig.6.8.1). As it has been shown above, some cone sheets open only under tension (Fig.6.7.5 and 6). As the net slip vector approaches pure shear, theoretically, an infinite number of net slip trajectories are possible (Fig.6.8.1), all of which involve an element of shear.

Cone sheets that opened by shear tend to be thicker than those which opened by tension. This is most probably caused by the movement of magma along the fracture resulting in shear displacement, there being little evidence of any shear occurring

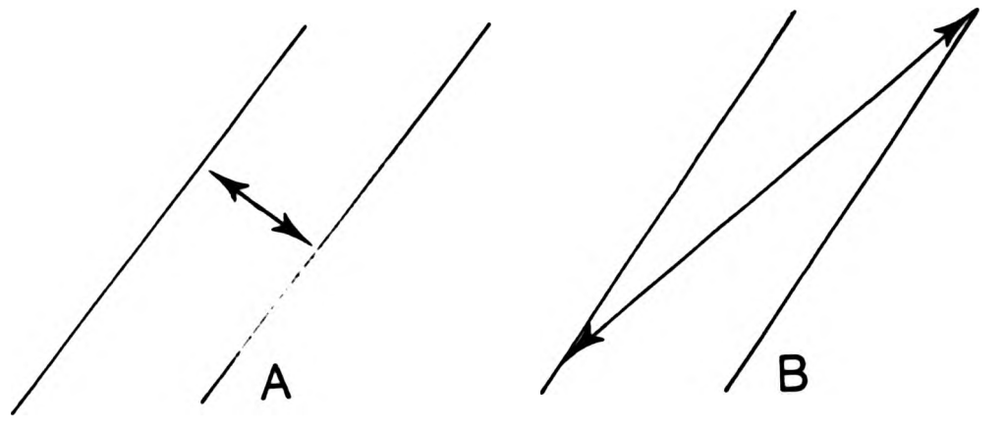

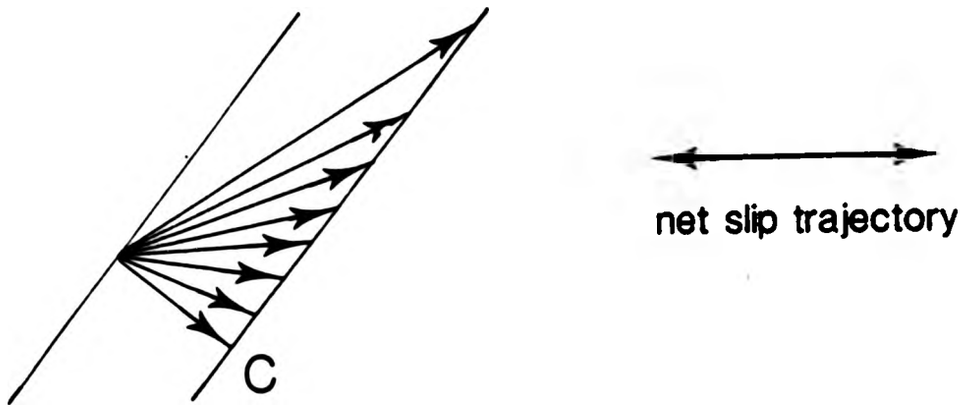

Fig.6.8.1 Diagramatic representation of the variation of net slip trajectories which vary with the amount of shear involved

A pure extension (tension) where the net slip is perpendicular to the cone sheet margin

B shear opening direction where the net slip becomes parallel to the cone sheet margin

C an infinite number of net slip trajectories that represent an increasing amount of shear as the net slip trajectory approaches parallelism to the cone sheet margin

along fractures prior to magma emplacement.

The confusion over the distinction between the two processes is marked by the overlap of the H values, between the values of 1 and 2. It is between these values that shear is in evidence and that the movement along the sheet becomes greater than the thickness of the sheet.

The location map (Fig.6.8.2) of the piercing point net slip vectors shows the prominence of a torque force, with an anti-clockwise element. The source of the torque could either originate as a local effect, that is, from the magma chamber, or a regional effect associated with the emplacement of the dyke swarms. The existence of a number of both dextral and sinistral en echelon cone sheet sets (Chapter 7) seems to support the suggestion that such a force exists.

The piercing point analyses for the small geniculate cone sheet (Fig.6.7.10) demonstrates that the amount of movement along an individual cone sheet can vary i.e. an individual cone sheet may open by different processes along it's length. Possibly this example demonstrates Phillips' theory, where by the mechanism of opening changes in the more distal regions. Or perhaps this example shows how at the leading edge of a cone sheet, wedging, or extension splitting is the most prominent process with shear occurring after this initial extension has taken place. There is no ubiquitous process for the opening of cone sheet fractures as demonstrated by the Ardnamurchan cone sheets. Regional and local conditions play important roles in both the type and amount of opening. The most probable cause of

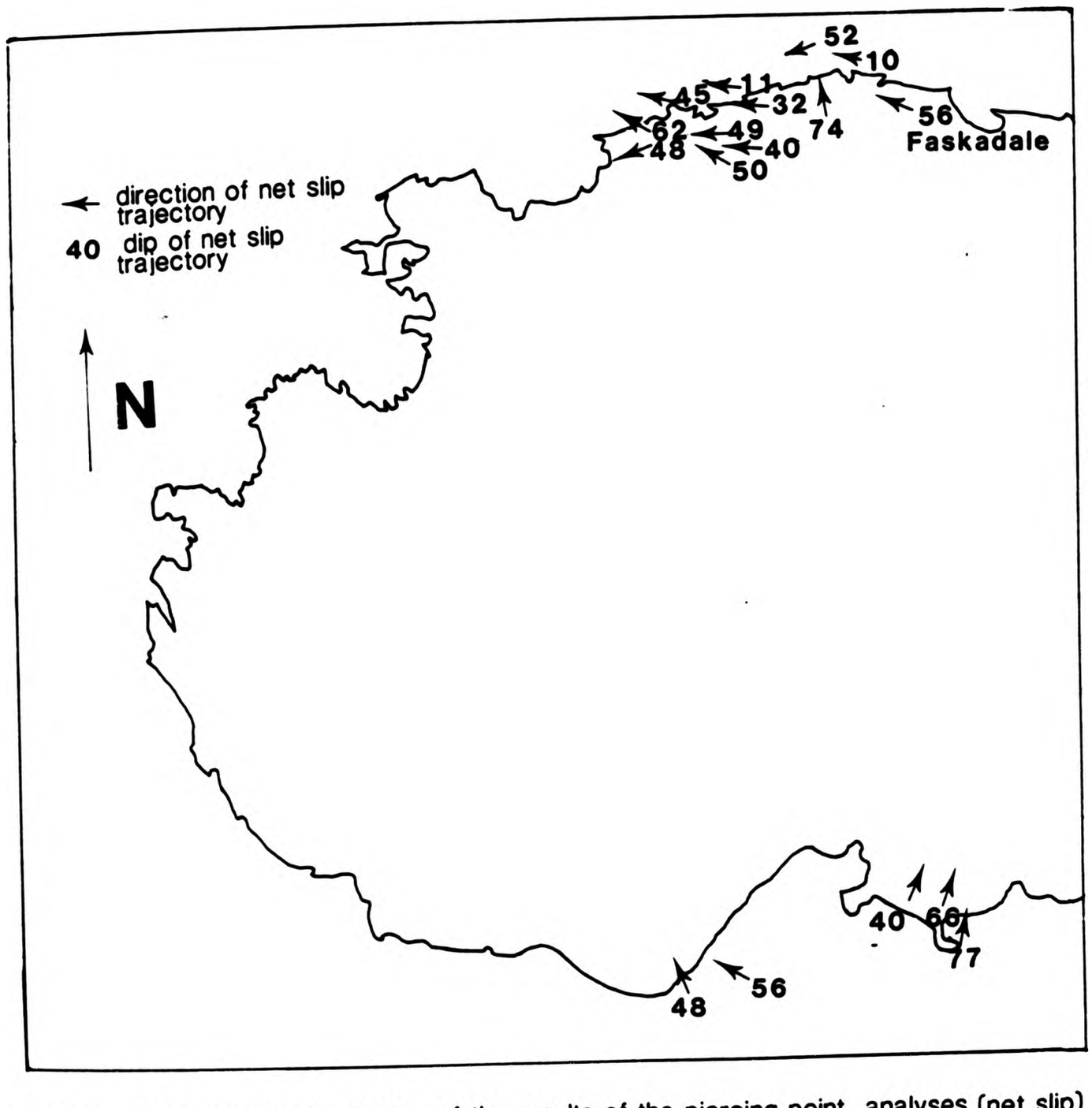

Fig.6.8.2 Geographical distribution of the results of the piercing point analyses (net slip) of the cone sheet opening directions

the fracture opening is the uplift of the central block above the magma chamber enabling the extension of the fractures by the emplacement of magma. Either continued supply of magma along the fracture and/or increased pressure on the magma chamber roof will result in reversed shear cone sheet fractures. A second component of shear may be caused by a torque force resulting in shear fracture movements. The third, and perhaps the least important cause, is the regional tensional system resulting in normal opening cone sheets.

CHAPTER 7

TERMINATIONS

7.1 INTRODUCTION

A termination is the begining and end of an intrusion, both vertically and laterally. Cone sheet terminations are rarely observed in Ardnamurchan and several reasons may account for this. Firstly, some of the sheets may have reached the surface and acted as feeders for vents from which lavas were erupted. Some of the Galapagos volcanoes have concentric rows of vents that have fed lava flows (Simkin, 1972) and it is conceivable that these concentrically arranged vents are the surface manifestation of cone sheets. In Ardnamurchan, the vents exposed at Ardtoe, Glas Eilean and near Ockle Point may thus be the surface expression of cone sheets as they have a similar arcuate form and parallel adjacent cone sheets. Secondly, it is possible that many sheets terminated at a higher level that the present erosion surface, without reaching the earths surface. In addition, on higher ground where terminations may be expected the amount of vertical exposure is limited, therefore decreasing the possibility of locating terminations. Also, it is possible that upwards the angle of dip of cone sheets may decrease until, near the surface of the earth, they become low-angle sills. Such sills representing this type of termination occur along the Centre One traverse, one particularly good example is seen at (546710). Cone sheets are best exposed along the coastal sections and even here the maximum vertical exposure is 76m at Sron Bheag. Thirdly, although the coastal sections provide an excellent cross-section, the maximum length of foreshore is 300m, which restricts the distance one can laterally trace a cone sheet and therefore locate lateral terminations. Finally, the focus of the sheets, thought to be located at a point 5.8km

beneath the present land surface, is not exposed. Richey (1932, p73) suggested that the Cuillin gabbro may have continued upwards to higher levels to form cone sheets: cone sheets may merge into large intrusions at depth. However, this dimension is not exposed within the Ardnamurchan complex.

7.2 THE FORM OF TERMINATIONS

The Ardnamurchan cone sheets show a variety of termination forms which have been classified as follows:-

A. Terminations with no fracture emanating from the cone sheet tip.
   i. Wedge-shaped termination,
   ii. Rectangular termination,
   iii. Rounded termination,
   iv. Irregularly shaped and branched termination,
   v. Hooked (horned) termination.
B. Terminations with fractures emanating from the cone sheet tip.
   i. Single fracture,
   ii. Multiple fractures.
C. En echelon lenses.

7.2.1 Terminations with no fracture at the tip

Figure 7.2.1A shows a tapering termination of a member of an en echelon set of sheets. Plate 7.1 illustrates the tapering of a narrow sheet that thins from 1cm to zero over a distance of 16cm. Commonly this type of termination is wedge-shaped (Plate 7.1) with one of the margins planar and the other curved (Plate 7.2). These wedge-shaped terminations are similar in form to the magma wedge described by Bradley (1965) and interpreted as a sheet fracture propagating by splitting along a bedding plane.

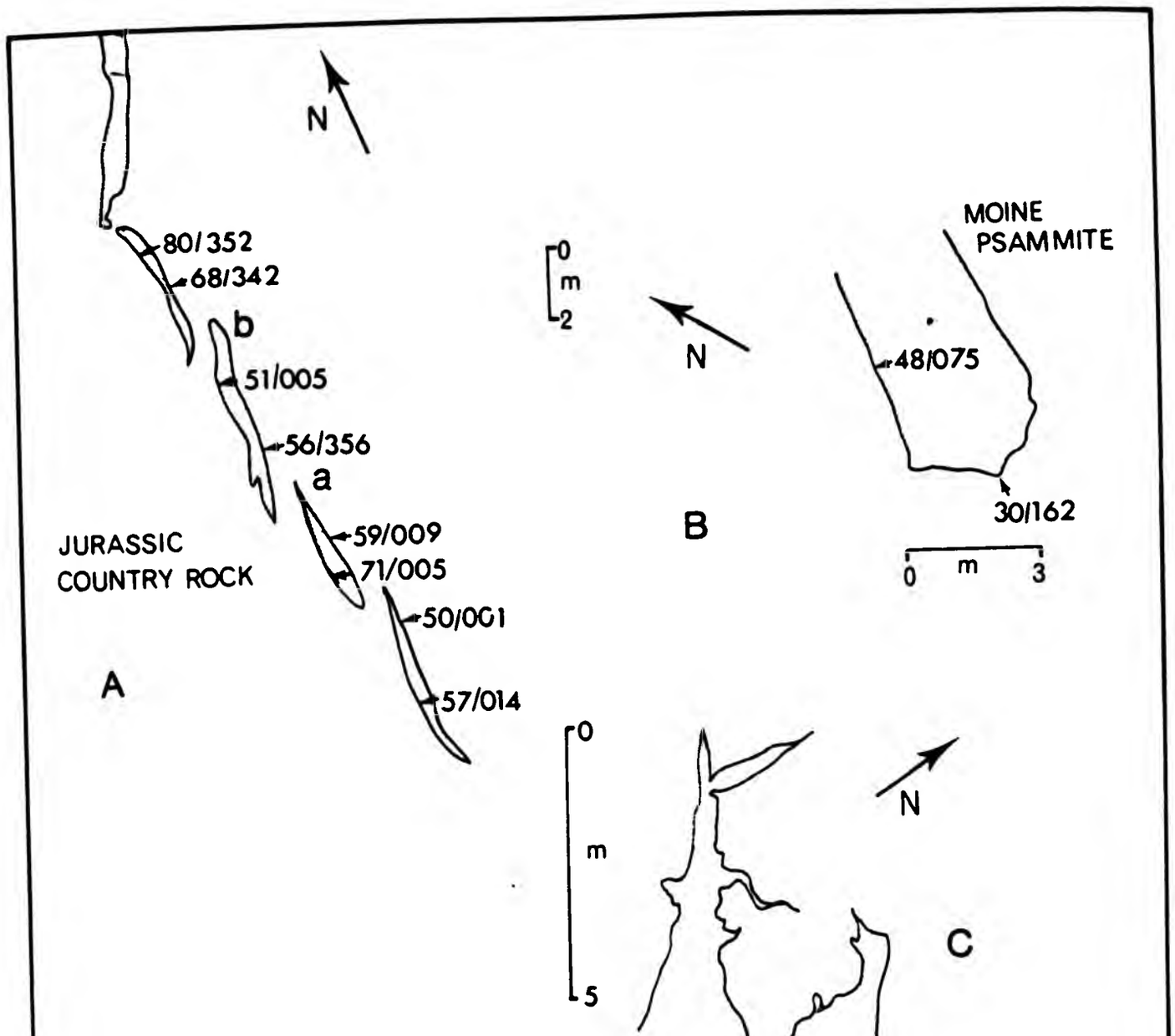

Fig.7.2.1. Forms of cone sheet terminations with no fracture emanating from the Tip

A. Outer Centre Two en echelon series of cone sheets exposed at Rubha Mhile showing a variety of forms of termination from a. simple tapering to b. rounded termination

B. Outer Centre Two cone sheet exposed W. of Mingary Pier which has a blunt termination and is rectangular in cross section

C. Inner Centre Two cone sheet on the slopes of Beinn Bhuidhe ,which has an irregular margin and has multiple terminations

Plate 7.1 Three sheets of an en echelon set, each having the form of a tapering termination, Inner Centre Two, Lighthouse section, Hypersthene Gabbro host rock.

faces

Plate 7.2 A pair of en echelon sheets, the form of which is like Bradley's (1965) theoretical magma wedge, with one surface planar and the other curved, Inner Centre Two, Lighthouse section, Hypersthene Gabbro host rock.

Plate 7.1 Three sheets of an en echelon set, each having the form of a tapering termination, Inner Centre Two, Lighthouse section, Hypersthene Gabbro host rock.

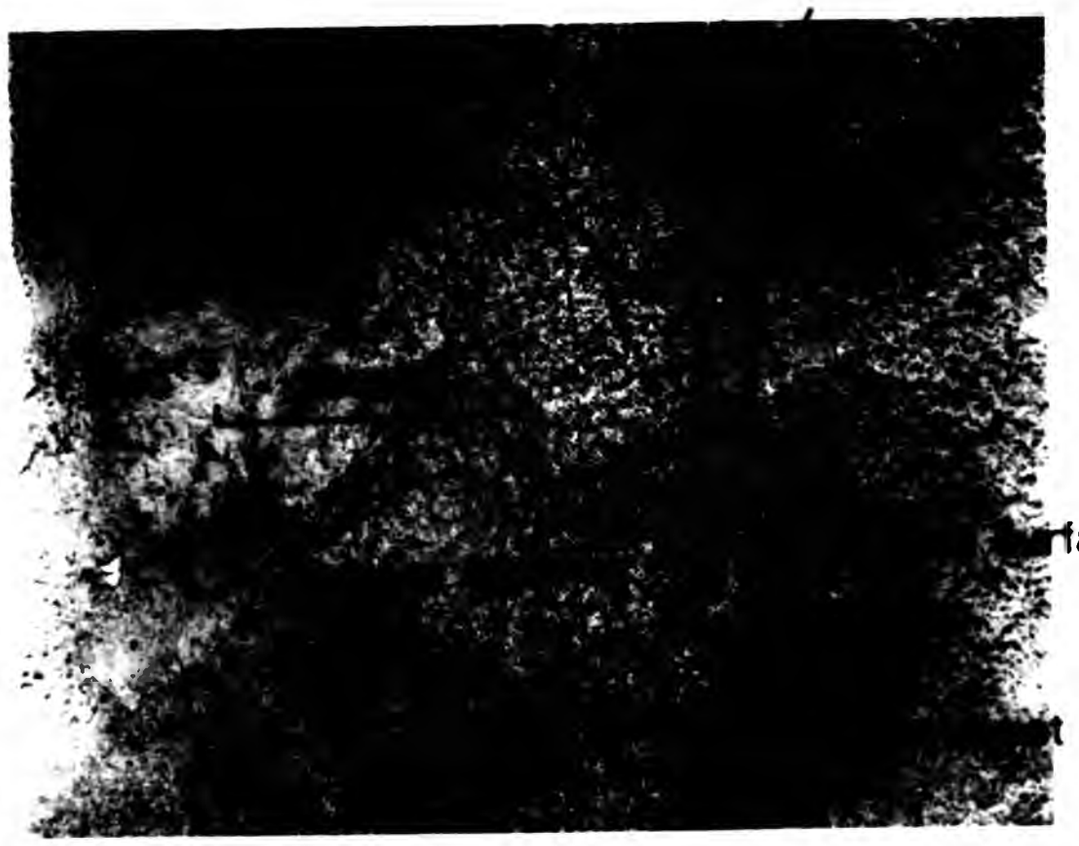

Plate 7.2 A pair of en echelon sheets, the form of which is like Bradley's (1965) theoretical magma wedge, with one surface planar and the other curved, Inner Centre Two, Lighthouse section, Hypersthene Gabbro host rock.

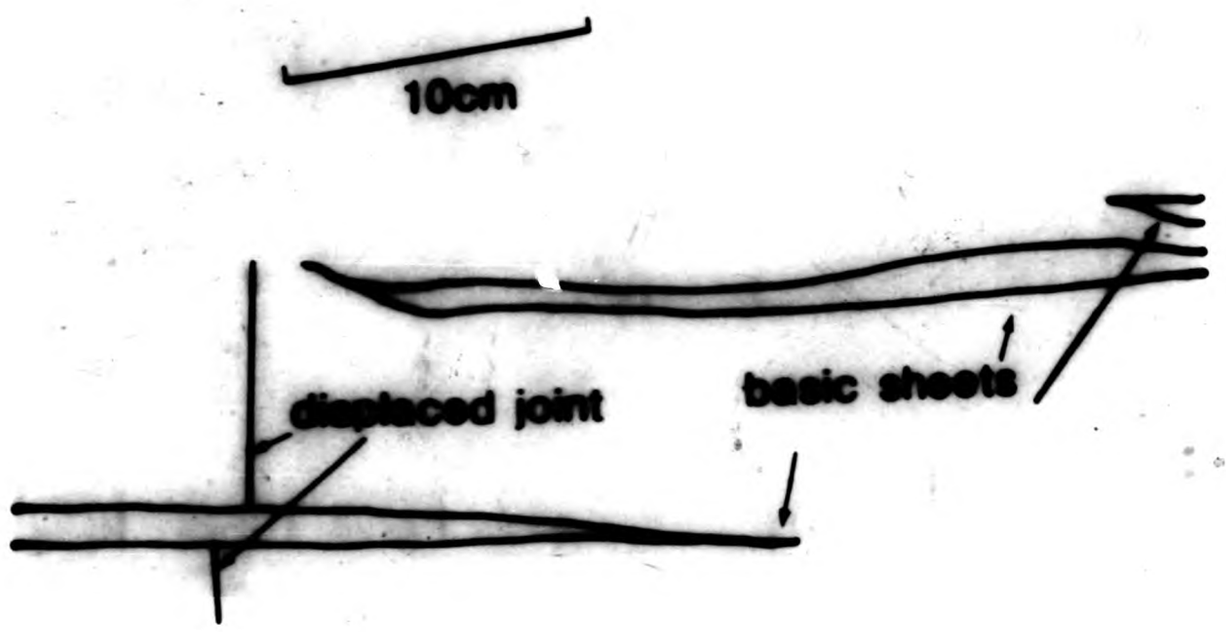
10cm
displaced joint
basic sheets

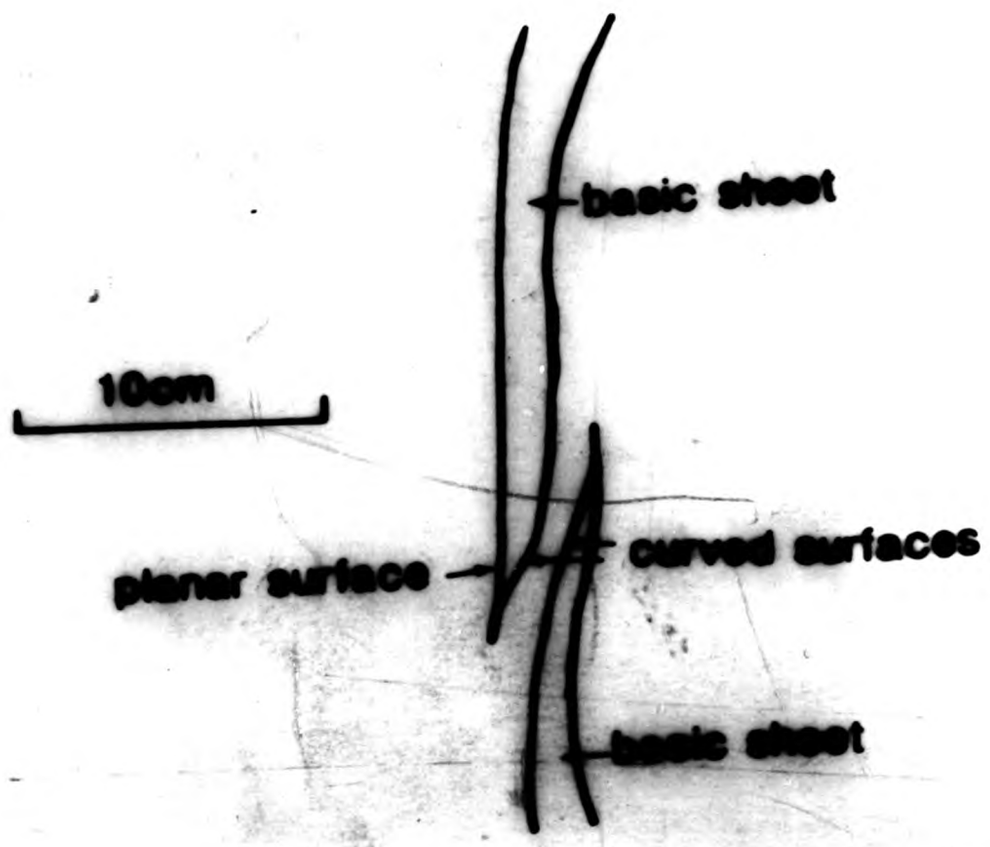
basic sheet
10cm
planer surface
curved surfaces
basic sheet

Plate 7.1 Three sheets of an en echelon set, each having the form of a tapering termination, Inner Centre Two, Lighthouse section, Hypersthene Gabbro host rock.

Plate 7.2 A pair of en echelon sheets, the form of which is like Bradley's (1965) theoretical magma wedge, with one surface planar and the other curved, Inner Centre Two, Lighthouse section, Hypersthene Gabbro host rock.

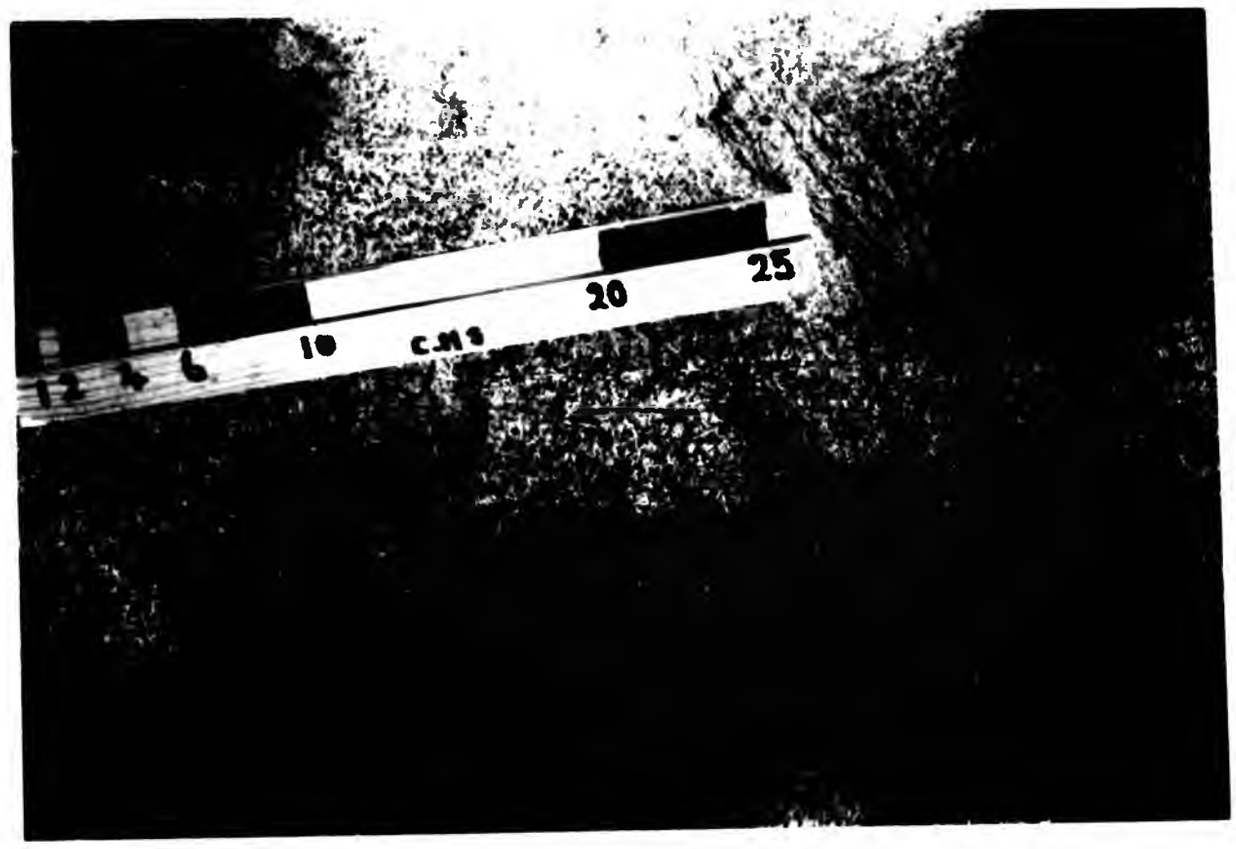

Plate 7.1 Three sheets of an en echelon set, each having the form of a tapering termination, Inner Centre Two, Lighthouse section, Hypersthene Gabbro host rock.

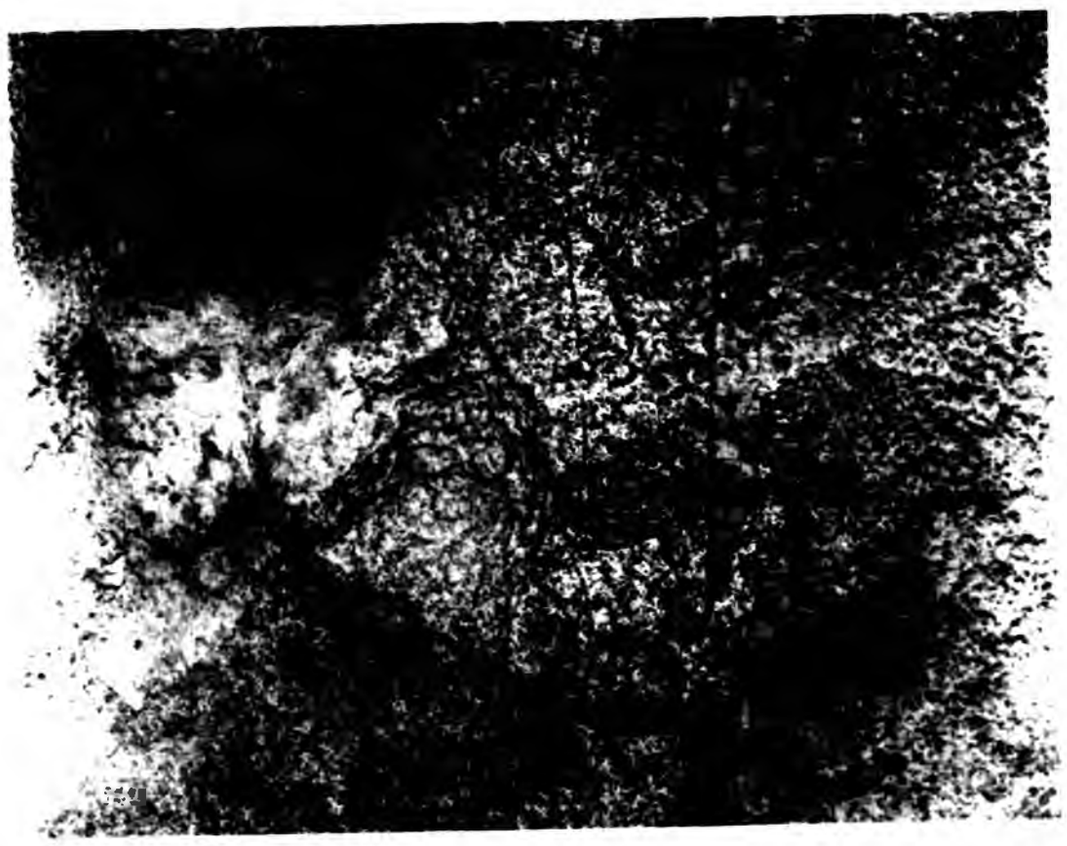

Plate 7.2 A pair of en echelon sheets, the form of which is like Bradley's (1965) theoretical magma wedge, with one surface planar and the other curved, Inner Centre Two, Lighthouse section, Hypersthene Gabbro host rock.

Figure 7.2.1B illustrates a rare type of termination, it is blunt ended (cone sheet intruded into Moine psammites). This type of termination is formed by the cone sheet utilizing a prominent joint plane.

Plate 7.3 illustrates a rounded termination which is similar to the blunt ended "fingered" periphery of the Shonkin Sag Sill (Pollard et al. 1975). Pollard (1973) postulates that the majority of terminations of all minor intrusions are curved, this being the simplest shape for the magma to form. In a wedge-shaped termination (Plate 7.3), curves of smaller radius can be successively advanced in to the space occurring ahead of the magma front, in this case, this may be accommodated by moulding of the partly solidified magma into the fracture space. The rounded form of the termination is emphasized by flow banding parallel to the margins.

Figure 7.2.1C shows the termination of a cone sheet by a number of small apophyses; the apophyses and the main termination have irregularly shaped margins (Plate 7.4).

A common type of termination is where the tip is o rientated at up to 90° to the trend of the main body of the sheet (Plates 7.4 and 7.5), this is particularly common in adjacent lenses of an en echelon series (Chapter 7.3).

The majority of the terminations described above occur in the horizontal (lateral) plane, but with type Ai (wedge-shaped) occurring also in the vertical plane (Plate 7.7).

Plate 7.3 A rounded sheet termination marked by flow banding parallel to the margins, Outer Centre Two, Rhubh 'a' Mhile, Triassic conglomerate host rock.

Plate 7.4 Irregularly shaped termination, consisting of a network of veinlets, Inner Centre Two, Lighthouse section, Hypersthene Gabbro host rock.

Plate 7.3 A rounded sheet termination marked by flow banding parallel to the margins, Outer Centre Two, Rhubh 'a' Mhile, Triassic conglomerate host rock.

Plate 7.4 Irregularly shaped termination, consisting of a network of veinlets, Inner Centre Two, Lighthouse section, Hypersthene Gabbro host rock.

5cm

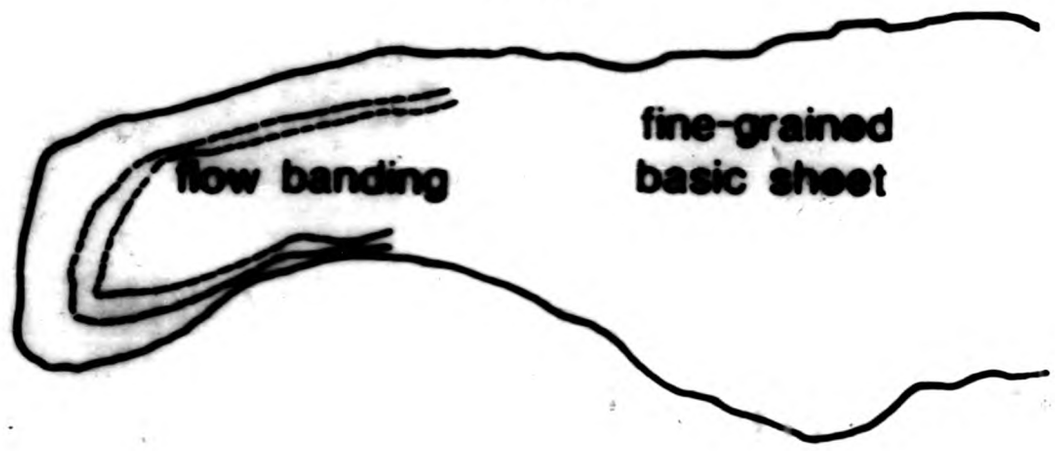
flow banding
fine-grained
basic sheet

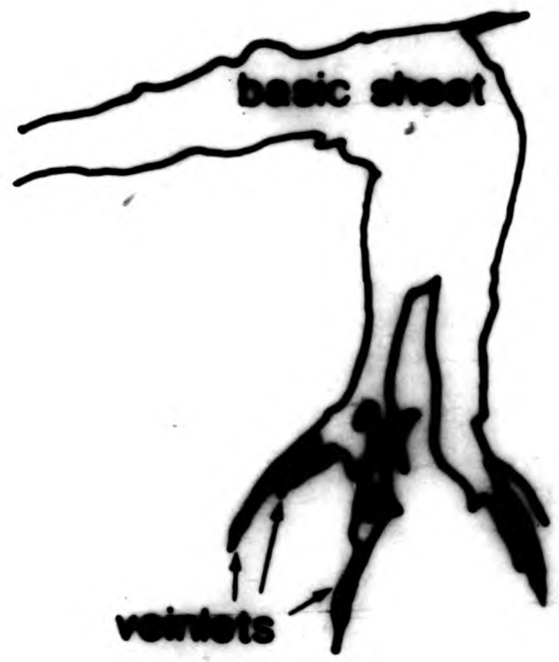
basic sheet
veinlets

5cm

Plate 7.3 A rounded sheet termination marked by flow banding parallel to the margins, Outer Centre Two, Rhubh 'a' Mhile, Triassic conglomerate host rock.

Plate 7.4 Irregularly shaped termination, consisting of a network of veinlets, Inner Centre Two, Lighthouse section, Hypersthene Gabbro host rock.

Plate 7.3 A rounded sheet termination marked by flow banding parallel to the margins, Outer Centre Two, Rhubh 'a' Mhile, Triassic conglomerate host rock.

Plate 7.4 Irregularly shaped termination, consisting of a network of veinlets, Inner Centre Two, Lighthouse section, Hypersthene Gabbro host rock.

Plate 7.5 A rounded termination which is combined with a 90° change in the orientation of the cone sheet, Outer Centre Two, north coast, granophyre host rock.

Plate 7.6 The termination of the sheet changes orientation by 45° from the main sheet, and follows a prominent joint set and trends towards an adjacent cone sheet, Inner Centre Two, Lighthouse section, Hypersthene Gabbro host rock.

Plate 7.5 A rounded termination which is combined with a 90° change in the orientation of the cone sheet, Outer Centre Two, north coast, granophyre host rock.

Plate 7.6 The termination of the sheet changes orientation by 45° from the main sheet, and follows a prominent joint set and trends towards an adjacent cone sheet, Inner Centre Two, Lighthouse section, Hypersthene Gabbro host rock.

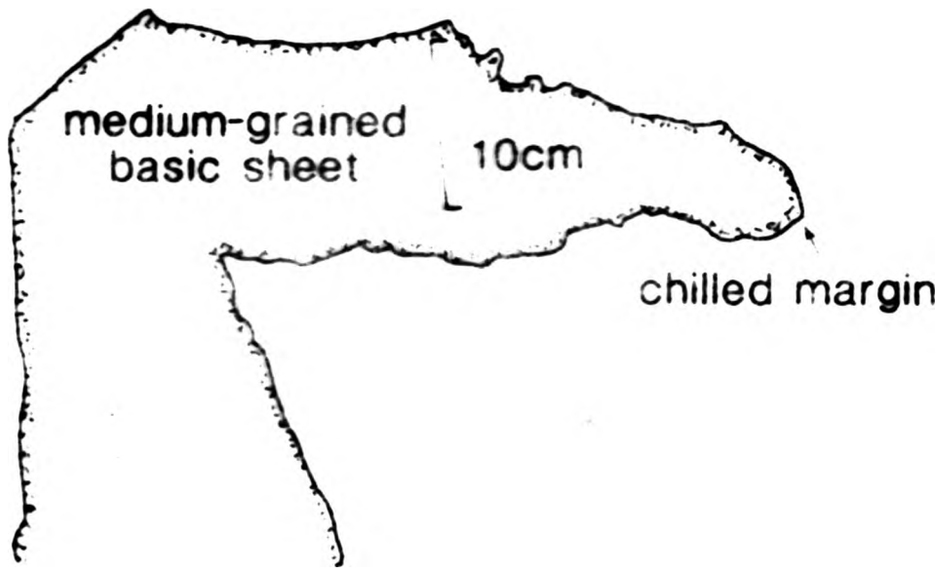
medium-grained
basic sheet
10cm
chilled margin

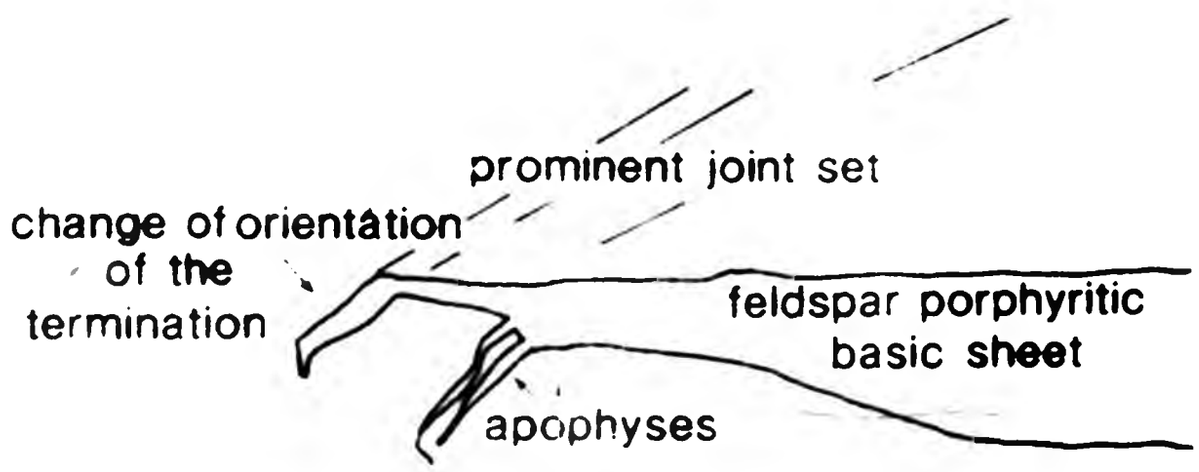
prominent joint set
change of orientation
of the
termination
feldspar porphyritic
basic sheet
apophyses
5cm
adjacent en
echelon sheet

Plate 7.5 A rounded termination which is combined with a 90° change in the orientation of the cone sheet, Outer Centre Two, north coast, granophyre host rock.

Plate 7.6 The termination of the sheet changes orientation by 45° from the main sheet, and follows a prominent joint set and trends towards an adjacent cone sheet, Inner Centre Two, Lighthouse section, Hypersthene Gabbro host rock.

Plate 7.5 A rounded termination which is combined with a 90° change in the orientation of the cone sheet, Outer Centre Two, north coast, granophyre host rock.

Plate 7.6 The termination of the sheet changes orientation by 45° from the main sheet, and follows a prominent joint set and trends towards an adjacent cone sheet, Inner Centre Two, Lighthouse section, Hypersthene Gabbro host rock.

7.2.2 Terminations with fractures at their tips

Sheets which terminate in fractures (Fig.7.2.2) unfilled by magma are not common. Two examples (Fig.7.2.2A and B) show a single fracture emanating from the tip of a cone sheet, the unfilled part of the termination in A is 5m and in B 7m in length; both sheets are 50cm thick. Figure 7.2.2 (C and D) show irregularly spaced terminations that have a series of branched fractures emanating from the tip of the cone sheet. In D (Fig.7.2.2) a number of small cracks occur in the area immediatley adjacent to the terminating fractures. Plate 7.8 shows a series of arcuate fractures radiating from the wedge-shaped, cone sheet tip.

7.2.3 En echelon lenses

The classification given above includes only the last few cm or metres of individual terminations. However, on a larger scale it may be interpreted that the termination of a cone sheet may be in the form of an en echelon series of igneous lenses (Plate 7.9).

7.3 EN ECHELON SETS

Offset or en echelon sets were described from the Cuillins of Skye by Harker (1904) as "the shifting of an inclined basic sheet". By "shifting" it may be interpreted that Harker envisaged the offsetting of the sheets as a method of propagation or a method of transgression. This is one of the few

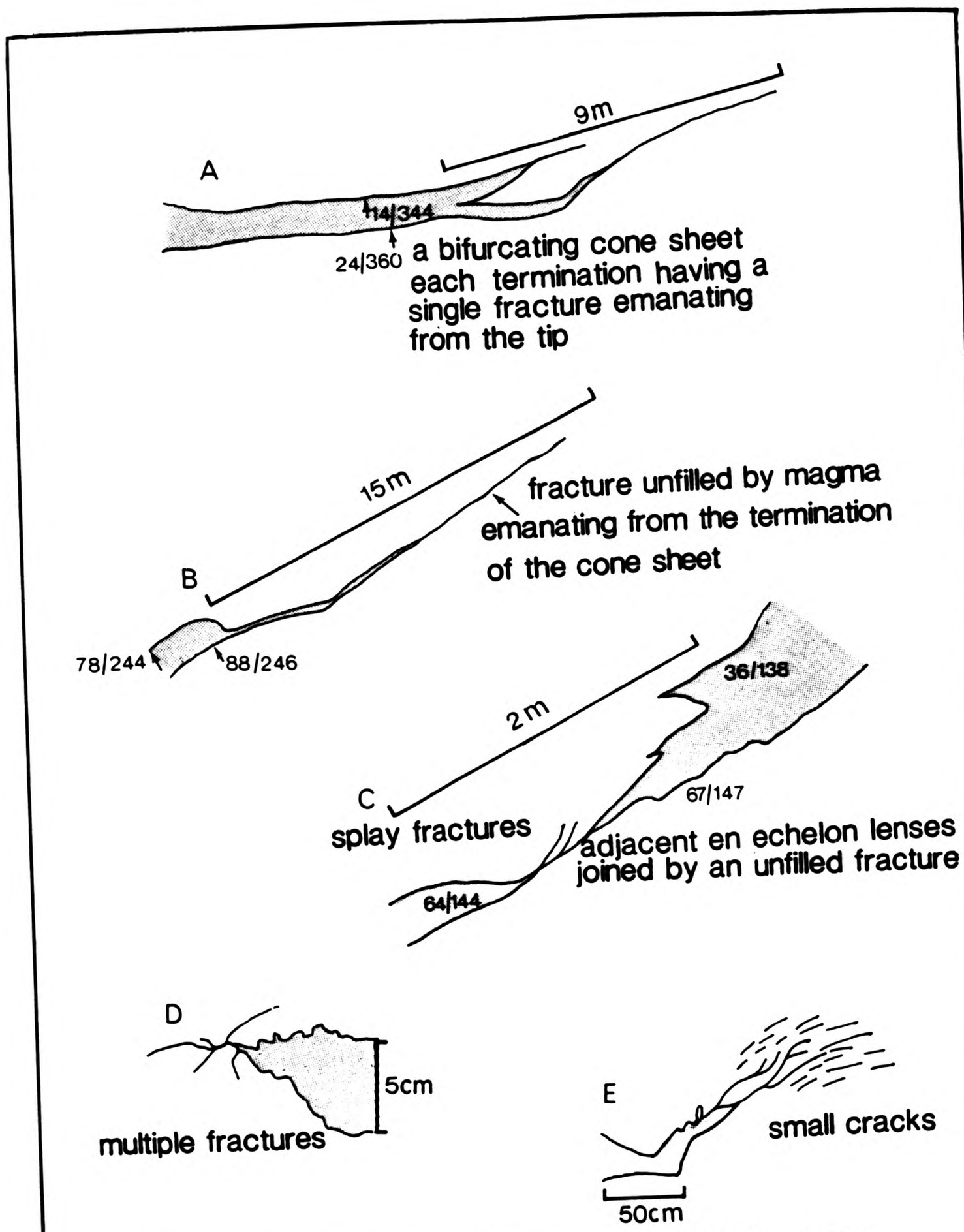

Fig.7.2.2. Cone Sheet Terminations which have fractures, unfilled by magma emanating from them

Plate 7.7 Two sheets follow the pronounced foliation in the Moine host rock. At it's termination the lower sheet tapers and cross cuts the foliation. Centre One, Rubha'Choit.

Plate 7.8 Small en echelon sheetlets. From the termination of the lower sheet a series of semi-arcuate fractures emanate and curve away from the upper sheet, Inner Centre Two, Lighthouse section, Hypersthene Gabbro host rock.

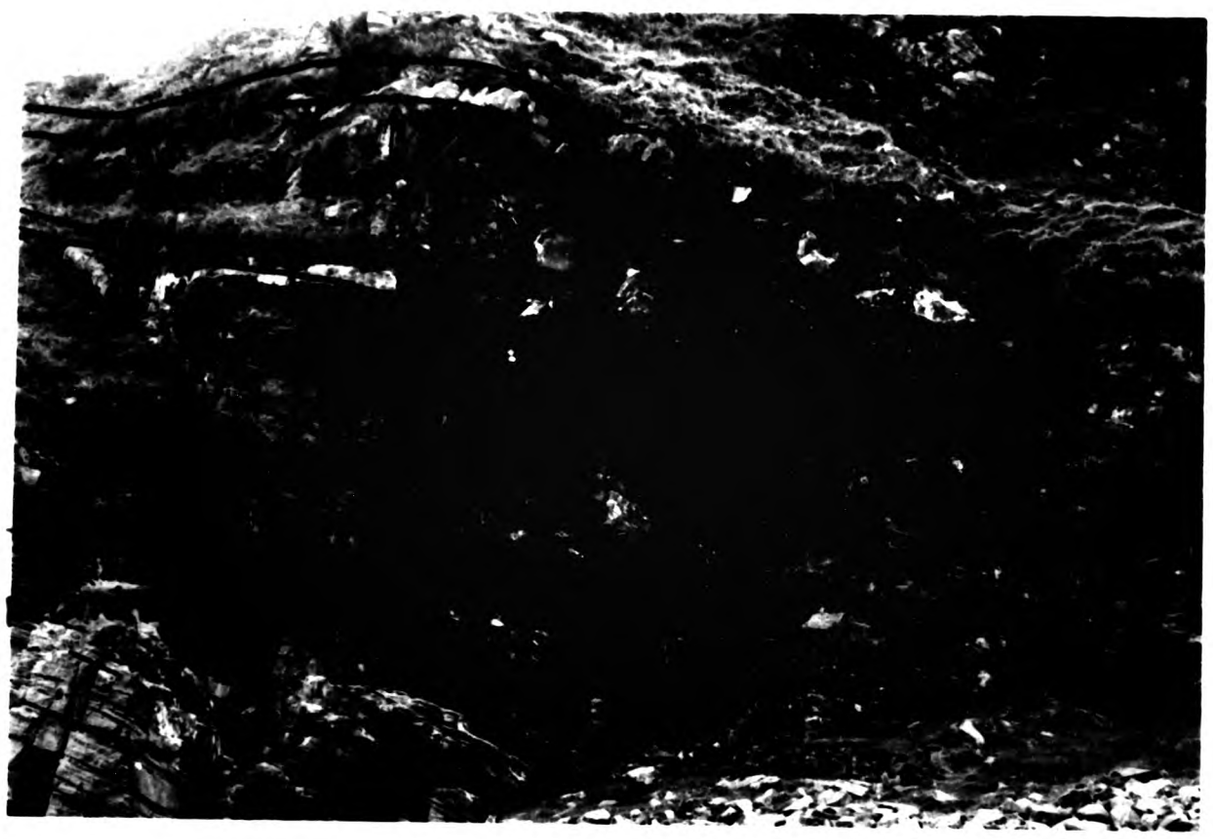

Plate 7.7 Two sheets follow the pronounced foliation in the Moine host rock. At it's termination the lower sheet tapers and cross cuts the foliation. Centre One, Rubha'Choit.

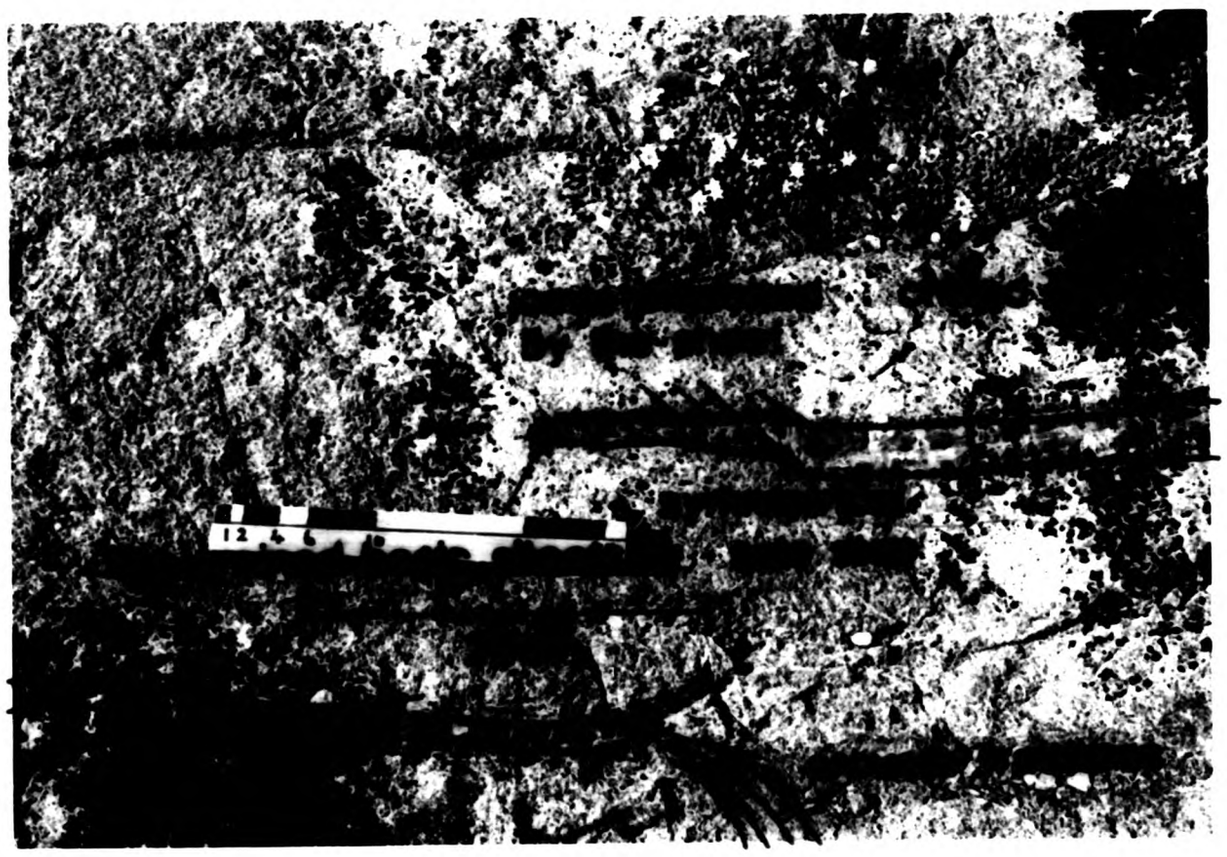

Plate 7.8 Small en echelon sheetlets. From the termination of the lower sheet a series of semi-arcuate fractures emanate and curve away from the upper sheet, Inner Centre Two, Lighthouse section, Hypersthene Gabbro host rock.

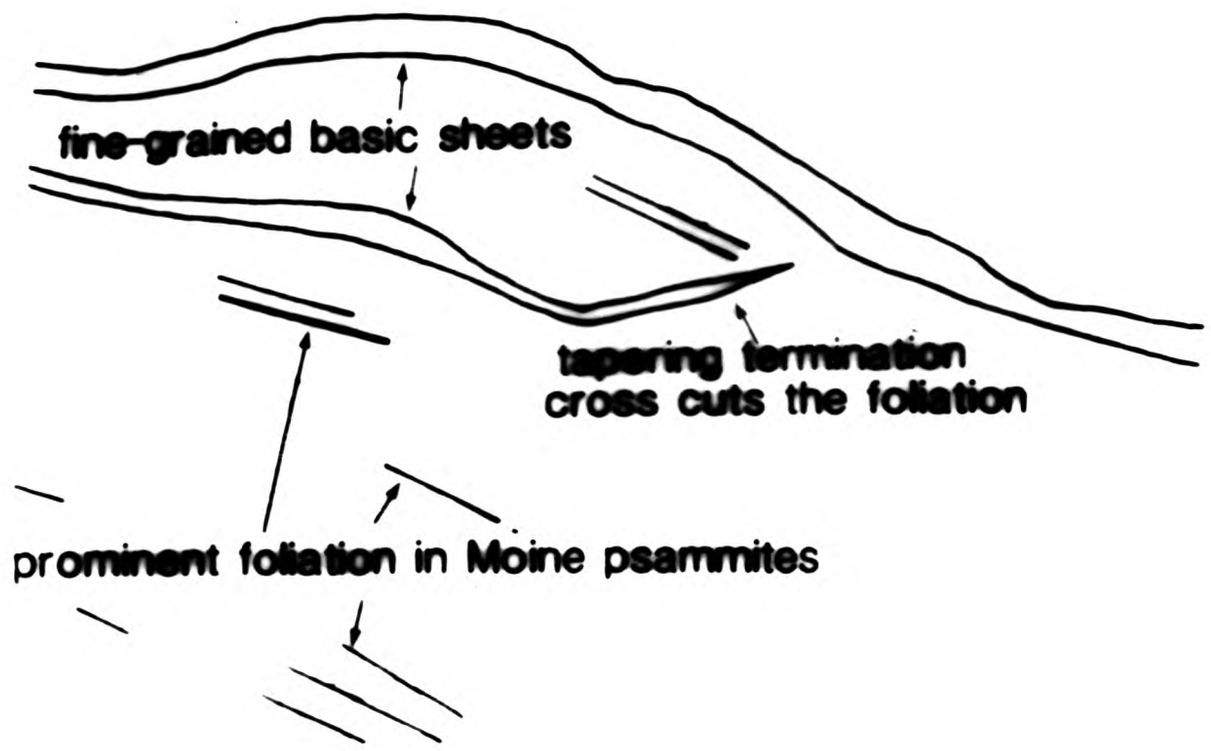
fine-grained basic sheets
tapering termination
cross cuts the foliation
prominent foliation in Moine psammites

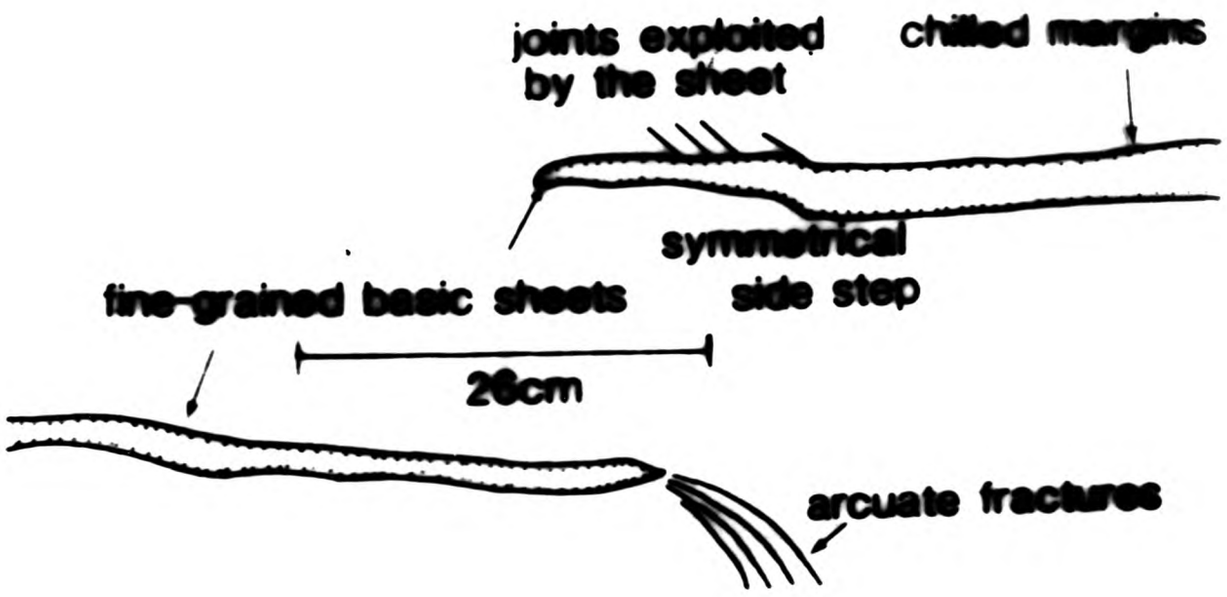
joints exploited
by the sheet
chilled margins
symmetrical
side step
fine-grained basic sheets
26cm
arcuate fractures

Plate 7.7 Two sheets follow the pronounced foliation in the Moine host rock. At it's termination the lower sheet tapers and cross cuts the foliation. Centre One, Rubha'Choit.

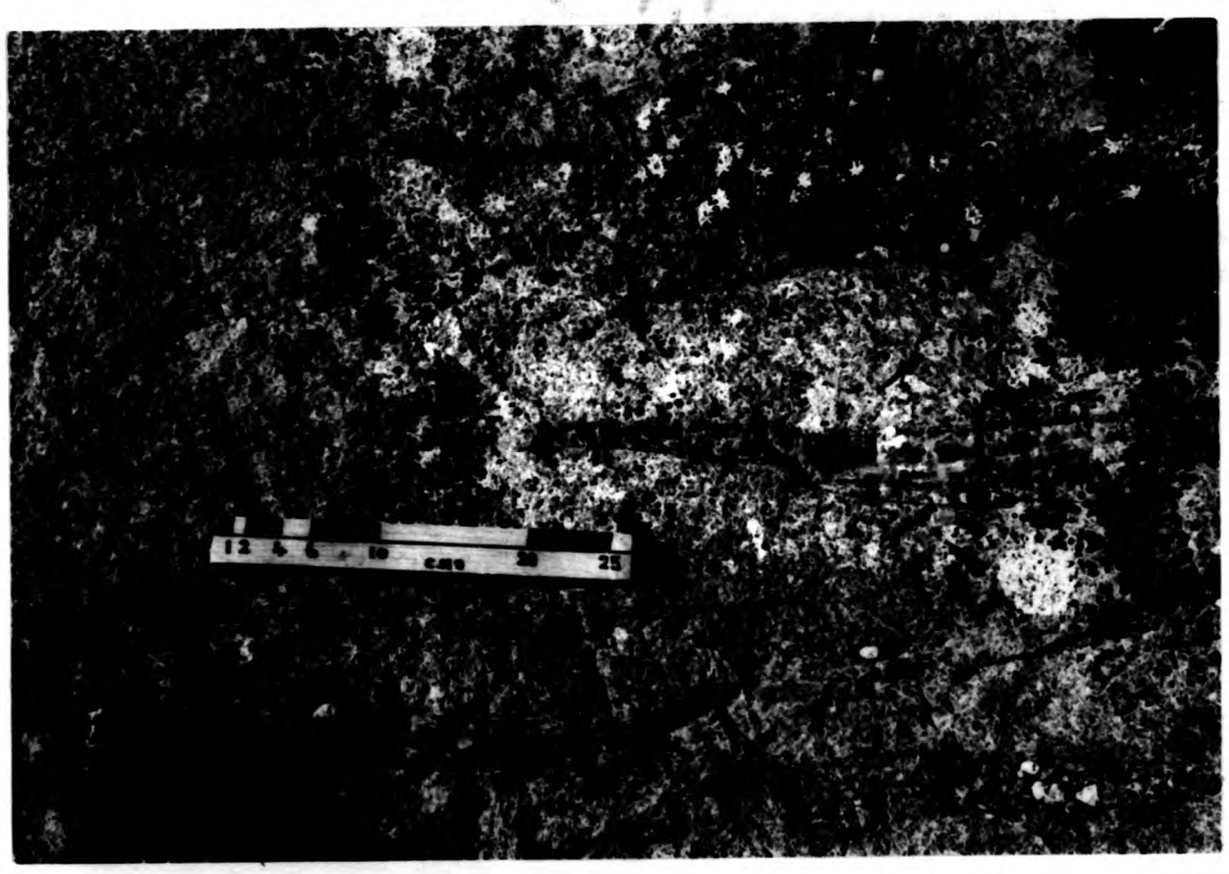

Plate 7.8 Small en echelon sheetlets. From the termination of the lower sheet a series of semi-arcuate fractures emanate and curve away from the upper sheet. Inner Centre Two, Lighthouse section, Hypersthene Gabbro host rock.

Plate 7.7 Two sheets follow the pronounced foliation in the Moine host rock. At it's termination the lower sheet tapers and cross cuts the foliation. Centre One, Rubha'Choit.

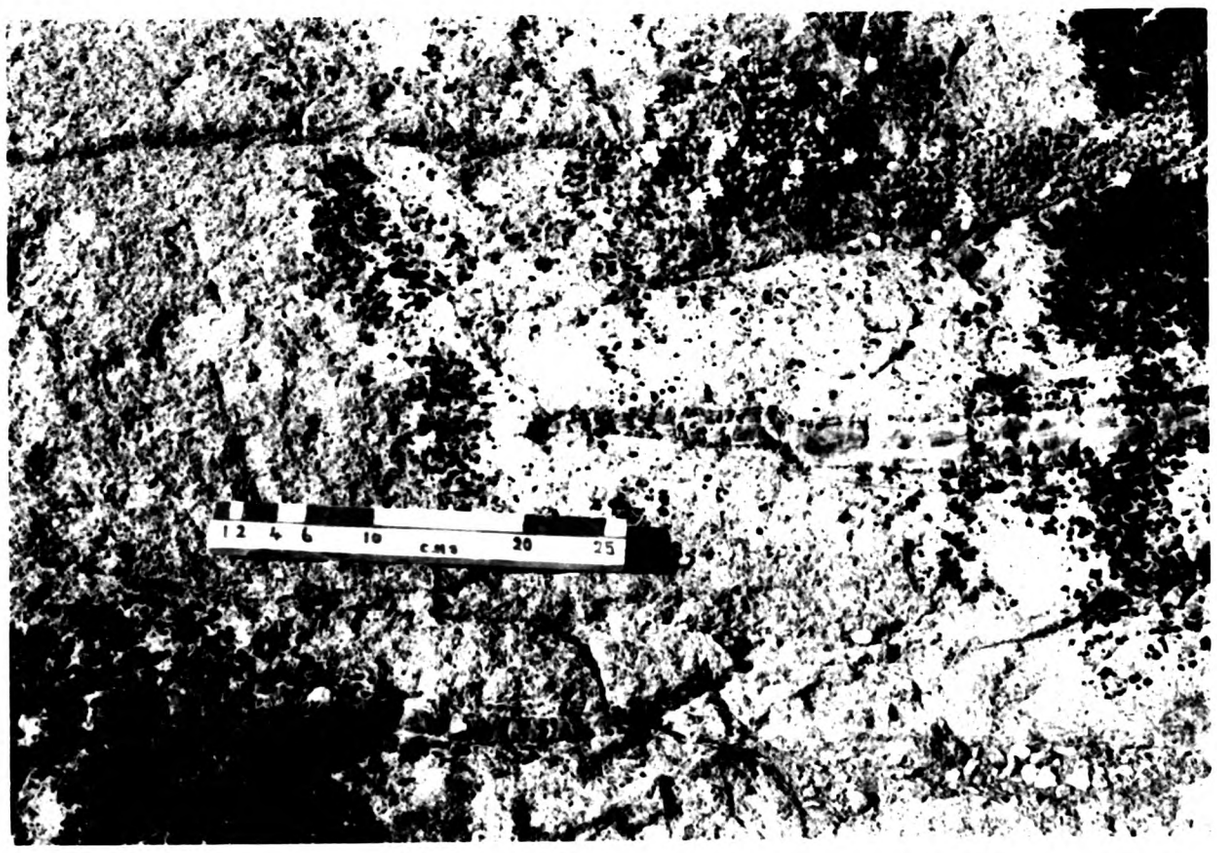

Plate 7.8 Small en echelon sheetlets. From the termination of the lower sheet a series of semi-arcuate fractures emanate and curve away from the upper sheet, Inner Centre Two, Lighthouse section, Hypersthene Gabbro host rock.

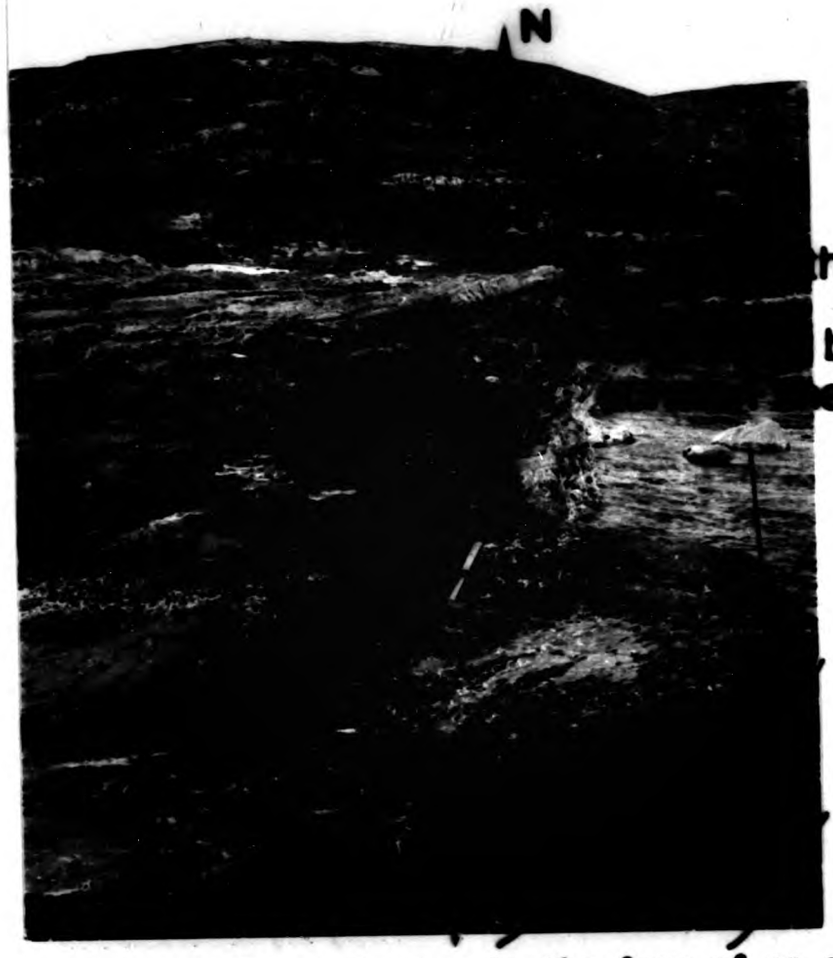

Plate 7.9 A cone sheet which terminates in the from of en echelon sheets Outer Centre Two, Rubha'a Mhile, Triassic conglomerate host rock (see also Fig.7.2.1A).

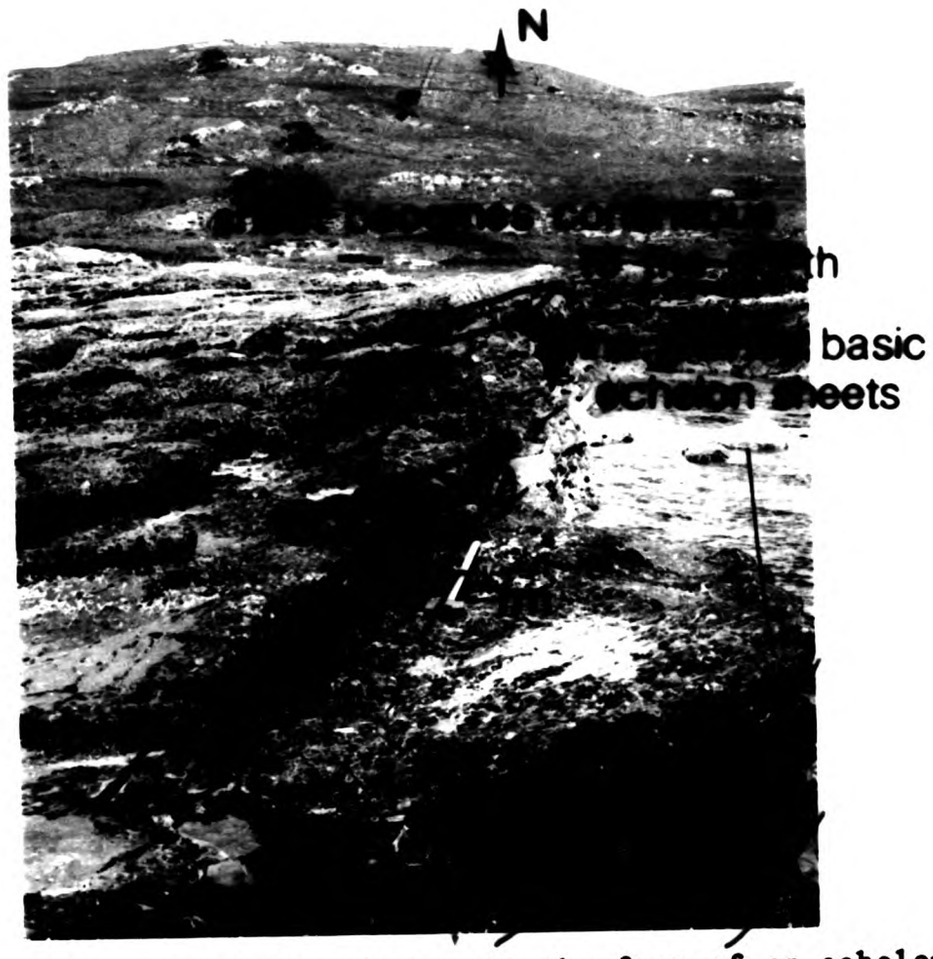

Plate 7.9 A cone sheet which terminates in the from of en echelon sheets Outer Centre Two, Rubha'a Mhile, Triassic conglomerate host rock (see also Fig.7.2.1A).

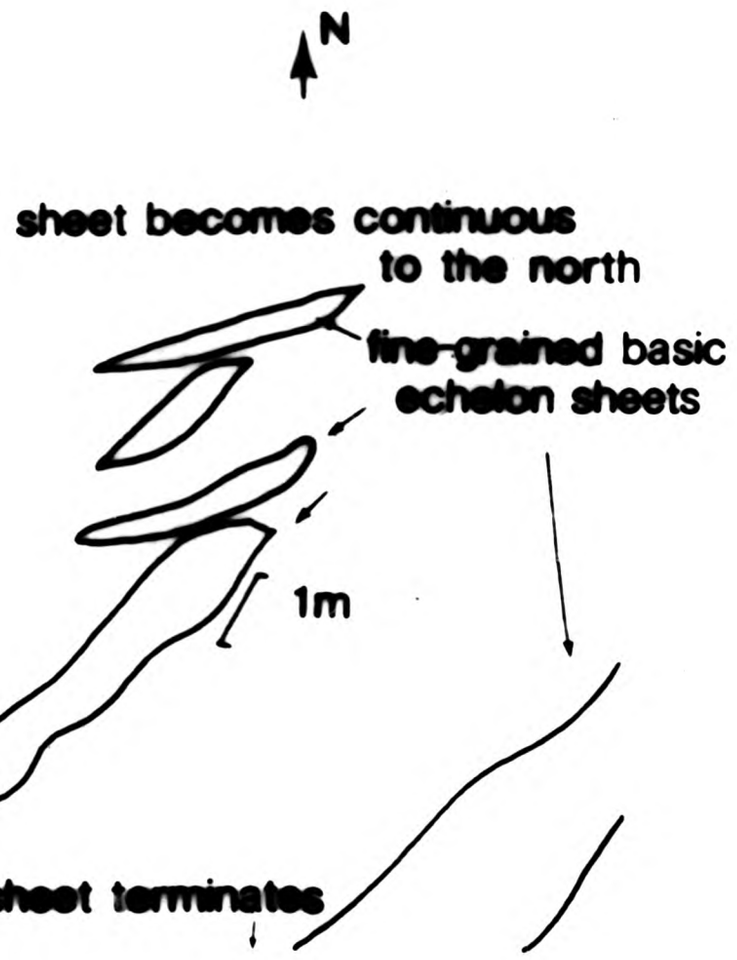
N
sheet becomes continuous
to the north
fine-grained basic
echelon sheets
1m
sheet terminates

Plate 7.9 A cone sheet which terminates in the from of en echelon sheets Outer Centre Two, Rubha'a Mhile, Triassic conglomerate host rock (see also Fig.7.2.1A).

Plate 7.9 A cone sheet which terminates in the from of en echelon sheets Outer Centre Two, Rubha'a Mhile, Triassic conglomerate host rock (see also Fig.7.2.1A).

examples of offset cone sheets described in the literature. However, many sills and dykes have been described as forming en echelon sets; Harker (1904, p303) illustrates offset dykes in Broadford Bay, Skye; Hills (1901), Griggs (1939) and Tweto (1951) give similar examples. Escher et al. (1976) show en echelon dykes in Greenland which also show directional asymmetry of apophyses (Chapter 4). Currie and Fergusson (1970) believed that dykes propagate along a series of en echelon fractures and Pollard et al. (1975) concluded that the fingered periphery of the Shonkin Sag Sill may be characteristic of the method by which sills propagate.

En echelon sets have been identified in all four cone sheet sets of Ardnamurchan. The best developed occur at the Point of Ardnamurchan (Lighthouse section) (Fig.7.3.1) where 9 en echelon sets are developed in an area measuring 100m x 30m. The number of sheetlets belonging to one en echelon set varies between three and six. There are a few sheets in this area which do not form part of an en echelon set. The presence of an en echelon set may indicate either that the exposed section marks the vertical extent of a cone sheet, or that a different stress regime existed at the point where the en echelon set occurs.

A total of 30 examples of en echelon sets have been identified in Ardnamurchan, a number of which are illustrated in Figs.7.3.2 - 4. Most of the en echelon sets occur within the Centre One and Inner Centre Two cone sheets. If it is assumed that en echelon sets mark both vertical and lateral termination of a cone sheet, then it is possible that the Centre One and Inner Centre Two cone sheet sets mark the location of traverses

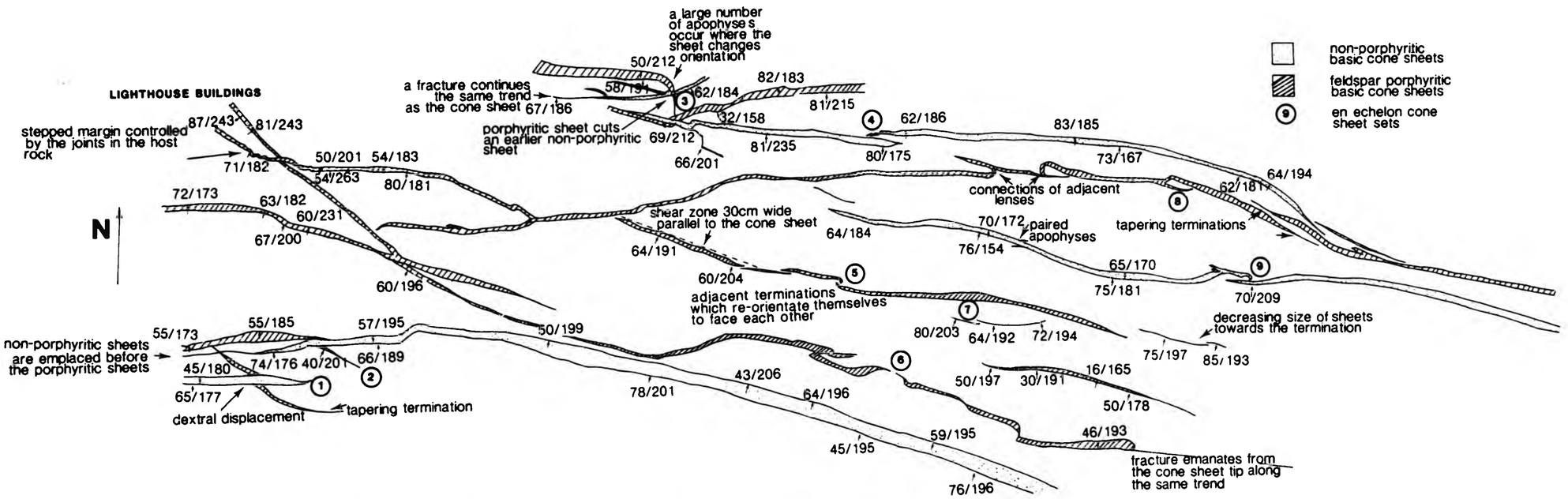

Fig.7.3.1 A map of the Inner Centre Two cone sheets which outcrop at the Lighthouse Nine en echelon cone sheet sets (① to ⑨) can be seen at this location the majority of which indicate dextral shear. Three phases of emplacement can be recognised ie. porphyritic non-porphyritic, porphyritic, which typifys the Inner Centre Two cone sheets. This diagram demonstrates a number of termination types.

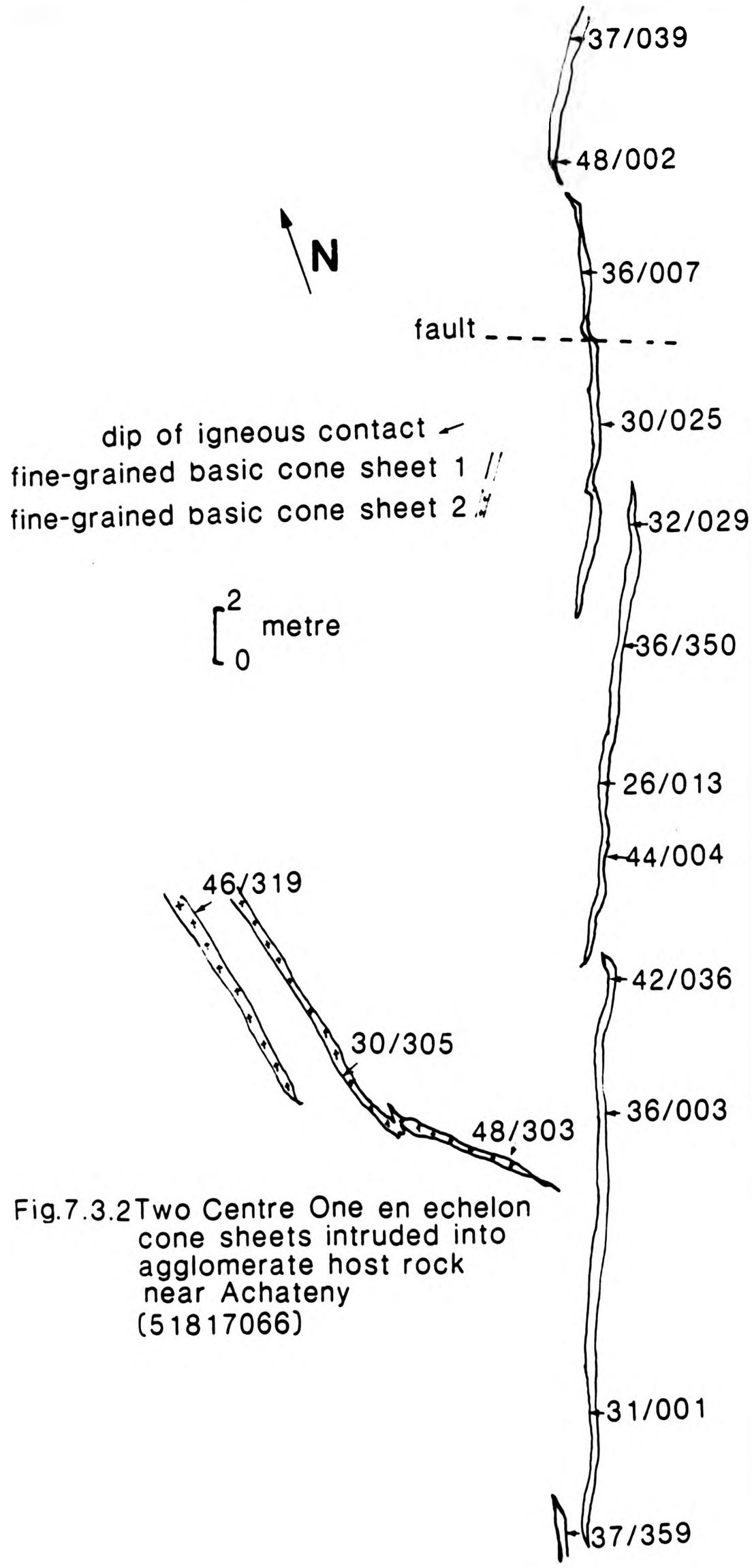

Fig.7.3.2 Two Centre One en echelon cone sheets intruded into agglomerate host rock near Achateny (51817066)

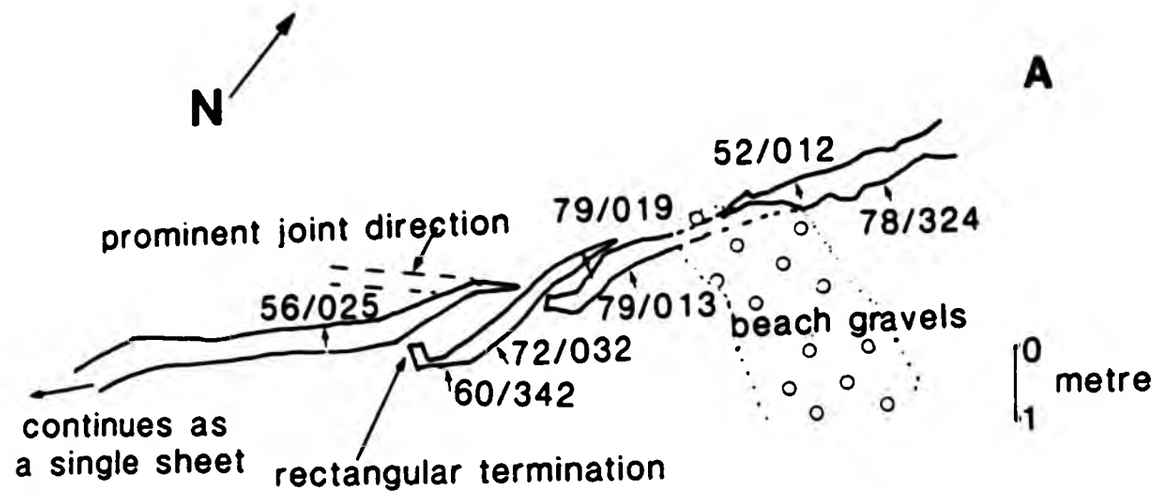

an Outer Centre Two en echelon cone sheet which has utilized the prominent joints of the Moine host rock (49146283)

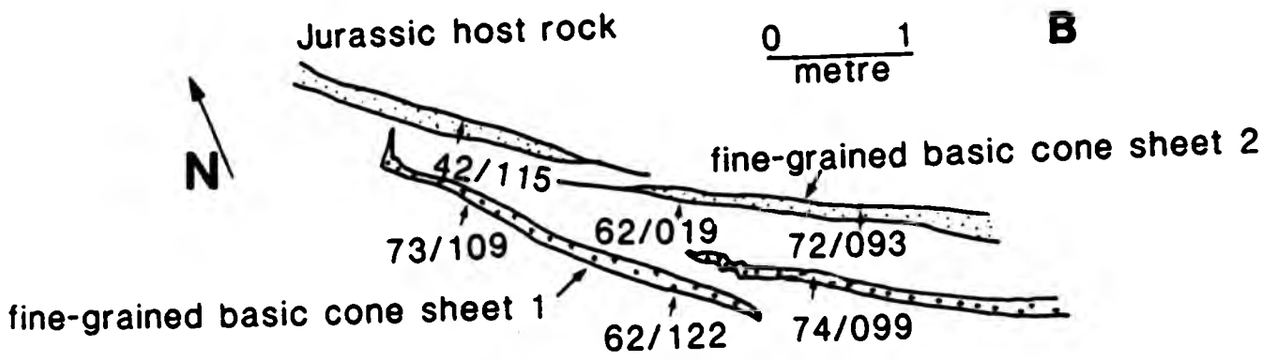

two en echelon Outer Centre Two cone sheets (44506280)

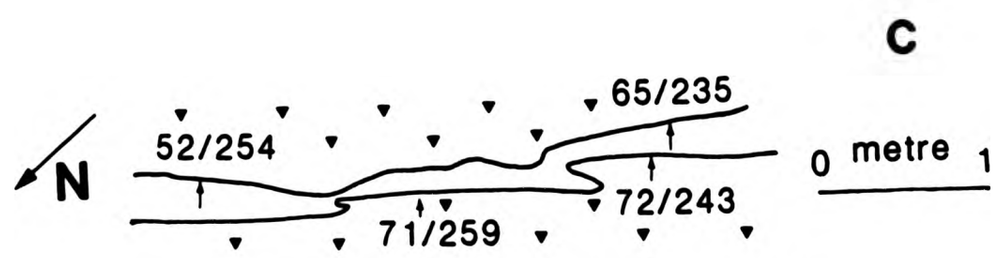

Centre One cone sheet (52017095)

Fig.7.3.3 Three examples of en echelon cone sheets emplaced into different host rocks

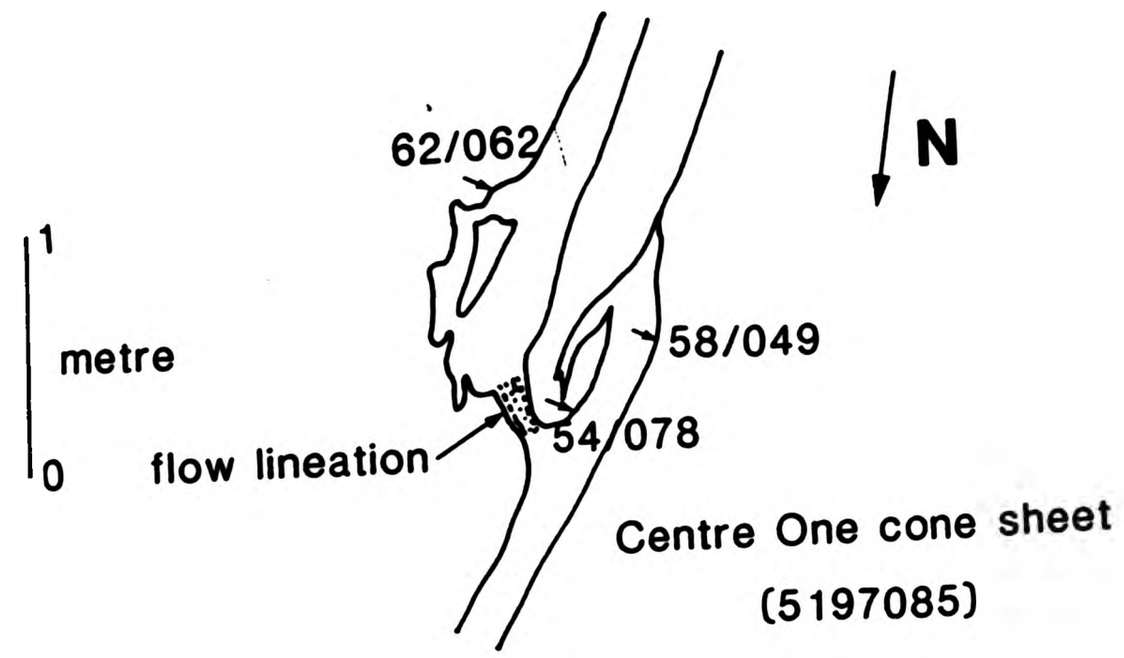

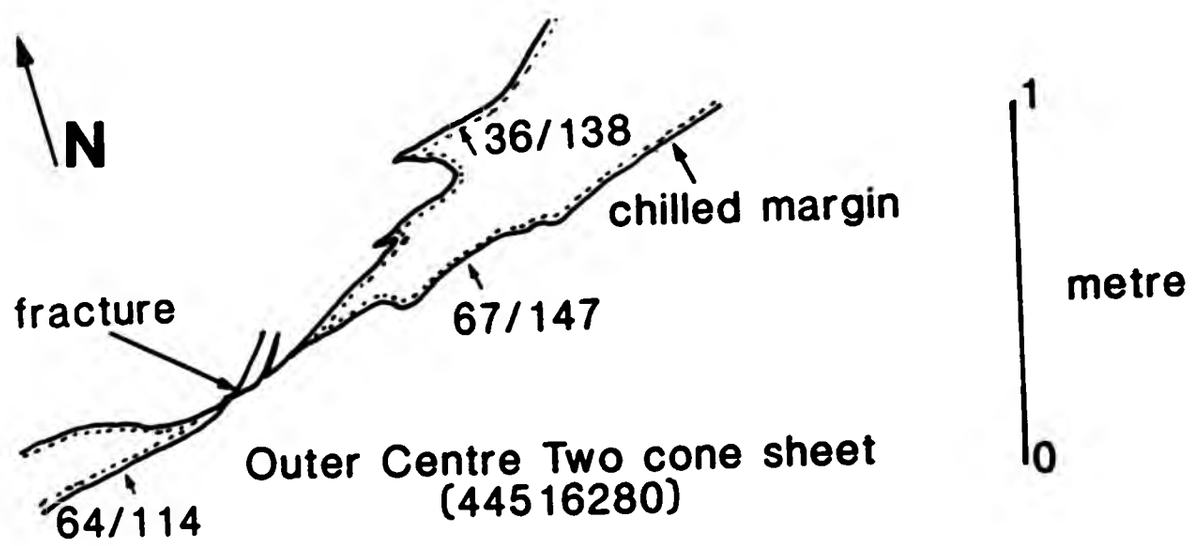

Fig.7.3.4 A diagram to show two types of connections between adjacent en echelon lenses

at a relatively high structural level within a cone sheet set. Thus, the presence of a large number of en echelon sets marks the distal parts of a cone sheet complex.

Individual sheetlets or lenses of an en echelon set maintain a constant thickness over most of their length before tapering. The lenses range in size from 26cm long x 1cm thick (Plate 7.2) to more than 70m long x 1m thick (Fig.7.3.1). Towards the periphery of an en echelon set the lenses decrease in size, both in length and thickness (Fig.7.3.1). They are usually filled with fine-grained basic/intermediate rock; the majority of sheets depicted in Fig.7.3.1 consist of feldspar porphyritic, fine-grained basic rock. No acid en echelon sets have been found, which may be a function of the paucity of acid sheets. Acid magma cannot easily rise to high levels in the earths crust because of its very high viscosity and it is of interest to note that the majority of acid cone sheets form parts of composite intrusions; to rise to high levels in the crust, acid magma needs basic magma to precede it and warm up the fracture. As en echelon sets only form a small percentage of the total number of sheets observed, coupled with the paucity of acid sheets in general, the probability of an acid en echelon set being developed is low and its subsequent exposure even lower.

The actual terminations of the lenses show the same variety of forms as described in Chapter 7.2. However, the lenses themselves may assume the following shapes:- sharply terminating elongate ellipse (Fig.7.3.1), teardrop, prolate ellipse with rounded terminations (Fig.7.2.1) and rectangular terminations

(Fig.7.3.3).

It was noted that the margins of some en echelon sheets are not planar, but are arcuate or cuspate in horizontal cross-section as seen in two en echelon Centre One sheets from Swordle Bay (Plates 7.10 and 7.11). In some exposures the en echelon sheets are seen to coalesce (Figs.7.3.3C and 7.3.4) (Plate 7.12 and Plate 7.13). Plates 7.14 and 7.15 show two views of an en echelon set which are joined in three-dimensions. Exposures developed parallel to the strike of the sheet show that the junction between the coalesced sheetlets forms a groove (Fig.7.4.7), and in one example the length of the groove is 3m long. However, the connections between sheetlets are rarely exposed to this extent. Plates 7.16 and 7.17 show the delicate connections between two adjacent sheetlets at their tapering terminations.

Where offset sheets have been eroded at an oblique angle to their trend, the connections can be seen more clearly. Figure 7.3.5 is a block diagram of the en echelon set shown in Plates 7.18, 7.19 and 7.20, emphasizing the three-dimensional connections of the sheetlets. Plate 7.9 shows a single sheet which terminates as a series of en echelon lenses.

Deformation of the host rocks can be seen around some of the en echelon cone sheets that are emplaced in the Liassic limestones in Swordle Bay (Plates 7.18 and 7.19). Centre One sheets are concordant with bedding when they occur in sediments, that is where splitting of the bedding planes forms the most prominent process of emplacement (Plate 7.18). Plate 7.18 shows

Plate 7.10 The cuspate form of the lower margin of a cone sheet intruded into Jurassic (Lias) limestones. Each cusp is 40cm in length, Centre One, Swordle Bay.

Plate 7.11 The cuspate form of the lower margin of a cone sheet intruded into Jurassic (Lias) limestone. Amplitude of the cusps is 20cm, Centre One, Swordle Bay.

Plate 7.10 The cuspate form of the lower margin of a cone sheet intruded into Jurassic (Lias) limestones. Each cusp is 40cm in length, Centre One, Swordle Bay.

Plate 7.11 The cuspate form of the lower margin of a cone sheet intruded into Jurassic (Lias) limestone. Amplitude of the cusps is 20cm, Centre One, Swordle Bay.

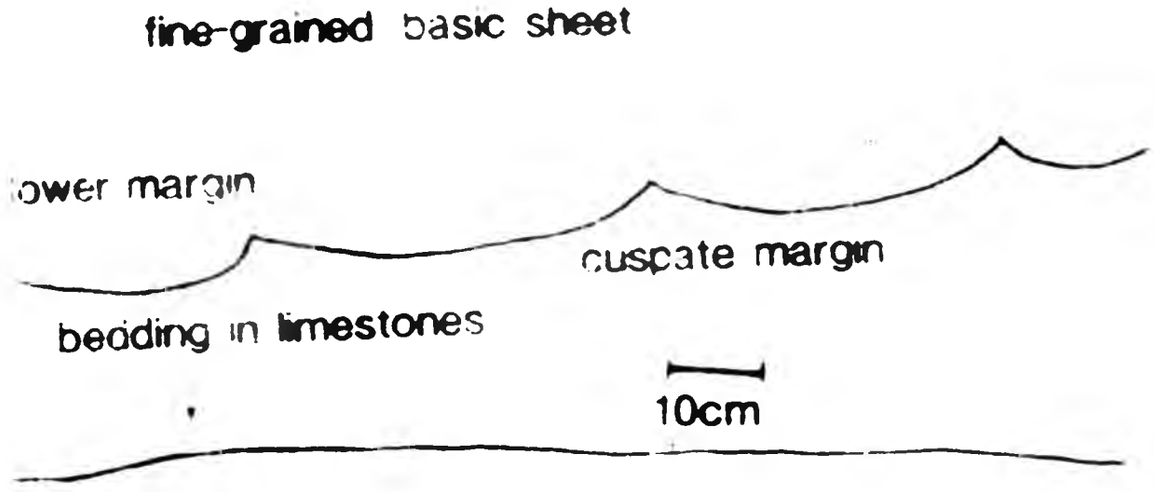
fine-grained basic sheet
lower margin
cuspate margin
bedding in limestones
10cm

5cm

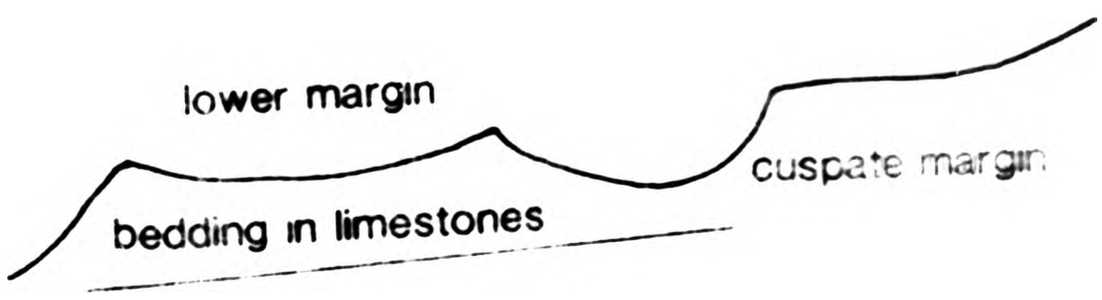
fine-grained basic sheet
lower margin
cuspate margin
bedding in limestones

Plate 7.10 The cuspate form of the lower margin of a cone sheet intruded into Jurassic (Lias) limestones. Each cusp is 40cm in length, Centre One, Swordle Bay.

Plate 7.11 The cuspate form of the lower margin of a cone sheet intruded into Jurassic (Lias) limestone. Amplitude of the cusps is 20cm, Centre One, Swordle Bay.

Plate 7.10 The cuspate form of the lower margin of a cone sheet intruded into Jurassic (Lias) limestones. Each cusp is 40cm in length, Centre One, Swordle Bay.

Plate 7.11 The cuspate form of the lower margin of a cone sheet intruded into Jurassic (Lias) limestone. Amplitude of the cusps is 20cm, Centre One, Swordle Bay.

Plate 7.12 Two en echelon lenses (A and B) are seen to join in three-dimensions and where this junction is visable, in the plane perpendicular to the photograph, a small groove is formed, Centre One, east of Garbh Rubha, Jurassic (Lias) limestone host rock.

Plate 7.13 Two adjacent en echelon lenses separated by a wedge of Jurassic (Lias) limestones. Where the two lenses coalesce there is formed a small groove. Centre One, Swordle Bay.

Plate 7.12 Two en echelon lenses (A and B) are seen to join in three-dimensions and where this junction is visable, in the plane perpendicular to the photograph, a small groove is formed, Centre One, east of Garbh Rubha, Jurassic (Lias) limestone host rock.

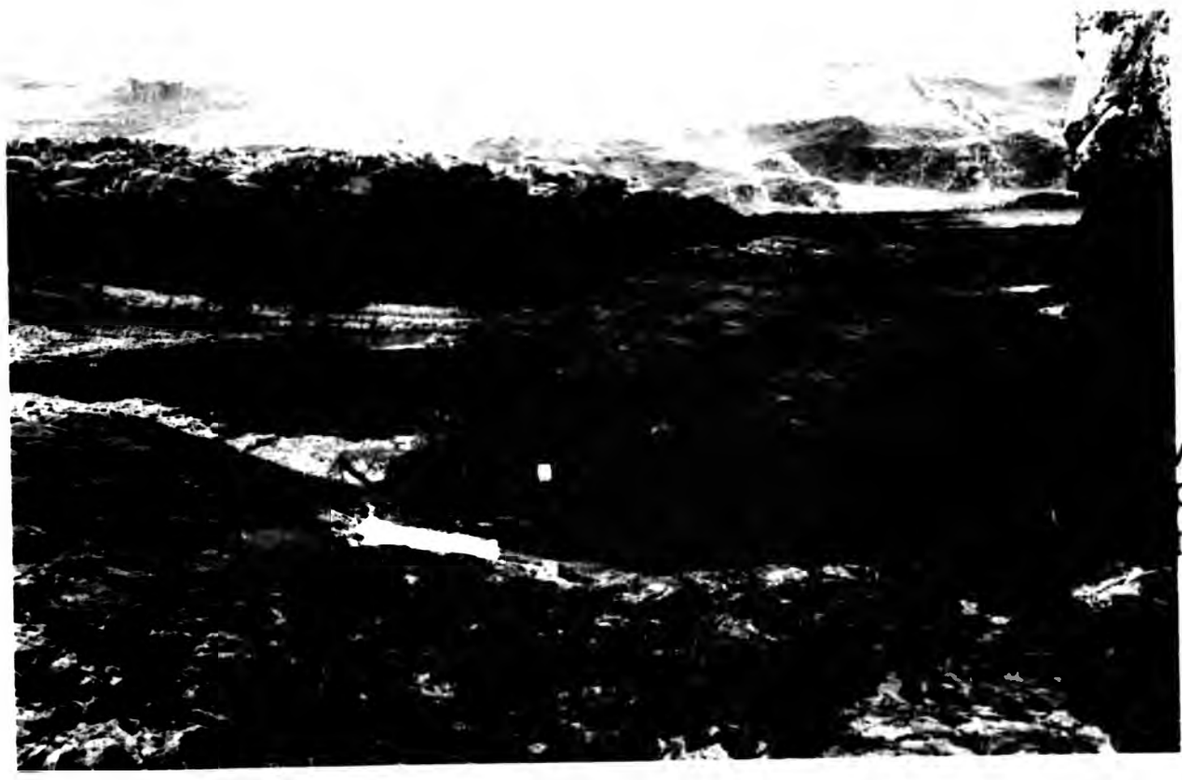

Plate 7.13 Two adjacent en echelon lenses separated by a wedge of Jurassic (Lias) limestones. Where the two lenses coalesce there is formed a small groove. Centre One, Swordle Bay.

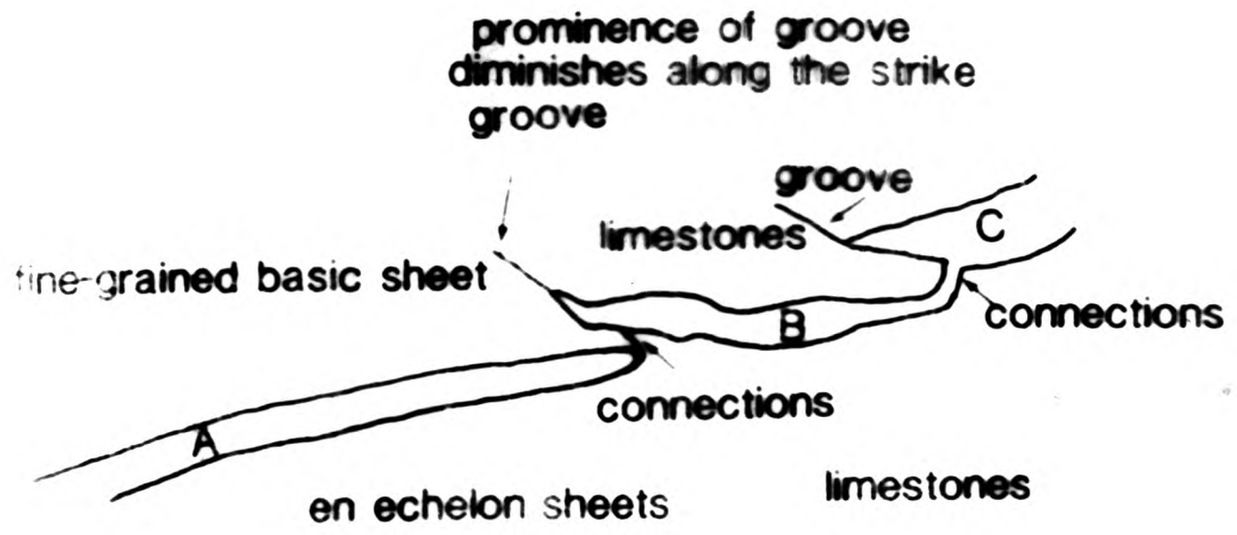

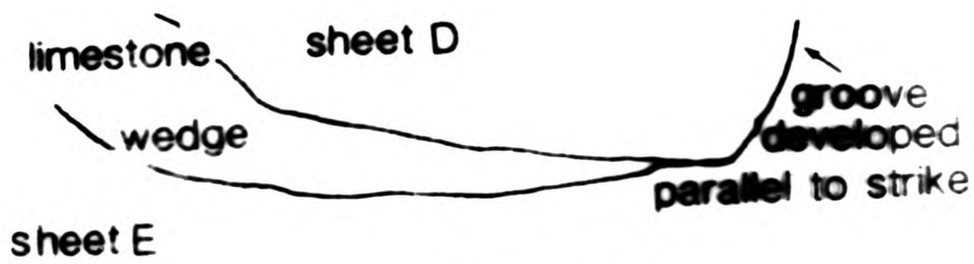

fine-grained basic sheet

Plate 7.12 Two en echelon lenses (A and B) are seen to join in three-dimensions and where this junction is visable, in the plane perpendicular to the photograph, a small groove is formed, Centre One, east of Garbh Rubha, Jurassic (Lias) limestone host rock.

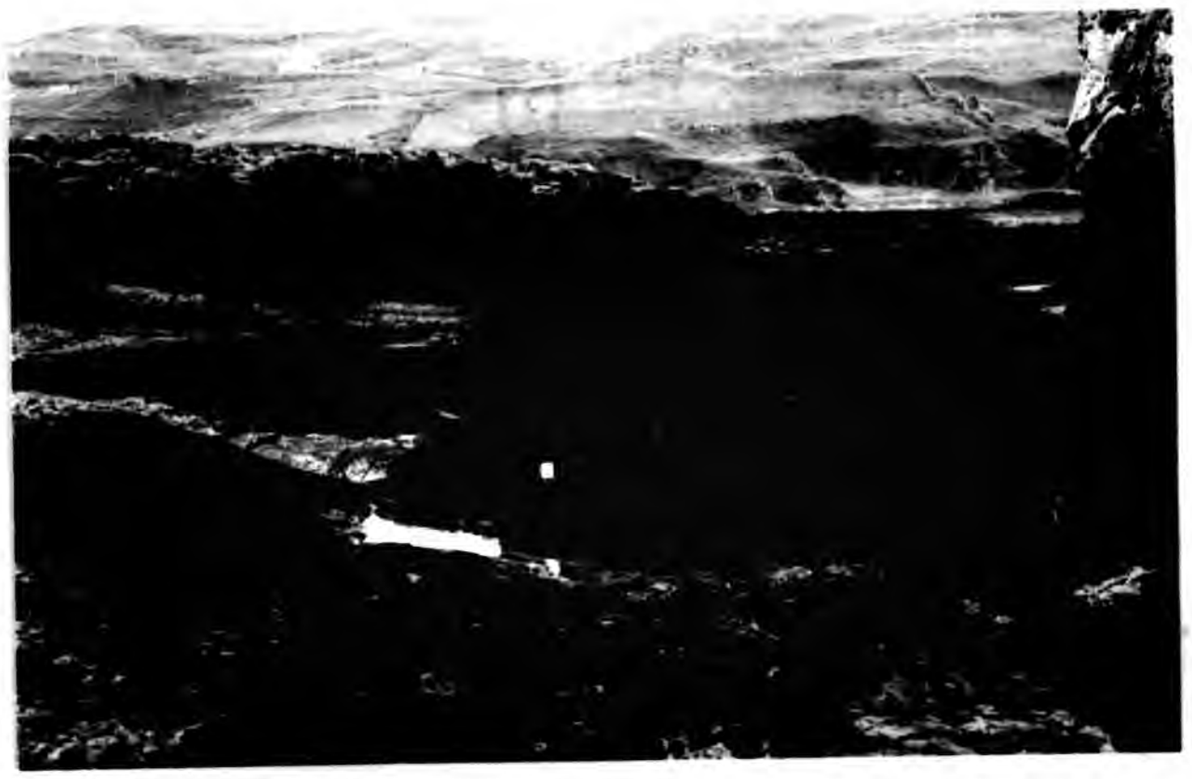

Plate 7.13 Two adjacent en echelon lenses separated by a wedge of Jurassic (Lias) limestones. Where the two lenses coalesce there is formed a small groove. Centre One, Swordle Bay.

Plate 7.12 Two en echelon lenses (A and B) are seen to join in three-dimensions and where this junction is visable, in the plane perpendicular to the photograph, a small groove is formed, Centre One, east of Garbh Rubha, Jurassic (Lias) limestone host rock.

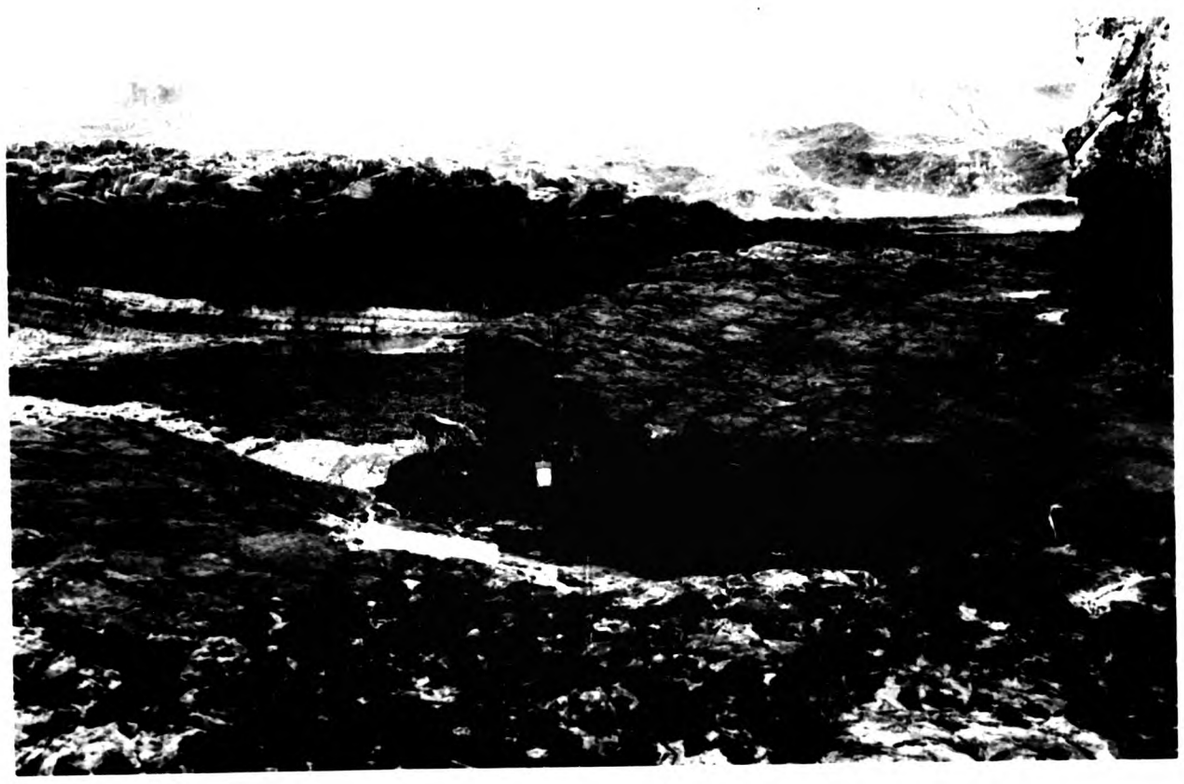

Plate 7.13 Two adjacent en echelon lenses separated by a wedge of Jurassic (Lias) limestones. Where the two lenses coalesce there is formed a small groove. Centre One, Swordle Bay.

Plate 7.16 A plan view of a pair of en echelon terminations. In cross section (Plate 7.17) it can be seen that the two sheets are connected, Inner Centre Two, Lighthouse section, Hypersthene Gabbro host rock.

Plate 7.17 The cross section of two sheetlets (Plate 7.16) which are joined in the third dimension, thus demonstrating the interconnections of the en echelon sets. Inner Centre Two, Lighthouse section, Hypersthene Gabbro host rock.

Plate 7.16 A plan view of a pair of en echelon terminations. In cross section (Plate 7.17) it can be seen that the two sheets are connected, Inner Centre Two, Lighthouse section, Hypersthene Gabbro host rock.

Plate 7.17 The cross section of two sheetlets (Plate 7.16) which are joined in the third dimension, thus demonstrating the interconnections of the en echelon sets. Inner Centre Two, Lighthouse section, Hypersthene Gabbro host rock.

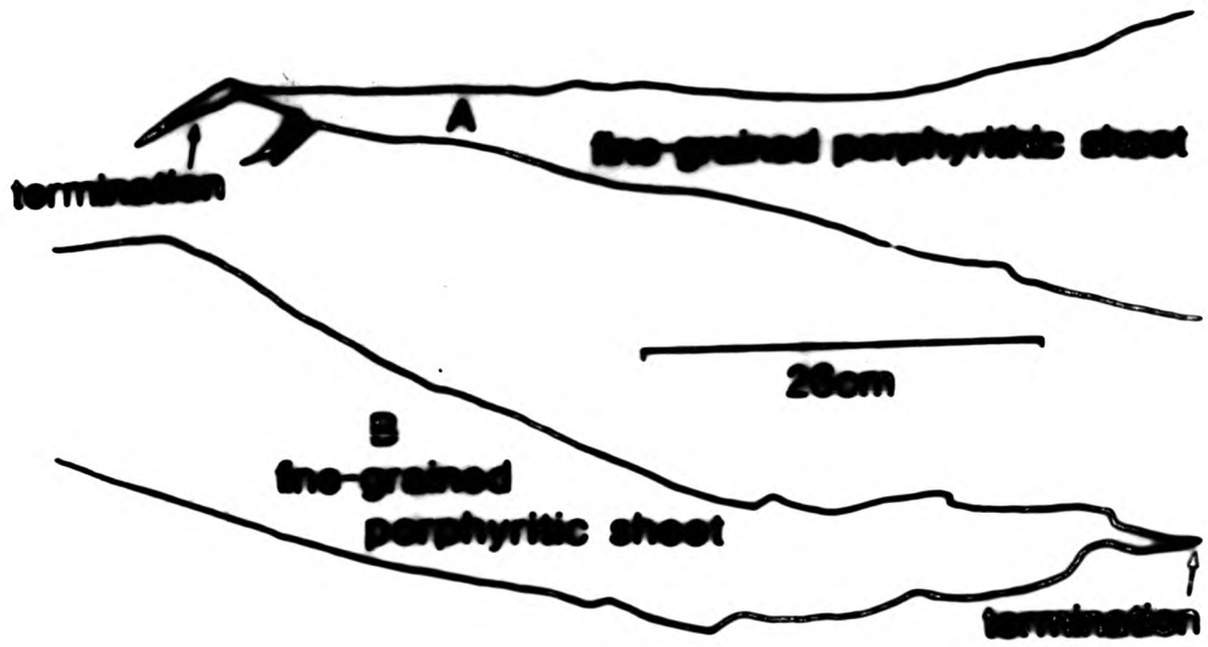
A
fine-grained porphyritic sheet
termination
26cm
B
fine-grained
porphyritic sheet
termination

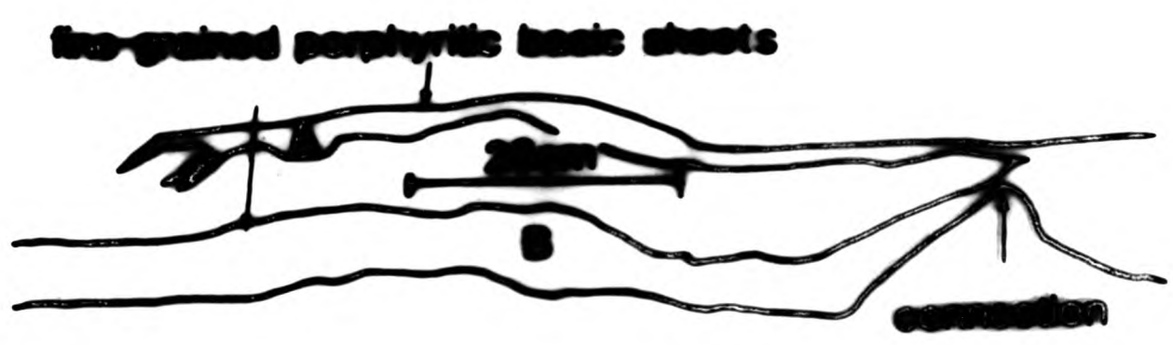
fine-grained porphyritic basic sheets
26cm
B
connection

Plate 7.16 A plan view of a pair of en echelon terminations. In cross section (Plate 7.17) it can be seen that the two sheets are connected, Inner Centre Two, Lighthouse section, Hypersthene Gabbro host rock.

Plate 7.17 The cross section of two sheetlets (Plate 7.16) which are joined in the third dimension, thus demonstrating the interconnections of the en echelon sets. Inner Centre Two, Lighthouse section, Hypersthene Gabbro host rock.

Plate 7.16 A plan view of a pair of en echelon terminations. In cross section (Plate 7.17) it can be seen that the two sheets are connected, Inner Centre Two, Lighthouse section, Hypersthene Gabbro host rock.

Plate 7.17 The cross section of two sheetlets (Plate 7.16) which are joined in the third dimension, thus demonstrating the interconnections of the en echelon sets. Inner Centre Two, Lighthouse section, Hypersthene Gabbro host rock.

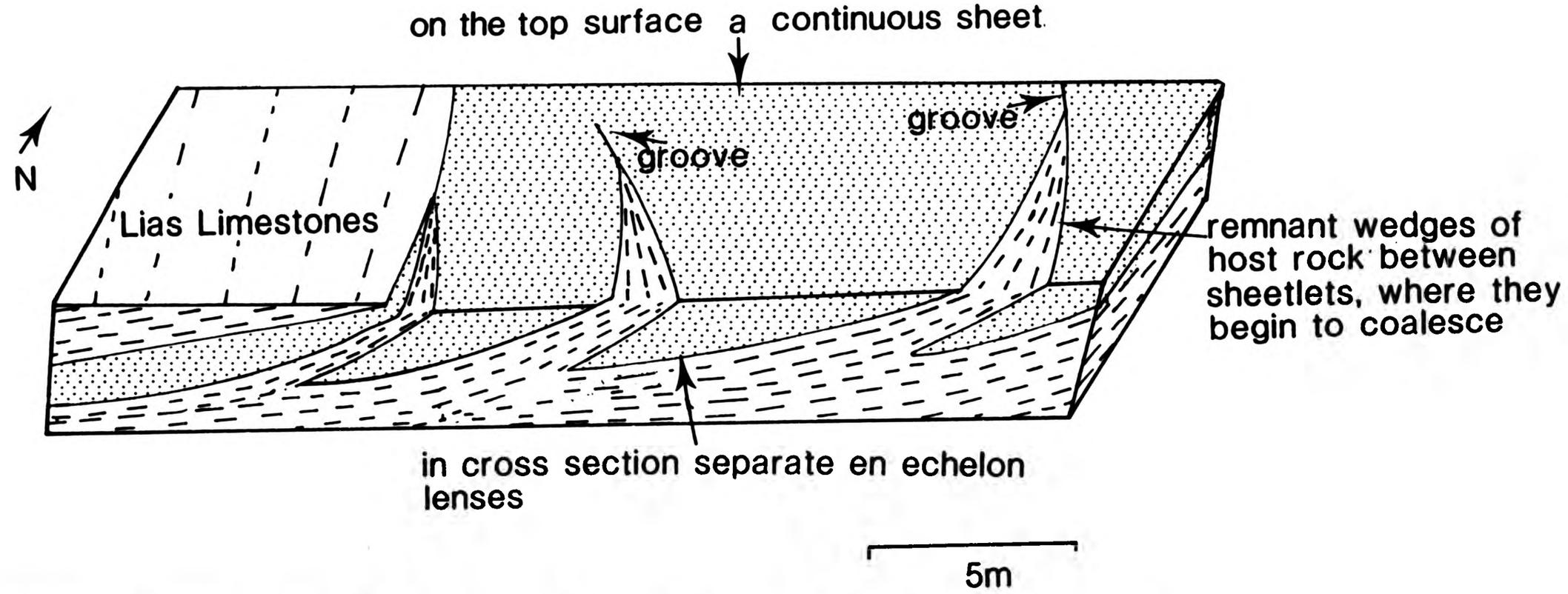

Fig.7.3.5 Block diagram showing a series of en echelon lenses that coalesce laterally (see also Plates 7.18 and 7.19).
Centre One Cone Sheet, Swordle Bay.

Plate 7.18 Two wedge-shaped en echelon sheetletsin which one surface of each sheetlet is planar and concordant with bedding whereas the other surface is inclined. Centre One, Swordle Bay, Jurassic (Lias) limestone host rock.

Plate 7.19 Bedding planes between two en echelon sheets have become distorted and assume the form of the termination of the lower sheet. Centre One, Swordle Bay, Jurassic (Lias) limestone host rock.

Plate 7.18 Two wedge-shaped en echelon sheetletsin which one surface of each sheetlet is planar and concordant with bedding whereas the other surface is inclined. Centre One, Swordle Bay, Jurassic (Lias) limestone host rock.

Plate 7.19 Bedding planes between two en echelon sheets have become distorted and assume the form of the termination of the lower sheet. Centre One, Swordle Bay, Jurassic (Lias) limestone host rock.

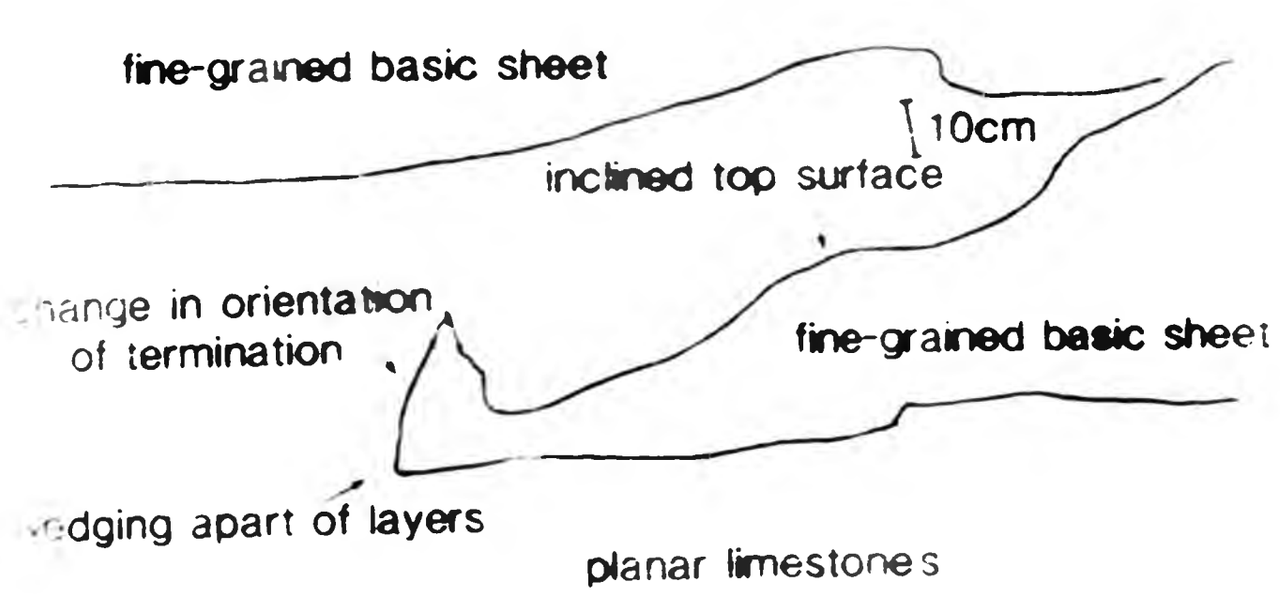

planar limestones

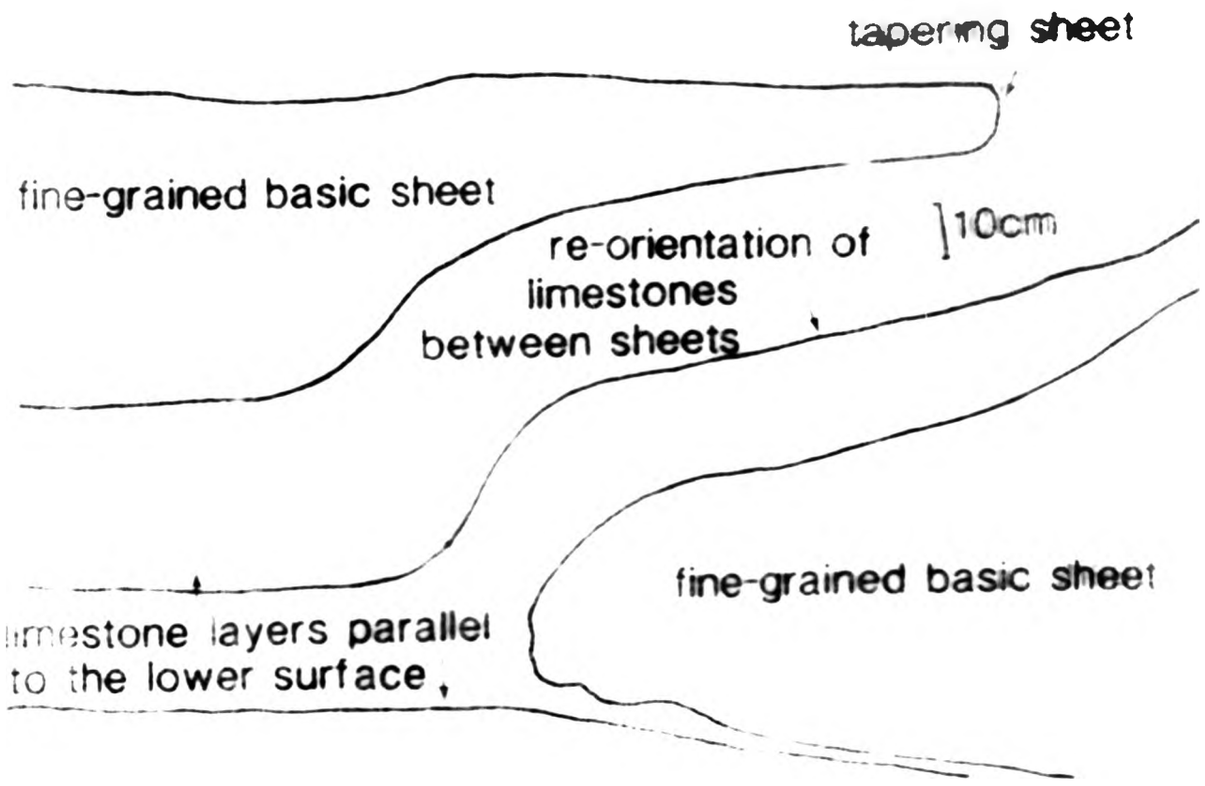

Plate 7.18 Two wedge-shaped en echelon sheetletsin which one surface of each sheetlet is planar and concordant with bedding whereas the other surface is inclined. Centre One, Swordle Bay, Jurassic (Lias) limestone host rock.

Plate 7.19 Bedding planes between two en echelon sheets have become distorted and assume the form of the termination of the lower sheet. Centre One, Swordle Bay, Jurassic (Lias) limestone host rock.

Plate 7.18 Two wedge-shaped en echelon sheetletsin which one surface of each sheetlet is planar and concordant with bedding whereas the other surface is inclined. Centre One, Swordle Bay, Jurassic (Lias) limestone host rock.

Plate 7.19 Bedding planes between two en echelon sheets have become distorted and assume the form of the termination of the lower sheet. Centre One, Swordle Bay, Jurassic (Lias) limestone host rock.

Plate 7.20 Cross section of a set of en echelon sheets, each sheet occupys a different layer within the Jurassic (Lias) limestones. Centre One, Swordle Bay (see Fig.7.3.5).

Plate 7.20 Cross section of a set of en echelon sheets, each sheet occupys a different layer within the Jurassic (Lias) limestones. Centre One, Swordle Bay (see Fig.7.3.5).

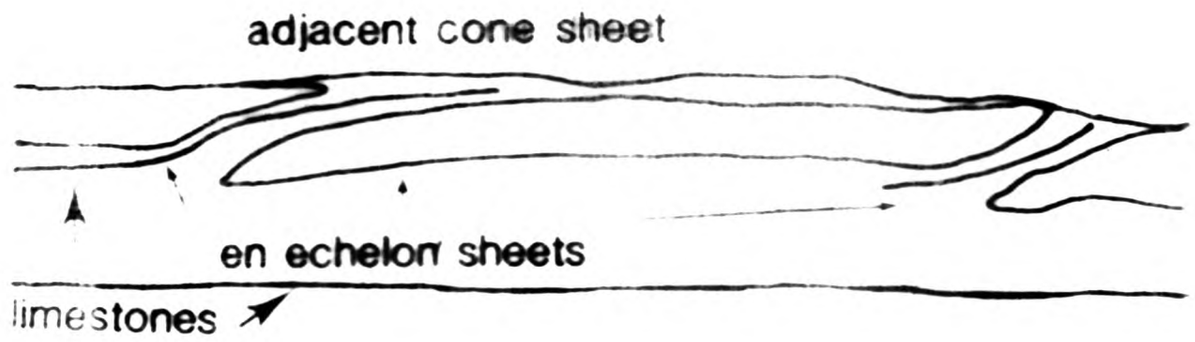
adjacent cone sheet
en echelon sheets
limestones

Plate 7.20 Cross section of a set of en echelon sheets, each sheet occupys a different layer within the Jurassic (Lias) limestones. Centre One, Swordle Bay (see Fig.7.3.5).

Plate 7.20 Cross section of a set of en echelon sheets, each sheet occupys a different layer within the Jurassic (Lias) limestones. Centre One, Swordle Bay (see Fig.7.3.5).

that the limestone beds between adjacent lenses assumes the attitude of the termination. As evidence of intrusion deformation is only preserved in sedimentary rocks, it is possible that deformation in igneous host rocks was either brittle or at the time of emplacement of some of the cone sheets the igneous host had not completed it's crystallization and deformation was ductile. It is interesting to note that Le Bas (1979) mentions the development of a pronounced cleavage in the country rock caused by the emplacement of carbonatite cone sheets.

7.4 EN ECHELON SETS AS A METHOD OF PROPAGATION

En echelon sets have been identified for all manner of minor intrusions and their existence may be indicative of a number of processes, either a ubiquitous process for the propagation of all sheet-like intrusions or they may be connected with conditions at the termination of the intrusion or they may be indicative of different stress orientations at different levels in the crust, or indicate the origin of a zone of hydraulic fracture. Two schools of thought exist as to the relationship between en echelon terminations and the direction of propagation of a sheet both in two- and three-dimensions.

The first school of thought believes that minor intrusions "break up" into en echelon sets towards their terminations. The second school of thought believe that minor intrusions begin as separate en echelon sets which merge together to form a continuous sheet.

Anderson (1951) explained the presence of en echelon sets

by assuming that different orientations of stress occur at different levels within the crust. Fig.7.4.1 illustrates Anderson's model, with the direction of tension changing from a NNW - SSE direction at the base, to a north - south direction at the top of the block. In this example, because dykes occupy the direction normal to the least principal stress they will therefore split into lobes which are discontinuous in a horizontal plane. This model only considers propagation in one direction, that is vertically upwards (Fig.7.4.1). Gilliland (1963) described a specimen of shale containing en echelon, quartz-filled tension fractures which merge at depth, as indicated by the continuous vein on the opposite side of the specimen. He follows Anderson's (1951) interpretation to account for the presence of the lenses: the vertical change in orientation of the vein being in response to an alteration in the direction of tension and a change in stress relief ; a decrease in total strain being recorded on the upper surface.

Beach (1975) describes two types of en echelon vein arrays which may equally well be applied to the en echelon arrangement of cone sheets. The two types are a) those formed in active ductile shear zones and b) those which form by the primary nucleation of fractures (hydraulic fracture) not connected with active shear zones. This latter type shows almost equal dilation along the length of the zone. Figure 7.3.1 depicts the en echelon cone sheets located along the Lighthouse traverse and demonstrates an almost equal dilation along the length of each en echelon set, where one sheetlet tapers out an adjacent one maintains the thickness. However, where connections between adjacent lenses are exposed the thickness of the zone may vary.

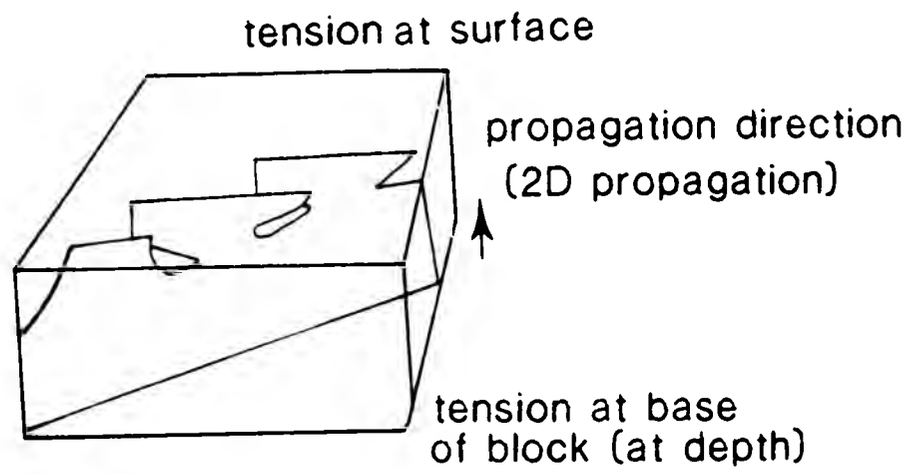

Fig.7.4.1 Diagram to illustrate the formation of en echelon sets at the termination of a sheet like intrusion (after Anderson,1951)

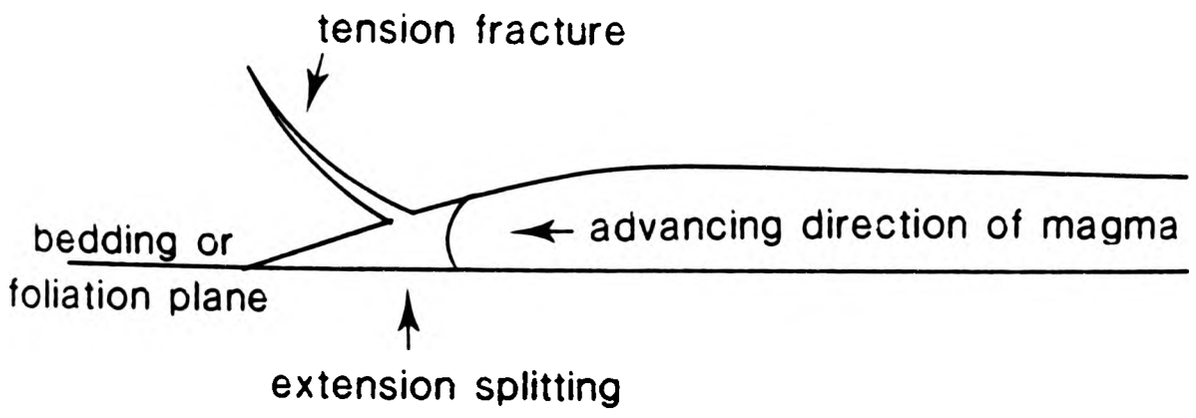

Fig.7.4.2 Diagram which explains the formation showing of en echelon lenses as steam filled extension spaces at the front of a sheet (after Bradley,1965)

Bradley (1965) explains the formation of en echelon lenses at the advancing front of a sheet as steam-filled extension spaces at an angle of 45° to the margin of the sheet body (Fig.7.4.2), thus accounting for the upturn commonly seen at the termination of a sheet (Plate 7.7). Figure 7.4.3 shows a set of en echelon lenses occurring at an angle to the main trend of the en echelon set, and is very similar to those described by Bradley.

Currie and Fergusson (1970) proposed a model of sheet propagation which requires the existance of en echelon fractures (Fig.7.4.4). One of the fractures is filled with a low viscosity, high velocity, volatile-rich material that has boiled off the magma and which preceeds the advance of the water-saturated magma. Currie and Fergusson (1970) maintain that the water is primary magmatic. However, water derived from a meteoric hydrothermal convective system (Taylor and Forrester, 1971) is thought to be the most important source of water in the Ardnamurchan Igneous Complex at the time of activity (Chapter 6). As such, the volatile phase is confined to the leading edge of the fracture and may therefore be redissolved into the magma, resulting in a magma of higher water pressure. In consequence, the magma can either cause or exploit the adjacent en echelon fracture (Fig.7.4.4). This pattern of advancement continues until enough water has been lost to the host rock walls to reduce the pressure of the magma and therefore it's activity. This theory indicates that propagation is along a series of fractures, again in two-dimensions, and also accounts for the presence of small apophyses composed largely of the rapidly chilled volatile phase at the point where the sheet

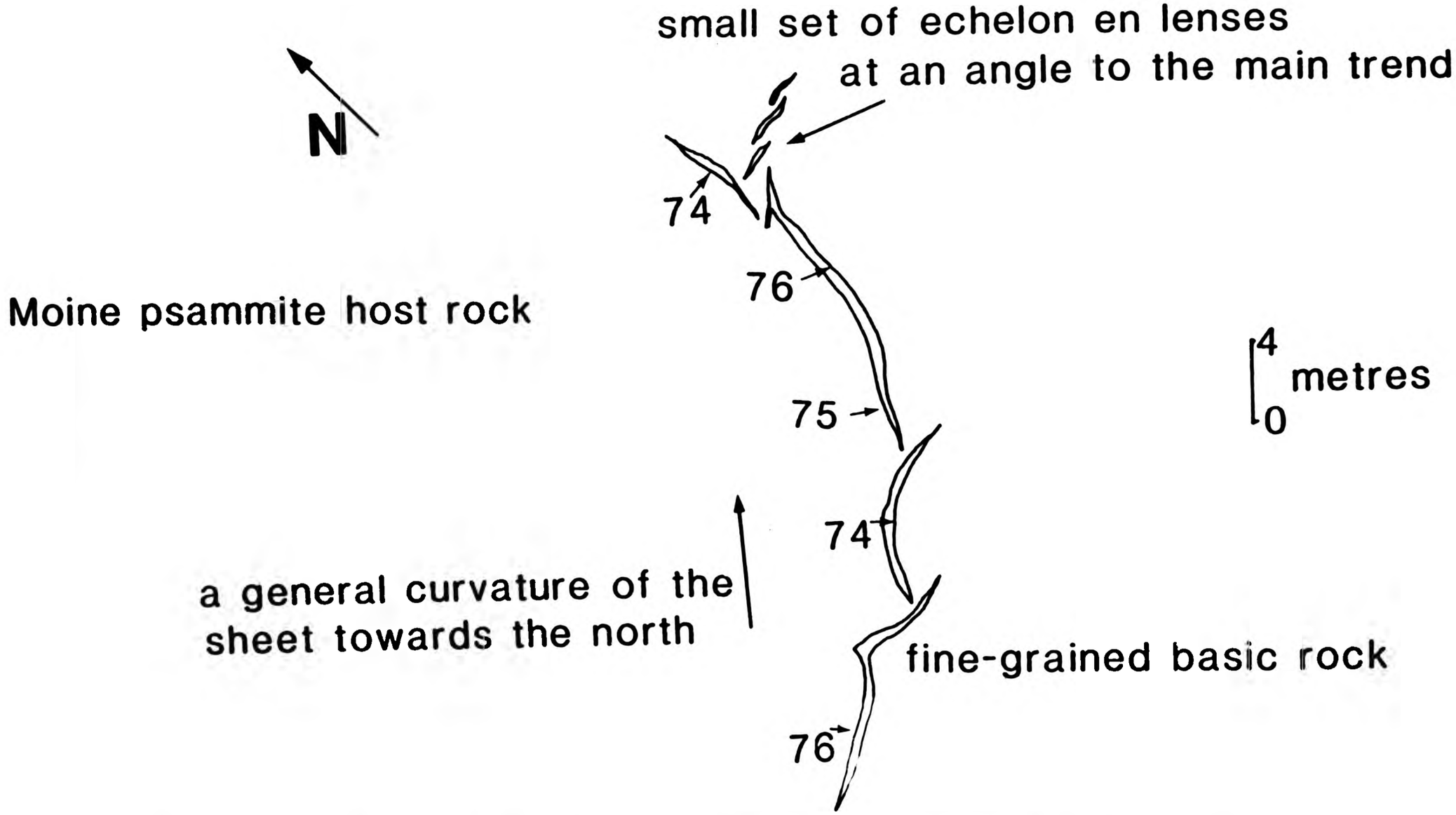

Fig.7.4.3 A diagram showing a set of en echelon lenses of an Outer Centre Two cone sheet developed at an angle to the main sheet (48936253)

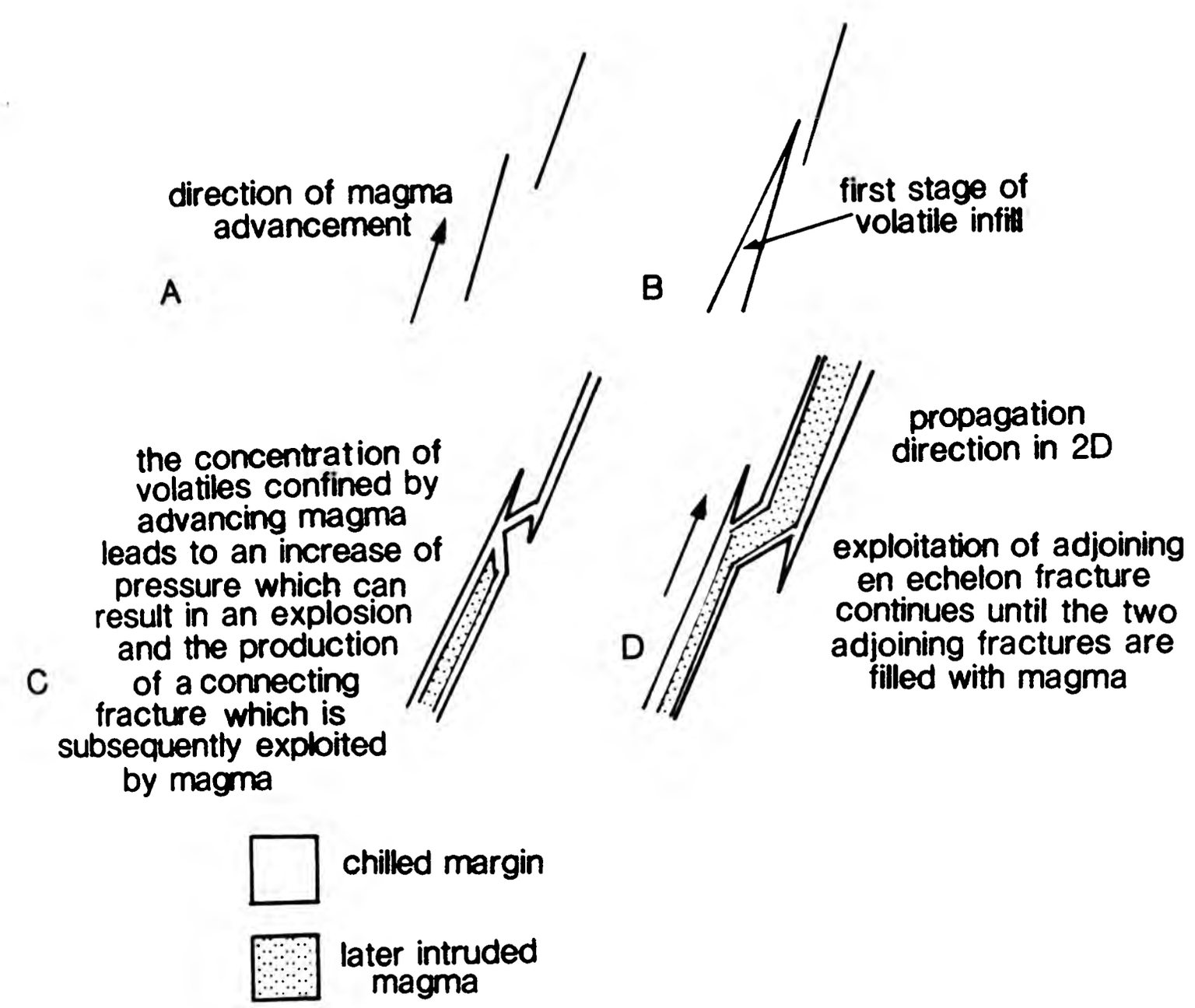

Fig.7.4.4 Four stages in the development of a set of en echelon fractures which then become a transgressive continuous sheet like intrusion, with apophyses continuing at the point of transgression (after Currie and Fergusson, 1970) . This method indicates propagation in 2D along the strike.

transgresses. An alternative hypothesis may be that the sheetlets were filled by magma and a connecting weakness was exploited by the magma in both sheetlets; lateral coalesence then formed the final stage (Fig.7.4.4).

Pollard et al. (1975), unlike the above authors, invoke a three-dimensional model to describe the propagation of sheets. They describe the margins of the Shonkin Sag Sill (porphyritic, fine-grained shonkinite) as a fingered periphery, that is, a large number of minor intrusions which when mapped are seen to be connected to each other in a direction perpendicular to their strike and eventually connected to the main body and, therefore, forming an integral part of the main body of the sill. They concluded that the fingers were a mechanism by which the sill was propagated. A number of characteristic features and terminology of the fingered periphery have been described by these authors. The fingers are ellipsoidal in cross-section and when seen to coalesce their ellipsoidal form is preserved as part of a cuspate margin (Fig.7.4.5). Trending perpendicular to the cuspate margin are grooves (Fig.7.4.5) which marks the line along which the fingers have coalesced. Figure 7.4.6 illustrates the termination which may develop in response to a change in orientation of the least principal stress (σ_3). Based on the ideas of Pollard et al. (1975), the offset sheetlets commonly observed in Ardnamurchan indicate that σ_3 is parallel to the strike of the cone sheets.

Two opinions therefore exist as to the significance of en echelon sets as terminations. Firstly, that the sheet has a rectilinear form and terminates in the form of lenses or second-

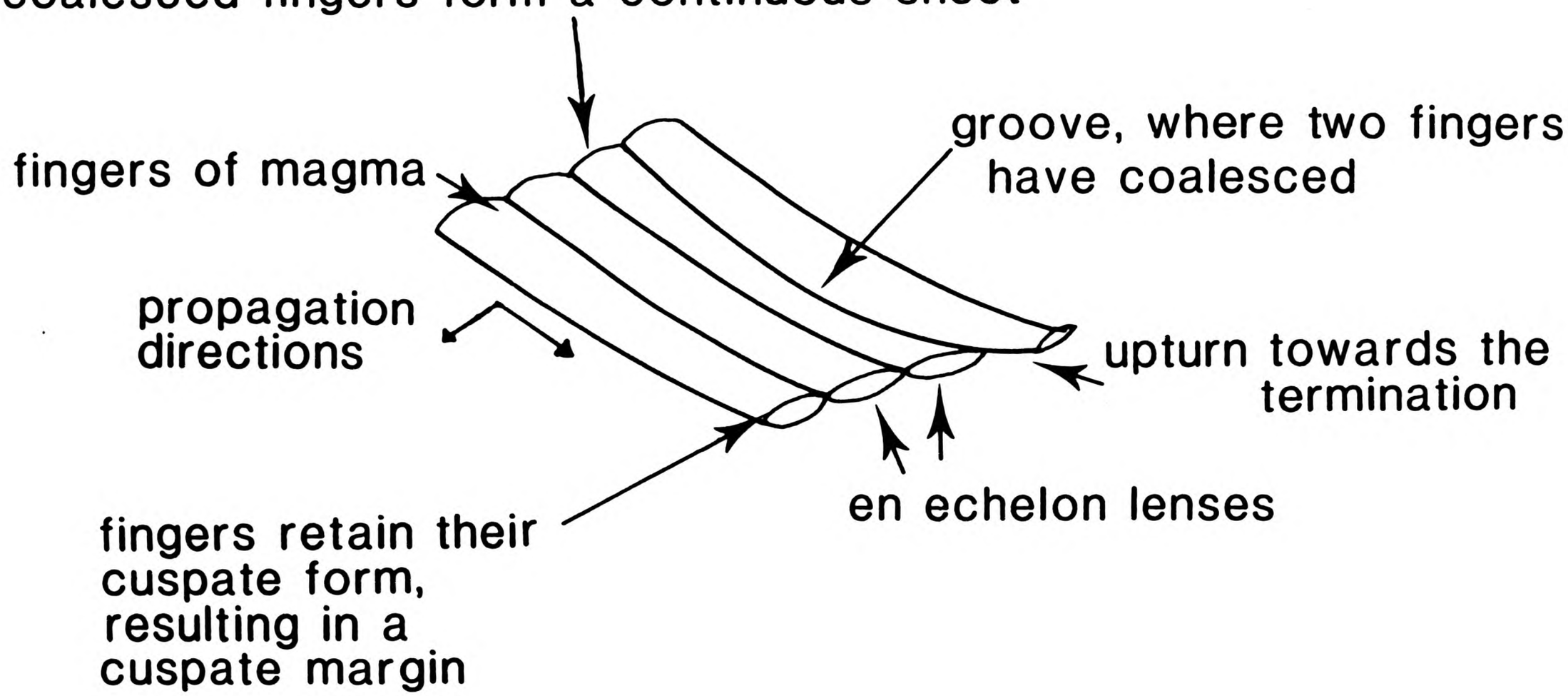

Fig.7.4.5 Terminology of sill terminations used by Pollard et.al. (1975)

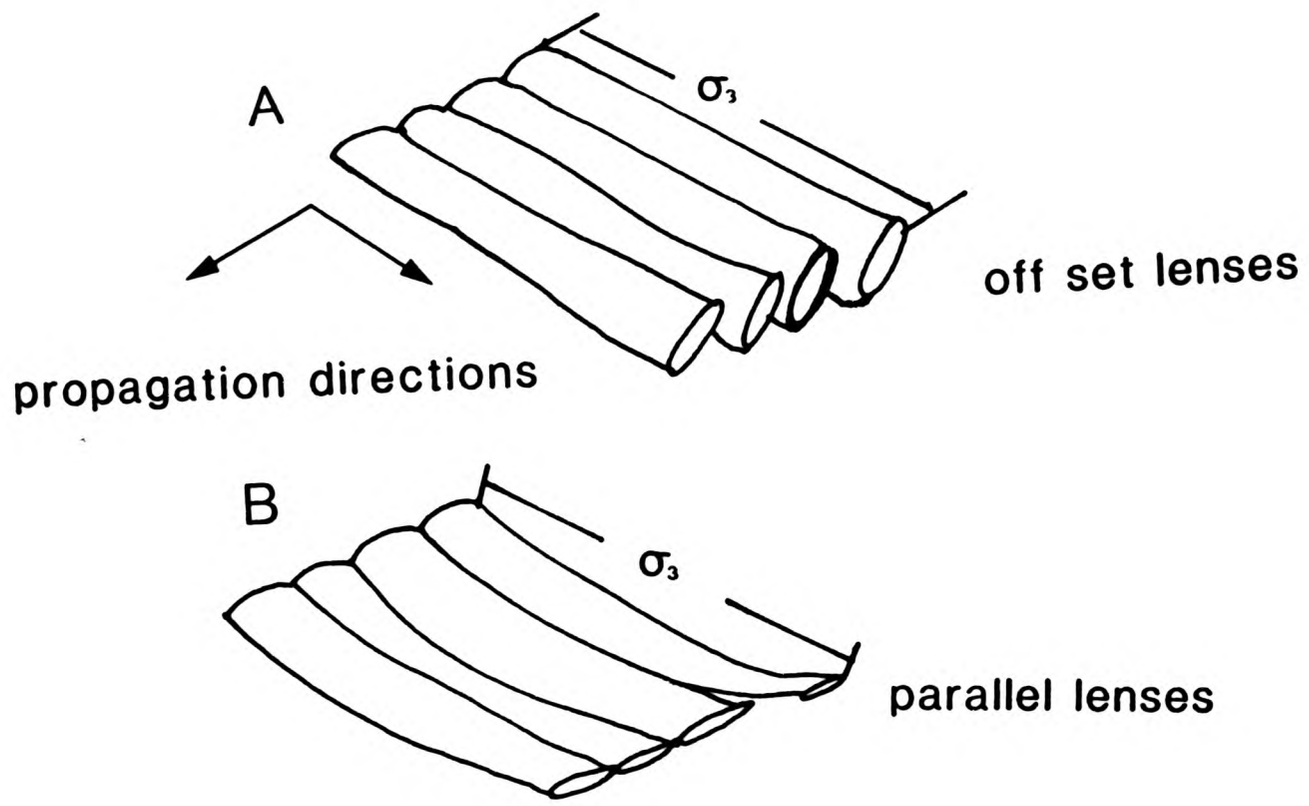

Fig.7.4.6 Two diagrams illustrate the distribution of stresses for two propagating fronts of sills. A change in the orientation of the least principal stress (σ_3) can result in
A an offset en echelon set
or B lenses which are not offset
(after Pollard et al., 1975)

ly, that each sheet constitutes a series of parallel tubes that have coalesced laterally and remain as seperate lenses at the leading edge of the sheet body.

Pollard (1973) proposed three mechanisms of sheet propagation which are characterised by the arrangement of fractures around the termination of a sheet body (Fig.7.4.7). The first mechanism is propagation by extension splitting along a fracture which is either caused by the magma or has been exploited by the magma. The second mechanism has surfaces of potential shear failure orientated at 30° to the σ_3 stress trajectories at the sheet termination, the magma advancing by intruding along the fractures and incorporating the blocks by stoping. The third mechanism consists of potential ductile faults oriented at 45° to the σ_1 trajectories of the termination of the sheet, propagation occurring when the host rock ruptures after ductile necking, following the blunting of the elliptical form of the original termination.

7.5 CONCLUSIONS

The geometry of the cone sheets of Ardnamurchan are controlled in part by previous structures, and in part by the intrusion mechanism. Exploitation of joint structures result in rectangular terminations (Fig.7.2.1.B). Shear stresses acting along the cone sheet fracture create a space to accommodate the wedge of magma, the fracture continuing ahead of the magma. If pressure of the magma decreases and therefore advancement of the fracture is halted, the rounded toe of the magma may be preserved (Plate 7.3). Of the terminations that have fractures

emanating from their tips only one of Pollards (1973) three mechanisms (mechanism 1) of sheet propagation can be recognised in Ardnamurchan. The cone sheets that show single fractures emanating from their tips and those which are emplaced along bedding and foliation planes (Plate 7.18) belong to Pollards mechanism 1. However, mechanisms 2 and 3 of Pollard are not represented by the Ardnamurchan sheets because the terminations which have multiple fractures at their tips are not conjugate and are often irregular in form, thus differing from the terminations of Pollards model. The most prominent mechanism for propagation as indicated by the form of the terminations of the Ardnamurchan sheets is extension splitting by brittle fracturing.

There is agreement in the literature that en echelon sets mark the termination of intrusions. However, there is disagreement as to whether en echelon sets represent the termination of an intrusion, that is a continuous sheet "breaks up" to form a series of separate lenses or that en echelon sets represent a series of tubes which have coalesced laterally to form a continuous sheet. A second item under discussion concerns the mechanism and direction of propagation of intrusions, whether in two- or three-dimensions.

Evidence to support the theory of different stresses at different levels is well demonstrated in Ardnamurchan. Figure 7.3.1 shows the cone sheets exposed at the Lighthouse section (Inner Centre Two) where there are at least nine separate examples of cone sheets which can be seen to pass from an apparently continuous sheet into a series of en echelon lenses, which

diminish in size towards their termination. At Swordle Bay (Centre One) and An Acairseid (Inner Centre Two) there are a group of cone sheets which show en echelon terminations. Isolated cases of cone sheets terminating in en echelon sets are observed at Rubh' a' Mhile (506628) and also at separate localities along the Glas Eilean to Mingary Pier section. A further piece of evidence to support the theory of different stresses at different levels within the crust is that some of the en echelon lenses show no connections with each other at the present level of erosion, each lens being a small, individual sheet (Fig.7.3.2 and Plate 7.9).

The theory of laterally coalescing tubes of magma to form a continuous sheet (Pollard et al. 1975) suggests that when propagation is arrested the fingers (or tubes) of magma form en echelon lenses that show some interconnection perpendicular to the strike of the sheet. Three-dimensional connections of adjacent en echelon lenses resulting in grooves are seen in the Ardnamurchan cone sheet complex at the Lighthouse section (Inner Centre Two) and Swordle Bay (Centre One).

Field evidence from Ardnamurchan lends support to all three theories, that of coalescing magma tubes, that of dissipation of a sheet into en echelon lenses, or an arrested developing fracture. An alternative explanation may be formed by amalgamating the first two theories. The first explanation for the occurrence of en echelon cone sheets at particular levels within the crust may be that the maximum vertical extent of an intrusion is reached when pressure from the source decreases, assuming that cone sheets exposed at one location belong to the same set, this

indicates that pressure at source is similar in the case of each cone sheet set. The second explanation is shown in Plates 4.10 and 7.5 in which one of the cone sheets of the Lighthouse section has paired apophyses, which indicate the existance of shear stresses at the time of emplacement. The majority of en echelon sets indicate a dextral shear component, the evidence of this is gained from the geometry of the en echelon sets. On the scale of the whole peninsula, the en echelon sets and the piercing point results (Chapter 6) indicate an anticlockwise shear movement, illustrating the existence of a torque force (Chapter 6). This may be caused by the development of spiral cracks (fractures) (Tolansky and Howes 1920) in the host rock.

Pollard et al. (1982) state that en echelon cracks grow by dilation and further, that directionally asymmetrical apophyses may be produced by internal pressures. Again this hypothesis can also be supported by the Ardnamurchan data in that Plate 4.11 shows matching of the wall rock and tensional displacement of an earlier porphyritic cone sheet, yet shows directionally asymmetrical apophyses.

The existance of grooves, steps and interconnections of adjacent lenses may alternatively be explained as an effect of superimposed stress systems, rather than the fingered periphery of Pollard et al. (1975). However, the latter hypothesis is thought to be more correct.

A prominent feature of the propagation theories described in the previous section is that few take into account the effects of propagation in three-dimensions. The work of Ander-

son (1951) considers propagation in two-dimensions only, in that he indicated that the en echelon set trends normal to the propagation directions (Fig.7.4.1). Whereas Currie and Fergusson (1970) propose that the propagation direction is along the en echelon sets, i.e. the sheet propagates from one echelon lens into the adjacent one. The hypothesis of Pollard et al. (1975) involves propagation in both directions, thus the sheet propagates both parallel and perpendicular to the en echelon set, that is, in three-dimensions.

In Ardnamurchan, evidence to support flow and propagation of cone sheets along the strike, as in the hypothesis of Currie and Fergusson (1970), is seen in the diminishing size of the sheetlets forming an en echelon set (Fig.7.3.1) towards their ultimate termination, thus indicating a decrease in pressure towards the extremities of the fractures now filled with basic rock. Flow direction of magma within each cone sheet cannot be ascertained for any of the Ardnamurchan cone sheets, as the only flow structure recorded is banding (Chapter 4.2). The banding,represented by amygdales and phenocrysts, records either temporary cessation of flow or accretion and with no flow alignment being in evidence only provides negative evidence for all proposed hypotheses. With no flow evidence to indicate the direction of propagation, the stepped profile of a transgressive sheet (Plate 7.20) may be equally well explained by either Currie and Fergusson's (1970) hypothesis or that of Pollard et al. (1975). However, evidence in support of the existence of lateral pressures in both directions is seen where both terminations of a sheetlet show ramifying veins (Fig.7.3.1), thus indicating that propagation continued in both lateral directions. Currie

and Fergusson's (1970) theory does not allow for separate en echelon lenses. In consequence of the connections seen between the following three phenomena, en echelon lenses (Plate 7.14), grooves and ramifying veins (Plate 7.4), the three-dimensional propagation mechanism of Pollard et al. (1975) seems to be the most probable. Also, the hypothesis of Pollard et al. allows for a variation in the position of σ_3 relative to the sheet body and therefore provides an explanation for both sinistral and dextral en echelon sets.

7.6 SUMMARY

Propagation of cone sheets involves several different processe. It has been demonstrated above that a cone sheet passes laterally from a continuous sheet into a series of en echelon lenses of diminishing size (length and thickness). The lenses show three-dimensional connections between adjacent sheetlets. The form of individual sheet margins sometimes show directionally asymmetrical apophyses, yet show tensional displacement of country rock structures.

The most simple explanation for the propagation of cone sheets is that elliptical flaws in the host rock develop by hydraulic fracture, which are then invaded by magma, which enlarges the fractures both along their length and laterally, thus, connecting adjacent sheetlets which ultimately form a single sheet. A shearing mechanism is obviously a prominent component in the propagation mechanism of cone sheets as has been demonstrates in an earlier chapter (Chapter 6).

CHAPTER 8

THE INFLUENCE OF COUNTRY ROCK STRUCTURES ON THE FORM OF CONE SHEETS

8.1 INTRODUCTION

In order to investigate the influence of host rocks and their associated structures on the form of cone sheets it is necessary to consider the following :-

rock type,
rock strength,
regional structure e.g.doming,
local structures (bedding, jointing, foliation),
distance from centre of igneous activity,
water content of host rock,
duration of intrusion,
explosivity index,
intrusion dynamics.

The influence that host rocks may have on the form of cone sheets may be considered as inhomogeneities on three scales, the largest scale, that of the whole peninsula, a medium scale, that of lithological groups and the smallest scale, within the lithological groups. Factors which are related to the act of intrusion are discussed later.

INHOMOGENEITIES

8.2 THE ARDNAMURCHAN PENINSULA

The peninsula is composed of a variety of rock types (Chapter 2) and to assess the homogeneity of the host rock distribution a Chi^2 test has been used. Figure 8.2.1 is a simplified geological map of the peninsula with all the cone sheets removed. For simplification, the following rock groups have been recognised:- Moine (metamorphic), Jurassic/Triassic (sedimentary); lavas and vent agglomerates (refered to hereafter as volcanics); basic intrusions; and acid intrusions. The classification is based on the assumption that the rock types

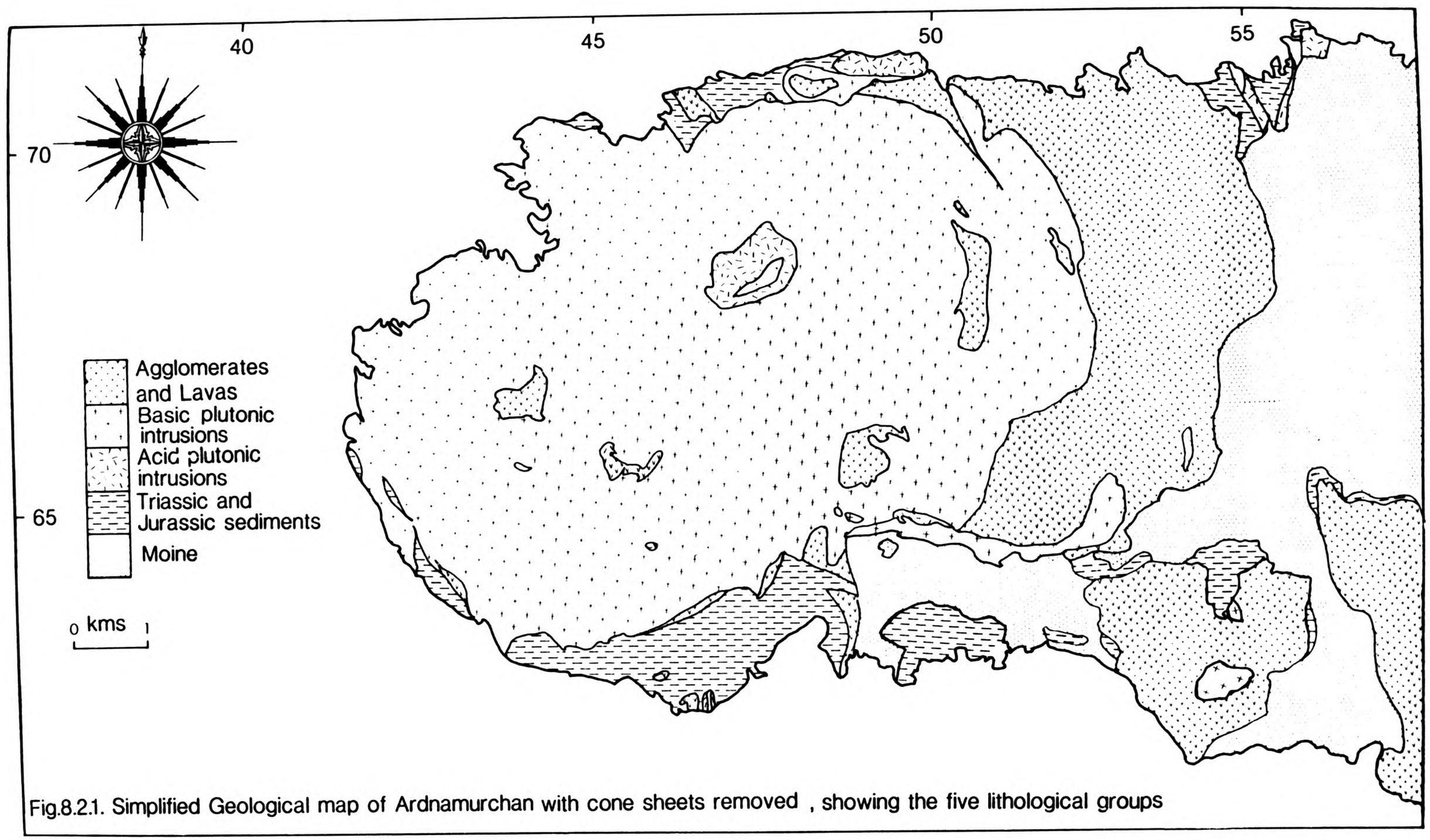

Fig.8.2.1. Simplified Geological map of Ardnamurchan with cone sheets removed , showing the five lithological groups

belonging to each group react characteristically in relation to cone sheet fracture formation. To establish whether the distribution of the lithological groups controls the distribution of the cone sheets a 2cm grid has been superimposed on a simplified 1:50000 geological map (Fig.8.2.1). Where an easting and northing grid line intersect, the rock type has been recorded, resulting in a point pattern of regular distribution (Fig.8.2.2). A seperate Chi^2 analysis has been made of each lithological group (Table 8.1), the results of which have enabled a comparison of the distribution types of each lithological group. A Chi^2 analysis enables a comparison of the observed frequency, that is the actual number of occurrences, of each lithological group to an expected frequency:-

$$\frac{\text{the total number of points of a particular rock type}}{\text{total number of points}}$$

The lower the Chi^2 value the more regular or uniform the distribution. The results of the analysis (Table 8.1) indicate that each lithology has a clustered distribution, the clustering of the Moine rocks is the most well developed. This result confirms the intuitive interpretation of Fig.8.2.1, that is, the distribution of the host rocks of the Ardnamurchan peninsula is heterogeneous.

8.3 LITHOLOGICAL GROUPS

If it is assumed that the form of a cone sheet is not influenced by the country rock which it intrudes then, disregarding the heterogeneity of the peninsula, the cone sheet

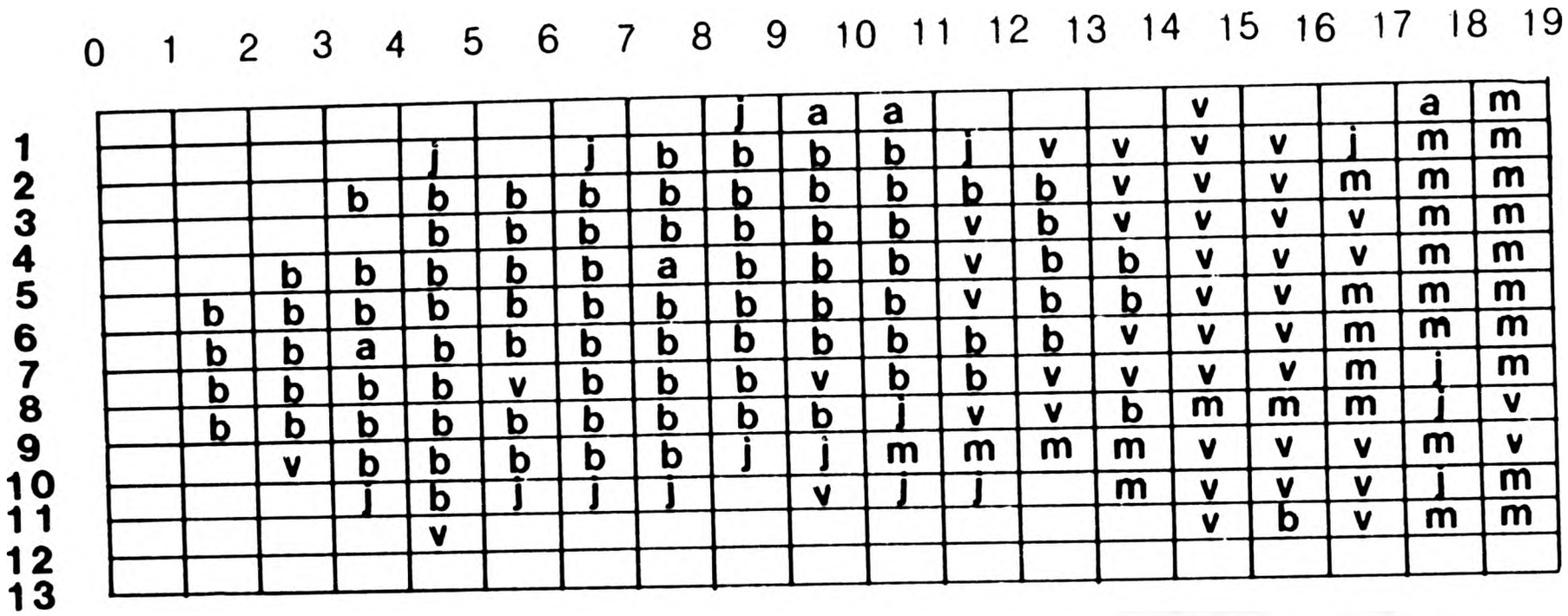

Lithological groups

- m Moine
- j Jurassic/Triassic
- v lavas and agglomerates
- b basic
- a acid

Fig. 8.2.2 Using the simplified geological map (Fig.8.2.1) a point pattern of lithological groups over the Ardnamurchan peninsula has been produced, to enable a Chi test to be applied to the distribution of lithological groups.

Table 8.1 Chi^2 values for each lithological group (Fig.8.2.2)

LITHOLOGY	Chi^2
Moine	138
Jurassic/Triassic	32
Lavas/agglomerates	83
basic intrusions	81
acid intrusions	19

should be at a constant distance from the centre and the annularity of the cone sheet should remain the same. Two indices have been used to assess the relationship between lithological groups and number of cone sheets contained within them:-

a) L.F.I. = Lithological Fracture Index
= for each lithological group the number of filled cone sheet fractures (n) per unit length

b) L.M.I. = Lithology Cone Sheet Magma Index

$$= \frac{\text{number of cone sheet fractures per unit length of the same lithology (n)}}{\text{amount of material emplaced within the cone sheet fractures per unit length (T)}}$$

$$= \frac{n}{T}$$

The unit lengths used in the calculations are as defined in Chapter 3, each unit length being 100m. Unit lengths which contain more than one rock type have been assigned to the dominant lithological group. The amount of material emplaced within the cone sheet fractures is calculated from the thicknesses of the cone sheets i.e. a two-dimensional measurement.

8.3.1 L.F.I.

Figure 8.3.1 shows the distribution of filled cone sheet fractures per unit length for each lithological group. The number of fractures has been classified into classes with intervals of 5 sheets. The sections in the Moine host rock vary from less than 5 sheets to a maximum of 15 sheets per unit length. However, the less than 5 class appears to form a secondary distribution. Similarly, the Jurassic unit lengths have a variation in the number of sheets they contain. There being little variation in the number of unit lengths which contain 5 to 25 sheets, but at the other end of the distribution, 36 to 40 class, a few unit lengths have a large number of sheets. Where the host rocks are volcanic, a large number of unit lengths (21)

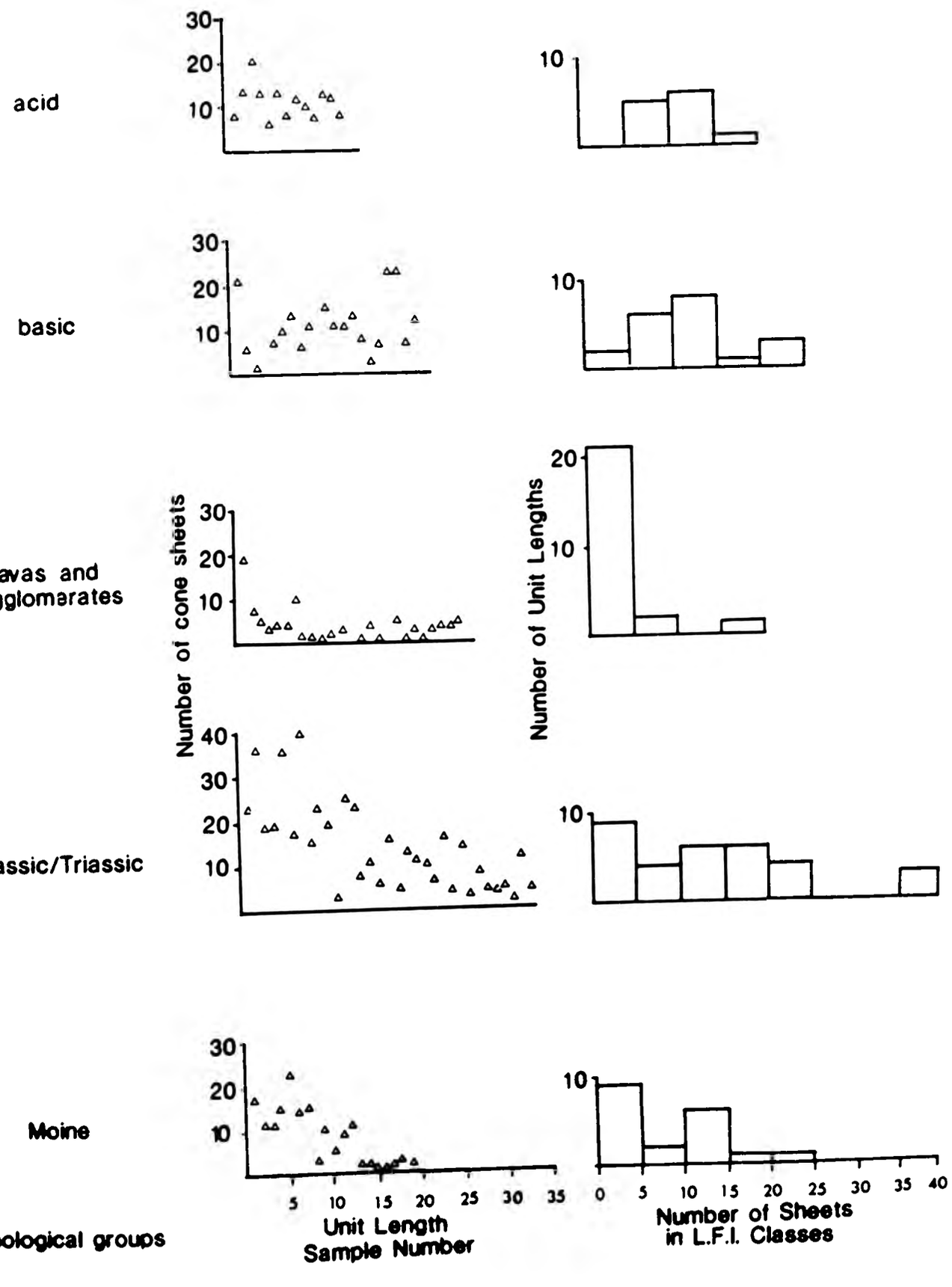

Fig.8.3.1 Number of cone sheets per unit length, per lithological group
Lithological Fracture Index (L.F.I.).

have less than 5 sheets, with the remaining three unit lengths having between 5 and 20 sheets. In the basic host rocks the number of filled cone sheet fractures per unit length varies from 0 to 25, being almost, normally distributed about the 15 sheet class. Acid intrusive host rocks differ from all other host rocks in that no unit length has less than 5 sheets, with the distribution ranging from 6 to 20 sheets.

Figure 8.3.1 shows that each lithological group has a different L.F.I., ranging from the volcanics with a large number of unit lengths having few fractures to the acid intrusive host rocks which have a larger number of sheets per unit length.

8.3.2 L.M.I.

There is a positive relationship between the number of cone sheets (n) per unit length and the amount of material (T) emplaced within each lithological group, that is, as the number of sheets increases so the cumulative amount of material along the traverses increases. For where the Moine forms the host rock, Fig.8.3.2 shows a plot of the number of sheets per unit length against the amount of material emplaced within the unit lengths.

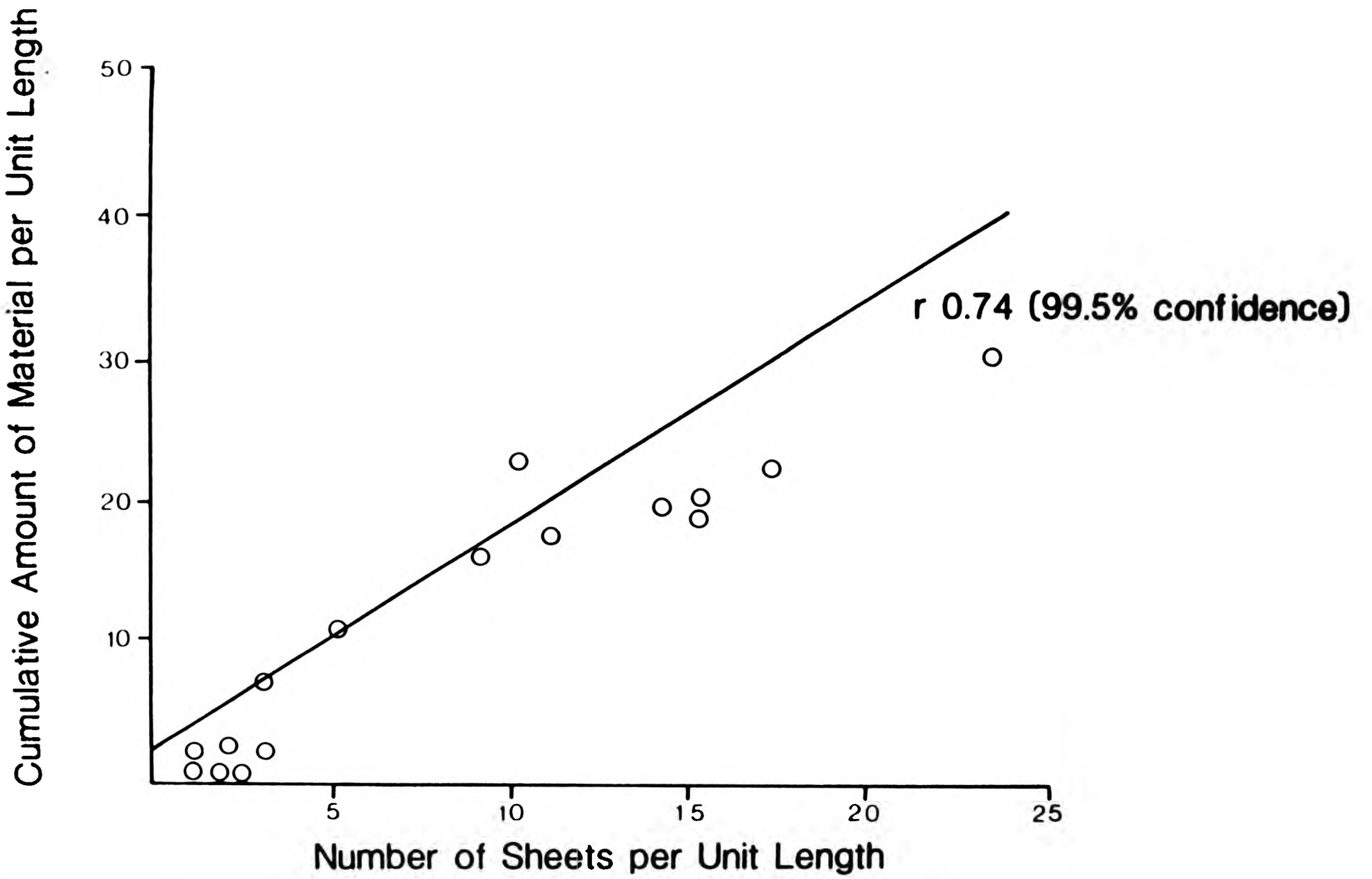

Fig.8.3.2 A plot of the cone sheets per unit length against the total amount of rock emplaced within each unit length, for all cone sheets occurring in Moine host rocks

For the Moine rocks the regression r = 0.74 has a 99.5% confidence limit (Table 8.2), although one example lies significantly off the regression. Data taken from from the Jurassic/Triassic sections (Fig.8.3.3) shows a well defined trend, with a regression r = 0.797 for the 99.95% confidence limit. Characteristically, there are few sheets in the unit lengths which occur in the volcanic host rocks, consequently the plot of the number of sheets against cumulative total thickness cluster around the origin (Fig.8.3.4), however, a 99.5% confidence limit can be applied to the regression (r = 0.57). Figure 8.3.5 shows the regression (r = 0.59) for both the basic intrusive host rock unit lengths at 99.5% confidence limit and for the acid intrusive host rocks (r = 0.61) at 97.5% confidence; the lower confidence limit emphasizes the misfit of one of the samples, unit length a (Fig.8.3.6) differs greatly from the remaining acid unit lengths and is the cause of the negative intercept of the regression line, if this sample is ignored a second regression line may be calculated (Fig.8.3.6). In Fig.8.3.6a the average total thickness of material emplaced in 10 cone sheet fractures per unit length for each lithological group is shown. The Moine host rocks contain the thickest cone sheets, whereas the volcanics and basic intrusive host rocks have much thinner cone sheets than the other lithological groups. Table 8.2 gives the regressions for the distributions of each lithological group emphasizing the differences between the groups. Based on these characteristics, n and T, it can be shown that the variation in number and cumulative thickness of the cone sheets are dependant on the host rock type. There is a sequential relationship from basic intrusive host rocks which contain only a few, thin sheets, through volcanic, Jurassic/Triassic, acid intrusive to

Table 8.2 THE STATISTICS OF REGRESSION FOR THE L.F.I. FOR EACH LITHOLOGICAL GROUP

Lithological group	n	r	L.F.I	av T
Moine	19	0.7388	1.04 ± 1.18	1.65
Jurassic/Triassic	34	0.7971	1.04 ± 0.54	1.27
volcanics	27	0.5715	1.74 ± 1.34	1.05
basic intrusions	21	0.5900	1.41 ± 0.93	2.19
acid intrusions	13	0.6100	0.84 ± 0.29	1.28

where n = the number of unit lengths occurring in each lithological group

r = the regression coefficient of the L.F.I. distribution for each lithological group

av T = the average thickness in metres of filled cone sheet for each lithological group

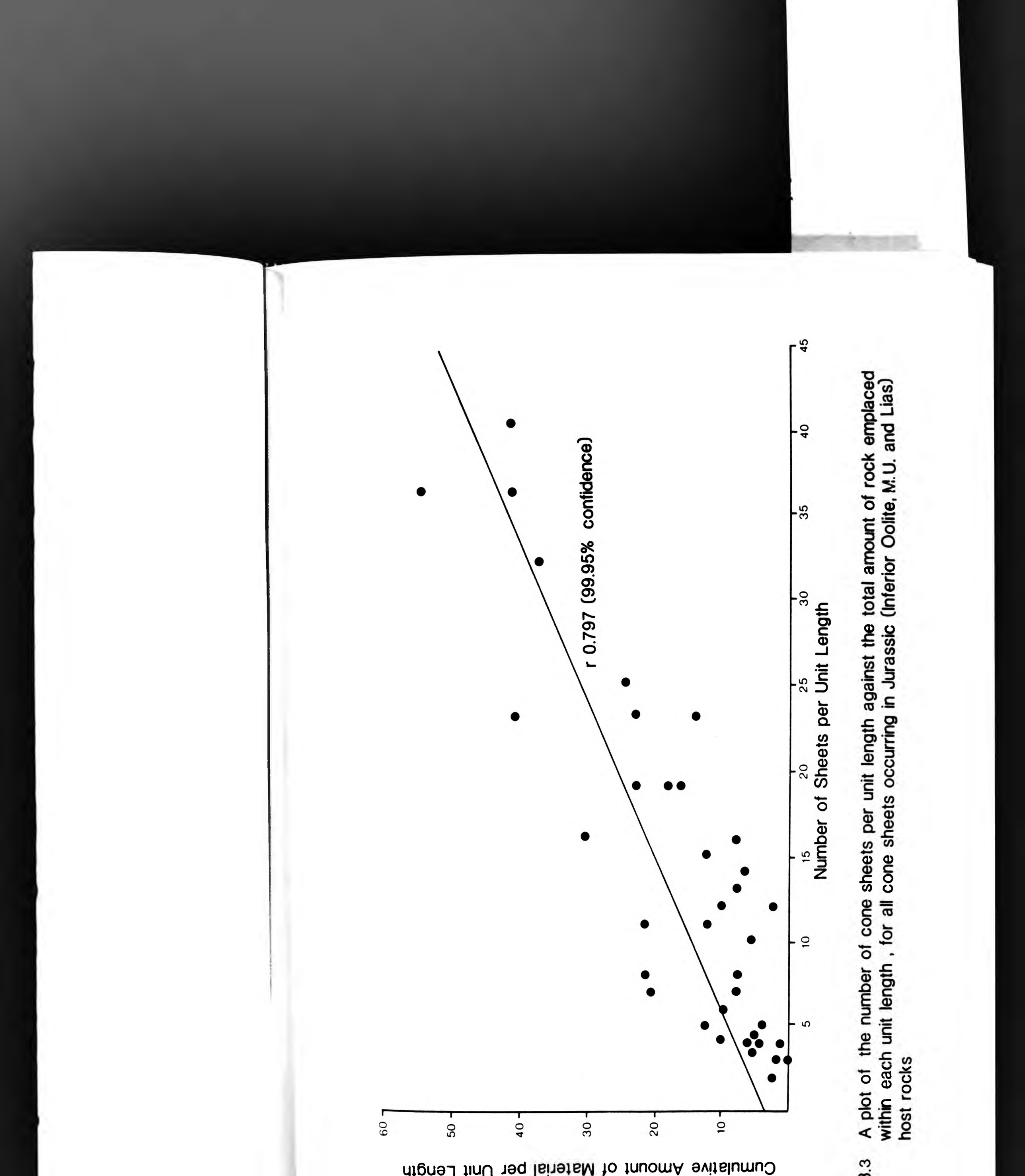

Fig.8.3.3 A plot of the number of cone sheets per unit length against the total amount of rock emplaced within each unit length , for all cone sheets occurring in Jurassic (Inferior Oolite, M.U. and Lias) host rocks

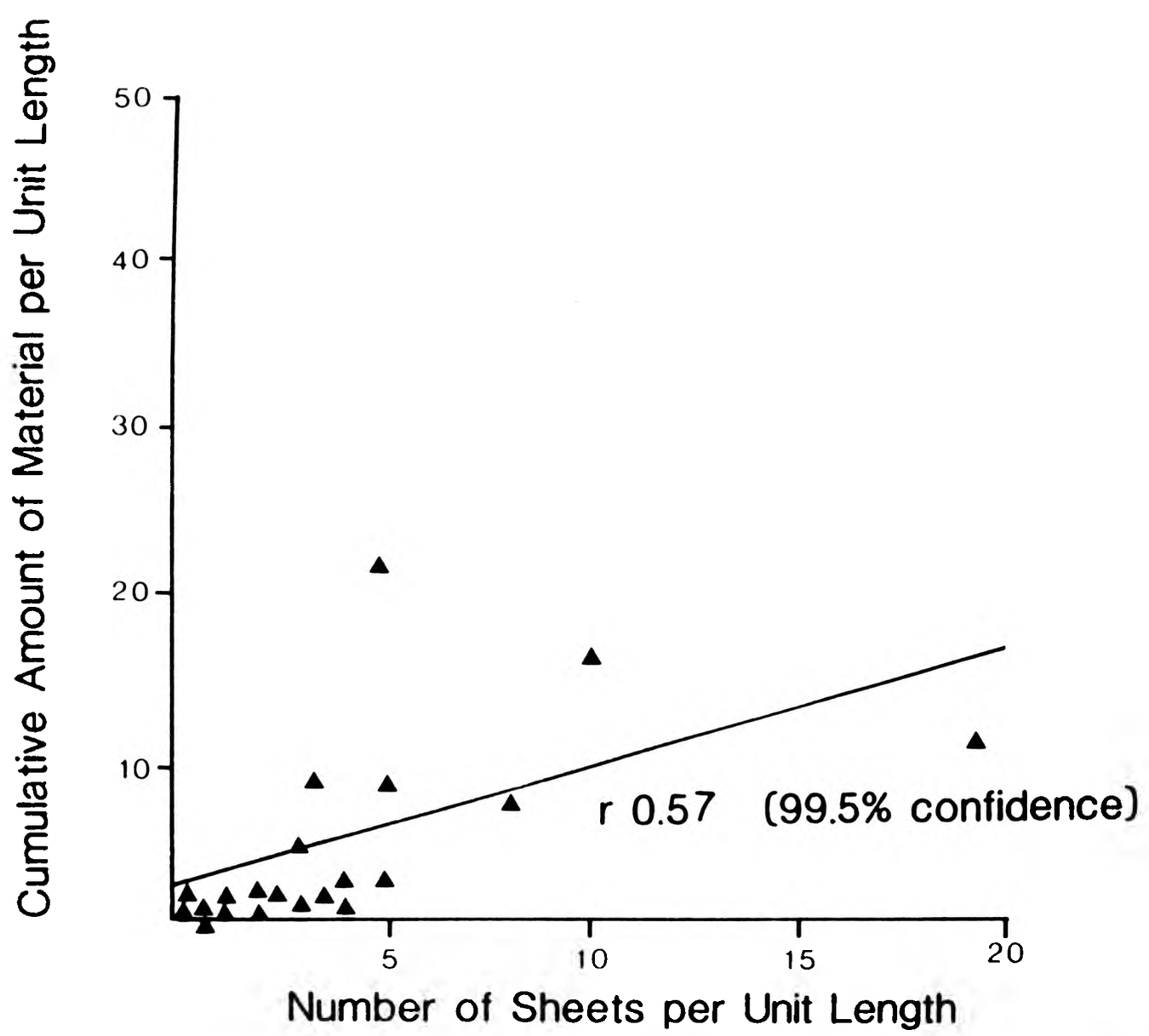

Fig.8.3.4 A plot of the number of cone sheets per unit length against total amount of rock emplaced along each unit length, for all cone sheets occurring in lavas and agglomerate host rocks

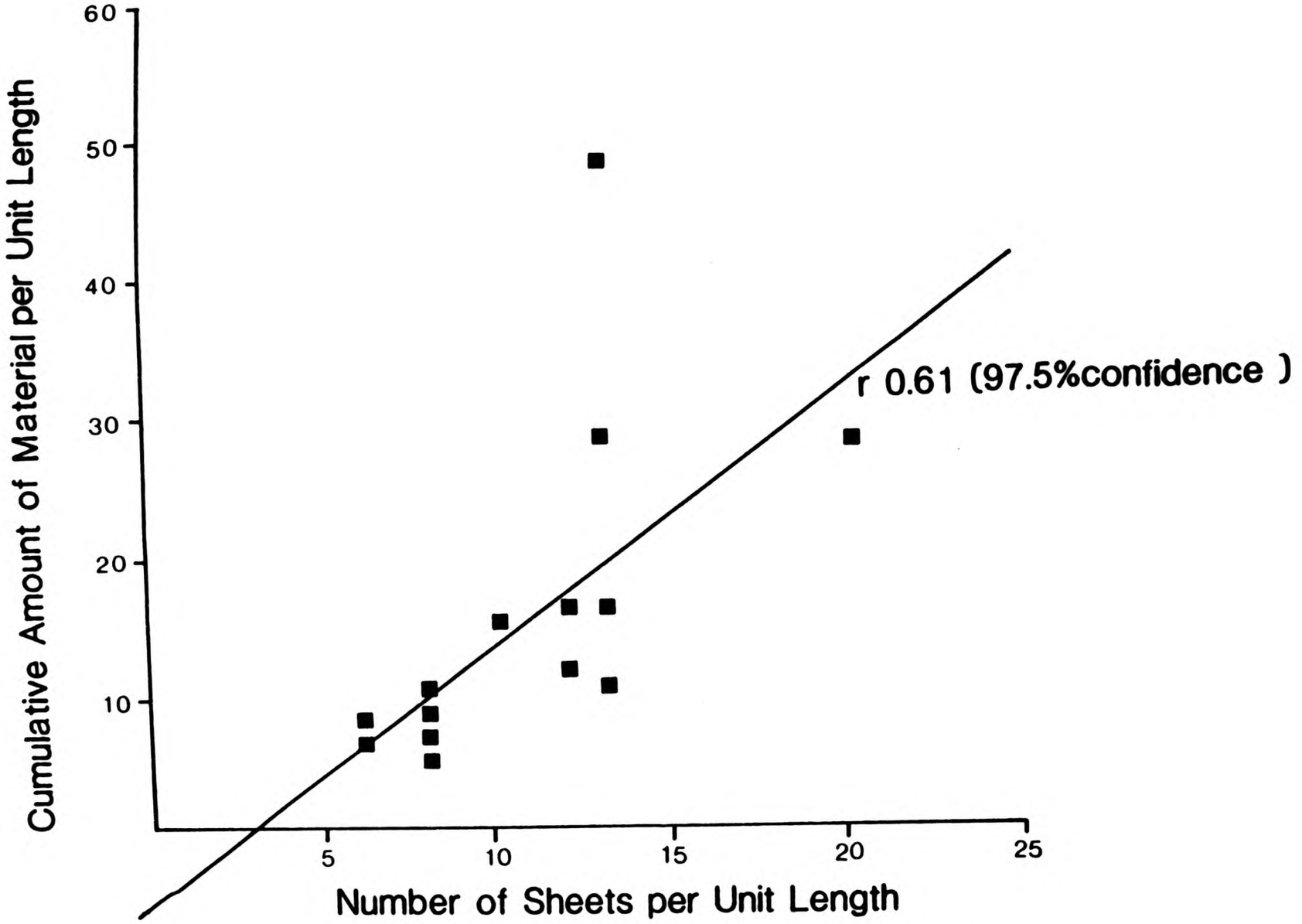

Fig.8.3.5 A plot of the number of cone sheets per unit length against total amount of rock emplaced along each unit length, for all cone sheets occurring in acid host rocks

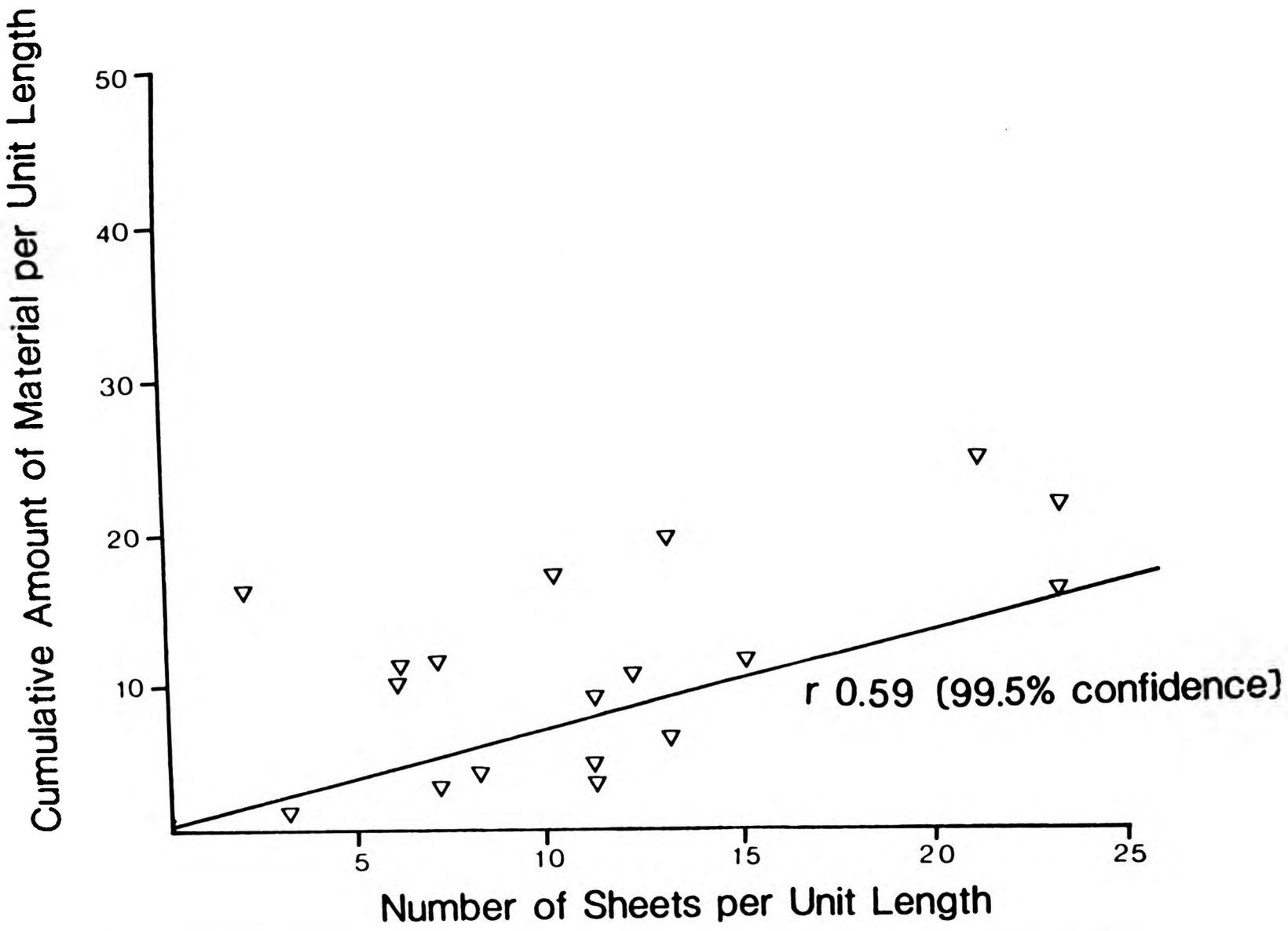

Fig. 8.3.6 A plot of cone sheets per unit length against total amount of rock emplaced along each unit length, for all cone sheets occurring in basic host rocks

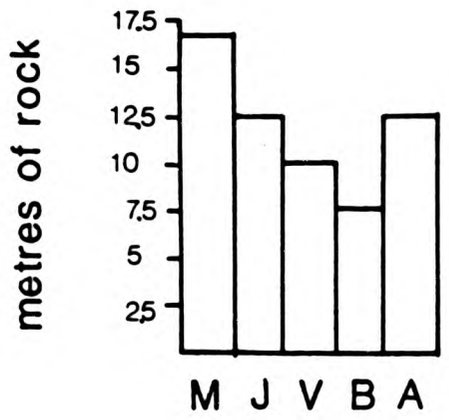

Fig.8.3.6a Average total cumulative thickness of 10 cone sheets emplaced in the different lithological groups

M - Moine
J - Jurassic/Triassic
V - lavas and agglomerates
B - basic
A - acid

Moine host rocks which contain the largest number of thicker sheets. Figure 8.3.6 highlights the regression line for the acid host rocks, which differs from the remaining host rocks in that it does not pass through the origin.

From both the original acid intrusive host rock regression (Fig.8.3.6) and the distribution of the number of sheets per unit length (Fig.8.3.1) it seems that a small number (less than 5) of thin sheets are difficult to accommodate. Conversely, when a large number (greater than 5) of sheets are emplaced they tend to be thick. This can perhaps be best illustrated by the analogy of inflating a balloon. That is the initial inflation takes a large amount of energy to overcome the resistance of the walls, further expansion of the balloon takes much less energy.

Table 8.3 shows the L.M.I. for each unit length in each lithological group. The index tends to 0 as n tends to 0 and to ∞ as T tends to 0. The L.M.I. enables a comparison of the number of fractures in each lithological group. Figures 8.3.7-9 show the L.M.I.'s for the Moine, Jurassic/Triassic and acid intrusive host rocks, all of which show that the spread of results are quite low, with low n and increasing T indicating thick sheets. However, the L.M.I. for the unit lengths occurring in volcanic and basic host rocks (Fig.8.3.10-11) are strongly contrasted with the L.M.I for the other host rocks and although the L.M.I. values show a wide range they tend to be high, indicative of thin sheets.

Figure 8.3.12 shows the mean and standard deviation (σ_n) of the L.M.I for each lithological group and therefore measures the

Table 8.3 Lithological Magma Fracture Index (L.M.I.), n and T for each unit length in each lithological group

MOINE				JURASSIC/TRIASSIC			
Ref	n	T	I	Ref	n	T	I
40	17	22.73	0.75	1	23	14.0	1.64
41	11	17.73	0.62	2	36	55.63	0.64
42	11	52.42	0.21	4	19	16.43	1.16
43	15	20.14	0.74	5	19	17.86	1.06
44	23	30.38	0.76	7	36	41.55	0.87
45	14	19.47	0.72	8	17	9.58	1.77
46	15	19.37	0.77	9	40	42.40	0.94
47	3	2.0	1.50	10	15	12.36	1.21
50	10	22.95	0.44	11	23	41.25	0.55
51	5	11.33	0.44	12	19	22.30	0.83
52	9	15.97	0.56	14	25	24.30	1.02
53	11	29.29	0.38	15	23	23.02	0.99
89	2	3.20	0.63	16	8	7.50	1.06
98	2	2.50	0.80	17	11	12.56	0.88
100	1	2.06	0.49	18	6	9.75	0.61
101	1	1.00	1.00	19	16	30.24	0.53
102	2	0.58	3.44	32	5	4.25	1.18
103	3	6.90	0.43	33	13	7.95	1.64
106	2	0.40	5.00	34	11	21.10	0.52
				35	10	5.73	1.75
LAVAS/AGGLOMERATES (VOLCANICS)				36	7	7.74	0.90
Ref	n	T	I	37	16	8.15	1.96
3	19	11.11	1.71	38	4	6.40	0.62
27	8	6.95	1.15	39	14	6.76	2.07
28	5	2.65	1.89	47	3	3.0	1.50
29	3	4.90	0.61	48	8	21.14	0.38
30	4	0.87	4.59	49	4	1.64	2.44
31	4	2.48	1.61	57	4	10.26	0.39
66	10	15.90	0.62	58	5	12.31	0.41
67	2	1.90	1.05	59	2	2.60	0.77
68	2	1.20	3.92	61	12	31.58	0.38
69	1	0.50	2.00	62	4	6.18	0.65
70	2	2.00	1.00				
72	3	8.30	0.36	BASIC INTRUSIONS			
74	1	0.30	3.30	6	21	24.25	0.87
75	4	1.32	3.03	93	6	9.18	0.65
76	1	0.50	2.00	94	2	16.10	0.13
78	5	21.55	0.23	107	7	10.80	0.65
79	1	0.70	1.42	108	10	16.95	0.59
80	3	8.30	0.36	109	13	5.88	2.20
81	1	0.20	5.00	110	6	9.45	0.36
82	3	1.05	2.86	112	11	3.62	3.03
83	4	2.20	0.58	113	15	11.05	1.36
84	4	2.60	1.54	114	11	8.35	1.32
85	5	8.60	0.58	115	11	3.42	3.22
86	1	1.10	0.91	116	13	19.00	0.68

Table 8.3 (contd)

Ref	n	T	I	Ref	n	T	I
				117	8	3.64	2.19
ACID INTRUSIONS				118	3	1.00	3.00
20	8	7.50	1.07	119	7	2.67	2.62
21	13	16.21	0.80	120	23	15.83	1.45
22	20	28.17	0.70	121	23	21.55	1.07
23	13	28.17	0.46	122	7	8.70	0.80
24	6	8.60	0.69	123	12	10.59	1.13
25	13	10.40	1.25				
26	8	7.79	1.02				
54	12	11.70	1.03				
55	10	14.80	0.68				
56	8	9.85	0.81				
63	13	48.35	0.27				
64	12	15.95	0.75				
65	8	5.92	1.35				

WHERE Ref Reference number
n number of sheets per unit length
T total thickness of all sheets within each unit length
I Lithological Magma Fracture Index (L.M.I.)

Fig.8.3.7 A figure showing the relationship between the number of cone sheets per unit length and the lithological magma fracture index (L.M.I.) for all cone sheets occurring in Moine host rock

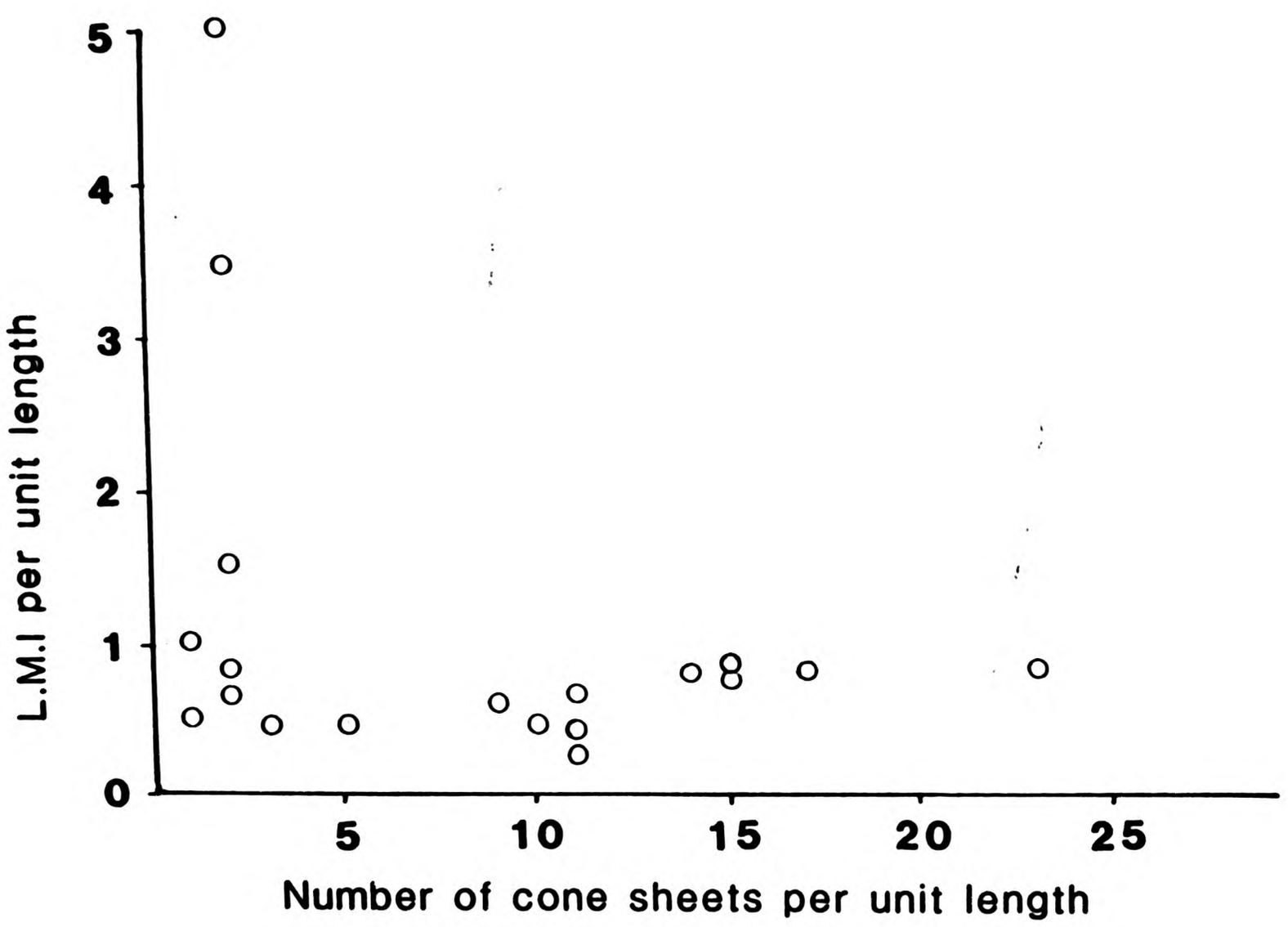

Fig.8.3.8 A figure showing the relationship between the number of cone sheets per unit length and the lithological magma fracture index (L.M.I.) for all cone sheets occurring in Jurassic/Triassic host rock

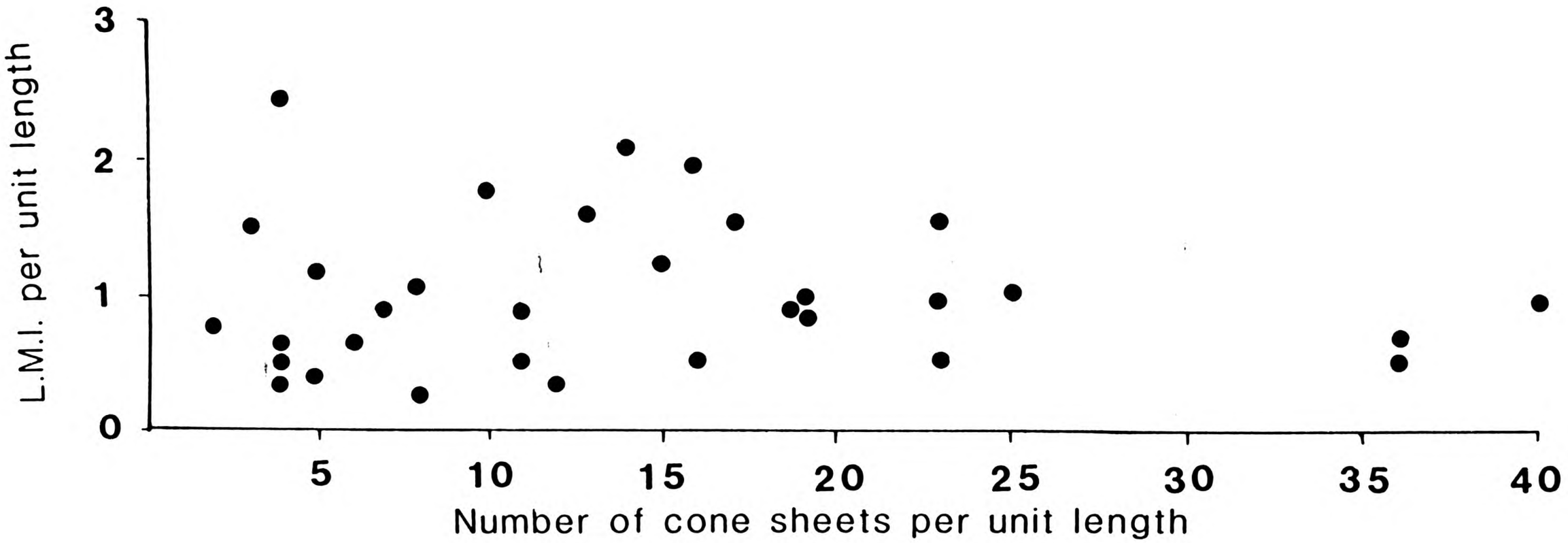

Fig.8.3.9 A figure showing the relationship between the number of cone sheets per unit length and the lithological magma fracture index (L.M.I.) for all cone sheets occurring in agglomerate and lava host rock

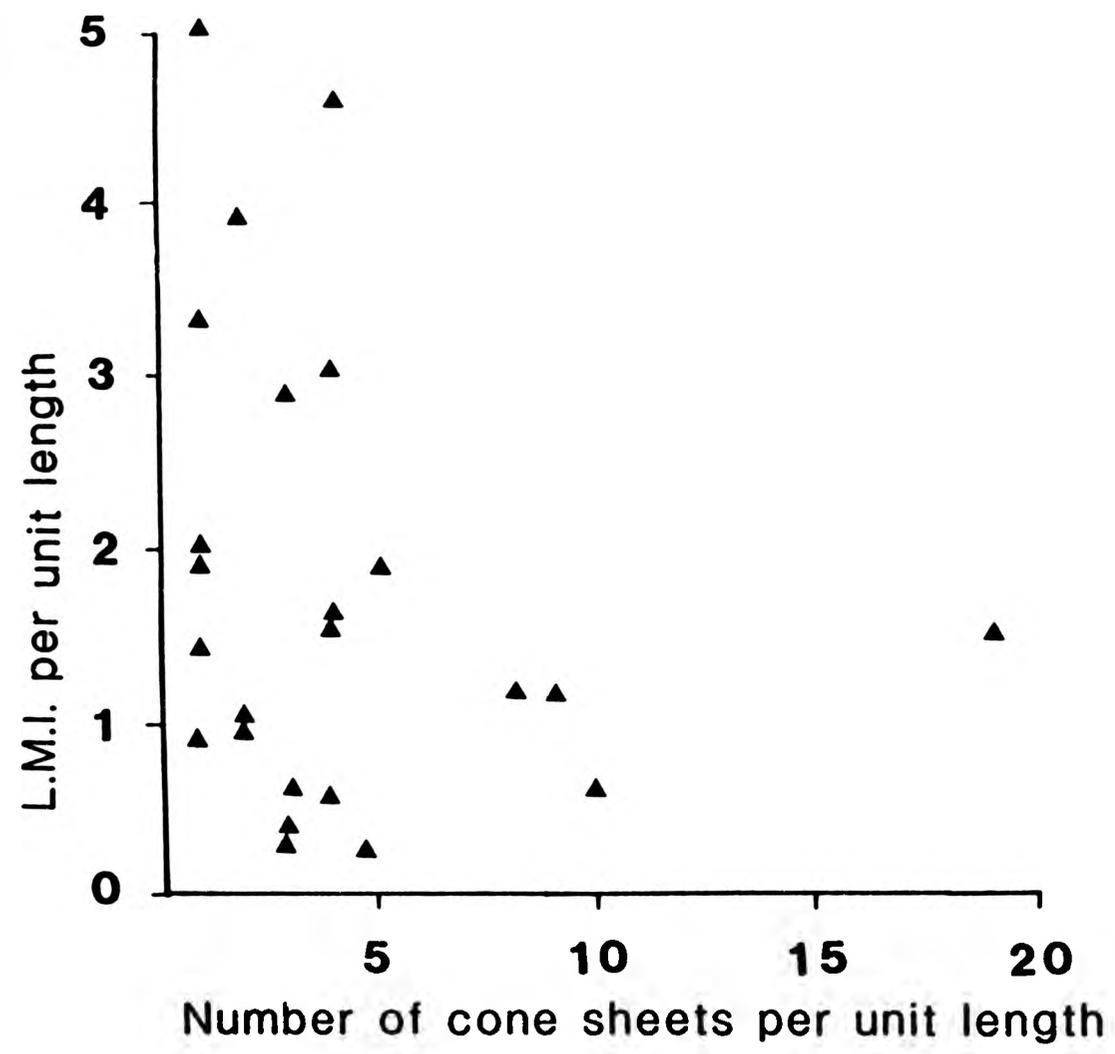

Fig.8.3.10 A figure showing the relationship between the number of cone sheets per unit length and the lithological magma fracture index (L.M.I.) for all cone sheets occurring in basic host rock

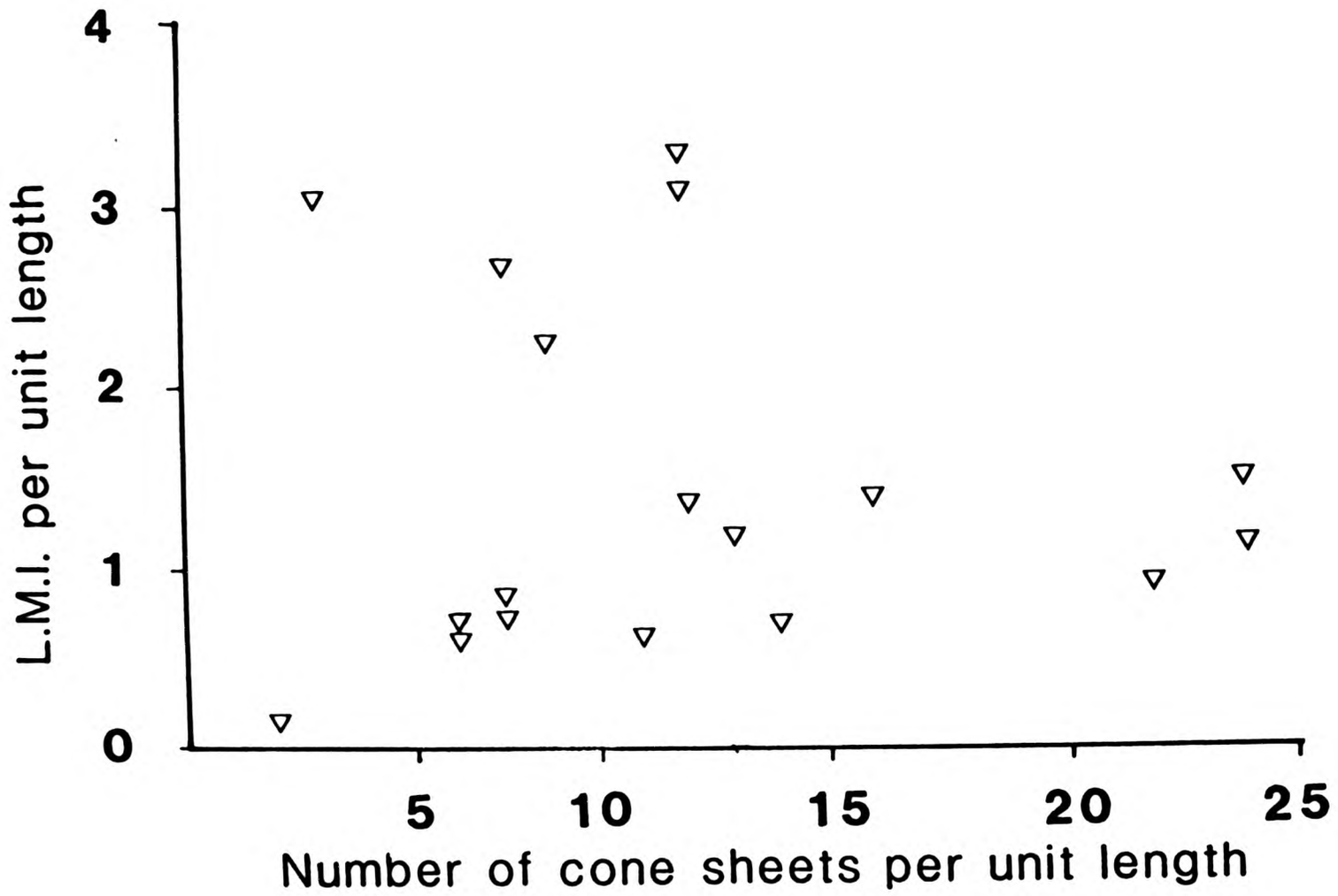

Fig.8.3.11 A figure showing the relationship between the number of cone sheets per unit length and the lithological magma fracture index (L.M.I.) for all cone sheets occurring in acid host rock

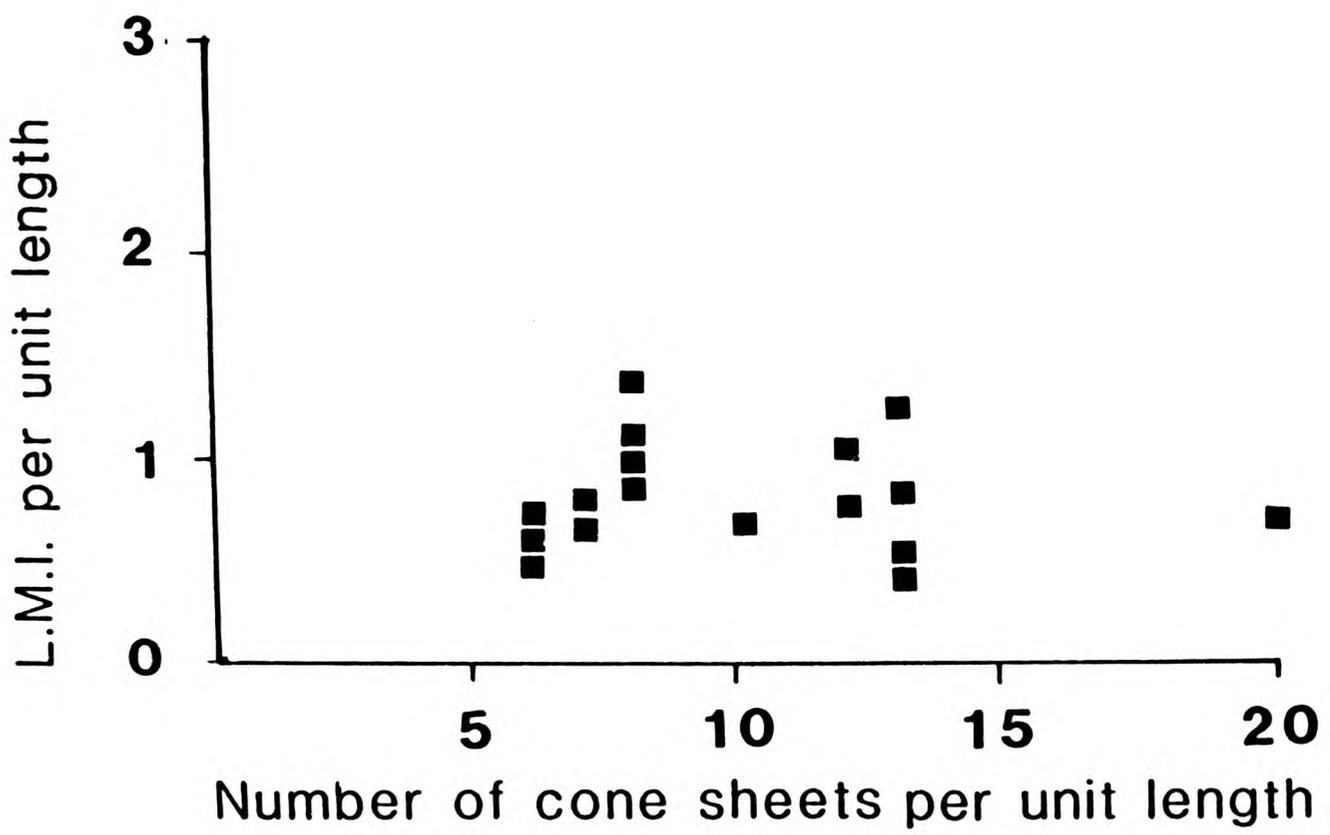

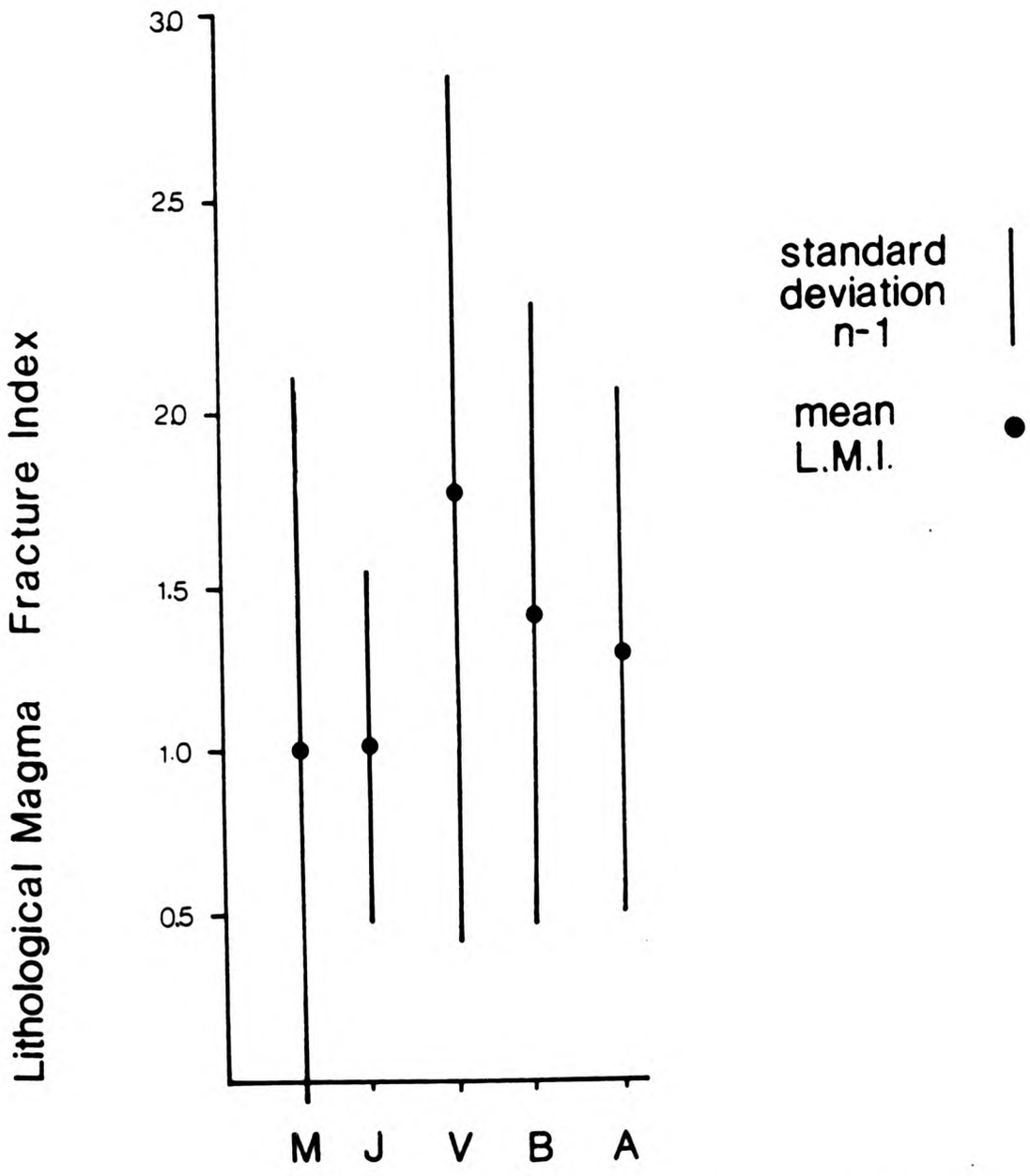

Fig.8.3.12 Mean and standard deviation of the L.M.I. for each lithological group

dispersion. It is significant that the mean L.M.I. of the Moine and Jurassic/Triassic rocks give similar low values. The acid, basic and volcanic host rock groups have high mean values and therefore differ from the sedimentary and metamorphic host rock groups.

Thus, on the basis of the L.M.I. the host rocks may be subdivided into a simple two fold division of sedimentary/metamorphic and igneous rocks, whilst the plot of n against T enables a distinction to be made between the lithologies, illustrating that the host rock lithology influences the mode of cone sheet emplacement.

8.4 DISTANCE BETWEEN CONE SHEET FRACTURES

As a measure of the frequency and distribution of fracture the distance between filled cone sheet fractures have been measured for each cone sheet set.

8.4.1 Centre One

In the west to east traverse across this cone sheet set the distance between cone sheet fractures tends to increase to the east with the maximum distance between cone sheet fractures occurring at the eastern extremity of the traverse (Rubha a' Choit)(Fig.8.4.1). East of Faskadale, the distances between fractures are low, with none exceeding 20m. This set shows the largest range of distance between fractures, that is from 0m to 360m. The eastern extremity of the traverse probably marks the

Fig.8.4.1 A diagram to show the distance between filled cone sheet fractures along a west to east traverse across the Centre One Cone Sheet Set

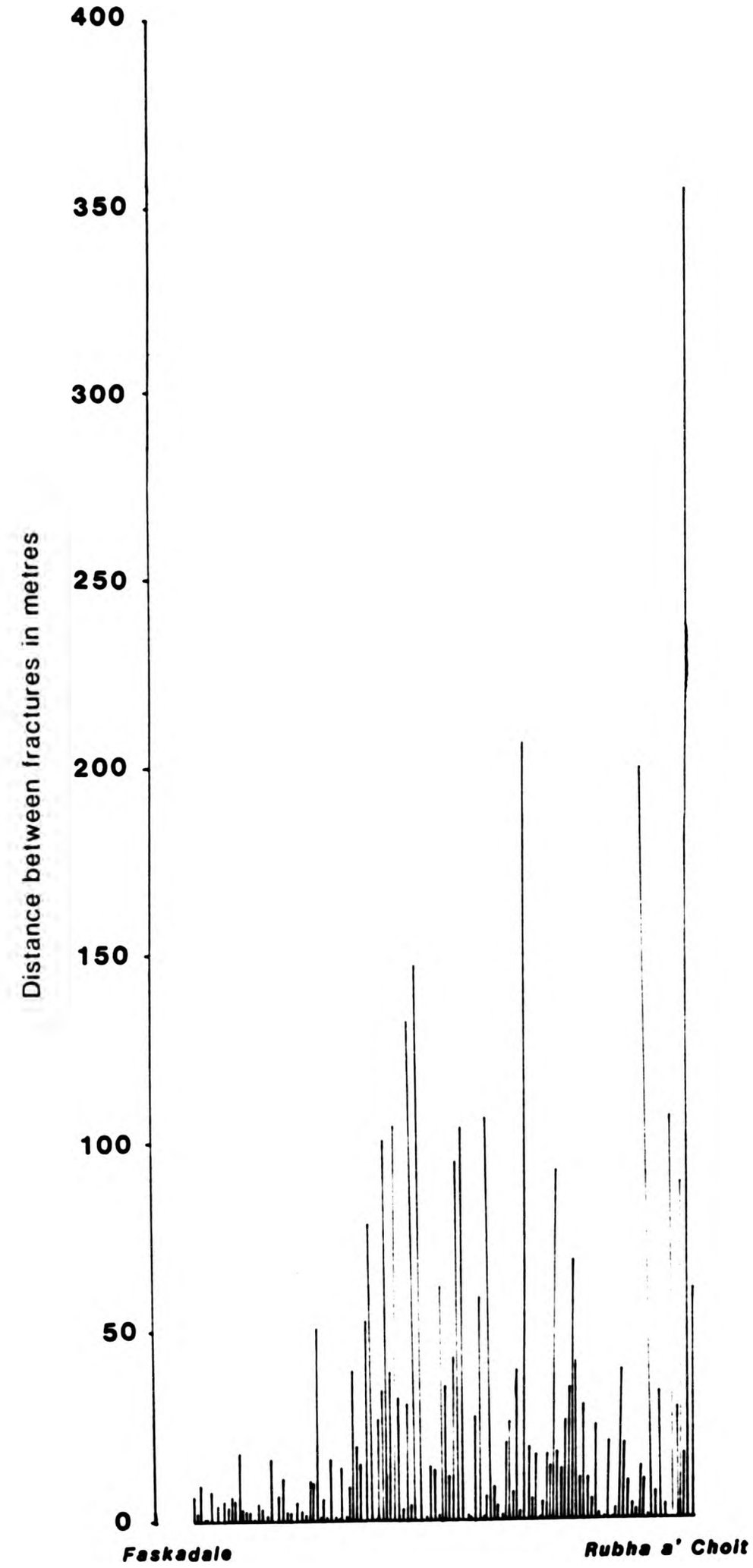

West to East traverse across the cone sheet set

natural end of a cone sheet set.

8.4.2 Outer Centre Two

North Coast. Cone sheet fractures along this section, most of which occur in Jurassic (Lias) sediments, are quite regularly spaced at approximately 5m intervals. The range is from 0.5m to 21m. The largest distances between cone sheet fractures occur at Glendrian and Rubha Carrach, which coincides with the outcrop of volcanic (agglomerates) host rock (Fig.8.4.2).

South Coast. In contrast to the north coast, the distances between cone sheet fractures along the south coast averages 9.75m and varies between 50cm and 119m. Overall, the pattern of distribution is saucer shaped (Fig.8.4.3) with the greatest distances between fractures occurring at Sron Bheag and to the east of Mingary Pier. At both these locations Jurassic/Triassic rocks are exposed. The central area of the saucer, where distance between cone sheet fractures is much less than the outer regions, consists of Moine host rocks (Fig.8.4.3).

8.4.3 Inner Centre Two

All sections occur in basic host rocks. On Beinn Bhuidhe (Fig.8.4.4) the distance between fractures increases down slope. Towards the southern locations i.e. towards Beinn na Seilg, the distance between fractures also increases. This may indicate that the Beinn Bhuidhe and Beinn na Seilg unit lengths either mark the outer limits of the set or that the cone sheet set is

Fig.8.4.2 A diagram showing the distance between filled cone sheet fractures along a west to east traverse across the north coast exposures of the Outer Centre Two Cone Sheet Set

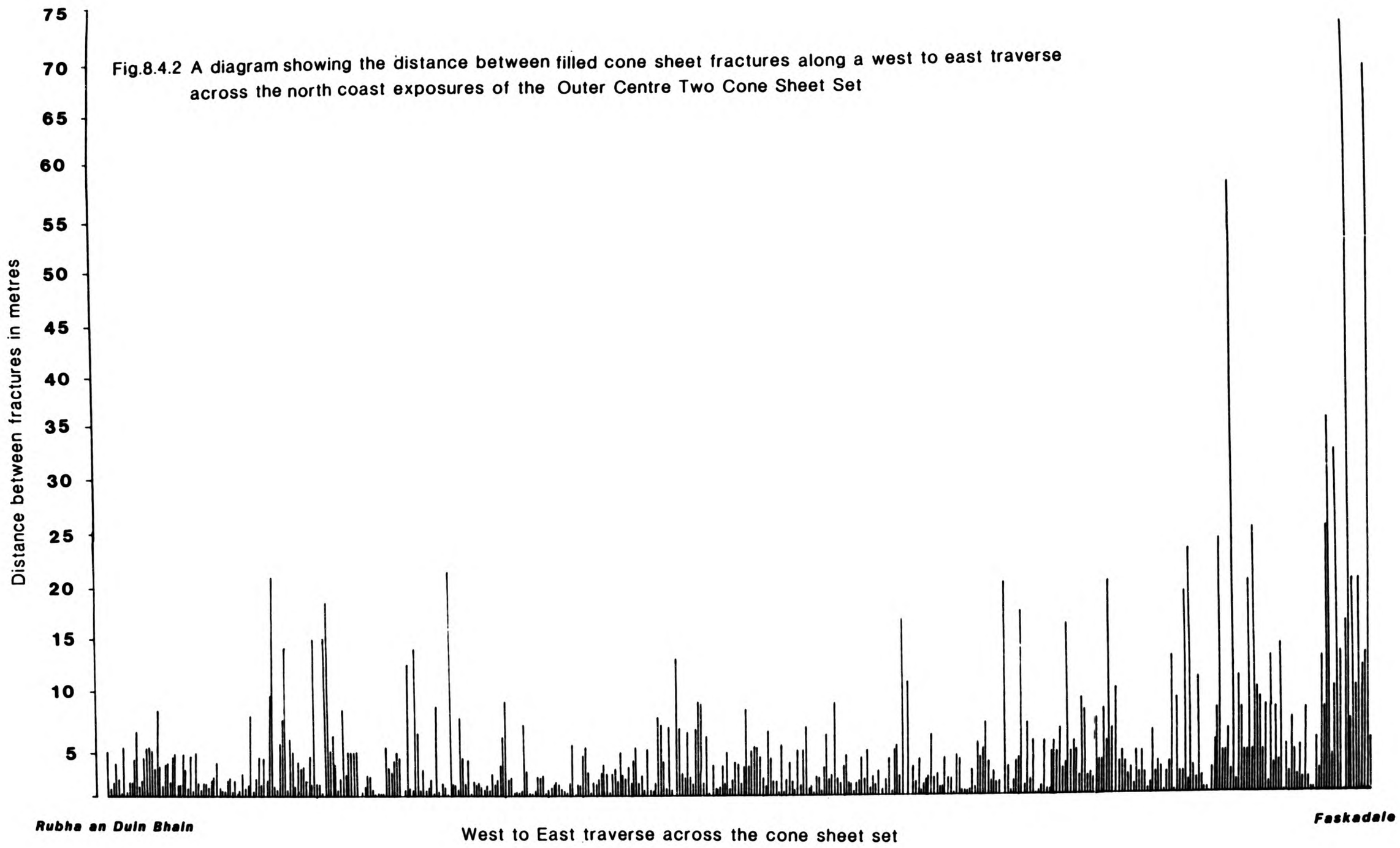

Fig.8.4.3 A west to east traverse across the Outer Centre Two Cone Sheet Set along the south coast to show the distance between filled cone sheet fractures

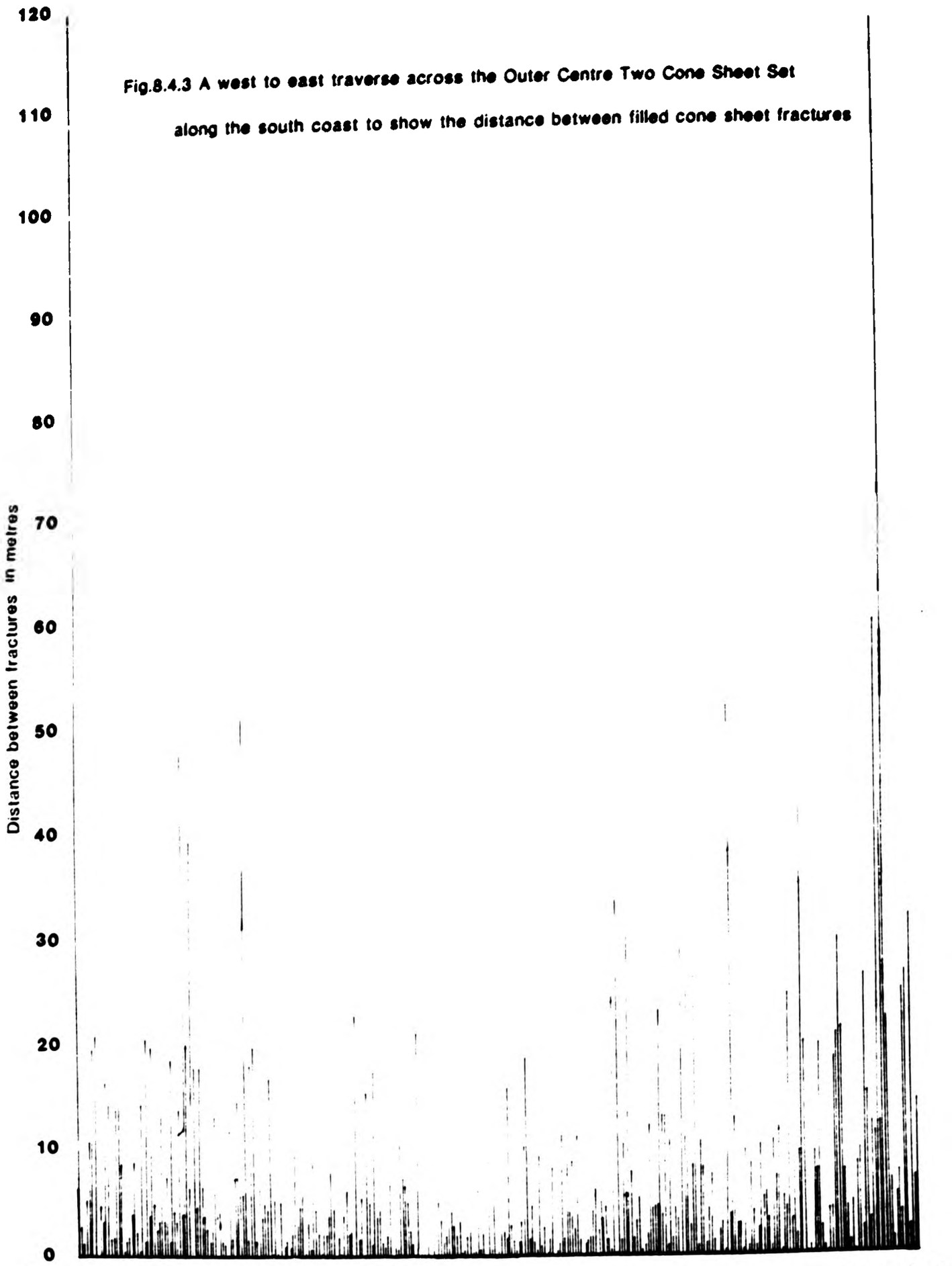

West to East traverse across the cone sheet set

Fig.8.4.4 A diagram showing the distance between filled cone sheet fractures along a North to South traverse across the Inner Centre Two Cone Sheet Set and a West to East traverse across the Centre Three Cone Sheet Set

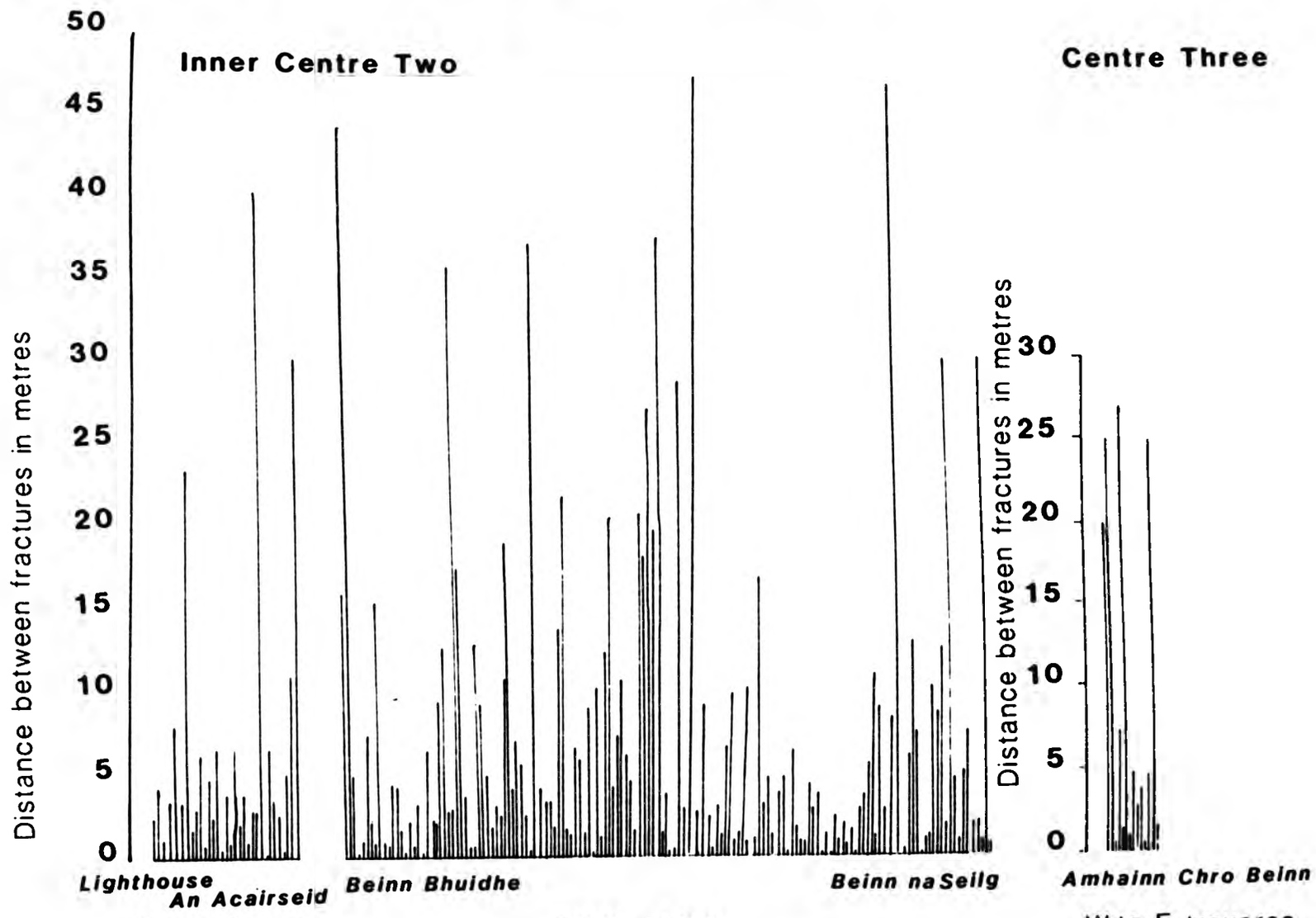

not equally developed at all locations.

8.4.4 Centre Three

Although the Centre Three cone sheets are not so profusely developed as the Outer Centre Two south coast section the distance between fractures shows a similar, saucer-shaped pattern (Fig.8.4.4). The central sheets are more closely spaced than those at the extremities of the section. Both sections occur in basic host rocks.

8.4.5 Summary

In general, the inner and outer most regions of a cone sheet set show large distances between fractures, whilst the region in the middle of the cone sheet set show much smaller distances between fractures, that is the sheets are more intense towards the centre of the cone sheet complex.

8.5 EXPLOITATION OF INHOMOGENEITIES BY CONE SHEETS

Exploitation of inhomogeneities by the cone sheets can be demonstrated within each host rock group. The main inhomogeneities exploited are bedding, foliation and joints.

8.5.1 Bedding and Foliation

Exploitation of both bedding and foliation planes is best

illustrated along the section from Rubha a' Choit to Ockle Point. Well foliated Moine psammites dipping at 70° to the SW form the host rock in the eastern part of the section, whilst Lias limestones form the country rock at Ockle Point. A series of thin basic sheets occur in the Moine host rock and parallel the dip of the 70° foliation (Fig.8.5.1). Plate 8.1 also illustrates the relationship between the foliation in the Moine (which dips at 70° S) and the dip of a cone sheet. At Ockle Point, just above the Moine/Jurassic unconformity, a 20m thick composite sheet lies parallel to bedding, which dips at 20° S (Plate 8.2). The two cone sheets depicted in the photographs are located approximately 500m apart along the section, both are Centre One sheets, yet one dips at 70° and is parallel to the foliation in the Moines, whilst the other dips at 20° and is parallel to the bedding in the Lias.

Pollard (1973) conducted a series of experiments to investigate the exploitation of layered host rocks by simulating intrusions into layered gelatine (Fig.8.5.2). He conducted two experiments to determine the effect of a well lubricated discontinuity in the path of an intrusion. Grease was intruded into gelatine at 90° to the plane of the discontinuity (Fig.8.5.2). The discontinuity is well lubricated and therefore transmits no shear stresses. The interface forms a small gap, as a result of normal stresses caused by the intrusion of grease. When the grease reaches the discontinuity it spreads in both directions. The second experiment involves the intrusion angle being $<90^{\circ}$. In this case, when the intrusion approaches the discontinuity, the effect is that the discontinuity to the left of the point where the intrusion intersects opens whereas the discontinuity

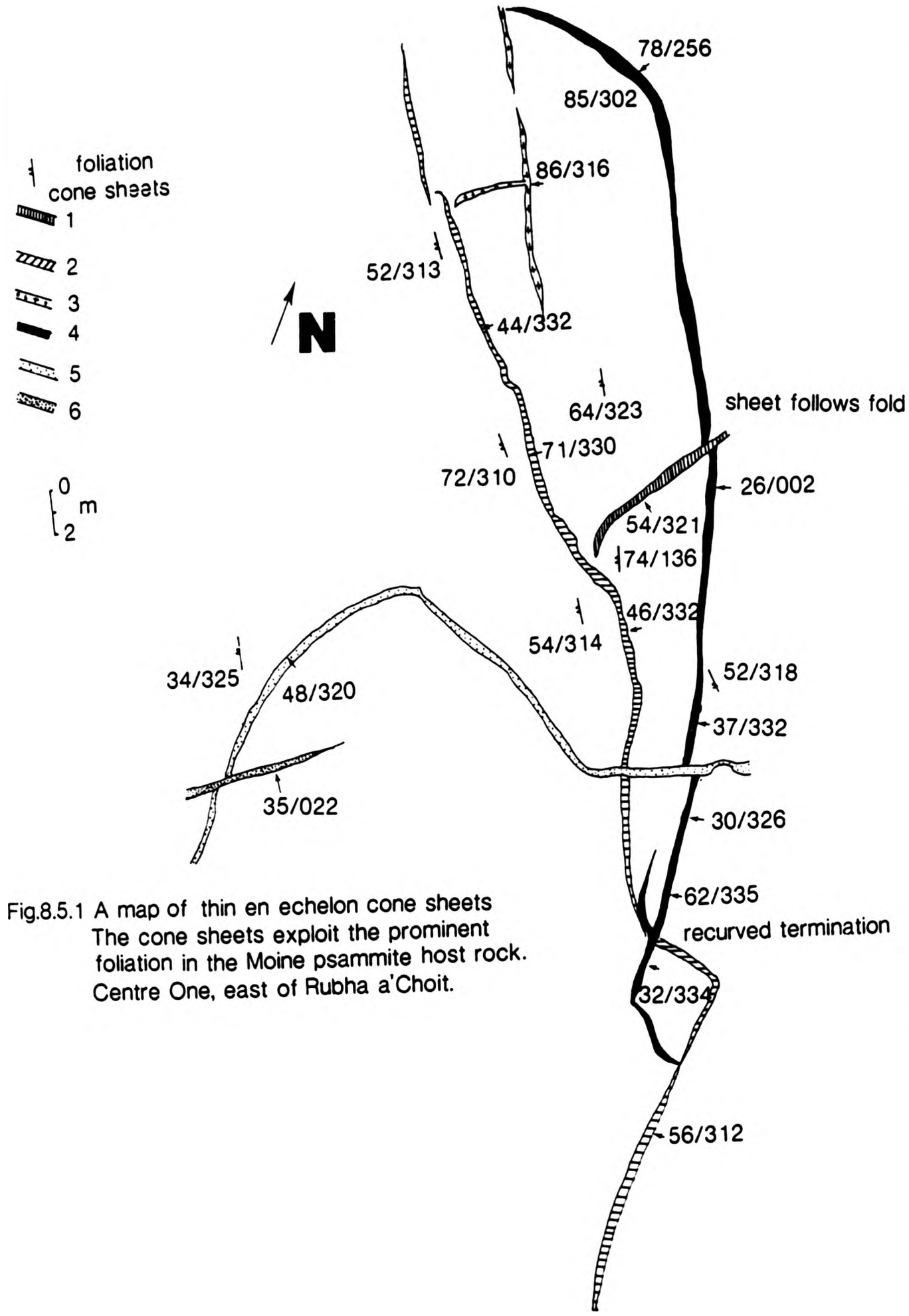

Fig.8.5.1 A map of thin en echelon cone sheets
The cone sheets exploit the prominent foliation in the Moine psammite host rock.
Centre One, east of Rubha a'Choit.

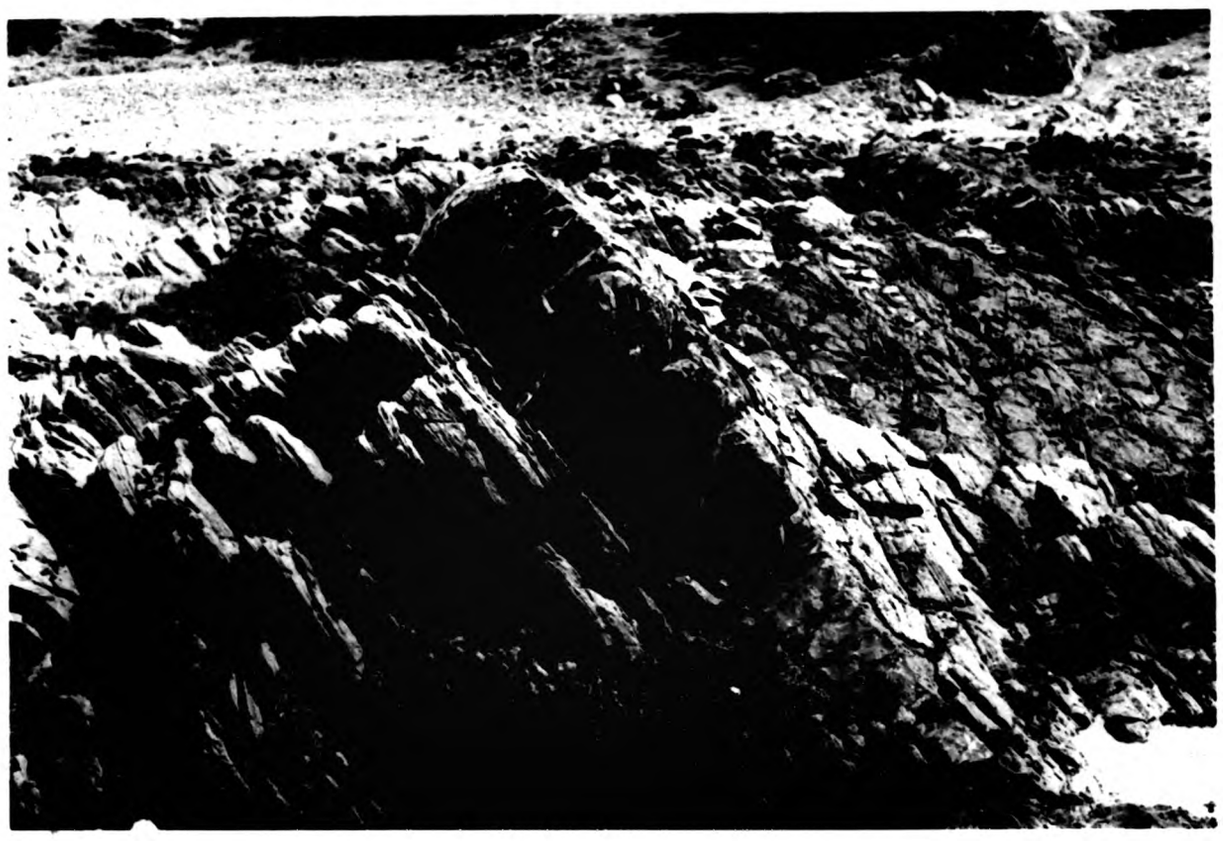

Plate 8.1 Exploitation of the foliation in the Moines by a cone sheet. Centre One, Rubha'Choit.

Plate 8.2 A thick composite sheet emplaced parallel to the bedding in the Lias limestones. Centre One, Ockle Point.

Plate 8.1 Exploitation of the foliation in the Moines by a cone sheet. Centre One, Rubha'Choit.

Plate 8.2 A thick composite sheet emplaced parallel to the bedding in the Lias limestones. Centre One, Ockle Point.

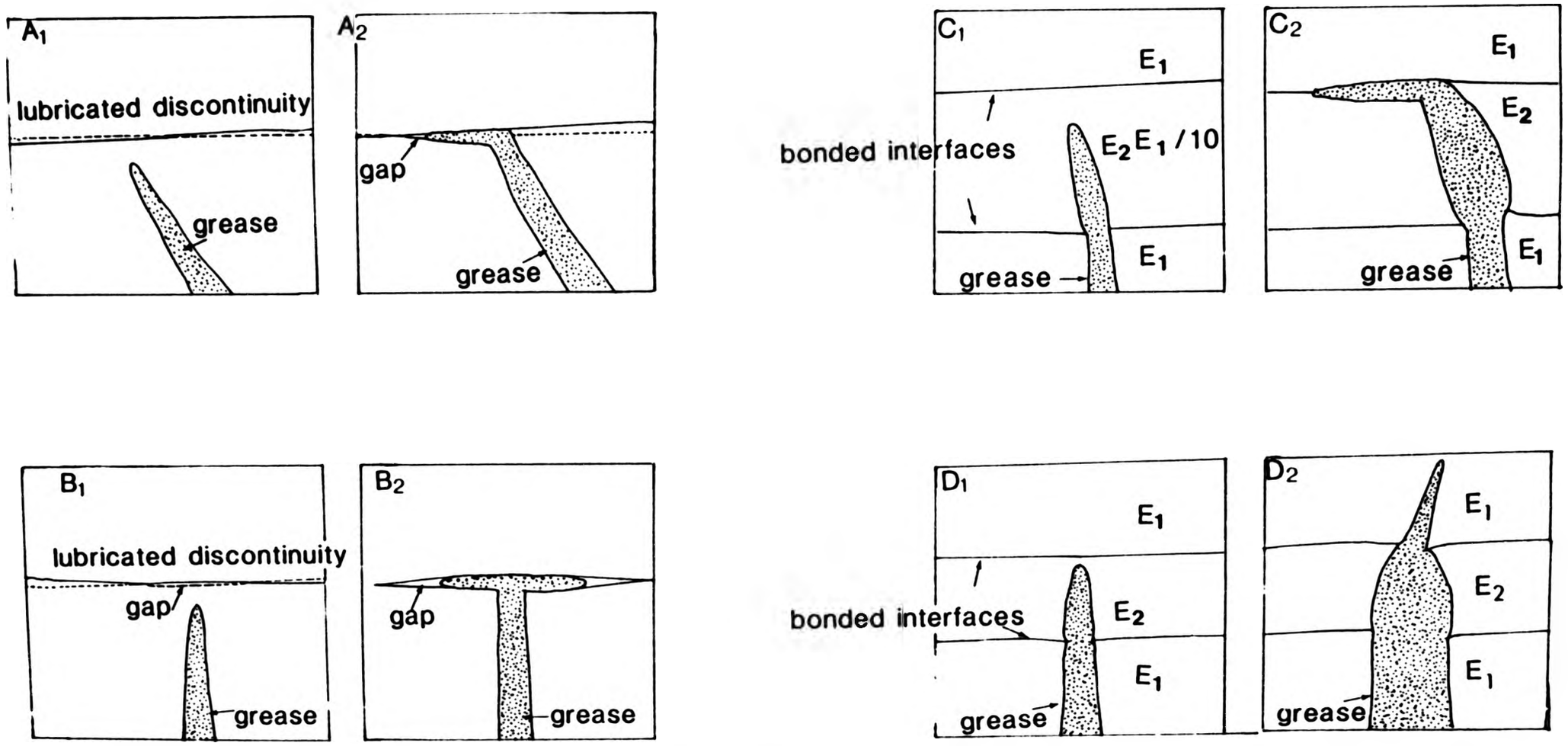

Fig.8.5.2 The paired diagrams represent a series of experiments performed by Pollard (1973) to investigate the intrusion mechanisms of minor intrusions intruded into a layered host. In diagrams A and B the boundary between the layers is lubricated. Diagrams C and D have three layers of host the central layer has a Youngs modulus greater than in C and less than in D the two outer layers, the boundaries between the layers are bonded The intrusion (grease) is intruded in A at an angle of greater than 90° to the layering,and in B C and D at 90°to the layering, the changes in form of the intrusions in response to the different Youngs moduli bonded and unbonded layers can be seen above. (after Pollard 1973)

to the right of the intersection closes. Thus the intrusion propagates along the discontinuity to the left (Fig.8.5.2).

Structures similar to those produced by Pollard (1973) (Fig.8.5.2 A and B) are seen at Ockle, where both steeply dipping and shallowly dipping country rock structures are exploited by hydraulic fracturing. The rocks may have contained ground waters which contributed to the formation of hydraulic fractures.

8.5.2 Joints

Keunen (1937) noted that certain cone sheets are parallel to conjugate joint sets (Plate 8.3) which he thought might represent unfilled cone sheet fractures. Undoubtedly, cone sheets do occupy large scale joints, especially where developed in Liassic rocks, although examples of joint exploitaion on a large scale are not common. Keunen's comments will be discussed later (Chapter 8). At present, therefore it will be assumed that the joints are pre-cone sheet fractures which have been exploited by magma. A more common exploitation of joint fractures is illustrated in Plates 8.4 and 8.5, where side steps in the cone sheet are facilitated by joints in the Jurassic host. Joints in the Tertiary major intrusions have been similarly exploited, as demonstrated by the sheet belonging to the Inner Set of Centre Two, Lighthouse section (Plate 8.6), where the sheet margin has the form of an open zig-zag.

Plate 8.3 Cone sheet emplaced parallel to well developed joint set in Jurassic limestones, west of Mingary Pier, Outer Centre Two, as referred to by Keunen (1937).

Plate 8.4 A conjugate joint set developed in Jurassic rocks which has been utilized by a cone sheet, giving a stepped profile in cross section. Outer Centre Two, east of Mingary Pier.

Plate 8.3 Cone sheet emplaced parallel to well developed joint set in Jurassic limestones, west of Mingary Pier, Outer Centre Two, as referred to by Keunen (1937).

Plate 8.4 A conjugate joint set developed in Jurassic rocks which has been utillized by a cone sheet, giving a stepped profile in cross section. Outer Centre Two, east of Mingary Pier.

Plate 8.5 Joint-controlled margins of an Outer Centre Two cone sheet containing a large number of anorthosite xenoliths. Jurassic limestones form the country rocks at Sron Bheag.

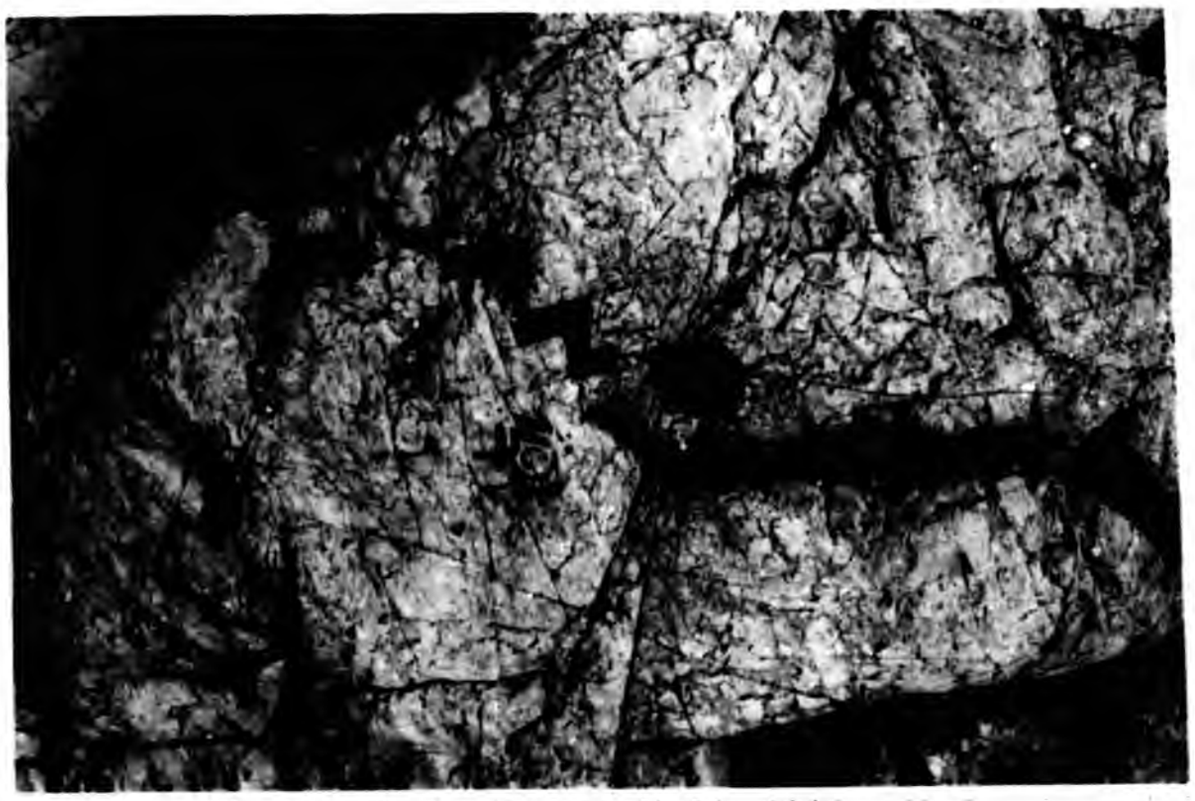

Plate 8.6 Joint controlled margins of an Outer Centre Two cone sheet resulting in a tight zigzag form, Rubha Groulin.

Plate 8.5 Joint-controlled margins of an Outer Centre Two cone sheet containing a large number of anorthosite xenoliths. Jurassic limestones form the country rocks at Sron Bheag.

Plate 8.6 Joint controlled margins of an Outer Centre Two cone sheet resulting in a tight zigzag form, Rubha Groulin.

8.5.3 Summary

On all three scales, that of the peninsula, the lithological groups and of the host rock structures, an amount of heterogeneity is displayed, from the heterogeneous distribution of the rock types throughout the peninsula, to the variable exploitation of the pre-existing host rock structures.

8.6 REGIONAL STRUCTURES

Doming

The country rocks dip radially away from the focus of Centre Two and similar doming is seen in other central complexes of the B.T.I.P., although in Mull the structures adjacent to the central intrusive complex are more complex. Table 8.2 summarises the interpretations of various authors on the relationship between doming and the development of cone sheets. These interpretations fall into two main categorys, the first category has two parts these being a) that cone sheets are a consequence of doming and b) that doming is a consequence of cone sheets and the second category is that there is no genetic relationship between the two phenomena.

Evidence for the existance of a dome around Centre Two is best shown by the radial dips observed throughout the Mesozoic rocks of the peninsula. Two traverses which show the best evidence for this are the one at Sron Bheag and the one between Rubha Carrach and Faskadale. Fig.8.6.1 is a contoured stereographic projection of the dip of all bedding planes collected in the field, and shows a small cluster close to the centre of the

Table 8.4 Historical review of the relationship between cone sheets and doming.

AUTHOR	YEAR	CONCLUSIONS
Anderson	1924	Doming caused by a localised magma pressure; doming predates cone sheet formation and is not essential to their formation. Cone sheets in general, in particular, west coast of Scotland.
Richey et al.	1930	Doming may be due to an increase in pressure in the magma - reservior which subsequently found relief in the emplacement of the Outer Centre Two cone sheets, Ardnamurchan.
Wells	1954	Doming preceeds cone sheet emplacement and is caused by a localised magma pressure. Ardnamurchan.
Walker	1975	Cone sheets only form when an acid diapir approaches the surface; doming is caused by the diapir and therefore is intimately linked with cone sheet formation: B.T.I.P. and present day Iceland.
Le Bas	1971	Flat topped domes are formed resulting from cone sheet emplacement
Le Bas	1977	Doming preceeds cone sheet formation and is unrelated, Kenya (Fig.8.6.3).
Bahat	1980	Doming is intimately connected with cone sheet formation; cone sheets can develop either before or after doming occurs. Cone sheets in general, in particular Kenya and B.T.I.P..

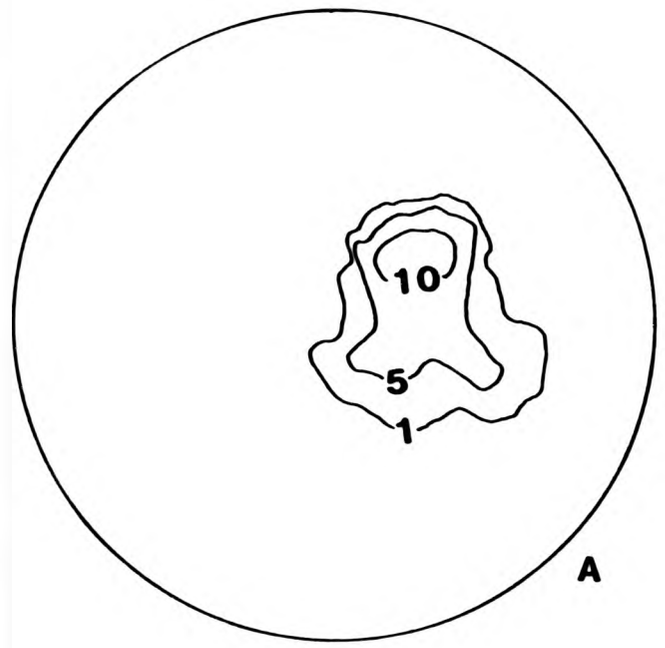

n 45

A

north coast measurements

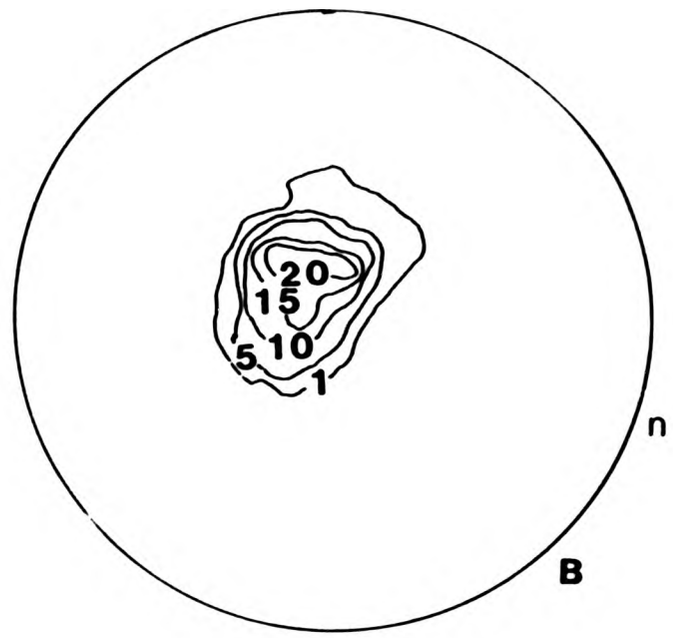

n 61

B

south coast measurements

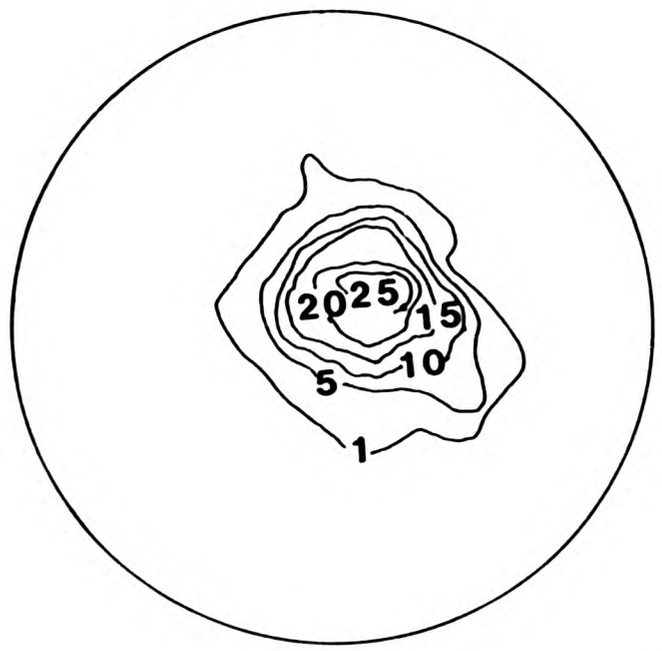

n number of bedding readings

contours at 1 then intervals of 5 cone sheets

n 106

AandB

Fig.8.6.1 Contoured stereographic projection of the dip and strike of the Jurassic sediments

plot, and therefore supports the doming hypothesis. However, in detail the dip of the sediments varies (Fig.8.6.2) in amount and direction. At a greater distance from the central complex the sediments show an even greater disparity (Fig.8.6.2), for example, the sediments on the shore at Swordle Bay dip at shallow angles to the north, although the direction is not constant and does not seem to have a close association with the foci of igneous activity. Often the sediments are faulted, as noted by Richey et al. (1930), with the dip of the sediments changing in the areas adjacent to the faults.

In the more easterly parts of the peninsula, the Moine rocks, which form the host rocks to the Centre One sheets, show quite complex deformation and do not afford any evidence to enable the effect of doming to be assessed. However, as described above, the sediments in this area do not indicate that doming has affected this area.

To the west of Sron Bheag the Hypersthene Gabbro truncates the folded sediments and timing of the doming can be further defined by the observation that the sheets cutting the sediments close to the junction with the Hypersthene Gabbro dip at similar angles to the Outer Centre Two cone sheets located near Kilchoan, that is 2 km away from the Hypersthene Gabbro. Doming therefore took place after the emplacement of the Centre One cone sheet set and before the Outer Set of Centre Two cone sheets were developed.

Richey et al. (1930) considered that the doming occurred as a separate event prior to the emplacement of the Outer Set of

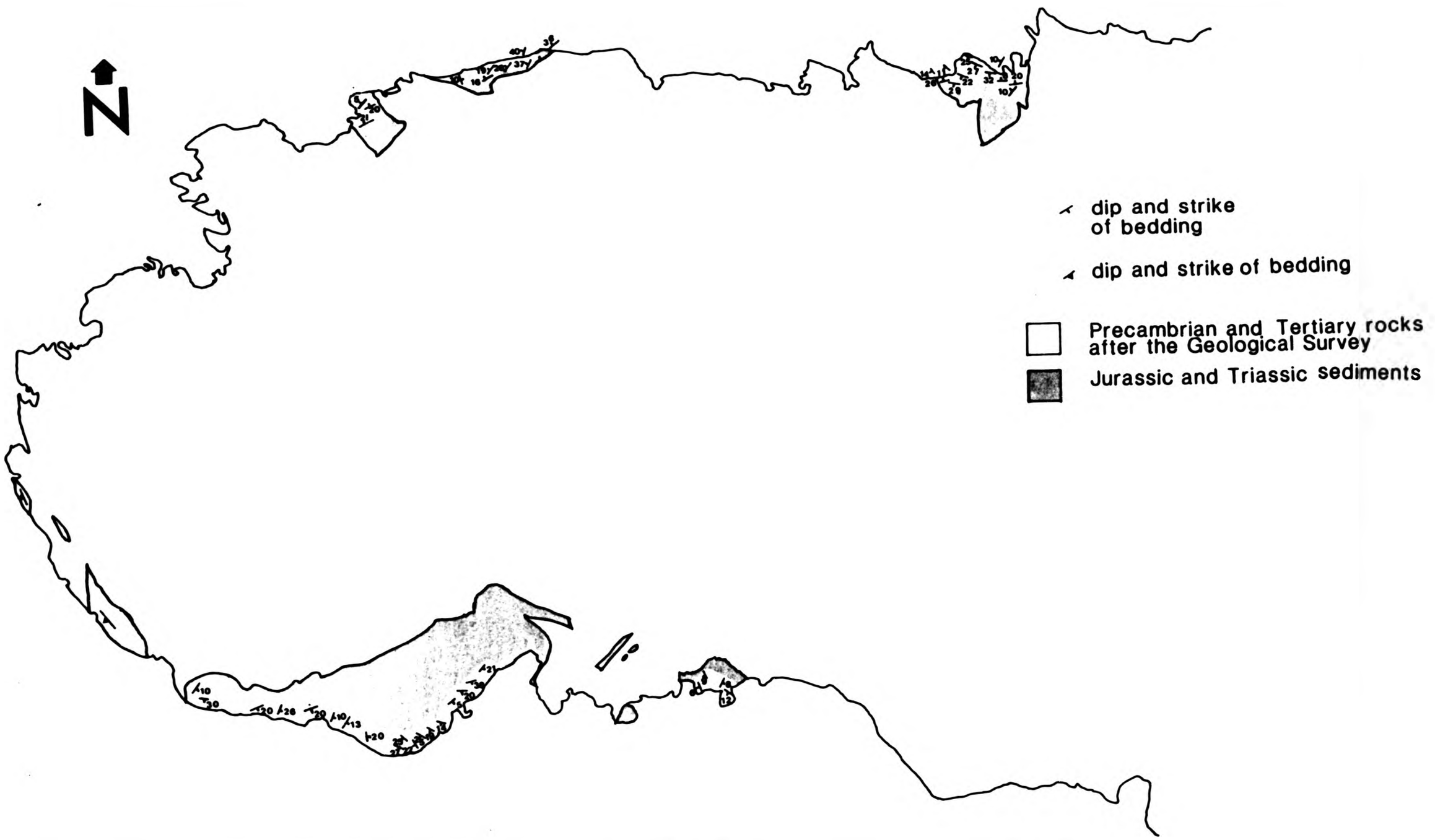

Fig.8.6.2 Diagram to show the distribution and the dip and strike of the Jurassic and Triassic sediments

Centre Two Cone Sheets, because they state (1930, p112) "...on the hillslopes west of Kilchoan Bay, the cone sheets cutting the domed Mesozoic are inclined towards Centre Two at no less an angle than others farther to the east outside the limits of the dome...". If the doming occurred post cone sheet emplacement, the cone sheets would presumably dip at very shallow angles within the area of doming. They conclude that an increase in magma pressure causing doming could be relieved by cone sheet formation. However, present day studies on the Kilauea volcano (Fiske and Kinoshita, 1969) show that inflation of the volcano summit occur periodically and can be measured, but deflation occurs as magma migrates laterally from the summit region into the rift zone, indicating that doming may occur and be totally unrelated to cone sheet emplacement. Phillips' (1974) model involved retrograde boiling of the magma resulting in fracturing of the roof of the magma chamber enabling cone sheet intrusion to take place. He considered doming a consequence of the slow upwelling of magma.

Bailey et al. (1924) attributed the doming associated with the Mull central intrusive complex to a localised magma pressure caused by the emplacement of the Derrynaculen and Glas Bheinn Granophyres which occurred prior to emplacement of cone sheets. The marginal folds around the Mull central intrusive complex are now thought to be due to the rise of a magma cylinder. Le Bas (1977) from his studies on the Nyasanja Complex subdivides the doming into a) that caused by the emplacement of the ijolite plug, which he terms general uplift and b) that caused by the emplacement of the carbonatite cone sheets (Fig.8.6.3 from Le Bas fig.14.23). He also noted that subsequent movements along

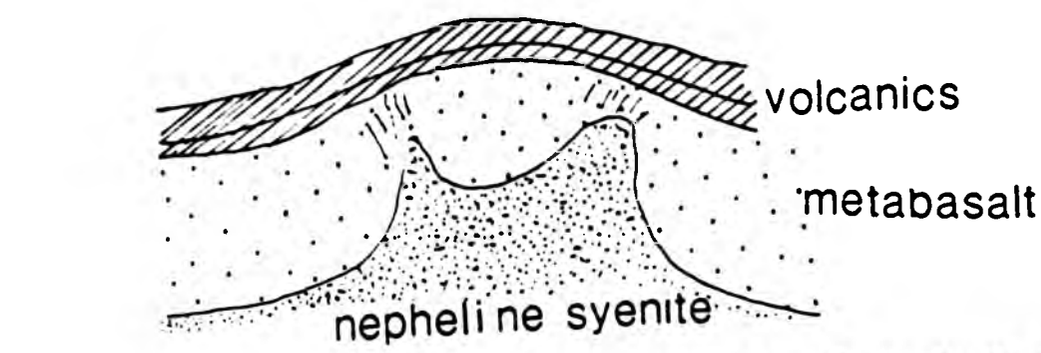

Up-doming and emplacement of nepheline syenite

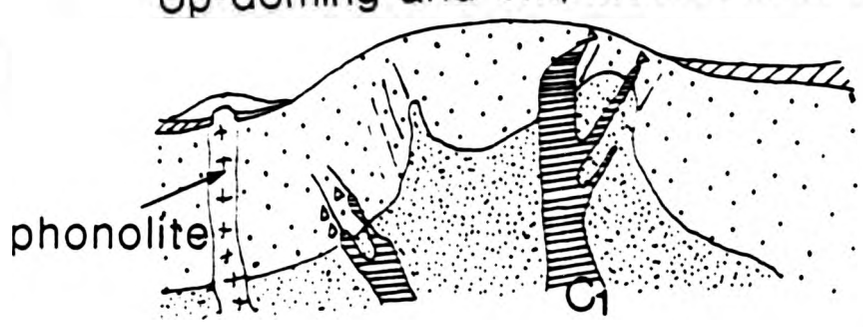

Erosion, intrusion of C_1 and phonolite

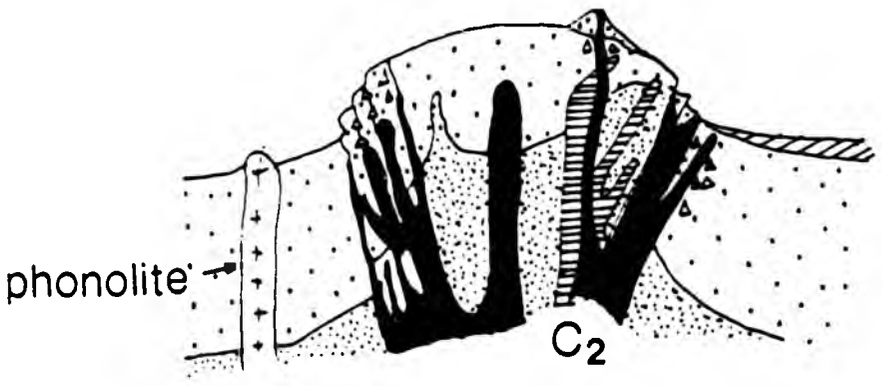

Intrusion of C_2 and uplift of central block

Emplacement of agglomerates

C cone sheets

Fig.8.6.3 Schematic stages in the development of the North Ruri volcanic centre illustrating the relationship between doming and cone sheet emplacement (after Le Bas, 1977)

concentric conical fractures are recorded as slickensides on the cone sheets.

Walker (1975) attributes doming in the B.T.I.P. to an uprising acid diapir resulting in the forceful shouldering aside of the country rock, and notes that "...each cone sheet swarm occurs where local updoming, now attributed to the early uprise of a granitic diapir, occurs." As evidence of this he refers to the fact that most cone sheet complexes are confined to the area of doming. However, this does not hold true for Ardnamurchan, as three out of four cone sheet sets occur outside the area of doming. Bahat (1980) follows Walker's hypothesis which invoked the presence of a rising acid diapir above a basic column. He summarises two mechanisms for the evolution of an intrusive centre. In both theories doming always develops, which therefore differs from the Centre One, Inner Centre Two and Centre Three cone sheets of Ardnamurchan. Mechanism I shows the development of cone sheets post doming, similar to the Outer Centre Two cone sheet set. Whereas via mechanism II, cone sheets develop prior to doming. No field evidence is given by Bahat, or can be found in the literature to support mechanism II.

The doming in Ardnamurchan is confined to the area surrounding Centre Two (Fig.8.6.2) whilst no evidence for doming can be found associated with the Centre One, Inner Centre Two or Centre Three cone sheet sets. This supports the observations of Richey et al. (1930) and Wells (1954) that doming is associated only with Centre Two activity. If a re-surgent uprise of magma was responsible for each cone sheet set, with associated doming, then several phases of movement would be expected on the cone

sheet margins. In the present study, only two examples of slickensides associated with cone sheets have been found and therefore it is assumed that very little doming has occurred after the main phase which occurred before the emplacement of the Outer Set of Centre Two cone sheets. All the examples of cone sheets sets of the B.I.T.P. are associated with central intrusive complexes, thus the relationships between ring dykes, cone sheets and doming are difficult to separate. However, I believe that the sequence described by Le Bas (1967), that is, doming preceeds cone sheet formation and is unrelated to the formation of cone sheets, may be applied to the Ardnamurchan complex, and that the doming may be the result of the rise of a cylinder of magma.

8.7 JOINTING

Keunen (1937) believed that the conjugate joint sets which occur in the Liassic rocks west of Mingary Pier represent unfilled cone sheet sets (Plate 8.3). In order to verify or deny this hypothesis the present author collected a large number of joint plane dip and strike measurements from the country rocks of the peninsula. The joints occur in large numbers and have a multitude of different orientations even on a small scale. This implies that stress systems of different orientations were operative. Consequently no clear simple stress pattern could be discerned for the whole area. However, this observation is compatable with the theory that cone sheets were emplaced in small groups, with each group having it's own stress pattern. Also, if localised swellings of the volcanic surface occurred, similar to the upwellings recorded on Kileaua

(Hawaii)(Fiske and Kinoshita, 1969) then perhaps a number of superimposed stress systems would result.

8.8 DISCUSSION AND CONCLUSIONS

In order to classify the form of cone sheets in relation to the heterogeneity present within the country rocks a flow diagram has been constructed (Table 8.5). If the host rock consisted of just one rock type, then the variations in the form of a cone sheet would be caused entirely by the emplacement mechanics. If the area consisted of a variety of rock types then other factors may be involved. On a large scale, the apparent annularity of the cone sheets indicates that the distribution of the different rock types did not influence cone sheet emplacement. However, on a smaller scale as shown in Table 8.5. the different rock types are classified into a simple two fold division of sedimentary/metamorphic and igneous rocks. Different types of inhomogeneities are present within each group, for example bedding occurs in sedimentary rocks, whereas joint structures occur in both sedimentary and igneous rocks. Each type of inhomogeneity found within the lithological groups has been exploited by cone sheets to a different degree.

Therefore, on a localised scale, the form of the cone sheets can be influenced by inhomogeneities in the country rock. Simultaneously, the form of the cone sheets are dependant upon the length of time that pressure is exerted and how the energy of the intruding magma is dissipated. For instance, where cone sheets are emplaced quickly with sustained magma pressure, the intrusions determine their own form, whereas when the magma is

Table 8.5 A flow diagram to illustrate the relationship between form of cone sheets and the heterogeneities of the host rocks.

Are the rock types of the area homogeneous?

YES
The form of the cone sheets are controlled by the intrusions

NO
What are the inhomogeneities?

SEDIMENTARY/ METAMORPHIC ROCKS
Moine, Jurassic/ Triassic

IGNEOUS ROCKS
Agglomerates and lavas, basic and acid intrusions

Are these groups heterogeneous?

YES
The form of the sheets are influenced by the inhomogeneities.
What are the inhomogeneities?

NO
The observed structures are controlled by some other unknown process.

BEDDING
e.g. Ockle Point Centre One.

FOLIATION
e.g. Rubha a' Choit, Centre One

JOINTING
e.g. west of Mingary Pier, Outer Centre Two.
e.g. Lighthouse, Inner Centre Two.

distant from source, pressure is low and therefore the magma tends to exploit inhomogeneities in the host rock (Fig.8.8.1).

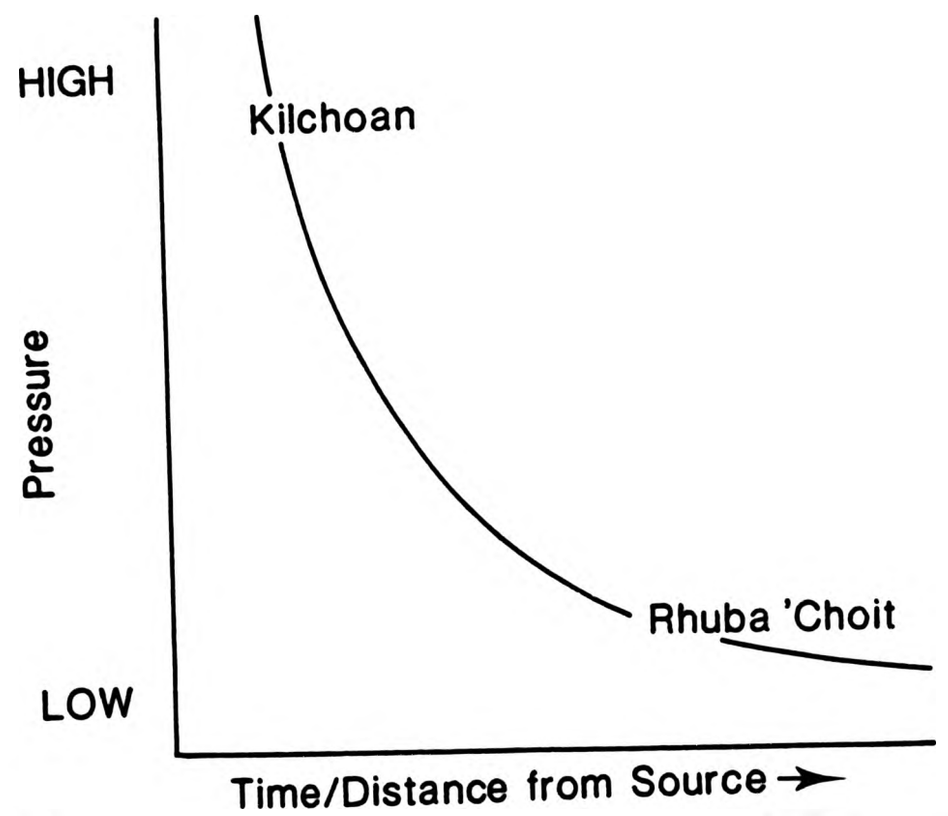

Fig.8.8.1 Relationship between pressure and distance from source of pressure, resulting in two extremes of cone sheet form
a) regular thin sheets cross cutting previous structures, e.g. Kilchoan
b) few, relatively thick sheets exploiting previous structures, e.g. Rhuba'Choit

CHAPTER 9

MODELLING

9.1 INTRODUCTION

A modelling programme has been undertaken to investigate the development, distribution and intensity of fractures within a cone sheet complex using photoelastic, numerical and mechanical models.

Photoelastic models were used to investigate the interactive stress systems of adjacent bodies, that is the influence of juxtaposed central intrusive complexes. Numerical models have been used to model an idealised cone sheet set, using figures gained from the field studies of this project, and also to investigate as to why a cone sheet set may deviate from the idealised form. Dip and strike are the most important properties in these models. A mechanical model which is principally involved with the formation of en echelon fractures has also been studied.

9.2 PHOTOELASTIC MODELS

9.2.1 Introduction

Sir David Brewster in 1816 was the first person to notice that when glass is stressed it exhibits birefringence, depicting the temporary stress distribution within the medium. Photoelasticity is the study of two-dimensional stress patterns in transparent substances and as such may be used as an indirect study of stress conditions in a scale model of a particular phenomenon. Although photoelasticity is a widely used technique in

engineering (Farquarsson and Hennes, 1940) little work has been done in the field of geology; only two studies on intrusions have been undertaken. The first was by Durrance (1968) who investigated the Ardnamurchan cone sheets and major ring intrusions. The second by Pollard (1973) who devised a series of photoelastic experiments to investigate the influence of adjacent sheets on the form of each sheet and the effects of superimposed stresses and the relationships between layered host rocks and the intruding sheets.

9.2.2 Previous Investigations

Durrance (1968) is the only author to apply photoelastic methods to the investigation of cone sheet intrusions. He undertook his study on the Ardnamurchan central intrusive complex in order to apply the analysis to both cone sheets and major ring intrusions. His photoelastic study incorporated the stress distribution of two two-dimensional models, one in axial compression and the second in compression at the two poles of the model, thus enabling a three-dimensional configuration of the maximum shear stress trajectory planes to be produced. Durrance (1968) applied the derived three-dimensional model to the cone sheet complex of Ardnamurchan. He examined the cone sheet pattern as depicted on the 1" Geological Survey map and interpreted the whole distribution as consisting of one cone sheet set, not four as proposed by Richey (1930) (Fig.9.2.1). Durrance united all the cone sheets of the peninsula into one cone sheet set with an inclined axis, such that cone sheets in the east (Centre One) of the peninsula dipping at 20° represent one limb, and those in the west (Inner Centre Two) dipping at

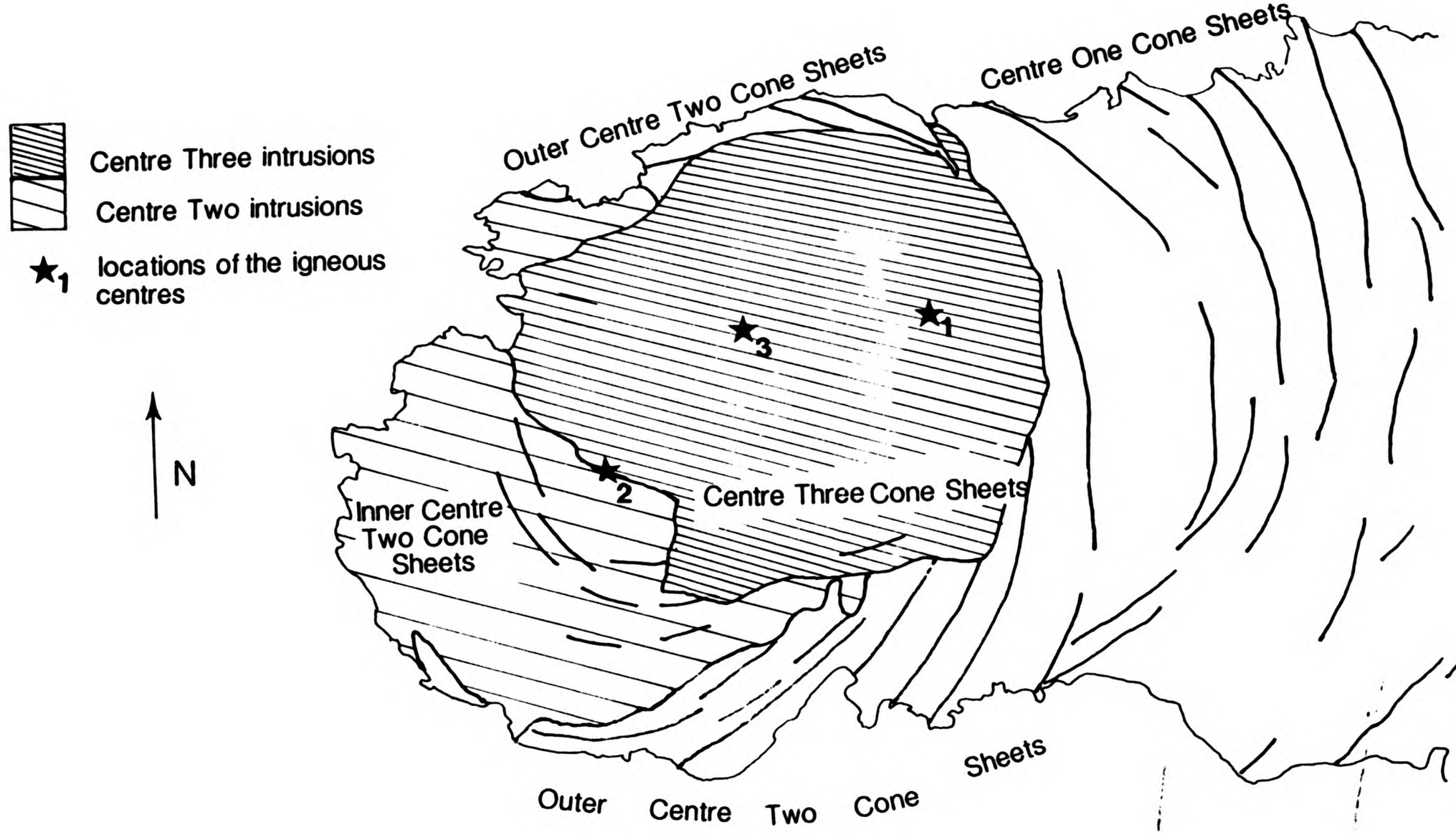

Fig.9.2.1 Diagram to show the distribution of the cone sheets and their related centres of activity as used by Richey et al (1930) in their three centred hypothesis

70°, representing the other limb (Fig.9.2.2). He also believed that the axis of this set was the centre of a single system of spiral fractures resulting in the development of all cone sheet fractures of the complex.

On a smaller scale, Pollard (1973) looked at propagation of individual minor intrusions (Fig.8.5.2). His first experiments investigated propagation of contemporaneous intrusions using photoelastic methods, the first pair of intrusions are parallel to each other and the second pair are parallel but offset perpendicular to their length, i.e. en echelon (Chapter 7). His second set of experiments involved a series of single intrusions which were emplaced into layered host rocks represented by gelatines having different poissons ratio's.

9.2.3 Modelling materials

The modelling substrate for photoelastic experiments needs to be transparent, deform elastically at relatively low stresses and produce temporary birefringence patterns when stressed. Two suitable substances are photoflex resin and gelatine. Gelatine has been used as a model substrate because it is cheap and re-usable, in addition to it's transparent properties. Gelatine has advantages over the hard modelling substances (e.g. photoflex resins) in that it does not require machining, which often imparts inherent stresses into the model, yet can be easily cut to shape. Therefore, gelatine is a useful model substrate to use in preliminary experiments and large models (e.g. Phillipe and Mellinger, 1948). As gelatine is of low strength it can be fractured quite easily, also fractures can be

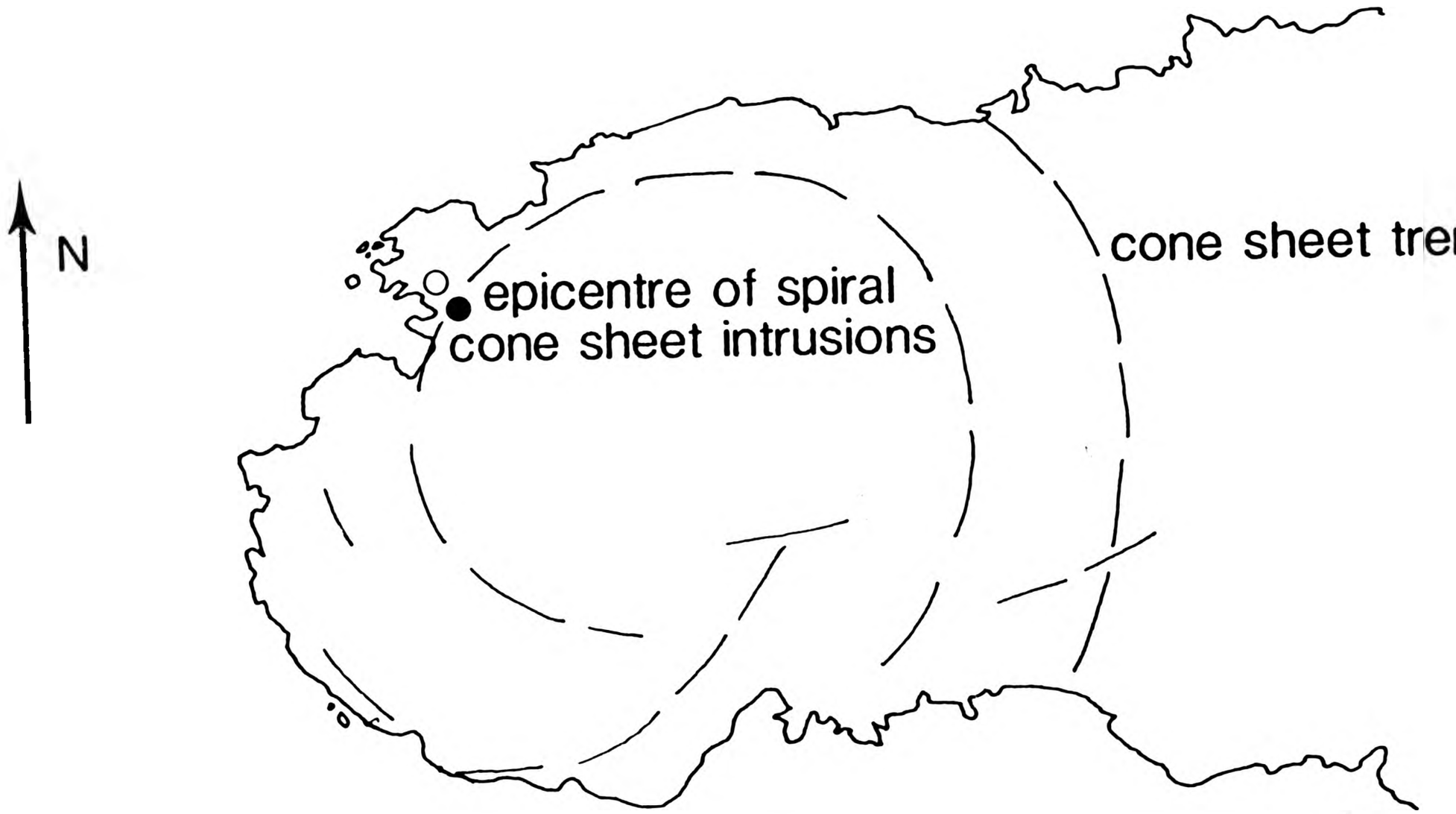

Fig.9.2 2 Diagram of Durrances (1968) generalised outcrop of cone sheets to show his single centred hypothesis

initiated and their subsequent propagation studied.

The composition of the gelatine is critical in that if it is too weak it does not hold it's shape and fractures with the slightest of pressures. Several experiments were conducted to determine the optimum proportions of gelatine and water. The recipe used by Heywood (1952) was found to be the optimum composition and consists of:- 15wt% gelatine, 25wt% glycerine and 60wt% water. The gelatine can be reused up to six times before growth of mould affects the properties of the substrate. An 11.5cm square slab (2cm thick) of gelatine is the maximum size that can be accommodated on the photoelastic bench.

Some different geometrical shapes of hard photoelastic models were studied in order to investigate the distribution of stresses within these models.

Also required for these experiments are a white light source, an overhead projector, a polariscope and a camera situated vertically above the photoelatic bench.

9.2.4 Models

A series of experiments were devised in order to investigate many of the factors thought to influence the emplacement of and form of cone sheets. The experiments designed fall into 6 categories:-

1. Simulation of intrusions (cf Pollards experiments) by injection of a liquid into the gelatine,
2. Simulation of inflation of a magma chamber (plan view),
3. Different shaped magma indentors of different relative strengths,
4. A number of closely spaced magma chambers and their

influence on each others stress pattern,
5.En echelon fractures, their form and propagation.

Unfortunately, due to the lack of time much of the work is incomplete because the length of time involved in setting up the apparatus and finding a suitable medium to use took longer than had been anticipated.

9.2.5 Results

Given below is a brief resume of the experiments highlighting the faults and possible improvements for future modelling.

1. An intrusion was simulated by injecting liquid gelatine into a slab of gelatine. The difference in strengths between the liquid and solid were too great, consequently insufficient pressure to allow intrusion could be maintained. An improvement to this experiment would involve the use of a wide bore syringe, "thicker" intruding material and a "weaker" gelatine slab.

2. Inflation of a magma chamber in plan view was simulated by setting a balloon in the gelatine slab, such that the balloon was sandwiched between "two" layers of gelatine, with a bung in the neck of the balloon to prevent the gelatine filling the balloon. Inflation of the balloon resulted in an inflation of the slab in the form of a dome. However, the gelatine began to fracture around the neck of the balloon. A thicker slab of gelatine is required.

3. In investigating the influence of different shaped magma chambers on the stress patterns in the country rock, a

semi-circular and a triangular (pointed) magma chamber were modelled. A semi-circular model results in stress patterns which would result in similar structures to those derived by Phillips (1974). The triangular shaped indentor, formed similar patterns with a narrower distance between "shoulder" areas, however, the experiment was curtailed due to the indentor fracturing the gelatine slab. A more extensive series of experiments could be conducted using various shapes and strengths of indentor.

4. In order to investigate the influence of adjacent central intrusive complexes a series of small circular holes were cut into a slab of gelatine, then stressed. Since the main external stress thought to affect the B.T.I.P. is the tension associated with the regional dyke swarms, the compressive force that can be applied to a gelatine slab seems inappropriate. An alternative would be to have a photoflex model made to represent the B.T.I.P. and therefore tensions could be applied and enable a more thorough investigation of the problem.

5. A set of en echelon fractures were initiated in a slab of gelatine then stressed, in order to study the direction of propagation, following the experiments of Pollard (1973). This experiment could be extended to study specifically the en echelon cone sheets found at the Lighthouse section, to determine the extent to which internal pressure (Pollard et al., 1982) and shearing (Chapter 7) have influenced the structures seen.

9.3 MECHANICAL MODELLING

9.3.1 Introduction

The aim of this type of model is to investigate the conditions of initiation and propagation of cone sheet fractures. Bahat (1981) studied the development of cone sheet fractures in glass using a non-solid indentor, with the result that a single, spirally developing, conical fracture develops. Field (1964) also studied fracture patterns in glass and his experiments simulated the development of a whole cone sheet complex. Field found that the rapid impact of a solid (metal) ball on glass results in a central region devoid of fractures with an outer region of intense circular fractures, the intensity of the fractures decreases towards the outer limits of the experimental area. Both of these studies have analogies in the Ardnamurchan cone sheet complex. Bahats single fractures are most similar to the poorly developed Outer Group of Inner Centre Two cone sheets, which developed after the emplacement of the Hypersthene Gabbro major ring intrusion. Field's intensively developed cone sheet set is most similar to the Outer Centre Two cone sheet set which is the most complete set of the whole complex. The present study, however, aims to illustrate the development of fractures under different conditions.

9.3.2 Experiment and Discussion

An experiment was carried out on a highly water-saturated sand sample on the sea shore. The sudden application of force,

by dropping a weight upon the sand, produces a series of en echelon fractures. Further application of pressure, by repeated dropping of the weight, results in the fractures "merging" to form a single arcuate fracture. Two stages of the experiment are shown in Fig.9.3.1. This type of fracturing only occurs where the model substrate is supersaturated: when the sand is dry and compacted the fractures do not develop. Beach (1980), in a numerical analysis of hydraulic fractures, discussed several structures that can be formed, one of which are en echelon fractures. Hydraulic fracturing is a process of fracturing in which tensile and shear fractures are produced through the action of a fluid under pressure. In a cone sheet analogy meteoric water contained within the host rock (Taylor and Forester, 1971) assisted the fracturing of the host rock as a result of a rise in pressure due to the advancing magma. The present experiment lends support to the hypothesis of hydraulic fracturing.

Field evidence in support of the hypothesis that hydraulic fractures develop firstly as a series of en echelon fractures which are subsequently joined to form a single sheet can be found in the cone sheets of Ardnamurchan. En echelon lenses of basic rock are seen to laterally coalesce to form a single sheet. On a smaller scale individual lenses which on one surface are seen as separate units can be seen on other surfaces to connect, perhaps frozen in the process of propagation.

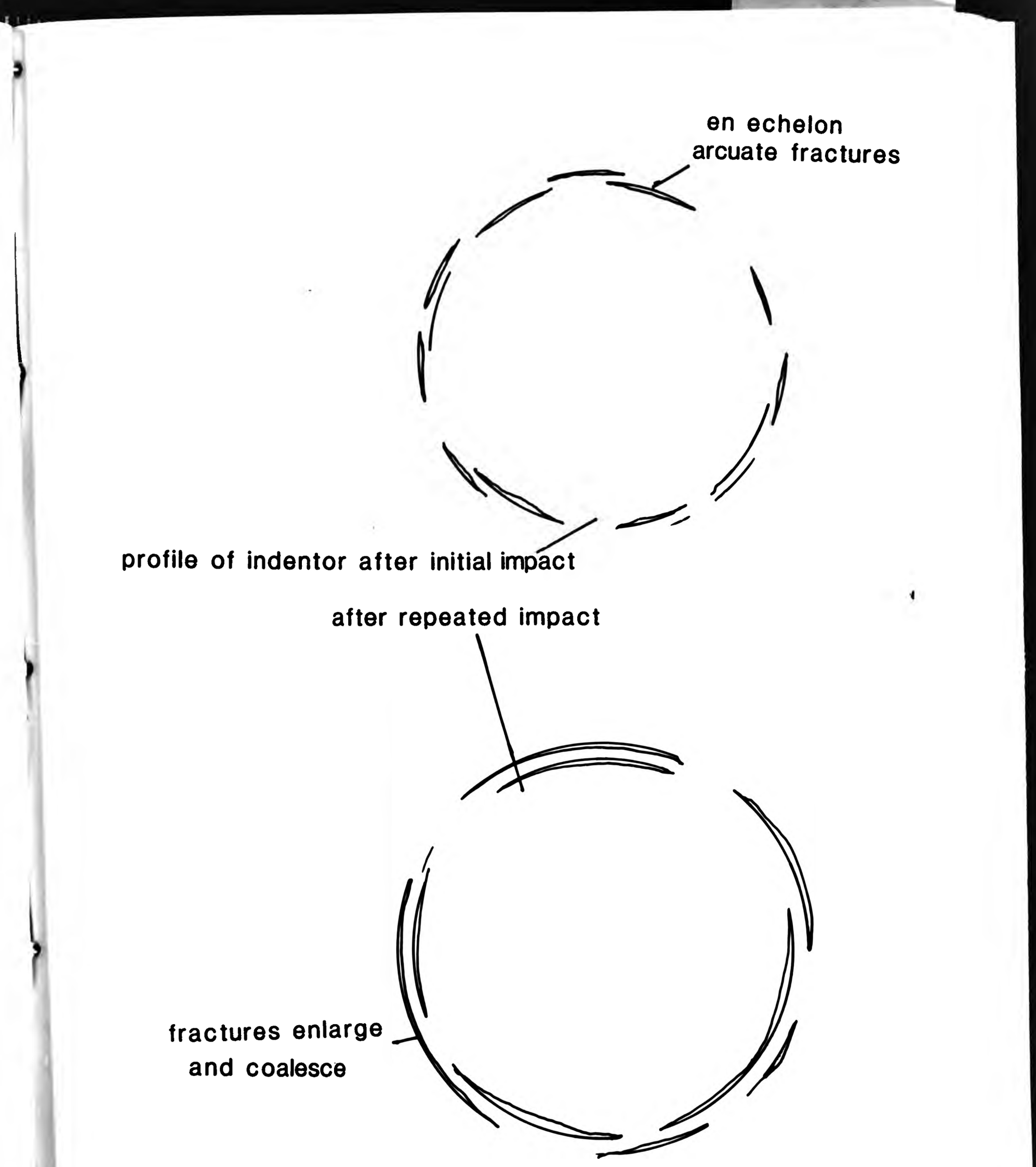

Fig.9.3.1 Mechanical model showing the development of circular fractures

9.4 NUMERICAL MODELLING

9.4.1 Modelling of cone sheet parameters

Theoretical modelling of physical characteristics of cone sheets has only been carried out once previously, to the knowledge of the present author, by Kresten (1980) who examined dip directions of cone sheets of the Alno complex, Norway, and concluded that the complex could be subdivided into two conjugate sets of sheets.

I have designed simple theoretical models for the strike and dip of cone sheets, as these are the most important characteristics of a cone sheet set.

9.4.2 Strike

A number of assumptions are made in order to investigate the strike of cone sheets, these being:-

1. the axis is vertical,
2. cone sheets are perfectly circular in plan view,
3. cone sheets of a set are equally developed around a centre of activity.

9.4.2.1 Model 1 -

In plan view the circular outline of a cone sheet set (A) may be subdivided into segments of 10° (Fig.9.4.1), cone sheets within each segment will have similar strikes and therefore a mean value will characterise each segment. Figure 9.4.1 shows the distribution of expected mean strike around the cone sheet

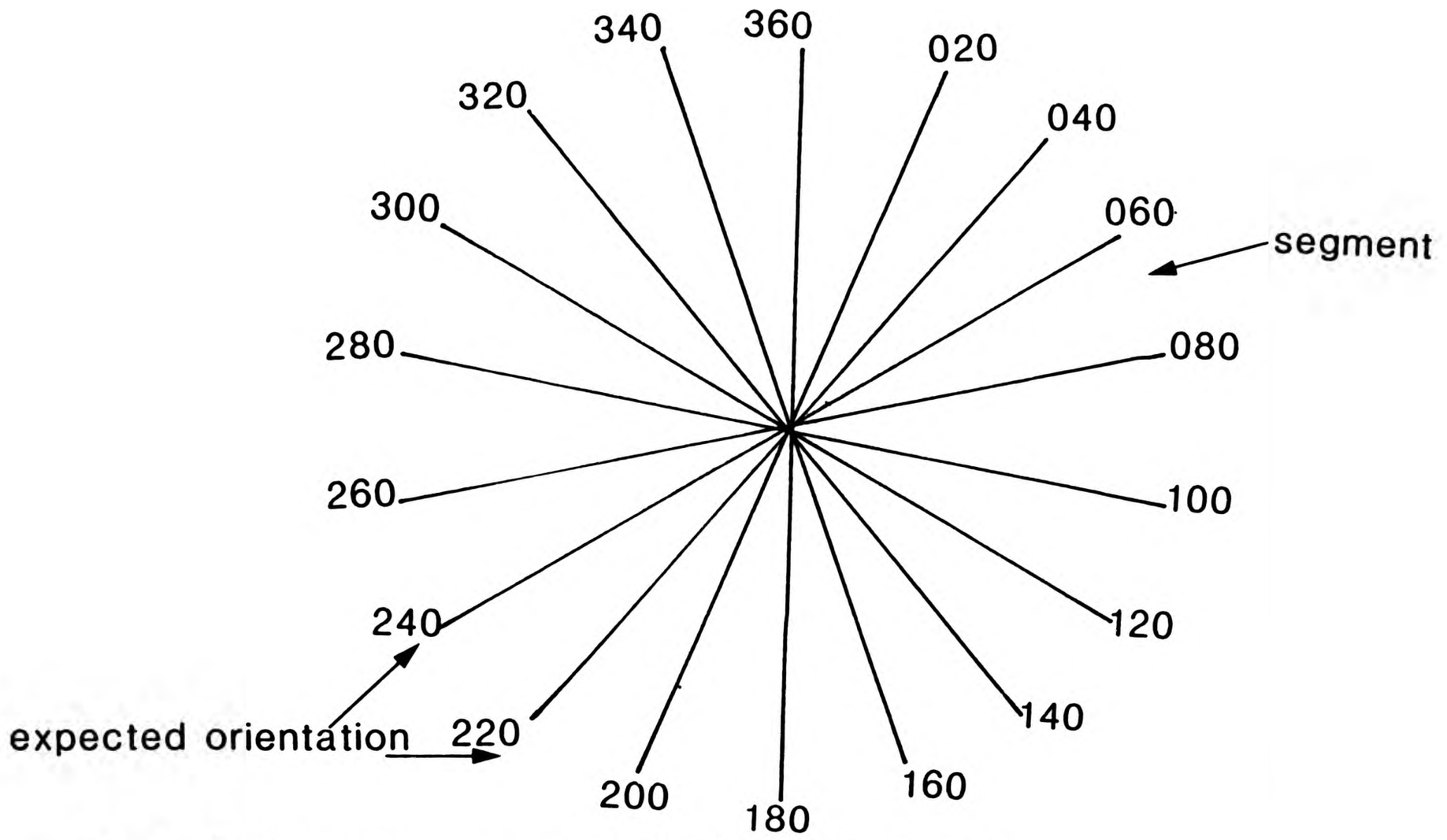

Fig.9. 4.1 Model 1, a series of radially distributed 20° segments . The expected orientation for cone sheets found within each segment shoud fall between the two values

set in each segment.

9.4.2.2 Testing Model 1 -

Model 1 (a radial grid in 20° intervals) was placed upon a 1:50000 topographic map of Ardnamurchan as the base map, Centres One and Two were handled separately (Centre Three is not used due to the limited amount of available data). The centre of the grid is located upon each centre of activity. The strike of the cone sheets collected in the field is recorded for each of the 20° segments. A comparison of the model derived strike distribution to that derived from the actual distribution is then carried out.

When the model is applied to the Centre One data, cone sheets only occur in five of the segments (Table 9.1). In one segment the model mean and the field data are the same, in the remaining segments the field data strikes in a more NE-SW direction than that derived from the model.

A more complete picture is obtained from the Centre Two data, where cone sheets occurring in 16 of the segments (Table 9.2). Approximately half of the model mean strike values equal the modal strike of the field data. In the remaining segments the spread of the strike frequency of the field data is often over several classes, so that 3 to 4 classes on either side of the model mean strike contain a large proportion of the sheets.

In both the examples used, Centre One and Centre Two, the simple model does not fit the field data and therefore indicates

set in each segment.

9.4.2.2 Testing Model 1 -

Model 1 (a radial grid in 20° intervals) was placed upon a 1:50000 topographic map of Ardnamurchan as the base map, Centres One and Two were handled separately (Centre Three is not used due to the limited amount of available data). The centre of the grid is located upon each centre of activity. The strike of the cone sheets collected in the field is recorded for each of the 20° segments. A comparison of the model derived strike distribution to that derived from the actual distribution is then carried out.

When the model is applied to the Centre One data, cone sheets only occur in five of the segments (Table 9.1). In one segment the model mean and the field data are the same, in the remaining segments the field data strikes in a more NE-SW direction than that derived from the model.

A more complete picture is obtained from the Centre Two data, where cone sheets occurring in 16 of the segments (Table 9.2). Approximately half of the model mean strike values equal the modal strike of the field data. In the remaining segments the spread of the strike frequency of the field data is often over several classes, so that 3 to 4 classes on either side of the model mean strike contain a large proportion of the sheets.

In both the examples used, Centre One and Centre Two, the simple model does not fit the field data and therefore indicates

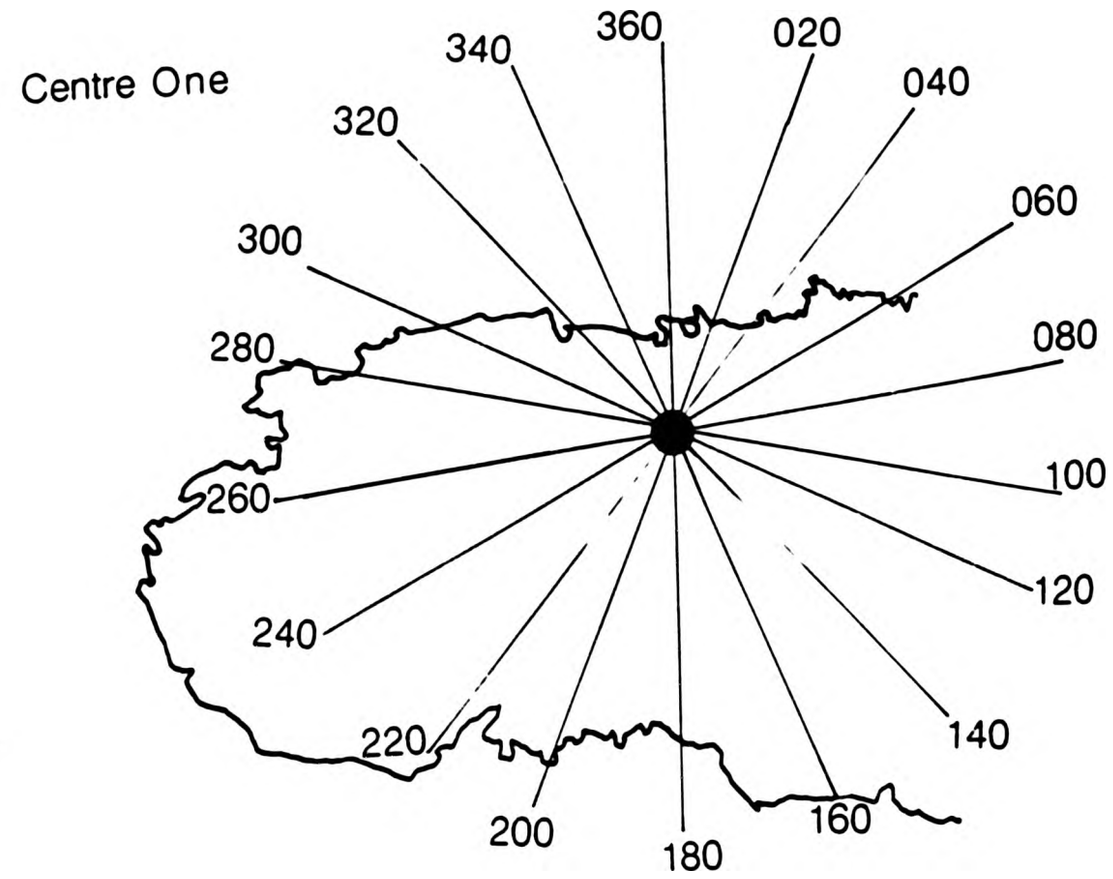

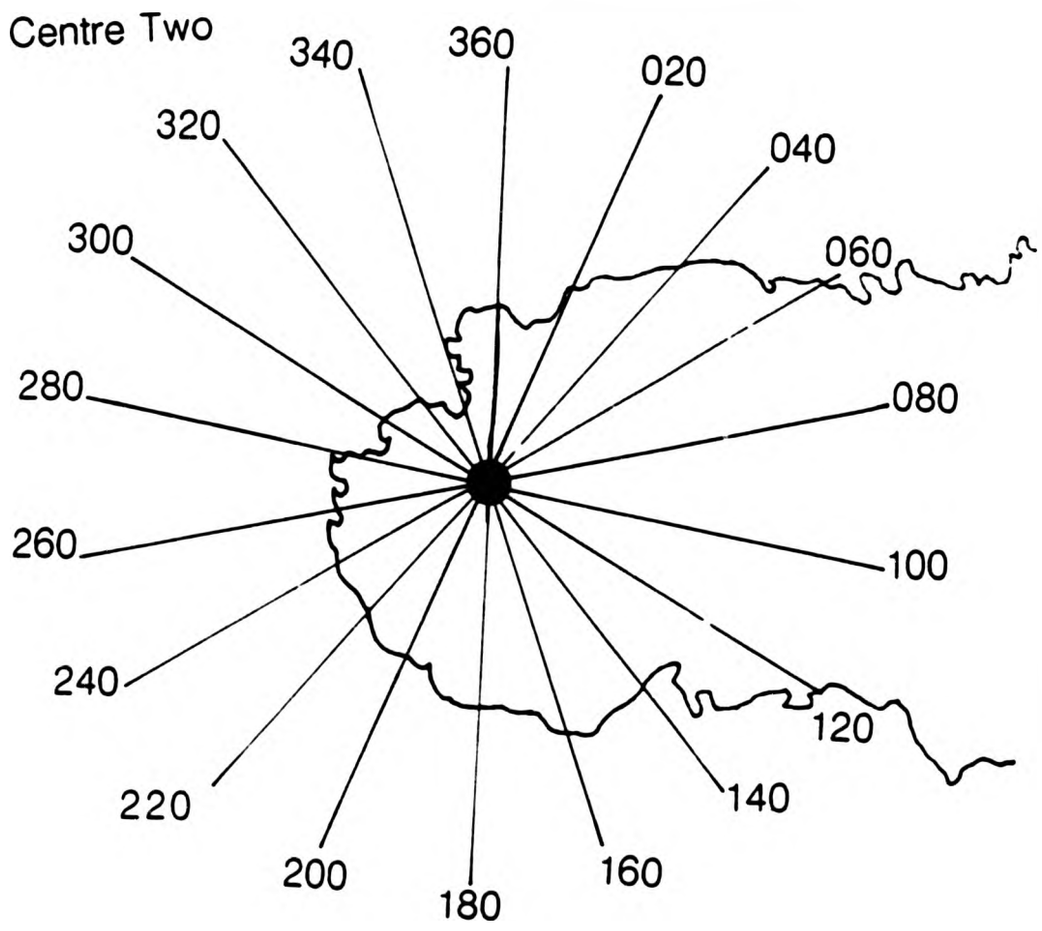

all orientations are measured clockwise from dip
expected orientation
focus of activity

Fig.9.4.2 Maps showing the location of Model 1 segments for the cone sheets of Centres One and Two

Table 9.1 Distribution of strike of the Centre One cone sheets (Model 1)

	Segment Orientation					
Strike classes	340°	360°	020°	040°	060°	080°
0 - 020	3	8	0	4	11	
021 - 040	0	17	0	0	0	
041 - 060	0	8	4	6	0	
061 - 080	0	17	0	0	0	
081 - 100	0	0	0	0	0	
101 - 120	0	0	8	0	0	
121 - 140	0	0	0	0	22	
141 - 160	0	0	0	4	11	
161 - 180	0	0	0	0	0	
181 - 200	0	17	0	0	0	
201 - 220	0	0	4	4	0	
221 - 240	0	0	4	2	0	
241 - 260	5	8	4	2	0	
261 - 280	5	8	8	4	0	
281 - 300	23	0	21	4	0	
301 - 320	38	8	25	18	0	
321 - 340	18	0	13	32	44	
341 - 360	10	8	8	16	11	

Figures given are percentage frequency per segment
Shaded areas indicate mean model strike values

Table 9.2 Distribution of strike of the Centre Two cone sheets (model 1)

Strike	Orientation of segments																
	-020	-040	-060	-080	-100	-120	-140	-160	-180	-200	-220	-240	-260	-280	-300	-320	-340	-360
000-020		5					50								3		2	
021-040	1	3	1				51								14	18		
041-060	7	3	2				47			1					14	34	3	
061-080	10	3	1				16		11	6					7	32		2
081-100	39	5					2		22	18						5	12	2
101-120	22	2	1				4		44	25					7		6	10
121-140	4	3					9		11	8					21	2	44	37
141-160	1	6					6								7		48	26
161-180	1						7		11	2							72	8
181-200							8			2							11	2
201-220	3	6					6			1								
221-240	7	3	6				2			1			1			2		
241-260	36	29					2									2		
261-280	53	51	2				3											
281-300	48	59	2				3								7		6	
301-320	22	44	4				8									2		
321-340	7	19	5				5								21		3	6
341-360		2					6									2		2

Actual distribution of sheets are indicated by the figures
The expected distribution of the sheets is indicated by shading

that either both Centre One and Centre Two cone sheets do not form a circle or that within the two sets there are sub-sets.

By moving the centre of the radial grid by 0.5km, either to the east or the west, results in a corresponding shift in the expected (model) mean strike value for each location. For example, if the centre of the grid is placed 0.5km to the east of the location of Centre Two activity (Aodainn), cone sheets outcropping on the north coast traverse now occupy segments with a more northerly strike than in the first model. However, cone sheets outcropping on the south coast traverse occupy the same segments as in the first model. A change in the position of the centre of the radial grid to the north or south of the location of Centre Two activity results in no change in the location of the segments. Thus, a number of closely spaced centres of cone sheets, whose general position is that of the "centre of activity", would result in a spread of strike values in each segment.

Model One has shown that a single set of cone sheets cannot account for the variation of strike values seen in the Centre Two data. Neither can model One explain the segment by segment variation seen in the Centre Two data.

9.4.2.3 Model 2 -

This model may be constructed by superimposing the plan of a second cone sheet set (B) upon the first cone sheet set (A, Model 1) with their centres being slightlt offset from each other (Fig.9.4.3). Measurement of the strike of sheets within the area defined by Set A will result in a distribution of mean

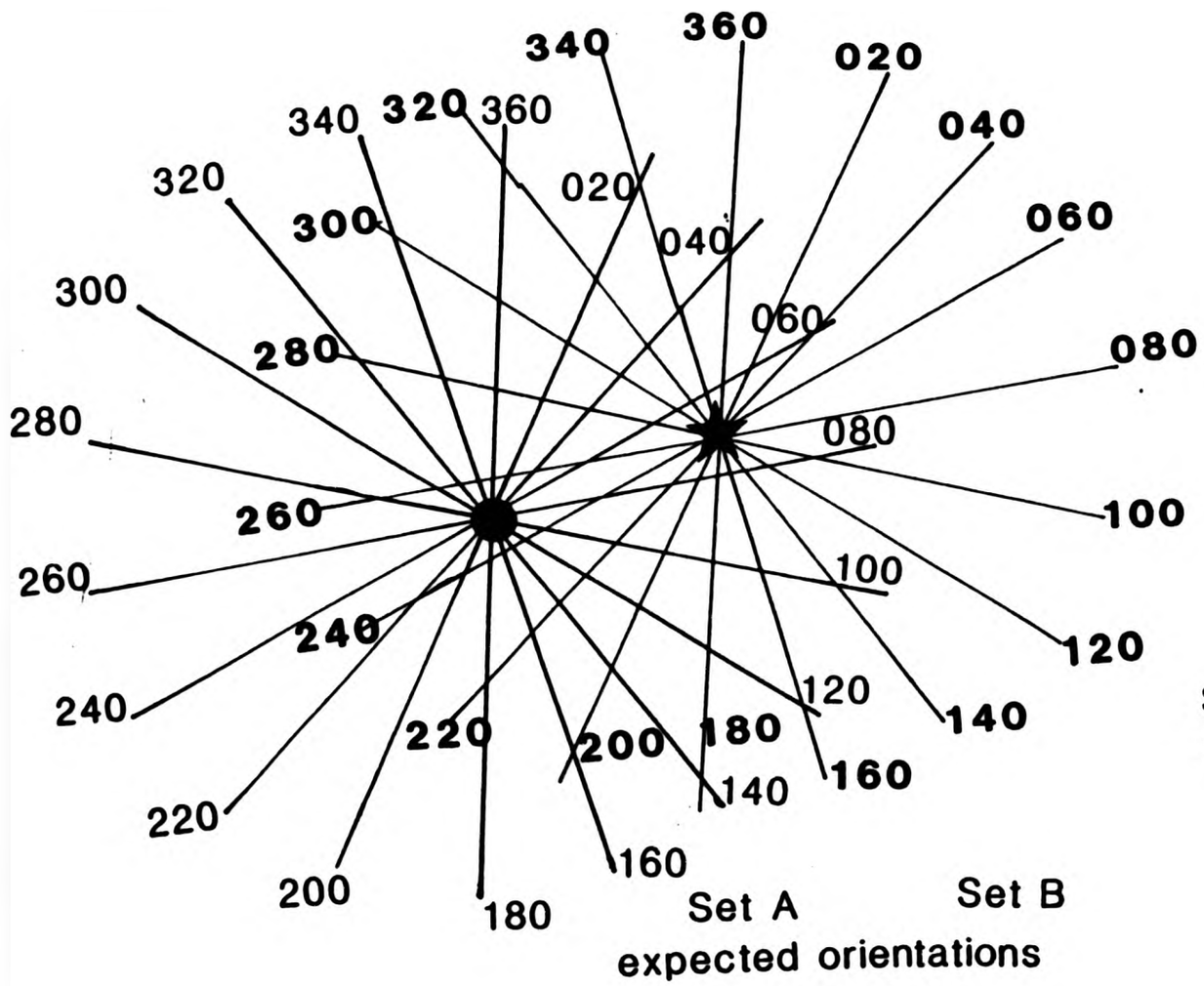

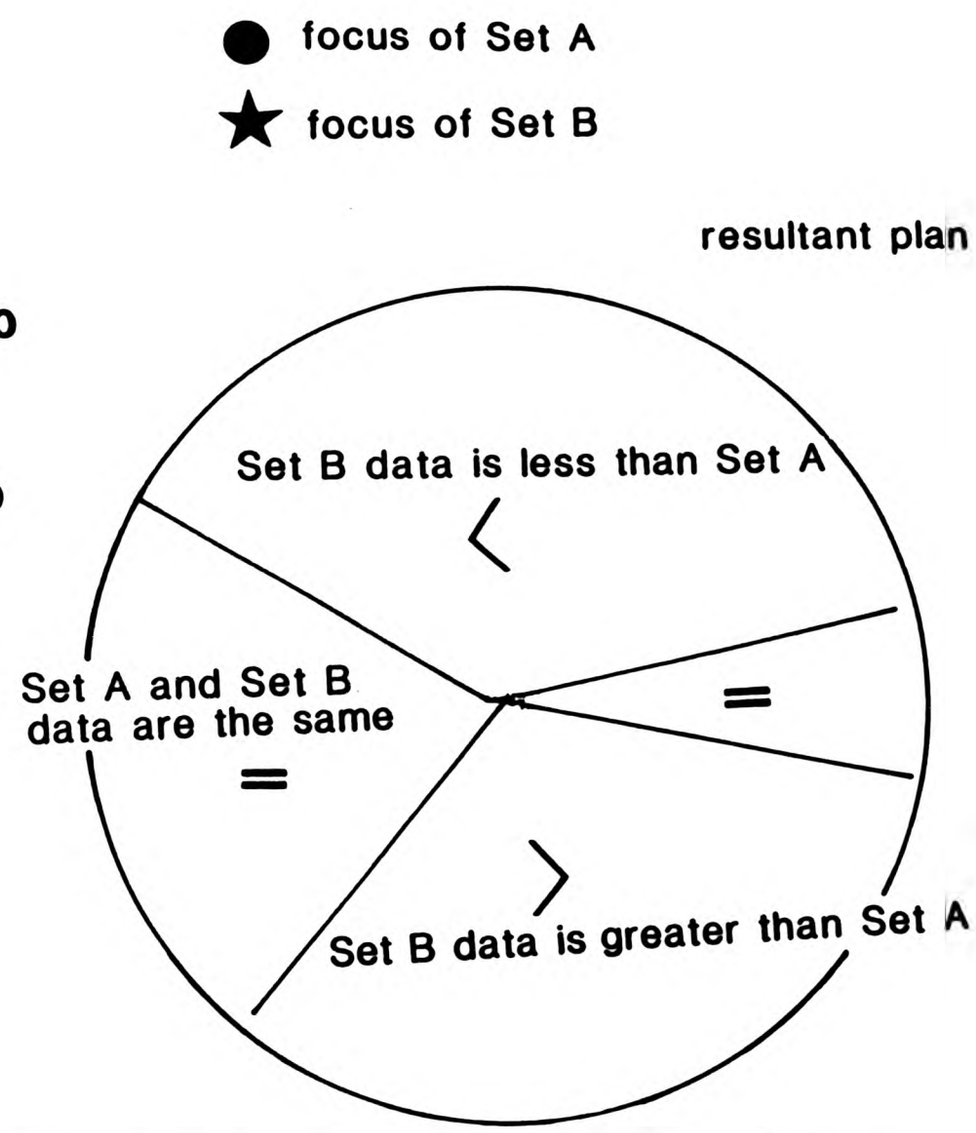

Fig.9.4.3 Model 2 Two overlapping cone sheet plans with their centres closely located

strike that differs from Set A alone (Model 1). The strike distribution can be subdivided into three sectors:-

1. where mean strike is less than in Model 1,
2. where mean strike is greater than in Model 1,
3. where mean strike is equal to Model 1.
(Fig.9.4.4)

The location and extent of these sectors depends on the amount and direction of the offsetting of the superimposed centre of Set B. Figure 9.4.4 shows a series of diagrams in which two cone sheet plans have been superimposed on each other, each diagram illustrating a different relative position of the two cone sheet plans. The result of these superimpositions is the relative location of the <, > or = sectors. By applying this model to the field data it is possible to determine if more than one cone sheet set is present.

9.4.2.4 Testing Model 2 -

When Model 2 is applied to the Centre Two data a number of sectors are formed. The series of diagrams representing Model 2 show four equally developed sectors subdividing the plan view of the cone sheet set. However, the sectors resulting from the Centre Two data do not correspond to that of the model, in that six sectors are formed (Fig.9.4.5). A similar pattern can be obtained by superimposing diagrams 2 and 5 of Fig.9.4.4 upon each other. It is therefore possible that three or more cone sheets sets with closely spaced centres of activity may be represented by the cone sheets of Centre Two.

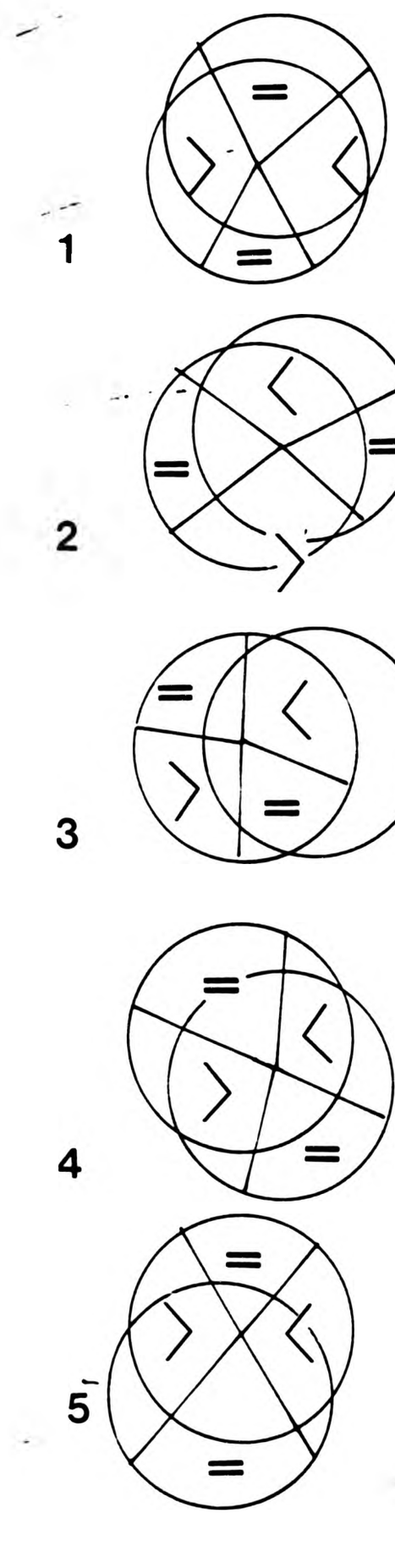

all orientations are measured clockwise from dip

= set A and set B data are the same

< set B data is less than set A

> set B data is greater than set A

Fig.9.4.4

Model 2 in which two cone sheet sets (A and B) are superimposed, their centres being slightly offset from each other. Diagrams 1 to 5 illustrate the variation in orientation distribution resulting from the progressive shift in position of set B. All orientation variations are measured with respect to Set A.

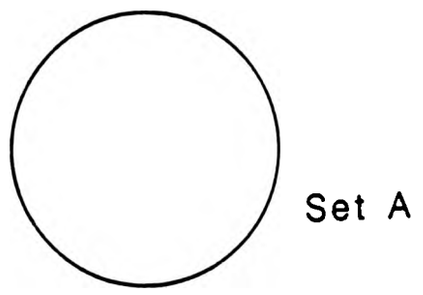

Set A

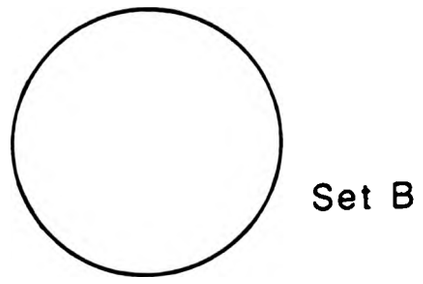

Set B

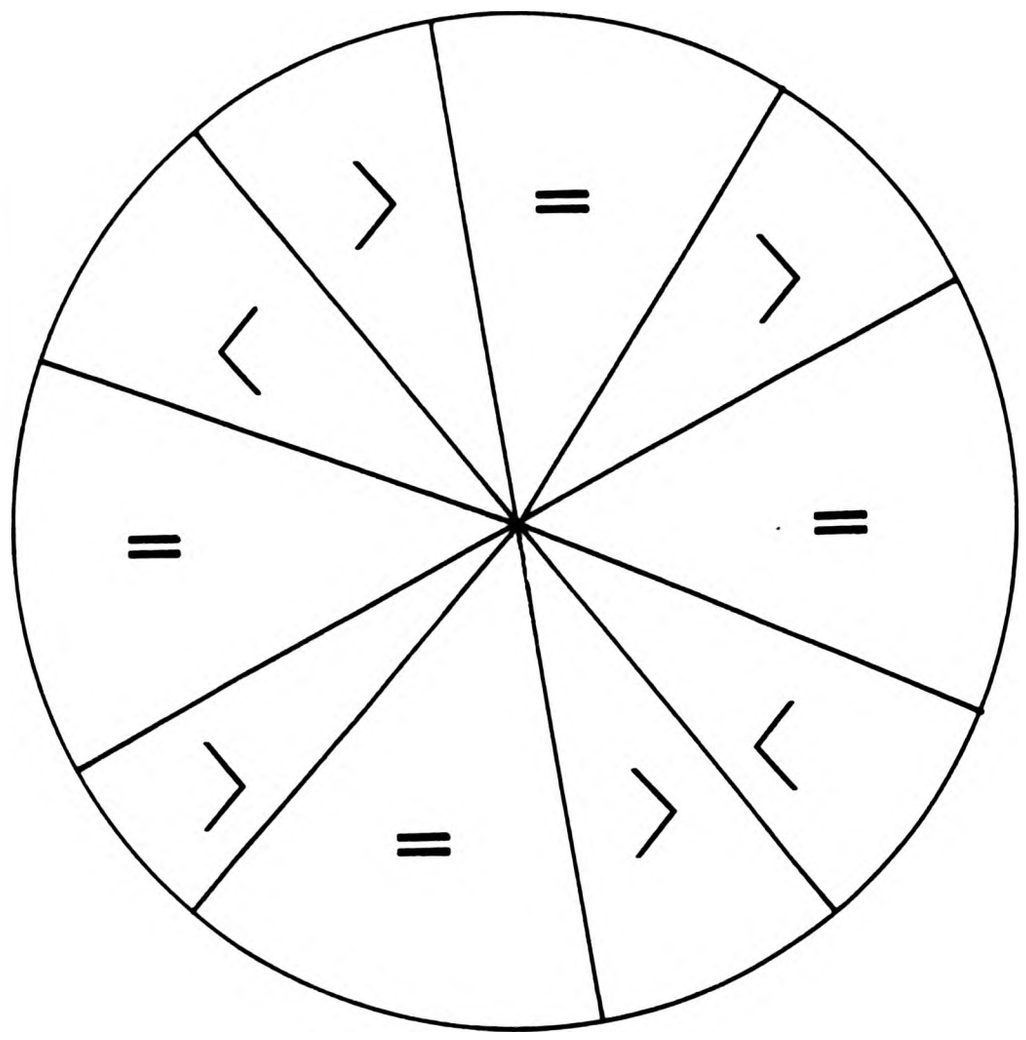

sector a number of similar segments

= field and model data are the same

< field data is less than the expected model value

> field data is greater than the expected model value

all orientations are measured clockwise from dip

Fig.9.4.5 Application of Model 2 to all the Centre Two data

9.4.3 Dip

The assumptions for a model of dip characteristics are:-

1. that the plan view is circular,
2. that the cone sheet axis is vertical,
3. that the sheets dip at a constant angle towards a central focus.

9.4.3.1 Model 3 -

In vertical section the model has a vertical axis, an apical angle of 90° with the limbs of the cone dipping at 45° (Fig.9.4.6). If the cone sheet axis were inclined relative to the horizontal the following angles of the dip of the limbs would result:

Dip of cone sheet axis	Dip of limbs	
	I	II
90°	45°	45°
85°	52°	38°
80°	56°	53°
70°	66°	24°

Accompanying this variation in dip is a change in the plan view of the sheets (Fig.9.4.6). The more shallowly the cone sheet axis dips, the more eccentric the elliptical plan view becomes. Also, the larger the ellipse is, the larger the geographical area over which the cone sheets occur.

9.4.3.2 Testing Model 3 -

Dip distributions of each cone sheet set show a wide variation in dip angle (Fig.5.4.10). Each set, except that of Centre Three, has sheets which dip at angles from 0° to 90°. However, Centre One cone sheets most commonly dip between 10°

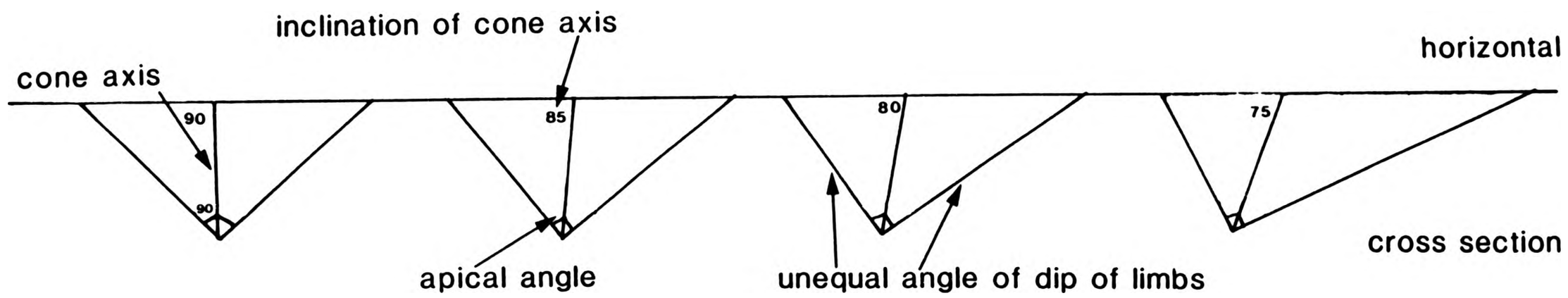

Fig.9.4.6 Model 3 Cross section and plan view of a series of theoretical cones with inclined axes and a constant apical angle of 90°

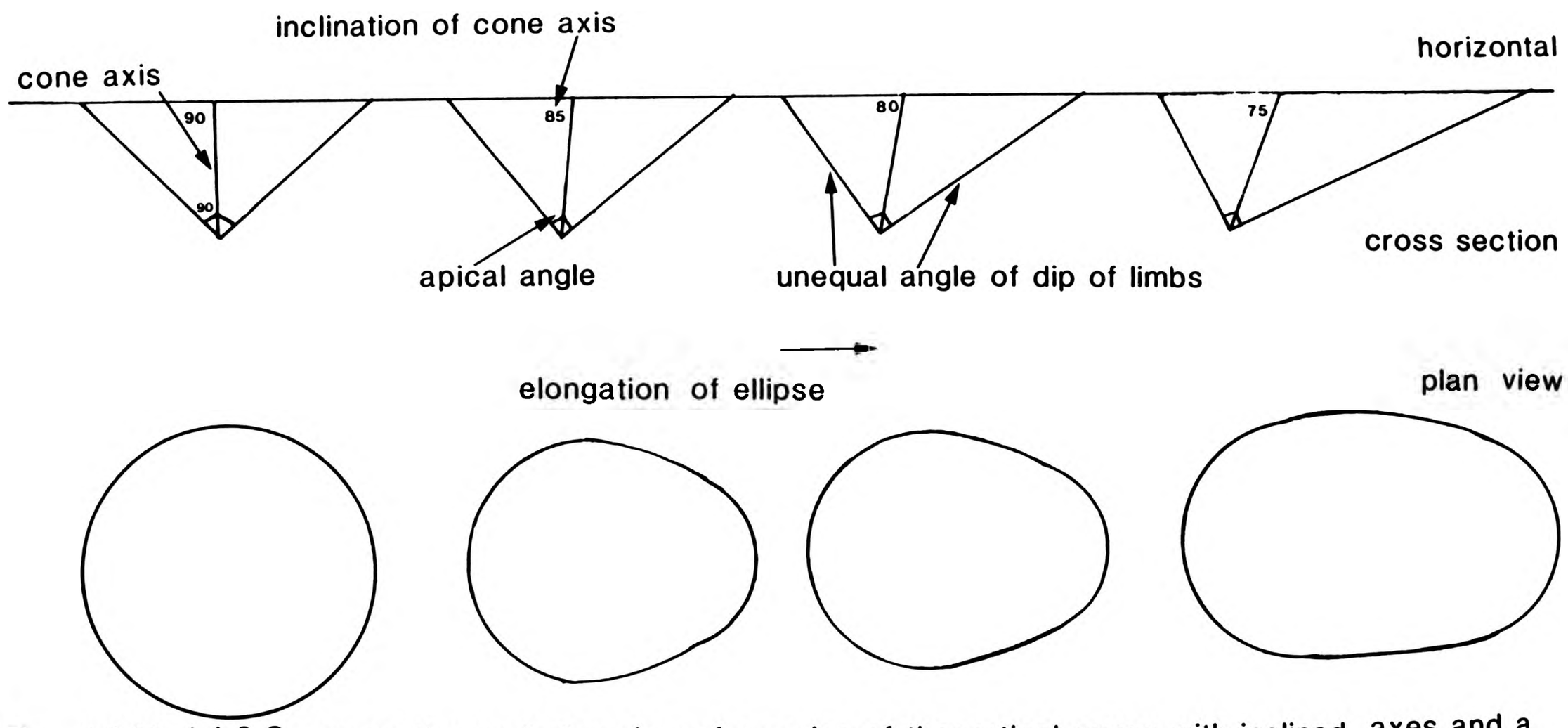

Fig.9.4.6 Model 3 Cross section and plan view of a series of theoretical cones with inclined axes and a constant apical angle of 90°

and 50°, Outer Centre Two cone sheets dip, commonly, between 30° and 70°, Inner Centre Two cone sheets dip between 60° and 80° and Centre Three sheets dip between 50° and 60°. To account for the variation, using Model 3, each cone sheet set would require several inclined cone sheet axes dipping at 85°, 80°, 75°, 70°and 65°. In this respect Model 3 is applicable to the one sheets of Ardnamurchan. Unfortunately, the associated elliptical plan view which would result from the emplacement of these inclined cone sheet axes do not fit the field data.

Model 3 shows that an inclined cone sheet axis or axes can account for the variation seen in the cone sheet sets. However, Model 3 implys elliptical plan views for all cone sheet sets. Eccentric ellipses are not seen in Ardnamurchan.

9.4.3.3 Model 4 -

Model 4 is formed by decreasing the apical angle of the cone sheet model and retaining a vertical cone sheet axis (Fig.9.4.7), consequently, the resultant cone sheets dip at steeper angles:-

Apical angle of cone	Dip of sheets
90°	45°
80°	50°
70°	55°
60°	60°
50°	65°
40°	70°
30°	75°
20°	80°
10°	85°
0°	90°

A circular plan view is still retained and dip angles may vary if the foci of cone sheet sets of varying apical angles

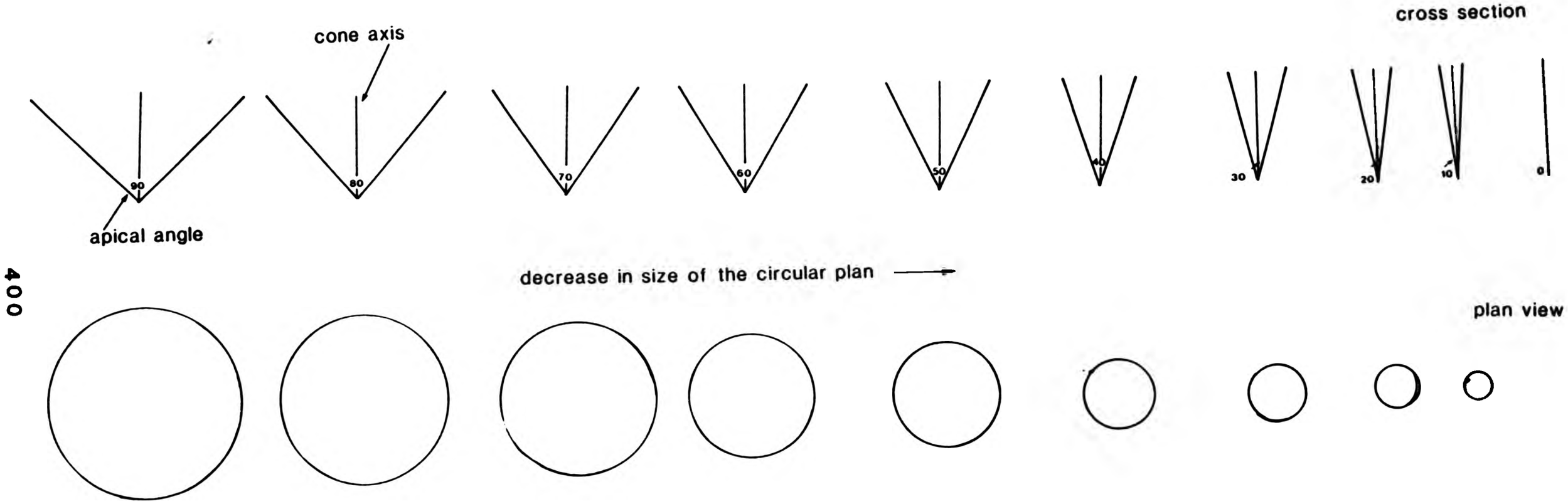

Fig.9.4.7 Model 4 Cross section and plan views of a series of theoretical cones with vertical axes and varying apical angles

originate at the same point. As the apical angle decreases so does the diameter of the circle in plan view.

9.4.3.4 Testing Model 4 -

Centre One sheets dip more shallowly than any of the other cone sheet sets and involves other factors, such as the utilization of host rock structures and therefore differs from a simple cone sheet model. However, Centre One cone sheets have a modal value of 45° which equates to a 90° apical angle.

The Outer Centre Two cone sheet data is more extensive than any other and shows a wide range in dip angles and more importantly there is a difference in angle of dip on the north and south coast traverses.

The Outer Group of Inner Centre Two cone sheets dip at a relatively constant angle of 55° to 60°, which implies a vertical cone sheet axis with an apical angle of between 70° and 60°. However, the more steeply dipping sheets of the Inner Group of Inner Centre Two would require cone sheet sets with a vertical axis and an apical angle of 40° to 20°. As the apical angle decreases the diameter of the cone sheet set in plan view also decreases, resulting in a more restricted distribtuion of cone sheets.

By combining elements of Models 3 and 4 a solution can be ascertained. Using a cone with an apical angle of 60° and inclining the axis at 80° the limbs of the cone dip at 70° and 50° respectively. If the axis is inclined at 70° then the limbs of

the cone dip at 82° and 38° respectively. In plan view the outcrop would form an ellipse. The cone sheet dips produced by this model are similar to the dip of the cone sheets which are exposed in the Inner Group of Inner Centre Two traverses and some of the cone sheets which occur on the north coast traverse. These two groups of cone sheets were grouped together as a result of cluster analysis (Chapter 5).

Centre Three sheets probably originate from a cone with an apical angle of 70° and a vertical axis.

9.4.4 Summary

The present distribution of cone sheets of Ardnamurchan may be explained in terms of superimposed and inclined cones of varying apical angles.

Centre One sheets with their sporadic distribution (Chapter 5) seem to support the theory that a number of cones of intrusion were the cause of the present distribution and perhaps supports Bahat's fracture model produced by a slow indentor. Alternatively, it may be that the present distribution represents a high structural level within the volcanic ediface and the sporadic occurrence results from the fact that few cone sheets actually reached this level.

The Outer Centre Two cone sheets seem to fit both the strike and dip numerical models such that a number of closely spaced vertical and sub-vertical cones with apical angles ranging from 90° to 60° would produce the observed distribution

patterns. The strike models showed that slight offsetting of the circular plan view can account for the distribution seen in the field.

The Outer Group of Inner Centre Two cone sheet set, along with the Centre Three cone sheet set, are perhaps examples of the most simple type. Both sets show a consistent angle of dip and indicate that they were probably formed by cones with vertical axes and apical angles of ~70°.

The Inner Group of Inner Centre Two cone sheet set is the set most dissimilar from all the others in that it approximates to a cone inclined at 70°, to the south west, to the present land surface, with an apical angle of 60°, and an elliptical outcrop.

CHAPTER 10

SUMMARY AND CONCLUSIONS

10.1 INTRODUCTION

As a culmination of this study a number of topics have been highlighted and will be discussed, these are the characteristics of an idealised cone sheet set; the redefinition of the cone sheet sets of Ardnamurchan; the extent to which country rock structures have influenced the cone sheet sets; the significance of cone sheet complexes within the B.T.I.P.; the amount of inflation of the volcanic land surface and lastly and perhaps most important of all the development of cone sheet fractures.

10.2 THE FORM AND STRUCTURE OF AN IDEALISED CONE SHEET SET

Field observations made during this study have enabled the present author to propose the structure of an idealised cone sheet set. Furthermore, the structure can be divided into three vertical zones, the cone sheets within each zone displaying unique characteristics. Throughout the following description a cone sheet set is assumed to have a vertical axis. Zone One consists of the most distal parts of the cone sheets, which may reach the surface. Zone Two consists of the middle area, halfway between the magma chamber and the uppermost extremities. Finally, Zone Three is the area closest to the magma chamber roof (Fig.10.2.1).

10.2.1 Zone One

This zone contains the distal parts of cone sheets, which may have reached the surface. The most prominent characteristic

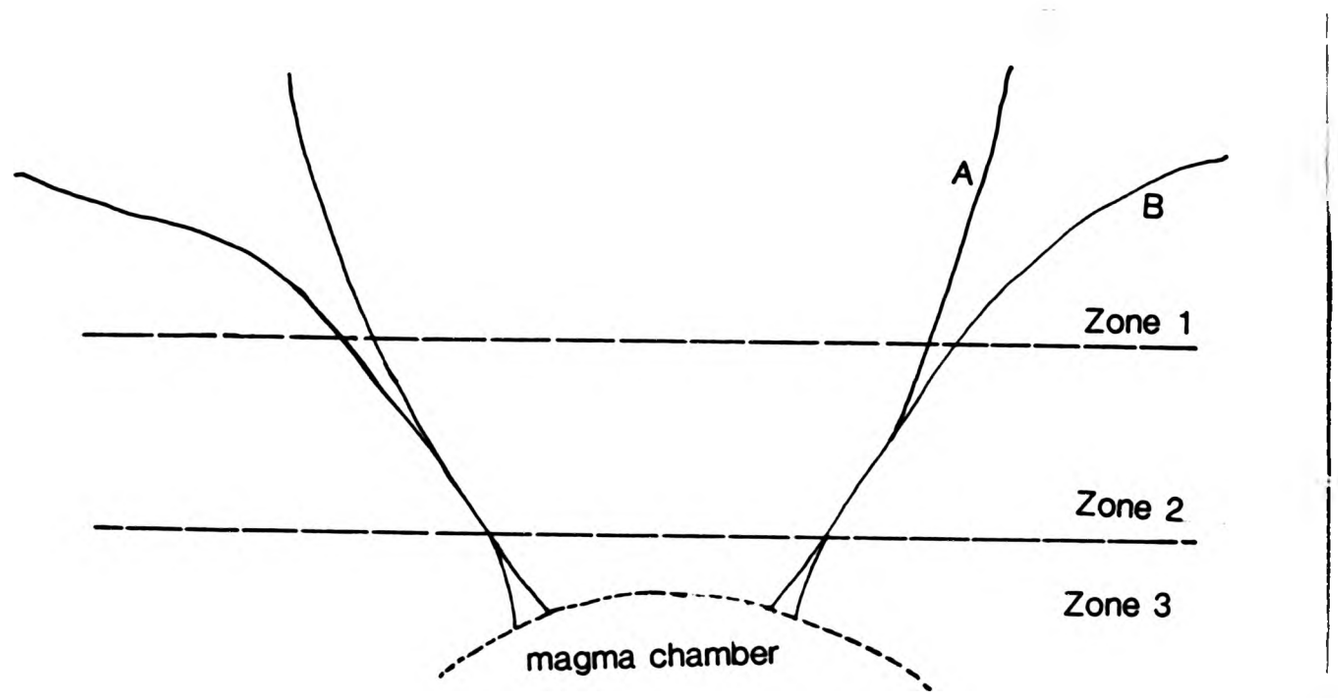

Fig.10.2.1 An idealised vertical profile of a cone sheet set

of the cone sheets in this zone is the common occurrence of termination structures. Two types of cone sheet may occur in this zone, cone sheets which have fairly steep dips and do not utilize country rock structures and cone sheets which are often shallowly dipping and may, to a large extent, utilize country rock structures. Zone One is principally divided on the dip of these two types of cone sheet.

10.2.1.1 Zone 1a -

This zone represents the more steeply dipping cone sheets in the distal parts of a cone sheet set and is an upward extension of Zone 2, with the main difference being that the intensity of cone sheets is less in Zone 1a than in Zone 2. This is due to the fact that Zone 1a is located higher within the volcanic ediface, and farther from the magma chamber. Angles of dip are slightly steeper (50°-60°) than those of Zone Two (45°-50°). A high percentage of cone sheets exhibit termination structures. Due to the lower intensity of intrusion in this zone it follows that strain profiles are also reduced. In addition, the area over which cone sheets are emplaced diminishes. As a consequence of distance from the focus of activity (5-8km) the thickness of the cone sheets (approximately 75cm) is less than that for Zone Two. These cone sheet fractures open both by shear and tension. The Outer Group of Inner Centre Two is an example of cone sheets which form in this zone.

10.2.1.2 Zone 1b -

The cone sheets of this zone differ from those of Zone 1a in that they utilize country rock structures, have less steep dips, are thicker, up to 20m, and occur over a large geographical area. The dip angles, 20°-40°, are lower than those of cone sheets in Zones Two and 1a. In a horizontal cross section these sheets occur between 4-6km and 6-10km from the epifocus. In contrast to those of Zone Two, the distance between cone sheets may be widely spaced. Cone sheet termination structures are abundant in this zone. Lower pressures in the more distal parts of a cone sheet complex result in less dynamic mechanisms of sheet propagation e.g. extension splitting. Cone sheets in this zone open by hydraulic tensile fracturing. Centre One cone sheets are an excellent example of Zone 1b cone sheets.

10.2.2 Zone Two

This zone is the most commonly exposed and recognised zone of a cone sheet complex. It is characterised by an intense array of cone sheets, the thickness distribution is positively skewed about 1m to 1.5m. Thick sheets (10-30m) are rare. The angle of dip is normally distributed about a mean value of 45°-50°; the mode has a similar value. Similarly, a normal distribution of strain in a plan view of the complex can be expected. The central area which is devoid of cone sheets varies from 2 to 4km in diameter, with the lateral parts of the complex occurring up to 7km radius from the epifocus. Both shear and tensile opening mechanisms occur in this zone. Few cone sheets in this zone show termination structures. An example of this zone is the Outer Set of Centre Two.

10.2.3 Zone Three

It is predicted that this zone occurs above the shoulder areas (Phillips, 1974; Fig.1.1.2) of the magma chamber. Because the zone is proximal to the area of indentation the principal stress system is tensile, with tension being the main opening mechanism of the cone sheets. Although no example of this zone has been recognised in Ardnamurchan, its characteristics may be inferred from other data. The geometrical constraints indicate that a radius of 1 to 2km would be the maximum and the zone probably contains thick, multiple sheets. It is possible that these sheets would resemble Pollard's et al. (1973) fingered periphery of a sheet, albeit on a larger scale.

10.2.4 Summary and Conclusions

Based on the field evidence gained from the Ardnamurchan cone sheets the structure of a cone sheet set can be identified. Two zones can be identified, and a third implied, in a vertical transect through an idealised cone sheet set (Table 10.1).

The applicability of this three fold zonation is, at present, somewhat limited due to the lack of detailed field studies available for other cone sheet sets. From map studies of the Mull and Skye cone sheet sets, it seems that both fall into the Zone Two category with the Loch Scridain Sills in SW Mull most likely representing Zone 1b; further field studies will be neccessary before any formal conclusions can be made. However, from the work of Siggurdson (1968) on the Snaefellsnes cone sheets in Iceland, a Zone Two can be identified from the large

Table 10.1 IDEALISED CONE SHEET SET – Three zone classification

CHARACTERISTICS	ZONE One A	One B	Two	Three
Dip	50°-60°	20°-40°	45°-50°	70°-90°
Thickness of cone sheets	0.75m	up to 20m	1-1.5m	10m?
Minimum radius of cone sheets from epifocus	3km	4-6km	2-4km	0-1km?
Maximum radius of cone sheets from epifocus	4km	6-10km	7km	1-2km?
Large number of termination structures present	YES	YES	NO	NO
Examples	Outer Group of Inner Centre Two	Centre One	Outer Centre Two	This zone is not exposed in Ardnamurchan

number of sheets within the traverse, the skewed thickness distribution, the thickness mode being 1m and the dip distribution having a modal value of 50°. To ascertain whether the three zone classification is applicable to other cone sheet sets requires detailed field work.

10.3 CONE SHEET SETS: the same or different structural levels?

Based on Anderson's (1936) trumpet-shaped cone sheet, Richey et al.(1930) concluded that the more steeply dipping Inner Centre Two cone sheets (average dip 60°) compared to the Outer Set of Centre Two (average dip 49°) represent a cross section close to the focus of a cone sheet set. The present author disagrees with this conclusion (Chapters 5 and 9) but, however, does believe that the cone sheet sets of Ardnamurchan depict different structural levels.

From the statistical analysis of the cone sheet data it has become evident that each cone sheet set has a distinguishing set of characteristics and it is, therefore, possible that these characteristics may be attributed to different structural levels of a cone sheet set.

A transect through an idealised cone sheet set, following Phillips' (1974) cone sheet model, finds two types of cone sheet in the upper extremities of a cone sheet complex. The cone sheets of the first type, occurring in Zone 1a, have dips of 55°-70° and probably opened by a shear mechanism. The second type is a shallowly dipping, 20°-30°, sheet which most probably developed by hydraulic tensile fracturing (Fig.10.2.1). The

various theories about the methods of propagation of intrusions (Chapter 7) agree that terminations of cone sheets, and minor intrusions in general, are often represented by en echelon sets. Therefore, the large number of en echelon sets in the Outer Group of the Inner Set of Centre Two cone sheets, combined with the high angle of dip (50°-70°), indicates that the first type of cone sheet in the upper extremities of the complex can be recognised.

En echelon sets are also a prominent feature of the Centre One cone sheets, which again point towards a location high in the profile of a cone sheet complex. In addition, there are a number of other features shown by the Centre One cone sheets which indicates that this set is located high within a cone sheet complex. In general, the intensity of the cone sheets over a large area is low, compared to that of the Outer Set of Centre Two. The large distance between Centre One cone sheet fractures may be because not all cone sheets reach the highest levels due to insufficient magma pressure, therefore, a lower intensity of numbers would be expected in the distal parts of the complex. Another feature of high level activity is the development of agglomerates. Along the Centre One traverse a number of cone sheet type intrusions are formed of intrusive agglomerates. In Phillips' (1974) cone sheet hypothesis when the magma pressure is reduced hydraulic fracturing occurs, resulting in the formation of sills. The low-dipping cone sheets found along a large part of the Centre One Traverse probably belong to this second type of cone sheet which occurs in the distal parts of a cone sheet complex. Also, utilization of country rock structures is common in the Centre One cone sheets,

irrespective of the dip of the structure. In combination, these factors point toward the conclusion that the Centre One cone sheets, at the present level of exposure, represent a high structural level within a cone sheet complex (Fig.10.2.1).

The next level of the vertical transect through an idealised cone sheet set is Zone 2 (Fig.10.2.1). This area, midway between the focus and the upper levels of the cross section, probably contains the largest number of cone sheets. As this area is close to the focus of activity, there are no restrictions with regard to loss of pressure or magma availability. Similarly, this zone is most probably the best location in which to view shear diplacements of structures in the country rocks caused by the emplacement of cone sheets, since it is above the zone of tension developed across the magma chamber roof and, therefore, following Phillips, shear fractures should be in evidence. Both the north and south coast Outer Centre Two cone sheets show a large number of cone sheets of similar thickness which may be thought to represent this central zone. The majority of both two- and three-dimensional displacement examples have been gained from the Outer Centre Two cone sheets. Therefore, not only at the present level of erosion but also within a vertical sense, the Outer Centre Two cone sheet set demonstrates the most intensively developed region of a cone sheet set.

The Inner Group of the Inner Centre Two cone sheets are thin, of a constant thickness (approximately 1m) and occur within a restricted area and have few termination structures. These features fit Zone 2 in all but one characteristic, that is dip.

These sheets dip at approximately 70°. To account for this data, the axis of the cone sheet set is required to be inclined towards the south with the result that the sheets of the south and western parts of the set are more steeply dipping than the sheets to the north and east, which in turn dip more shallowly than the idealised cone sheet set (Chapter 10.2). This group of cone sheets therefore occur at a similar structural level as the Outer Set of Centre Two cone sheets.

In conclusion, the cone sheet sets of Ardnamurchan illustrate three different cross sections through an idealised cone sheet complex. The lowest level exposed is that of Zone 2, for example, the Outer Set of Centre Two. At higher levels two different types are exposed, firstly where no fanning of the cone sheet "trumpet" occurs is represented, for example, by the Outer Group of Inner Centre Two and, secondly, where there is some fanning of the cone sheet "trumpet", is represented by the Centre One cone sheets.

10.4 THE ARDNAMURCHAN CONE SHEET SETS REDEFINED

10.4.1 Previous Investigations

Richey et al.(1930) recognised four cone sheet sets in Ardnamurchan; these being Centre One, Outer Centre Two, Inner Centre Two and Centre Three, which belong to three centres of activity (Fig.9.2.1). Conversely, Durrance (1967) attributed all cone sheet sets to a single centre which displays an inclined axis (Fig.9.2.2). Based on the statistical analysis

and field relationships of the cone sheets, Durrance's idea has been rejected whereas the theory of Richey et al. (1930) has been modified, particularly with regard to the Centre Two cone sheets.

Durrance's (1967) proposal is refuted on the basis of field evidence, cross cutting relationships, annular outcrop, conjugate fractures, strike and dip and utilization of country rock structures. The subsequent analysis of the data indicates that the central intrusive complex has within it a number of individual cone sheet sets that belong to separate fracture systems. Further evidence to refute Durrance's classification is gained from the geochemical evidence of Gribble (1974) and Holland and Brown (1973).

Durrance (1967) bases much of his theory on the attitude of the cone sheets belonging to the Inner Centre Two set (70°av.dip) (Fig.10.4.1) and those of Centre One (20°-40°av.dip). He unites the two sets together as being representative of the cross section of the single event fracture system and proposed that these two cone sheet sets represent the eastern and western limbs, respectively, of an inclined cone axis, disregarding their separation by several intrusive events. Evidence will be given later which separates the cone sheets in these two areas in terms of time, space and structural level. Also, Durrance failed to consider that the low dipping sheets of the Centre One cone sheet set, particularly those occurring at Ockle Point, are controlled largely by the bedding in the Jurassic (Lias) host rock. The control by pre-existing structures in the country rocks of the attitude of cone sheets in the Ockle

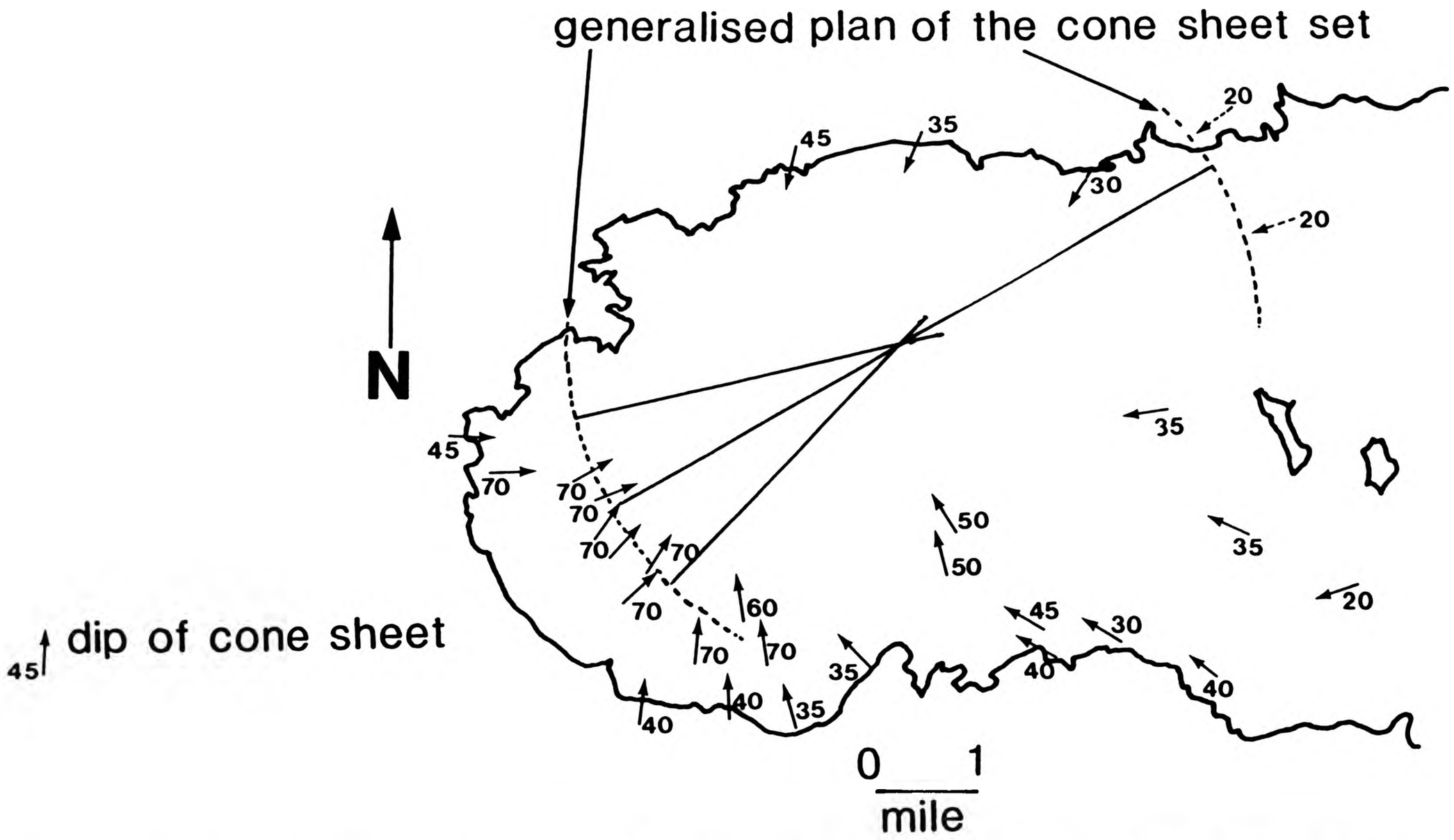

Fig.10.4.1 The interpretation by Durrance (1967) of the dip direction and value of the cone sheets of Ardnamurchan

Point area is pronounced, with both the shallowly dipping Jurassic bedding and the steeply dipping foliation in the Moine rocks being utilized by the sheets. This may be explained in either or both of the following two ways, 1) this location marks the distal part of the Centre One cone sheet complex, being in a region of low magmatic and lithostatic pressure, or 2) these sheets occupy hydraulic tension fractures (after Phillips, 1974). Durrance's single simple cone model is able to accommodate the 20° dip, 30m thick sheets parallel to bedding in the area of Ockle Point but does not account for the steeply dipping (70°), thin (0.50m) cone sheets which parallel the Moine foliation in this area.

The geochemical analyses by Holland and Brown (1973) of cone sheets sampled from selected traverses results in several groupings. The location of these grouped regional analyses on a factor analysis diagram (Fig.4.4.1) tends to support the subdivision of cone sheet sets as given by Richey et al. (1930). Gribble's (1974) geochemical analyses of the dolerites of Ardnamurchan shows a slight iron-enrichment trend for each of the three centres of activity and the plot of normative data on an Olivine-Nepheline-Quartz diagram for each of the centres indicates overlap. Thus, both the geochemical evidence of Holland and Brown (1973) and Gribble (1974) shows that the chemistry and iron-enrichment trends for the intrusions of all three centres are very similar. Based on this evidence it seems that the initiation of activity associated with each centre and it's cone sheets was caused by different magma bodies and that each magma body had a similar composition and was therefore derived from the same source.

Both field and geochemical evidence point to separate centres of activity with associated cone sheets. It will be shown later that the steeply dipping cone sheets of the Inner Centre Two can be accounted for by an inclined cone sheet axis which dips to the south.

10.4.2 The concept of three centres

Evidence to support the existence of three successive centres of activity is obtained both from field studies and the subsequent analysis of the collected cone sheet data. The types of data which substantiate the concept of three centres are; cross cutting relationships; geographical distribution of the annular outcrops; conjugate fractures; stereonet plots of strike and dip; dilation maps, along with the geochemical evidence discussed above.

The cross cutting relationships between cone sheets and other igneous intrusions is admirably demonstrated by Richey et al. (1930) who proposed four phases of cone sheet emplacement (Table 2.2).

From the geological map (Plate 2.1) the annular outcrop of the cone sheet sets can best be identified for both the Inner and Outer Cone Sheet Sets of Centre Two, both of which have the same epifocus. The Centre One cone sheets form an indistinct arc and because the Centre Three cone sheets are so poorly developed no arc is formed. However, in general the annular pattern of cone sheet sets can be recognised.

Figure 5.5.3 shows the strike and dip data for all four cone sheet sets displayed on stereographic plots. Well developed arcs are shown by three of the sets with Centre Three showing a small cluster.

Similarly, the dilation maps (Figs 6.3.1-4) constructed from both field and Geological Survey map data delineate a number of cone sheet sets, marked by intensity of dilation and orientation.

Collectively all the items stated above identify the presence of three centres of activity.

10.5 MORE THAN FOUR CONE SHEET SETS?

During the analysis of the field data it became apparent that the cone sheets of Centre Two do not form two distinct sets, the Outer and Inner Sets as defined by Richey et al. (1930) rather they form three sets (Table 10.2).

Data for the Outer Centre Two cone sheets as defined by Richey et al. (1930) show a series of discrepancies which depart from that of an idealised cone sheet set (Chapter 10.3). That is, the average number of cone sheets per unit length on the north coast is double that on the south coast, also, unlike the south coast traverse that on the north coast contains a large percentage of feldspar porphyritic basic cone sheets. The dip distribution for the north coast cone sheets varies along the traverse and has, in general, higher average dip values than those on the south coast traverse. Despite the individual vari-

ations of dip of cone sheets in each traverse when plotted on a stereonet each traverse results in an arc (Fig.5.5.2). When all the Outer Centre Two data are plotted onto one diagram (Fig.5.5.3) an overall annular profile results. The strike of the cone sheets contained within the north coast traverse show a range of modal classes, whilst the sheets of the main south coast traverse (Glas Eilean-Mingary Pier) have a single modal class. The variation in strike is emphasized by the Chi^2 results which tend to highlight the more westerly striking sheets located near Faskadale, as distinct from the more northerly trending sheets located near Rubha Carrach. Again these differ from the south coast traverse which shows a change in orientation, the cone sheets possessing a more northerly strike towards the east of the traverse. Despite the larger number of sheets on the north coast traverse, the sheets are thinner, being 1-2m, compared with those from the south coast traverse which are 2m-3m. A plot of thickness against strike for the north coast cone sheets gives two peaks, at 300°-260° and 280°-320°, for the western and eastern parts of the section, respectively, which probably indicates two subsets of cone sheets. For the Sron Bheag traverse, a plot of thickness against strike gives two peaks at 060° and 100°, whereas the Glas Eilean to Mingary Pier traverse has a single peak. The two peaks at Sron Bheag may indicate the presence of another cone sheet set.

The increased number of cone sheets, together with the existence of feldspar porphyritic basic cone sheets, occurring on the north coast indicates the presence of a subsidiary cone sheet set. This is further emphasized when the cumulative

thickness of cone sheets is plotted against strike. The subsidiary cone sheet set consists of feldspar porphyritic cone sheets and suggests links with the Inner Group of Inner Centre Two cone sheets. This theory is further substantiated by cluster analysis (Chapter 5).

In Chapter 5, the Inner Centre Two data was subdivided into an Outer Group (An Acairseid, Lighthouse and Sgurr nam Meann) and an Inner Group (Upper and Lower slopes of Beinn Bhuidhe, Garbdhail valley, Upper Garbdhail valley and Beinn na Seilg) on the basis of differences of dip, geographical location and intensity of intrusion with the additional characteristic of termination structures present in the Outer Group.

The data given above indicates that the Centre Two cone sheets can be grouped into three sets (Table 10.2).

Table 10.2 The location of the three cone sheet sets of Centre Two

SET A

Sron Bheag, Glas Eilean to Mingary Castle (south coast) and Rubha an Duin Bhain to Faskadale (north coast),

SET B

West of Sron Bheag, An Acairseid, Lighthouse, Sgurr nam Meann, Rubha an Duin Bhain,

SET C

Beinn Bhuidhe, Garbdhail, Beinn na Seilg and on the north coast from Rubha Carrach to Sgeir Ghibeach.

Therefore, five cone sheet sets can be identified in the cone sheet complex of Ardnamurchan:-

1. Centre One cone sheet set
2. Centre Two cone sheet set A
3. Centre Two cone sheet set B
4. Centre Two cone sheet set C
5. Centre Three cone sheet set.

10.6 WHY ARE CONE SHEETS A FEATURE OF THE B.T.I.P.?

The B.T.I.P. contains the most intensively developed cone sheet complexes in the world, with the Ardnamurchan complex possessing the most complete cone sheet complex. The best examples of intensively developed cone sheet complexes which have so far been described outside of the B.T.I.P are from Snaefellsnes, Western Iceland, Kroksfjordur, Northern Iceland and Kenya. The first two examples are formed of basic material like the vast majority of cone sheets of the B.T.I.P. with the Kenyan complex being composed of carbonatite. It should be noted that Iceland, although active at present, forms part of the Thulean Province and is therefor allied to the B.T.I.P.. It would seem, therefore, that large numbers of thin, basic cone sheets are a characteristic feature of the Thulean Province. A number of factors may in combination be responsible for this, such as: 1) form of the magma chamber; 2) repeated rapid rise of the magma chamber; 3) regional (tectonic) structure and thickness of the crust; 4) the physical state of the country rocks, such as, the structural state or the level of water saturation which may influence the type of fracturing within the host rocks.

1) The first of these factors is the form and size of the magma chamber which exerts two controls on the geometry of cone sheets, that is the diameter and shape of the cone sheets in a horizontal plane.

Cone sheet fractures are thought to develop in the shoulder areas of a magma chamber (Phillips, 1974). Consequently, the horizontal dimensions of the magma chamber would therefore con-

trol the internal diameter of the cone sheets. Field observations indicate that the number and intensity of cone sheets intruded after the emplacement of a major ring intrusion is less than those emplaced before the development of the first major ring intrusion. After a major ring intrusion has been intruded the magma reservoir is depleted, assuming no additional influx of magma into the reservoir. Therefore, a resurgence of activity within the smaller volumed magma chamber, possibly by retrograde boiling, results in cone sheet fractures of a smaller internal diameter than those which formed before the major ring intrusion. An example of this type of cone sheet is the Outer Group of the Inner Set of Centre Two (Fig.1.1.1) which outcrops within the limits of the Hypersthene Gabbro.

Based on a gravity survey of the B.T.I.P., Bott and Tuson (1973) concluded that the central intrusive complexes are underlain by cylinders of basic/ultrabasic rock. Their findings for Ardnamurchan indicate a cylinder of 6km radius extending to a depth of 2.1km for a density contrast of 0.35gmcm or to 4.5km for a density contrast of 0.21gmcm. Similarly, a finite element analysis of the structure beneath Kilauea volcano (Dietrich and Decker, 1973) concluded that the volcano was probably underlain by a magma chamber having a cylindrical form. Because this cylindrical form of magma chamber appears to be rare, it may be concluded that Hawaii may contain cone sheet complexes similar to those of the B.T.I.P..

It is possible that the form of the magma chamber controls the horizontal profile of the cone sheets. For example, Plate IV of Richey et al. (1961) shows the pattern of the Late Basic

Cone Sheets of Mull as having the profile of a dumpy pear, as has the Loch Ba Felsite Ring Dyke. Although the majority of cone sheets have a circular profile, it is possible that a horizontally elongated magma chamber would exert controls on the horizontal profile of the sheets. Alternatively, it may be the interaction of regional forces modified by individual complexes which may result in an elongated magma profile, or the migration of the centre of intrusion may influence the form of the horizontal profile of cone sheets.

It does appear from geophysical evidence that the large cylindrical basic/ultrabasic magma chamber that underlay each of the B.T.I.P. central intrusive complexes is, on a world wide scale, very rare.

2) Bahats (1981) model for cone sheet fracture formation involved a re-surgent indentor acting on numerous times on the magma chamber roof and as each fracture is formed it is filled with magma. A possible mechanism for this type of emplacement is a continually rising magma chamber, such that a cone sheet complex indicates evidence that the magma chamber was rising. This model could explain the numerous cone sheets of the Thulean Province which tend to be thin, less than 1.5m thick. Photoelastic (Durrance,1967; Pollard, 1973) and theoretical studies (Field, 1964) imply that potential fractures for cone sheet development are large in number. This is further supported by field evidence which indicates that adjacent cone sheets develop simultaneously (Chapter 5). Similarly, the observation that adjacent groups of cone sheets, up to 10 approximately, are composed of a similar rock type, lends credit to the suggestion

that small groups of cone sheets develop simultaneously.

A consequence of the rise of the magma chamber is that different structural levels of a cone sheet set could outcrop at the same level. This can be seen in Ardnamurchan, where Centre One cone sheets represent a cross section through a high level of a cone sheet set and those of the Outer Centre Two represent a lower-level (Chapter 10.2).

3) The regional structure and thicknesss of the crust in conjunction with the prevailing tectonic forces may have determined the location of the central intrusive complexes. It was shown in Chapter 2 that most of the central intrusive complexes of the B.T.I.P. lie along a line. It has been suggested from the presence of Mesozoic sedimentary basins in NW Scotland (Hallam, 1972) that there has been thinning of the crust and that this may have been a factor in the location of the sites of Tertiary igneous activity.

On a smaller scale the type and structure of the host rocks exerts controls on the cone sheets. In Ardnamurchan, the country rocks into which the cone sheet complexes have been emplaced are a low-grade, regionally metamorphosed Precambrian (Moinian) psammite with pelitic layers, with a prominent foliation and secondary crenulation cleavage in the pelitic layers, thin sequences of Triassic and Jurassic sediments, Tertiary basalt lavas and various members of the central intrusive complex. The main Skye cone sheet complex is emplaced predominantly in the Cuillin Gabbro complex, whereas the Mull cone sheets are found within a combination of sediments, metasediments and igneous

host rocks.

External controls on the B.T.I.P. cone sheet complexes include the tensile forces related to the emplacement of dyke swarms which were forming throughout the evolution of the central intrusive complexes (Speight et al.,1982). One possible effect of this tensile force could have resulted in normal displacements of structures in the country rocks at the margins of cone sheets (Chapter 6); this is particularly well developed in the cone sheets of the north coast traverse.

4) The country rocks into which the Ardnamurchan cone sheets are emplaced have had a varied and sometimes intense structural history. In particular, the Moine rocks which contain stretched feldspar grains, a prominant foliation and secondary crenulation cleavage and numerous joints. Jurassic host rocks are less deformed but show inclined bedding, due in part to doming, and several sets of joints. The Tertiary igneous host rocks are well jointed, with the intensity varying with the rock type. Thus, before the emplacement of the cone sheets the host rocks contained numerous, well-developed planar structures which, in places, locally controlled the form of individual cone sheets.

As shown in Chapter 8, on a local scale the different host rocks control, to a certain extent, the variation in numbers and thicknesses of cone sheets. This may be attributed to how susceptable each rock type is to fracturing. In high levels of a cone sheet complex (Chapter 10.2), fractures open by hydraulic fracturing produced by the interaction of meteoric water (Taylor

and Forester, 1971) within the host rocks and the advancing magma.

10.6.1 Summary

Mesozoic thinning of the crust, repeated rapid rise of a cylindrical shaped magma chamber into a fractured host rock produced the intensively developed cone sheet complexes of the B.T.I.P.. However, no single factor in isolation can account for the development of the cone sheet sets of Ardnamurchan, each of the factors discussed exerts some influence on the cone sheet fractures.

10.7 RELATIONSHIP BETWEEN CONE SHEETS AND AN INTRUSIVE COMPLEX

The relationship between cone sheets and the evolution of a central intrusive complex is not simple. This is emphasized by the two models proposed by Bahat (1981) (Fig.1.1.1). Three aspects of this problem will be discussed, they are timing of events, the geochemical and the structural controls on the development of the complex.

Bahat's (1981) models demonstrate two alternative sequences of events (Chapter 1), each involving cone sheet formation, doming and ring dyke formation. In both sequences cone sheets are formed before the emplacement of ring dykes and, in general, this seems to be the case in the B.T.I.P.. However, for the Ardnamurchan central intrusive complex these simple models do not adequately explain all of the following facts:-

1. The first set of cone sheets (Centre One) occur in agglomerates, Moine and Jurassic host rocks and there is no associated doming or ring dyke emplacement.
2. The second cone sheet set (Outer Centre Two) was intruded before the emplacement of the first major ring intrusion (Hypersthene Gabbro) associated with Centre Two.
3. The third set crop out both within and adjacent to the Hypersthene Gabbro, indicating that they developed after the major ring intrusions of Centre Two had begun to form.
4. The fourth set (Inner Centre Two) outcrop within the major ring intrusions of Centre Two, i.e. during the development of the major ring intrusions.
5. The fifth cone sheet set outcrop within the margins of the first major ring intrusion of Centre Three.

These five sets of cone sheets recognised by the present author can be classified on the basis of their location, both in time and place, relative to the associated major ring intrusions. Sets 1 and 2 were emplaced before the development of the first major ring intrusions of the complex whereas Sets 3 and 5 were emplaced within the first major ring intrusions of the associated centre of activity. The fourth set differs from the others in that it occurs within the later ring intrusions of the centre and is located close to the centre of activity (Centre Two).

Sets 1 and 2 fit Bahat's (1981) theory in that they developed before the major ring intrusions were emplaced. Sets 3 and 5, which were emplaced after the development of the major ring intrusions, indicates that a resurgence of pressure was necessary for cone sheet emplacement following a decrease in pressure associated with the emplacement of a major ring intrusion. Sets 3 and 5 have a narrower diameter (max 3km and 1.5km respectively) than earlier cone sheet sets e.g. Set 2 (max 7km). This difference may be related to a rise in the magma chamber in the crust or a shift in position of the centre of

activity. Set 4 is similar to sets 3 and 5 in terms of it's total volume and yet differs in that it occurs after the emplacement of a number of major ring intrusions. This may either be caused by the uprise of new magma resulting in a cone sheet set having a vertical axis and located at a higher structural level as suggested by Richey et al. (1930), or possibly that another magma chamber developed which produced a cone sheet set, the axis of which was inclined. If the latter suggestion is accepted, then Set 4 is similar to Sets 1 and 2 in that it formed before the development of associated major ring intrusions.

Geochemically, the major ring intrusions of Centres Two and Three show an evolution from basic to more acid with time (Gribble et al. 1976). The cone sheets are predominantly basic to intermediate in composition and each centre exhibits a similar iron-enrichment trend (Gribble et al. 1976). Each cone sheet set, therefore, indicates a new supply of magma, supporting the field evidence that cone sheet sets are emplaced in the early stages in the evolution of each centre. Also, that a new influx of magma resulted in the Set 4 cone sheets at a late stage in the evolution of Centre Two.

Theories of development of cone sheet complexes, indeed central intrusive complexes, involve an initial upward increase in pressure. In most theories (cf.Kaitro, 1982), cone sheets are thought to result from the upward increase in pressure, followed by a decrease in pressure due to a) the migration of magma into the cone sheet fractures b) the cessation of retrograde boiling (Phillips, 1974), or c) the migration of magma into

another part of the complex. Following an episode of major ring intrusion emplacement the magma reservoir would be depleted, assuming there was no replenishment of magma. A resurgence of pressure in the magma chamber would result in a less extensive (numerically, geographically and volumetrically) cone sheet set, e.g. Sets 3 and 5.

In the Ardnamurchan complex, cone sheet Sets 1 and 2 form the most abundant and areally extensive group of cone sheets. Although, to a large extent, this intensity may be attributed to the structural level presently exposed, it may also be because these sets were emplaced very early in the evolution of the central intrusive complex. Perhaps these two sets of cone sheets are typical examples of cone sheet formation in that they represent the first stage in the evolution of a central intrusive complex. This is supported by the geochemical evidence of Gribble (1968). Resurgence of activity, in which sets 3 and 5 were formed, following the formation of the first major ring intrusion, is always minor in relation to the first phase of cone sheet formation (e.g. Sets 1 and 2).

10.8 VOLUME OF MAGMA

In order to calculate the volume of magma emplaced as cone sheets a number of factors have to be considered, these being:-

1. The structure and intensity of cone sheets with depth.
2. The thickness of the cone sheet complex removed by erosion.
3. The amount of magma erupted at the surface by cone sheets.

10.8.1 Present level to the focus

A number of assumptions have to be made before the volume of magma can be calculated, such as:-

1. The measured traverses are a representative cross section of the cone sheet set.
2. That the limits of the measured traverses are similar to the limits of the original cone sheet set.
3. The thickness of cone sheets is constant with depth.
4. Cone sheets dip at a constant angle.
5. An average angle of dip may be used for the whole set.
6. The intensity of cone sheets is maintained with depth.

There are two stages in the calculation of the volume of magma. The first stage consists of two parts. The first part is to calculate the volume of the cone (cone 1) as defined by the outer limits of the set and the second part is to calculate the volume of an inner cone (cone 2) defined by an absence of cone sheets.

volume of cone 1 - volume of cone 2 = volume of cone sheets plus the host rock

The second stage is to calculate the proportion of country rock to cone sheet material.

Table 10.3 shows the volume of magma emplaced for each cone sheet set and highlights the variation between each set. Two separate calculations, one for each of the two traverses, have been performed for the Outer Set of Centre Two cone sheets in order to investigate the differences previously described between the two traverses. The north coast traverse (I) gives a higher volume (51.75km^3) than that calculated for the south coast traverse (II = 43.8km^3). The difference of 8km^3 may be attributed to analytical error, although this is rather a large amount. The increased volume on the north coast section lends

Table 10.3 Volume of magma emplaced as cone sheets

CONE SHEET SET	Volume A	Volume B
Centre One	15.6km³	7.9 km³
Outer Centre Two I based on the north coast traverse	51.8km³	23.2km³
Outer Centre Two II based on the south coast traverse	43.8km³	17.9km³
Inner Centre Two		
Outer Group;Lighthouse,An Acairseid, Sgurr nam Meann	0.664km³	0.18km³
Inner Group:Beinn Bhuidhe, Garbhdhail, Beinn na Seilg	0.824km³	0.34km³
Centre Three	1.168km³	0.48km³
Total volume of magma	66.56km³	29.80km³

where Volume A = volume of magma emplaced as cone sheets calculated from the focus to the present level of erosion

Volume B = volume of magma emplaced as cone sheets in a 1km high block above the present erosion level

In the calculations for total volume of magma an average value was used for the Outer Centre Two traverse

support to the existence of another, overlapping cone sheet set, that is the Inner Group of Inner Centre Two. However, the Inner Group of Inner Centre Two cannot account for the 8km^3 difference between the north and south coast calculations and therefore indicates that more magma was emplaced in the north than in the south.

The Outer Group and Inner Group of Inner Centre Two and the Centre Three cone sheets represent only a small percentage (4%) of the total volume of cone sheet material intruded within the central intrusive complex.

The total volume of cone sheet material emplaced in the complex is 66.556km^3 of basic magma, which caused a 22% inflation of the country rock (calculated as a percentage of the volume of cone I).

10.8.2 Present level to the upper limits

Definition of the upper limits of the cone sheet complex presents a number of problems. Firstly, dip of the cone sheets may change, as described in section 10.3, some sheets becoming almost horizontal in the upper levels. Secondly, only a few scattered remnants of the lava pile that once covered Ardnamurchan exist at the present and therefore no indication of the upper extent of the cone sheets can be ascertained. As the amount of erosion cannot be stated then a minimum value of erosion has been estimated - the maximum amount of inflation caused by the emplacement of the cone sheets is 820m, the minimum estimated amount of erosion is, therefore,a minimum of 1km.

Table 10.3 shows the volume of magma emplaced as cone sheets in 1km above the present level. The proportions of the individual cone sheet sets remains the same, with the two Outer Centre Two calculations containing the majority of the volume. The Outer Centre Two calculation based on the north coast section is 30% larger than that based on the south coast traverse. This larger proportion of cone sheet material amplifys the suggestion that a subsidiary set is present along the north coast traverse.

10.8.3 Amount of magma erupted at the surface by cone sheets

There is no conclusive evidence in Ardnamurchan that cone sheets acted as feeders for lava flows, although there are examples of vents which have an annular form. If cone sheets flatten with height above their origin (Zone 1B, Table 10.1), then the chance of them intersecting the surface is less than if they had a uniform dip (Zone 1A, Table 10.1). As both Zone 1A and 1B occur in Ardnamurchan it is possible that cone sheets may have fed flows at the surface. However, the author considers that the volume of basaltic magma erupted at the surface from cone sheets was insignificant.

10.8.4 Volume of magma emplaced as cone sheets

The volume of magma emplaced as cone sheets, compared to the volume emplaced as major ring intrusions, is approximately 10%. The figures used for this calculation are derived from the 1" Geological Survey Map (Sheet 51 and 52).

10.9 DO CONE SHEETS REACH THE SURFACE?

In an earlier section the vertical extent of cone sheets has been discussed. However, whether some cone sheets actually reached the surface has not. In order to conclude that cone sheets reached the surface and acted as feeders evidence is required in the form of exposures where sheets are seen to continue into lava flows or into agglomerates. Alternatively, connections between surface activity and cone sheets may be gained from the study of recent volcanoes.

The volcanoes of the Galapagos Islands possess well-defined circumferential fractures (Simkin, 1972; Delaney et al., 1973; Banfield et al. 1956). Simkin (1972) postulates that these circumferential fractures are modern day equivalents to the products of the central intrusive complexes of the B.T.I.P.. Situated at various points around the circumferential fractures of the Galapagos volcanoes are vents, from which lavas issue. Simkin (1973) believes that magma erupted from the circumferential fractures lead to the formation of a guyot by ponding of lava in the central depression. A characteristic feature of these circumferential fractures are a parallel series of collapse depressions up to 125m long as seen on the Sierra Negra Volcanoe. Delaney et al. (1973) concluded that these depressions are formed by subsidence which is related to the formation of the adjacent fractures.

It is highly likely that the circumferential fractures seen in the Galapagos volcanoes represent cone sheet fractures, in that they are annular outcropping features filled with magma and

are centrally inclined to a focus beneath the present level.

Work by Rittman (1971) on Etna indicated that a series of inclined sheets exposed beneath the volcano may be cone sheets.

Speaking in terms of the Ardnamurchan cone sheets, Richey (1932) also suggested that "...others may perhaps reach the surface and act as feeders for parasitic vents...". Evidence gained from the Ardnamurchan cone sheets, relating to their upper extensisons is limited. Most terminations of cone sheets are in the form of simple wedges and en echelon sets. However, the Centre One traverses include linear vents, which are parallel to and are similar in form to cone sheets. A similar occurrence is seen to the east of the Glas Eilean vent (Outer Centre Two, south coast). All examples of linear vents occur close to the more extensive vents which may indicate that the linear vents represent parasitic vents closely allied to the major vents. With the form of the linear vents and cone sheets being similar it follows that cone sheet fractures may have reached the surface and fed small surface vents.

10.10 INFLATION OF VOLCANOES - does this indicate intrusion of cone sheets?

Detailed studies of present day active volcanoes reveal that the surface changes shape in a cyclical pattern. Kilauea volcano (Hawaii) has been intensively studied since 1912 when evidence for tilting was first obtained (Jaeger and Finch, 1929). Fiske and Kinoshita (1969) measured migrating centres of uplift over the surface, and during the period January 1966 to

October 1967 they located 10 centres of uplift which were grouped into 3 regions of inflation. The periods of slow inflation terminate with episodes of rapid deflation which were equated with either rift eruptions on the flanks of the volcano or the emplacement of shallow intrusions, such as sills. Dietrich and Decker (1975) analysed the observations of movements of the Kilauea volcano, using a finite element model. This work tried to relate the surface deformations to the type of intrusion envisaged at depth, and they concluded that the most likely shape of the intrusions beneath Kilauea is a series of cylindrical shapes, which may consist of a plexus of dykes and sills, located 1km below the surface. The models investigated by Dietrich and Decker (1975) included sills and dykes of various inclinations, horizontal lenses, spheres and vertical plugs.

Field observations of present day volcanic activity indicate a migration of magma from its source to chambers located approximately 2 to 4km beneath the volcano, before it is ultimately erupted or intruded. The theoretical models proposed by Dietrich and Decker (1975) cannot determine or distinguish whether the intrusion is a large, single cylinder or a large number of smaller intrusions, such as cone sheets. Together the field and theoretical works cannot prove conclusively that cone sheets are being emplaced but there is no evidence which says that cone sheets are not being emplaced at depth beneath active volcanoes.

10.11 INFLATION OF THE ARDNAMURCHAN VOLCANIC LAND SURFACE

To calculate minimum values for the inflation of the land surface due to emplacement of the cone sheets, a minimum aggregate thickness for the cone sheets was used together with mean dip angles for each cone sheet set (Table 10.4).

A comparison of the figures calculated by Richey *et al.* (1930) for the total uplift (1250m) with that derived from this study (maximum 820m) indicates that the figure calculated by Richey *et al.* (1930) is 30% greater than that derived from the present study. This is because Richey *et al.* based their figures for the total uplift of the central intrusive complex purely on the Glas Eilean - Mingary Pier traverse, which shows the most intensive development of cone sheets in Ardnamurchan. My calculations based on this traverse gives a value of 524m uplift for the Outer Centre Two Set only, whilst Richey's *et al.* (1930) figure represents uplift for the whole complex i.e. Centres One, Two and Three.

Using an average angle of dip of 42° and a radius of 5.5km, the Centre One sheets raised the land surface by 212m (Fig.10.11.1). Two calculations for the Outer Set of Centre Two cone sheets have been performed. That based on the south coast traverse indicates an uplift of 524m of the surface, whereas the calculation for the north coast traverse gives a value of 763m. The difference of 240m may be explained in two ways. Firstly, the Inner Centre Two cone sheet set represents the southern exposures of a tilted cone sheet set, with the northern extremities occurring along the Outer Centre Two north coast traverse.

Table 10.4 A table to show the amount of inflation caused by the emplacement of each cone sheet set

Cone Sheet Set	Min Agg thickness	Av dip	Inflation
Centre One	235.6m	42	212m
Outer Centre Two			
north coast	663.9m	49	763m
south coast	446.9m	49	524m
Inner Centre Two			
Inner Group	27.9m	72	85m
Outer Group	9.6m	57	14m
Centre Three	10.5m	50	22m

Table 10.5 Volume of magma emplaced in each high and low pressure event of the evolution of the central intrusive complex

High/Low pressure	Type of intrusion	Volume of magma emplaced km^3
H	cone sheets (C1)	8.3×10^6
H	cone sheets (O.C2)	8.7×10^6
L	major ring intrusion	45.2×10^6
H	cone sheets (O.G.)	0.2×10^6
L	major ring intrusion	11.7×10^6
L	major ring intrusion	1.9×10^6
L	major ring intrusion	0.9×10^6
L	major ring intrusion	10.9×10^6
H	cone sheets (I.G.)	0.2×10^6
L	major ring intrusion	2.6×10^6
L	major ring intrusion	4.1×10^6
H	cone sheets (C3)	0.4×10^6
L	major ring intrusion	65.3×10^6
L	major ring intrusion	3.6×10^6
L	major ring intrusion	4.3×10^6
L	major ring intrusion	1.2×10^6
L	major ring intrusion	1.6×10^6
L	major ring intrusion	1.1×10^6

C1 Centre One
O.C2 Outer Centre Two
O.G. Outer Group of Inner Centre Two
I.G. Inner Group of Inner Centre Two
C3 Centre Three

Volumes were calculated from the 1" Geological Survey Map

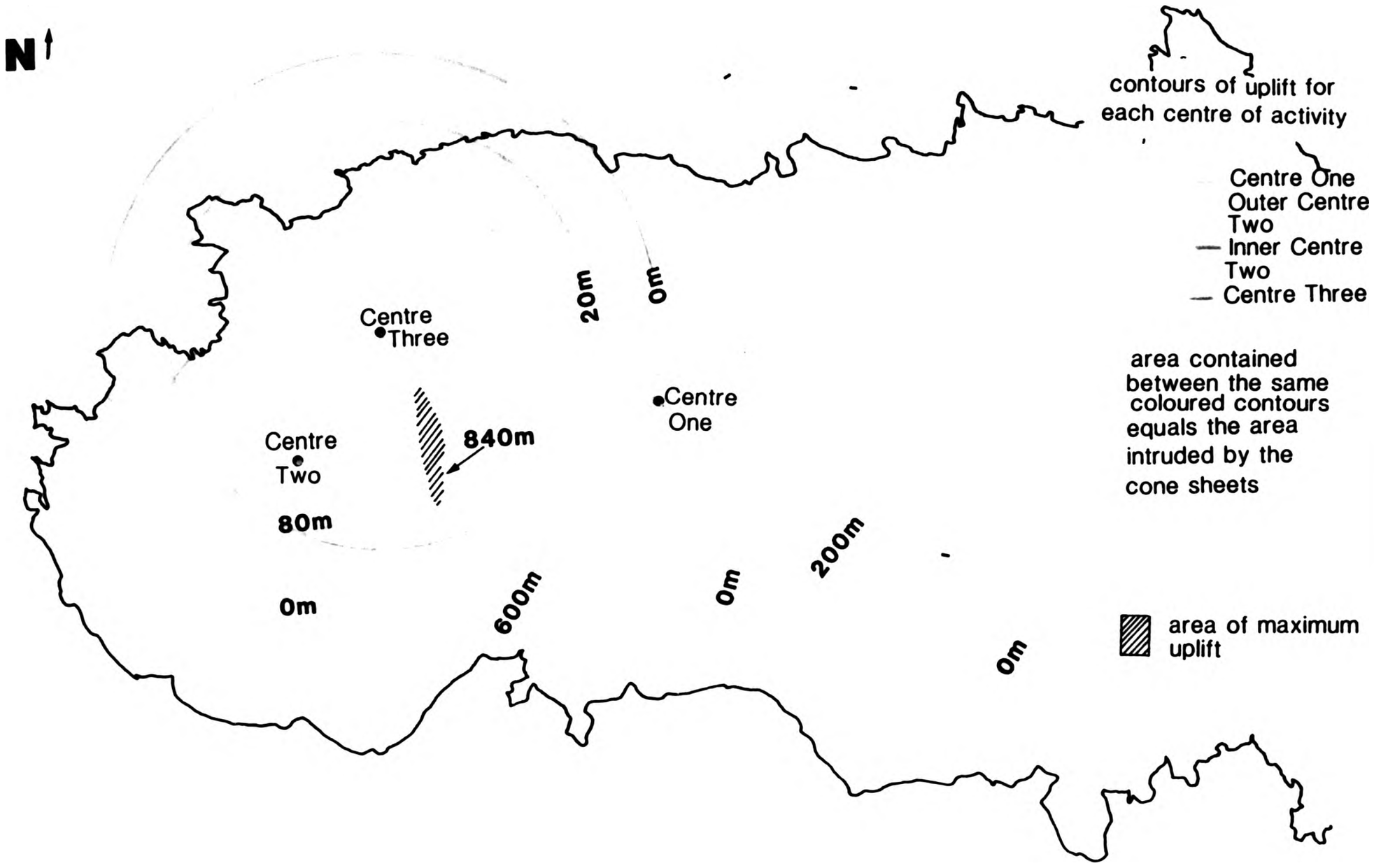

Fig.10.11.1 Areas of uplift caused by the emplacement of the cone sheet sets of Ardnamurchan

Or, secondly, that the north coast represents an area where cone sheets belonging to the Outer Set of Centre Two have been more intensively intruded than in the area of the south coast. When the volume of magma is also taken into account (Chapter 10.10) it becomes clear that both of these explanations could be correct. I believe that the effects of both these explanations are seen.

The Inner Centre Two cone sheets were responsible for an increase in the height of the volcanic land surface by 100m, the Outer Group caused an inflation of 15m whereas the Inner Group produced one of 85m. Finally, the Centre Three cone sheet set caused an uplift of 22m (Fig.10.11.1).

Figure 10.11.1 shows the limits of each cone sheet set and emphasizes the effects of the cone sheet sets on the amount of inflation of the surface. In Fig.10.11.1 an average value of the north and south coast traverses was used to estimate the total uplift caused by the emplacement of the Outer Centre Two cone sheet set. The maximum uplift caused by the emplacement of all cone sheet sets is 820m and not 878m (Table 10.4) as the maximum limits of each cone sheet set do not overlap. In general, the area represented by Centre Three would have been increased in height by at least 820m, approximating to a ridge trending from Glendrian to Meall an Tarmachain. Locations farther eastward would have been less inflated principally as the number of Centre One cone sheets decrease to the east. It must be stated that the volcanic land surface may never have been inflated by 820m, due to possible intermittent cauldron subsidence and/or erosion between episodes of cone sheet

emplacement.

10.12 RELATIONSHIP BETWEEN CONE SHEETS AND MAJOR RING INTRUSIONS

The central intrusive complexes of the B.T.I.P. are witness to an intimate relationship between emplacement of cone sheets and major ring intrusions. Richey et al. (1930) and Anderson (in Bailey et al., 1924) concluded that upward pressures within the magma chamber formed cone sheets, with the consequent decrease in pressure resulting in the emplacement of major ring intrusions. Subsequent work has supported these ideas, particularly that cone sheet emplacement is usually one of the first events in the evolution of a central intrusive complex.

Figure 10.12.1 shows an idealised sequence of events in the evolution of the Ardnamurchan central intrusive complex, in terms of pressure changes. The first event is one of high pressure, that is when the Centre One and Centre Two Set A cone sheet sets are emplaced, followed by a series of pressure oscillations finishing with a low pressure event marking the emplacement of the major ring intrusions of Centre Three. It is significant that the first event is a high pressure event and the last event a low pressure one. In general, there is a decline in the quantity of magma emplaced in each of the successive events, with the exception of the final event.

The first event is one of high pressure, resulting from a rapidly rising magma chamber. Cone sheets were formed at this peak of pressure, that is when magma pressure is greater than

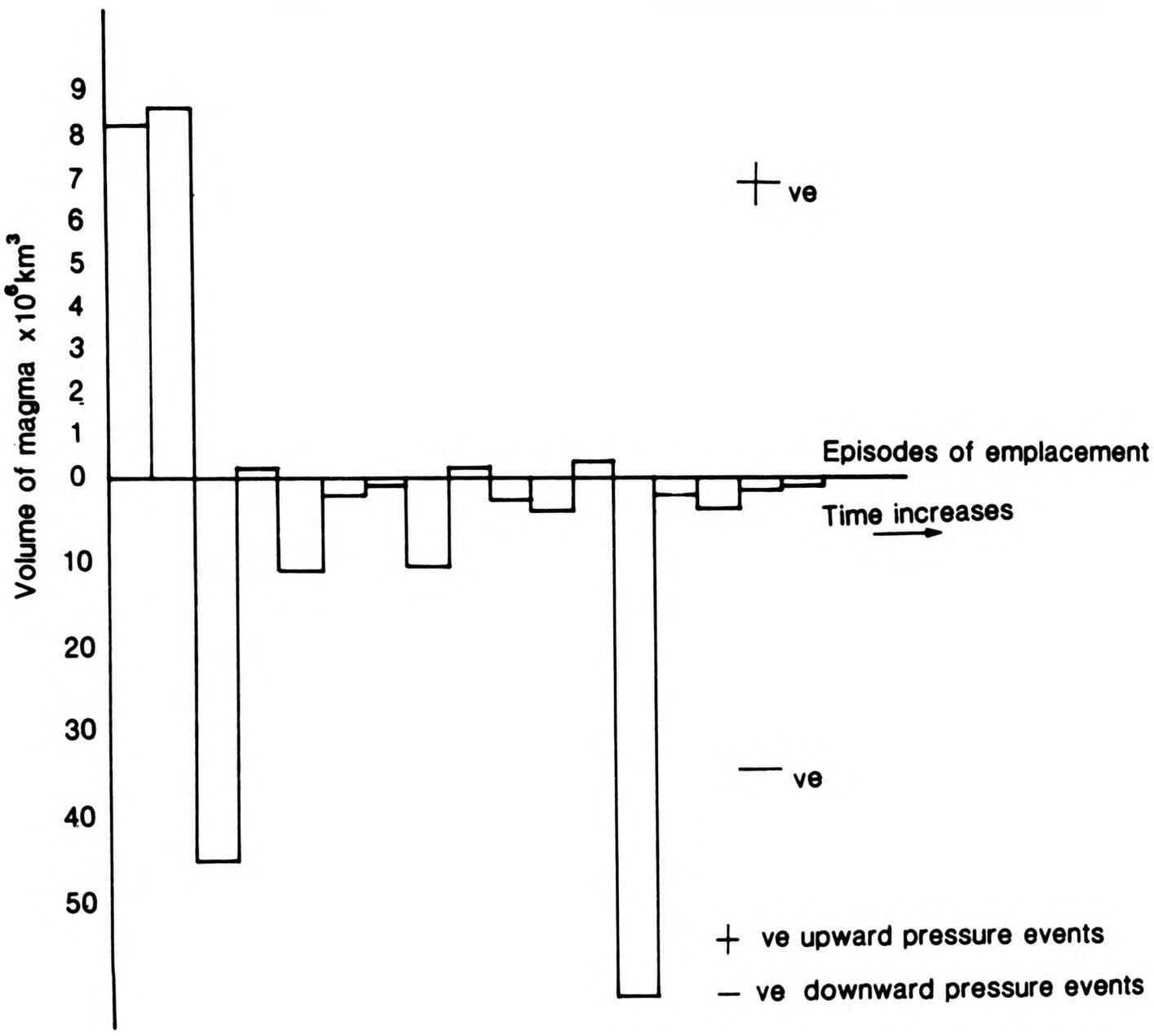

Fig.10.12.1 Diagram showing volumes of magma emplaced as cone sheets (+ve) and major ring intrusions (-ve) in Ardnamurchan

fracture pressure (Fig.10.12.2). Following the emplacement of a large number of cone sheets, the next event is a low pressure one, resulting in subsidence of a central block to form a major ring intrusion, that is the Hypersthene Gabbro.

It can be suggested that it is the relative change in pressure, from high to low, which results in the subsidence of a central block allowing the ingress of a large volume of magma to form a major ring intrusion to be emplaced into the "pre-fractured" area caused by the preceding cone sheet event. However, on the margins of some of the major ring intrusions (eg. at the margin of the Centre Three Quartz Gabbro) net veining occurs which is evidence for a positive pressure, albeit on a microscale, which is something of a paradox. Figure 10.12.3 and Table 10.5 show the volume totals of magma emplaced for each high and low pressure event for the whole of the Ardnamurchan Central Intrusive Complex. In terms of the volume of magma, the first event is very large (a high pressure event), that is the emplacement of the Centre One and Centre Two Set A cone sheet sets, which is then followed by an even larger volume of magma emplaced during a low pressure event, that is the emplacement of the Hypersthene Gabbro major ring intrusion. A series of small high pressure events occur throughout the evolution of the whole complex, these are the Centre Two Set B, Set C and the Centre Three cone sheet sets. Low pressure events occur between these high pressure events, which correspond to the major ring intrusions of Centres Two and the start of Centre Three activity. Finally, the evolution of the whole complex is terminated by a large low pressure event when the major ring intrusions of Centre Three were formed after the emplacement of the last cone

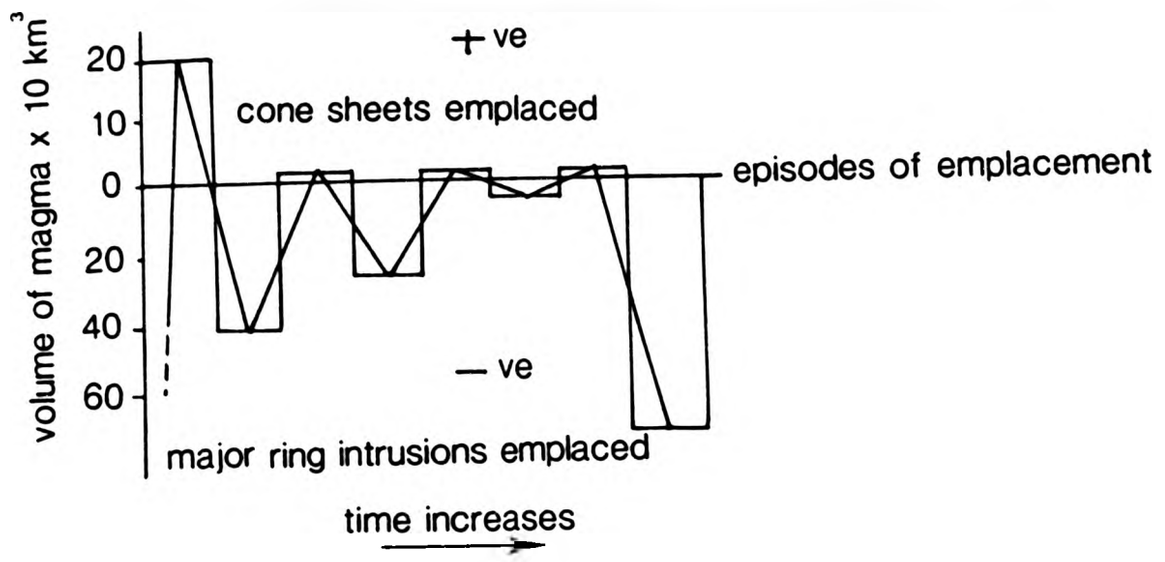

Fig.10.12.2 Diagram of the simpified+ ve and -ve pressure sequence of the intrusions of the Ardnamurchan central intrusive complex

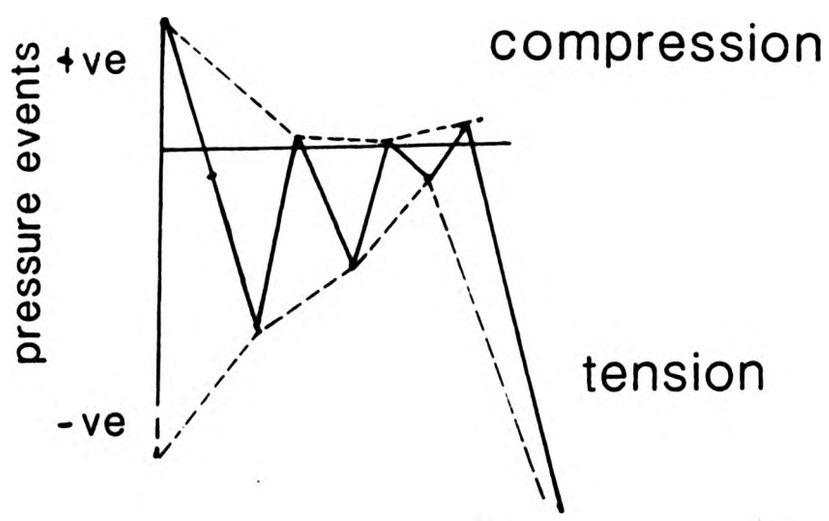

Fig.10.12.3 A summary of the rock fracture pressure throughout the evolution of the Ardnamurchan central intrusive complex

sheet set.

The end event may be due to cooling of the complex with the local dynamic equilibrium which existed between the magma pressure and the lithostatic pressure being destroyed resulting in massive emplacement of major ring intrusions.

Figure 10.12.3 summarises the relative pressure differences marked by each of the intrusive episodes and shows that the rock fracture pressure and the tensional fracture pressures decrease with time.

10.13 PHYSICAL CHARACTERISTICS OF EACH CONE SHEET SET

10.13.1 Centre One

This set of cone sheets outcrops along the north coast eastwards from Faskadale to Rubha a'Choit and also along the south coast of the peninsula from Mingary Castle eastwards (Fig.10.13.1). On the south coast these sheets are distinguished from those of the Outer Centre Two Set by their more northerly strike and low intensity of intrusion e.g. as found along the Allt Choire Mhuilinn (Fig.5.3.6). The inland exposures of Centre One cone sheets are generally poor. With the exception of four unit lengths immediately west of Faskadale, the Centre One traverse typically shows a low distribution of sheets per unit length. Large tracts of the traverse contain no or few (5) cone sheets with a small number of punctuated occurrences of relatively high distributions (10 - 15 sheets). The

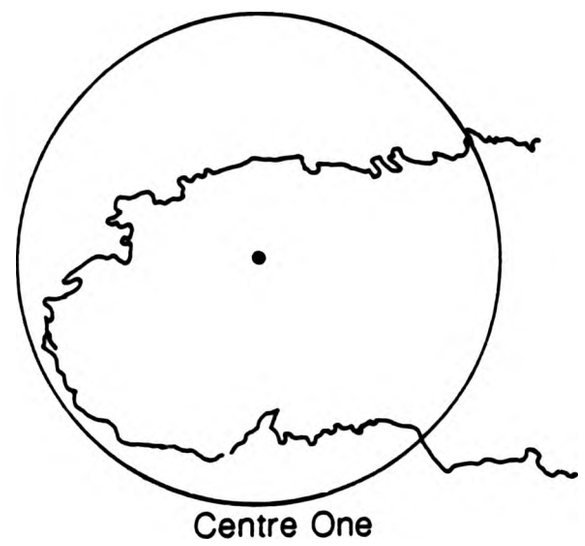

Centre One

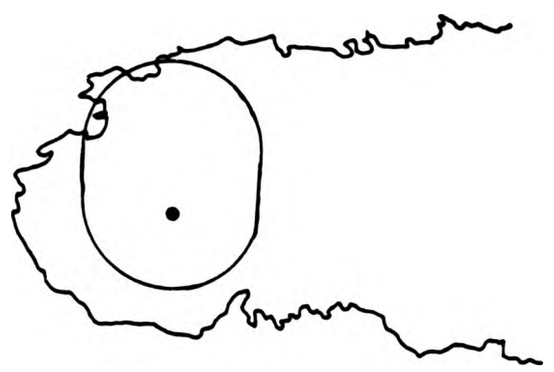

Centre Two Set 3

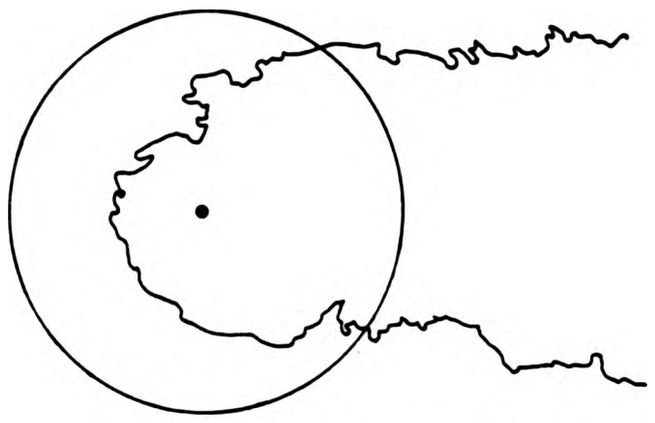

Centre Two Set 1

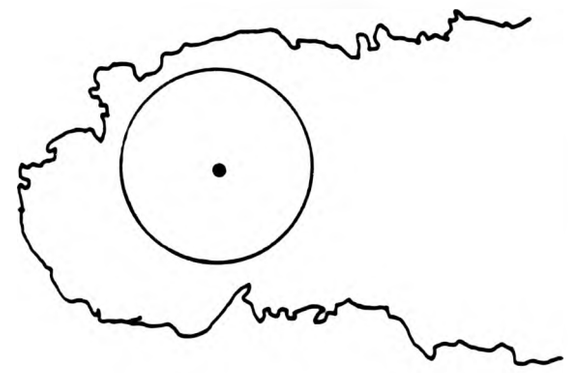

Centre Three

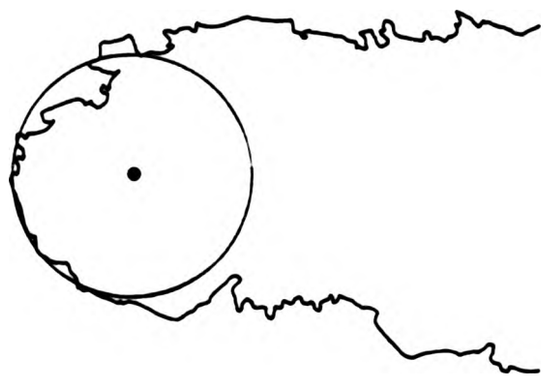

Centre Two Set 2

outline of cone sheets

• focus of activity

Fig.10.13.1 Generalised out line of the 5 sets of cone sheets of Ardnamurchan

Centre One cone sheets outcrop in an arcuate zone between 3 and 6km from the epicentre of activity.

Along the north coast traverse mean dip values change from 50° in the east to 30° in the west. However, this variation is not prominent in the dip distribution per unit length. The total dip distribution is skewed towards the low angled classes, although no sheets occur in the 0°-10° class. On the south coast, dip decreases from 60° at Mingary Pier to 20° at Rubh'a'Mhile. On the north coast, in the eastern extremities, the dip and strike data form a small cluster in the NE quadrant of a stereonet projection with the more westerly exposed cone sheets spreading the cluster into the NE and SE quadrants. The south coast data for Centre One is obscured by the large number of Outer Centre Two cone sheets in this area.

The strike of the sheets and of the host rock structures (e.g. bedding, foliation, joints) are coincident indicating that the cone sheets exploited pre-existing weaknesses in the host rock during their development (Chapter 8). For example, unit lengths which occur in volcanic agglomerates and lavas show a wide range of strike values whereas unit lengths in Moine and Jurassic host rocks show a well developed modal class. Chi^2 values of the strike of Centre One cone sheets indicate a change of average strike from 340° in the east to 310° in the west, part of the change in the west may be due to the presence of Centre Two cone sheets. This is again emphasized by the analysis of the distribution of strike to thickness, the western section shows a large, widespread, peak from 280° to 360° and a smaller one at 060°, whereas the eastern section has one peak at

340° containing 52% of the data and four smaller peaks of thin sheets at 020°,160°, 220° and 260°. The south coast Centre One sheets (Fig.5.10.3b) are represented by a small peak at 320°.

10.13.2 Centre Two

Centre Two cone sheets have been subdivided into three sets. As described in an earlier section (10.5) cone sheet sets can be vertically zoned. All Centre Two cone sheets fall into Zones 1A and 2 (Fig.10.2.1). These two zones have similar characteristics but 1A possesses large numbers of en echelon sets. In consequence, the physical characteristics of dip, strike, thickness of all three sets of Centre Two are similar, yet different. Division into the three sets is based largely on distribution and cross cutting relationships which is further substantiated by cluster analysis and intensity of intrusion, the natural limits of each set being marked by a decrease in intensity.

Set A This set is approximately equivalent to Richey's Outer Set of Centre Two cone sheets. The traverses consist of a) the south coast from Sron Bheag to Rubh' a' Mhile, eastwards of this location the Centre One cone sheets are present and b) the north coast section from Rubha an Duin Bhain to Faskadale. Set C is also present along part of the north coast traverse. A broad arc of sheets is exposed between the north and south coast traverses.

In studying the two traverses separately, a number of signficant details have emerged. The north coast section contains a large number of cone sheets per unit length, average

n=24, which is twice that for the south coast traverse. More particularly, in unit lengths 1 to 16 of the north coast traverse, a larger number of cone sheets occur compared with farther east where the traverse from east of Sgeir Ghibeach to Faskadale resembles the south coast distribution. In general, the number of sheets decrease towards the extremities of the traverses, which most probably demonstrates the original limits of the set. This is particularly well marked in the eastern extremities of both traverses. The difference between the two traverses is again emphasized by the distribution of sheets, the north coast has a maximum peak of 40 at Rubha Groulin, with a subsidiary peak on either side (n=30). Whereas on the south coast the maximum peak (n=23) is located halfway between Glas Eilean and Mingary Pier with two adjacent peaks of 15 sheets.

The dip of cone sheets on the north coast is shallow in the west, modal class of 31°-40°, with some higher angled sheets at Rubha Carrach (61°-70°) and at (404732). The south coast sheets dip at 41°-50°, with some variation. When the dip and strike data for the cone sheets of each traverse are plotted on a stereonet it shows the arcuate form of the cone sheets (Fig.5.5.6). Due to the large number of readings and variation in dip, the clusters, although well defined, are widespread. The strike of cone sheets on the north coast, particularly to the west of Sgeir Ghibeach, show some oscillation between 270° and 310°,whilst to the east the strike is 290°. It is assumed that the cone sheets striking 310° belong to Set C (see below). The south coast sheeets have a strike of 080° at Sron Bheag, 030° from Glas Eilean to Mingary Pier and east of the Pier values between 350° and 010° occur but are more inconsistent due

to the presence of Centre One sheets. The Chi^2 mean values refine the strike values yet they still show a difference along the traverses. This analysis also shows how the strike of the cone sheets within the first two unit lengths from Rubha an Duin Bhain trend to the west, with the strike for the next two unit lengths trending more northerly. Chi^2 mean values for the strike of the south coast sheets indicate a gradual change in orientation from ENE to NNE. Average thicknesses of sheets on the north coast varies from 1 to 2 metres, whereas thickness of sheets on the south coast varies between 0.5m and 3m. In both traverses, sheets in the east are thicker than those in the west. Figures 5.10.3-5 illustrate the variation of cumulative thickness of cone sheets (expressed as a percentage of the total thickness of cone sheets) along the north coast traverse which was subdivided into two subsections. The first subsection is west of Sgeir Ghibeach and shows two peaks, one of 30% total thickness at 300° and 18% total thickness at 260°. The second subsection is east of Sgeir Ghibeach where the data is less well defined and consists of a large group spreading from 220° to 360°. The south coast traverse was subdivided into three sections, the first at Sron Bheag, shows two main peaks at 060° and 100° with 28% and 27% total thickness respectively. From Glas Eilean to Mingary Pier is the second data set and shows a single dominant peak at 040°. The third data set, based on cone sheets east of Mingary Pier, has a main peak at 020°, with subsidiary peaks at 060°, 140°, 200° and 320°.

Set B This group was identified principally on the basis of geographical location and petrological characteristics. It occurs around the marginal parts of the Hypersthene Gabbro (Fig.10.13.1) and consists largely of feldspar porphyritic basic

cone sheets. At the western extremities of the Sron Bheag traverse, where it approaches the Hypersthene Gabbro margin, feldspar porphyritic basic cone sheets are also present. It was noted (Set A, above) that the Sron Bheag traverse shows a double peaked distribution and part of the 060° peak consists of feldspar porphyritic basic sheets, which belong to Set B. It is possible that the non-porphyritic basic cone sheets of Sron Bheag which have a trend 060° also belong to Set B because of their similar strike to the An Acairseid cone sheets. Figure 10.13.2 shows that the number of porphyritic basic sheets increases to the west along the 600m Sron Bheag traverse. On the north coast the first two sections contain porphyritic basic cone sheets (5 and 9, respectively) with fewer porphyritic sheets occurring farther east. These north coast sections fall on the lateral extension of the arc which joins the two locations of An Acairseid and the Lighthouse. The Set B basic cone sheets occur marginally to and just within the boundary of the Hypersthene Gabbro.

The average number of sheets for the Sgurr nam Mean, Lighthouse and An Acairseid unit lengths is 10. From west to east along the Sron Bheag section the average number of sheets decrease from 5 to 1, indicating an approach to the limits of cone sheet intrusion. On the north coast at Rubha an Duin Bhain and (404732), 5 and 9 porphyritic basic cone sheets are present respectively and equal the most intense areas of intrusion of the Set seen at the Lighthouse, An Acairseid and Sgurr nam Mean. The modal class dip of all Set B sheets is 51°-60°, with mean dips of 54° and 56°, which is significantly different from the Inner Group of Inner Centre Two (70°) with which they have pre-

viously be allied. Strike distributions of the set show peaks at 060° at Sron Bheag, 070° at An Acarseid and 190° at the Lighthouse and Sgurr nam Mean, 270° at Rubha an Duin Bhain and 090° at (404732) unit length. Together, these values demonstrate the arcuate outcrop of the Set. The Set B cone sheets have a mean thickness of less than 1m. Further evidence to unite the cone sheets of Sron Bheag to the other sheets of Set B is gained from the geochemical analyses reported by Holland and Brown (1973). In their principal factor matrix, the Sron Bheag cone sheets plot very closely to the Inner Centre Two cone sheets (Fig.4.4.1).

Set C This Set consists of the Inner Group of Inner Centre Two cone sheets and, in addition sheets which occur along the north coast traverse. Figure 10.13.2 shows the distribution of porphyritic and non-porphyritic basic cone sheets which occur in these locations. It should be noted that porphyritic basic sheets are very rarely found within Set A along the south coast traverse. However, the Inner Group of Centre Two consists of approximately 30% porphyritic basic cone sheets. The presence of porphyritic basic cone sheets on the north coast indicates that a different magma source is tapped. The north coast traverse, as has been described in Set A, contains a larger number of cone sheets than it's south coast equivalent with the maximum number of sheets occurring towards the west in unit lengths 1-16. The maximum number of sheets in the Inner Group of the Inner Centre Two is 23. Dip distribution on the north coast traverse consists of shallowly dipping sheets, with a modal class of 31°-40°, whilst the Inner Group consists mainly of steeply dipping sheets (71°-80°). If these two groups of cone sheets belong to the same set then the two different dip classes

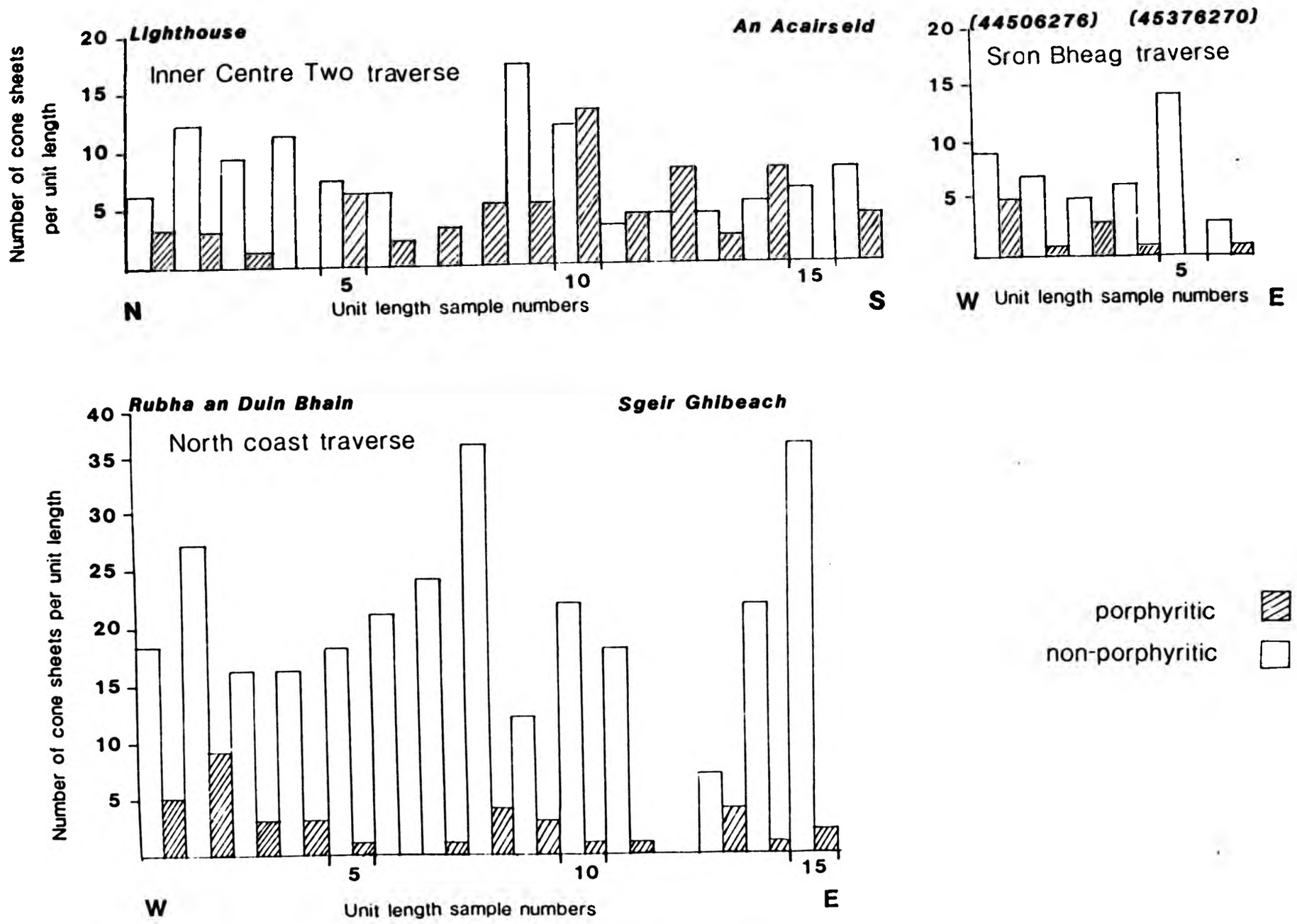

Fig.10.13.2 Distribution of porphyritic cone sheets along the traverses in which they occur

indicate an inclined cone sheet axis. Two modal strike directions (270° and 310°) are well pronounced along the north coast traverse, similarly the Chi² analysis shows two prominent directions which are 280° and 310°. The modal strike of the Inner Group shows a gradual change from 160° on the upper slopes of Beinn Bhuidhe to 110° at Garbdhail and Beinn na Seilg and the Chi² analysis shows a similar change. Strike to thickness data for the north coast traverse also shows two peaks in the distribution, these being 300° (30% total thickness) and 260° (18% total thickness). The existance of two groups on the north coast traverse which are of different orientations indicates the presence of more than one cone sheet set. The more northerly trending set is not as well marked in the more easterly extremities and therefore it may be concluded that this set is restricted to the western parts of the traverse.

Recognition of Set C has been principally identified by the occurrence of feldspar porphyritic basic cone sheets in both locations, which is further supported by their geochemistry (Holland and Brown, 1973). The next piece of evidence is gained from the strike data which when plotted on a map do not lie on a circular outline. However, the data does suggest an elliptical form, largely due to the elongated form of the Inner Centre Two data (Fig.10.12.1). Cluster analysis (Chapter 5) gives further support for the existence of Set C in that the analysis grouped the data from the two locations into two very similar terminal clusters. The dip of the two groups indicates a 70° dipping westerly limb of the cone and a 40° dipping easterly limb, thus implying an inclined axis, dipping at approximately 70° to the SW.

10.13.3 Centre Three

This poorly developed cone sheet set crops out over a restricted area on the northern slopes of Abhain Chro Beinn.The two measured sections have a mean number of 10 sheets per unit length. The dip is towards the north at 52° and 57° for the west and east unit lengths respectively. Modal and Chi² strike values are 070° in the west and 090° in the east. Thickness to strike analysis shows one single peak at 100°.

10.14 CONE SHEETS:FRACTURE INITIATION AND DEVELOPMENT

Controls on the intiation and development of cone sheet fractures include a) the presence of fluids in the host rock which controls whether dry or hydraulic fractures are formed, b) the duration, volume and acceleration of the magma indentor and c) the influence of adjacent stress systems.

The superimposed effect of the spreading dyke axis (Speight et al., 1982) located to the north of the peninsula would have facilitated the emplacement of normally displaced cone sheet margins. However, the dyke swarms are less intense in Ardnamurchan than in the adjacent centres of activity and the number of normally displaced sheet margins is greater than would be expected, in relation to the number of dykes emplaced.

Controls exerted by the magma indentor have been modelled (Chapter 9) with the result that three models of cone sheet fractures have been investigated, which can be classified into two types. The first type requires a rapid indentor on either a

glass or saturated sand host, which produces a number of circular fractures simultaneously. The second type is by slow indentation on a glass host which produces a single fracture, repeated indentation produces more fractures of similar orientation. Both types of model produce a central zone where no fracturing is observed. It seems, therefore, in order to produce a large number of conical fractures simultaneously, the host material requires to be indented rapidly. A possible mechanical example of this is a rapidly ascending magma chamber. The volume of the indentor or geometry of the magma chamber is important as has been highlighted by the Set B Centre Two cone sheets which occur over a restricted area, following the emplacement of the Hypersthene Gabbro.

Indentation of the magma chamber roof creates, firstly, a system of tension around the roof of the chamber; photoelastic experiments demonstrate how these stress patterns are produced at the time of indentation. Secondly, indentation causes increased pressure on the fluids contained within the host rock. The result of these two processes along with the indentation, is the production of fractures in the shoulder areas of the magma chamber. Hydraulic fracturing is the process by which fractures are produced through the action of a fluid under pressure. Fracturing may be caused by one of two ways, which are by increasing the effective stress (the difference between the maximum and minimum stresses) or by decreasing the deviatoric stress (the actual value of the stress) by increased pore fluid pressure.

According to Phillips (1972) the concept of effective

stress can be applied to a porous medium which has a tensile strength and to the stresses at the edge of a fluid filled fracture. Under conditions of low deviatoric stress,that is less than approximately 4x the tensile strength of the rock, a hydraulic tensile fracture will form perpendicular to the minimum principal stress when the fluid pressure exceeds the combined minimum principal stress and the tensile strength of the rock. When a porous rock is subjected to a high and increasing deviatoric stress under conditions of relatively low fluid pressure, it will eventually fail by displacements along shear fractures. The inclination of shear fractures to the maximum principal stress will depend partly on the magnitude of the pore fluid pressure at the time of the fracture, the greater the fluid pressure the more closely the shear plane approaches the plane of tensile fracture which is perpendicular to the minimum principal stress. If fluid accumulates on the shear fracture and forms a sufficently large sheet which transmits pressure from below to the leading edge of the fracture, then the shear fracture may be extended at constant or decreasing deviatoric stress and this could be described as hydraulic shear fracture. As the deviatoric stress decreases the hydraulic shear fracture curves into a simple hydraulic tensile fracture. In summary, hydraulic tensile fractures initiate and propagate under conditions of high fluid pressure and low deviatoric stress and shear fractures initiate under conditions of low fluid pressure and high deviatoric stress.

10.14.1 Cone sheet evidence for the type of fracture

Bradley (1968), Escher et al. (1976) and Pollard (1973)

all give evidence of hydraulic fracturing as a mode of propagation of magmatic sheets. Beach (1980) also lists features associated with hydraulic fracture, one of which are en echelon sets.

Taylor and Forester (1971) have established the presence of meteoric water in the host rocks of Ardnamurchan, which facilitated the fracturing of the host rock. More than thirty examples of en echelon sets have been found within the cone sheet sets of the complex. The en echelon sets occur mainly in two of the cone sheet sets, Centre One and Centre Two Set B.

Two- and three-dimensional evidence (piercing point analysis) obtained from country-rock structures adjacent to cone sheet margins indicates that opening of all cone sheets involves, perpendicular to their margins, tension to some extent, in order to accommodate the magma emplaced. Consequently, calculations for the inflation caused by the emplacement of cone sheets was based on simple tensional openings. Cone sheets which open by tension are generally thin (Chapter 8).

However, some cone sheets demonstrate displacements along their fractures which indicate shear movements, both normal and reversed. On both the north and south coast Outer Centre Two traverses, the ratio of reversed to normal shear is 2:1. Another feature indicative of shear are the paired apophyses which "face" in opposite directions to each other and which occur in the Centre Two Set B cone sheets at An Acairseid and the Lighthouse section (Fig.7.1.3). The large number of en

echelon lenses occurring mainly in Centre One and Centre Two Set B and also occurring in fewer numbers in the other cone sheet sets also indicate some shearing. This, together with the existence of a zone of shear in the Hypersthene Gabbro host rock (Fig.7.1.3), and the predominantly dextral shear displacement associated with the en echelon sets, suggests that shearing was a prominent mechanism. Piercing point analyses have shown that both tension and shear operate to accommodate cone sheets and the net slip direction of the sheets indicates the presence of horizontal forces acting during emplacement of cone sheets, which result in a general anticlockwise movement of the central block. En echelon sheets, piercing point analyses and "facing apophyses" all indicate an anticlockwise movement of the central block. This may be evidence in support of spirally developing cone sheets (Tolansky and Howes, 1901; Bahat, 1979). It should be noted that these workers worked on single fractures which develop spirally. Therefore, the mechanism of emplacement cone sheets is not a simple one, as it has to explain the presence of cone sheets some of which have been emplaced under tensional regimes whereas others were emplaced in a shear regime, producing both normal and reversed movement.

10.14.2 Development of cone sheet fractures

Previous workers have concluded that cone sheet fractures are shear fractures which in general are reversed fractures, therefore the emplacement of a cone sheet set would result in the uplifting of the central block. Robson and Barr (1968) and Phillips (1974) discuss theories of normal shear displacements and tensional displacements, respectively, although Phillips

concludes that normal displacements cannot occur.

Phillips (1974) states that if no shear movements on the fractures occurred then in order to emplace magma into fractures a large radial compression would develop in the adjacent rocks. Alternatively, he suggests an outward radial displacement of the host rock.

Robson and Barr's (1968) theory involved a vertical maximum principal stress and that the magma body be sufficiently buried that a zone of shear existed in it's vicinity. The consequential failure is in the shape of a cone, whose apex is located within the magma chamber, with the central block descending to give normal displacements on the cone sheet fractures. These fractures originate at the earths surface and propagate down towards the magma chamber.

It is possible that both Phillips and Robson and Bar are correct, to some extent. Cone sheets involving normal displacement may be formed when the magma roof is inflated, however, in the theory of Robson and Bar these normally displaced fractures form at the surface and propagate down towards the magma chamber, therefore the fracture must be completely developed before any magma is emplaced. No field evidence of complete fractures existing before cone sheets were emplaced have been found in Ardnamurchan.

The space problem is a difficult one, in terms of opening cone sheet fractures under tension, due to the circular nature of the fracture the tension cannot be accommodated in the cen-

tral zone without resulting in central uplift. However, if the relationships between thickness of cone sheet and type of dilation are investigated (Chapter 8) it is shown that thin sheets (<1m) open by tension. Emplacement of these sheets would involve a build up of an excessive compression in the country rocks, as stated by Phillips. Conversley, the cone sheets which open by shear are often thick (>1m) and show a large amount of displacement, for example, a 2.8m thick sheet is associated with a displacement of 8m. Therefore, a possible solution to the problem of both tensional and shear displacements occurring within the same cone sheet set is that the emplacement of a series of thin cone sheets, opening purely by tension, produces compression in the host rock which is relieved by the emplacement of thicker sheets with large shear displacements along their margins.

Rapid indentation of the magma on the magma chamber roof firstly sets up the possbile stress trajectories for all the cone sheets of the set, increases the pore fluid pressure in the country rocks and acts as a buffer, that is it protects the contact area of the magma chamber roof against fracture, resulting in fracture in the "shoulder" areas where hydraulic tension fractures are formed. A repeated rise of magma results in either an increase of pressure, or a sustaining of the pressure, which produces the large number of sheets characteristic of Zone 2.

If throughout this time the adjacent dyke axis was active, which is substantiated by the presence of dykes which cut and are cut by cone sheets, then normal displacements would occur.

It is possible that the periodic stretching of the crust responsible for either dyke emplacement, or due to a rise of the magma chamber, was relieved by the downfaulting of the central block, forming cone sheet fractures with normal displacement.

10.15 FUTURE WORK

Plans for future work are two fold. Firstly to investigate the other cone sheet complexes of the B.T.I.P., particularly the Mull and Skye sets, in order to compare them to the Ardnamurchan cone sheet sets and to test my model. Secondly, based on the field and statistical subdivision of the cone sheet sets, I would like to collect and geochemically analyse the cone sheet rocks of Ardnamurchan. In particular, I would like to study the trace element patterns for each cone sheet set.

REFERENCES

Anderson, E.M. 1924. In Tertiary and post Tertiary geology in Mull, Loch Aline and Oban Eds. Bailey, E.B., Clough, C.D., Wright, B.A., Richey, J.E. and Wilson, G.V. Mem. Geol. Surv. Scotland. 445pp.

Anderson, E.M. 1936. The dynamics of the formation of cone-sheets, ring-dykes and cauldron-subsidences. Proc. R. Soc. Edin. 56 128-157.

Anderson, E.M. 1951. The dynamics of faulting and dyke formation. 2nd ed. London, Oliver and Boyd, 206pp.

Bahat, D. 1978. Hertzian fracture: a sound physical basis for the explanation of carbonatite structure. Mem. B.R.C.H. 91 275-283.

Bahat, D. 1979. Interpretation on the basis of Hertzian theory of a spiral carbonatite structure at Homa Mountain, Kenya. Tectonophysics 60 235-246.

Bahat, D. 1980. Hertzian fracture, a principal mechanism in the emplacement of the British Tertiary intrusive centres. Geol. Mag. 117 463-470.

Bailey, E.B., Clough, C.D., Wright, B.A., Richey, J.E. and Wilson, G.V. 1924. Tertiary and post Tertiary geology of Mull, Loch Aline, and Oban. Mem. Geol. Surv. Scotland, 445pp.

Bailey, E.B. 1958. Some aspects of igneous geology 1908-1958. Trans. geol. Soc. Glasgow. 23 29-52.

Baker, I. 1968. Small scale arcuate intrusions on Saint Helena, South Atlantic. Bull. Volcanol. 371-397.

Banfield, A.F., Behre, C.H. and St. Clair, D. 1956. Geology of Isabela (Albemarle) Island, Archipelago de Colon (Galapagos). Bull. geol. Soc. Am. 67 215-234.

Beach, A. 1979. The analysis of deformed belemnites. J. Struc. Geol. 1 127-136.

Beach, A. 1980. Numerical models of hydraulic fracturing and the interpretation of syntectonic veins. J. Struc. Geol. 2 425-438.

Bott, M.H.P. and Tuson, J. 1973. Deep structure beneath the Tertiary volcanic regions of Skye, Mull and Ardnamurchan, north-west Scotland. Nature. Phys. Sci. 242 114-116.

Boulter, M.C. 1978. In A correlation of Tertiary rocks in the British Isles. Eds. Curry, D., Adams, C.G., Boulter, M.C., Dilley, F.C., Eames, F.E., Funnell, B.M. and Wells, M.K. London: Geol. Soc. 72pp.

Bradley, J. 1965. Intrusions of major dolerite sills. Trans. R. Soc. N. Z. 3 27-55.

Cloos, H. 1936. Einfuhrung. Die Geologie, Berlin. 198-200.

Coker, E.G., Finlon, L.N.G. and Jessop, H.T. 1957. A treatise on photoelasticity Cambridge University Press, 550pp.

Currie, K.L. and Fergusson, J. 1970. The mechanics of intrusion of lamprophyre dikes indicated by

offsetting of dykes. Tectonophysics 9 525-535.

Dagley, P., Mussett, A.E. and Skelhorn, R.R. 1984. The palaeomagnetism of the Tertiaty igneous complex of Ardnamurchan. Geophys. J. R. astr. Soc. 79 911-922.

Davis, J.C. 1973. Statistics and data analysis New York, London, John Wiley and Sons, 550pp.

Delaney, J.R., Colony, W.E., Gerlach, T.M. and Nordlie, B.E. 1973. Geology of the Volcan Chico Area on Sierra Negra volcano, Galapagos Islands. Bull. geol. Soc. Am. 84 2455-2470.

Delaney, P.T. and Pollard, D.D. 1981. Deformation of host rocks and flow of magma during growth of minette dikes and breccia - bearing intrusions near ship rock, New Mexico. Geol. Surv. Prof. Paper 1202.

Dietrich, J.B. and Decker, R.W. 1975. Finite element modeling of surface deformation associated with volcanism. J. geophys. Res. 80 4094-4102.

Durrance, E.M. 1967. Photoelastic stress studies and their application to a mechanical analysis of the Tertiary ring-complex of Ardnamurchan, Argyllshire. Proc. Geol. Assoc. London 78 289-318.

Escher, A., Jack, S. and Watterson, J. 1976. Tectonics of the North Atlantic Proterozoic dyke swarm. Phil. Trans. R. Soc. London. A 280 529-539.

Farquharson, F.B. and Hennes, R.G. 1940. Gelatin

models for photoelstic analysis of stress in earth masses. Civil Eng. 10 211-214.

Field, J.E. 1964. Fracture in solids. Times Sci. Rev. No 51 5-9.

Fiske, R.S. 1969. Anatomy of an active volcaono - Kilauea, 1965-1968. Eos. Trans. A.G.U. 50 113.

Fiske, R.S. and Kinoshita, W.T. 1969. Inflation of Kilauea volcano prior to its 1967-1968 eruption. Science 165 341-349.

Garson, M.S. 1959. Stress pattern of carbonatite and alkaline dykes at Tundulu ring structure southern Nyasaland. Int. geol. Congr. Mexico 303.

Garson, M.S. 1966. Carbonatites in Malawi. In Carbonatites Ed. Tuttle, O.F. and Gittins, J. New York, Wiley Interscience, 33-71.

Gilliland, W.N. 1963. A minature πdykeπ echelon. Geol. Mag. 100 424-427.

Gribble, C.D., Durrance, and Walsh, J.N. 1976. Ardnamurchan a guide to geological excursions. Edinburgh Geol. Soc. 122pp.

Gribble, C.D. 1974. The dolerites of Ardnamurchan. Scott. J. Geol. 10 71-89.

Hald, N., Noe-Nygaard, A. and Pedersen 1971. The Kroksfjordur Central Volcano in north-west Iceland. Acta. Nat. islandica 2 5-29.

Hallam, A. 1972. Relation of Palaeogene ridge and basin structures and vulcanicity in the Hebrides and Irish sea regions of the British Isles to the opening of the North Atlantic. Earth planet.

Sci. Lett. 16 171-177.

Harker, A. 1904. The Tertiary Igneous rocks of Skye. Mem. Geol. Surv. U.K. 481pp.

Harrison, P.W. 1957. New technique for the three-dimensional fabric analysis of till and englacial debris containing particles from 3 to 40mm in size. J. Geol. 65 98-105.

Heywood, R.P. 1978. Designing by Photoelasticity London, Chapman and Hall, 303pp.

Hills, E.S. 1972. Elements of Structural Geology. London, Chapman and Hall, 502pp.

Holland, J.G. and Brown, G.M. 1972. Hebridean tholeiitic magmas: a geochemical study of the Ardnamurchan cone sheets. Contib. Mineral. Petrol. 37 139-160.

Holmes, A. 1924. Practical Methods. 125pp.

Irvine, T. 1982. Terminology for layered intrusions. J. Petrol. 23 127-162.

Jeffreys, H. 1936. Note on fracture. Proc. R. Soc. Edinburgh. 56 158-163.

Jessop, H.T. and Harris, F.C. 1960. Photoelasticity - Principals and Methods. New York, Dover Publications. Inc. 185pp.

Judd, J.W. 1874. The secondary rocks of Scotland. On the ancient volcanoes of the Highlands and the relations of their products of the Mesozoic strata. Q. J. geol. Soc. London 30 220-302.

Johnson, A.M. and Pollard, D.D. 1973. Mechanics of growth of some laccolithic intrusions in the Henry Mountains, Utah. Tectonophysics 18

261-309.

Kaitaro, S. 1953. Geologic structures of the late Precambrian Intrusives in the Ava area, Aland Islands. Bull. Comm. geol. Finl. No. 162 4-69.

Keunen, P.H. 1937. Intrusion of cone sheets. Geol. Mag. 74 177-183.

Kinoshita, W.T. 1967. May 1963 earthquakes and deformation in the Koae fault zone, Kilauea volcaono, Hawaii. U.S. geol. Surv. Prof. Paper. 575-C 173-176.

Kresten, P. 1980. The Alno complex: tectonics of dyke emplacement. Lithos 13 153-158.

Le Bas, M.J. 1971. Cone-sheets as a mechanism of uplift. Geol. Mag. 108 373-376.

Le Bas, M.J. 1977. Carbonatite-Nephelinite Volcanism. London, J. Wiley and Sons., 347pp.

Leeder, M. 1975. Lower Border Group (Tournasian) limestones from the Northumberland Basin. Scott. J. Geol. 11 151-167.

MacGregor, A.G. 1967. Faults and fractures in Ardnamurchan, Moidart, Sunart and Morven. Bull. geol. Surv. G.B. 27 1-14. I -5 Macintyre, R.M., Menamin, T. and Preston, J. 1975. K-Ar results from western Ireland and their bearing on the timing and siting of Thulean magmatism. Scott. J. Geol. 11 227-249.

Middleton, G.V. 1965. The Tukey chi-square test. J. Geol. 73 547-549.

Mitchell, J.G. and Reen, K.P. 1973. Potassium-Argon

ages from the Tertiary Ring Complexes of the Ardnamurchan peninsula, Western Scotland. Geol. Mag. 110 331-340.

Mussett, A.E., Dagley, P. and Skelhorn, R.R. 1980. Magnetostratigraphy of the Tertiary igneous succession of Mull, Scotland. J. geol. Soc. London 137 349-357.

Phillipe, R.R. and Mellinger, F.M. 1948. A study of photoelastic models of foundations. Proc. Sec. Conf. Soil. Mech. Found. Engg. 5 58-62.

Platten, I.M. and Watterson, J.S. 1969. Orientated crystal growth in some Tertiary dykes. Nature, London. 223 286-287.

Phillips, W.J. 1974. The dynamic emplacement of cone sheets. Tectonophysics 24 69-84.

Pollard, D.D. 1973. Derivation and evaluation of a mechanical model for sheet intrusions. Tectonophysics 19: 233-269.

Pollard, D.D., Muller, O.H. and Dockstader, D.R. 1975. The form and growth of fingered sheet intrusions. Bull. geol. Soc. Am. 86 351-363.

Pollard, D.D., Segall, P. and Delaney, P.T. 1982. Formation and interpretation of dilatant echelon cracks. Bull. geol. Soc. Am. 93 1291-1303 .

Ramsey, J.G. (1967). Folding and fracturing of rocks. New York: McGraw-Hill. 568pp.

Richey, J.E., Thomas, H.H. with contributions by Bailey, E.B., Simpson, J.B., Eyles, W.A., Lee, G.W., Radley, E.G. and Dixon, B.E. 1930. The geology of Ardnamurchan, northwest Mull and Coll. Mem.

Geol. Surv. Scotland, 378pp.

Richey, J.E. 1932. Tertiary ring structures in Britain. Trans. Geol. Soc. Glasgow 19 42-140.

Richey, J.E. 1934. Guide to the geological model of Ardnamurchan. Mem. Geol. Surv. Scotland, 49pp.

Richey, J.E. 1937. Some features of Tertiary volcanicity in Scotland and Ireland. Bull. Volcanol. 1 13-34.

Richey, J.E. 1961. Scotland: The Tertiary volcanic districts. British Regional Guide. Edinburgh, H.M.S.O. 120pp.

Rittmann, A. 1973. Structure and evolution of Mount Etna. Phil. Trans. R. Soc. Lond. A 274 5-16.

Robson, G.R. and Barr, K.G. 1964. The effect of stress on faulting and minor intrusions in the vicinity of a magma body. Bull. Volcanol. 27 315-330.

Rusnak, G.A. 1957. The orientation of sand grains under conditions of "unidirectional" fluid flow. J. Geol. 65 384-409.

Schminke, H.U. 1967. Cone sheet swarm resurgence of Tejeda Caldera, and the early geologic history of Gran Canaria. Bull. Volcanol. 31 153-162.

Sigurdsson, H. 1966. Geology of the Setberg area, Snaefellsnes, western Iceland. Greinar IV2 Societas Scientianum Islandica. IV2 1-54.

Simkin, T. 1972. Origin of some flat-topped volcanoes and guyots. Mem. geol. Soc. Am. 32

183-193.

Simpson, J.B. 1961. The Tertiary pollen flora of Mull and Ardnamurchan. Trans. R. Soc. Edinburgh. 64 421-464.

Speight, J.M. 1972. The form and structure of the Tertiary dyke-swarms of Skye and Ardnamurchan. Ph.D. Thesis (unpublished). Univ. London.

Speight, J.M., Skelhorn, R.R., Sloan, T. and Knapp, R.J. 1982. The dyke swarms of Scotland. In Igneous rocks of the British Isles (Ed. Sutherland, D.S. Chichester, John Wiley and Sons) 449-460.

Taylor, H.P. and Forrester, R.W. 1971. Low O igneous rocks from the Intrusive Complexes of Skye, Mull and Ardnamurchan, western Scotland. J. Petrol. 12 465-497.

Thompson, R.N. 1982. Magmatism and the British Tertiary Igneous Province. Scott. J. Geol. 18 49-107.

Tolansky, S. and Howes, V.R. 1954. Optical studies of ring cracks in glass. Proc. Phys. Soc. London. B67 467-472.

Tomkieff, S.I. 1958. Isle of Arran G. A. Guide. No.32.

Van Bemmelen, R.W. 1937. The cause and mechanism of igneous intrusion:- with some Scottish examples. Trans. geol. Soc. Glasgow 19 453-492.

Vann, I.R. 1978. The siting of Tertiary vulcanicity. In Crustal Evolution in northwestern Britain and adjacent regions. (Eds. Bowes, P.R. and Leake,

B.E.) Geol. J. Special Issue 10, 393-414.

Von Eckermann, H. 1948. The alkaline district of Alno Island. Sver. Geol. Unders. Ser. C A36.

Von Eckermann, H. 1966. Progress of research on the Alno carbonatite. In Carbonatites Eds. Tuttle, O.F. and Gittings, G. New York, Interscience 3-31.

Walker, G.P.L. 1975. A new concept of the evolution of the British Tertiary intrusive centres. J. Geol. Soc. London 131 121-141.

Wells, M.K. 1954. The structure and petrology of the Hypersthene-Gabbro intrusion, Ardnamurchan, Argyllshire. Q. J. geol. Soc. London 109 367-397.

Wishart, D. 1969a. Fortran II programs for 8 methods of cluster analysis (CLUSTAN 1). Computer Contribution 39, State Geological Survey. Kansas University.

Wishart, D. 1969. Numerical classification method for deriving natural classes. Nature. London. 221 97-98.

Wishart, D. 1978. Clustan user manual. 3rd ed. Edinburgh University, 123pp.

APPENDIX A
TABLE OF THE PHYSICAL DATA COLLECTED FROM THE ARDNAMURCHAN CONE SHEET COMPLEX FOR THE PRESENT STUDY

The following is a list of the cone sheet characteristics for all the measured traverses for all cone sheet sets.

where

LOCATION	location of the start of each traverse, * indicates the end of each traverse
N	number assigned to each cone sheet for identification in cluster analysis
D	angle of inclination of the cone sheet contact
S	orientation of the cone sheet, measured clockwise from dip
T	true thickness of the cone sheet, in metres
DS	distance from the focus of each centre of activity (after Richey et al. 1930) in kilometres
P	porphyritic cone sheets, 1 = presence 0 = absence
A	1 = acidic cone sheets 0 = basic cone sheets

CENTRE ONE

All cone sheets of Centre One were measured sequentially along a west to east traverse from Faskadale to Rubha ' a ' Choit

LOCATION	D	S	T	DS	P	A
Faskadale	57	308	0.35	2.30	0	0
	76	294	0.20	2.30	0	1
	30	310	1.20	2.30	1	0
	41	290	0.80	2.30	0	0
	33	311	0.16	2.30	0	0
	43	293	0.16	2.30	0	0
	45	287	1.00	2.30	1	0
	45	302	7.17	2.30	0	1
	63	284	5.08	2.30	0	0
	49	278	11.16	2.30	0	0
	35	339	0.85	2.30	0	0
	37	309	1.00	2.30	0	0
	30	045	19.2	2.30	0	1
	35	327	2.00	2.35	0	0
	40	307	0.45	2.35	1	0
	38	311	0.90	2.35	0	0
	40	323	0.34	2.35	0	0
	36	006	1.35	2.35	0	0
	44	273	1.50	2.35	0	0
	56	249	1.91	2.35	0	0
	42	307	3.15	2.35	0	0
	67	343	0.65	2.35	0	1
	50	321	0.50	2.35	0	0
	30	325	0.45	2.35	0	0
	23	321	0.60	2.35	0	0
	34	345	0.75	2.35	1	0
	30	317	1.60	2.35	1	0
	29	293	0.52	2.35	0	0
	42	310	0.50	2.35	0	0
	30	243	0.75	2.40	0	0
	46	345	0.20	2.40	0	0
	56	312	2.00	2.40	0	0
	52	289	0.30	2.40	0	0
	46	285	0.75	2.40	0	0
	27	289	0.80	2.40	0	0
	34	293	7.00	2.40	0	0
	34	302	3.00	2.40	0	0
	42	312	0.40	2.40	0	0
	32	317	0.70	2.40	0	0
	42	314	0.40	2.35	0	0
	44	346	1.50	2.35	0	0
	42	028	0.32	2.40	0	0
	56	161	0.70	2.40	0	0
	30	354	0.50	2.35	0	0
	40	077	1.30	2.35	0	0
	78	245	0.48	2.80	0	0
	52	319	5.40	2.80	0	0
	65	275	2.50	2.80	0	0

LOCATION	D	S	T	DS	P	A
	63	282	0.30	2.80	0	0
	56	256	0.40	2.80	0	0
	42	337	0.40	2.80	0	0
	39	295	0.22	2.80	0	0
	68	305	0.30	2.80	0	0
	30	284	0.50	2.80	0	0
	39	122	2.10	2.80	0	0
	58	312	3.20	2.80	0	0
	30	331	13.35	2.80	1	0
	43	343	0.40	2.80	0	0
	31	310	2.50	3.05	0	0
	49	317	0.70	3.10	0	0
	45	317	6.00	3.25	0	0
	41	335	1.20	3.25	1	0
	58	300	1.70	3.25	0	0
	38	079	0.20	3.40	0	0
	60	314	0.10	3.50	0	0
	44	146	0.66	3.50	1	0
	50	283	0.35	3.50	0	0
	48	206	0.20	3.45	0	0
	70	240	0.40	3.45	1	0
	60	320	0.22	3.45	0	0
	43	268	1.20	3.45	0	0
	48	166	0.60	3.45	0	1
	47	294	0.30	3.65	0	0
	49	319	1.20	3.65	0	0
	45	296	0.50	4.05	0	0
	41	288	0.40	4.05	0	0
	41	313	1.20	4.05	0	1
	54	312	0.05	4.05	1	0
	41	351	1.00	4.05	0	0
	30	340	6.00	4.05	0	0
	31	355	0.60	4.80	0	0
	42	326	1.40	4.80	0	0
	82	144	0.50	4.80	0	0
	32	313	2.50	4.80	0	0
	28	325	3.06	4.30	0	0
	12	321	0.20	4.30	0	0
	20	325	8.00	4.20	0	0
	24	349	0.10	4.20	0	0
	30	317	5.00	4.20	0	1
	36	313	2.20	4.20	0	0
	36	337	0.35	4.20	0	0
	25	341	2.11	4.20	0	0
	44	264	1.20	4.20	0	0
	14	022	1.10	4.20	0	0
	20	213	1.00	5.75	0	0
	33	228	1.00	5.75	0	0
	24	360	0.30	5.75	0	0
	40	336	0.50	5.75	0	0
	72	322	0.16	5.75	0	0
	67	313	0.20	5.75	0	0
	90	327	0.50	5.75	0	0
	57	331	0.90	5.75	0	0

LOCATION	D	S	T	DS	P	A
	75	313	0.70	5.75	0	0
	40	331	2.50	5.75	0	0
	16	052	0.38	5.75	0	0
	15	336	1.50	5.75	0	0
	26	359	1.50	5.75	0	0
	12	007	1.30	6.00	0	0
	56	266	0.90	6.00	1	0
	30	045	0.80	6.00	0	0
	30	305	0.50	6.00	1	0
	22	283	0.45	6.00	0	0
	70	204	0.50	6.00	0	0
	32	009	0.40	6.00	0	0
	38	343	0.25	6.00	0	0
	70	204	1.00	6.00	0	0
	50	225	1.10	6.00	0	0
	54	251	6.00	6.00	0	0
	20	323	15.00	6.15	0	0
	22	039	1.10	6.15	0	0
	50	049	0.25	6.30	0	0
	22	353	0.32	6.30	0	0
	48	305	0.90	6.30	0	0
	27	324	1.00	6.50	0	0
	28	340	1.10	6.50	1	0
	38	327	1.40	6.50	0	0
	34	334	2.00	6.50	0	0
	82	154	1.00	6.50	0	0
	52	132	0.18	6.55	0	0
	76	329	0.40	6.55	0	0
	44	333	6.00	6.55	0	1
	24	007	0.60	6.55	0	0
	28	327	0.30	6.60	0	0
	82	350	0.20	6.80	0	0
	54	121	0.20	6.80	1	0
	52	124	0.30	4.10	0	1
	67	005	0.30	4.10	1	0
	52	329	2.36	4.10	0	0
	34	343	2.50	4.10	0	0
	59	346	3.50	4.10	0	0
	40	322	0.70	4.10	0	0
	54	222	0.40	4.10	0	0
	35	359	0.30	4.10	0	0
	46	317	0.80	4.10	1	0
	58	146	0.60	4.10	0	0
	43	142	0.20	4.10	0	0
	90	027	0.20	4.10	0	0
	41	306	1.00	4.10	0	0
	50	331	0.90	4.10	0	0
	52	264	0.50	4.10	0	0
	49	058	2.00	4.10	1	0
	58	126	0.90	4.10	0	0
	42	114	2.00	4.10	0	0
	40	136	0.50	4.10	0	0
	40	129	0.70	4.10	0	0
	24	119	0.15	4.10	0	0

LOCATION	D	S	T	DS	P	A
	58	126	0.80	4.10	0	0
	50	112	0.90	4.10	0	0
	26	128	1.50	4.10	0	0
	40	156	0.30	4.10	0	0
	38	298	2.50	4.10	0	0
	43	116	0.30	4.10	1	0
	48	121	0.15	4.10	0	0
	21	009	0.10	3.75	0	0
	50	154	0.25	3.75	1	0
	36	294	0.40	3.75	0	0
	62	137	0.10	4.10	0	0
*Rubha a'Choit	48	069	0.60	3.75	0	0

OUTER CENTER TWO

Both the north and south coast traverses across the Outer Centre Two cone sheets are from the west to the east

LOCATION	N	D	S	T	DS	P	A
W of Sron Bheag	1	40	088	1.05	3.50	0	0
	2	81	177	0.20	3.50	0	0
	3	50	245	1.00	3.50	0	0
	4	45	328	1.00	3.50	0	0
	5	36	126	1.00	3.50	0	0
	6	66	084	0.30	3.80	0	0
*	7	68	077	0.50	3.80	1	0
(44506276)	8	08	068	0.05	3.80	0	0
	9	60	100	0.10	3.80	0	0
	10	30	241	2.00	3.80	0	0
	11	44	089	1.50	3.80	0	0
	12	38	049	1.00	3.80	0	0
	13	64	085	0.45	3.80	0	0
	14	50	084	0.25	3.80	0	0
	15	50	074	0.30	3.80	0	0
	16	51	087	0.40	3.80	1	0
	17	50	153	0.30	3.80	0	0
	18	46	076	0.80	3.80	1	0
	19	40	080	1.00	4.00	0	0
	20	43	073	0.50	4.00	0	0
	21	25	089	6.20	4.00	0	0
	22	54	064	0.80	4.00	0	0
	23	24	228	1.50	4.00	0	0
	24	42	047	2.00	4.00	0	0
	25	46	065	2.00	4.00	0	0
	26	25	093	2.00	4.00	0	0
	27	50	072	3.98	4.00	0	0
	28	62	055	0.10	4.00	1	0
	29	52	062	1.02	4.00	1	0
	30	68	091	0.20	4.25	0	0
	31	48	073	0.20	4.25	1	0
	32	44	095	0.40	4.25	0	0
	33	60	100	0.30	4.25	1	0
	34	52	080	0.50	4.25	0	0
	35	00	312	0.50	4.25	0	0
	36	30	121	1.83	4.25	1	0
	37	40	111	0.10	4.25	0	0
	38	81	349	0.20	4.35	1	0
	39	30	095	1.50	4.35	0	0
	40	38	082	0.35	4.35	0	0
	41	33	085	0.80	4.35	0	0
	42	42	045	2.00	4.35	1	0
	43	40	052	3.45	4.35	0	0
	44	62	065	0.40	4.35	0	0

OUTER CENTER TWO

Both the north and south coast traverses across the Outer Centre Two cone sheets are from the west to the east

LOCATION	N	D	S	T	DS	P	A
W of Sron Bheag	1	40	088	1.05	3.50	0	0
	2	81	177	0.20	3.50	0	0
	3	50	245	1.00	3.50	0	0
	4	45	328	1.00	3.50	0	0
	5	36	126	1.00	3.50	0	0
	6	66	084	0.30	3.80	0	0
*	7	68	077	0.50	3.80	1	0
(44506276)	8	08	068	0.05	3.80	0	0
	9	60	100	0.10	3.80	0	0
	10	30	241	2.00	3.80	0	0
	11	44	089	1.50	3.80	0	0
	12	38	049	1.00	3.80	0	0
	13	64	085	0.45	3.80	0	0
	14	50	084	0.25	3.80	0	0
	15	50	074	0.30	3.80	0	0
	16	51	087	0.40	3.80	1	0
	17	50	153	0.30	3.80	0	0
	18	46	076	0.80	3.80	1	0
	19	40	080	1.00	4.00	0	0
	20	43	073	0.50	4.00	0	0
	21	25	089	6.20	4.00	0	0
	22	54	064	0.80	4.00	0	0
	23	24	228	1.50	4.00	0	0
	24	42	047	2.00	4.00	0	0
	25	46	065	2.00	4.00	0	0
	26	25	093	2.00	4.00	0	0
	27	50	072	3.98	4.00	0	0
	28	62	055	0.10	4.00	1	0
	29	52	062	1.02	4.00	1	0
	30	68	091	0.20	4.25	0	0
	31	48	073	0.20	4.25	1	0
	32	44	095	0.40	4.25	0	0
	33	60	100	0.30	4.25	1	0
	34	52	080	0.50	4.25	0	0
	35	00	312	0.50	4.25	0	0
	36	30	121	1.83	4.25	1	0
	37	40	111	0.10	4.25	0	0
	38	81	349	0.20	4.35	1	0
	39	30	095	1.50	4.35	0	0
	40	38	082	0.35	4.35	0	0
	41	33	085	0.80	4.35	0	0
	42	42	045	2.00	4.35	1	0
	43	40	052	3.45	4.35	0	0
	44	62	065	0.40	4.35	0	0

LOCATION	N	D	S	T	DS	P	A
	45	58	073	0.60	4.35	0	0
	46	42	054	0.14	4.35	0	0
	47	43	099	0.20	4.50	0	0
	48	47	083	0.05	4.50	0	0
	49	63	062	1.00	4.50	0	0
	50	54	055	1.20	4.50	0	0
	51	72	049	1.00	4.50	0	1
	52	65	055	0.20	4.50	0	0
	53	42	079	0.20	4.50	0	0
	54	32	082	1.60	4.50	0	0
	55	40	074	0.30	4.50	0	0
	56	32	082	0.30	4.50	0	0
	57	44	068	0.50	4.50	0	0
	58	33	039	0.20	4.50	0	0
	59	56	108	0.50	4.50	0	0
	60	50	066	0.20	4.50	0	0
	61	40	035	0.70	4.50	0	0
	62	43	072	0.70	4.55	1	0
	63	32	067	1.40	4.55	0	0
	64	42	084	1.60	4.55	0	0
*(45376250)	65	30	042	2.70	4.55	0	0
(46856251)	66	59	329	0.59	4.25	1	0
	67	42	297	1.50	4.25	0	1
	68	20	326	0.30	4.25	0	0
	69	34	326	2.40	4.25	1	0
	70	80	154	0.25	4.25	0	0
	71	48	144	0.30	4.25	0	0
	72	37	080	0.12	4.25	0	0
	73	47	136	0.27	4.25	0	0
	74	24	055	0.55	4.25	0	0
	75	70	099	0.30	4.25	0	0
	76	18	158	0.20	4.25	0	0
	77	42	053	1.50	4.25	0	1
	78	42	067	0.60	4.25	1	0
	79	52	075	1.24	4.60	0	0
	80	41	047	1.05	4.60	0	0
*	81	44	021	0.49	4.60	0	0
Glas Eilean	82	50	052	0.19	4.60	1	0
	83	33	002	0.20	4.60	0	0
	84	56	011	4.44	4.60	0	0
	85	52	026	0.30	4.60	0	0
	86	20	354	1.37	4.60	0	0
	87	52	037	3.60	4.60	0	0

LOCATION	N	D	S	T	DS	P	A
	88	56	037	0.40	4.60	0	0
	89	46	029	0.94	4.60	0	0
	90	58	020	1.87	4.60	0	0
	91	39	012	1.45	4.60	0	0
	92	30	007	0.40	4.60	0	0
	93	22	012	1.78	4.60	0	0
	94	45	026	0.04	4.60	0	0
	95	61	038	1.05	4.60	0	0
	96	42	028	0.40	4.60	0	0
	97	46	019	0.65	4.60	0	0
	98	42	027	1.84	4.60	0	0
	99	30	018	2.00	4.60	0	0
	100	84	124	0.30	4.70	0	0
	101	90	334	0.70	4.70	0	0
	102	82	337	6.00	4.70	0	0
	103	33	024	2.56	4.70	0	0
	104	50	034	1.30	4.70	0	0
	105	27	076	0.44	4.70	1	0
	106	42	050	0.60	4.70	0	0
	107	31	044	1.29	4.70	0	0
	108	41	020	0.40	4.70	0	0
	109	42	035	0.54	4.70	0	0
	110	40	024	0.15	4.80	0	0
	111	32	026	0.31	4.80	0	0
	112	48	015	1.49	4.80	0	0
	113	44	029	5.45	4.80	1	0
	114	59	044	0.26	4.80	0	0
	115	42	065	0.20	4.80	0	0
	116	52	034	0.71	4.80	0	0
	117	40	077	10.61	4.80	0	0
	118	42	257	0.20	4.80	0	0
	119	40	056	0.19	4.80	0	0
	120	32	039	32.85	4.80	0	0
	121	52	060	0.30	4.90	0	0
	122	50	036	0.66	4.90	0	0
	123	40	024	1.67	4.90	0	0
	124	33	273	5.55	4.90	0	0
	125	90	014	0.30	4.90	0	0
	126	58	046	0.42	4.90	0	0
	127	90	068	0.27	4.90	0	0
	128	86	052	0.30	4.90	0	0
	129	84	040	0.20	4.90	0	0
	130	90	053	0.20	4.90	0	0
	131	72	219	6.10	4.90	0	0
	132	33	066	2.42	4.90	0	0
	133	18	218	0.37	4.90	0	0
	134	50	010	1.23	4.90	0	0
	135	32	026	0.15	4.90	0	0
	136	34	051	0.40	5.00	0	0
	137	36	047	4.29	5.00	1	0
	138	44	056	0.50	5.00	0	0
	139	20	059	0.30	5.00	0	0

LOCATION	N	D	S	T	DS	P	A
	140	42	080	4.82	5.00	0	0
	141	40	047	0.35	5.00	1	0
	142	36	035	0.15	5.00	1	0
	143	18	069	0.74	5.00	1	0
	144	22	058	0.79	5.00	0	0
	145	36	058	0.50	5.00	1	0
	146	42	063	3.10	5.00	1	0
	147	30	039	0.30	5.00	0	0
	148	52	040	2.29	5.00	1	0
	149	41	046	1.31	5.00	1	0
	150	18	240	0.15	5.00	0	0
	151	36	025	2.41	5.00	0	0
	152	30	035	0.10	5.00	0	0
	153	20	008	0.30	5.00	0	0
	154	20	012	1.54	5.00	1	0
	155	60	038	0.70	5.00	0	0
	156	58	028	1.50	5.00	0	0
	157	54	030	1.34	5.00	0	0
	158	70	084	0.20	5.00	0	0
	159	30	026	1.30	5.10	0	0
	160	36	035	2.00	5.10	1	0
	161	60	036	0.75	5.10	0	0
	162	44	066	0.20	5.10	0	0
	163	50	032	0.70	5.10	1	0
	164	40	031	0.60	5.10	0	0
	165	56	045	4.89	5.10	1	0
	166	40	056	0.25	5.10	0	0
	167	40	048	0.30	5.10	0	0
	168	39	079	0.50	5.10	0	0
	169	41	041	6.69	5.10	0	0
	170	40	052	0.74	5.10	1	0
	171	38	038	0.30	5.10	0	0
	172	42	030	0.25	5.10	0	0
	173	47	009	0.80	5.20	0	0
	174	64	018	0.08	5.20	0	0
	175	48	022	1.00	5.20	0	0
	176	44	031	2.20	5.20	0	0
	177	58	174	0.70	5.20	0	0
	178	54	198	3.07	5.20	0	0
	179	44	019	0.49	5.20	0	0
	180	34	019	0.60	5.20	0	0
	181	40	185	0.20	5.20	0	1
	182	76	032	1.50	5.20	1	0
	183	47	142	1.83	5.20	0	0
	184	44	144	3.60	5.20	0	0
	185	42	030	0.74	5.20	0	0
	186	40	024	0.16	5.20	0	0
	187	42	044	0.60	5.30	0	0
	188	42	097	1.00	5.30	0	0
	189	46	024	0.40	5.30	0	0
	190	42	021	2.50	5.30	1	0
	191	68	016	1.40	5.30	1	0

LOCATION	N	D	S	T	DS	P	A
	192	41	022	5.25	5.30	0	0
	193	40	020	2.18	5.30	0	0
	194	32	179	3.00	5.30	0	0
	195	46	070	3.96	5.30	0	0
	196	34	180	0.80	5.30	0	0
	197	54	064	0.55	5.30	0	0
	198	42	288	0.30	5.40	1	1
	199	37	274	1.00	5.40	0	0
	200	58	313	0.18	5.40	0	0
	201	50	077	0.16	5.40	0	0
	202	60	036	2.00	5.60	0	0
	203	40	028	1.50	5.60	0	0
	204	40	027	1.29	5.60	0	0
Mingary Pier	205	40	029	1.10	5.60	1	0
	206	32	066	4.50	5.45	0	0
	207	82	025	0.60	5.45	0	0
	208	49	012	1.00	5.45	0	0
	209	68	038	3.80	5.45	0	0
	210	44	018	0.90	5.45	0	0
	211	78	328	1.42	5.45	0	0
	212	46	005	5.97	5.45	0	0
	213	60	119	1.47	5.45	0	0
	214	67	125	1.11	5.45	0	0
	215	67	103	2.21	5.45	0	0
	216	90	316	0.50	5.45	0	0
	217	58	015	0.12	5.45	0	0
	218	30	010	1.65	5.45	0	0
	219	70	120	2.91	5.45	0	0
	220	34	262	6.15	5.45	0	0
	221	54	299	0.81	5.45	0	0
	222	50	316	4.83	5.50	0	0
	223	68	011	0.80	5.50	0	0
	224	24	134	0.73	5.50	0	0
	225	57	018	3.24	5.50	0	0
	226	77	210	0.10	5.50	0	0
	227	56	011	0.05	5.50	0	0
	228	85	133	0.36	5.50	0	0
	229	82	133	5.05	5.50	0	0
	230	48	355	9.77	5.50	0	0
	231	50	353	0.45	5.05	0	0
	232	58	353	0.20	5.05	0	0
	233	55	001	1.14	5.05	0	0
	234	52	356	6.66	5.05	0	0
	235	37	341	5.24	5.05	0	0
	236	36	341	0.12	5.05	0	0
	237	90	194	2.30	5.05	0	0
	238	34	017	0.70	5.05	0	0
	239	42	351	2.41	5.05	0	0
	240	33	192	0.35	5.15	0	0
	241	45	011	0.40	5.15	0	0
	242	30	012	0.90	5.15	0	0
	243	27	012	0.14	5.15	0	0

LOCATION	N	D	S	T	DS	P	A
	244	15	048	1.37	5.15	0	0
	245	48	135	0.50	5.15	0	0
	246	70	125	0.55	5.15	0	0
	247	17	301	1.00	5.15	0	0
	248	08	348	0.20	5.15	0	0
	249	13	019	0.25	5.15	0	0
	250	66	135	2.10	5.25	0	0
	251	74	005	0.20	5.25	0	0
	252	72	307	0.21	5.25	0	0
	253	78	058	6.36	5.25	0	0
	254	56	037	0.45	5.25	0	0
	255	50	045	0.23	5.25	0	0
	256	78	031	0.34	5.25	0	0
	257	60	039	0.04	5.25	0	0
	258	80	210	0.02	5.25	0	0
	259	82	213	0.06	5.25	0	0
	260	56	009	0.30	5.25	0	0
	261	68	027	3.70	5.25	0	0
	262	56	198	1.65	5.25	0	0
	263	86	319	0.59	5.25	0	0
	264	41	360	1.50	5.35	0	0
	265	14	319	1.50	5.35	0	0
	266	19	310	1.50	5.35	0	0
	267	28	048	0.10	5.35	0	0
	268	50	051	0.21	5.35	0	0
	269	38	054	4.00	5.35	0	0
Rubh' a' Mhile	270	20	020	5.47	5.90	0	0
	271	20	041	1.12	5.35	0	0
	272	32	337	1.00	5.90	0	0
	273	39	007	0.45	5.90	0	0
	274	48	055	3.34	5.90	0	0
	275	39	016	1.38	6.00	0	0
	276	72	145	0.38	6.00	0	0
	277	38	029	1.10	6.00	0	0
	278	44	002	8.60	6.00	0	0
	279	42	034	0.93	6.00	0	0
	280	08	288	1.50	6.10	0	0
	281	44	011	2.00	6.10	0	0
	282	90	339	5.40	6.20	0	0
	283	50	321	2.06	6.20	0	0
	284	57	355	3.35	6.30	1	0
	285	62	008	2.90	6.30	0	0
	286	78	046	1.37	6.30	0	0
	287	45	011	1.50	6.30	0	0
	288	52	013	0.75	6.30	0	0
	289	84	052	4.70	6.30	0	0
	290	60	052	0.95	6.30	0	0
	291	54	037	5.80	6.30	0	0
	292	35	014	0.18	6.30	0	0
	293	57	018	3.18	6.30	0	0
	294	66	176	2.00	6.30	0	0
	295	16	007	4.00	6.30	0	0

LOCATION	N	D	S	T	DS	P	A
	296	64	048	0.63	6.45	0	0
	297	36	002	2.05	6.45	0	0
	298	40	007	1.92	6.45	0	0
	299	52	152	1.58	6.45	0	0
	300	43	031	4.00	6.35	0	0
	301	41	335	3.00	6.35	0	0
	302	43	313	2.00	6.35	0	0
	303	42	002	4.10	6.35	0	0
	304	56	048	2.00	6.35	0	0
	305	40	357	0.70	6.35	0	0
	306	63	153	0.10	6.35	0	0
Sgeir nan Eun	307	20	268	1.00	6.35	0	0
	308	42	033	0.40	7.00	0	0
	309	30	179	0.70	7.00	0	0
	310	32	212	1.00	7.00	0	0
	311	71	064	0.60	7.00	0	0
	312	63	131	4.00	7.00	0	1
	313	42	227	3.00	7.00	0	0
	314	44	040	2.00	7.00	0	0
*end of S trav	315	26	131	2.00	7.00	0	0
N coast trav	316	66	061	0.70	7.00	0	0
Rubha an Duin	317	28	201	1.50	4.10	0	1
Bhain	318	90	042	0.10	4.10	0	0
	319	76	088	1.00	4.10	0	0
	320	86	097	0.70	4.10	0	0
	321	62	091	0.20	4.10	1	0
	322	82	073	1.80	4.10	1	0
	323	84	088	0.20	4.10	0	0
	324	76	097	0.87	4.10	0	0
	325	78	088	1.00	4.10	0	0
	326	74	079	0.63	4.10	0	0
	327	76	096	1.00	4.10	0	0
	328	60	098	2.00	4.10	1	0
	329	40	273	0.77	4.10	0	0
	330	77	093	0.20	4.10	0	0
	331	90	103	0.90	4.10	0	0
	332	66	090	0.14	4.10	0	0
	333	90	084	0.45	4.10	0	0
	334	72	089	1.71	4.10	0	0
	335	69	096	1.59	4.10	0	0
	336	85	108	3.00	4.10	1	0
	337	84	125	1.50	4.10	1	0
	338	80	104	1.57	4.10	0	0
	339	77	108	1.46	4.10	0	0
	340	82	102	1.19	4.10	0	0
	341	64	074	2.06	4.10	0	0
	342	58	285	1.90	4.10	0	0
	343	52	110	0.55	4.10	1	1
	344	46	108	3.34	4.10	1	0
	345	44	104	1.39	4.10	0	0
	346	70	275	0.70	4.10	1	0
	347	45	098	1.00	4.10	0	0

LOCATION	N	D	S	T	DS	P	A
	348	52	306	4.30	4.10	1	0
	349	90	056	0.20	4.10	0	0
	350	60	270	2.77	4.10	0	0
*	351	88	281	1.00	4.10	0	0
Rubha Carrach	352	47	252	10.90	4.10	0	0
	353	74	273	0.50	4.35	1	0
	354	70	285	0.80	4.35	0	1
	355	50	272	0.20	4.35	0	0
	356	52	000	0.40	4.35	0	0
	357	10	000	0.50	4.35	0	0
	358	25	000	1.00	4.35	0	0
	359	30	000	0.15	4.35	0	0
	360	72	282	0.30	4.35	0	0
	361	69	162	1.50	4.35	0	1
	362	81	245	0.25	4.35	0	0
	363	49	256	0.65	4.35	0	0
	364	23	000	0.27	4.35	0	0
	365	41	250	1.00	4.35	0	0
	366	25	244	0.30	4.35	0	0
	367	77	257	0.40	4.35	0	0
	368	46	236	1.00	4.35	1	0
	369	38	258	0.06	4.35	0	0
	370	70	238	1.20	4.35	1	0
	371	56	250	0.90	4.35	0	0
	372	33	287	2.00	4.35	1	0
	373	28	300	3.30	4.35	0	0
	374	59	248	0.50	4.35	0	0
	375	70	234	0.03	4.35	0	0
	376	69	270	0.40	4.35	1	0
	377	44	213	0.50	4.35	0	0
	378	90	270	0.60	4.35	0	0
	379	72	246	0.80	4.35	0	0
	380	60	266	0.30	4.35	0	0
	381	76	250	0.75	4.35	0	0
	382	50	262	0.70	4.35	0	0
	383	65	263	0.70	4.35	1	0
	384	48	274	0.35	4.45	0	0
	385	42	282	0.50	4.45	0	0
	386	66	294	1.00	4.50	0	0
	387	60	282	1.78	4.50	0	0
	388	70	280	1.12	4.50	0	0
	389	74	282	2.30	4.50	0	0
	390	68	245	0.25	4.50	0	0
	391	60	289	0.50	4.50	0	0
	392	72	281	0.40	4.50	0	0
	393	65	279	0.70	4.50	1	0
	394	40	289	2.60	4.50	0	0
	395	50	250	0.40	4.50	0	0
	396	49	283	1.10	4.50	0	0
*	397	90	340	4.00	4.50	0	0
Alt Glendrian	398	46	301	0.15	4.55	0	0
	399	42	316	1.70	4.55	0	0

LOCATION	N	D	S	T	DS	P	A
	400	45	300	0.20	4.55	0	0
	401	36	284	0.60	4.55	0	0
	402	46	312	0.15	4.55	0	0
	403	50	287	0.50	4.55	0	0
	404	50	324	0.20	4.55	0	0
	405	46	280	0.80	4.55	0	0
	406	36	265	1.30	4.55	0	0
	407	38	280	0.10	4.55	0	0
	408	34	260	0.30	4.55	0	0
	409	34	317	2.00	4.55	0	0
	410	38	309	0.90	4.55	0	0
	411	26	263	1.00	4.55	0	0
	412	33	305	0.90	4.55	0	0
	413	20	323	0.80	4.55	0	0
	414	62	317	0.30	4.55	0	0
	415	48	302	1.00	4.55	0	0
	416	63	327	9.35	4.55	0	0
*	417	42	301	0.50	4.65	0	0
(46497068)	418	45	298	1.40	4.65	0	0
	419	14	039	0.48	4.65	0	1
	420	42	287	3.00	4.65	0	0
	421	68	235	2.00	4.65	0	0
	422	40	298	0.50	4.65	0	0
	423	79	314	0.30	4.65	0	0
	424	68	120	0.57	4.65	0	0
	425	55	269	2.07	4.65	0	0
	426	67	263	0.55	4.65	0	0
	427	38	278	0.85	4.65	0	0
	428	52	240	0.30	4.65	0	0
	429	78	217	0.50	4.65	0	0
	430	72	131	0.50	4.65	0	0
	431	80	230	0.60	4.65	0	0
	432	42	333	0.84	4.65	0	0
	433	32	265	0.39	4.65	0	0
	434	29	295	0.68	4.65	0	0
	435	29	295	1.28	4.65	0	0
	436	29	090	2.39	4.65	0	0
	437	27	246	1.50	4.65	0	0
	438	30	255	2.00	4.65	0	1
	439	36	269	0.80	4.65	0	0
	440	35	271	4.50	4.65	0	0
	441	52	267	0.15	4.65	0	0
	442	30	267	1.26	4.65	0	0
	443	42	247	0.28	4.65	1	0
	444	36	232	3.80	4.65	0	0
	445	34	244	2.01	4.65	0	0
	446	22	267	0.90	4.65	0	0
	447	67	041	0.27	4.65	0	0
	448	46	261	0.40	4.65	0	0
	449	35	279	0.35	4.65	0	0
	450	57	275	1.42	4.65	0	0
	451	42	282	1.14	4.65	1	0

LOCATION	N	D	S	T	DS	P	A
	452	37	257	0.07	4.65	0	0
	453	49	261	0.25	4.65	0	0
	454	31	264	0.17	4.65	0	0
	455	32	266	0.40	4.65	0	0
	456	32	253	0.40	4.65	0	0
	457	25	260	0.36	4.65	0	0
	458	36	259	0.80	4.65	0	0
	459	32	254	0.30	4.65	0	0
	460	30	262	0.55	4.65	0	0
	461	20	254	0.27	4.65	0	0
	462	31	248	0.31	4.65	0	0
	463	32	254	0.16	4.65	0	0
	464	43	261	0.21	4.65	0	0
	465	52	262	0.87	4.65	0	0
	466	39	303	0.63	4.65	0	0
	467	33	255	2.17	4.65	0	0
	468	24	271	0.57	4.65	0	0
	469	20	281	1.16	4.65	0	0
*	470	50	283	3.80	4.90	0	0
(46707093)	471	40	295	2.00	4.90	0	0
	472	30	301	2.00	4.90	0	0
	473	37	252	0.54	4.90	0	0
	474	39	272	2.50	4.90	0	0
	475	38	259	1.00	4.90	0	0
	476	28	271	0.20	4.90	0	0
	477	72	285	1.10	4.90	0	0
	478	28	274	0.10	4.90	0	0
	479	47	279	0.15	4.90	0	0
	480	48	285	1.04	4.90	1	0
	481	52	293	0.10	4.90	0	0
	482	82	271	0.20	4.90	0	0
	483	46	310	1.44	4.90	0	0
	484	56	273	0.20	4.90	0	0
	485	59	285	0.60	4.90	0	0
	486	40	292	3.00	4.90	0	0
	487	60	274	1.00	4.90	0	0
	488	36	300	0.10	4.90	0	0
	489	35	283	0.10	4.90	0	0
	490	62	289	0.80	4.90	0	0
	491	54	295	0.40	4.90	0	0
	492	53	279	1.50	4.90	0	0
	493	36	285	0.20	4.90	0	0
	494	41	259	0.60	4.90	0	0
	495	30	293	0.20	4.90	0	0
	496	48	290	0.30	4.90	0	0
	497	40	247	0.40	4.90	0	0
	498	46	275	0.40	4.90	0	0
	499	62	063	2.64	4.90	0	0
	500	22	252	0.40	4.90	0	0
	501	30	250	0.15	4.90	0	0
	502	54	075	0.50	4.90	0	0

503	57	319	0.60	4.90	0	0

	N	D	S	T	DS	P	A
	504	45	020	6.00	4.90	0	0
	505	38	257	0.50	4.90	0	0
	506	42	289	0.60	4.90	0	0
*	507	53	311	0.20	4.90	0	0
Rubha Dubh an	508	30	265	0.30	4.90	0	0
Aige	509	30	259	0.25	4.95	0	0
	510	40	277	0.20	4.95	0	0
	511	45	301	0.30	4.95	0	0
	512	21	272	0.25	4.95	0	0
	513	41	302	0.50	4.95	0	0
	514	37	321	0.21	4.95	1	0
	515	26	288	1.00	4.95	0	0
	516	42	301	0.08	4.95	0	0
	517	36	229	0.12	4.95	0	0
	518	38	287	0.60	4.95	0	0
	519	35	279	2.35	4.95	0	0
	520	35	287	0.70	4.95	0	0
	521	21	291	1.50	4.95	1	1
	522	56	281	5.10	4.95	0	0
	523	39	289	0.38	4.95	0	0
	524	44	287	3.75	4.95	0	0
	525	32	261	1.54	4.95	0	0
	526	59	262	1.28	4.95	0	1
	527	72	271	0.09	4.95	0	0
	528	54	245	4.60	4.95	0	0
	529	44	273	0.16	4.95	0	0
	530	37	299	6.00	4.95	0	0
	531	45	279	0.99	4.95	0	0
	532	34	295	3.30	4.95	0	1
	533	36	311	0.17	4.95	0	0
	534	26	305	0.78	4.95	0	0
	535	30	273	2.20	4.95	0	0
	536	32	282	0.20	4.95	0	0
	537	30	291	0.10	4.95	0	0
	538	30	276	0.60	4.95	0	0
	539	34	305	0.60	4.95	0	0
	540	55	243	5.25	4.95	0	0
	541	41	274	1.70	4.95	0	0
	542	43	300	0.25	4.95	0	0
	543	18	258	0.87	4.95	0	0
	544	50	267	1.00	4.95	0	0
	545	54	261	0.50	4.95	0	0
	546	45	266	0.50	4.95	0	0
	547	12	243	2.60	4.95	0	0
	548	64	079	0.50	4.95	0	0
	549	34	279	2.01	4.95	0	0
	550	30	281	0.35	4.95	0	0
	551	25	304	0.92	4.95	0	0
	552	28	283	3.20	4.95	0	0
	553	45	284	0.25	4.95	1	0
	554	41	289	0.30	4.95	0	0
	555	44	333	0.35	4.95	0	0

LOCATION	N	D	S	T	DS	P	A
	556	42	289	3.00	4.95	0	0
	557	19	246	0.55	4.95	0	0
	558	32	283	2.33	4.95	0	0
	559	87	104	1.59	4.95	0	1
	560	43	336	1.00	4.95	0	0
	561	14	072	1.00	4.95	0	0
	562	41	281	0.80	4.95	0	0
	563	70	303	0.40	4.95	0	0
	564	74	334	0.55	4.95	0	0
	565	32	300	0.20	4.95	0	0
	566	50	209	2.00	5.05	0	0
	567	50	273	1.00	5.05	0	0
	568	02	309	0.10	5.05	0	0
	569	42	275	0.30	5.05	0	0
	570	75	302	0.76	5.05	0	0
	571	40	298	0.35	5.05	0	0
	572	54	305	0.30	5.05	0	0
	573	32	287	0.63	5.05	0	0
	574	45	296	2.80	5.05	0	0
	575	61	283	0.80	5.05	0	0
	576	57	105	0.60	5.05	0	0
	577	47	236	4.10	5.05	0	0
	578	49	291	0.35	5.05	0	0
	579	50	288	1.38	5.05	0	0
	580	37	301	0.40	5.05	0	0
	581	67	329	2.76	5.05	0	0
	582	71	267	1.15	5.05	0	0
	583	52	323	0.50	5.05	0	0
	584	70	283	0.93	5.05	0	0
	585	39	263	0.20	5.05	0	0
	586	66	233	0.45	5.05	0	0
	587	64	287	0.55	5.05	0	0
	588	54	149	1.05	5.05	0	0
	589	55	288	2.53	5.05	0	1
	590	38	283	1.90	5.05	0	0
	591	59	209	0.50	5.05	0	0
	592	47	272	0.85	5.05	0	0
	593	42	304	0.40	5.05	0	0
	594	47	306	1.00	5.05	0	0
	595	67	283	1.00	5.05	0	0
*	596	30	284	2.30	5.05	0	0
(47177109)	597	21	269	1.18	5.05	0	0
	598	47	311	0.50	5.10	0	0
	599	48	287	0.20	5.10	0	0
	600	35	324	0.34	5.10	0	0
	601	37	307	0.25	5.10	0	0
	602	31	306	0.77	5.10	0	0
	603	56	299	0.90	5.10	0	0
	604	55	287	3.00	5.10	0	0
	605	32	256	0.48	5.10	0	0
	606	34	338	0.31	5.10	0	0
	607	45	343	0.46	5.10	0	0

LOCATION	N	D	S	T	DS	P	A
	608	45	310	0.64	5.10	0	0
	609	82	296	0.79	5.10	0	0
	610	44	285	1.00	5.10	0	0
	611	58	312	4.40	5.10	0	0
	612	35	253	2.50	5.10	0	0
	613	53	276	0.35	5.10	0	0
	614	40	268	0.30	5.10	0	0
	615	60	326	0.20	5.10	0	0
	616	48	210	0.80	5.10	0	0
	617	82	120	0.60	5.10	0	0
	618	42	282	0.94	5.10	0	0
*	619	58	312	0.89	5.10	0	0
(47397106)	620	52	143	17.00	5.10	0	0
	621	40	295	0.20	5.20	0	0
	622	67	312	0.17	5.20	0	0
	623	64	339	0.03	5.20	0	0
	624	40	306	2.00	5.20	0	0
	625	48	291	1.30	5.20	0	0
	626	38	297	0.17	5.20	0	0
	627	53	294	0.50	5.20	0	0
	628	67	252	0.40	5.20	0	0
	629	78	252	0.30	5.20	0	0
	630	69	285	1.87	5.20	0	0
	631	43	287	1.36	5.20	0	0
	632	59	295	3.88	5.20	0	0
	633	51	304	0.50	5.20	1	0
	634	39	287	2.71	5.20	0	0
	635	43	282	2.80	5.20	0	0
	636	62	303	0.15	5.15	0	0
	637	57	313	0.75	5.15	0	0
	638	39	312	0.38	5.15	0	0
	639	47	300	0.13	5.15	0	0
	640	58	267	0.67	5.15	0	0
*	641	43	317	2.50	5.15	0	0
Sgeir Ghibeach	642	62	017	0.70	5.15	0	0
	643	60	303	0.40	5.15	1	0
	644	63	307	0.18	5.15	0	0
	645	49	293	0.90	5.15	0	1
	646	62	294	1.00	5.15	0	0
	647	74	065	0.40	5.15	0	0
	648	70	297	0.60	5.15	0	0
	649	55	271	0.40	5.15	0	0
	650	76	130	0.10	5.25	1	0
	651	54	297	1.13	5.25	0	0
	652	62	317	0.70	5.25	1	0
	653	53	306	1.52	5.25	0	0
	654	50	309	0.15	5.25	0	0
	655	50	310	0.31	5.25	0	0
	656	40	300	0.42	5.25	0	0
	657	84	328	1.40	5.25	0	0
	658	68	303	1.69	5.25	0	0
	659	70	327	4.70	5.25	0	0

LOCATION	N	D	S	T	DS	P	A
	660	70	154	0.80	5.50	0	0
	661	84	205	1.50	5.50	0	0
	662	42	144	0.40	5.50	1	0
	663	40	039	0.90	5.50	1	0
	664	56	266	0.20	5.50	0	0
	665	52	325	6.00	5.50	0	0
	666	56	311	0.60	5.50	0	0
	667	76	145	1.00	5.50	0	0
	668	62	309	11.00	5.50	0	0
	669	62	297	3.00	5.50	0	0
	670	80	337	0.50	5.50	1	0
	671	83	099	0.90	5.50	0	0
	672	83	135	0.29	5.50	1	0
	673	70	155	0.40	5.50	0	0
	674	32	303	0.25	5.50	0	0
	675	61	321	2.50	5.50	0	0
	676	53	113	1.00	5.50	1	0
	677	32	009	0.40	5.50	0	0
	678	38	343	0.25	5.50	0	0
	679	70	204	1.00	5.50	0	0
	680	50	225	1.10	5.50	1	0
*	681	54	251	6.00	5.50	0	1
Sloch na	682	35	275	0.20	6.00	0	0
Brach	683	52	266	1.50	6.00	0	0
	684	40	255	2.50	6.00	0	0
	685	34	283	0.17	6.00	0	0
	686	45	251	0.08	6.00	0	0
	687	55	268	0.10	6.00	0	0
	688	28	276	1.10	6.00	0	0
	689	26	242	1.00	6.00	0	0
*	690	40	272	0.40	6.00	0	0
(49127121)	691	50	287	0.60	6.00	0	0
	692	46	275	0.50	6.00	0	0
	693	53	287	1.05	6.00	0	0
	694	40	284	2.00	6.00	0	0
	695	62	283	0.25	6.00	1	0
	696	32	276	0.90	6.00	0	0
	697	45	279	1.50	6.00	0	0
	698	55	255	1.00	6.00	0	0
	699	56	260	0.70	6.00	0	0
	700	54	245	0.50	6.00	0	0
	701	40	284	1.54	6.00	0	0
1000m	702	37	263	1.00	6.00	0	0
	703	44	336	1.70	6.00	0	0
	704	46	308	0.05	6.00	0	0
	705	47	324	1.00	6.00	0	0
	706	36	276	4.10	6.00	0	0
	707	46	288	0.80	6.00	0	0
	708	30	280	1.20	6.00	0	0
	709	40	273	0.30	6.00	0	0
	710	60	290	0.50	6.00	0	0
	711	35	309	0.52	6.00	0	0

LOCATION	N	D	S	T	DS	P	A
	712	50	307	2.90	6.00	0	0
	713	60	272	0.60	6.00	0	0
	714	52	293	0.60	6.00	0	0
	715	55	321	1.23	6.00	0	0
	716	40	312	0.72	6.00	0	0
	717	55	310	2.30	6.00	0	0
	718	46	309	0.80	6.00	0	0
	719	82	302	2.57	6.00	0	0
	720	36	291	0.10	6.00	0	0
	721	48	291	0.42	6.00	0	0
	722	42	251	1.20	6.00	0	0
	723	46	291	2.40	6.00	0	0
	724	32	265	0.15	6.00	0	0
	725	70	091	6.20	6.00	0	0
	726	68	096	0.15	6.00	0	0
	727	66	266	1.00	6.00	0	0
	728	44	273	3.00	6.00	0	0
	729	52	262	0.13	6.00	0	0
	730	60	279	0.90	6.00	0	0
	731	62	267	2.50	6.00	0	0
	732	54	281	0.40	6.00	0	0
	733	58	319	2.00	6.00	0	0
	734	39	279	3.00	6.00	0	0
	735	58	289	0.20	6.00	0	0
	736	72	277	0.32	6.00	0	0
	737	56	310	0.30	6.00	0	0
	738	82	062	0.80	6.00	0	0
	739	70	052	0.30	6.00	0	0
	740	27	289	0.40	6.20	0	0
	741	46	326	0.25	6.20	0	0
	742	55	325	0.30	6.20	0	0
	743	46	307	0.30	6.20	1	0
	745	44	301	0.16	6.20	1	0
	746	62	270	0.20	6.20	1	0
	747	34	091	5.00	6.20	0	0
	748	76	002	0.10	6.20	0	0
	749	68	358	2.20	6.20	0	1
	750	74	014	0.20	6.20	0	0
	751	80	041	0.40	6.20	1	0
	752	62	286	0.70	6.20	0	0
	753	41	321	0.10	6.20	0	0
	754	64	021	0.20	6.20	0	0
	755	75	260	0.77	6.20	1	0
	756	42	262	3.00	6.20	0	0
	757	45	281	2.50	6.20	0	0
	758	77	049	0.40	6.20	0	0
	759	78	026	0.50	6.20	0	0
	760	62	322	0.32	6.20	1	0
	761	66	228	2.40	6.40	0	0
	762	71	233	1.30	6.40	0	0
	763	60	230	1.20	6.40	0	0

LOCATION	N	D	S	T	DS	P	A
	764	56	261	0.50	6.40	0	0
	765	89	237	0.55	6.40	0	0
	766	82	221	0.70	6.40	0	0
	767	48	328	0.10	6.40	0	0
	768	60	045	0.20	6.40	0	0
	769	52	321	0.30	6.40	0	0
	770	57	316	0.25	6.40	0	0
	771	42	332	0.50	6.40	0	0
	772	46	029	0.60	6.40	0	0
	773	52	284	1.00	6.40	0	0
	774	44	234	3.00	6.40	1	0
	775	22	261	0.90	6.40	1	0
	776	42	057	1.00	6.30	0	0
	777	62	331	0.40	6.30	0	0
	778	54	339	0.27	6.30	0	0
	779	28	106	0.10	6.30	0	0
	780	28	080	0.10	6.30	0	0
	781	62	319	0.36	6.30	0	0
	782	42	291	0.32	6.30	0	0
	783	55	304	0.20	6.20	0	0
	784	49	319	0.80	6.30	1	0
	785	38	313	1.00	6.30	1	0
	786	90	042	0.10	4.10	0	0
(46047032)	787	76	088	1.00	4.10	0	0
	788	86	097	0.70	4.10	0	0
	789	62	091	0.20	4.10	1	0
	790	82	073	1.80	4.10	1	0
	791	84	088	0.20	4.10	0	0
	792	76	097	0.87	4.10	0	0
	793	78	088	1.00	4.10	0	0
	794	74	079	0.63	4.10	0	0
	795	76	090	1.00	4.10	0	0
	796	60	098	2.00	4.10	1	0
	797	40	273	0.77	4.10	0	0
	798	77	093	0.20	4.10	0	0
	799	90	103	0.90	4.10	0	0
	800	66	090	0.14	4.10	0	0
	801	90	084	0.45	4.10	0	0
	802	72	089	1.71	4.10	0	0
	803	69	096	1.59	4.10	0	0
	804	85	108	3.00	4.10	1	0
	805	84	125	1.50	4.10	1	0
	806	80	104	1.57	4.10	0	0
	807	77	108	1.46	4.10	0	0
	808	82	102	1.09	4.10	0	0
	809	64	074	2.06	4.10	0	0
	810	58	285	1.90	4.10	0	0
	811	52	285	1.90	4.10	1	1
	812	40	108	3.34	4.10	1	0
	813	44	104	1.39	4.10	0	0
	814	70	275	0.70	4.10	1	0
	815	52	306	4.30	4.10	1	0

LOCATION	N	D	S	T	D	P	A
	816	90	056	0.20	4.10	0	0
	817	60	270	2.77	4.10	0	0
*	818	88	281	1.00	4.10	0	0
Rubha an	819	47	252	10.90	4.10	0	0
Duin Bhain	820	42	280	1.20	4.10	0	0
	821	76	261	0.25	4.10	0	0
	822	46	255	1.50	4.10	0	0
	823	72	257	0.50	4.10	1	0
	824	90	263	0.20	4.10	0	0
	825	40	248	1.00	4.10	0	0
	826	42	064	0.20	4.10	0	0
	827	46	239	0.20	4.10	0	0
	828	84	287	0.40	4.10	1	0
	829	64	288	1.20	4.10	0	0
	830	54	268	0.10	4.10	0	0
	831	90	275	0.14	4.10	0	0
	832	40	247	0.40	4.10	0	0
	833	45	275	0.80	4.10	1	0
	834	82	278	0.40	4.10	1	0
	835	81	279	0.70	4.10	0	0
	836	70	242	0.50	4.10	0	0
	837	85	264	0.80	4.10	0	0
	838	62	240	0.30	4.10	0	0
	839	44	255	1.00	4.10	1	0
	840	54	261	0.10	4.10	0	0
*	841	50	089	1.00	4.10	0	0

LOCATION	N	D	S	T	D	P	A
	816	90	056	0.20	4.10	0	0
	817	60	270	2.77	4.10	0	0
*	818	88	281	1.00	4.10	0	0
Rubha an	819	47	252	10.90	4.10	0	0
Duin Bhain	820	42	280	1.20	4.10	0	0
	821	76	261	0.25	4.10	0	0
	822	46	255	1.50	4.10	0	0
	823	72	257	0.50	4.10	1	0
	824	90	263	0.20	4.10	0	0
	825	40	248	1.00	4.10	0	0
	826	42	064	0.20	4.10	0	0
	827	46	239	0.20	4.10	0	0
	828	84	287	0.40	4.10	1	0
	829	64	288	1.20	4.10	0	0
	830	54	268	0.10	4.10	0	0
	831	90	275	0.14	4.10	0	0
	832	40	247	0.40	4.10	0	0
	833	45	275	0.80	4.10	1	0
	834	82	278	0.40	4.10	1	0
	835	81	279	0.70	4.10	0	0
	836	70	242	0.50	4.10	0	0
	837	85	264	0.80	4.10	0	0
	838	62	240	0.30	4.10	0	0
	839	44	255	1.00	4.10	1	0
	840	54	261	0.10	4.10	0	0
*	841	50	089	1.00	4.10	0	0

INNER CENTRE TWO

All unit lengths are measured from north to south

LOCATION	D	S	T	D	P	A
Lighthouse	58	182	1.50	3.80	1	0
	43	151	0.20	3.80	0	0
	30	178	0.50	3.80	0	0
	75	179	0.70	3.80	1	0
	72	189	0.50	3.80	0	0
	80	198	0.70	3.80	1	0
	68	204	0.40	3.80	1	0
	72	197	0.20	3.80	0	0
	70	193	0.15	3.80	1	0
	52	193	0.30	3.80	1	0
	28	198	0.30	3.80	1	0
*	40	197	0.40	3.80	0	0
Sgurr nam	47	186	0.80	3.80	0	0
Mean	48	217	3.00	3.80	0	0
	59	165	1.00	3.80	0	0
	60	187	0.30	3.80	0	0
*	80	334	0.10	1.85	0	1
U. Beinn	70	149	0.15	1.85	1	0
Bhuidhe	54	162	0.24	1.85	0	0
	76	296	0.15	1.85	0	0
	74	297	1.15	1.85	1	0
	75	082	0.03	1.85	0	1
	64	154	0.10	1.85	0	0
	90	165	0.10	1.85	0	0
	74	155	0.20	1.85	0	1
	75	130	0.40	1.85	1	0
	68	158	1.00	1.85	0	0
	71	138	0.56	1.80	1	0
	72	172	0.55	1.80	0	0
	84	334	0.22	1.80	0	0
	76	151	1.84	1.80	0	1
	75	185	2.80	1.80	0	0
	80	197	0.16	1.80	0	0
	84	154	0.20	1.80	0	0
	80	171	0.45	1.80	0	0
	90	348	0.05	1.80	0	0
	76	152	1.00	1.80	0	0
	75	160	0.30	1.80	0	0
	77	168	2.00	1.60	0	1
	70	152	1.20	1.80	1	0
	71	160	0.50	1.60	0	0
	82	143	2.50	1.60	0	1
	76	152	0.40	1.60	0	1
	64	164	0.02	1.60	0	0
	56	183	1.00	1.60	0	0
	76	155	0.03	1.60	0	0
	53	123	0.40	1.60	1	0
	70	152	0.03	1.60	0	0
	55	165	0.05	1.60	0	0
	72	163	0.15	1.60	0	0

LOCATION	D	S	T	DS	P	A
	76	171	0.15	1.60	0	0
	58	122	0.22	1.60	0	1
	70	185	0.15	1.60	0	0
	76	168	0.80	1.60	0	0
	78	148	0.30	1.60	0	0
	84	140	0.10	1.60	0	0
	75	161	0.30	1.60	0	0
*	79	149	1.00	1.70	0	0
L. Beinn	70	173	2.00	1.50	1	0
Bhuidhe	85	166	1.00	1.50	0	0
	82	165	0.50	1.50	1	0
	70	146	3.00	1.50	0	0
	80	162	0.20	1.50	0	0
	74	174	2.45	1.50	1	0
	78	193	3.30	1.50	0	1
	89	157	0.17	1.60	1	0
	81	162	2.65	1.60	1	0
	78	146	3.08	1.60	1	0
	80	170	0.26	1.60	0	0
	78	156	1.91	1.70	0	0
	73	137	0.35	1.70	0	0
	84	148	0.10	1.70	1	0
	40	201	0.15	1.70	0	0
	88	101	0.20	1.80	1	0
	56	153	0.25	1.80	1	0
	60	167	0.12	1.80	0	0
	72	130	0.10	1.80	1	0
	40	118	0.12	1.80	1	0
	60	146	0.65	1.80	0	0
	88	329	0.10	1.80	1	0
	70	150	0.20	1.80	1	0
*	64	119	1.00	1.80	1	0
Garbdhail	74	147	0.26	1.80	0	1
	70	247	1.00	1.50	1	0
	66	330	0.15	1.50	0	0
	70	287	0.05	1.50	0	0
	77	293	0.30	1.50	0	0
	79	299	0.70	1.50	0	0
	70	139	0.70	1.50	1	0
	70	078	0.07	1.50	0	0
	85	127	1.10	1.50	0	0
	66	311	0.50	1.50	0	0
	70	104	0.60	1.50	1	0
	73	301	1.00	1.50	0	0
	35	229	1.50	1.50	0	0
	64	216	1.20	1.50	0	0
	80	059	0.50	1.50	0	0
	50	080	2.00	1.50	0	0
	80	193	0.70	1.50	0	0
	64	292	0.20	1.50	0	0
	48	268	0.12	1.50	0	0

LOCATION	D	S	T	D	P	A
	90	086	0.06	1.50	0	1
	77	274	1.50	1.50	1	0
	69	282	0.50	1.60	0	0
	76	258	0.12	1.60	1	0
	79	284	0.40	1.60	0	0
	65	279	1.00	1.60	0	0
	68	299	3.90	1.60	1	0
	62	068	0.80	1.60	1	0
	72	136	3.00	1.60	0	0
	65	287	0.15	1.60	0	1
	67	281	0.30	1.60	0	1
	66	274	0.90	1.60	1	0
	62	285	0.85	1.60	1	0
	61	310	0.55	1.60	0	0
	74	288	0.45	1.60	0	0
	65	267	0.30	1.60	1	0
	69	103	0.70	1.60	1	0
	75	101	0.70	1.60	1	0
	73	100	0.28	1.60	1	0
	67	112	0.05	1.60	0	0
	57	129	4.00	1.60	0	0
	80	074	0.20	1.60	1	0
	70	082	0.12	1.60	1	0
	85	101	0.20	1.60	1	0
	76	107	0.40	1.60	1	0
	70	233	0.60	1.60	0	0
	66	136	0.90	1.60	1	0
	90	103	0.50	1.60	1	0
	70	103	0.15	1.60	0	0
	76	116	0.15	1.60	1	0
	83	100	2.50	1.60	0	0
*	83	182	0.60	1.60	1	0
U. Garbdh-	70	097	2.00	2.10	1	0
ail	74	193	1.00	2.10	0	0
	40	113	2.00	2.10	1	0
	60	115	1.00	2.10	0	0
	90	113	0.80	2.10	1	0
	70	094	0.60	2.10	0	0
	88	085	1.30	2.10	1	0
	80	095	1.50	2.05	1	0
	60	102	0.09	2.05	0	0
	88	104	1.00	2.05	1	0
	78	111	2.00	2.05	1	0
	54	123	1.00	2.05	0	0
	56	109	0.23	2.05	1	0
	62	105	0.30	2.05	1	0
	80	140	0.90	2.05	0	0
	68	165	0.12	2.05	1	0

LOCATION	D	S	T	DS	P	A
	75	090	1.15	2.05	0	0
	64	093	1.30	2.05	1	0
*	60	107	2.50	2.05	1	0
Beinn na	51	117	0.40	2.35	1	0
Selig	63	097	0.50	2.35	1	0
	63	097	0.30	2.35	1	0
	44	115	0.25	2.35	0	0
*	50	088	0.30	2.35	0	0
An Acar-	50	102	2.00	2.20	0	0
seid	46	107	1.60	2.20	0	0
	70	136	0.90	2.20	0	0
	48	105	0.50	2.20	0	0
	44	076	0.15	2.25	0	0
	58	100	0.40	2.25	0	0
	54	117	1.10	2.25	1	0
	60	096	0.10	2.25	1	0
	56	101	0.50	2.25	1	0
	64	101	0.50	2.25	0	0

CENTRE THREE

Both unit lengths are N-S

LOCATION	D	S	T	DS	P	A
Abhain	62	072	1.00	2.55	1	0
Chro	62	072	1.20	2.55	1	0
Beinn	54	097	1.20	2.55	1	0
	70	079	2.30	2.55	1	0
	54	063	3.00	2.55	1	0
	60	060	0.10	2.55	0	0
*	40	065	2.00	2.55	1	0
200m	65	059	2.00	2.55	1	0
	73	085	1.20	2.55	1	0
	45	072	3.00	2.55	1	0
	48	075	0.75	2.55	1	0
	56	071	4.00	2.55	0	0
	49	064	0.70	2.55	0	0
	50	079	1.75	2.55	0	0
	60	071	0.05	2.55	0	0
	60	083	2.00	2.55	1	0
*	46	103	1.50	2.55	1	0

APPENDIX B

CLUSTER ANALYSIS

B1.1 INTRODUCTION During the course of the field study a variety of characteristics (six) were measured on a large number of cone sheets. Recognition of important features or groupings in such a large data set is difficult and prone to gross subjectivity if attempted manually. Computer based statistical analysis provides the potential for synthesizing such large data sets. Cluster analysis was chosen as the analytical method since it is both objective and yields relatively simple graphical results (Fig.B1.1.1) Leeder (1975) used this type of analysis in petrographic analysis of limestones and Davis (1973) outlines general geological uses for this type of analysis. The cluster analysis for this work was run on the City of London Polytechnic's DEC10 computer, using CLUSTAN (Wishart, 1969a, 1969 and 1978)

B1.2 Method The mathematics of cluster analysis are relatively complex (Davis, 1973). However, it works by plotting the characteristics for each case in a multidimensional space and then checks to see if the data falls into groupings (clusters, Fig.B1.1.1). Unlike manual methods where it is difficult to deal with three variables simultaneously, cluster analysis can use any number of variables - plotting the clusters in n-dimensional hyperspace. The most common and most objective way of displaying the results is as a dendrogram. Whereby individuals are progressively grouped with closest neighbours until one cluster embracing all samples is formed (Fig.B1.1.1). Data which has a cluster tendency groups within major "branches" of the dendrogram (Fig.B1.1.1).

B1.3 RESULTS Listed below are the results of the cluster ana-

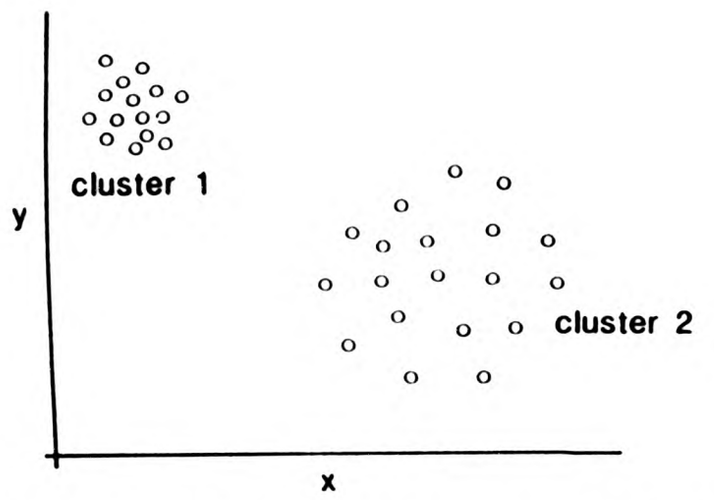

Cluster differentiaton of two data sets using parameters x and y
Cluster 1 is more tightly clustered than cluster 2

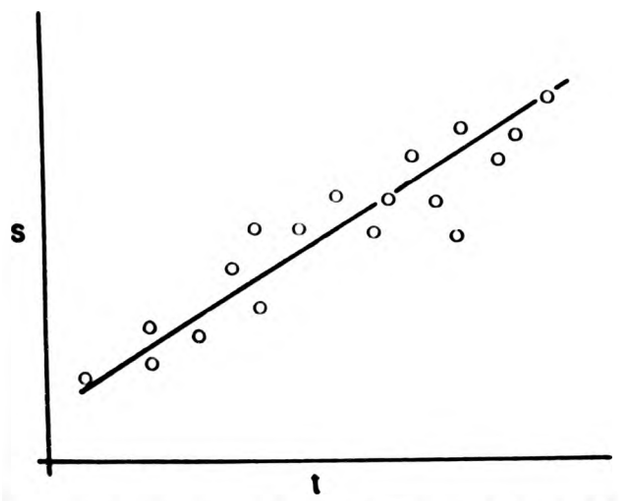

Parameters s and t are highly correlated. The program informs the user that both parameters are not required to define the cluster

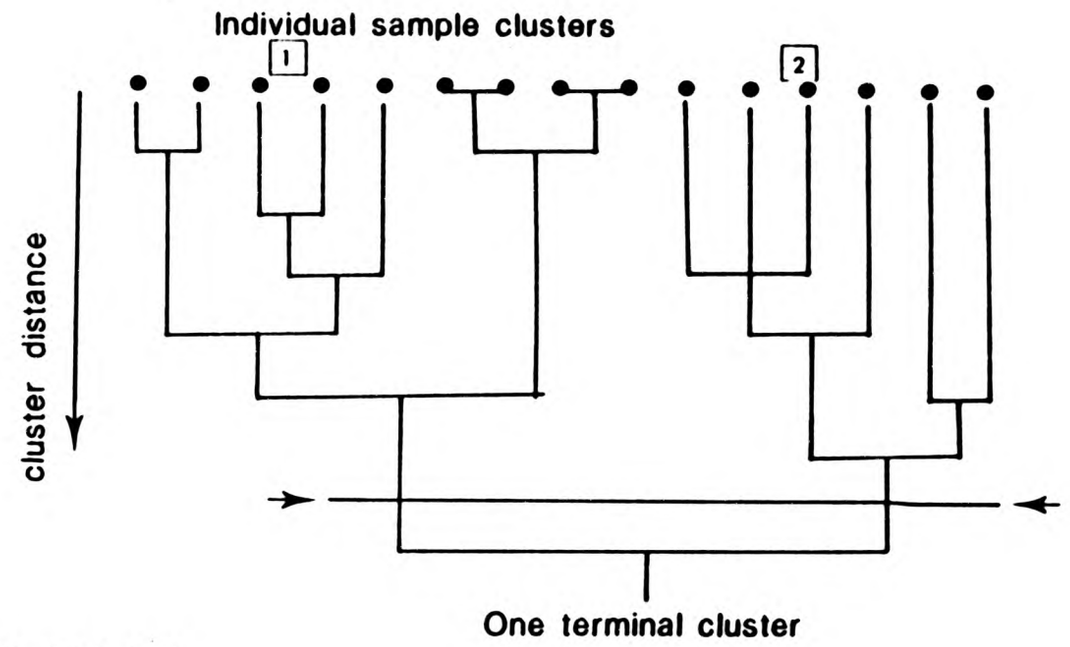

Fig.B1.1.1

Cluster analysis Dendrogram or tree, the branches represent ties between adjacent clusters The distance between fractures increases from top to bottom of the tree . At → ← two clusters are defined. Cluster distance for cluster [1] is shorter than for cluster [2] indicating that the defining parameters of cluster [1] are more homogeneous than those of cluster [2] and thus [1] is more tightly clustered.

lysis of the Centre Two cone sheets. Ten clusters were formed. The cone sheets of each cluster are listed as case numbers (given in Appendix A), and the characteristics of each cluster are given.

where VAR variable

1 Dip

2 Orientation

3 Thickness of sheet in metres

4 Distance from focus of activity

MN-ORIG mean of the cone sheet data

SD-ORIG standard deviation of the cone sheet data

CLUSTER ONE NUMBER OF CASES = 82

CASE NUMBERS

680 682 683 684 685 686 687 688 689 690 691 692 693 694

696 697 698 699 700 701 702 703 704 705 707 708 709 710

711 712 713 714 715 716 717 718 720 721 722 723 724 728

729 730 731 732 733 734 735 737 740 741 742 744 745 748

751 752 755 756 759 760 761 762 763 766 768 769 770 772

773 774 776 777 778 779 780 782 783 784

CLUSTER DIAGNOSIS

VAR	F-RATIO	T	MN-ORIG	STD-ORIG
4	0.0574	1.5662	6.1085	0.1679
2	0.1326	0.8225	282.5122	41.6031
3	0.1922	-0.1849	0.9369	0.8482
1	0.3633	-0.1590	47.4878	10.7097

CLUSTER TWO NUMBER OF CASES = 13

CASE NUMBERS

231 283 640 649 651 653 654 655 664 666 695 727 736

CLUSTER DIAGNOSIS

VAR	F-RATIO	T	MN-ORIG	STD-ORIG
2	0.0533	0.9331	295.1538	26.3813
3	0.0893	-0.3087	0.6969	0.4018
1	0.1459	0.3374	56.3077	6.7871
4	0.3284	0.7038	5.5038	0.4018

CLUSTER THREE NUMBER OF CASES = 98

CASE NUMBERS

200 211 216 221 226 228 232 237 252 258 259 263 276 306
351 353 354 360 362 367 370 375 376 378 381 383 386 388
389 390 391 392 397 414 421 423 426 429 431 477 482 485
487 526 527 559 563 564 570 575 581 582 584 586 587 595
609 615 617 622 623 628 629 630 636 643 644 648 652 657
658 661 670 719 787 790 798 800 803 804 805 806 807 813
815 817 820 822 823 827 830 833 834 835 836

CLUSTER DIAGNOSIS

VAR	F-RATIO	T	MN-ORIG	STD-ORIG
3	0.1311	-0.2660	0.7796	0.7006
1	0.2938	1.3475	74.2551	9.6306
2	0.3742	0.5670	253.3265	69.8716
4	0.5606	-0.3503	4.7648	0.5250

CLUSTER FOUR NUMBER OF CASES = 140

CASE NUMBERS

10 23 35 67 68 69 86 118 133 150 198 199 236 239
247 248 264 265 266 272 280 302 305 307 309 310 317 366
372 373 409 411 412 413 433 434 435 437 438 439 442 445
446 449 454 455 456 457 458 459 460 461 462 463 466 467
468 469 471 472 473 474 475 476 478 486 488 489 490 493
494 495 497 500 501 505 506 508 509 510 512 513 514 516
517 518 519 520 521 523 525 532 533 534 535 536 537 538
539 541 542 543 547 549 550 551 552 554 557 558 560 562
565 568 569 571 573 580 585 590 593 596 597 600 601 602
605 606 612 614 618 621 624 626 631 638 656 674 678

CLUSTER DIAGNOSIS

VAR	F-RATIO	T	MN-ORIG	STD-ORIG
2	0.0731	0.8270	283.0357	30.89.05
3	0.1693	-0.1963	0.9144	0.7960
1	0.2337	-1.0524	31.6143	8.5894
4	0.4061	-0.0857	4.9504	0.4468

CLUSTER FIVE NUMBER OF CASES = 9

CASE NUMBERS

8 191 196 224 240 588 616 662 676

CLUSTER DIAGNOSIS

VAR	F-RATIO	T	MN-ORIG	STD-ORIG
3	0.0342	-0.3600	0.5978	0.3578
2	0.1620	-0.3045	153.7778	45.9722
4	0.5647	0.1595	5.1222	0.5268
1	0.6866	-0.7305	37.3333	14.7224

CLUSTER SIX NUMBER OF CASES = 109

CASE NUMBERS

4 38 66 101 329 342 346 348 350 355 363 365 368 369
371 374 377 380 382 384 387 394 395 396 398 399 400 401
402 403 404 405 406 407 408 410 415 417 418 420 422 425
427 428 432 441 443 448 450 451 452 453 464 465 479 480
481 483 484 491 492 496 498 503 507 511 529 531 544 546
553 555 567 572 578 579 583 592 594 598 599 603 607 608
610 613 619 625 627 633 637 639 645 796 809 810 819 821
824 826 828 829 831 832 837 838 839

CLUSTER DIAGNOSIS

VAR	F-RATIO	T	MN-ORIG	STD-ORIG
2	0.0483	0.8275	283.0826	25.0950
3	0.1230	-0.2674	0.7769	0.6785
1	0.2213	-0.0760	48.9633	8.3588
4	0.2685	-0.5514	4.6239	0.3633

CLUSTER SEVEN NUMBER OF CASES = 270

CASE NUMBERS

1	2	3	5	6	7	9	11	12	13	14	15	16	17
18	19	20	22	24	25	26	27	28	29	30	31	32	33
34	36	37	39	40	41	42	43	44	45	46	47	48	49
50	51	52	53	54	55	56	57	58	59	60	61	62	63
64	65	70	71	72	73	74	75	76	77	78	79	80	81
82	83	84	85	87	88	89	90	91	92	93	94	95	96
97	98	99	100	103	104	105	106	107	108	109	110	111	112
114	115	116	119	121	122	125	126	127	128	129	130	132	134
135	136	138	139	141	142	143	144	145	146	147	148	149	151
152	153	154	155	156	157	158	159	160	161	162	163	164	166
167	168	170	181	172	173	174	175	176	179	180	182	185	186
187	188	189	190	191	193	197	201	202	203	204	205	207	208
210	217	218	223	227	233	238	241	242	243	244	245	249	251
254	255	256	257	260	267	268	271	273	275	277	279	281	287
288	290	292	296	297	298	308	318	319	320	321	322	323	324
325	326	327	330	331	332	333	334	335	336	337	338	339	340
341	343	344	345	347	349	356	357	358	359	361	364	419	424
430	436	447	499	502	548	561	576	642	647	663	677	785	786

788 789 791 792 793 794 795 797 799 801 802 808 811 812

825 840

CLUSTER DIAGNOSIS

VAR	F-RATIO	T	MN-ORIG	STD-ORIG
2	0.1082	-1.1428	58.0259	37.5663
3	0.1648	-0.2066	0.8945	0.7855
4	0.7425	-0.4512	4.6941	0.6041
1	1.0010	0.0132	50.5481	17.7767

CLUSTER EIGHT NUMBER OF CLUSTERS = 17

CASE NUMBERS

183 524 556 566 574 589 604 611 632 634 635 641 659 669

675 814 816

CLUSTER DIAGNOSIS

VAR	F-RATIO	T	MN-ORIG	STD-ORIG
2	0.1523	0.8252	282.8235	44.5775
3	0.1846	0.9263	3.0865	0.8313
1	0.2465	0.0983	52.0588	8.8209

CLUSTER NINE NUMBER OF CASES = 28

CASE NUMBERS

177 213 214 246 262 591 650 660 667 671 672 673 679 726

738 739 747 749 750 753 754 757 758 764 765 767 771 775

CLUSTER DIAGNOSIS

VAR	F-RATIO	T	MN-ORIG	STD-ORIG
3	0.0428	-0.3489	0.6193	0.4001
1	0.4011	1.1100	70.0357	11.2529
4	0.4255	1.1618	5.8250	0.4573
2	0.4306	-0.6553	113.7143	74.9572

CLUSTER TEN NUMBER OF CASES = 74

CASE NUMBERS

21 102 113 117 120 124 131 137 140 165 169 178 184 192
194 195 206 209 212 215 219 220 222 225 229 230 234 235
250 253 261 269 270 274 278 282 284 286 289 291 293 294
295 299 300 301 303 304 311 312 313 314 315 316 352 416
440 444 470 504 522 528 530 540 577 620 665 668 681 706
725 746 818

CLUSTER DIAGNOSIS

VAR	F-RATIO	T	MN-ORIG	STD-ORIG
1	0.7755	0.0333	50.9054	15.6469
2	1.0546	-0.3447	149.1892	117.3033
4	1.1071	0.7571	5.5412	0.7377
3	4.7251	2.0935	5.3447	4.2057

D

D58144 '85

END